GEORGIA INSTITUTE OF TECHNOLOGY
OFFICE OF RESEARCH ADMINISTRATION

Date: 3 March 1969

RESEARCH PROJECT INITIATION

Project Title: Behavior of Nozzles and Acoustic Liners in Three-Dimensional Acoustic Fields

Project No.: B-214 - (E-16-607)

Project Director: Dr. B. T. Zinn

Sponsor: National Aeronautics and Space Administration, Washington, D. C.

Agreement Period: From 1 March 1969 until 28 February 1970

Type Agreement: Grant No. NGR 11-002-085

Amount: $48,980 NASA Funds (B-214)
2,748 GIT Contribution (E-205)
$51,728 Total Budget

Grant Administrator

National Aeronautics and Space Administration
Office of University Affairs (Code Y)
Washington, D. C. 20546

Address for Reports

National Aeronautics and Space Administration
Office of Scientific and Technical Information (Code US)
Washington, D. C. 20546

Reports Required

Quarterly Status - 1Jun69, 1Sep69, and 1Dec69 - Five (5) copies required.

Final Technical - 1Mar70 - Five (5) copies required.

Note: In addition to the above, two (2) copies of all technical reports shall be sent to:

Propulsion & Vehicle Engr. Laboratory
George C. Marshall Space Flight Center
National Aeronautics and Space Administration
Huntsville, Alabama 35812

Assigned to: School of Aerospace Engineering

COPIES TO:

- [ ] Project Director
- [ ] School Director
- [ ] Dean of the College
- [ ] Administrator of Research
- [ ] Associate Controller (2)
- [ ] Security-Reports-Property Office
- [ ] Patent Coordinator
- [X] Library
- [ ] Rich Electronic Computer Center
- [ ] Photographic Laboratory
- [ ] EES Machine Shop
- [ ] EES Accounting Office

Other Mr. R. A. Martin
File B-214

Reports 300. B214 (Sch)

RA-3 (4/65)

N11-28 ... N-

Posted
ALG
OH

GEORGIA INSTITUTE OF TECHNOLOGY

OFFICE OF RESEARCH ADMINISTRATION

RESEARCH PROJECT TERMINATION

Date: May 26, 1975

Project Title: Behavior of Nozzles and Acoustic Liners in Three-Dimensional Acoustic Fields

Project No: E-16-607 (Formerly B-214)

Principal Investigator: B. T. Zinn

Sponsor: NASA - Lewis Research Center

Effective Termination Date: 2/28/75

Clearance of Accounting Charges: 3/31/75

~~XXXXX~~ Grant/~~Contract~~ Closeout Actions Remaining:

1. Final Invoice
2. Final Report of Inventions
3. Gov't. Prop. Inven. & Related Cert.
4. Classified Material Certificate

Assigned to School of Aerospace Engineering

COPIES TO:

Principal Investigator	Library, Technical Reports Section
School Director	Computer Sciences
Dean of the College	Photographic Laboratory
Director of Research Administration	Terminated Project File No. ________
Office of Financial Affairs (2)	Other ________
Security - Reports - Property Office ✓	
Patent and Inventions Coordinator	

RA-4 (3/70)

E-16-601

NASA GRANT NGR 11-002-085

BEHAVIOR OF NOZZLES AND ACOUSTIC LINERS IN THREE-DIMENSIONAL ACOUSTIC FIELDS

Quarterly Report for Period 1 March 1969 to 31 May 1969

Prepared by: Ben T. Zinn, Principal Investigator
Allan J. Smith, Jr., Research Engineer
B. Robert Daniel, Research Engineer

School of Aerospace Engineering
Georgia Institute of Technology
Atlanta, Georgia

I. PROGRAM OBJECTIVES

The possibility of exciting a given acoustic mode in a liquid-propellant rocket motor depends on the nature of the interaction that occurs between this mode and the various physical processes and mechanical components that are present in the system. While some of the physical processes (e.g., the combustion process) will tend to "feed" energy into the wave and hence excite it, other processes will "act" as energy sinks and thus tend to attenuate the wave. The excitation of a given acoustic mode depends on the balance that exists among the various "gain" and "loss" mechanisms. Quantitative information about the various "gain" and "loss" mechanisms, as they are related to various modes, must become available before a reliable design procedure for liquid-propellant rocket engines can be established.

Of special importance is the need for quantitative understanding of the effect that the presence of a converging-diverging nozzle at one end of the combustor has upon the behavior of the natural modes of the combustion chamber. While it is generally accepted that the presence of a converging-diverging nozzle will tend to damp the longitudinal modes, its influence upon the transverse and three-dimensional modes is still open to question. Analytical studies[1,2] indicate that the response of a nozzle that is subjected to transverse or three-dimensional acoustic oscillations depends on its geometry, the mode and frequency of the oscillations, and the Mach number of the entering mean flow. Surprisingly, the results of these analytical studies also point out the possibility that under certain conditions the nozzle might actually "pump" energy into

the combustion chamber and thus have a destabilizing effect. These analytical predictions have never been verified experimentally; they have nevertheless been used in design by several major rocket manufactures. To improve existing design procedures it is important that these analytical predictions be checked experimentally.

The experimental determination of the response of several converging-diverging nozzles that are subjected to three-dimensional or transverse acoustic oscillation is one of the objectives of the present study. More specifically, it is the aim of this study to experimentally determine the dependence of the nozzle admittance relation, which quantitatively describes the wave-nozzle interaction, upon the nozzle shape, frequency and mode of oscillation, and upon the Mach number of the entering mean flow. Attaining this goal requires the development of special experimental facilities as well as new measurement techniques. Work performed during the first quarter of investigation was devoted to the design of the experimental facilities and the development of a theory that will provide the foundation for the new measurement techniques.

The second objective of this program is the investigation of the behavior of acoustic liners in simulated rocket environment. The majority of past studies of wave attenuation by Helmholtz resonators were limited to one-dimensional oscillations while the presence of mean flow past or through the resonators was not properly accounted for. There exists a need to experimentally determine the effect of various design parameters upon the attenuation caused by a liner when it is subjected to three-dimensional or transverse acoustic oscilla-

tions. Such information should be obtained from carefully controlled experiments in which the flow conditions inside an unstable rocket engine will be simulated as closely as possible. The cold flow rocket simulator that is presently being designed at Georgia Tech will provide the environment in which such experiments can be conducted. It is one of the objectives of this program to combine theory and experiments in the quantitative determination of the influence of liner design parameters and engine flow conditions upon the damping effectiveness of acoustic liners that are subjected to three-dimensional and/or transverse pressure oscillations. Such information is a prerequisite for the establishment of reliable design procedure for effective acoustic liners.

II. PROGRESS TO DATE

A. Theoretical Studies

1. Theoretical Considerations of Impedance Tubes For Three Dimensional Oscillations.

Classical theory which provides the foundation for the design of impedance tube experiments[3] assumes that the pressure oscillations are one-dimensional and that they are superimposed upon a quiescent medium. In order to achieve the objectives outlined in the introduction of this report the classical theory had to be modified to account for the presence of one-dimensional mean flow and three-dimensional pressure oscillations. It was the objective of this theoretical study

to obtain expressions that will describe the dependence of the amplitude of the three-dimensional pressure oscillations upon the "end-wall" admittance, the Mach number of the mean flow and the frequency and transverse mode of oscillation. Since this expression will depend upon the acoustic admittance presented to the waves at one end of the tube, then a change in this admittance will result in changes in the axial distribution of the pressure amplitude. If a relationship between the pressure amplitude and admittance function at one end of the tube is known, then for given experimental conditions the measurement of the axial variation of the pressure amplitude along the tube can be used to determine the admittance function at the end of the tube. In the present investigation such a method will be used in the experimental determination of the admittance function of supercritical nozzles that are subjected to pressure oscillations that depend on more than one space dimension.

During the first quarter of investigation a theory that resulted in an analytical expression that describes the axial variations of the amplitude of a three-dimensional pressure oscillation has been developed. This expression can be considered as the counterpart of the classical one-dimensional expression that is used in the design of one-dimensional impedance tubes. The theory shows that the standing three-dimensional wave pattern can be considered as a superposition of incident and reflected waves. Knowing the ratio of reflected and incident pressure amplitudes and the phase shift upon reflection, the standing three-dimensional wave pattern in the tube can be established.

The analysis that produced the expression for the amplitude of the three-dimensional pressure oscillations was based on the following

assumptions: (1) the unsteady flow is inviscid and irrotational; (2) the mean flow is one-dimensional, and its Mach number does not vary along the tube; and (3) wave attenuation along the tube is neglegible. An investigation is presently under way to determine whether some of these assumptions may be relaxed, and the analysis extended to consider more general flow situations.

The results obtained in the above-mentioned investigation were used to develop a computer program that will determine the admittance at the end of the tube (i.e., the nozzle admittance) from available experimental data. This computer program is divided into several parts. In the first part the variation of the pressure amplitude along the tube, for a given admittance at the end of the tube and for given operating conditions, can be determined. In another part of the program the admittance at the end of the tube can be computed from input data that consists of the values of the pressure amplitude at three locations along the tube. This computer program is used at present to determine the optimum axial locations of the pressure transducers that will be used in the actual experiments. In addition this program is currently utilized in an investigation directed at the determination of the errors in the calculated admittance function that will result from experimental errors in the measured pressure amplitude.

In a different study, another computer program that was originally used in combustion instability studies[2] has been modified to compute the nozzle admittance function for a given nozzle configuration and given operating conditions. This program computes the admittance function by numerically solving a system of differential equations originally de-

rived by Crocco[4] in his study of wave propagation in supercritical converging-diverging nozzles. The admittance functions computed in this program will be compared with those measured experimentally. Such comparison will shed the necessary light upon the applicability in rocket design of available nozzle theories.

2. Acoustic Liner Studies

During the first quarter all relevant literature on acoustic liners has been surveyed. This has been done in order to avoid unnecessary duplication of effort. It has been found that although several excellent theoretical studies (e.g., ref. 5) of the problem are presently available, no experimental study aimed at direct verification of the theoretical findings has been conducted to date. The literature survey revealed an interesting theoretical study[6], conducted by Brillouin, in which the liner response was related to properties (e.g., the effective mass and the effective resistance) of a single resonator. This study[6] which has been restricted to longitudinal oscillations has since been extended to consider the case of transverse oscillations. The theoretical results obtained in this study are presently being programmed for numerical computations. These results will serve as guidelines in the planning of the acoustic liner experiments.

Additional study on the interaction of a single Helmholtz resonator with finite amplitude sound waves has also been conducted. In this study the model of the resonator's flow field that was used in an earlier study[7] has been modified to better fit experimental

observations of the flow field[8]. The results produced in this experimental study are in excellent agreement with available experimental data on resonator resistance. The results obtained in this study will be used as guidelines in the experimental determination of the impedance of a single Helmholtz resonator that is subjected to transverse and three-dimensional pressure oscillations. It is also hoped that the results obtained in this study will serve as a first step in the development of a more comprehensive theory that will describe the behavior of arrays of Helmholtz resonators when the latter are subjected to finite amplitude pressure oscillations.

It has recently been found that the Russian literature contains a considerable number of studies that may be relevant to our investigations of acoustic liners. These papers are presently being reviewed, and all relevant information will be gathered.

B. Design of Experimental Facilities

The main objective of this portion of the program was the design of an acoustic facility capable of closely simulating the flow conditions in an unstable liquid-propellant rocket engine. The choice of rocket simulator chamber diameter was determined by three factors: (1) the upper limit of frequency at which the acoustic power output of the acoustic driver drops off (1000 cps), (2) the frequency spacing between the various transverse acoustic modes of the chamber and (3) the blow-down time of the air supply system at the test Mach numbers. The chamber length (10 ft.) was selected to be consistent with previous impedance tube work at Georgia Tech. The selection of a chamber dia-

meter and chamber Mach numbers fixed the nozzle throat diameter. The remainder of the nozzle dimensions were selected to fit the requirements of available theoretical studies on the subject[4] as well as reflect current nozzle design practices. An injector with a showerhead orifice pattern is included as an integral part of this test apparatus. The driving characteristics of the combustion process are simulated by acoustic drivers that are placed 4-in. downstream of the injector. The chamber pressure has been determined by the requirement that the flow at the nozzle throat be sonic during the experiment. It can be seen from this short discussion that the design of this cold-flow facility attempted to simulate every aspect of the flow in an unstable rocket engine with the exception of the combustion process.

Airflow requirements for the experiment will be provided by an existing 3000 psia air supply with a storage capacity of 500 cubic feet. The testing time available for a continuous run is approximately 200 seconds with a 11.375-inch diameter impedance tube with a chamber pressure of 30 psia and a mean flow Mach number of 0.16.

The test apparatus and supporting facility are shown in Figure 1. The test apparatus consists of the injector, chamber (i.e., impedance tube), exhaust nozzle, acoustic liner, and acoustic drivers. The intended operating conditions for this facility include chamber Mach numbers up to 0.20 at total pressures in the chamber up to and including 50 psia. Regulator valves will maintain the desired pressure levels in the impedance tube and across the acoustic drivers.

The injector will be fabricated from a 12-in. ips blind flange with a 150 lb. ASA rating. The air will pass through the injector

plate via a showerhead injector orifice pattern. The main objective of this design is to keep the velocity distribution of the entering air as uniform as possible and at the same time keep the acoustic impedance of the injector as high as possible. The latter can be achieved by uniformly-spaced holes and a large pressure drop across the injector.

The chamber (i.e., the impedance tube) is fabricated from an aluminum pipe that has an inner diameter of 11.375-in., a wall thickness of 0.687-in., and an overall length of 10-ft. The acoustic drivers can be mounted on the chamber at a location 4-in. downstream of the injector face at three different tangential positions: 0°, 90°, and 180°. The first tangential mode can be made to spin or stand by properly selecting two of these three ports. Pressure oscillations within the chamber will be monitored by 7 or 8 - depending on the mode - pressure transducers, Photocon Model 403. There are 9 axial locations at which 2 transducers can be mounted at 0° and 270°. A tenth axial position, 5-inches upstream of the exhaust nozzle (or liner), has 4 pressure ports located at 0°, 120°, 180°, and 270°. Because a given mode has established characteristics, the selection of pressure transducer position will be determined by the mode to be tested. To date the chamber has been designed and ordered and we are presently rechecking our original design.

Two exhaust nozzles have been designed. The first nozzle has an entrance design Mach number of 0.08 while the second has an entrance design Mach number of 0.16. Both nozzles have a radius of curvature at the inlet and radius of curvature at the throat equal

to the chamber radius of 5.688-in. However, the convergent half-angle of the first nozzle is 15° while that of the second nozzle is 30°. The test results of the first nozzle are expected to agree more closely to Crocco's Nozzle Admittance Theory than the results of the second nozzle because of the small angle assumption of that theory. Originally, the design of both nozzles called for aluminum to be the nozzle material but subsequent cost analyses indicated that a reinforced plastic (i.e., fiberglass) would cut the cost of fabrication by a factor of three. Consequently, both nozzles are being redesigned for the new manufacturing technique. Both nozzle designs will be submitted to the NASA project engineer for his approval prior to the initiation of the final phase of the fabrication cycle.

Two different types of acoustic drivers will be used. For the no-flow experiments (reference data), two 75-watt, electro-magnetic University acoustic drivers will be used. For those experiments with flow, two 4000 watt, electro-pneumatic Ling drivers will be used.

There is one area of great concern at this time, namely the noise generated within the air stream by the normal shocks in the valves. The required pressure drops across the valves require the valves to operate critically, thereby inducing a considerable amount of noise to the entire system. Various techniques to suppress this noise are being investigated and show that this problem can be circumvented to a great extent. The residual noise can then be tolerated.

C. Expected Progress During Next Report Period

During this quarter theoretical investigations aimed at improv-

ing existing impedance tube theories and available measurement techniques will continue. Computer programs developed to date will be used in an error analysis that will determine the accuracy and reliability of the experimental data. The nozzle computer program will be used to numerically calculate the theoretical nozzle admittance function. The predictions provided by these calculations will be used for comparison with the experimental data. Theoretical investigations of acoustic liners will continue and liner experiments will be planned and designed.

Design and fabrication of all components of the experimental facility will be completed. Installation and preliminary checkout of various support systems will be initiated.

REFERENCES

1. "Three Dimensional Combustion Instability in Liquid Propellant Rocket Engines: A Parametric Study," co-authored with C. T. Savell and W. Mikolowsky, Proceedings of the 5th ICRPG Combustion Conference, CPIA publication No. 183, Dec., 1968.

2. "A Theoretical Study of Three Dimensional Combustion Instability in Liquid Propellant Rocket Motors," co-authored with C. T. Savell, to appear in the proceedings of the Twelfth International Symposium on Combustion.

3. Kinsler, L. E., Frey, A. R., "Fundamentals of Acoustics," second edition, John Wiley and Sons, New York, 1962.

4. Crocco, L., Sirignano, W. A., "Behavior of Supercritical Nozzles Under Three Dimensional Oscillatory Conditions" AGARDograph 117, 1967.

5. Oberg, C. C., Kuluva, N. M., "Acoustic Liners For Large Engines," Rocketdyne Report R-7792, March 1969.

6. Brillouin, J., "Sound Absorption By Structures With Perforated Panels," translated from French (by T. J. Schultz) appeared in Sound and Vibration during 1968 (exact issue unknown).

7. "A Theoretical Study of Nonlinear Dissipation in Acoustic Liners," Proceedings of the 4th ICRPG Combustion Conference, CPIA Publication No. 166, Vol. I, December, 1967, pp. 135-150.

8. Ingard, U., Labate, S., "Acoustic Circulation Effects and Nonlinear Impedance of Orifices," J. Acoust. Soc. of Amer., Vol. 22, No. 2, March 1950, pp. 211-218.

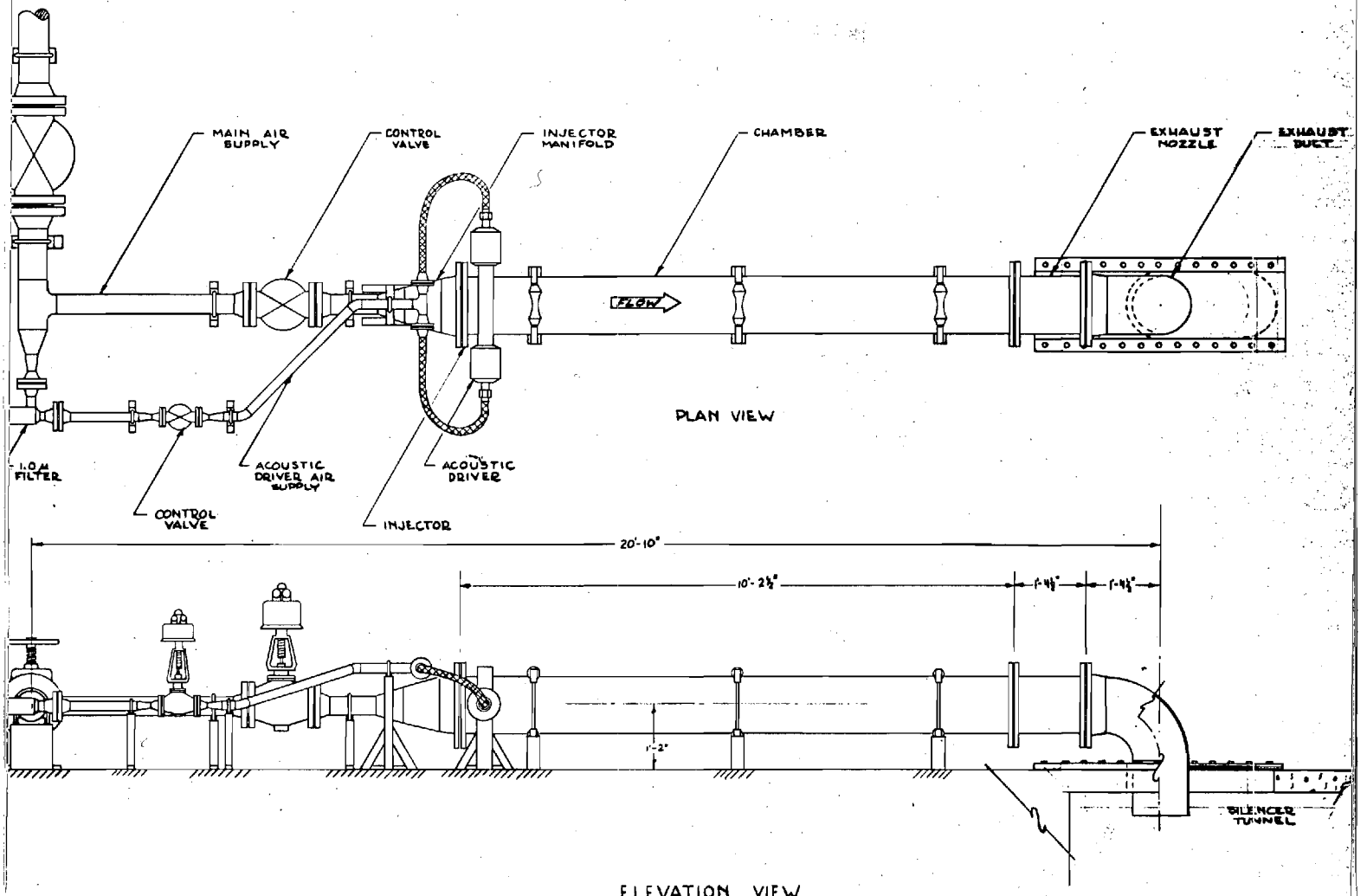

FIG. 1 EXPERIMENT EQUIPMENT SCHEMATIC

NASA GRANT NGR 11-002-085

BEHAVIOR OF NOZZLES AND ACOUSTIC LINERS IN THREE-DIMENSIONAL ACOUSTIC FIELDS

Quarterly Report for Period 1 June 1969 to 31 August 1969

Prepared by: Ben T. Zinn, Principal Investigator
Allan J. Smith, Jr., Project Engineer
B. Robert Daniel, Research Engineer

School of Aerospace Engineering
Georgia Institute of Technology
Atlanta, Georgia

I. PROGRAM OBJECTIVES

The possibility of exciting a given acoustic mode in a liquid-propellant rocket motor depends on the nature of the interaction that occurs between this mode and the various physical processes and mechanical components that are present in the system. While some of the physical processes (e.g., the combustion process) will tend to "feed" energy into the wave and hence excite it, other processes will "act" as energy sinks and thus tend to attenuate the wave. The excitation of a given acoustic mode depends on the balance that exists among the various "gain" and "loss" mechanisms. Quantitative information about the various "gain" and "loss" mechanisms, as they are related to various modes, must become available before a reliable design procedure for liquid-propellant rocket engines can be established.

Of special importance is the need for quantitative understanding of the effect that the presence of a converging-diverging nozzle at one end of the combustor has upon the behavior of the natural modes of the combustion chamber. While it is generally accepted that the presence of a converging-diverging nozzle will tend to damp the longitudinal modes, its influence upon the transverse and three-dimensional modes is still open to question. Analytical studies[1,2] indicate that the response of a nozzle that is subjected to transverse or three-dimensional acoustic oscillations depends on its geometry, the mode and frequency of the oscillations, and the Mach number of the entering mean flow. Surprisingly, the results of these analytical studies also point out the possibility that under certain conditions the nozzle might actually "pump" energy into the combustion chamber and thus have a destabilizing effect. These analytical predictions have never been verified experimentally; they have nevertheless been used in design by several major rocket manufactures. To improve existing design procedures it is important that these analytical predictions be checked experimentally.

The experimental determination of the response of several converging-diverging nozzles that are subjected to three-dimensional

or transverse acoustic oscillation is one of the objectives of the present study. More specifically, it is the aim of this study to experimentally determine the dependence of the nozzle admittance relation, which quantitatively describes the wave-nozzle interaction, upon the nozzle shape, frequency and mode of oscillation, and upon the Mach number of the entering mean flow. Attaining this goal requires the development of special experimental facilities as well as new measurement techniques.

The second objective of this program is the investigation of the behavior of acoustic liners in simulated rocket environment. The majority of past studies of wave attenuation by Helmholtz resonators were limited to one-dimensional oscillations while the presence of mean flow past or through the resonators was not properly accounted for. There exists a need to experimentally determine the effect of various design parameters upon the attenuation caused by a liner when it is subjected to three-dimensional or transverse acoustic oscillations. Such information should be obtained from carefully controlled experiments in which the flow conditions inside an unstable rocket engine will be simulated as closely as possible. The cold flow rocket simulator that is presently being designed at Georgia Tech will provide the environment in which such experiments can be conducted. It is one of the objectives of this program to combine theory and experiments in the quantitative determination of the influence of liner design parameters and engine flow conditions upon the damping effectiveness of acoustic liners that are subjected to three-dimensional and/or transverse pressure oscillations. Such information is a prerequisite for the establishment of reliable design procedure for effective acoustic liners.

II. PROGRESS DURING REPORT PERIOD

A. Summary of Program Status

The program is partitioned into time-sequenced areas of effort

similar to the familiar milepost chart. These areas include design, fabrication, installation and checkout, test, data reduction, and final report. At this time, the design phase of the program has been completed, the manufacturing phase is near completion and the installation phase has just begun. Only the fabrication of the fiberglass exhaust nozzles and acoustic liners remains, and it is expected that both items will be ready for the checkout tests that are scheduled for the end of September.

At present the program is approximately on schedule. There is, however, some concern that the various target dates during installation will be subjected to slippage because several vendor-supplied components have not been delivered on schedule. For example, delivery of the control valves for the main air supply for the chamber and the air supply for the pneumatic acoustic drivers is four weeks overdue. Some provision was made in the time table for such slippages but only in modest terms.

B. Theoretical Studies

1. Theoretical Considerations of Impedance Tubes For Three Dimensional Oscillations.

During the first quarter from March 1, 1969 to May 31, 1969 an analysis of three dimensional wave oscillations in a cylindrical tube with steady mean flow was performed. One of the by-products of this analysis was an analytical expression that describes the spatial dependence of the three-dimensional wave pattern. It has been shown that the standing-wave pattern depends on both the mean flow Mach number as well as the value of the admittance of one end of the tube. In the derivation of this expression it has been assumed that: (1) the unsteady flow in the tube is inviscid and irrotational; (2) the mean flow is one-dimensional and its Mach number does not vary along the tube; and (3) wave attenuation along the tube is negligible. This expression was used to develop a computer program that can determine

the admittance of a device situated at the end of the tube (e.g., an exhaust nozzle) from available experimental data.

The analytical studies performed during this quarter concentrated on the following three problems: (1) efforts were made to develop an appropriate theory that will enable the experimentalist to quantitatively determine the wave attenuation along the walls of the tube; (2) an investigation aimed at the evaluation of the errors associated with the experimental determination of the nozzle admittances was conducted; and (3) the optimum location of the pressure transducers along the tube was investigated.

The investigation of wall attenuation is still in progress and it appears that analytical expressions that can account for side wall attenuation can be derived for travelling waves only. The difficulties associated with the determination of the standing wave attenuation is due to the fact that the latter is comprised of two travelling waves that move in opposite directions and experience different wall attenuation due to the presence of mean flow.

In the second investigation it has been found that the errors in the experimental determination of the nozzle admittance will be largely due to the errors in measuring the sound pressure level at the various axial positions along the length of the chamber. The aforementioned computer program was used to determine how various sound pressure level errors affected the measured values of the nozzle admittance function. In order to establish an "exact" test case, assumed values of the admittance parameters were used to calculate a typical three-dimensional standing wave pattern along the length of the chamber thereby providing "exact" reference sound pressure levels at the various transducer locations. It was then assumed that a "measured" sound pressure level consisted of the "exact" reference sound pressure level plus an error, usually $\pm$ 1 decibel. These "measured" values were then used to determine the nozzle admittances and the comparison of these admittances with the "exact" known admittances provided an estimate of the errors

associated with the experimental determination of the nozzle admittance functions. The maximum admittance error, ± 100%, occurred when all the "measured" sound pressure levels were approximately the same whereas the minimum admittance error, ± 1%, occurred when at least one sound pressure was 5 decibels different than the remaining sound pressures. Additionally, these errors decreased as the reflected wave decreased in amplitude.

The error analysis also yielded useful information about the optimum placement of the dynamic pressure transducers. Inasmuch as the maximum admittance error occurred when the sound pressure levels were approximately the same, then it follows that the transducers should be distributed along the tube in such a way that this condition is not fulfilled. This requirement necessitated the provisions of more transducer ports in the tube in order to facilitate moving the transducers whenever the values of their outputs become similar in magnitude.

C. Test Facility

The results of an investigation to determine the noise level that will be induced into the airstream by the control valves indicated a negligible effect on the data quality. In the event that the noise level does become intolerable, provisions have been made for the inclusion of a noise suppression device into the flow system. All major components of this system, except the air control valves, have been received and the installation of this system has been initiated.

The instrumentation system has been designed and installation has just begun. All major components of this system have been purchased and received.

The injector for this experiment has been fabricated. This injector is comprised of 1,627 orifices of 0.073-in. diameter. The

injector has been designed to flow critically in order to achieve an infinite impedance and minimize wave attenuation at the injector face. Additionally, the injector has been designed to provide a uniform flow distribution inside the chamber.

The chamber, shown in Figure 1, and the wooden mandrils, which provide the inner contour for the exhaust nozzles, have been fabricated. The nozzles, shown in Figure 2, will be made out of fiberglass and they are presently being built by a local manufacturer.

It is planned that four different acoustic liners will be tested during this first year's effort. These four liners are interchangeable combinations of two inside perforated shells and two outer casings. The shells and casings are shown in Figure 3. All liners are designed for a resonant frequency of 717 Hertz, which corresponds to the first tangential mode of the chamber. The liners are 16-in. long and the perforated shells have a fixed inner diameter of 11.375-in. The casings have a fixed outer diameter of 19-in. The following tabulation presents the shell and casing dimensions:

UNIT	t	d	σ
Shell #1	1.5	0.291	7.5
Shell #2	1.25	0.334	10.4
Casing #1	1.892	---	---
Casing #2	2.112	---	---

where t is the wall thickness in inches, d is the hole diameter in inches and σ is the open area ratio. The following table describes the four liners that can be made up out of the above casings and shells:

LINER	SHELL/CASING	Δr
1	1/1	0.42
2	1/2	.20
3	2/1	.67
4	2/2	.45

In this table Δr is the cavity backing distance and it is equal to the casing inner radius minus the outside radius of the shell. The admittances and absorption coefficients of these liners will be determined by simultaneous measurements of the chamber and cavity pressure amplitudes and the phase angle between these pressures. The theoretically predicted responses of these four liners are shown in Figure 4.

D. PROGRESS DURING NEXT QUARTER

The installation and preliminary checkout of the system will be completed. Both nozzles will have been tested and preliminary data analysis of these results will have begun. Both problems associated with the theoretical phase will have been resolved.

REFERENCES

1. "Three Dimensional Combustion Instability in Liquid Propellant Rocket Engines: A Parametric Study," B. T. Zinn, C. T. Savell, and W. Mikolowsky, Proceedings of the 5th ICRPG Combustion Conference, CPIA publication No. 183, Dec., 1968.

2. "A Theoretical Study of Three Dimensional Combustion Instability in Liquid Propellant Rocket Motors," B. T. Zinn and C. T. Savell, to appear in the proceedings of the Twelfth International Symposium on Combustion.

3. Crocco, L., Sirignano, W. A., "Behavior of Supercritical Nozzles Under Three Dimensional Oscillatory Conditions," AGARDograph 117, 1967.

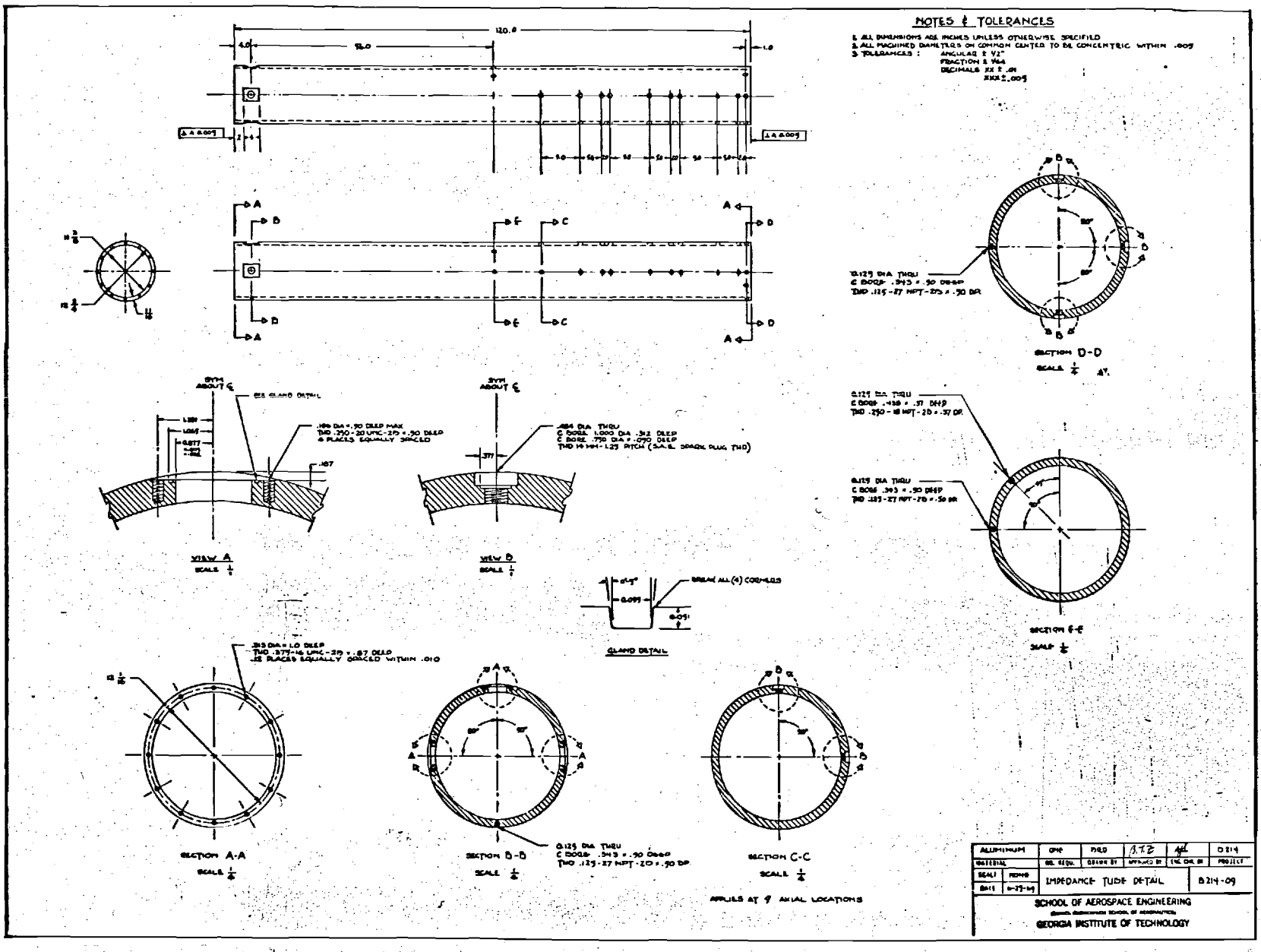

FIGURE 1: CHAMBER DETAIL

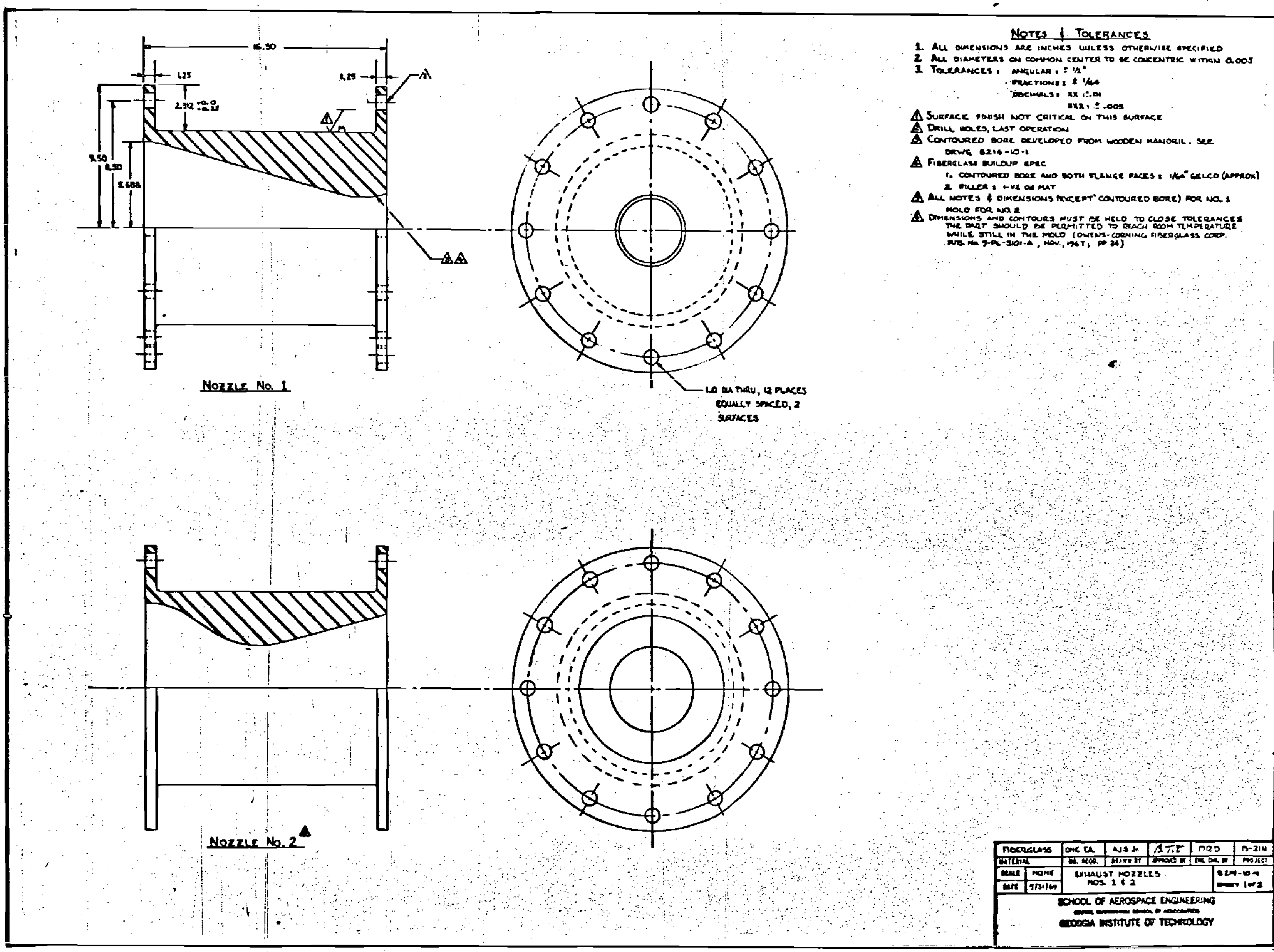

FIGURE 2A: EXHAUST NOZZLE DETAIL.

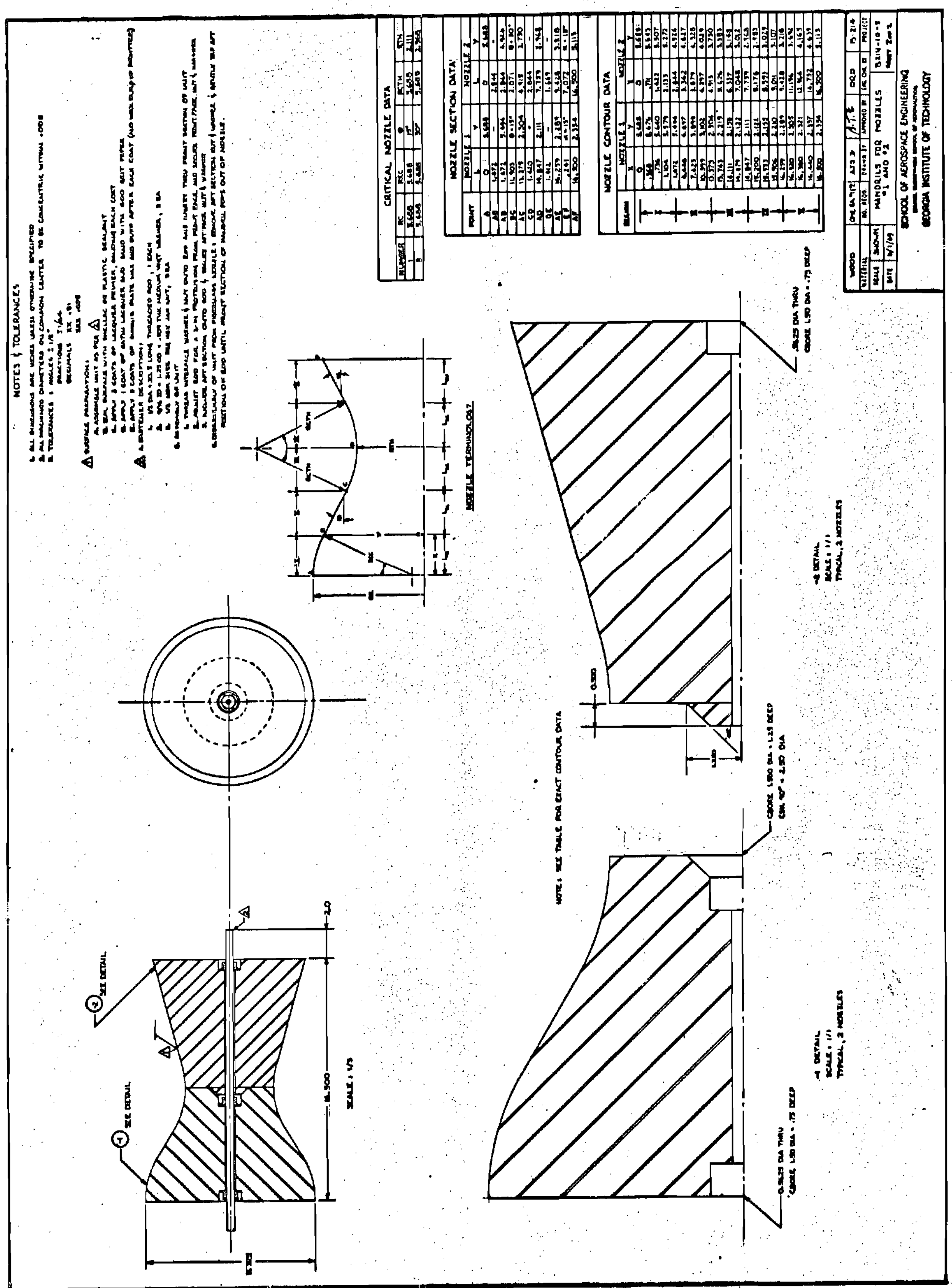

FIGURE 2B: EXHAUST NOZZLE DETAIL

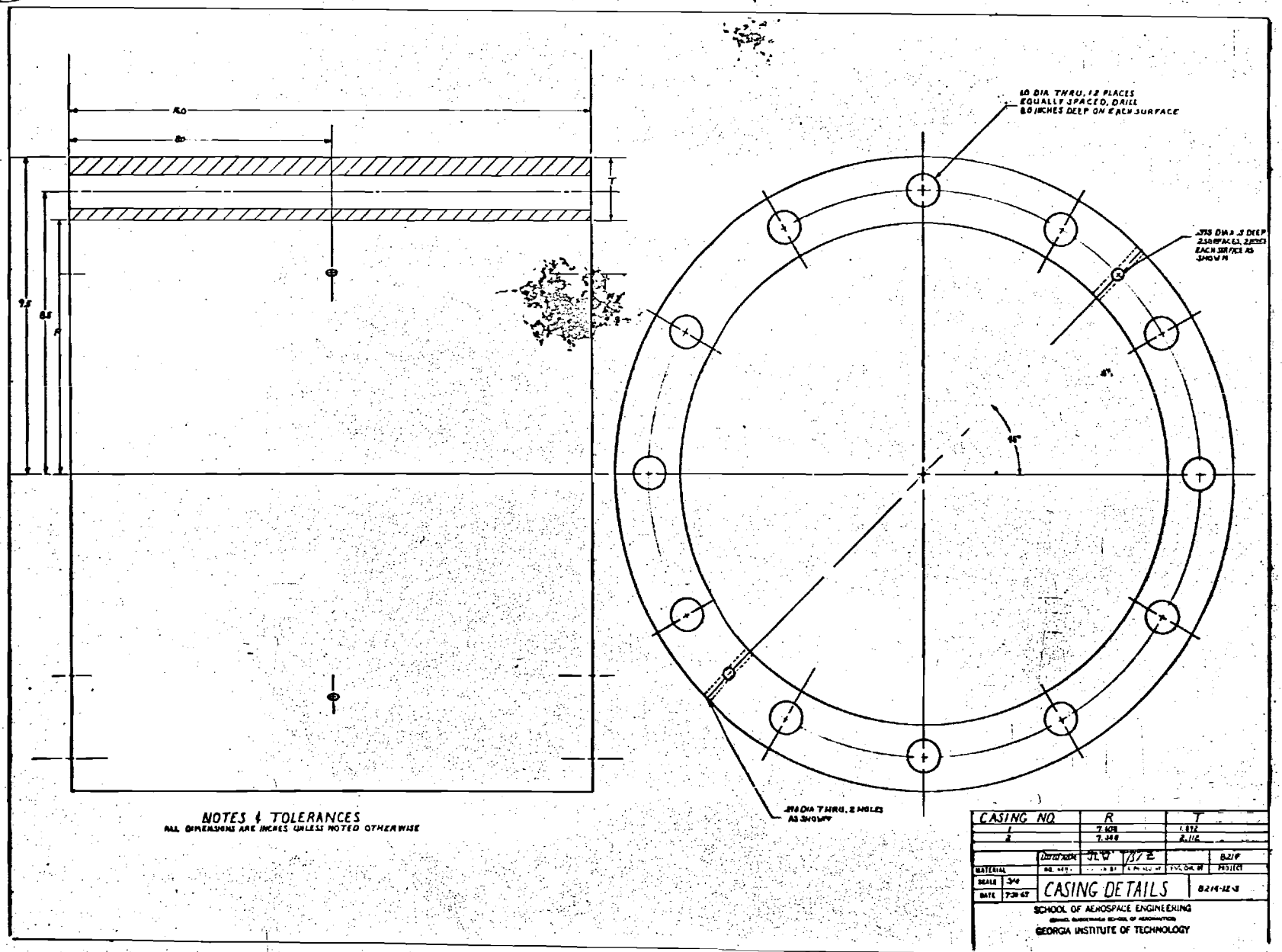

FIGURE 3A: ACOUSTIC LINER DETAIL

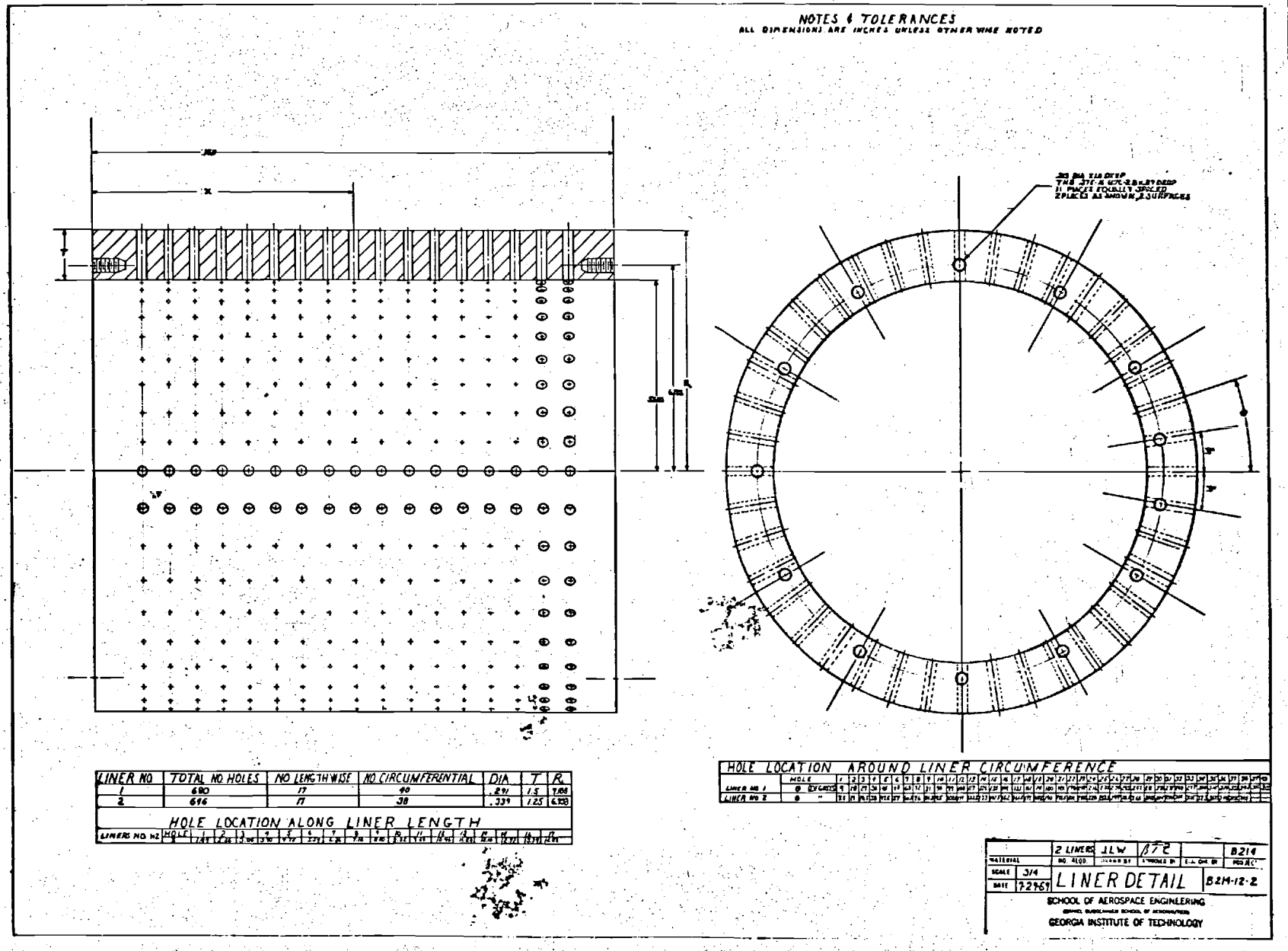

FIGURE 3B: ACOUSTIC LINER DETAIL

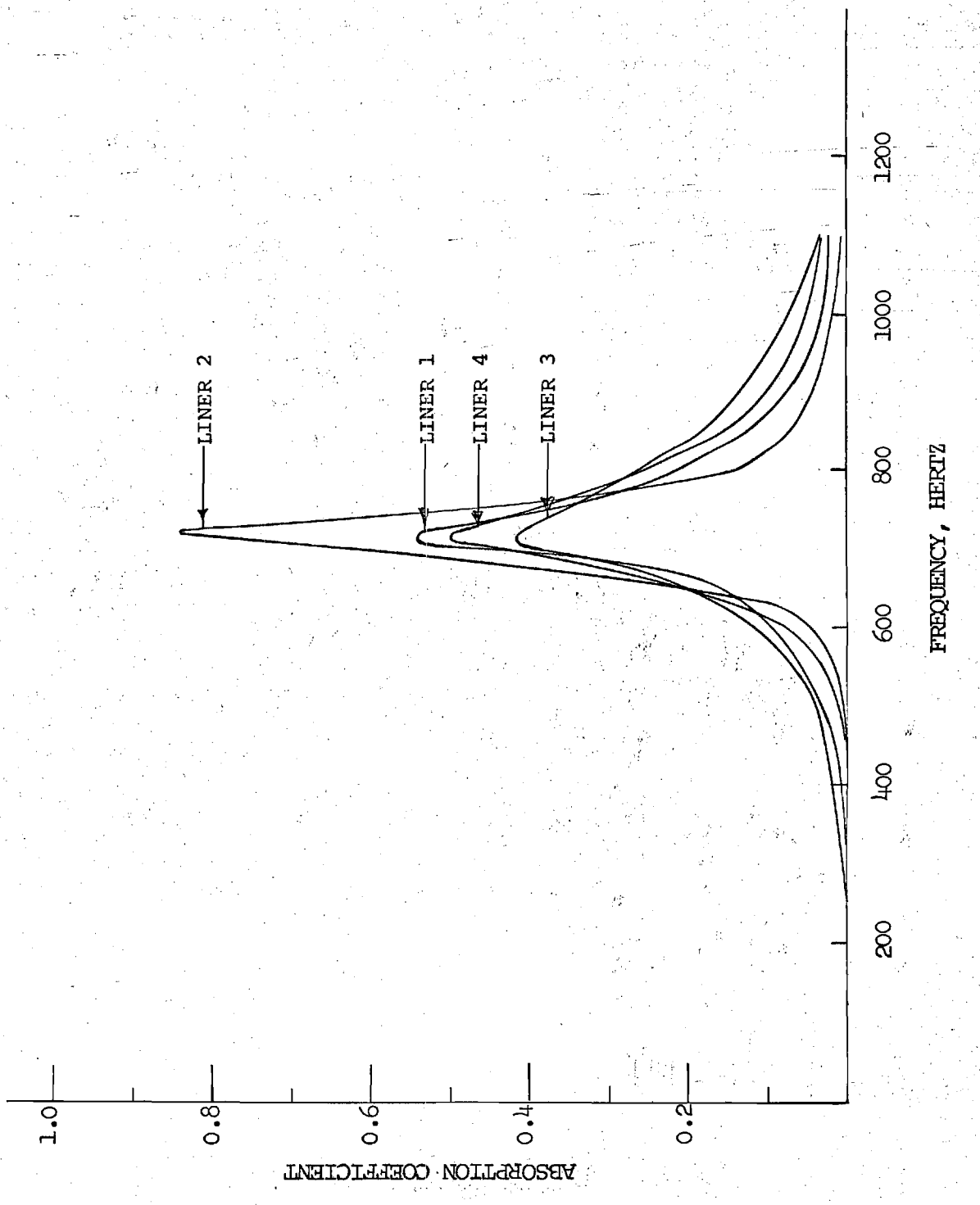

FIGURE 4: RESPONSE CURVES FOR THE FOUR ACOUSTIC LINERS

NASA GRANT NGR 11-002-085

BEHAVIOR OF NOZZLES AND ACOUSTIC LINERS IN THREE-DIMENSIONAL ACOUSTIC FIELDS

Quarterly Report for Period 1 September 1969 to 31 December 1969

Prepared by: Ben T. Zinn, Principal Investigator
Allan J. Smith, Jr., Project Engineer
B. Robert Daniel, Research Engineer

School of Aerospace Engineering
Georgia Institute of Technology
Atlanta, Georgia

I. PROGRESS DURING REPORT PERIOD

A. Summary of Program Status

One of the primary objectives of this program was the development of an experimental facility in which the flow conditions inside an unstable liquid propellant rocket motor could be simulated. This facility is to be used in the quantitative determination of the admittance functions of supercritical converging-diverging nozzles. In addition this facility is to be used in the investigation of the damping characteristics of acoustic liners. Performing the above-mentioned experiments requires the development of an appropriate theory, adequate experimental facilities, and proper measurement and data reduction techniques.

To date the efforts devoted to this program proceeded in two directions; i.e., development of an appropriate theory and measurement techniques as well as the construction of proper experimental facilities. As reported in our earlier progress reports the appropriate theory has been developed early in the program and it has since been used as a guide in the development of the experimental facilities. Further theoretical work that was performed as part of this program was primarily devoted to extensions and refinements of the basic theory. With the basic guiding theory available, the development of the desired experiments required the design, fabrication, installation and checkout of the mechanical hardware. Alongside this effort appropriate instrumentation system and data reduction techniques had to be developed.

At this time, the design of the experimental facility,

the manufacturing of the various mechanical components (with the exception of the acoustic liners) and the installation of the mechanical hardware is completed. In addition the necessary instrumentation has been purchased and installed and the set up of the appropriate electrical networks has been completed. At present the whole experimental facility, including both the mechanical and electrical hardware, is undergoing a thorough check out as it is being prepared for the actual testing, which is expected to take place in the very near future.

B. Theoretical Studies

During the third quarter of this program the theoretical efforts continued in two directions. As reported in our previous progress reports work continued on the analysis of three dimensional wave propagation in a circular duct containing a through steady state flow and attenuating side walls. Although this is a very difficult problem it is believed that its solution, once obtained, will enable engineers to develop more effective procedures for the design of acoustic liners.

Our other theoretical effort is directed towards obtaining admittance functions for nozzles of arbitrary shape. Presently available theories are only applicable to nozzles with slowly converging walls whose mean flow may be assumed to behave in a quasi one dimensional manner. As is well known, most practical nozzles are <u>not</u> slowly converging and the applicability of existing theories to calculate their admittance functions is at best questionable. In the analysis of the case when the nozzle walls are slowly converging solutions can be obtained by means of separation of variables technique. This is no longer the case when the convergence of the nozzle walls is fast so that

the steady state flow cannot be assumed to be one dimensional. We are presently exploring the possibility of obtaining numerical solutions for this case. Once obtained these solutions will be of considerable use in the analysis of various combustion instability problems. It is believed that the analysis and solution of this problem will require a considerable amount of time.

C. Test Facility

The installation and preliminary checkout of the entire system has been completed; however, the final checkout is still underway. At the outset of this program it was planned that at this point in the program the facility would have been completed and testing would be underway. Unfortunately failures in various components of the system (e.g., system dryer and valves) and delay in deliveries of major system components resulted in unexpected delays. In February, 1969, two valves were ordered for the system. One of these valves controls the air flow into the chamber of the rocket motor while the other controls the air flow through the sound generating system. The manufacturer promised delivery of these valves in mid-July whereas the actual delivery occurred at the end of October. As a result our whole working schedule had to be changed in order to minimize delays in the planned program.

The final installation of the system was completed when the valves arrived. Initial operation of these valves disclosed two discrepancies: (1) the hydraulic power unit for these valves (also purchased from the same manufacturer) had an output pressure of 1500 psig instead of 3000 psig; (2) the electric controller for the valve had a faulty printed circuit. Two weeks were

required to correct the difficulty with the hydraulic power unit and one week to repair the electric controller. Once these difficulties were corrected the valve functionals were completed. The delays and difficulties encountered with the delivery, installation and operation of the valves are the main reasons for the slippage in the program schedule. It is hoped that through a concentrated effort we shall be able to make up for this delay.

When the valve functionals were completed, the new air pressurization and storage facility was activated for the first time. Additional minor problems that resulted in minor slippage were encountered. These problems included leakage of compressor intake valves, leaks in the discharge system and clogged air dryers. To date all of these problems have been resolved. The experimental facility is undergoing its final checkout and is being prepared for the initiation of the nozzle testing.

In addition to the effort required to develop the hardware and its associated systems, a similar effort was required for the instrumentation associated with this experiment. Both the steady state and the dynamic circuits had to be designed, developed, and installed into an area where no instrumentation had previously existed. Major instrumentation items such as an automatic tracking filter, tape recorder, oscillograph, strip-chart recorders, and dynamic pressure transducers had to be purchased, calibrated, and installed into the system. Special attention was given to calibration, recording, and data processing techniques.

All of the instrumention and its circuitry have been installed. The majority of the circuits have been checked out. As to be expected, some problems with ground-loop currents, faulty cables, and guard loop modes were encountered; however,

these were eliminated as they appeared. A few circuits remain to be checked but these will be ready when nozzle testing is begun.

II. PROGRESS DURING NEXT REPORT PERIOD

Final checkout of the entire experimental facility will be completed. Testing of the nozzles will be completed and nozzle data analysis will be performed during the time that the acoustic liners will be tested. All data reduction will then be completed. The final report will follow thereafter.

NASA GRANT NGL 11-002-085

BEHAVIOR OF NOZZLES AND ACOUSTIC LINERS IN THREE-DIMENSIONAL ACOUSTIC FIELDS

Quarterly Report for Period 1 December 1969 to 28 February 1970 4

Prepared by: Ben T. Zinn, Principal Investigator
Allan J. Smith, Jr., Project Engineer
B. Robert Daniel, Research Engineer

School of Aerospace Engineering
Georgia Institute of Technology
Atlanta, Georgia

I. SUMMARY OF PROGRAM OBJECTIVES

The growth or decay of a disturbance that is accidentally introduced into a propulsion device depends on the nature of its interaction with the various processes and components that are present in the system. While some processes respond by adding energy to the disturbance (e.g., the combustion process), others tend to act as energy sinks and hence cause an attenuation of the disturbance. To be able to predict whether a given disturbance will amplify or attenuate it is necessary to know the frequency response of the various processes and components with whom the disturbance is bound to interact. As long as such information is not known, a quantitative prediction of the stability of liquid propellant rocket motors will not be possible.

To obtain the desired information separate theoretical and experimental investigations aimed at the determination of the frequency responses of the various processes and components that contribute to engine stability must be conducted. These investigations should be performed under conditions that closely simulate the flow inside unstable liquid propellant rocket motors. In the present study the frequency responses of supercritical nozzles and acoustic liners are investigated.

At present, the only available investigation of the nozzle frequency response is theoretical in nature[1]. In spite of their importance in the design[2] of stable liquid propellant rocket engines these theoretical predictions have never been verified experimentally; hence their applicability and usefulness are open to question. It is one of the objectives of the present investigation to experimentally determine the frequency response of various practical nozzles. Nozzles of various shapes and area

ratios will be tested and a special effort will be made to determine the dependence of the nozzle response function upon these design parameters. A comparison between the experimental data and theoretical predictions will provide a check on the validity and range of applicability of the theoretical predictions.

It is the objective of the acoustic liner study to determine the response of acoustic liners under controlled conditions that simulate, as closely as possible, the flow conditions inside unstable liquid propellant rocket motors. In this connection it should be mentioned that available data on acoustic liners response was obtained in experiments where either careful control was not possible[3] or the experimental set up did not simulate the flow conditions inside unstable liquid propellant rocket motors[4].

It is the long range objective of this program to provide propulsion engineers with reliable data about the frequency responses of typical nozzles and acoustic liners when they are subjected to flow oscillations similar to the ones that can be found in unstable liquid propellant rocket motors.

II. SUMMARY OF PROGRAM STATUS

The various tasks performed under this program involved the cooperation of three faculty members, Dr. B. T. Zinn, and Messrs. A. J. Smith, Jr. and B. R. Daniel and three graduate students, Messrs. W. A. Bell, J. M. Walsh and D. C. Kooker. These individuals were responsible for performing various design tasks as well as various theoretical and experimental investigations that had to be carried out as part of this program.

Since results obtained in the theoretical studies were used to guide the design and planning of the experiments, the results of these investigations will be discussed first. Initial theoretical studies involved the development of a three dimensional impedance tube theory that accounts for the presence of a one dimensional mean flow in the tube. The new theory represents a major extension of the classical impedance tube theory that is limited to considerations of one dimensional oscillations in tubes without mean flow. The new theory provides expressions that describe the dependence of the three dimensional wave pattern, that is generated inside the combustion chamber, upon the impedance at the tube end (e.g., the nozzle impedance) and upon the magnitude of the mean flow Mach number. It has been theoretically shown that by measuring instantaneous pressure amplitudes at various locations along the tube and then substituting the experimental data into the theoretical expressions results in a set of equations that can be used in the determination of the nozzle admittance function. As part of this investigation a special computer program capable of converting the experimental data into meaningful results (i.e., nozzle admittance functions) has been developed.

Other related analytical studies included the development of a computer program that uses Crocco's nozzle theory[1] to compute the theoretical nozzle admittance functions. The applicability of these theoretically predicted admittance functions will be checked by comparing them with the experimentally determined admittance functions. Another phase of this program was the study of acoustic liners. As part of this investigation a thorough literature search was conducted and the results were used as a guide in the design of the liners that will be tested in the program. In

addition an approximate theory for investigating acoustic liner response has been developed. Other relevant theoretical investigations are in progress and they will be discussed in another section of this report.

The results of the above investigations were used to guide the design of a cold flow facility capable of simulating the flow conditions in unstable liquid propellant rocket motors. The facility uses high pressure air that is stored in a 500 cubic feet, 3000 psia storage system. During a run the air leaves the storage facility, passes through a series of control valves that reduce its pressure to a desirable level, and enters the simulated combustion chamber through a showerhead injector. Two 4000 watt electro-pneumatic drivers, that are attached to the combustion chamber walls, are used to generate the desired three dimensional pressure oscillations. The behavior of these waves is monitored by a series of pressure transducers located at various locations along the tube. The transducers' signals are recorded on tape and later processed for conversion into impedance data. A schematic of this system is presented in Fig. 1.

To be able to perform the various tasks demanded by these experiments a specialized instrumentation system had to be designed and assembled. Todate considerable amounts of money, effort and time have been invested in the purchase, installation and calibration of the various components that comprise this instrumentation system.

As part of the planning of the experimental program the various components that were to be tested (i.e., nozzles and acoustic liners) had to be designed. Two nozzles of practical shape were designed and built. These nozzles have different geometries and were chosen in a way that will enable the investi-

gators to determine the validity of some of the assumptions used in the theoretical predictions of the nozzle admittance function. The problem of designing acoustic liners has been studied in depth. After several modifications, the present design of the acoustic liners are based on results obtained in investigations conducted at NASA Lewis[5] and Pratt & Whitney[4]. The testing of these liners is expected to produce data that will shed additional light about the applicability of available liner theory.

Considerable delays in delivery and malfunction of major system components resulted in corresponding delays in the initiation of the test program. It appears, however, that all major difficulties have been solved and preliminary testing has begun. These temporary delays will not affect the productivity and results of the overall program.

III. PROGRESS DURING REPORT PERIOD

A. Theoretical Studies

The analytical investigations concentrated in several areas. One of the investigations was concerned with the evaluation and improvement of the experimental results. To perform this investigation values of nozzle admittance function, that were determined by using Crocco's nozzle theory, were substituted into the expressions that determine the three-dimensional wave amplitude. The resulting expression could be used to calculate the pressure amplitude at any location in the chamber. The theoretically computed amplitudes were then modified by the introduction of intentional positive or negative errors. It was then assumed that the modified amplitudes had been determined experi-

mentally and they were then used to compute the nozzle admittance functions. The computed values were then compared with the known correct values. These studies revealed that the accuracy of the experimental predictions depends upon several variables that include the magnitudes of the real and imaginary parts of the nozzle admittance, the frequency of the oscillation and the locations chosen for measurement. This investigation is in progress and various possibilities for improving the accuracy of results obtained from experimental data are being investigated.

In a recent study of lined cylindrical chambers[5] it has been shown that the inclusion of liners may have the additional effect of "detuning" the chamber. This information has been used in the design of the acoustic liners that will be tested in the present program. To obtain a better appreciation of the problem two liners having different characteristics were designed. One of these liners was designed to be a poor absorber (over the range of frequencies that will be tested) but a good "detuner", while the other liner was designed to be primarily a good absorber. The testing of these liners should help to shed light about the relative importance of these two effects as well as the applicability of the theories that guided the designs of these liners.

Two additional theoretical investigations are in progress. One of these is concerned with the investigation of three dimensional standing-wave behavior in chamber with lined walls. The second investigation is concerned with the prediction of the admittance function of nozzles with fast converging walls. Both investigations are aimed at improving existing theories and providing better theoretical approaches for the design of future liquid propellant rocket motors.

B. Test Facility

The final facility checkout phase has been completed and preliminary testing has been initiated. The main objectives of the preliminary tests were to determine the system characteristics with all control valves and instrumentation operating simultaneously, measure the background noise level that is induced in the chamber by the mean flow, and determine the limitations and characteristics of the dynamic pressure transducers that will be used to measure the sound pressure levels.

Measurements of the flow noise and its spectral analysis showed that, in the frequency range that will be used in actual experiments, there are six predominant frequencies that are contributing the major portion of the noise. The sound pressure levels recorded at these frequencies were all above 120 db (re. 2×10^{-4} DYNES/cm^2) and the highest had the level of 138 db. A detailed analysis of system characteristics showed that the major portion of the noise was being generated by the flow control valves. To alleviate this difficulty a muffler has been designed to suppress these upstream noise sources. The estimated sound pressure level of the noise generated by the valves is 160 db. Design calculations show that the addition of the muffler will decrease the sound pressure level in the chamber from 138 db to 70 db in spite of the fact that the valve noise output is 160 db. The necessary muffler has been designed and fabrication has begun. Estimated time necessary for muffler completion is approximately one month.

During the period that the muffler is being fabricated, all of the no-flow tests will be completed. The first series of tests will be conducted with an infinite impedance termination. This data will be used to provide an additional check

on the operation of the computer program that has been specially formulated to reduce the experimental data. Once program verification is completed, the admittance of the nozzles, with and without steady flow, will be determined.

IV. PROGRESS DURING THE NEXT REPORT PERIOD

The admittance of the nozzles with no mean flow will be completed. The muffler will be installed and the admittance of the nozzles with mean flow will be determined. Testing of the liners will be initiated. Work on various reported theoretical investigations will continue.

REFERENCES

1. Crocco, L., Sirignano, W. A., "Behavior of Supercritical Nozzles Under Three Dimensional Oscillatory Conditions," AGARDograph 117, 1967.

2. Smith, A. J., Jr., Reardon, F. H., et. al., "The Sensitive Time Lag Theory and Its Application To Liquid Rocket Combustion Instability Problems," Aerojet-General Corp. Technical Report No. AFRPL-TR-67-314, Volume I, March 1968.

3. Oberg, C. C., Kuluva, N. M., "Acoustic Liners For Large Engines," Rocketdyne Report R-7792, March 1969.

4. Garrison, G. D., Schnell, A. C., Baldwin, C. D., Russell, P. R., "Suppression of Combustion Oscillations with Mechanical Damping Devices," Pratt and Whitney Report PWA FR-3299, August 1969.

5. Philips, B., "On the Design of Acoustic Liners For Rocket Engines: Maximum Damping as a Design Objective," NASA TM X-1720, January 1969.

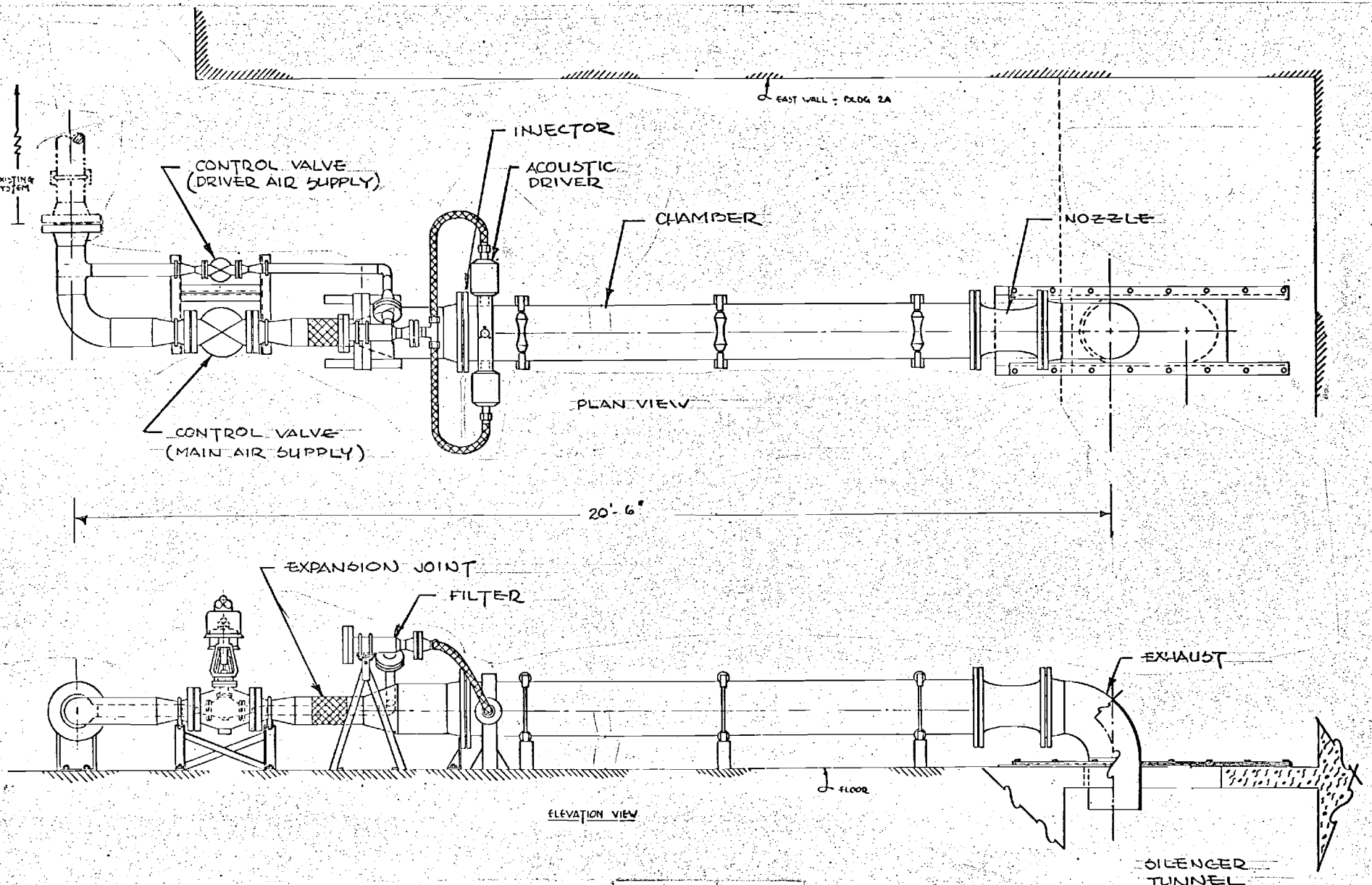

EXPERIMENT ASSEMBLY

Figure 1

NASA GRANT NGL 11-002-085

BEHAVIOR OF NOZZLES AND ACOUSTIC LINERS IN THREE-DIMENSIONAL ACOUSTIC FIELDS

Quarterly Report for Period 1 March 1970 to 31 May 1970

Prepared by: Ben T. Zinn, Principal Investigator
Allan J. Smith, Jr., Project Engineer
B. Robert Daniel, Research Engineer

School of Aerospace Engineering
Georgia Institute of Technology
Atlanta, Georgia

PROGRESS DURING THE REPORT PERIOD

A. Theoretical Studies

An analytical investigation concerned with the evaluation and improvement of the original measurement and data reduction methods indicated that the originally planned method of attack should be replaced by a more accurate experimental scheme. This investigation was triggered by the observation that when the original method was used, small experimental errors caused disproportionate errors in the determination of the exhaust nozzle admittance functions. The new experimental scheme considerably reduces the errors associated with the determination of the nozzle admittance functions. Other analytical investigations that were conducted during this period were:

(1) The determination and elimination of the flow noise that is superimposed on the measured sound signal.

(2) The determination of the behavior and possible orientation (relative to the drivers) of a standing three-dimensional wave pattern.

(3) The investigation of three-dimensional standing wave behavior in chambers with lined walls.

(4) The development of a theory for the prediction of the admittance values of nozzles with rapidly converging walls.

The error analysis (i.e., the evaluation and improvement analysis) of the original experimental scheme showed that for certain nozzles small errors in experimental measurements would result in very large errors in the calculated admittance functions. The analytical expression for the sound pressure level measured at a point in the cylindrical chamber is a function of the transducer position, the frequency and mode of oscillation, the fluid temperature, the two parameters that relate to the nozzle admittance and the mode amplitude at the driven end of the chamber. With the exception of the last two items, which represent two unknowns, the remainder of the above-mentioned quantities can be measured experimentally. Inasmuch as the expression for the

pressure amplitude contains three unknowns, the original experimental scheme called for three pressure amplitude measurements to determine the two parameters related to the nozzle admittance and the mode amplitude at the driven end. The analysis conducted last quarter showed that the errors associated with the measurements of position, frequency, and temperature could be neglected. This is primarily due to the fact that these quantities could be measured with a high degree of accuracy; also, the error in the calculated nozzle admittance function was insensitive to experimental errors in these quantities. The same analysis showed that the accuracy of the pressure amplitude measurements determines the accuracy of the calculated admittance functions. The magnification of the experimental error in the measurement of the pressure amplitude is due to the fact that the pressure amplitude is related to the admittance function through a hyperbolic cosine function. Using this functional relationship, it has been shown that for nozzles with small admittance values (which according to Crocco's nozzle theory describe the majority of practical nozzles) small errors in pressure measurements could result in admittance errors in excess of 50 percent. This observation pointed out the need for modifications in both the original experimental measurement techniques as well as the data reduction method.

The alternative experimental scheme was dictated by a modification to the analytical approach to the solution of the problem. It was shown that the desired admittance function may be determined from knowledge of amplitude and phase angle (referenced to any arbitrary source) at various axial positions. It was also shown that the desired nozzle admittance function may be determined by measurements of pressure amplitudes at two axial positions along the tube and measurement of the difference between the corresponding phase angles. The use of phase angle data had the effect of relating the desired nozzle admittance function to the experimented data through a hyperbolic sine function. It has been shown that use of the new functional

relationship produces significantly smaller errors (by an order of magnitude) in the calculated values of the admittance functions, than the use of the hyperbolic cosine function. The error analysis for the use of this measurement technique is in the final stages of completion. However, the results obtained to date are most encouraging as far as minimizing the resultant admittance errors are concerned.

Another analysis, that is concerned with the proper interpretation of the measured data, has indicated that an axial mode can coexist simultaneously with the three-dimensional mode. Present studies are concerned with the determination of the experimental conditions under which the effects of the axial mode can be neglected.

Previous test results have indicated that the presence of flow noise and possible rotation of the transverse pressure wave nodal lines should be accounted for in the analytical investigations and the resulting computer programs. Both the elimination of flow noise effects and the determination of the effect of the rotation of the nodal surfaces of the three-dimensional pressure wave were investigated and the appropriate modifications are presently added to existing computer programs.

The two studies concerned with the investigation of three-dimensional standing wave behavior in chambers with lined walls and with the prediction of the admittance values of nozzles with rapidly converging walls were continued during the report period. Inasmuch as these studies are still in their preliminary stages, no results can be presented at this time.

B. Test Facility

The muffler, which was designed to suppress valve-generated flow noise, has been fabricated and is presently being installed into the system. A portion of the system had to be disassembled in order to accommodate final "field fitting" of the muffler. Some minor modifications will have to be included in system components that are located in the vicinity of the muffler.

The major portion of the acoustic liner fabrication has been completed. The only task that remains to be completed is the drilling of the holes in the inner liner shell. All other aspects of the liner fabrication have been completed.

A number of tests have been conducted in an effort to answer such fundamental questions as:

(1) Is it possible to distinguish between the driven oscillations and the flow noise during the operation of the experiment?

(2) What is the nature of the excited three-dimensional mode when the acoustic drivers are driven in and out of phase in a no-flow environment?

(3) What is the wave phase angle difference between two transducers separated by 90° (at a given axial location) as the driver's frequency is swept through the range from 100 hertz to 1000 hertz?

The first series of tests showed that there is no difficulty in distinguishing between sound and flow noise. When a wave with a given frequency was excited in the chamber containing steady air flow, it was observed that the unfiltered sound-plus-flow noise signal was approximately 20 db larger than the corresponding flow noise signal. Processing the signals through a tracking filter showed a greater difference between these two sets of signals. This experiment suggested that the flow noise contributes an insignificant portion of the total measured sound pressure level. This difference can be further augmented by the use of the muffler and by increasing the power output of the drivers. In addition, the analytical elimination of the flow noise in the data reduction portion of the computer program will further improve the reliability of the data.

The characteristics of the three-dimensional wave, regardless of the driver phasing, were shown to be more complicated than one would expect. In some instances the pressure antinode of the three-dimensional wave did not appear to establish itself where classical acoustics would have predicted. Instead, it appeared to have been

skewed (or rotated) to some degree. In other instances, the pressure antinode appeared to align itself properly. These conclusions are based on superficial analysis of test data that was monitored while the test was in progress. After the installation of the muffler, this test will be rerun and the proper data recorded and analyzed with more sophisticated instrumentation.

The test related to the determination of the wave phase angle differences has been conducted and the results were recorded on a magnetic tape. These results have not been analyzed at this time. This test is intended to check whether the presence of an axial wave, that coexists with a three-dimensional wave, can be neglected. The data from this experiment will determine the range of frequencies for which the presence of axial modes may be neglected. These frequencies will be used to obtain experimental data for the determination of the nozzle admittance function.

PROGRESS DURING THE NEXT REPORT PERIOD

The error analysis will be completed. Unless unforeseen difficulties arise, testing of the nozzles will be conducted. The acoustic liners will complete their fabrication cycle and their testing will begin after the nozzles complete their test program. Work on the development of data reduction computer programs will continue. The various theoretical investigations will also continue.

NASA GRANT NGL 11-002-085

BEHAVIOR OF NOZZLES AND ACOUSTIC LINERS IN THREE-DIMENSIONAL ACOUSTIC FIELDS

Quarterly Report for Period 1 June 1970 to 31 August 1970

Prepared by: Ben T. Zinn, Principal Investigator
Allan J. Smith, Jr., Project Engineer
B. Robert Daniel, Research Engineer

School of Aerospace Engineering
Georgia Institute of Technology
Atlanta, Georgia

PROGRESS DURING THE REPORT PERIOD

A. Summary of Progress

The computer program that uses experimental data to determine the nozzle admittances has been updated in order to (1) eliminate a double-root solution and (2) to statistically curve-fit the resultant admittance data. Prior to actual nozzle testing preliminary tests were conducted in order to determine (1) the effectiveness of the installed muffler; (2) the best mode of chamber frequency excitation; (3) the chamber acoustics under flow and no-flow conditions; and (4) the quality of the data measured by various transducers located at different locations along the chamber. Due to the failure of its predecessor, a different tape recorder is presently being added to the system, and actual nozzle testing will take place shortly.

B. Theoretical Studies

A considerable amount of work has been devoted to final modifications of the computer program that calculates the desired nozzle admittances from experimental sound pressure level and phase measurements. Studies conducted during this period showed that for a given set of input data the computer program may calculate two solutions for the nozzle admittance function. In order to eliminate this difficulty an additional subroutine, capable of selecting the proper solution, has been added to the computer program. In its present form the developed computer program can use available experimental data to compute the desired nozzle admittance function.

In addition to the aforementioned computer update, a parallel effort to statistically curve-fit the admittance data has been conducted. During the test, five axial pressure transducers are employed to sample the acoustic wave within the chamber. During data analysis, three pressure measurements are required to determine

the nozzle admittance at that particular frequency. By using the five pressure measurements in combinations of three, ten values of the admittance are generated at each frequency. In the event that the five pressure measurements are perfect, all ten nozzle admittance values will be equal. As a result of experimental inaccuracies the computed admittances, at each frequency, will differ from one another. In order to treat the data-scatter, the computer program will apply various statistical methods at each frequency and then curve-fit the admittance data over the frequency range.

Additional efforts associated with the analytical investigation of three-dimensional standing wave behavior in chambers with lined walls as well as the prediction of the admittance values of nozzles with rapidly-converging walls have continued during this report period; the studies have, however, not progressed to the point where significant results can yet be presented.

C. Experimental Investigations

The installation of the muffler together with system modifications required to accommodate the muffler have been completed. Preliminary results of the tests conducted to determine the amount of chamber noise reduction due to the insertion of the muffler into the system indicate approximately 20 db reduction in the chamber flow noise. Based on this "quick-look" data, additional testing of the muffler to generate more specific information was deemed unnecessary, and the muffler will be retained as an integral part of the flow system.

The acoustic liner has been fabricated, and it will be tested once the exhaust nozzles have completed their test cycles.

The experimental efforts conducted during this report period were directed at the determination of the admittance values of the

manufactured convergent-divergent nozzles, whereas the previous report period efforts were directed at understanding the control and operating characteristics of the simulated rocket cold-flow system. As a prelude to the current effort, the following questions had to be answered:

(1) Could the desired experimental data be obtained by using a continuous frequency sweep? In this case the frequency of the excited three-dimensional waves will be changed in a continuous pre-assigned rate. An alternative to this method of operation would be to run separate tests at various discrete frequencies that are of interest to rocket designers.

(2) Is there a significant difference between the acoustic properties of the cold-flow rocket simulator under flow and no-flow conditions?

(3) Is there a significant difference in the characteristics and quality of the data obtained from pressure transducers located at different locations along the tube (e.g., transducers located at the mid-section of the chamber and near the nozzle entrance)?

A total of seven complete tests were conducted during this report period, and the data was analyzed in order to answer the aforementioned questions. The use of an automated frequency sweep during the test is the preferred mode of operation because it provides data at many more frequencies from which admittances can be determined. This mode of operation also conserves on the limited supply of air available for the blowdown tests. The sweep cannot, however, be used if the sweep-rate exceeds the maximum sweep-rate that is acceptable to the data processing equipment (e.g., the tracking filter). The filter employed for data processing has a 1.5 Hz bandwidth when the signal level is 3 db down from its maximum level and 6.0 Hz bandwidth when the signal is 60 db below its maximum value. By recording the test data at a tape recorder

speed of 30 ips (i.e., inches per second) and reducing the data at a tape speed of 1-7/8 ips, the tracking filter senses a sweep rate of 0.009 Hz/sec that is sufficiently slow to satisfy filter requirements.

Some considerations were given to investigating the acoustics of the system under no-flow conditions and then using this information as a guide during actual flow experiments. To check the feasibility of this approach the acoustic properties of the system under flow and no-flow conditions had to be compared. Comparisons of acoustic data obtained during flow and no-flow tests revealed that the introduction of flow into the system results in a significant modification of the acoustic properties of the system. When no air is flowing in the system, neither the injector holes nor the nozzle throat are choked. Under these conditions, the portions of the system located upstream of the injector plate and downstream of the nozzle throat can affect the acoustic properties of the chamber. When flow is introduced into the system, the influence of that portion of the system that is located upstream of the injector plate is changed whereas the influence of the system downstream of the nozzle throat is eliminated. As a result the acoustic properties of the system under no-flow conditions are entirely different from the acoustic properties of the system during actual testing. Another difference between flow and no-flow testing is associated with changes in the speed of sound. The electropneumatic acoustic drivers used in the experimental setup require relatively little air flow. Consequently, during no-flow testing the rate of discharge from the air supply tanks is small while the rate of decrease in air temperature, due to the expansion of the compressed air, is negligible. This is not the case during flow testing when the air flows through the main chamber and the temperature changes between 60°F at the start of the test and -30°F at the end of the

test. This wide temperature excursion results in a rapid change in the speed of sound (that in turn results in a change in wavelength) during the test; a change that greatly affects the acoustic properties of the system. In view of the above-described observations, the previously-mentioned possibility of using no-flow data to determine the acoustic properties of the system should be discarded.

Comparisons of data recorded by various transducers located at different locations along the chamber indicated qualitative similarity in the observed frequency spectrum as well as the sound pressure level. The recorded signals were also qualitatively similar to data obtained in related sound-flow interaction experiments.

Based on the above findings it was decided that the investigation of the system as well as the actual nozzle testing should be conducted under flow conditions. The frequency of the excited waves will be changed in a continuous manner over a predetermined frequency range, and any of the transducer locations can be used with the same degree of confidence. It was expected that the actual testing would have been completed at this date; a massive failure of the system's tape recorder unfortunately resulted in a temporary postponement of the scheduled testing. Another tape recorder is presently being incorporated into the system, and acquisition of the desired data is expected to begin shortly.

D. Expected Progress During Next Report Period

The computer program will be finalized. The new tape recorder will be inserted into the system, and nozzle admittance tests will be conducted. Testing of the acoustic liner will be initiated, and work on the other analytical investigations will continue.

E-16-601
B-214

NASA GRANT NGL 11-002-085

BEHAVIOR OF NOZZLES AND ACOUSTIC LINERS IN THREE-DIMENSIONAL ACOUSTIC FIELDS

Quarterly Report for Period 1 December 1970 to 28 February 1971

Prepared by: Ben T. Zinn, Principal Investigator
Allan J. Smith, Jr., Project Engineer
B. Robert Daniel, Research Engineer

School of Aerospace Engineering
Georgia Institute of Technology
Atlanta, Georgia

PROGRESS DURING REPORT PERIOD

A. Summary of Progress

The analytical investigations during this report period have concentrated on the investigation of wave motion in fast converging nozzles, the development of a nonlinear regression analysis for the reduction of the experimental data, and on the computation of theoretical nozzle admittance values. The nonlinear regression analysis and the nozzle admittance studies have resulted in computer programs that are either in operation or in final checkout; the nozzle wave motion study is in progress.

Eleven tests have been conducted and analyzed. The frequency response of nozzles 1 and 2 was the subject of ten tests while the frequency response of a nozzle-acoustic liner combination was considered in one of the tests. These test results are discussed herein as well as the fabrication of three additional nozzles. The use of the analog-to-digital conversion technique for data reduction has been examined. The results of this study indicate that the use of an analog-to-digital data reduction technique is an excellent alternative method of data reduction. The application of this method is under investigation.

B. Theoretical Studies

Analytical studies conducted under this program have concentrated on the development of a new nonlinear regression analysis for data reduction and the improvement of an existing computer program that predicts theoretical nozzle admittance values. In addition, the development of a theory for the prediction of the admittance values of nozzles with rapidly-converging walls has continued.

The nonlinear regression analysis, which has been discussed in the last Quarterly Progress Report, was programmed during this report period and its checkout was initiated. Several problems, that are associated with the mathematical aspects of the solution, were encountered during the checkout phase. These problems were corrected and the checkout of the program was completed. The nonlinear regression technique was used to reduce data that had been obtained in earlier nozzle tests; the calculated nozzle admittance data is being analyzed and these results will be reported in the next quarterly progress report.

The work on the computer program that calculates the theoretical nozzle admittance values was instigated by the discovery that the integration subroutine that was used in the program could become numerically unstable under certain conditions. This problem was solved by replacing the previously-used numerical integration scheme (viz., Runge Kutta of order four) by a more stable integration subroutine that depends on the use of predictor-corrector techniques (viz., the Adams integration scheme). The resulting program has begun its final checkout.

Some preliminary results from the analysis to predict the admittances of nozzles with rapidly convergent walls are now available. This theoretical development solves the linear equations for the perturbed flow field in the region between an acoustic driver at the upstream end of a combustion chamber and the choked throat of the nozzle as an elliptic boundary value problem.

No attempt has been made to separate the analysis of the nozzle from that of the combustion chamber. The steady mean flow is considered to be one-dimensional and isentropic, as is the perturbed flow. The finite difference solution is accomplished with a computer program based on a special numerical technique originally formulated in Reference 1. One of the

early check-out runs was the simple problem of a longitudinal standing wave in a chamber with closed ends. The numberical results were in excellent agreement with available analytical solutions.

Under investigation, at the present time, is the unsteady behavior of a system comprizing of a full nozzle and a combustion chamber problem. The solution of this problem will enable a comparison between the nozzle admittances predicted by this analysis and those predicted by Crocco and Sirignano[2]. These results should be available soon.

C. Experimental Investigation

Eleven tests have been conducted and analyzed during this report period. Ten tests were conducted with either nozzle 1 or nozzle 2 (see Reference 3, Figure 1) in the system and one test was conducted with the acoustic liner in the system. The objectives of the nozzle tests were as follows:

1. Determine the test-to-test repeatibility of the resultant nozzle admittance data.
2. Test nozzle 2 (M = 0.16) with 5 pressure transducers and obtain multiple admittance data for this nozzle.
3. Measure the overall flow noise associated with each nozzle and determine the spectral content of this noise.
4. Determine if tests conducted by driving an oscillation of a given frequency, over a period of several seconds, yield the same admittance data as tests in which the frequency of the driven waves is varied continuously at a very slow rate.
5. Determine the dependence of the admittance data upon the choice of transducer locations in the chamber.

The acoustic liner test was conducted to obtain a rough estimate regarding the changes in data that might be expected during the liner studies.

The test-to-test repeatibility of the admittance data has been found to be good. Figure 1 presents the data taken from two separate tests conducted at identical test conditions. For $k \leq 5.5$, the two test yielded approximately the same values of nozzle admittance. However, this data must be supplemented for the following reasons: (1) the analysis of the data recorded in both tests failed to provide data points for the ranges $k = 5.0 \pm 0.2$ and $k = 5.9 \pm 0.2$ - the missing data is needed for the determination of the missing portion of the admittance curve; (2) the analysis of the first test data yielded no data for the range $k > 5.5$; (3) the data scatter becomes large when $k > 5.5$. Additional analysis of the two test records will provide the needed data at $k = 5.0$ and $k = 5.9$. The increased data scatter must be investigated.

It is important to qualify data presented in Figure 1 as well as in the other figures. All experimental programs must eventually relate the quality of the data to acceptable statistical standards. Statistical confidence in experimental data can be related directly to the number of samples obtained at a particular value of the independent variable. In this experiment, the use of five transducers results in a maximum of ten values of nozzle admittance for each value of k. Consequently the maximum sample size is ten, which puts the statistics of this problem in the category of "Small Sampling Theory". Due to experimental errors and the nature of the computations that are associated with the reduction of the experimental data, the number of admittances computed for each value of k varies from zero to ten. In view of this fact it is necessary to select a minimum sample size that should be used for the presentation of the experimental data.

Using one of the small sampling theories (viz., the Students t Distribution) at a confidence level of 95 percent, a sample size of four was selected as the minimum sample size for the data presented in the figures.

There was some concern about the quality of the measured sound pressure level (SpL) due to the contribution of flow noise in the frequency range of interest. In order to investigate this point the experiments conducted with each of the nozzles were repeated and the noise generated by the flow, in the absence of any driven signal, was recorded. The unfiltered flow noise associated with nozzle 1 (M = 0.08) indicated a SpL of approximately 155 db whereas the filtered flow noise indicated an overall SpL of approximately 115 db and random spectral contributions up to 125 db. Consequently, the flow noise can be ignored as long as the measured SpL is in the range 145 db to 170 db. Nozzle 2 (M = 0.16) showed a 5 db increase in flow noise level; consequently, recorded SpL in the range, $150 \leq \text{SpL, db} \leq 170$ will yield acceptable results without worrying about the flow noise contributions.

Test results indicate that there is no variation in the quality of the admittance data obtained in tests where an oscillation of a given frequency is driven over a period of few seconds and admittance data obtained in tests where oscillations of different frequencies are generated by automatically sweeping the driver through a prescribed frequency range. Figure 2 presents a comparison of these test results for nozzle 1. The data points in that figure represent the "fixed-frequency" test results and the curve, taken from Figure 1, represent the "frequency-sweep" test results. As can be seen relatively good agreement exists between these two sets of data.

The admittance values have been found to be insensitive to the choice of locations for pressure measurement thereby

reinforcing the validity of the assumption that the wave attenuation in the axial direction is negligible. Figure 3 presents a comparison of admittance data obtained from measurements taken near the nozzle end of the chamber, which are represented by the data symbols, and admittance data obtained from measurements taken close to the midsection of the chamber, which are represented by the curve taken from Figure 1. It can be seen from this figure that these two sets of data agree with one another over the entire k-range. As in the case of the data presented in Figure 1, the data scatter at $k \gtrsim 5.5$ becomes bothersome and must be further investigated.

Whereas Figures 1 through 3 describe the behavior of the real part of the admittance, Figure 4 presents the measured imaginary part of the nozzle admittance. The conclusion reached from this figure is that the imaginary part of the admittance does show good test-to-test repeatibility and is equally insensitive to the manner of excitation and the choices of pressure measurement locations.

The acoustic liner was inserted into the system between the end of the chamber and the entrance to nozzle 1 and the combined liner-nozzle combination was tested to determine the admittance of the combined system. The design parameters[4] of this liner are as follows:

maximum absorption coefficient = 45% @ 700 Hz
open area ratio = 3%
number of holes = 650
hole diameter = 0.159, in.
orifice thickness = 0.50, in.
backing distance = 0.435, in.

Because of the need to monitor other effects, only four pressure transducers were used in the chamber to measure the liner-nozzle admittance; consequently, the statistical requirement of four

samples had to be discarded for the discussion of this test result. Figures 5 and 6 present comparisons of the real and imaginary parts of the admittances of the liner-nozzle combination, indicated by the symbols, and the nozzle, indicated by the curve taken from Figures 1 and 4. The effect of the liner is clearly indicated in these figures. Of particular significance is the fact that the insertion of the liner into the system has apparently resulted in improved damping over selected frequency ranges; however, the interpretation of this data needs further study.

Nozzle 2 (M = 0.16) has been tested using multiple transducers and the reduction of the data is in progress. This data will be presented in the next quarterly report.

In addition to the above-mentioned experimental work, work has begun on the fabrication of additional nozzles and the incorporation of an analog-to-digital data reduction scheme into the existing program.

After considering various alternatives it has been decided to build three additional nozzles to be denoted by the numbers 3, 4 and 5. Nozzle 3 has a 15 degree convergent half-angle whereas nozzles 4 and 5 have 30 and 45 degree convergent half-angles. All three nozzles have equal radii of curvature at the chamber and at the throat; viz., 2.5-inches. These nozzles will be fabricated from billets of cast aluminum. All three nozzles will be initially machined for an entrance Mach number of 0.08 and tested. Upon the completion of these series of tests each of these nozzles will be remachined for an entrance Mach number of 0.16 and then tested. This sequence of remachining and testing will be concluded when all nozzles have entrance Mach numbers of 0.32. The technique of using one nozzle billet for numerous Mach number configurations is illustrated in Figure 7. The principle advantage of this method is that it provides a

substantial amount of data at relatively low cost.

The processing of dynamic data by completely digital techniques has been made practical in the last five years by advances in the required equipment. Georgia Tech presently owns a 14 channel, Analog-to-Digital Conversion System manufactured by the Radiation Corporation. An investigation was undertaken to determine the feasibility of incorporating such a method of data reduction in this program and to determine the relative advantages and disadvantages associated with the use of such a method. The principle advantage of such a system is that it will reduce the "per-test" data reduction time from 720 minutes to twelve minutes and provide both amplitude and phase data. The ability to obtain accurate phase data is particularly important in liner studies where local liner admittance is determined from phase and amplitude measurements. In view of these facts it has been decided to acquire capability in the area of analog-to-digital data conversion and develop a computer program that would use the digitized data to compute the desired nozzle, liner and liner-nozzle combination admittances. This work is in progress.

D. Expected Progress During the Next Report Period

The nonlinear regression analysis will be used to analyze the experimental admittance data. Theoretical admittance values will be determined over the frequency range of interest. Nozzle testing and data analysis will be continued. The new nozzles will have begun their test phase. The analog-to-digital technique will be programmed and in its final check-out.

REFERENCES

1. Prozan, R. J. and Kooker, D. E., "The Error Minimization Technique with Application to a Transonic Nozzle Solution," J. Fluid Mech. vol. 43 (1970) part 2, pp. 269-277.

2. Crocco, L., Sirignano, W. A., "Behavior of Supercritical Nozzles Under Three Dimensional Oscillatory Conditions," AGARDograph 117, 1967.

3. Zinn, B. T., Smith, A. J., Jr., and Daniel, B. R., "Behavior of Nozzles and Acoustic Liners in Three-Dimensional Acoustic Fields," Quarterly Report for Period 1 September 1970 to 31 November 1970, Georgia Institute of Technology, School of Aerospace Engineering, December, 1970.

4. Walsh, J. L., Jr., "The Design of Acoustic Liners for Three-Dimensional Instability Studies in a Cold-Flow Rocket Engine," Georgia Institute of Technology, School of Aerospace Engineering, Publication Pending.

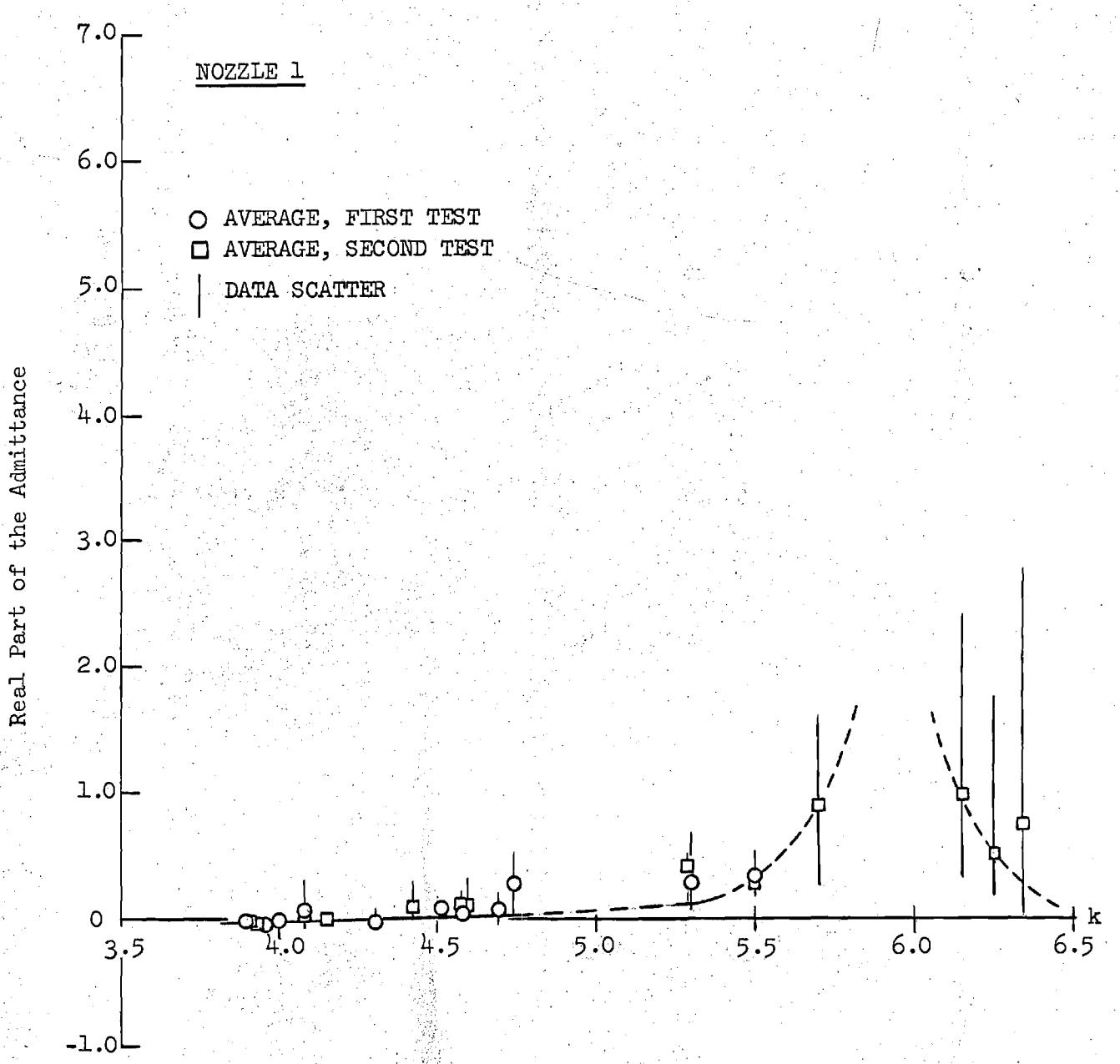

Figure 1. Demonstration of test-to-test repeatibility.

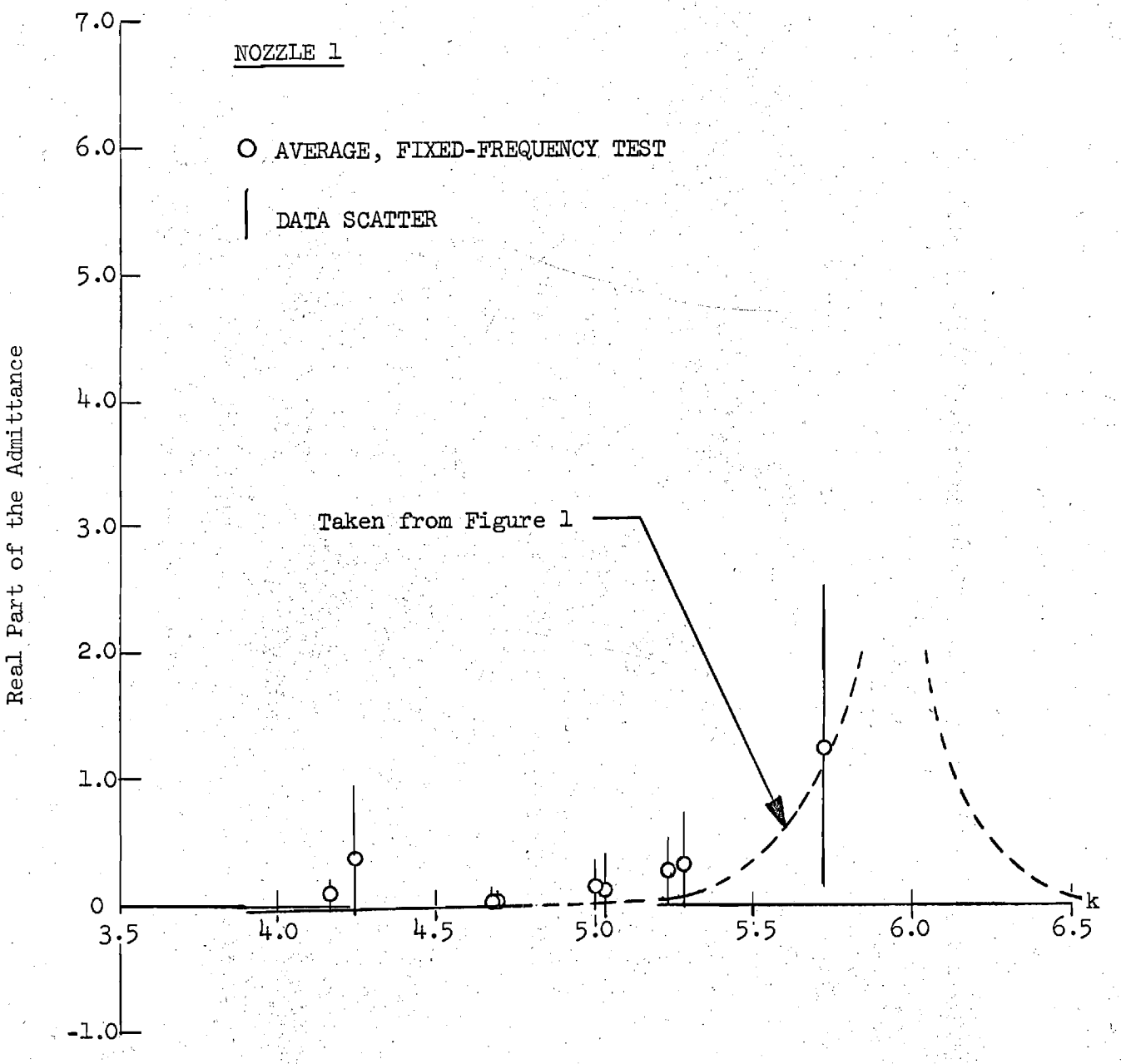

Figure 2. Comparison of fixed-frequency test results and swept-frequency test results.

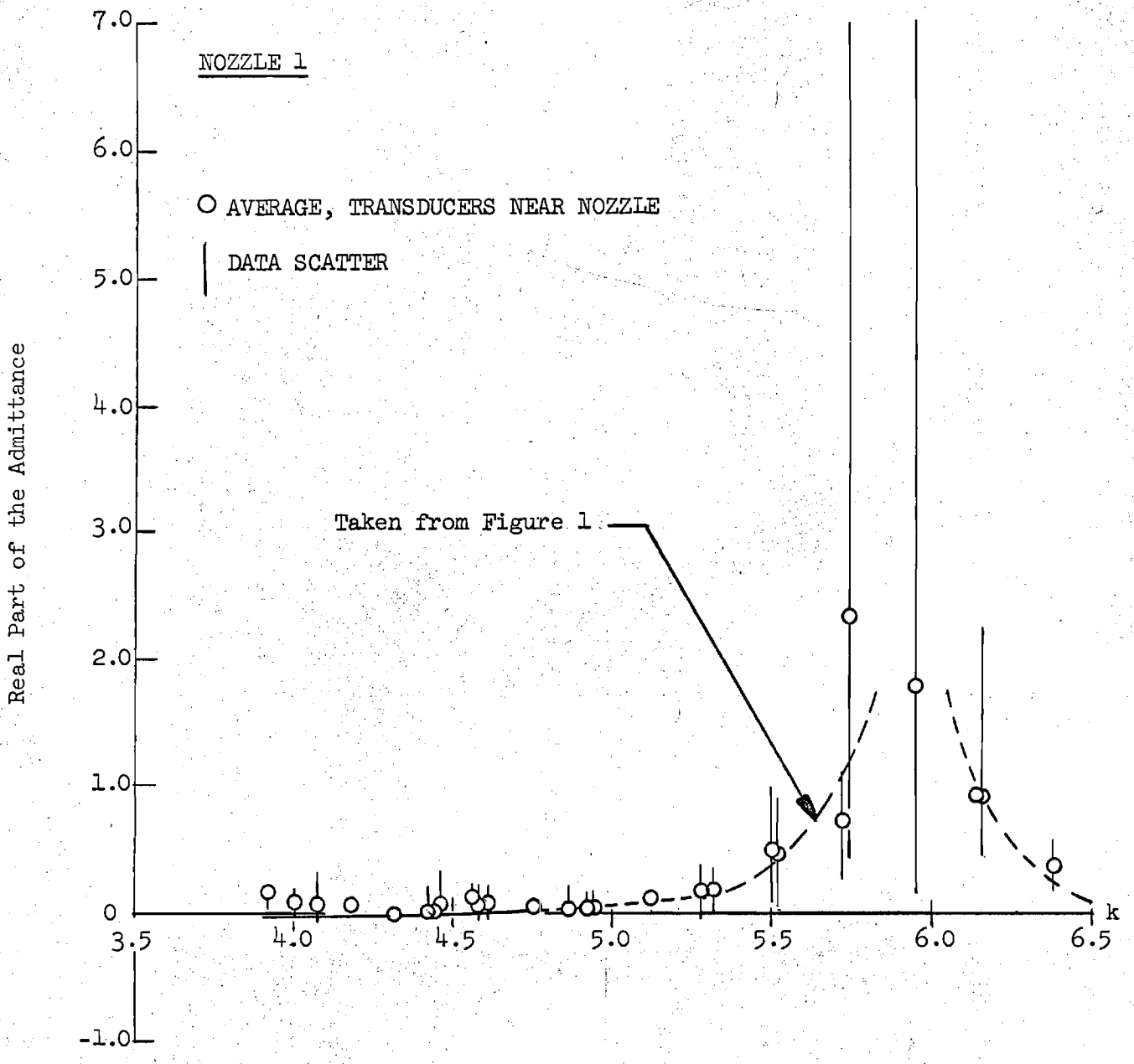

Figure 3. Comparison of admittance values measured at different chamber locations.

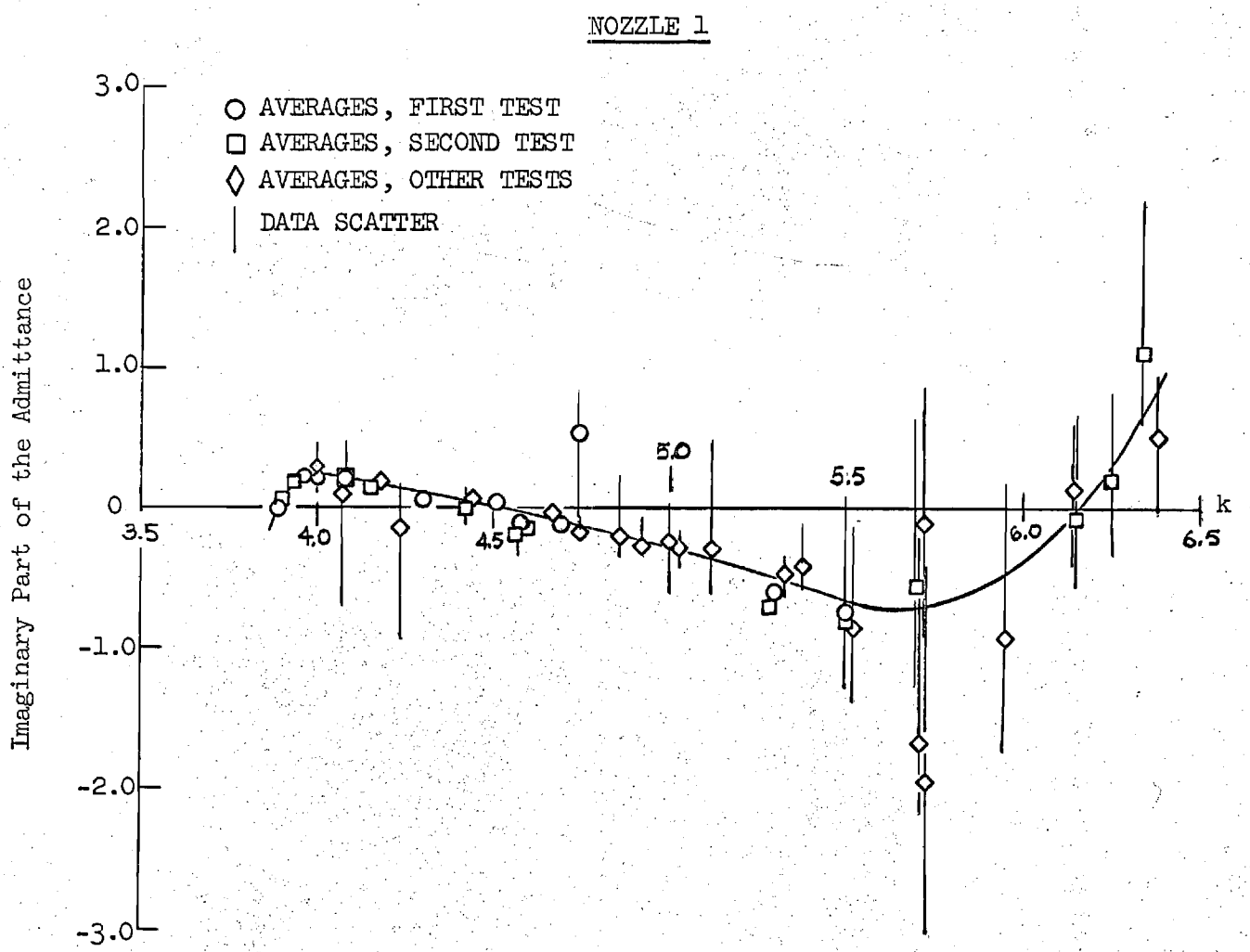

Figure 4. Imaginary part of the admittance values for Nozzle 1.

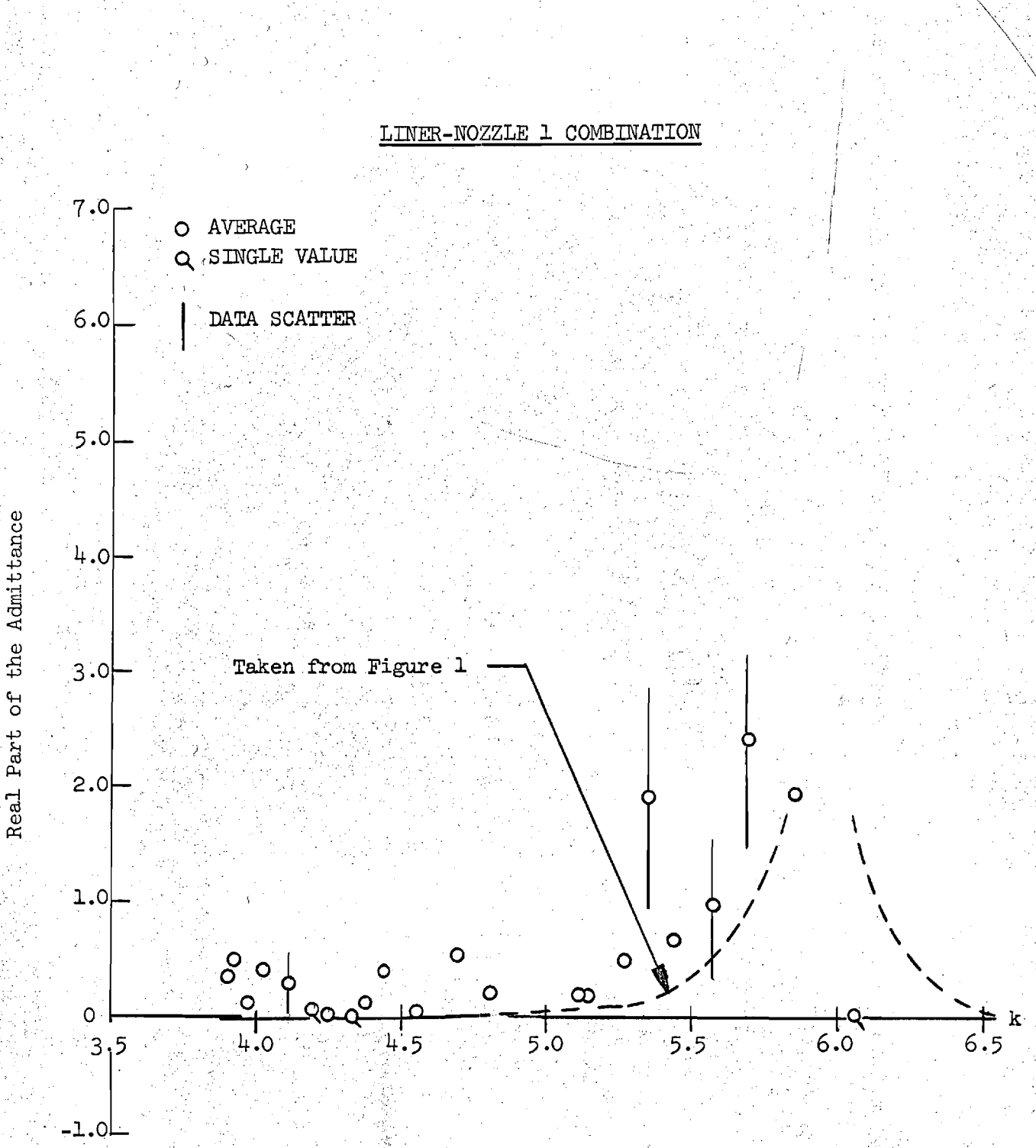

Figure 5. Comparison of the Liner-Nozzle 1 combination test results with the Nozzle 1 test results.

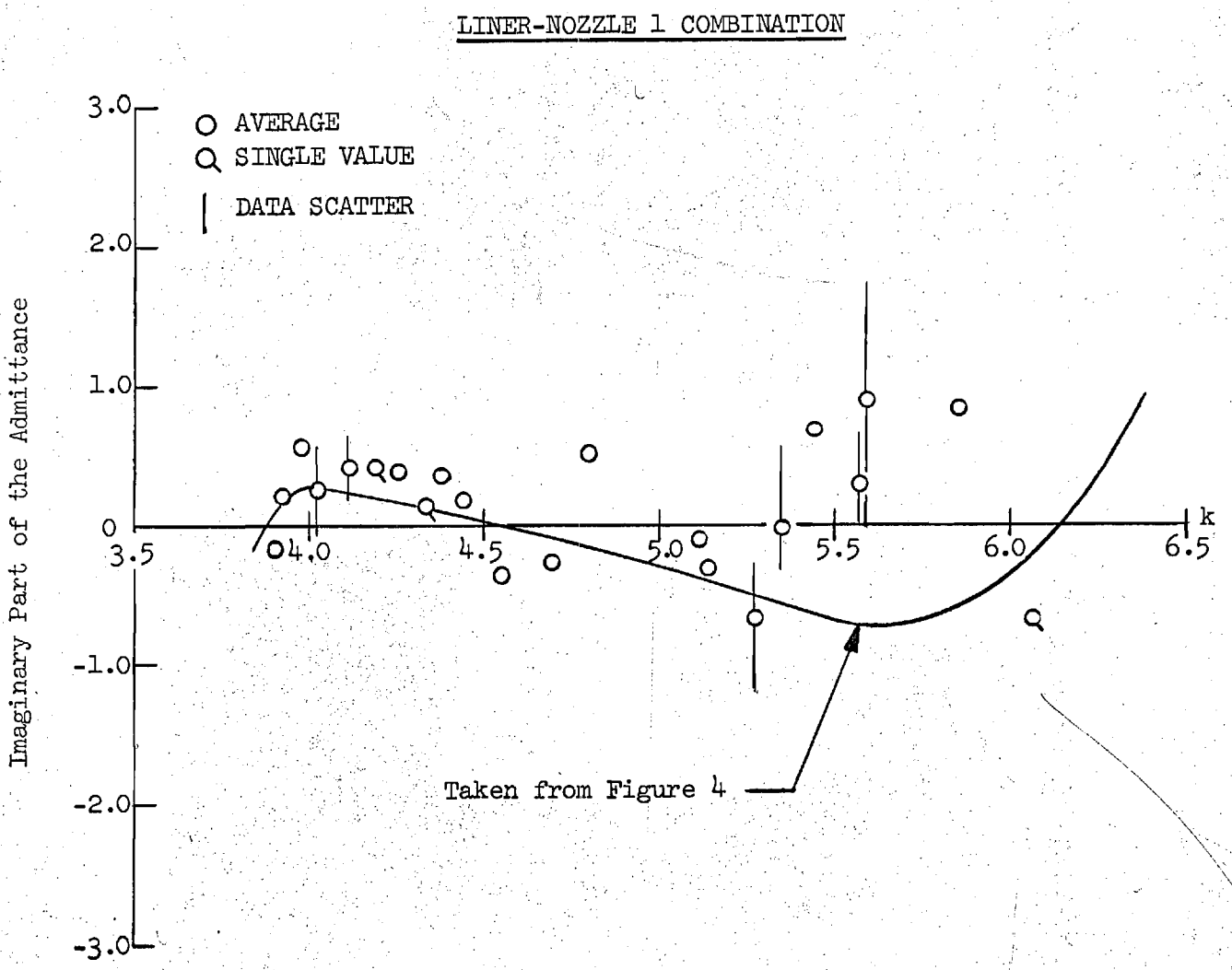

Figure 6. Comparison of the Liner-Nozzle 1 combination test results with the Nozzle 1 test results.

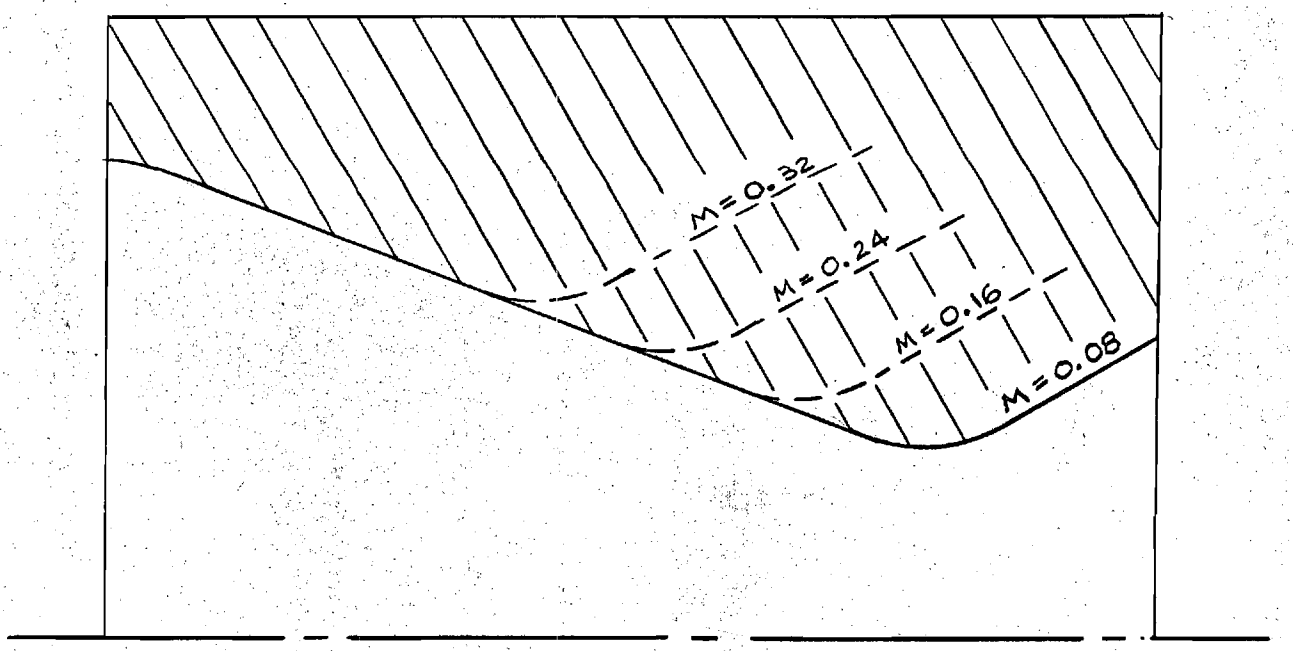

Figure 7. The technique of obtaining more than one nozzle from a given nozzle billet.

E-16-607

NASA GRANT NGL 11-002-085

BEHAVIOR OF NOZZLES AND ACOUSTIC LINERS IN THREE-DIMENSIONAL ACOUSTIC FIELDS

Quarterly Report for Period 1 March 1971 to 31 May 1971

Prepared by: Ben T. Zinn, Principal Investigator
Allan J. Smith, Jr., Project Engineer
B. R. Daniel, Research Engineer

School of Aerospace Engineering
Georgia Institute of Technology
Atlanta, Georgia

PROGRESS DURING REPORT PERIOD

A. Summary

The analytical studies during this report period have concentrated on the development of the nonlinear regression analysis for the reduction of experimental data and the initiation of work on the development of an analog-to-digital data conversion technique to be incorporated into the existing data reduction program. Work also continued on the checkout and correction of a computer program to determine theoretical admittances of slowly-converging nozzles and the development of an analysis for the prediction of the admittances of rapidly-converging nozzles.

The experimental investigations conducted during this period include eleven nozzle tests. Admittance data were obtained for a nozzle with a convergent half angle of 45 degrees and an entrance Mach number of 0.08. Additional data were also obtained for the two nozzles which were discussed in a previous report[2]. The effects of the sweep rate of the acoustic driver frequency on the accuracy of the measured data was investigated. Finally, a series of tests aimed at the determination of the behavior of the oscillations inside the tube were performed. These tests indicated the absence of circumferential wave rotation and wave skewedness.

B. Theoretical Studies

The Nonlinear Regression Technique[3] was used to reduce the data that was presented in Figures 1 through 6 in the previous progress report[2]. An initial examination of the results indicates that the values of nozzle admittance computed by using the Nonlinear Regression Technique provide better agreement between the predicted and measured pressure amplitudes than the straight forward solution technique that was used hitherto. This investigation is in progress and the results will be presented in the next progress report.

The efforts associated with the development of a computer program to determine the theoretical admittance values of slowly-converging nozzles and the development of a theory for the prediction of admittance values of rapidly-converging nozzles continued.

The development of an analog-to-digital data reduction program has been completed and a checkout has been initiated. Preliminary results indicate the program is very accurate and requires only 40 seconds of computer execution time per test.

C. Experimental Investigations

Eleven tests were conducted during the period of this report, however, several of these tests involved component failures which invalidated the data. Other tests were made to check out the data aquisition system in an effort to improve data quality and reduce data scatter.

Nozzle admittance data were obtained for a recently fabricated aluminum nozzle with a convergent half angle of 45 degrees, a radii of curvature of 2.5 inches, and an entrance Mach number of 0.08. The admittance of this nozzle will be presented in the next progress report after additional tests of the same nozzle will have been completed. These results will then be compared with admittance data obtained from testing of additional nozzles.

During the last quarter additional testing of the two fiberglass nozzles has been accomplished. An inconsistancy exists between the results obtained from tests conducted earlier in the program and the more recent test results. This discrepancy is currently being investigated and any discussion of these test results will be delayed until the present study is completed.

In the current study the dependence of a given nozzle admittance upon frequency is determined by continuously changing the frequency of the waves in the chamber. During the last quarter

the dependence of the accuracy of the data upon the frequency sweep rate has been investigated. In this study the testing of the available nozzles has been repeated with two different sweep rates. In the first experiment the frequency of the driven waves was continuously changed at a rate of 2.5 Hertz/sec while in the second experiment the frequency of the driven waves was swept at the slower rate of 1.25 Hertz/sec. Both tests yielded data of comparable quality. This comparison has indicated that tests conducted with the faster sweep rate of 2.5 Hertz/sec provide accurate data and there is no need to further reduce this sweep rate.

Tests were also conducted to investigate the possibility of circumferential standing wave rotation or skewness. The results of these tests indicate no evidence of measurable wave rotation or skewness.

There was a significant delay in the planned testing schedule for this period because of modifications and failures associated with the acoustic drivers and the main airflow control valves. These problems are being corrected at this time and testing should be resumed soon.

D. Expected Progress During the Next Report Period

The computer program used for the prediction of admittances for slowly-converging nozzles will be operational and work will continue on the analysis for the prediction of rapidly-converging nozzles. The analog-to-digital data reduction program is expected to become fully operational.

Testing and data analysis will continue on the recently fabricated family of nozzles and the results of these tests should become available for the next progress report.

REFERENCES

1. Zinn, B. T., Smith, A. J., Jr., and Daniel, B. R., "Behavior of Nozzles and Acoustic Liners in Three-Dimensional Acoustic Fields," Quarterly Report for Period 1 September 1970 to 31 November 1970, Georgia Institute of Technology, School of Aerospace Engineering, December, 1970.

2. Zinn, B. T., Smith, A. J., Jr., and Daniel, B. R., "Behavior of Nozzles and Acoustic Liners in Three-Dimensional Acoustic Fields," Quarterly Report for Period 1 December 1970 to 28 February 1971, Georgia Institute of Technology, School of Aerospace Engineering, March, 1971.

3. Pfahl, R. C., Jr. and Mitchel, B. J., "Nonlinear Regression Methods for Simultaneous Property Measurements," AIAA Journal, Vol. 8, No. 6, June 1970, pp. 1046-1053.

E-16-607

NASA GRANT NGL 11-002-085

BEHAVIOR OF NOZZLES AND ACOUSTIC LINERS IN THREE-DIMENSIONAL ACOUSTIC FIELDS

Quarterly Report for Period 1 June 1971 to 31 August 1971

Prepared by: Ben T. Zinn, Principal Investigator
Allan J. Smith, Jr., Research Engineer
B. R. Daniel, Research Engineer
W. A. Bell, Graduate Research Assistant

School of Aerospace Engineering
Georgia Institute of Technology
Atlanta, Georgia

PROGRESS DURING REPORT PERIOD

A. Summary

The computer program used for the prediction of admittances of slowly-converging nozzles has been checked out and is operational. An investigation of oscillatory flows in rapidly-converging nozzles is encountering difficulties satisfying the imposed boundary conditions. Various numerical schemes for circumventing this difficulty are being considered. The checkout of the analog-to-digital data reduction program has been continued and is being finalized. Twenty-one nozzle tests have been conducted during this report period.

B. Theoretical Studies

The computer program used for the prediction of admittances of slowly-converging nozzles has been checked out and is operational. The computation of theoretical admittance values has been delayed by a heavy test and data analysis schedule and by the need to recheck the mathematical derivations that are used in the development of the nozzle admittance theory. This check is near completion and it will be followed by computations of the theoretical nozzle admittances. The next Quarterly Progress Report will show comparisons between theoretical admittance values and experimental admittance values.

A parallel study is concerned with the development of an analytical technique for the prediction of the admittances of rapidly-converging nozzles. Recent efforts in this area concentrated on the development of an appropriate numerical solution technique. The chosen numerical solution technique uses an iteration scheme whose aim is to minimize the error that is associated with previous iterations. Application of this technique to predict the nozzle admittance in the case of axial oscillations has experienced considerable difficulties; the latter were traced to the numerical

treatment of the problem's boundary conditions. Present efforts in this area are concerned with the development of improved analytical means for numerically satisfying the imposed boundary conditions.

The checkout of the analog-to-digital data reduction program has been continued. The purpose of this program is twofold. First, the program will reduce the time associated with the data reduction process from 720 minutes to 12 minutes. Second, the program scheme (i.e., Fourier analysis of digitized data) is the best way to obtain accurate phase data, which is particularly important in liner studies. The checkout scheme called for the determination of the frequency, amplitude, and phase resolution of "unknown" signals with the following characteristics: a simple periodic signal; a complex periodic signal; and a nonperiodic signal.

The results of the simple periodic signal checkout compared well with the reference signal. For example, the maximum amplitude and phase error encountered was 0.2% and 0.02%, respectively. The frequency error was 0.02%. The results of the complex periodic signal (i.e., a given periodic signal with noise) showed that the maximum amplitude and phase error increased to 32% and 6%, respectively, when the signal amplitude and the noise amplitude were equal. When the signal amplitude was 100 times greater than the noise amplitude, the amplitude and phase error decreased to 0.3% and 0.08%, respectively. Inasmuch as low signal amplitudes constitute an important area of data reduction, work has been initiated to improve the resolution of the signal. The checkout of the complex periodic signal and nonperiodic signal should be completed soon; consequently, the analog-to-digital data reduction program should be operational by the next Quarterly Progress Report.

C. Experimental Investigations

Twenty-one tests were conducted during this report period. Five tests were conducted for system checkout. Ten tests were

conducted for nozzle admittance data in a frequency range that include two-dimensional and three-dimensional waves. One of these ten tests was conducted without flow in the chamber. Six tests were conducted for nozzle admittance data in the frequency range of the one-dimensional (i.e., axial) waves.

It was reported in the last Quarterly Progress Report that an inconsistency had recently arisen in the data and that a serious valve failure had occurred. The valve had to be returned to the California manufacturer for repair. After the valve was repaired and installed into the system, five tests were conducted to checkout the system. The data inconsistency was traced to a bad thermocouple; consequently, ten tests that had previously been conducted had to be invalidated. The thermocouple was replaced and the flow system was readjusted for the new operating characteristics of the valve. Testing was resumed.

Ten tests were conducted to obtain admittance data associated with nozzles with convergent half-angles of 15, 30, and 45 degrees, radii of curvature (i.e., the radius of curvature at the chamber is equal to the radius of curvature at the throat) of 2.5 and 5.7 inches, and entrance Mach number of 0.08 and 0.16. Some of the results are presented herein.

Before presenting these results, a brief review of background information is included to relate to the reader how the measurement of sound wave amplitudes can provide the nozzle admittance.

The standing wave pattern inside the chamber depends upon the interaction of the incident wave and the reflected wave which in turn depend upon the amplitude and phase change upon reflection from the end termination. This statement introduces the two parameters, α and β, which serve to define the admittance of the termination and appear in the expression that relates the sound pressure anywhere in the chamber to the Mach number, the frequency, and the velocity of sound.

It can be shown[1] that the amplitude change upon reflection is a function of α whereas the phase change is a function of β. It is shown in Reference 1 that the ratio of the reflected amplitude P_R to

the incident amplitude P_I at the location whose admittance is measured is given by the following expression

$$\frac{P_R}{P_I} = e^{-2\pi\alpha} \tag{1}$$

A similar relationship for the sound energy, W, is given by

$$\frac{W_R}{W_I} = e^{-4\pi\alpha} \tag{2}$$

When $\alpha = 0$, both energies are equal implying that no sound energy is lost from the system. When $\alpha = \infty$, no reflected wave is present implying that all the sound energy is removed from the system. The phase change upon reflection θ is given by[1]:

$$\theta = \pi(1 + 2\beta) \tag{3}$$

where β must satisfy the following relationship $-0.5 \leq \beta \leq 0.5$.

The values of α and β are determined with the aid of the following expression that describes the behavior of the standing wave pattern inside the tube:

$$|p(z,r,\theta)| = P_o\left[J_m\left(S_{mn}\right)\right]\cos m\theta\left[\cosh^2\alpha - \cos^2\pi\left(\beta + \frac{2d}{\lambda}\right)\right]^{\frac{1}{2}} \tag{4}$$

where

$\lvert p(z,r,\theta)\rvert$	:	magnitude of the pressure at the point z,r,θ, psia (RMS)
P_o	:	amplitude of the pressure oscillation at the driven end of the chamber, psia (RMS)
$J_m(x)$	:	Bessel function of first kind of order m
S_{mn}	:	transverse mode eigenvalue
m	:	index counting the number of diametrical nodel surfaces in the transverse oscillating pattern

n	:	index counting the number of radial nodal surfaces in the transverse oscillating pattern.
d	:	distance from the nozzle entrance, ft
λ	:	wavelength, ft

Equation (4) contains three unknowns: P_o, α, and β. Consequently, if three pressure measurements are taken, each at a different axial position, then these three pressures can be used together with Equation (4) to simultaneously solve for P_o, α, and β.

Typical experimental values of α and β determined by such a scheme are shown in Figure 1. The nondimensional angular frequency, s, is the independent variable where

$$s = 2\pi f\left(\frac{r_c}{c}\right)$$

and f is the frequency of oscillation (cycles/sec), r_c is the chamber radius (ft), and c is the speed of sound (ft/sec) in the chamber. The nozzle used to generate this data has a 15° half-angle, entrance Mach number of 0.08, and radii of curvature of 2.5 inches. The low value of α, over the entire range of s, suggests that little sound energy is transmitted out of the system by this nozzle. However, the phase change upon reflection is significant.

Once the parameters α and β have been determined, they are used to determine the nozzle admittance Y which is given by the relationship[2]

$$Y = \frac{g}{\rho c}\left(\frac{a}{b}\right)\left(\Gamma + i\eta\right) \tag{5}$$

where

$$a = \left(\frac{\omega}{c}\right)\sqrt{\left(\frac{\omega}{c}\right)^2 - \left(\frac{S_{mn}}{r_c}\right)\left(1-M^2\right)}$$

$$b = \left(\frac{\omega}{c}\right)^2 + \left(\frac{S_{mn}}{r_c}\,M\right)^2$$

ω : angular frequency, radians/sec

c : speed of sound, ft/sec

r_c : chamber radius, ft

M : steady state chamber Mach number

g : gravitational constant, $(lb_m\text{-ft})/(lb_f\text{-sec}^2)$

ρ : gas density, lb_m/ft^3

$(\frac{1}{g}\rho c)$: characteristic impedance of the gas, $ft^3/(lb_f\text{-sec})$

$$\Gamma = \frac{\tanh(\pi\alpha)\sec^2(\pi\beta)}{\tanh^2(\pi\alpha) + \tan^2(\pi\beta)} + \frac{1}{a}\left(\frac{S_{mn}}{r_c}\right)^2 M$$

$$\eta = \frac{\operatorname{sech}^2(\pi\alpha)\tan(\pi\beta)}{\tanh^2(\pi\alpha) + \tan^2(\pi\beta)}$$

Figures 2 and 3 show the real and imaginary parts of the experimental admittance obtained from the α and β data presented in Figure 1. For $s \leq 2.6$, the real part of the admittance has a small constant value while the imaginary part decreases at a constant rate. For $s > 2.6$, the real part of the admittance increases and the rate of change of the imaginary part with respect to s fluctuates considerably.

Hereafter, the three-dimensional admittance results will be presented for the nozzles shown in the following tabulation:

		Chamber Mach Number			
		0.08	0.16	0.24	0.32
Convergent Half-Angle	15°	2*,3			
	30°	4	1*		
	45°	5	6		

*Radii of Curvature = 5.7 inches (all others = 2.5 inches)

Table I. Nozzle Configurations

Since they are of little interest in engine design, the measured values of α and β will not be considered in the following discussion that will only consider the measured nozzle admittances.

The effect of the convergent half-angle upon the real and imaginary parts of the admittance can be determined by examining the test results obtained with nozzles 3, 4, and 5. These results are shown in Figures 4 and 5. For $s \leq 2.6$, the real part of the admittance is independent of the half-angle. For $s > 2.6$, the 30° and 45° nozzles do not exhibit the behavior of the 15° nozzle, which has much higher admittance values in this range than in the previous range. The imaginary part of the admittance, shown in Figure 5, indicates a similar characteristic for these three nozzles; namely, the 30° and 45° nozzles do not exhibit the behavior of the 15° nozzle.

A comparison of the test results of nozzles 2 and 3 substantiates the admittance results associated with the 15° nozzles and indicates the effect of radius of curvature on the admittance. These results are shown in Figures 6 and 7. Figure 6 shows similar "spikes" associated with the real part of the admittance. However, increasing the radius of curvature has not only decreased the frequency at which this effect begins to occur but also increased the number of spikes. Figure 7 shows an increase in the radius of curvature causes a similar frequency shift in the imaginary part of the admittance.

Before proceeding with the discussion of additional test results, it is of interest to compare the test results in Figures 4 through 7 with the theoretical predictions[3] available at this time. Qualitatively, the test results are in agreement with the theoretical predictions. During the next report period, the theory presented in Reference 3 will be used to predict the admittances of the nozzles tested in this program and comparisons of theoretical vs. experimental admittance values will be presented.

The effect of Mach number upon the real and imaginary parts of the nozzle admittance is shown in Figures 8 and 9 for nozzles

5 and 6. These figures suggest the Mach number has little influence on the admittance of these nozzles. Future testing with the 15° and 30° nozzles will determine whether the above conclusion is applicable to all nozzles.

EXPECTED PROGRESS DURING NEXT REPORT PERIOD

The theoretical admittance values will be determined for the tested nozzles and compared with the experimental values. The analysis concerned with the admittance of rapidly converging nozzles will continue. Barring any unexpected difficulties, the analog-to-digital data reduction program will be operational. The testing of nozzles with an entrance Mach number of 0.16 will be completed and the testing of the 0.24 nozzles will be initiated.

REFERENCES

1. Morse, P. M. and Ingard, K. U., Theoretical Acoustics, McGraw-Hill, New York, 1968.

2. Bell, W. A., "Theoretical Considerations of Impedance Tubes for Three-Dimensional Oscillations," M.S. Special Problem, Georgia Institute of Technology, June, 1970.

3. Zinn, B. T., Savell, C. T., and Mikolowsky, W., "Three Dimensional Combustion Instability in Liquid Propellant Rocket Engines: A Parametric Study," Proceedings of the 5th ICRPG Combustion Conference, CPIA Publication No. 183, Dec., 1968.

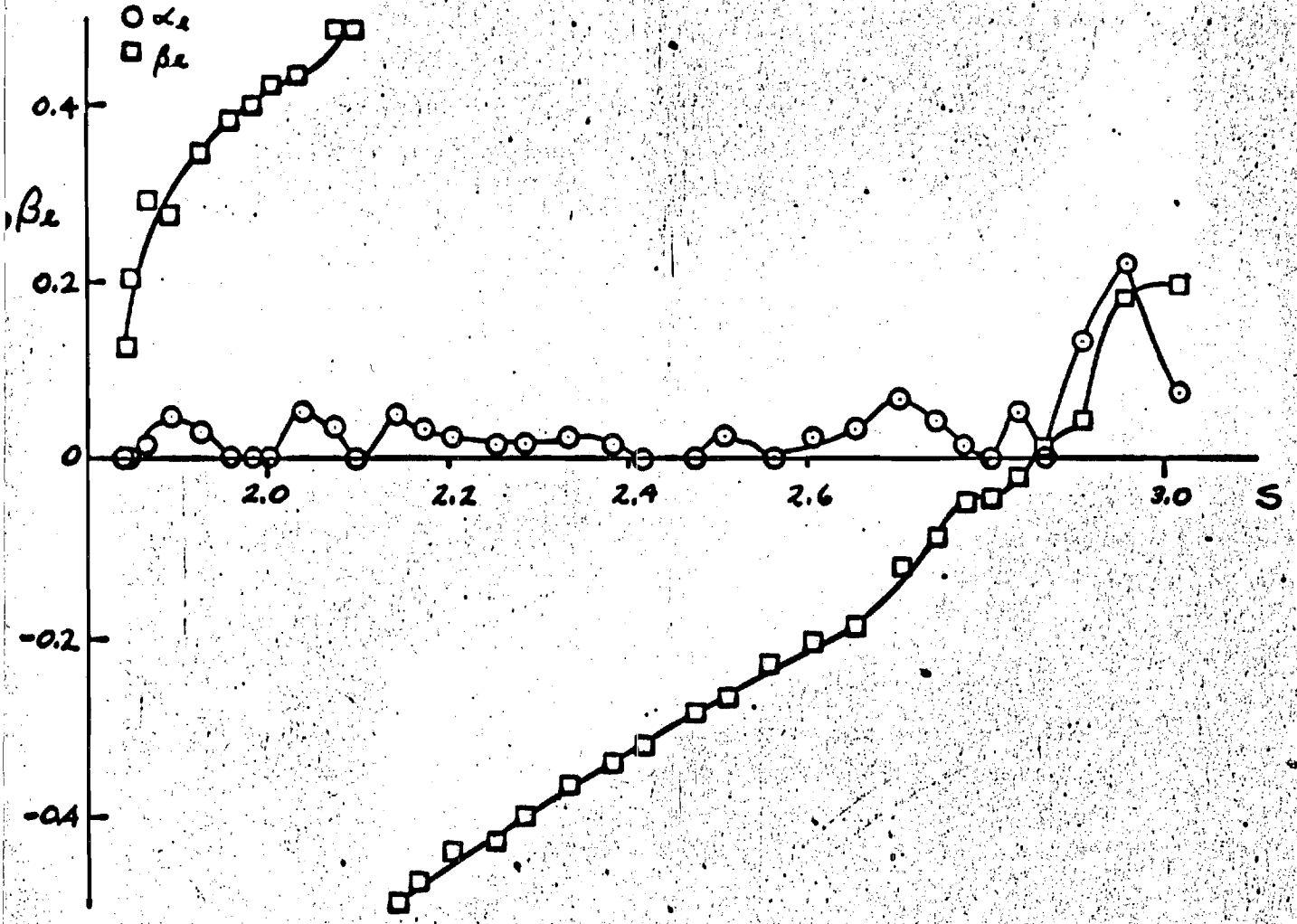

Figure 1. Experimentally Determined Values of α and β.

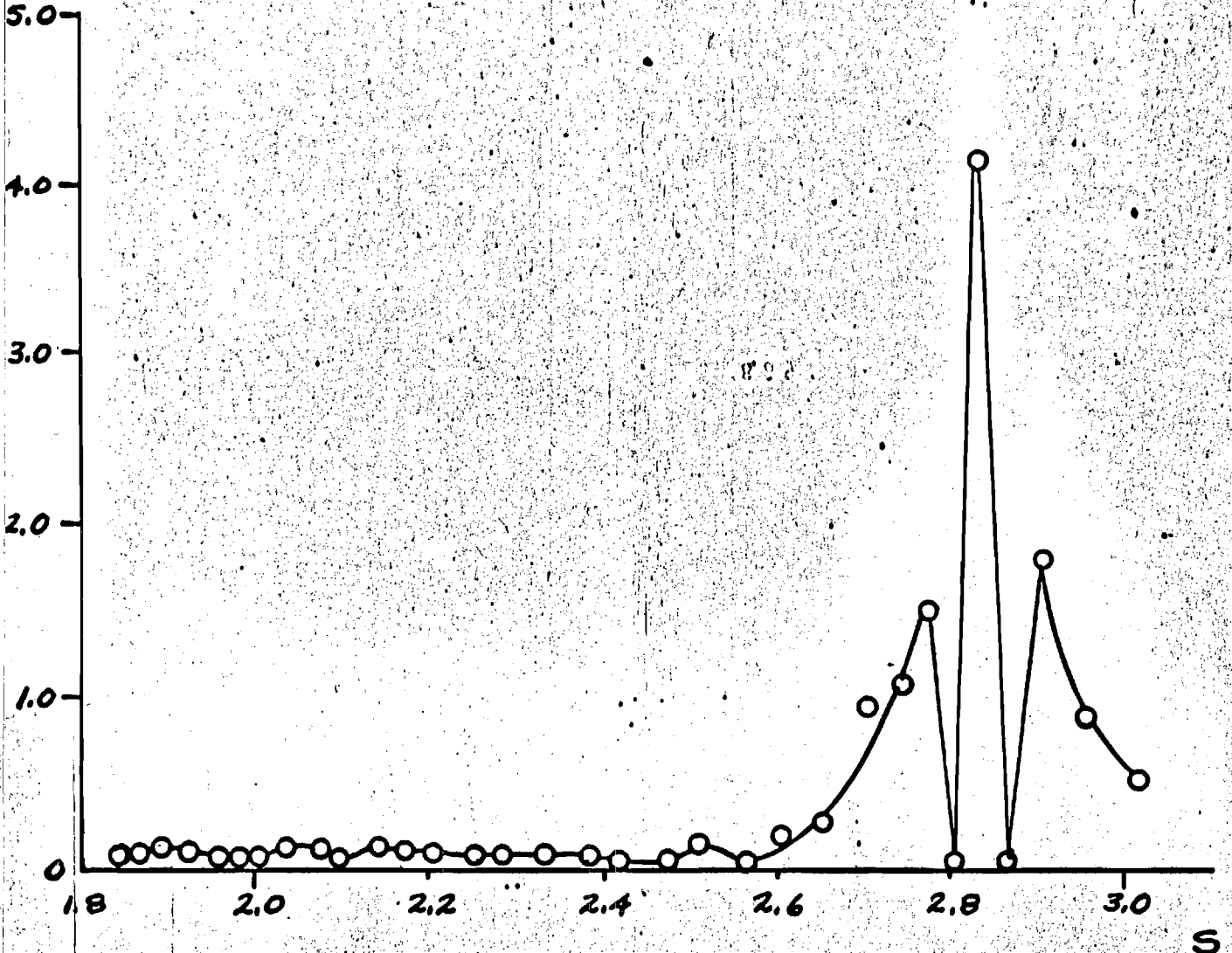

Figure 2. Experimentally Determined Admittances (Real).

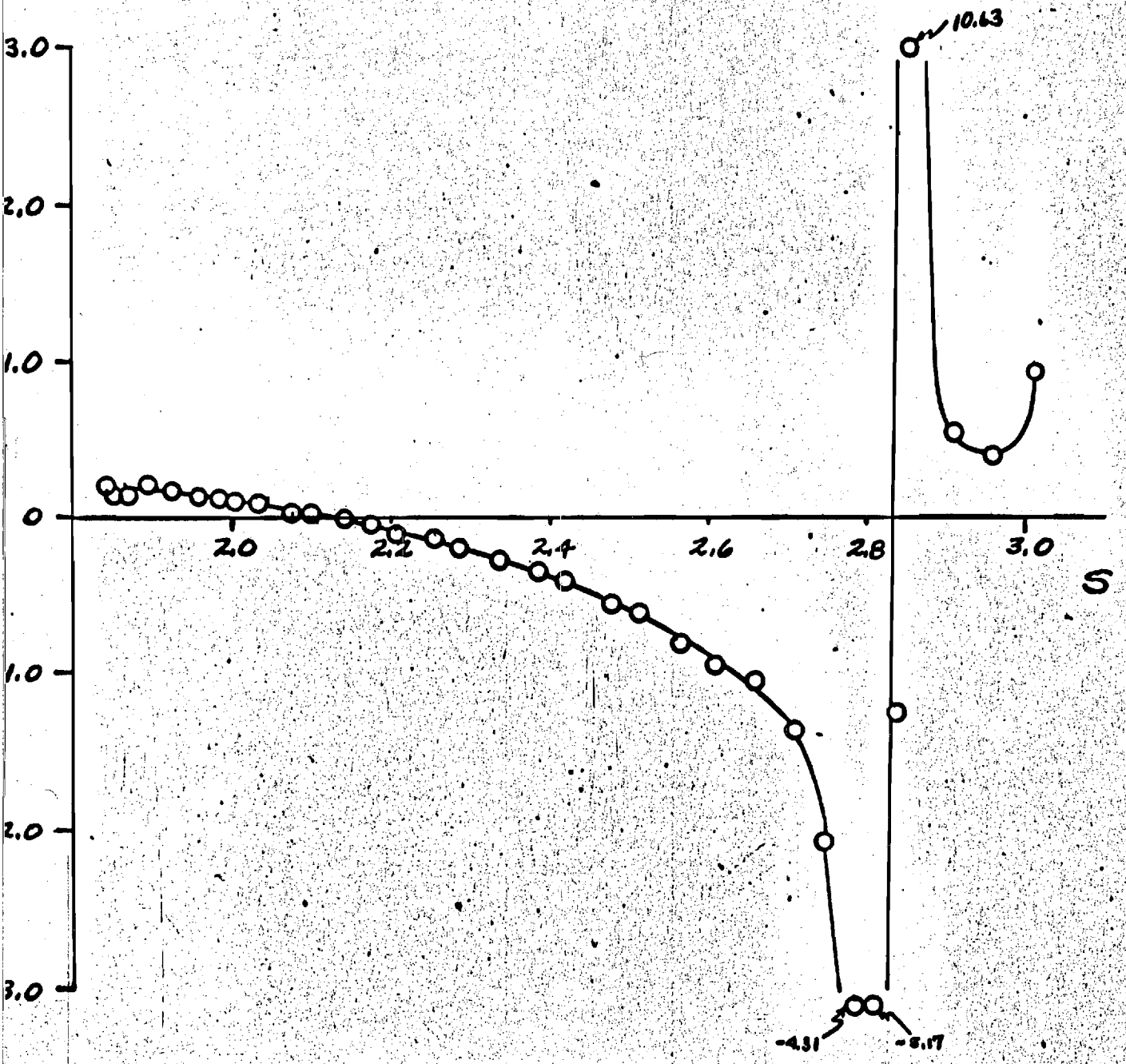

Figure 3. Experimentally Determined Admittances (Imaginary).

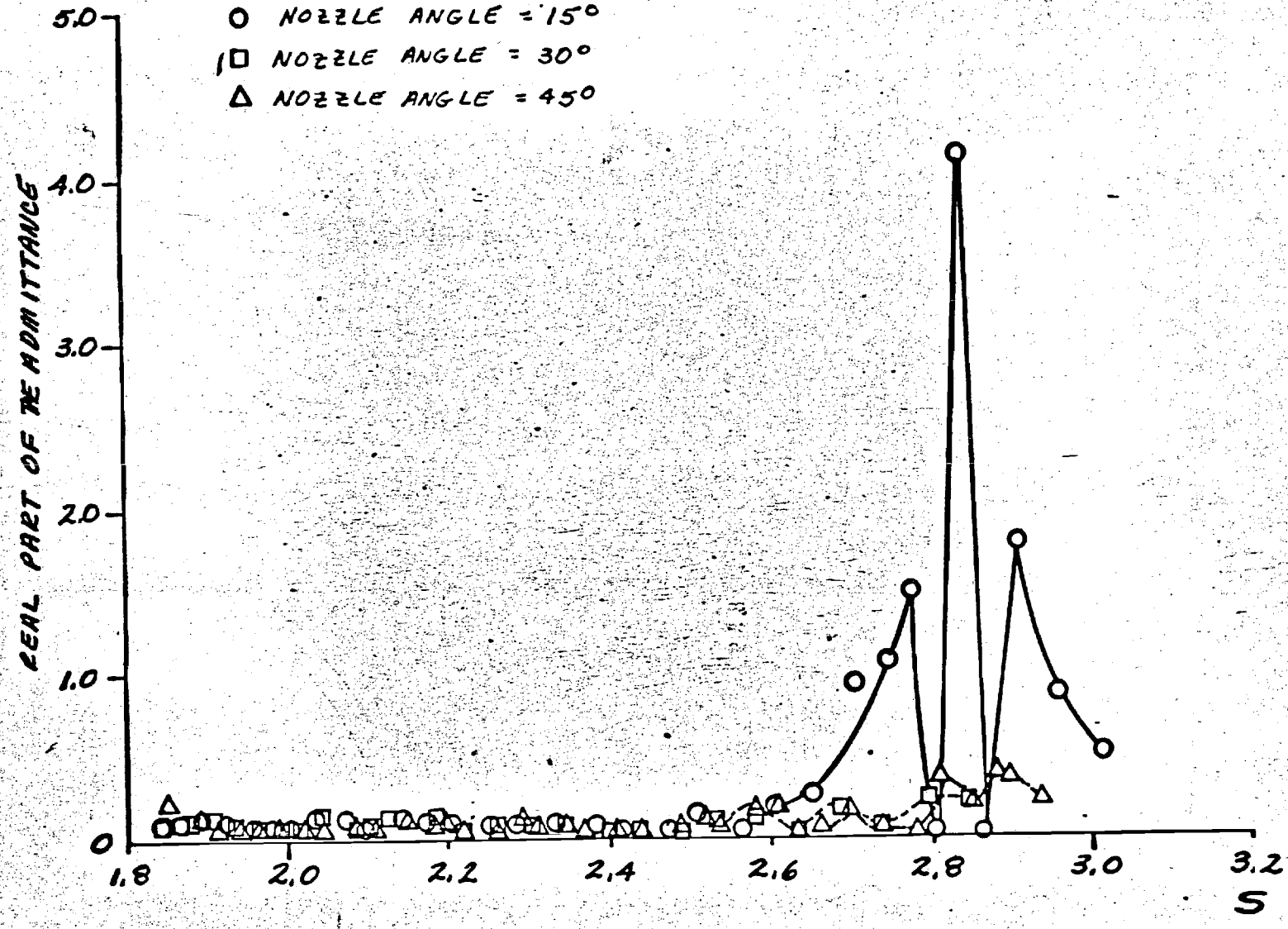

FIGURE 4. EFFECT OF NOZZLE ANGLE AT A MACH NUMBER OF .08 AND A RADIUS OF CURVATURE OF 2.5"

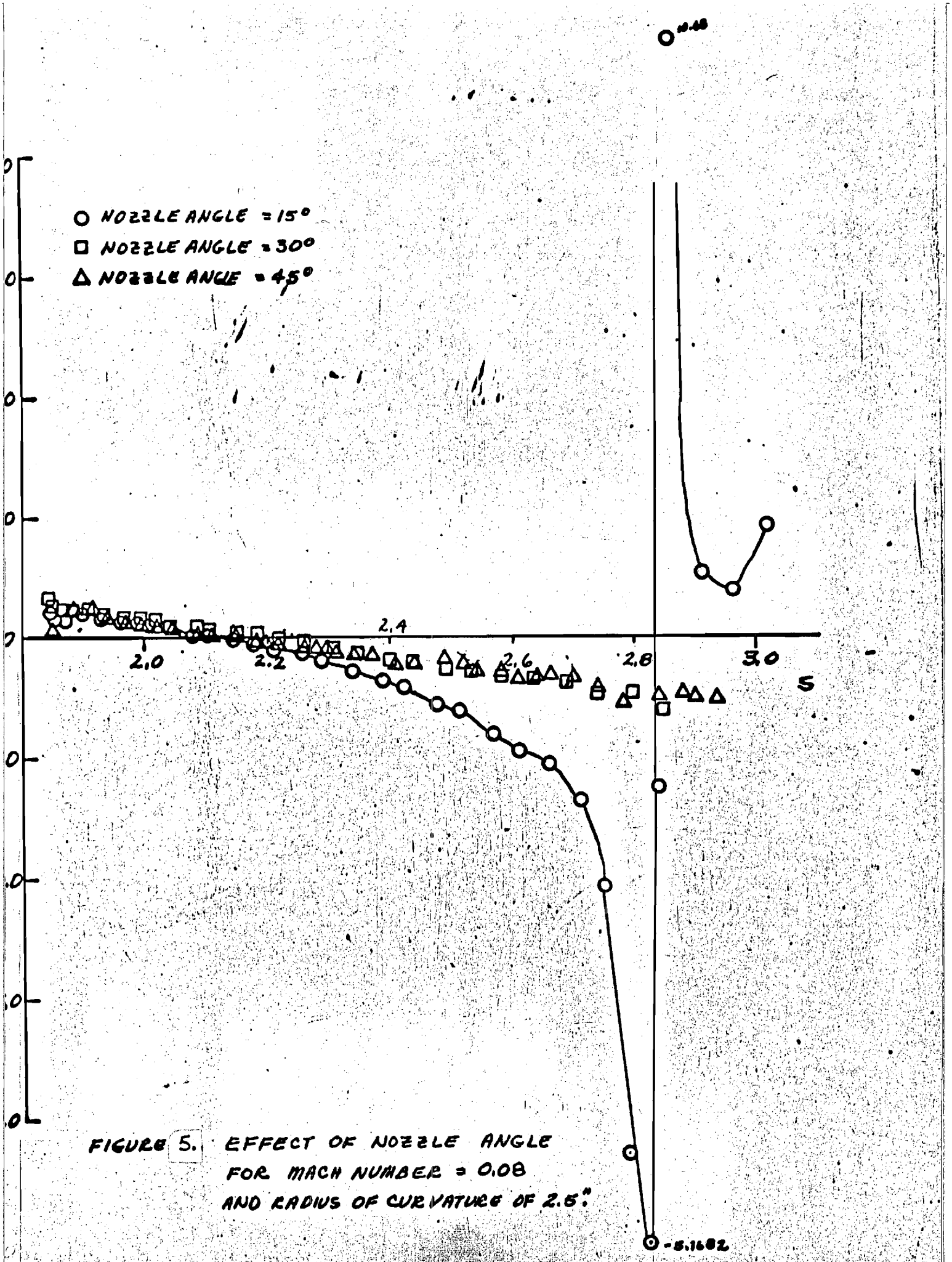

FIGURE 5. EFFECT OF NOZZLE ANGLE FOR MACH NUMBER = 0.08 AND RADIUS OF CURVATURE OF 2.5".

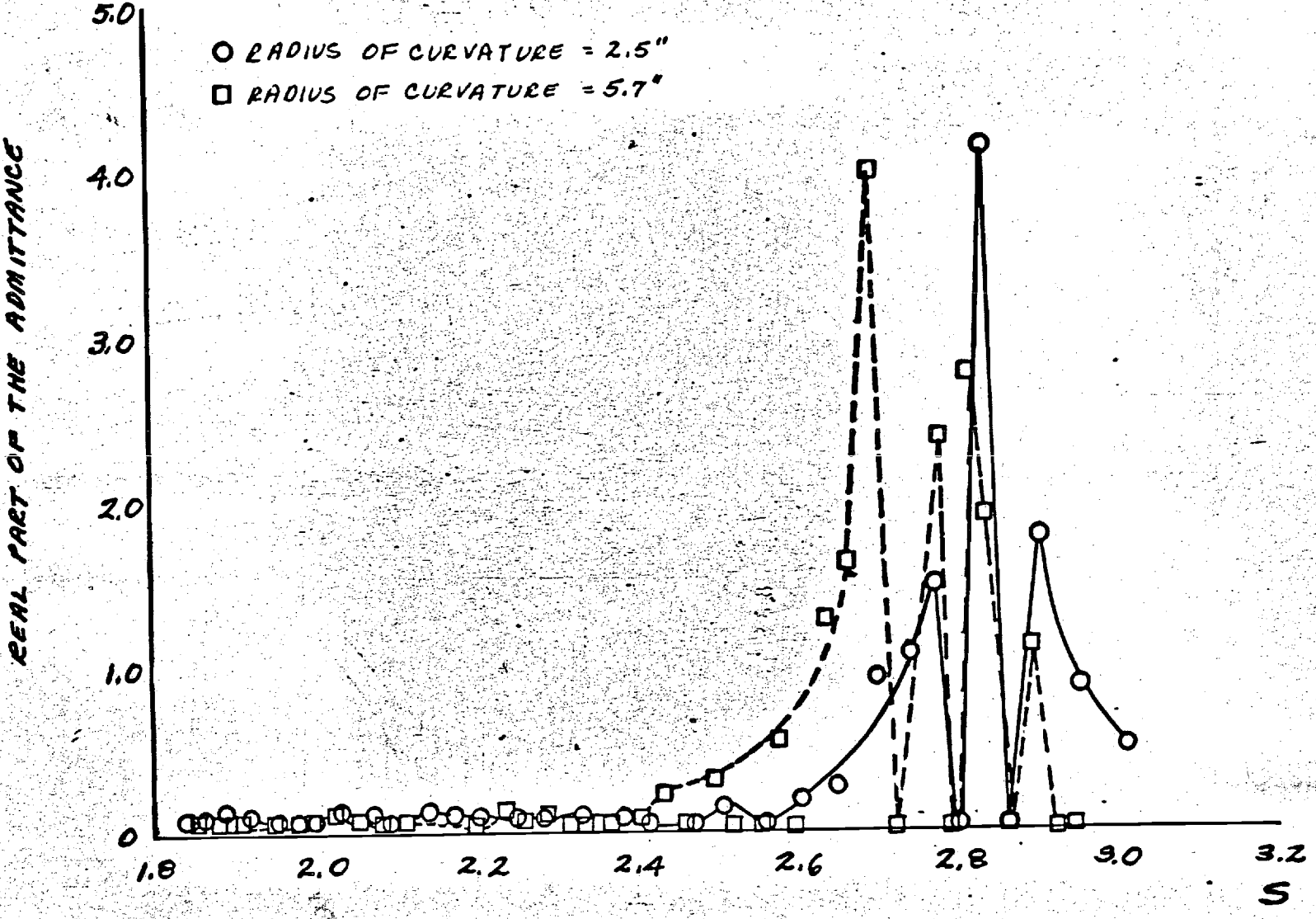

FIGURE 6. EFFECT OF RADIUS OF CURVATURE AT A MACH NUMBER OF .08 AND A NOZZLE ANGLE OF 15°

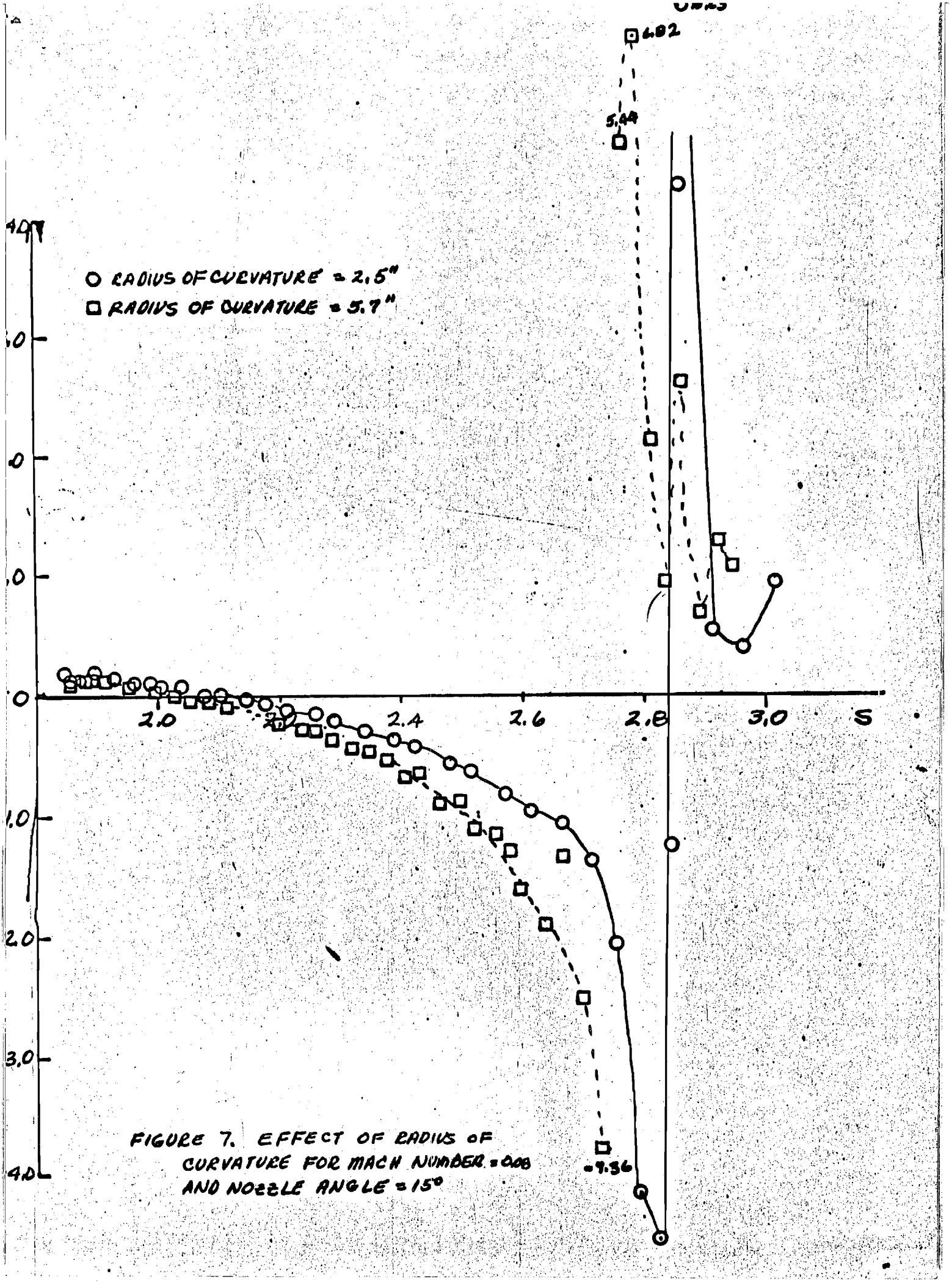

FIGURE 7. EFFECT OF RADIUS OF CURVATURE FOR MACH NUMBER = 0.08 AND NOZZLE ANGLE = 15°

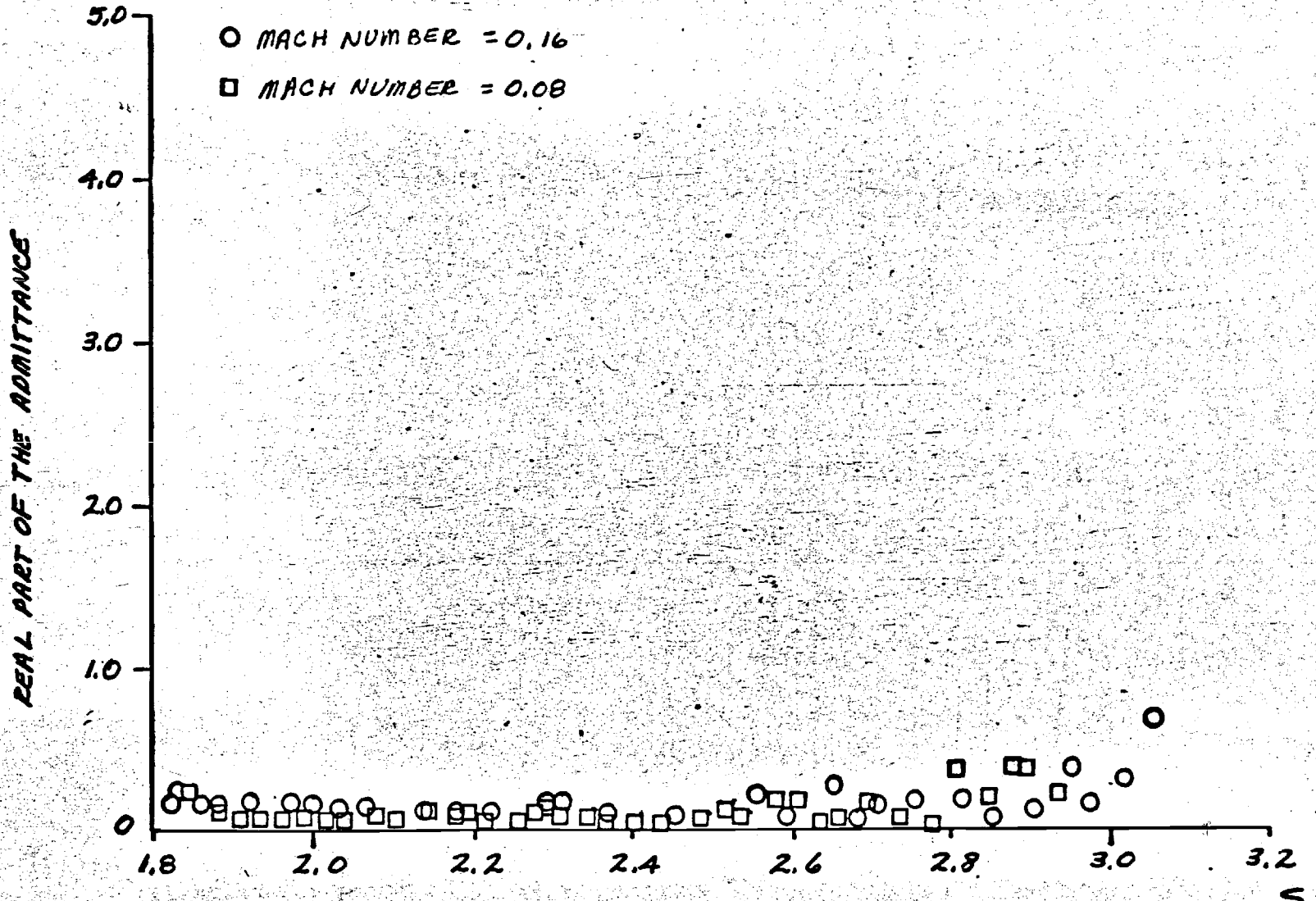

FIGURE 8. EFFECT OF MACH NUMBER AT A NOZZLE ANGLE OF 45° AND RADIUS OF CURVATURE OF 2.5".

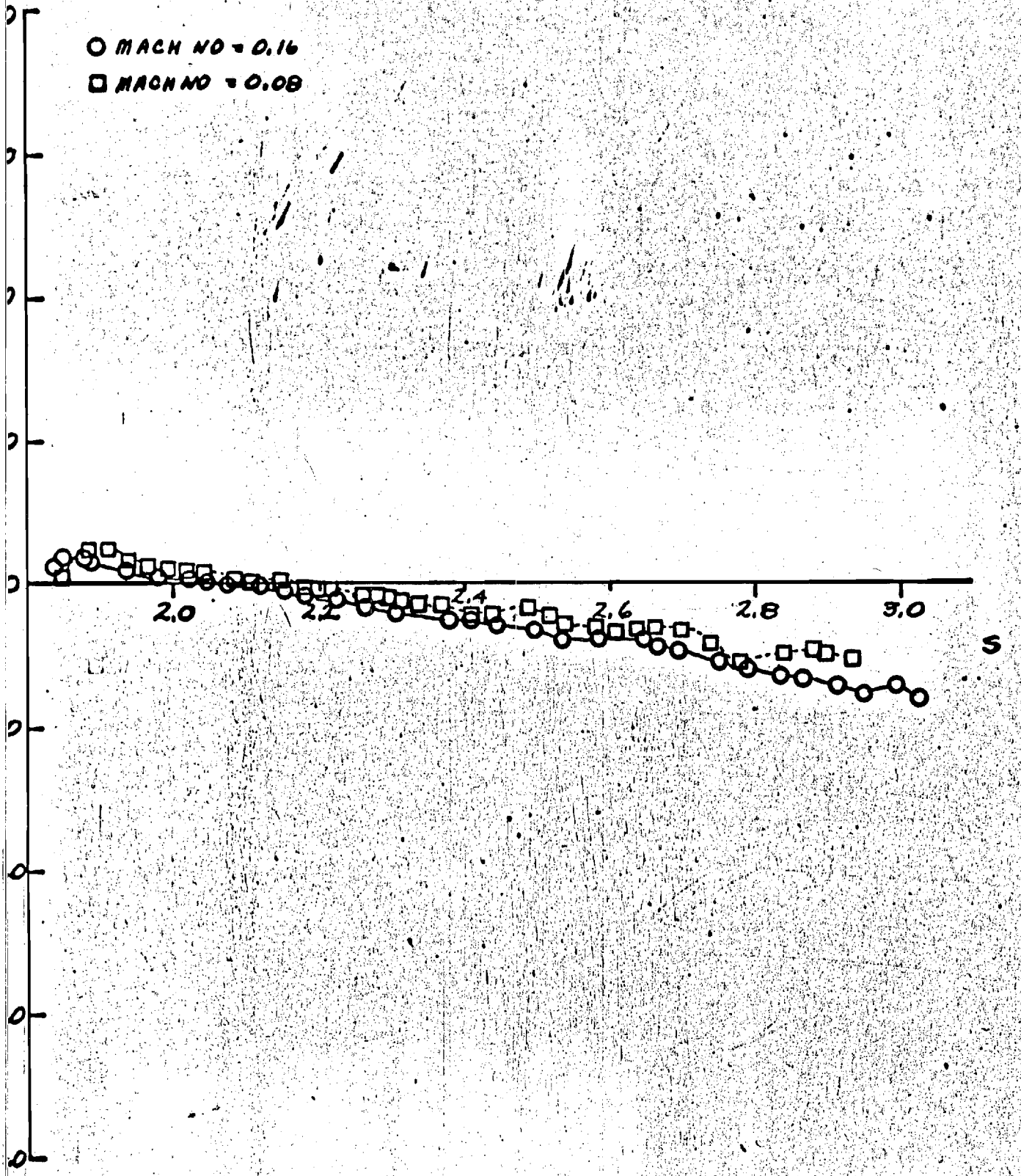

FIGURE 9. EFFECT OF MACH NUMBER

E-16-607

NASA GRANT NGL 11-002-085

BEHAVIOR OF NOZZLES AND ACOUSTIC LINERS IN THREE-DIMENSIONAL ACOUSTIC FIELDS

Quarterly Report for Period 1 September 1971 to 30 November 1971

Prepared by: Ben T. Zinn, Principal Investigator
W. A. Bell, Graduate Research Assistant
B. R. Daniel, Research Engineer
Allan J. Smith, Jr., Research Engineer

School of Aerospace Engineering
Georgia Institute of Technology
Atlanta, Georgia

PROGRESS DURING REPORT PERIOD

A. Summary

Theoretical values of the admittances of various nozzles have been computed and compared with the corresponding experimental values. The existing data reduction scheme has been corrected and all available experimental data has been rechecked and corrected whenever necessary; the updated experimental admittance values are presented in this report. An analysis associated with the frequency sensitivity of experimental admittance values has been initiated. The Analog-To-Digital Data Reduction Program has become operational. Fourteen nozzle tests have been conducted during this report period.

B. Theoretical Studies

Theoretical values of the nozzle admittance have been computed based on the three dimensional nozzle admittance theory of Crocco.[1] The development of a computer program which employs this theory to predict nozzle admittances has been completed; this program was then used to predict the admittance values for all the nozzles tested to date. Before presenting the results, a brief description of the theory used in developing this computer program will now be given.

According to Crocco's theory[1], the admittance Y is given by the expression

$$Y = \frac{-Z}{q^2 Z + is} \qquad (1)$$

where

$$Z = \frac{\text{axial dependence of the axial velocity perturbation}}{\text{axial dependence of the radial velocity perturbation}}$$

q = nondimensionalized mean flow velocity

s = nondimensionalized frequency

Once Z is known and q and s are specified, the admittance can be found from Eq. (1). The problem is to compute Z. Values of this parameter can be determined by numerically integrating the following complex, nonlinear equation (called the Riccati Equation):

$$\frac{dZ}{d\bar{\Phi}} = A(\bar{\Phi})Z - B(\bar{\Phi}) - Z^2 \tag{2}$$

where the independent variable $\bar{\Phi}$ is the steady state flow potential, and $A(\bar{\Phi})$ and $B(\bar{\Phi})$ are coefficients whose form depends upon s and the mean flow properties in the converging section of the nozzle. The major difficulty in integrating Eq. (2) is that Z can take on very large values whenever the radial velocity approaches zero. These large values can occur for the nozzles under investigation, and can cause numerical instabilities in the integration scheme. This problem is circumvented by transforming the dependent variable as follows:

$$T = \frac{1}{Z} \tag{3}$$

Thus, when Z becomes large T becomes small. Substituting for Z in Eq. (2) gives the following Riccati Equation for T:

$$\frac{dT}{d\bar{\Phi}} = 1 - A(\bar{\Phi})T + B(\bar{\Phi})\ T^2 \tag{4}$$

In order to avoid numerical instabilities in the computer program which predicts theoretical admittance values, the following procedure is used. Starting at the nozzle throat, Eq. (2) is integrated until the magnitude of Z becomes larger than a specified value at a certain value of $\bar{\Phi}$; T is then found from Eq. (3) and Eq. (4) is integrated. Similarly, when $|T|$ exceeds a certain value, Z is computed from Eq. (3) and the integration is carried out using Eq. (2).

This process is repeated until Φ equals the value at the nozzle entrance. The admittance is then determined from Eq. (1) using the value of Z or T at that point.

When the theoretical admittance values were computed it was found that a discrepancy existed between the theoretical predictions and the experimental results. This discrepancy was traced to the improper interpretation of the incident and reflected waves in the theory used for the reduction of the experimental data. The discrepancy was corrected and all the experimental data that had been previously taken was rerun. While correcting the data reduction scheme, it was found that the equations presented in the last quarterly report remain unchanged with the exception of the expression for the real part of the admittance whose corrected form is given by Eq. (5). The corrected admittance data indicates that increasing the mean flow Mach number decreases the value of the real part of the admittance for three dimensional modes which is in agreement with nozzle admittance theory. Data presented in earlier reports shows the opposite trend. In addition, the signs of the corrected values of the imaginary parts of the nozzle admittance are the negative of the values reported earlier.

The comparisons of the experimental admittances with the corresponding theoretical predictions are presented in figures 1 through 24. Except for figures 3 and 7 the theory and experiment are in qualitative agreement. Before any conclusions, concerning the validity of the theory or the experimental data, are drawn, further analysis of these results will be performed. Included in this analysis will be the study of the accuracy of the frequency measurements and its effect upon the experimental results. The findings of this analysis will be reported in the next progress report.

Figures 3 and 7 show that the experimental values for the real part of the admittance approach large positive numbers whereas the theory predicts large negative values. This discrepancy could be due to the inability of the present data reduction scheme to

determine the proper sign of α. This point may become clearer if one considers the following equations:

$$Y_r = \frac{S\sqrt{S^2 - S_{mn}^2(1-\bar{m}^2)}\ \tanh \pi\alpha\ \sec^2\pi\beta\ \bar{\sigma}\ S_{mn}^2 M}{(S^2 + S_{mn}^2 M^2)\ (\tanh^2\pi\alpha + \tan^2 \pi\beta)} \qquad (5)$$

where

$$e^{-2\pi\alpha} = \left(\frac{\text{reflected wave amplitude}}{\text{incident wave amplitude}}\right)_{\text{nozzle entrance}}$$

$\pi(1 + 2\beta)$ = phase change of the incident wave upon reflection

r_c = chamber radius

S_{mn} = 0 for longitudinal modes
S_{mn} = 1.8413 for transverse modes

M = chamber Mach number

In order for the theoretical and experimental admittances, in Figs. 3 and 7, to agree α must take on negative values. However, the present data reduction scheme is not capable of determining the sign of α from the perturbation pressure amplitude measurements at various locations along the tube. The sign of α can, however, be determined from perturbation pressure phase measurements; as a matter of fact the phase measurements can be used to determine both the sign and magnitude of α.

A computer program using the Nonlinear Regression Technique for the computation of α, β, and the admittance from phase measurements taken at discrete points along the tube is in preparation. This program is currently undergoing preliminary checkouts and

admittance values obtained from this program will be presented in the next report.

The checkout of the analog-to-digital data reduction program has been completed and the program is operational at this time. The principal motivation for the development of the A-to-D program was the desire to obtain accurate phase data, which is an important consideration for both the present nozzle testing program and the anticipated acoustic liner work. Other advantages associated with the use of the A-to-D program are: (1) the data reduction time is reduced by several orders of magnitude; (2) the frequency resolution is improved; and (3) the possibility of human errors affecting the data accuracy are virtually eliminated.

A brief description of the use of the A-to-D program follows. First, the analog data taken during the test must be digitized. This is accomplished by a 14 channel Analog-To-Digital Conversion System manufactured by the Radiation Corporation. This unit is made available, free-of-charge, to users of the Rich Electronic Computer Center, which is an integral part of Georgia Tech. The unit has been programmed to sample 25,000 samples/second. For ten channels of analog data (viz., two frequency channels and eight dynamic pressure transducer channels), this sample rate provides 2,500 samples/second/channel, which represents 0.4 milliseconds between samples on each channel. The maximum frequency recorded on the analog tape is 1,000 Hz; however, the maximum frequency of the Conversion System is restricted to 250 Hz at this sample rate for ten channels. Consequently, the analog tape recorder speed must be reduced by 4:1 during the playback into the A-to-D Conversion System. This selection of sample rate and maximum frequency insures that the signal with the shortest period (viz., the real-time frequency of 1,000 Hz) will be sampled 10 times during the period, which is considered to be an absolute minimum for good statistical confidence. The minimum frequency is not limited by the Conversion System but is limited by the available core size associated with the computer that is used to process the digitized

data. In this case, the computer is a Univac 1108 that has a total available core of 60,000 words. This amount of core results in a minimum real-time frequency of 56 Hz, which implies that this period is sampled 179 times during one cycle by the Conversion System. The frequency limits can be summarized as follows:

$$\text{Real-time;} \quad 56 \leq f, \ \text{Hz} \leq 1{,}000$$

$$\text{Reduced-time;} \quad 14 \leq f, \ \text{Hz} \leq 250$$

The end product of the A-to-D conversion is a tape of digitized test data.

The digitized test data is then transferred to the Univac 1108 system where it is used to determine all needed information. The data reduction program is written in the Fortran V compiler and executed by the Univac 1108. After this program reads a block of digitized data, it proceeds to determine the frequency associated with that block of data. This is accomplished by checking for the zero-crossings of a reference (sinusoidal) frequency signal. Inasmuch as the frequency signal will not be digitized at the exact instant when the signal is identically zero, the instant when the signal crosses the zero line must be interpolated by using the last two positive values and the first two negative values. The use of an interpolation routine suggests that an error might be introduced. A checkout of the interpolation schemed showed that it produces a maximum error of 0.5 Hz, which represents a 0.05% error.

The frequency that has just been determined is the frequency of the driven oscillation at that instant of time during the test. Therefore, it represents the fundamental frequency for that block of digitized pressure data. For one period of the fundamental mode, the Fourier Series representation of the time-dependent signal is given by:

$$p(t) = A \cos \omega t + B \sin \omega t$$

where

$p(t)$: time-dependent pressure amplitude, psi

ω : angular frequency, radians/sec

$$A = \frac{2}{T} \int_0^T p(t) \cos \omega t \, dt$$

$$B = \frac{2}{T} \int_0^T p(t) \sin \omega t \, dt$$

T : period of the fundamental mode, seconds

The program determines the Fourier Coefficients A and B for each of the pressure signals. The signal amplitude is determined from the expression:

$$\text{Amplitude} = (A^2 + B^2)^{1/2}$$

and the phase is determined from the expression:

$$\text{Phase} = \tan^{-1}(B/A)$$

Each test can be divided into 500 data reduction points. After the frequency, amplitude, and phase have been determined for the entire digital tape, this information is fed into a special subroutine that uses this data to compute the nozzle admittance and related data. An example of the data reduction results is presented in Appendix A.

The data reduction program was checked out with and without a digitized tape data. The first checkout was without a digitized tape data. In this case, signals of known frequency, amplitude, and phase were generated using a sine function. These continuous signals were synthetically digitized in a manner similar to that used by the Conversion System when it digitizes the analog data. This data was processed by the program and the program results were compared to the input values. For both simple periodic signals and complex periodic signals (i.e., signals composed of a sum of a fundamental oscillation and its various harmonics), the error in amplitude and phase appeared as a "round-off" error, which represents an error of less than 0.2%. For a nonperiodic signal (i.e., two periodic signals whose frequencies are not related by an integer constant), the amplitude error was less than 5% and the phase error was approximately 5° for the case when the two signal amplitudes were equal. This case approximates conditions when the signal-to-noise ratios equal to one. These errors decreased rapidly as the signal-to-noise ratio approached 10:1.

The second checkout of the program involved the use of digitized data obtained from an actual test. A comparison of the program's results with the results obtained by the previous data reduction method disclosed that there was general agreement between the two methods. The concensus of opinion is that the new data reduction scheme is more accurate than the one used to date; furthermore, the new program is considerably more efficient.

C. Experimental Investigations

During this report period fourteen tests have been run. One test was conducted for checking the analog-to-digital data reduction program. All of the nozzles fabricated thus far were retested in order to include the entire frequency range for 1T modes ($1.84 < s < 3.05$) and most of the longitudinal frequency range ($.1 < s < 1.84$). The results of these tests are included in

figures 1 through 24. In addition, two tests were run with a quasi-steady nozzle and two more with a nozzle whose half-angle is 45° and radius of curvature of 2.5 inches. The Mach number of the latter nozzle was increased to a value of .20. The data obtained in these tests is being reduced and it will be presented in the next progress report.

Other efforts have resulted in the improvement of the precision of the frequency measurements. This improvement allowed a significant increase in the number of data points taken per run.

EXPECTED PROGRESS DURING NEXT REPORT PERIOD

During the next quarter, two more microphones will be added to the data acquisition system. This addition will bring the number of pressure amplitudes sampled along the standing wave pattern to ten. This will improve the accuracy of the admittance values by providing more information about the wave structure.

The nozzle with a half-angle of 45° and radius of curvature of 2.5 inches will be tested at various Mach numbers starting at M = .24 and proceeding to M = .32. These series of tests will be conducted to determine whether there are any unexpected problems associated with testing at higher Mach numbers. Assuming that no major problems are encountered, the other nozzles will be tested and the experimental admittance values along with the corresponding theoretical predictions will be determined. These results will be compared in the next quarterly report.

REFERENCES

1. Crocco, L., Sirignano, W. A., "Behavior of Supercritical Nozzles Under Three Dimensional Oscillatory Conditions," AGARDograph 117, 1967.

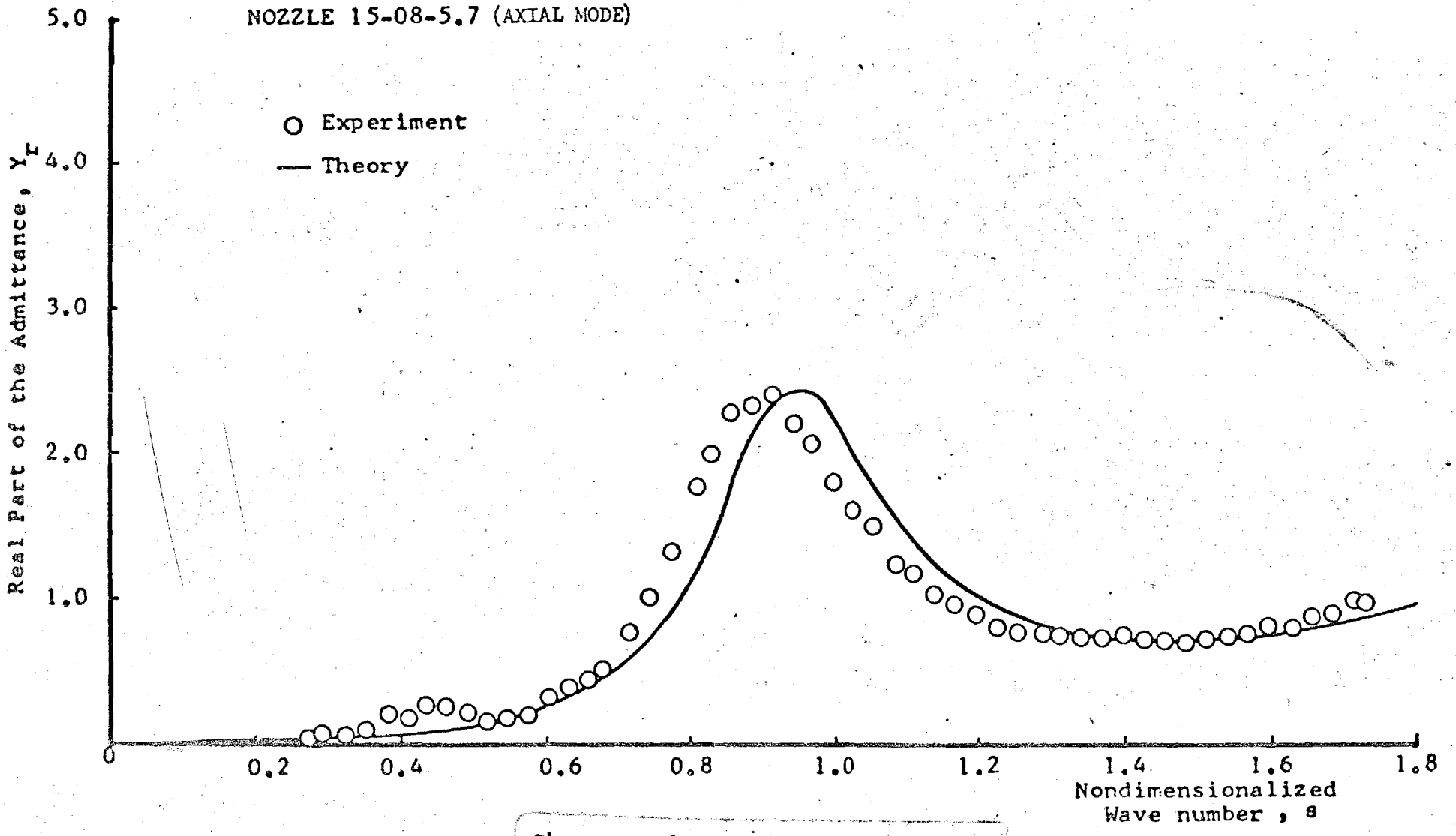

Figure 1. Comparison of the theory and experimental values of the real part of the admittance for the nozzle with a half-angle of 15 degrees, entrance Mach number of .08, and radii of curvature at the throat and entrance of 5.7 inches.

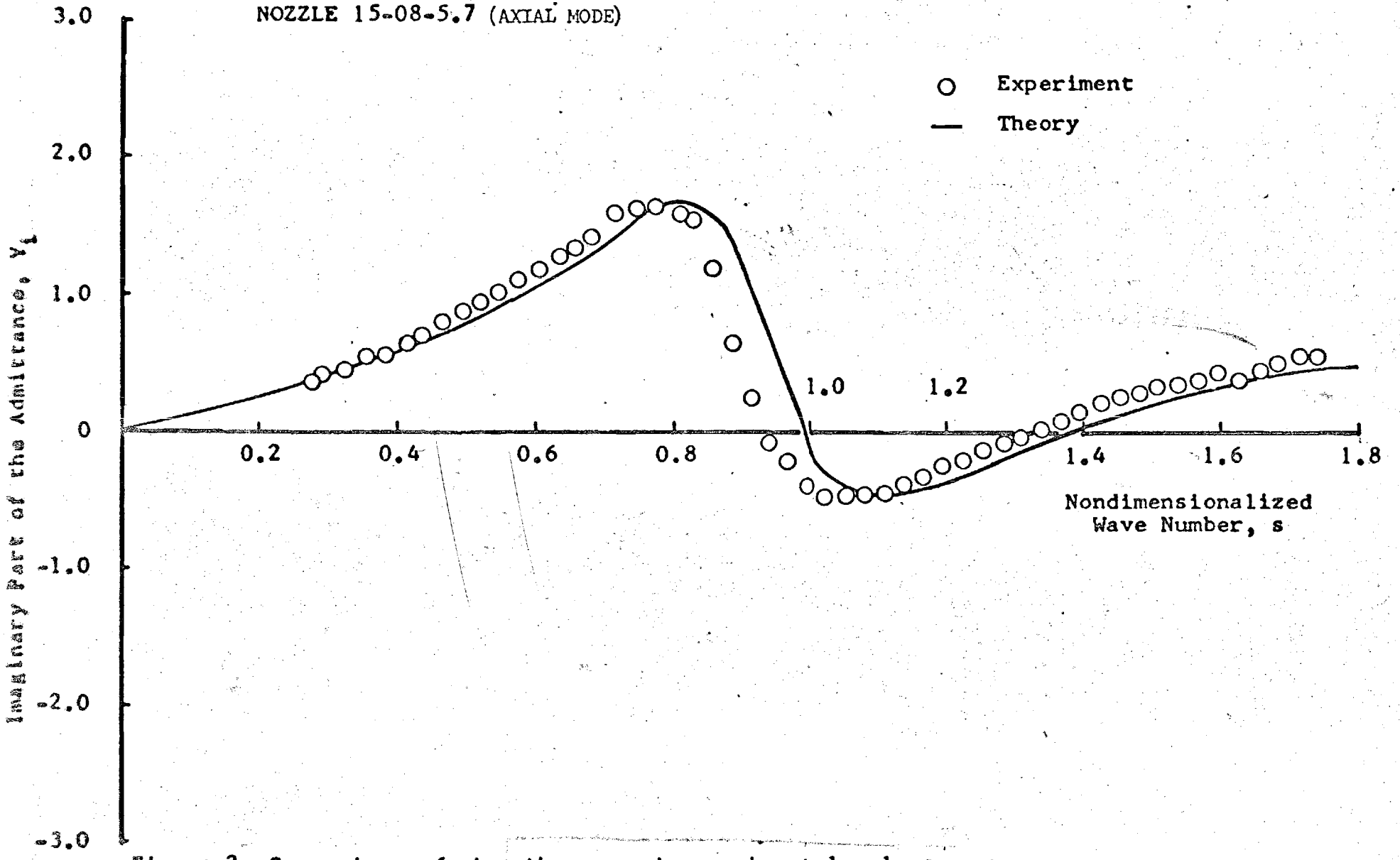

Figure 2. Comparison of the theory and experimental values of the imaginary part of the admittance for the nozzle with a half-angle of 15 degrees, entrance Mach number of .08, and radii of curvature at the throat and entrance of 5.7 inches.

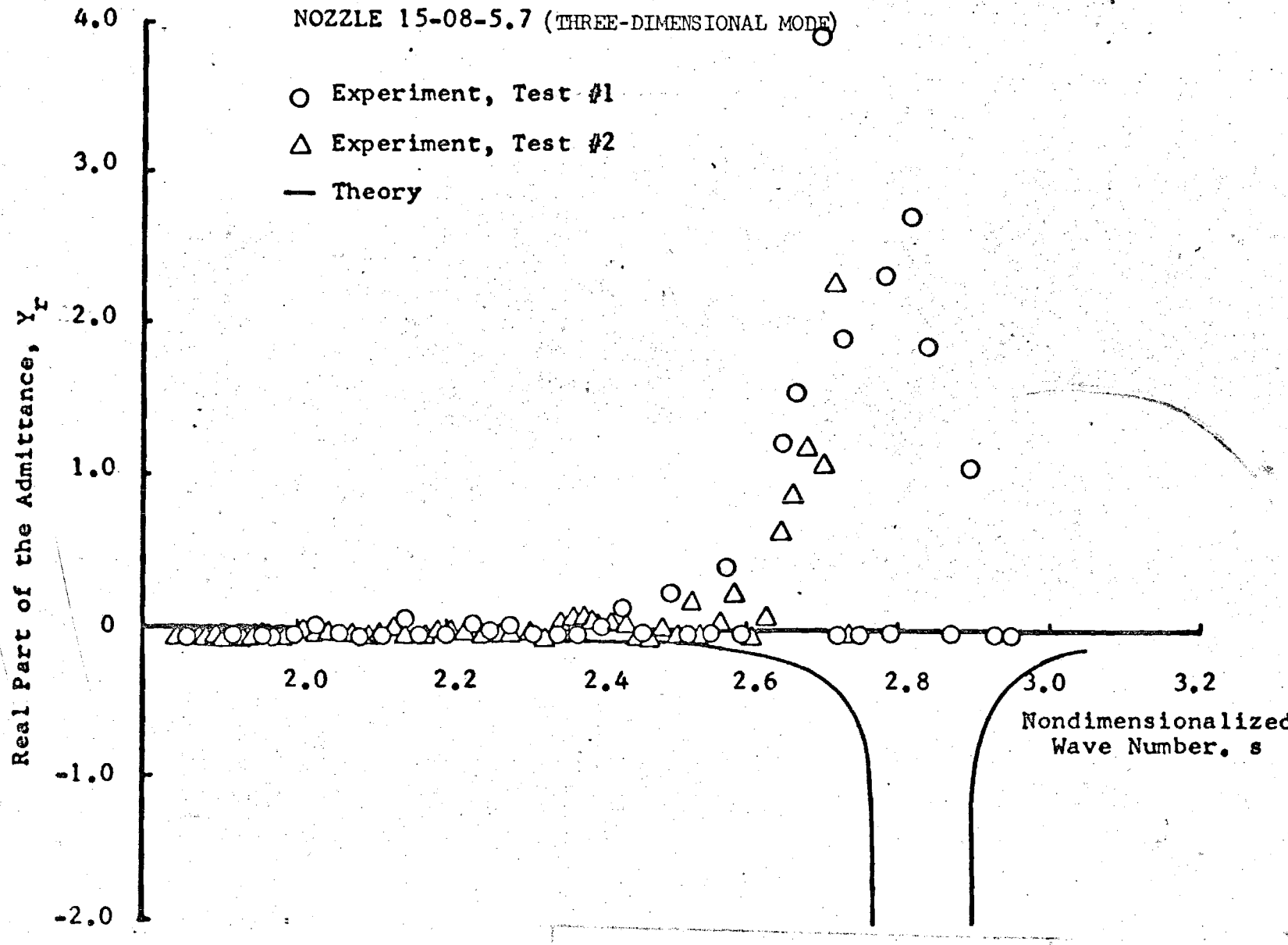

Figure 3. Comparison of the theory and experimental values of the real part of the admittance for a nozzle with a half-angle of 15 degrees, entrance Mach number of .08, and radii of curvature at the throat and entrance of 5.7 inches.

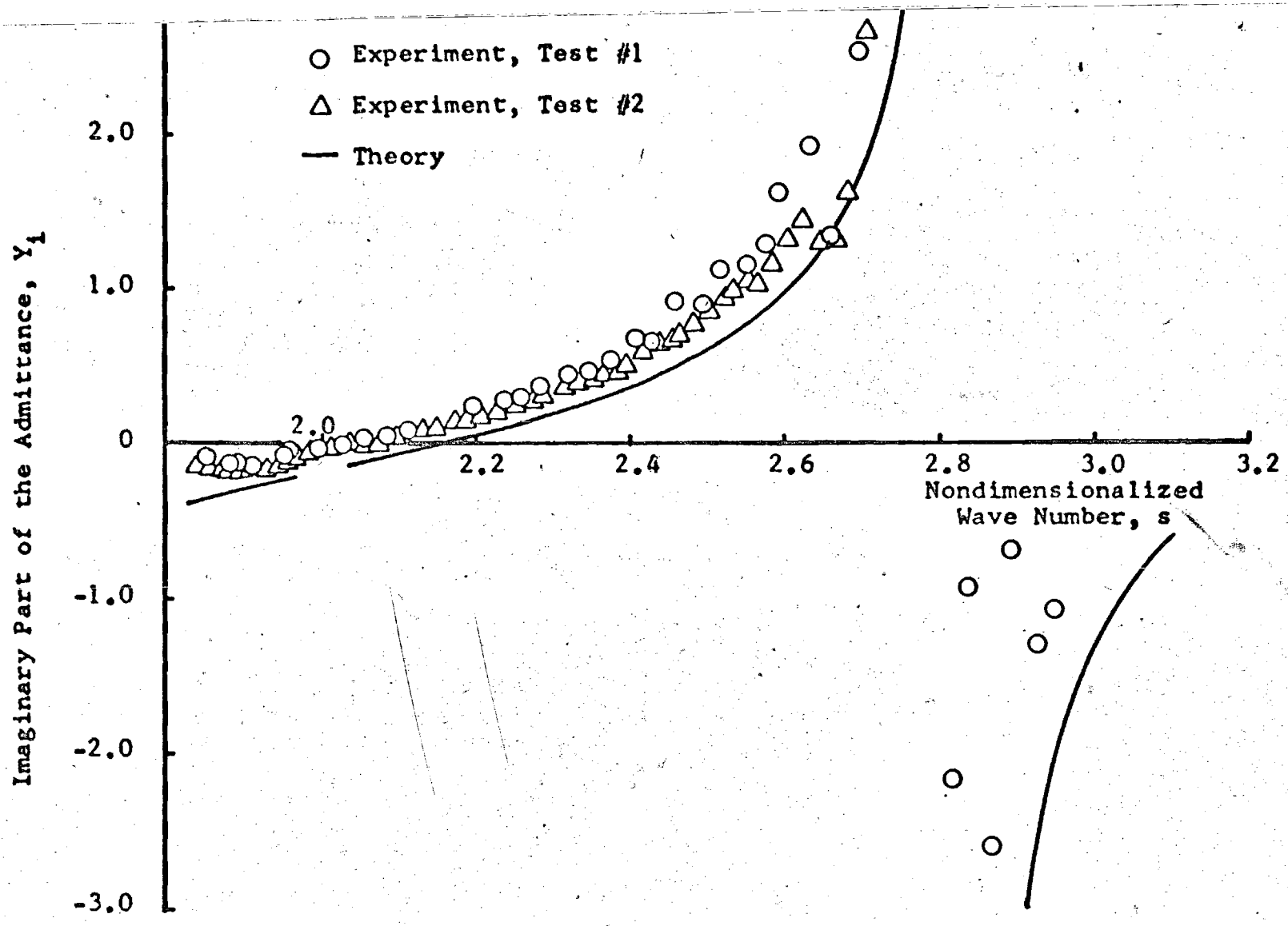

Figure 4. Comparison of the theoretical and experimental values of the imaginary part of the admittance for a nozzle with a half-angle of 15 degrees, entrance Mach Number of .08, and radii of curvature at the throat and entrance of 5.7.

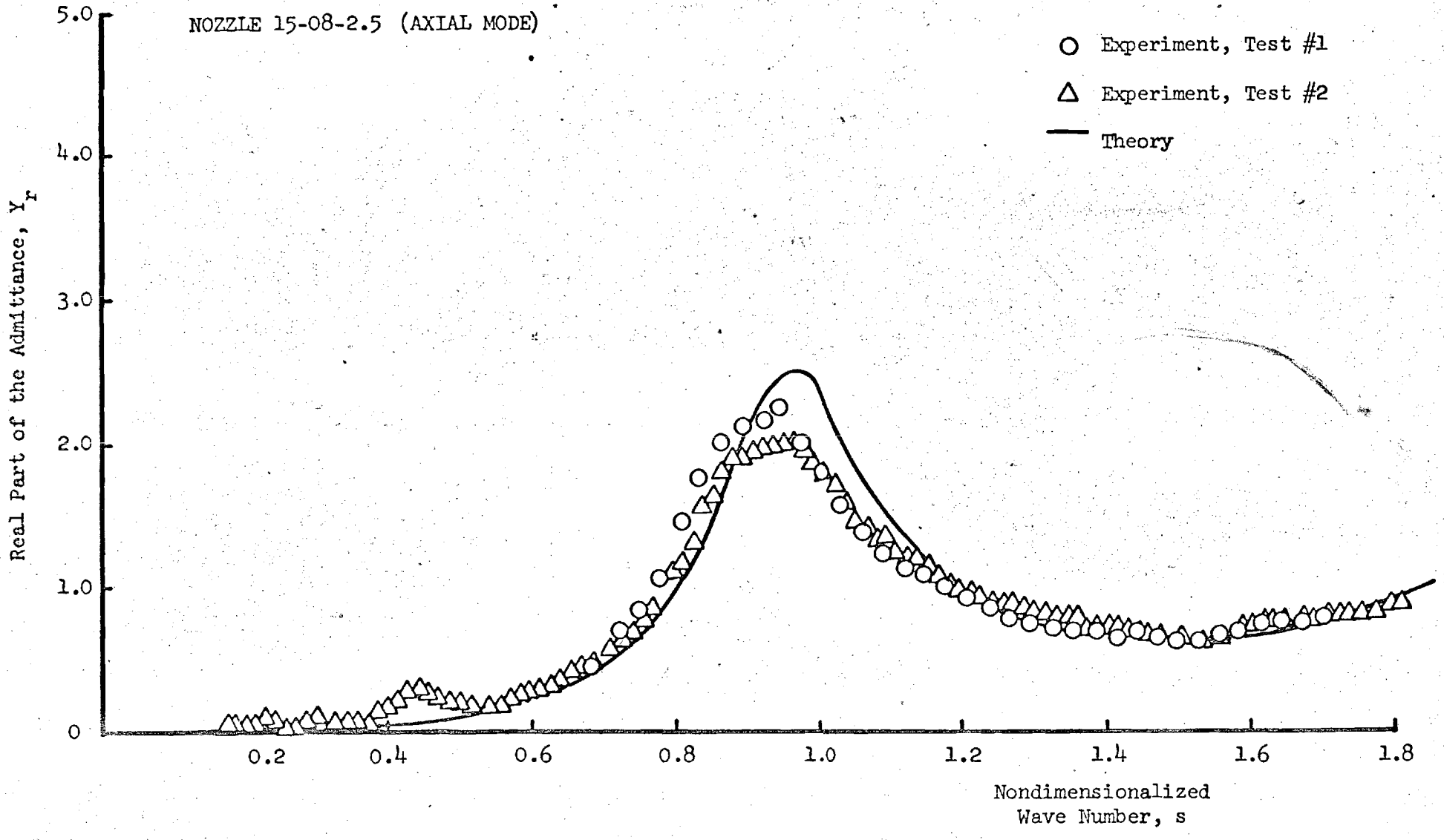

Figure 5. Comparison of the theoretical and experimental values of the real part of the admittance for a nozzle with a half-angle of 15 degrees entrance Mach number of .08 and radii of curvature at the entrance and throat of 2.5 inches.

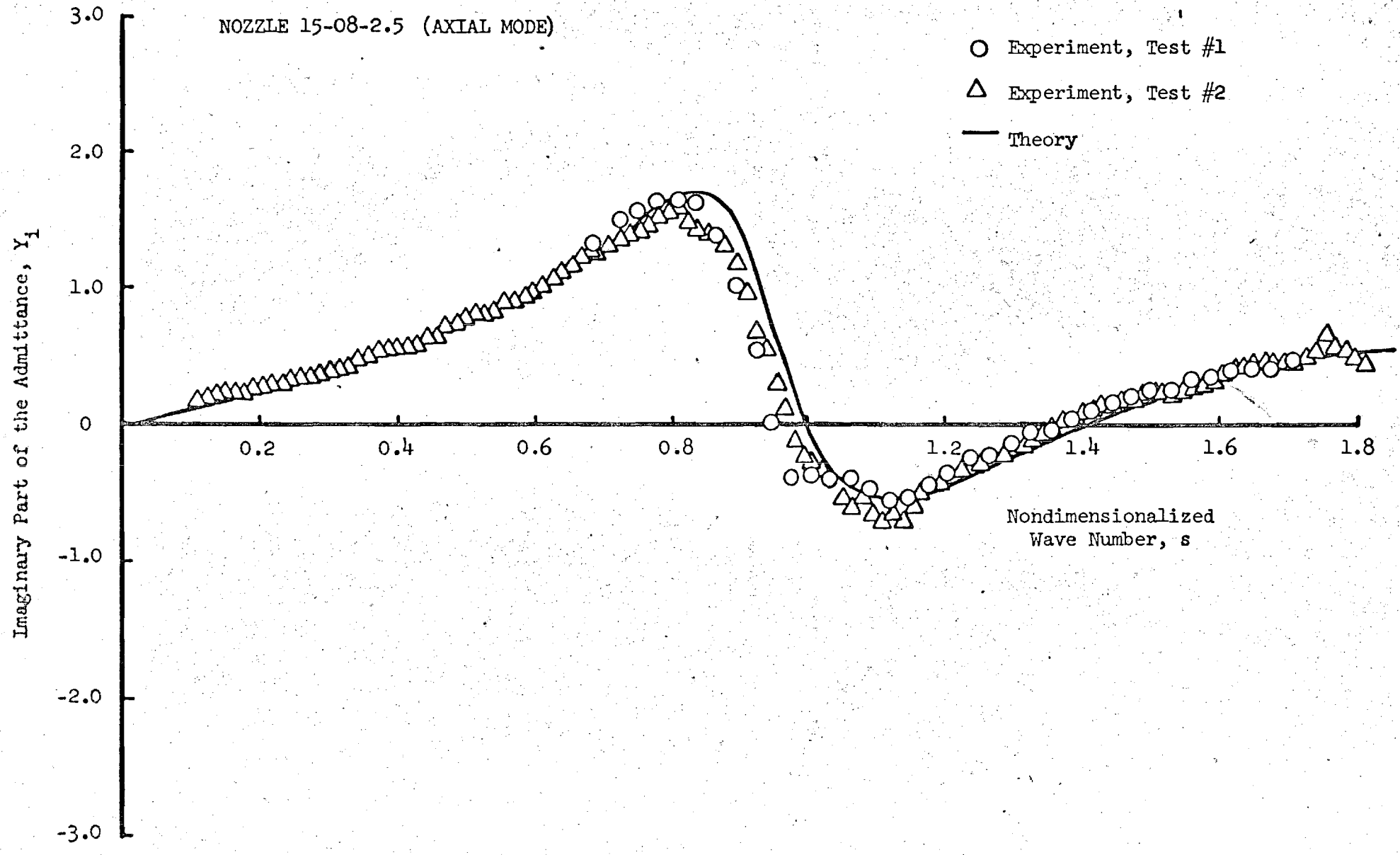

Figure 6. Comparison of the theoretical and experimental values of the imaginary part of the admittance for a nozzle with a half-angle of 15 degrees, entrance Mach number of .08 and radii of curvature at the entrance and throat of 2.5 inches.

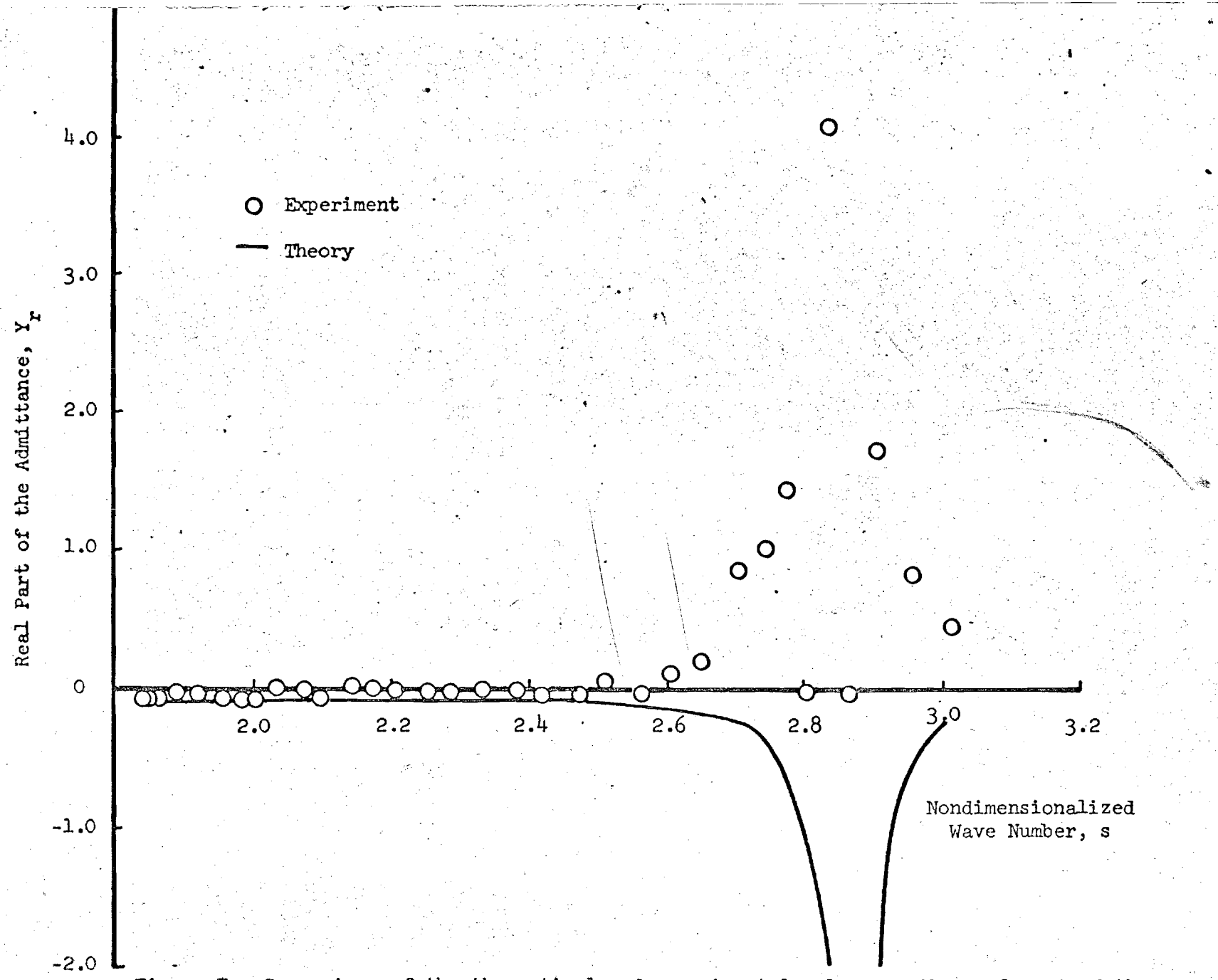

Figure 7. Comparison of the theoretical and experimental values of the real part of the admittance for a nozzle with a half-angle of 15 degrees, entrance Mach number of .08, and radii of curvature at the throat and entrance of 2.5 inches.

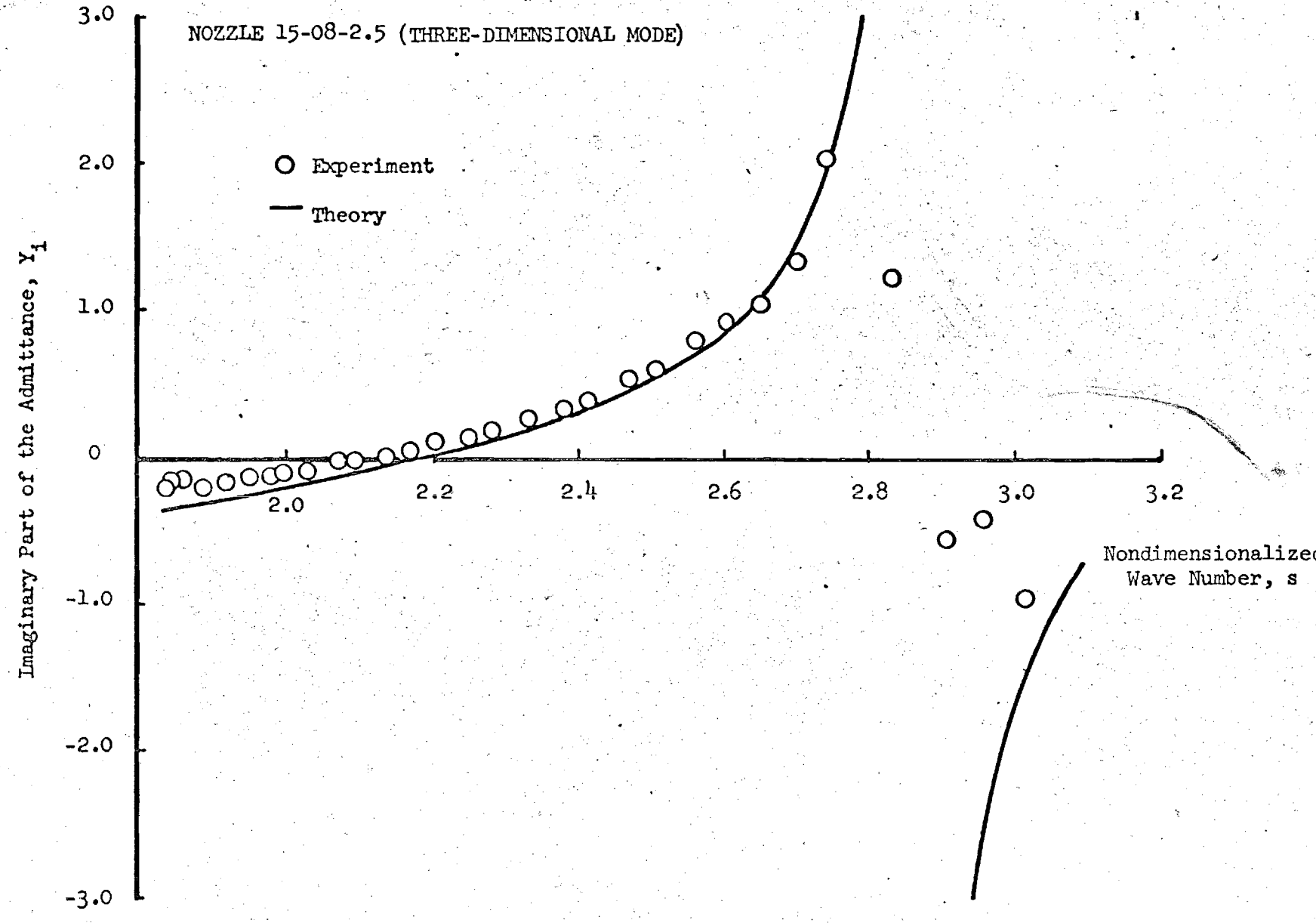

Figure 8. Comparison of the theoretical and experimental values of the imaginary part of the admittance for a nozzle with a half-angle of 15 degrees, entrance Mach number of .08, and radii of curvature at the throat and entrance of 2.5 inches.

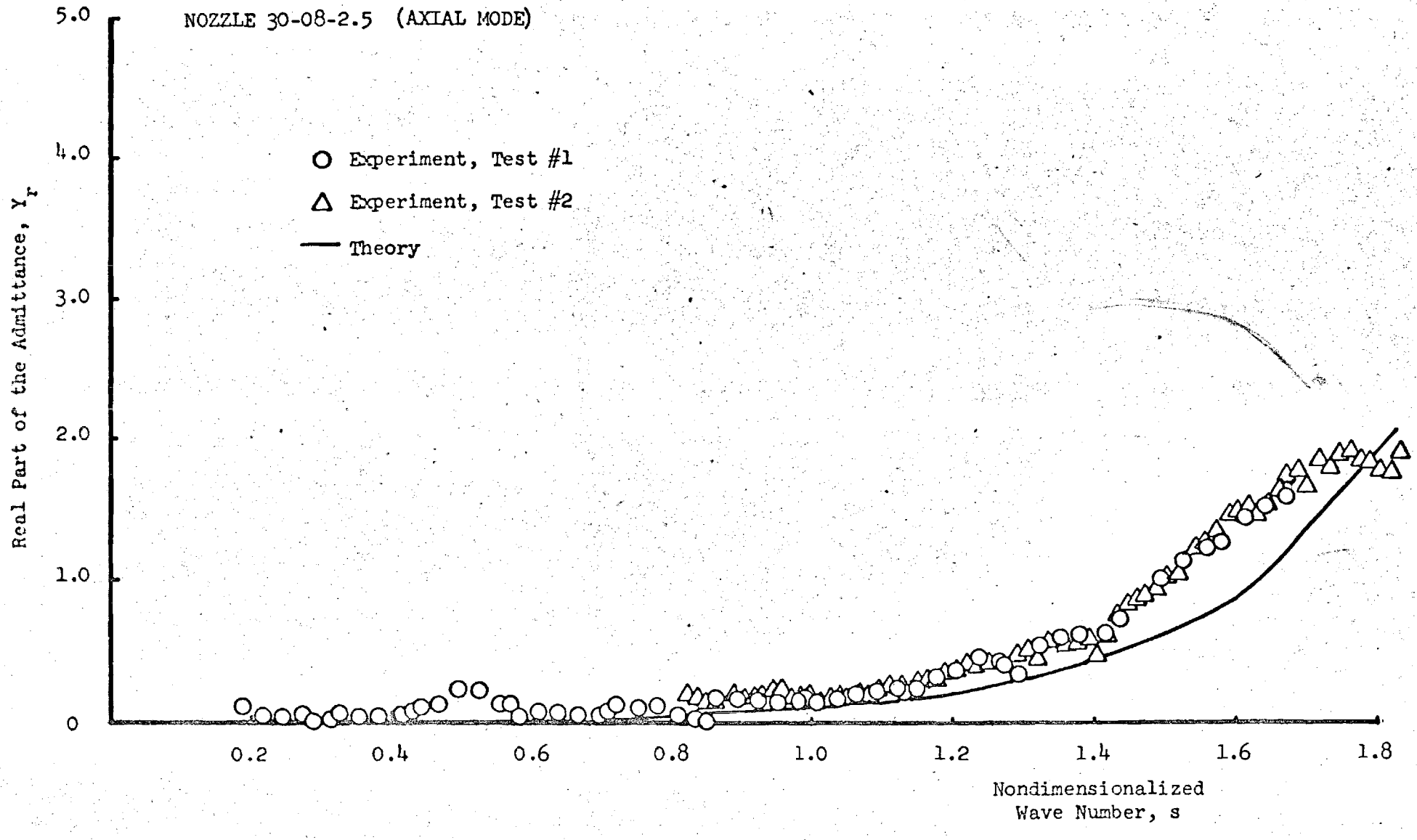

Figure 9. Comparison of the theoretical and experimental values of the real part of the admittance for a nozzle with a half-angle of 30 degrees, entrance Mach number of .08, and radii of curvature at the throat and entrance of 2.5 inches.

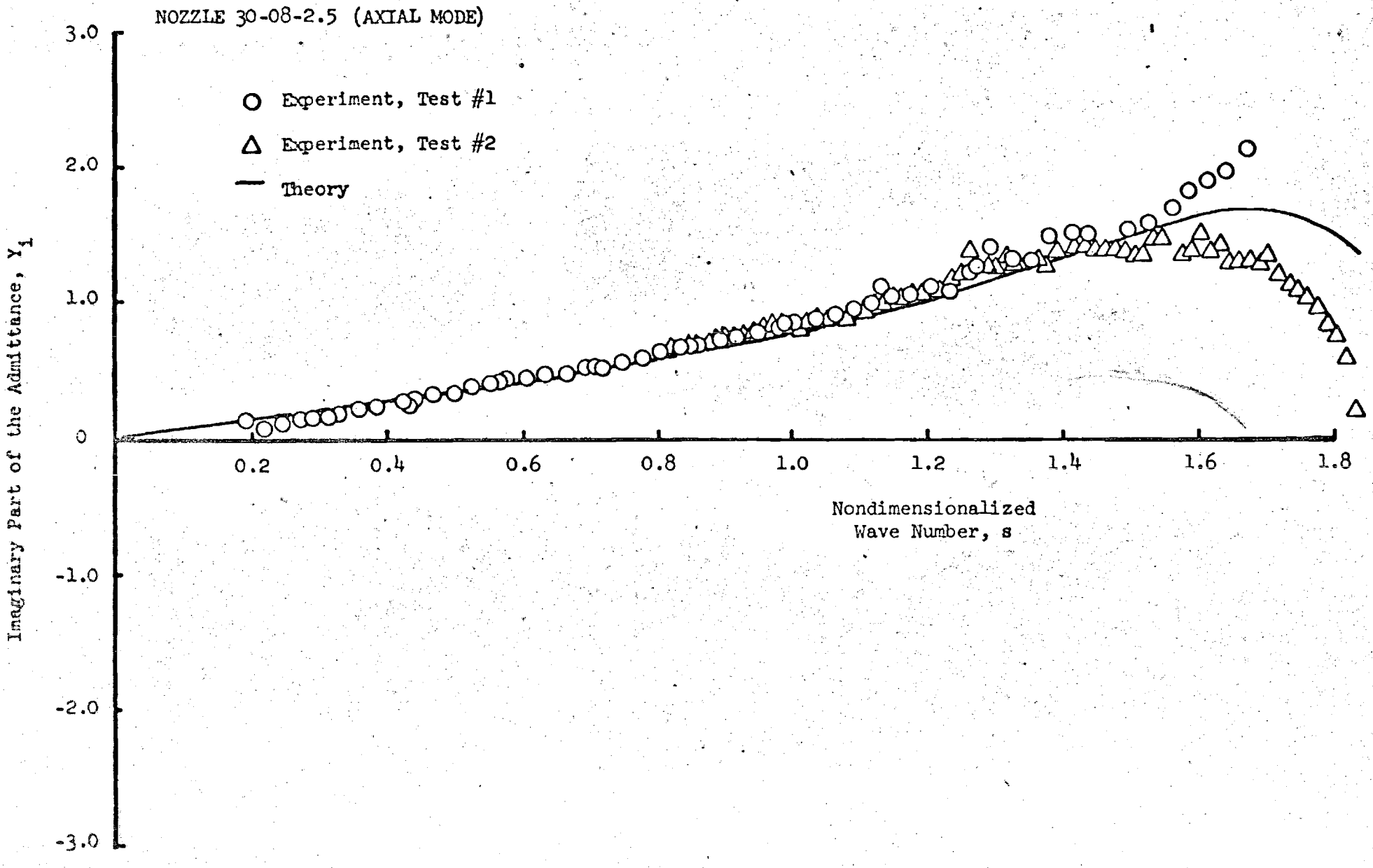

Figure 10. Comparison of the theoretical and experimental values of the imaginary part of the admittance for a nozzle with a half-angle of 30 degrees, entrance Mach number of .08, and radii of curvature at the throat and entrance of 2.5 inches.

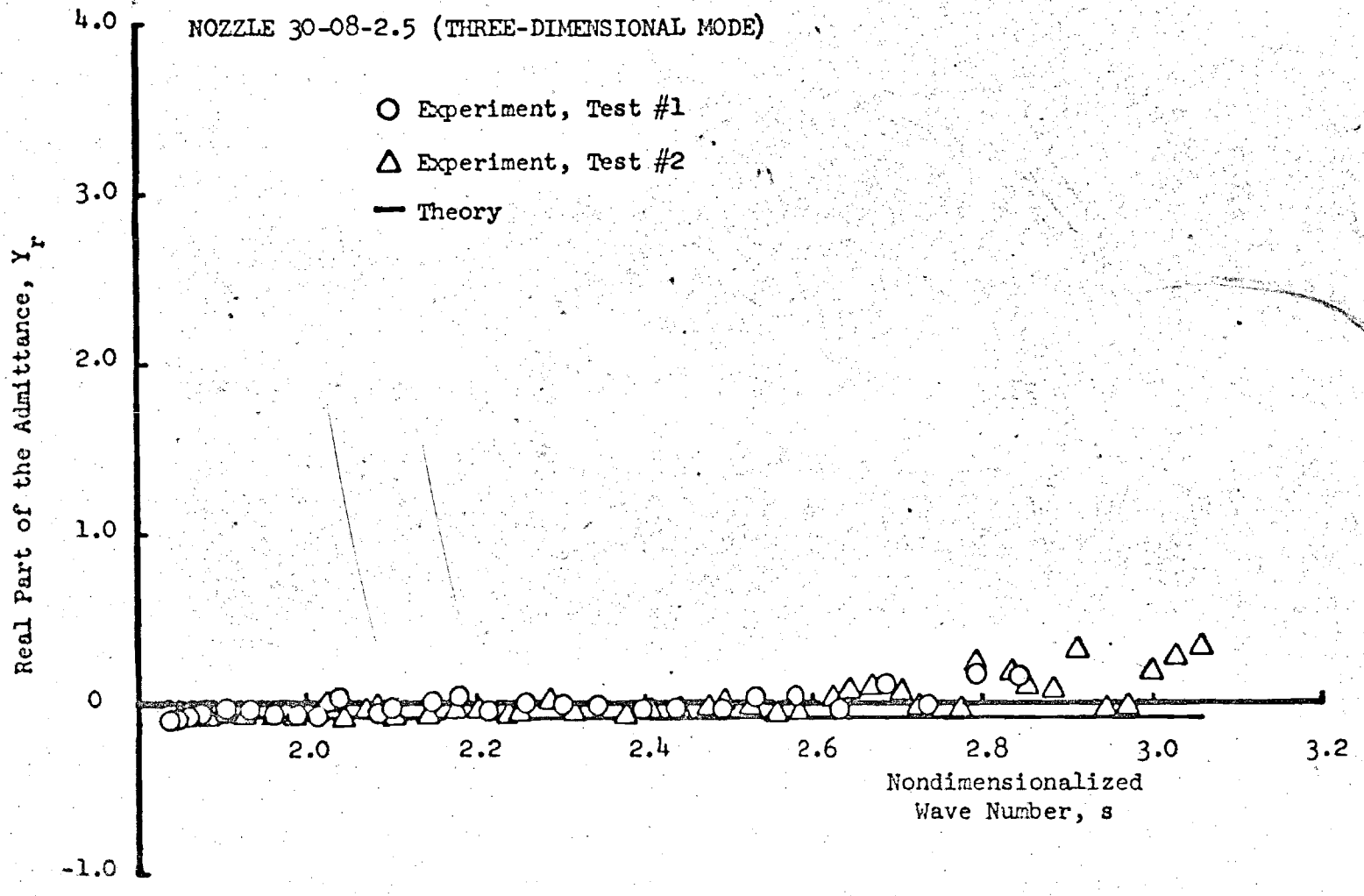

Figure 11. Comparison of the theoretical and experimental values of the real part of the admittance for a nozzle with a half-angle of 30 degrees, entrance Mach number of .08, and radii of curvature at the throat and entrance of 2.5 inches.

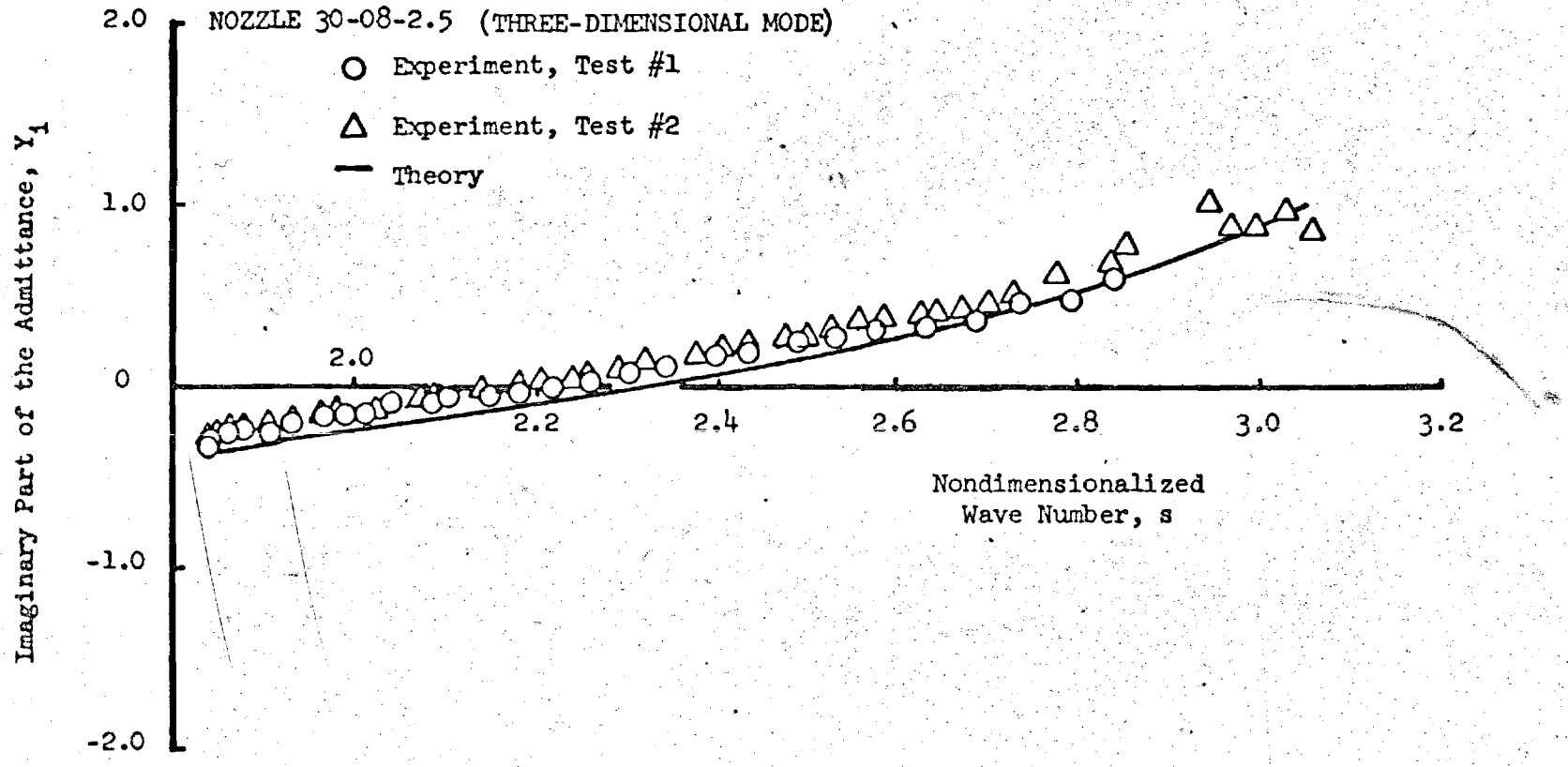

Figure 12. Comparison of the theoretical and experimental values of the imaginary part of the admittance for a nozzle with a half-angle of 30 degrees, an entrance Mach number of .08, and radii of curvature at the throat and entrance of 2.5 inches.

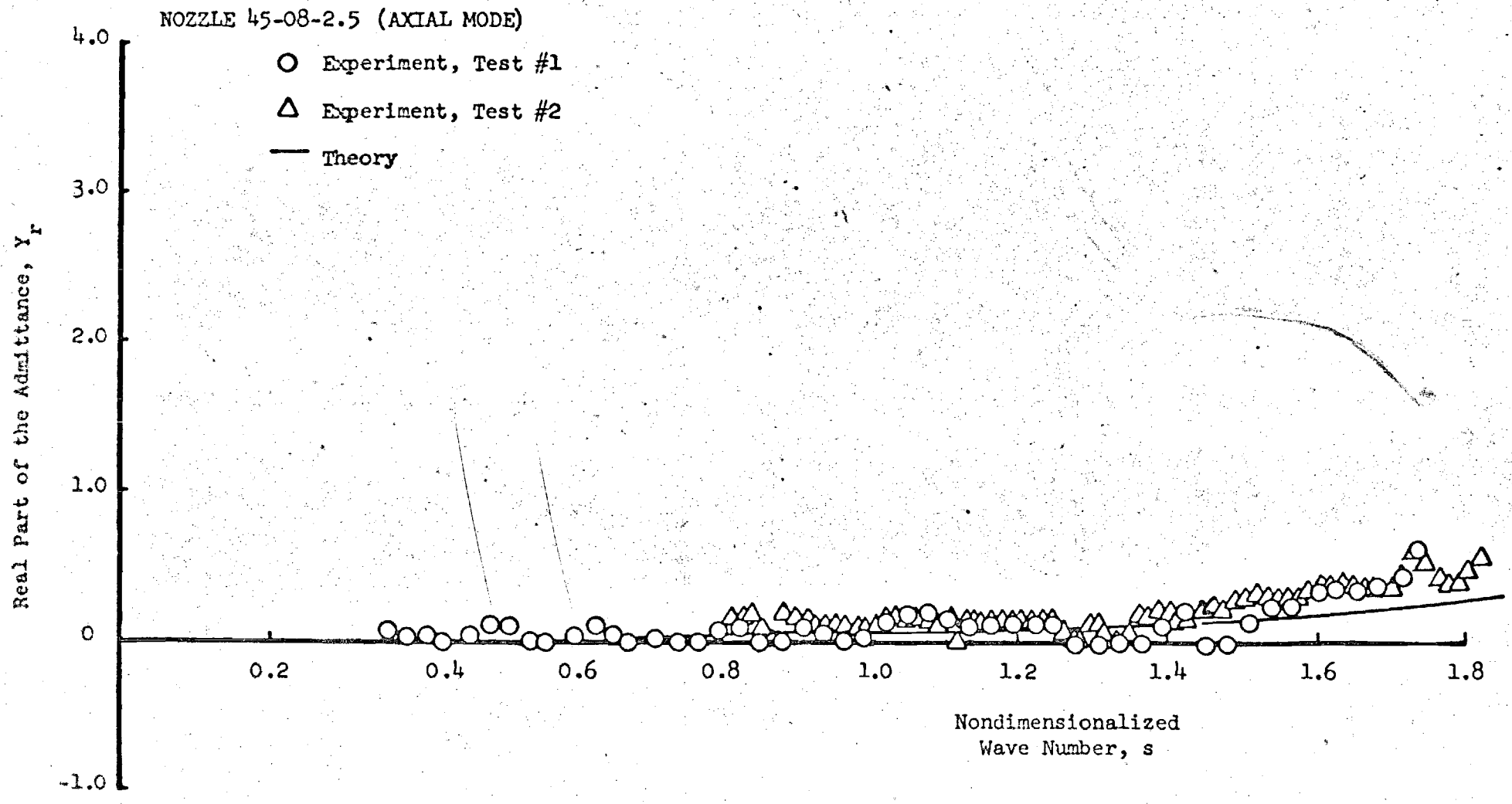

Figure 13. Comparison of the theoretical and experimental values of the real part of the admittance for a nozzle with a half-angle of 45 degrees, entrance Mach number of .08, and radii of curvature at the throat and entrance of 2.5 inches.

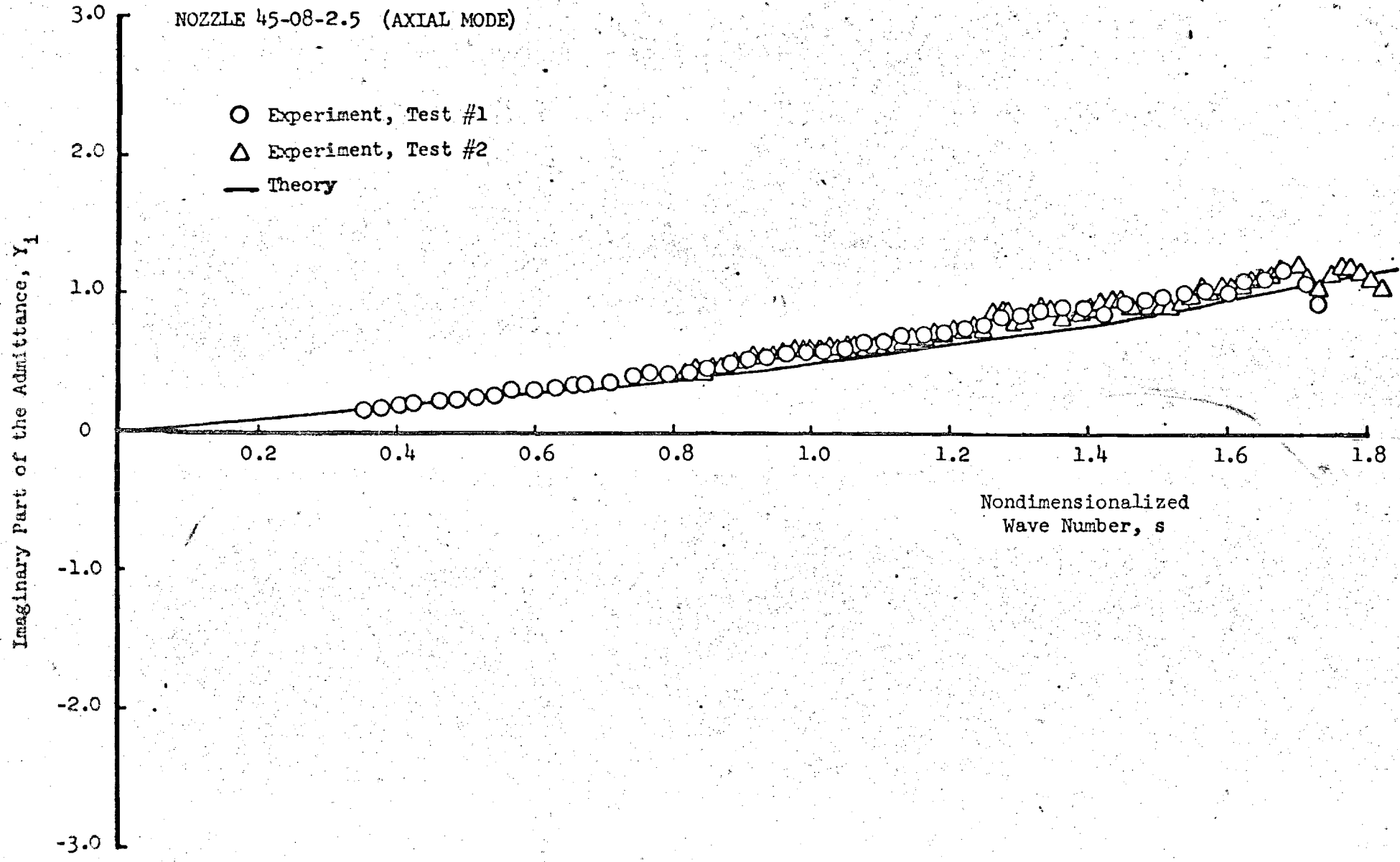

Figure 14. Comparison of the theoretical and experimental values of the imaginary part of the admittance for a nozzle with an entrance Mach number of .08, half-angle of 45 degrees, and radii of curvature at the throat and entrance of 2.5 inches.

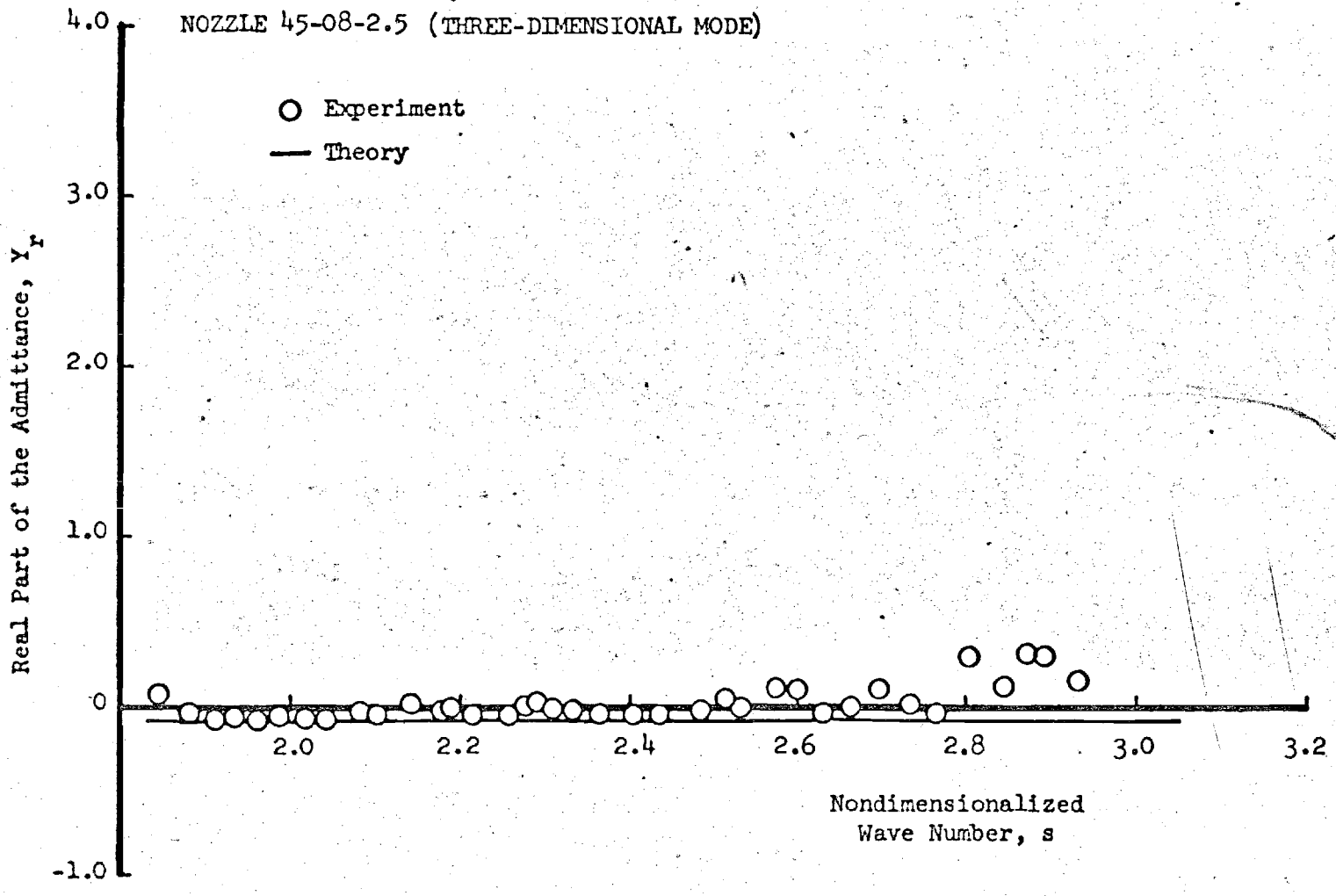

Figure 15. Comparison of the theoretical and experimental values of the real part of the admittance for a nozzle with a half-angle of 45 degrees, entrance Mach number of .08, and radii of curvature at the throat and entrance of 2.5 inches.

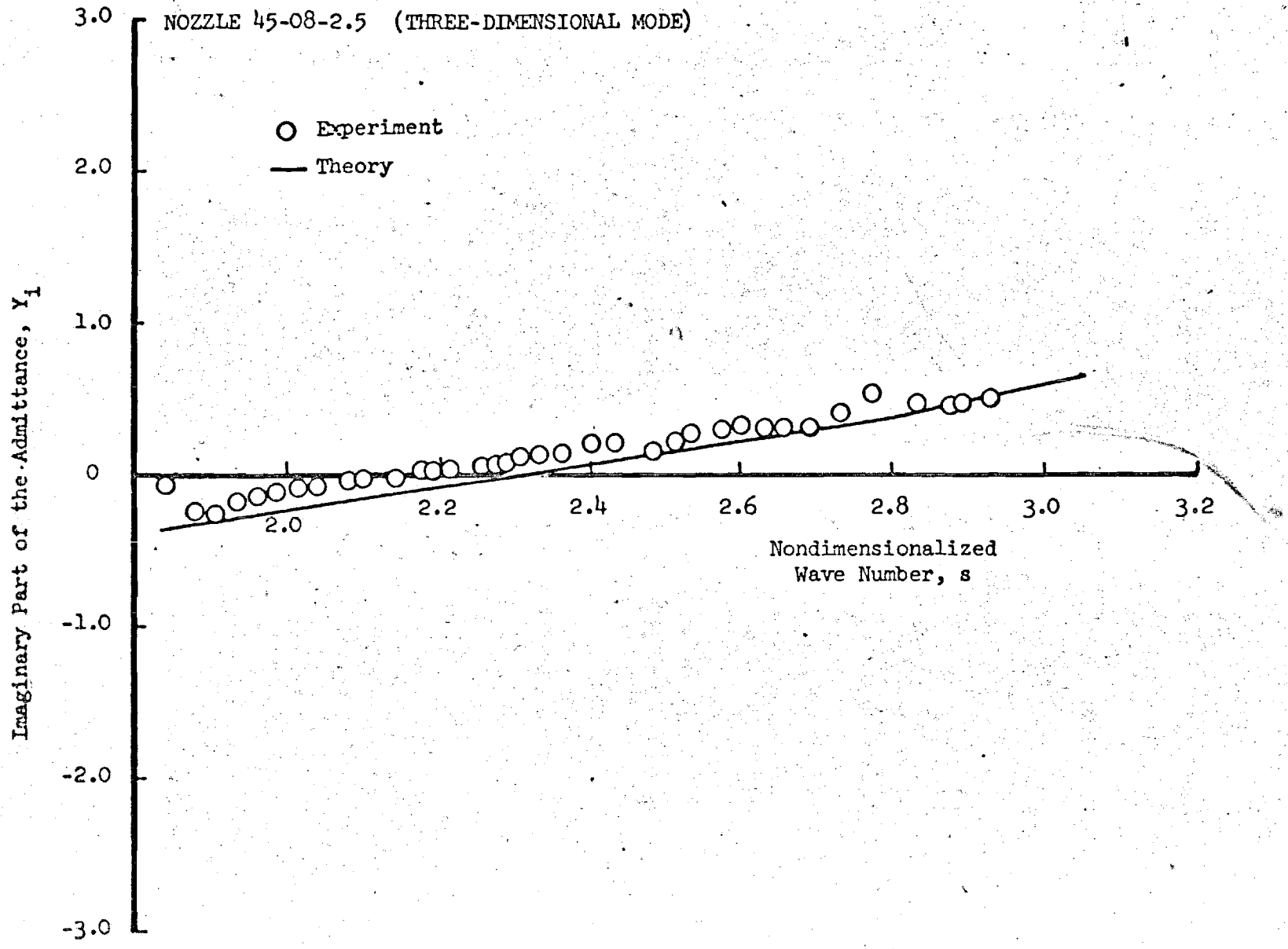

Figure 16. Comparison of the theoretical and experimental values of the imaginary part of the admittance for a nozzle with an entrance Mach number of .08, half-angle of 45 degrees, and radii of curvature at the throat and entrance of 2.5 inches.

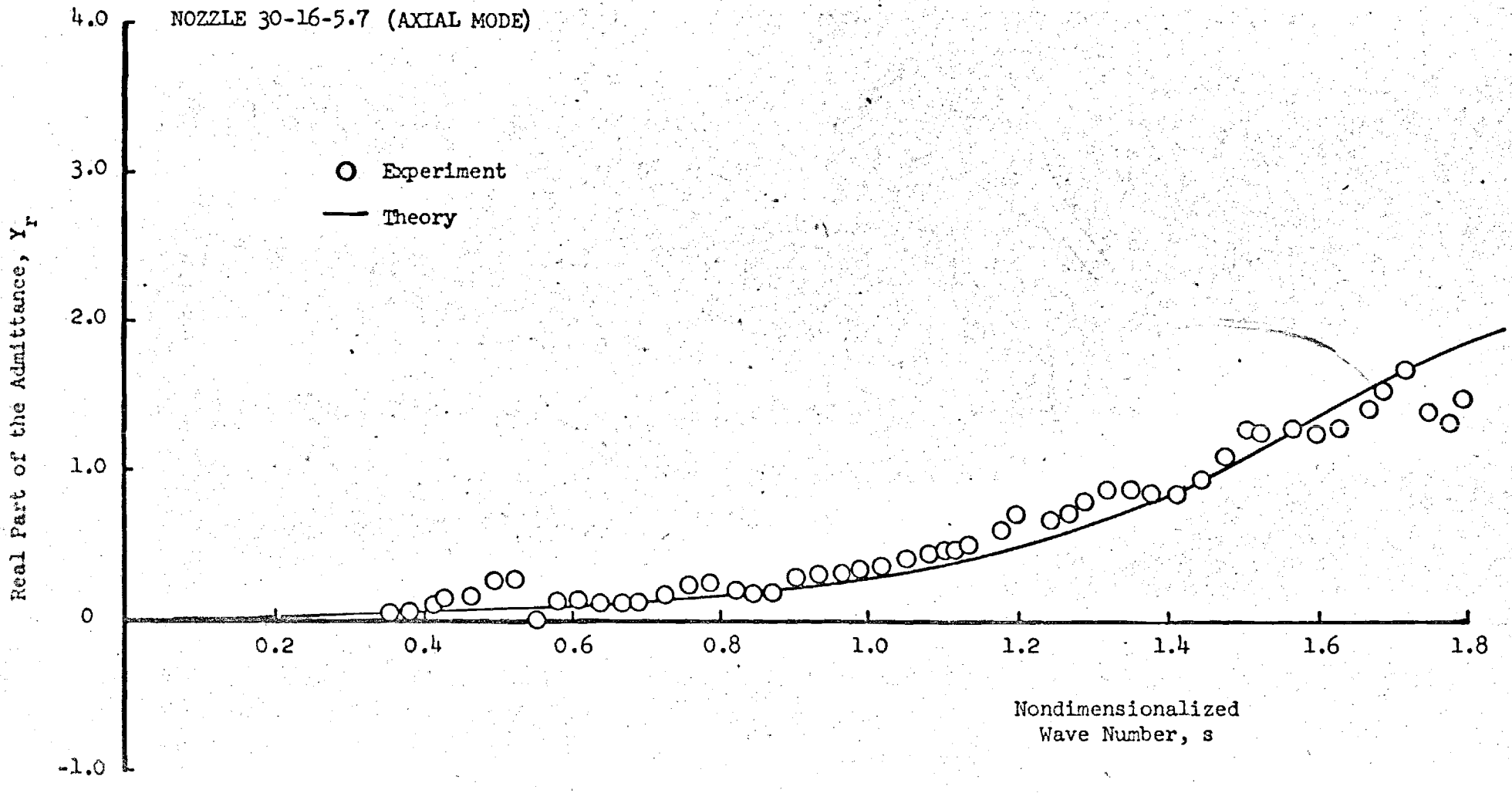

Figure 17. Comparison of the theoretical and experimental values of the real part of the admittance for a nozzle with a half-angle of 30 degrees, entrance Mach number of .16, and radii of curvature at the entrance and throat of 5.7 inches.

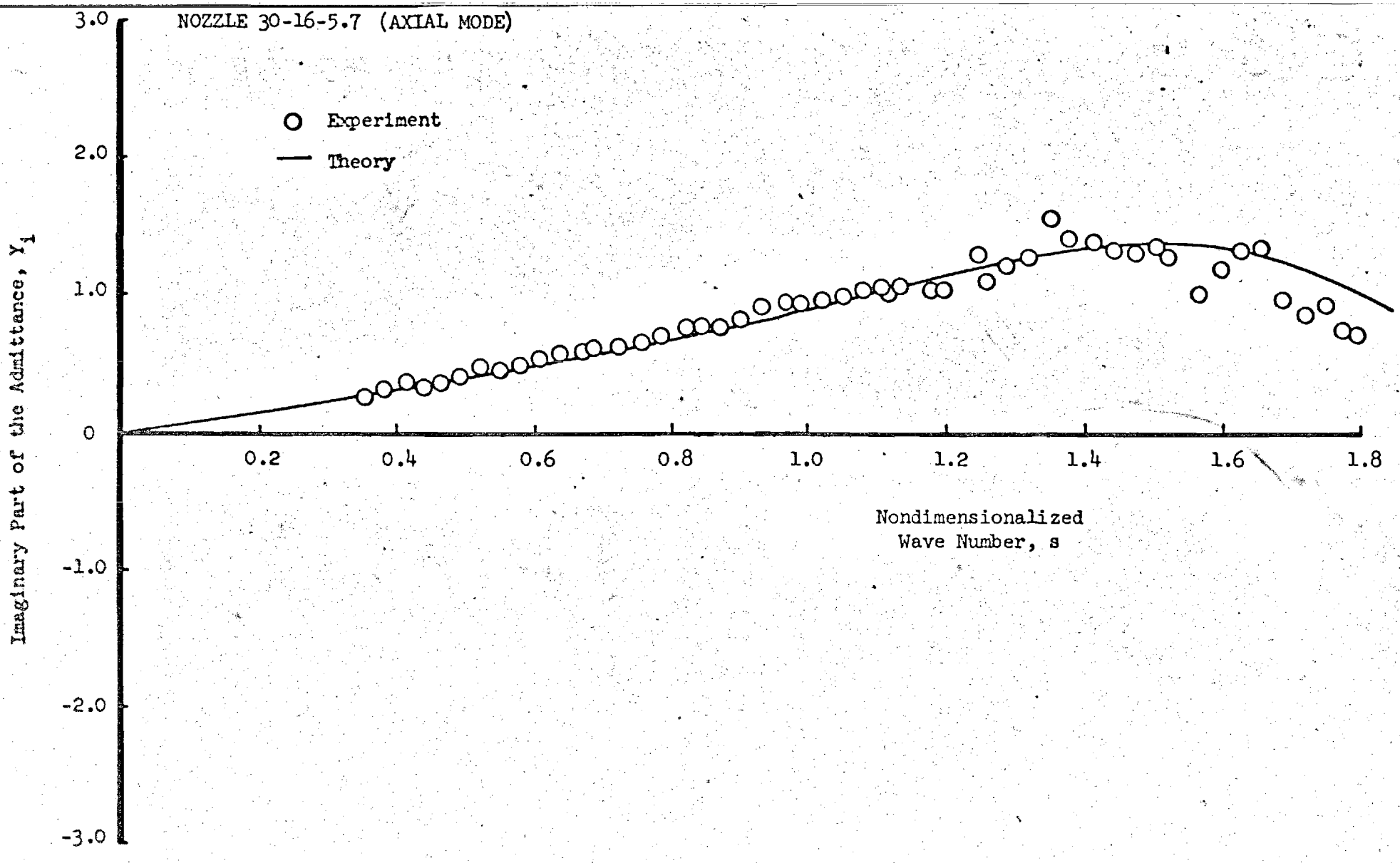

Figure 18. Comparison of the theoretical and experimental values of the imaginary part of the admittance for a nozzle with a half-angle of 30 degrees, entrance Mach number of .16, and radii of curvature at the throat and entrance of 5.7 inches.

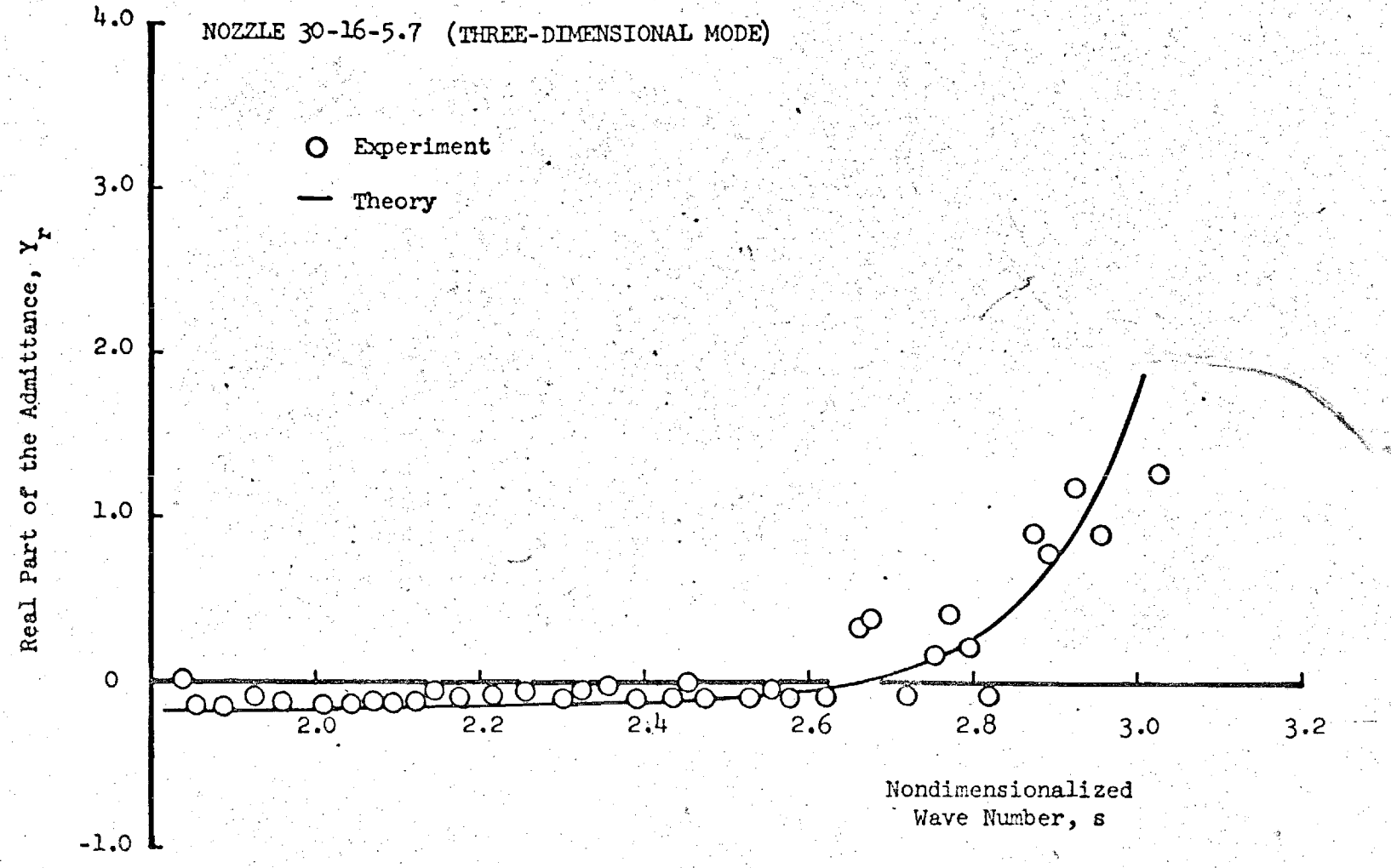

Figure 19. Comparison of the theoretical and experimental values of the real part of the admittance for a nozzle with a half-angle of 30 degrees, entrance Mach number of .16, and radii of curvature at the throat and entrance of 5.7 inches.

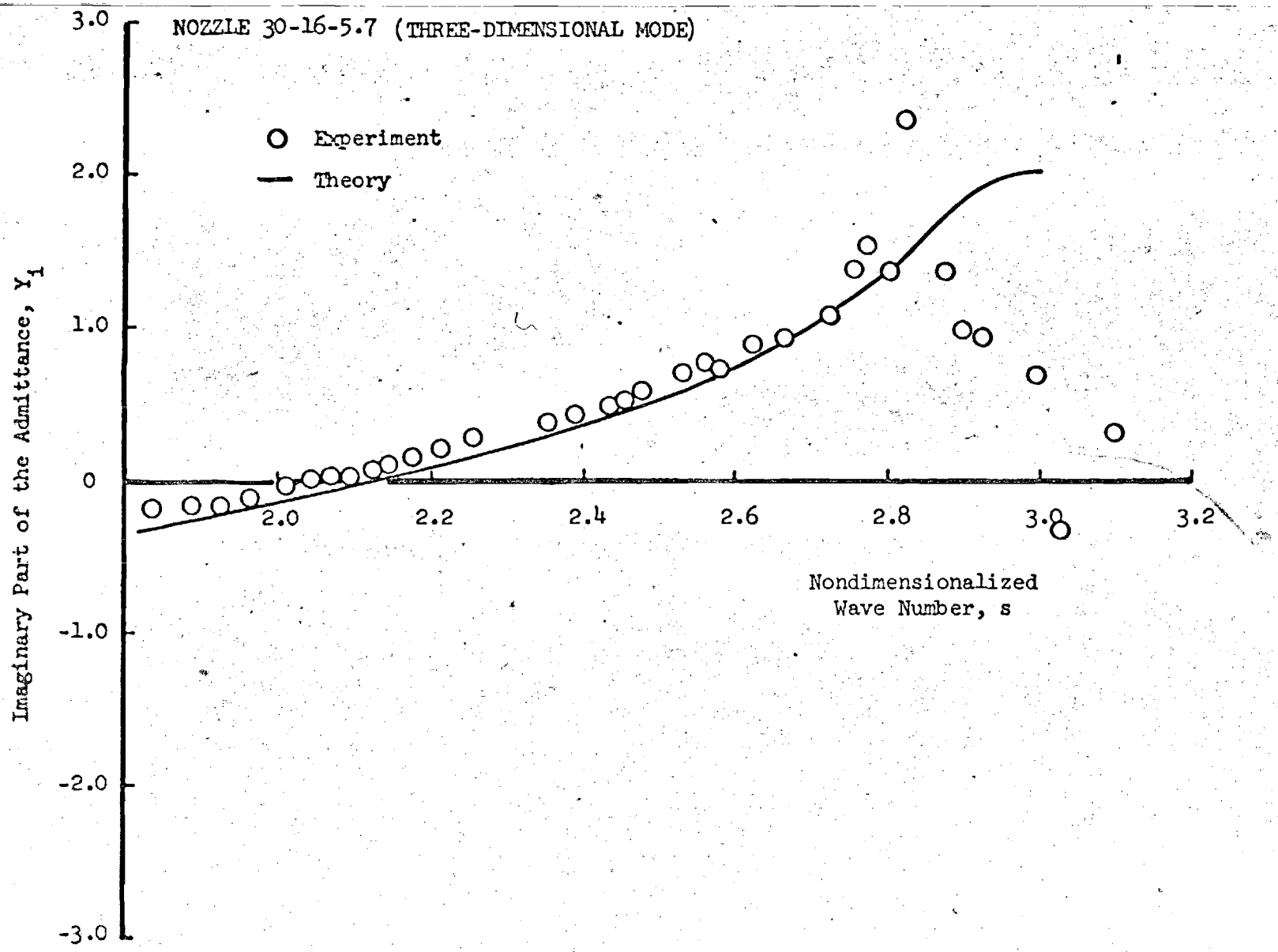

Figure 20. Comparison of the theoretical and experimental values of the imaginary part of the admittance for a nozzle with a half-angle of 30 degrees, entrance Mach number of .16, and radii of curvature at the throat and entrance of 5.7 inches.

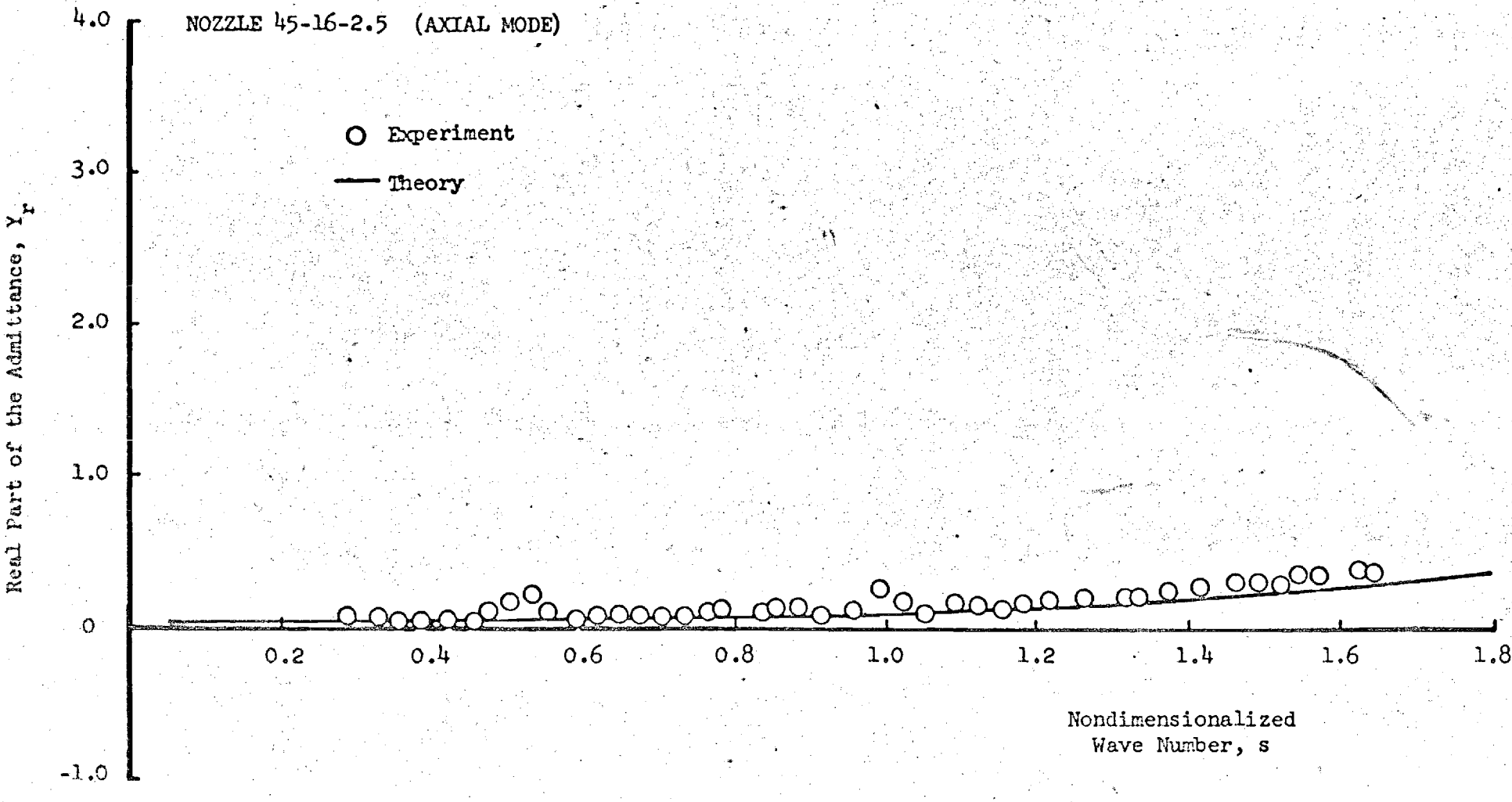

Figure 21. Comparison of the theoretical and experimental values of the real part of the admittance for a nozzle with a half-angle of 45 degrees, entrance Mach number of .16, and radii of curvature at the throat and entrance of 2.5 inches.

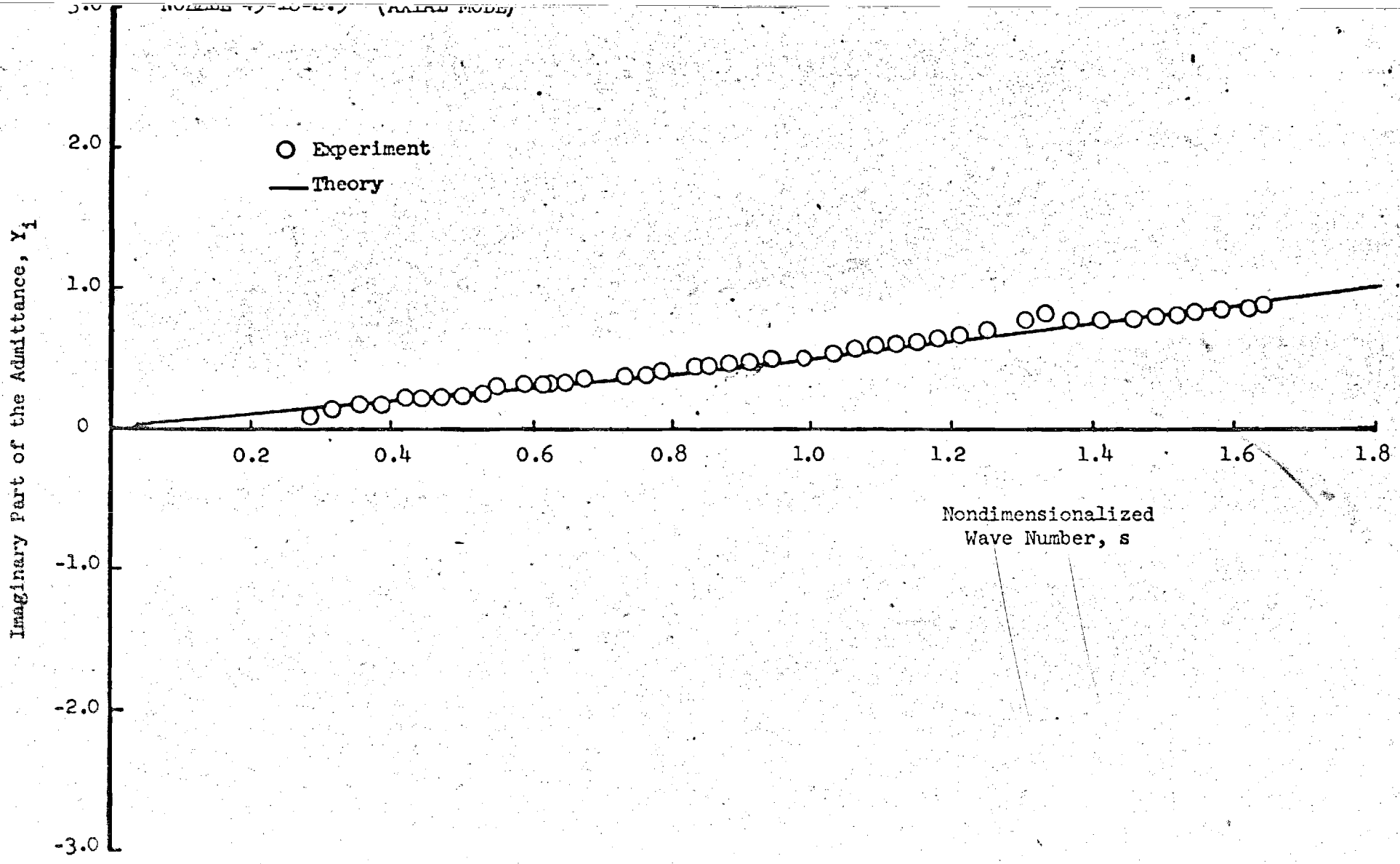

Figure 22. Comparison of the theoretical and experimental values of the imaginary part of the admittance for a nozzle with a half-angle of 45 degrees, entrance Mach number of .16, and radii of curvature at the throat and entrance of 2.5 inches.

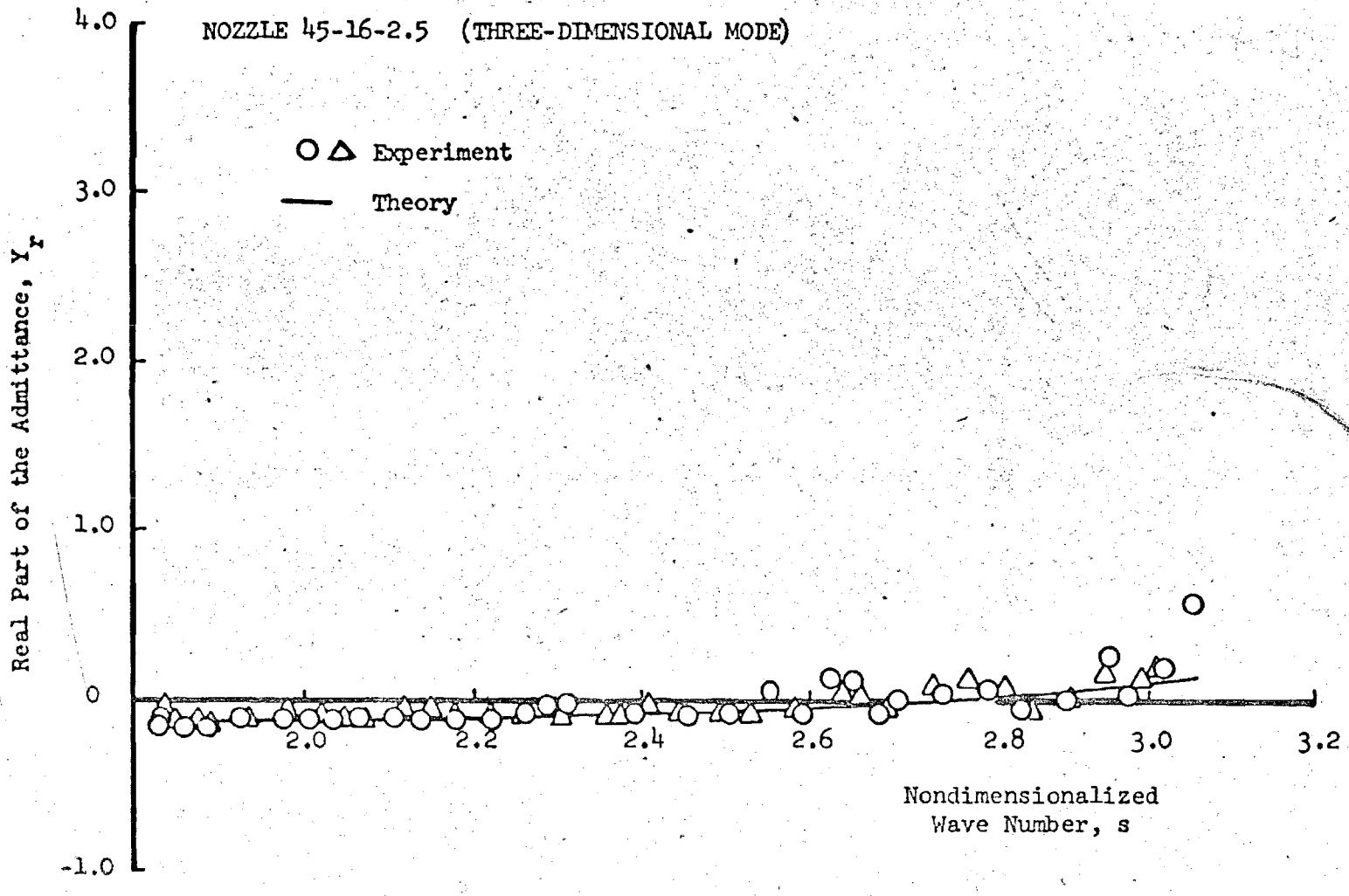

Figure 23. Comparison of the theoretical and experimental values of the real part of the nozzle admittance of a nozzle with a half-angle of 45 degrees, entrance Mach number of .16, and radii of curvature at the throat and entrance of 2.5 inches.

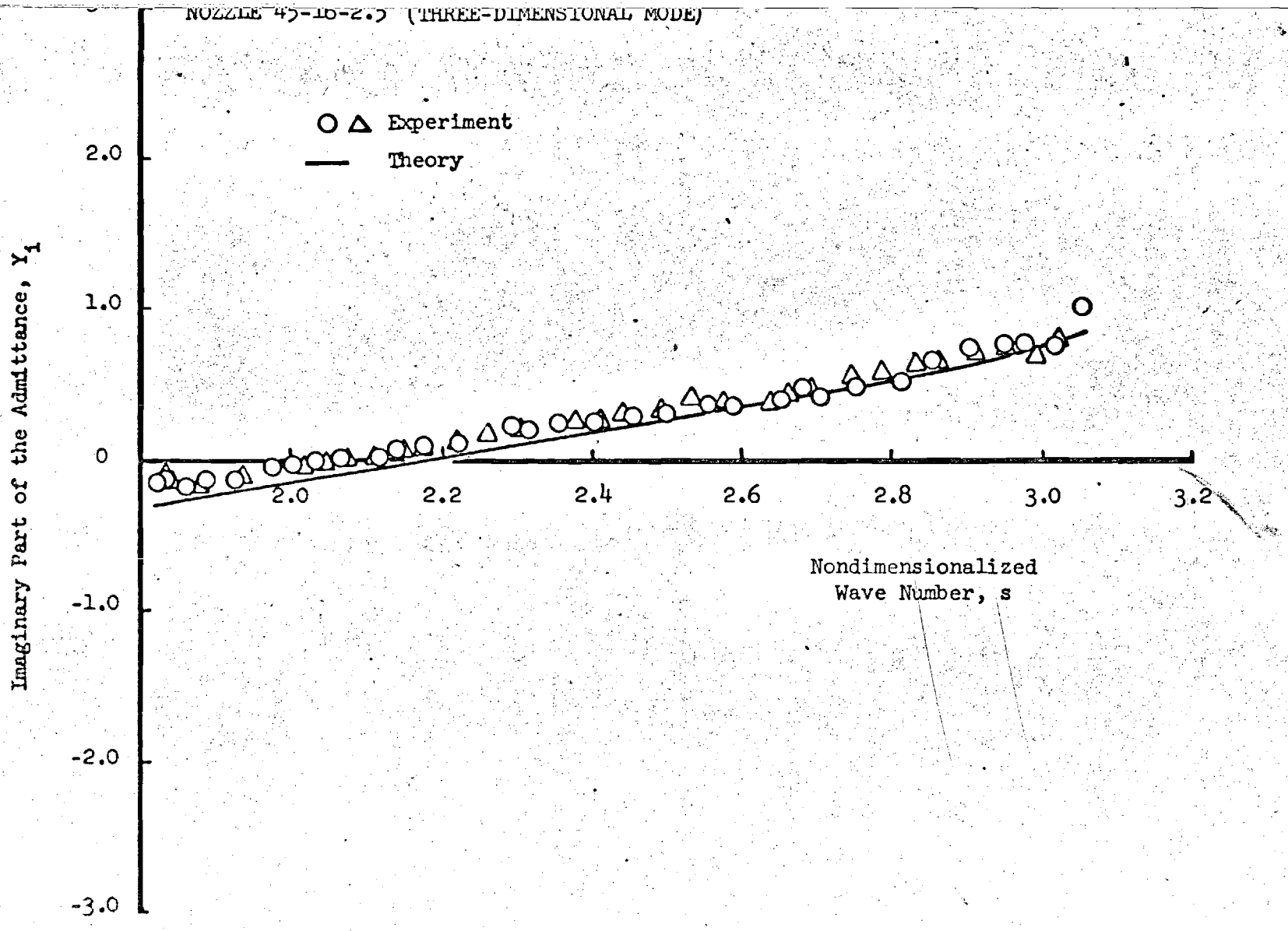

Figure 24. Comparison of the theoretical and experimental values of the imaginary part of the admittance for a nozzle with a half-angle of 45 degrees, entrance Mach number of .16, and radii of curvature at the throat and entrance of 2.5 inches.

APPENDIX A: OUTPUT OF ANALOG-TO-DIGITAL DATA REDUCTION PROGRAM

FOURIER ANALYSIS RESULTS OF A-TO-D DATA, EXAMPLE CASE, A-TO-D PROGRAM AEDPP, TEST B214-61

	HF-FREQ	HF- 8/9	HF-33/9	HF-19/9	HF-40/9	HF-FREQ	HF-35/9	HF-24/9	HF-17/9	HF- 3/9
FREQUENCY = 1000.0, HZ RUN POINT	1									
AMPLITUDE, SPL(DB) =	.99	160.00	160.00	160.00	160.00	.99	160.00	160.00	160.00	160.00
PHASE, DEGREES =	.00	231.96	237.65	175.14	234.60	3.85	258.10	274.64	219.10	331.19
FREQUENCY = 609.1, HZ RUN POINT	2									
AMPLITUDE, SPL(DB) =	1.00	124.28	124.06	100.00	100.00	1.00	128.70	127.54	120.95	134.17
PHASE, DEGREES =	.00	40.46	113.40	68.75	75.07	3.49	126.26	129.12	109.22	10.84
FREQUENCY = 616.7, HZ RUN POINT	3									
AMPLITUDE, SPL(DB) =	.99	131.64	131.62	100.00	100.00	1.00	128.95	121.00	100.00	124.08
PHASE, DEGREES =	.00	214.81	219.08	112.47	32.12	3.87	222.58	219.90	284.46	241.05
FREQUENCY = 625.0, HZ RUN POINT	4									
AMPLITUDE, SPL(DB) =	1.00	124.50	100.00	100.00	125.37	1.00	121.55	124.87	100.00	128.61
PHASE, DEGREES =	.00	275.73	344.24	348.98	37.72	3.53	42.20	332.25	110.17	345.26
FREQUENCY = 632.6, HZ RUN POINT	5									
AMPLITUDE, SPL(DB) =	1.00	130.95	130.74	100.00	130.93	1.00	132.32	129.14	100.00	129.83
PHASE, DEGREES =	.00	169.99	10.58	34.70	44.43	3.31	43.90	351.11	124.97	211.59
FREQUENCY = 640.7, HZ RUN POINT	6									
AMPLITUDE, SPL(DB) =	1.00	127.65	126.52	100.00	126.43	1.00	126.40	100.00	127.51	100.00
PHASE, DEGREES =	.00	77.37	290.09	98.95	22.82	4.14	328.85	88.34	105.09	129.33
FREQUENCY = 648.1, HZ RUN POINT	7									
AMPLITUDE, SPL(DB) =	1.00	126.70	133.30	131.73	127.71	1.01	133.67	131.78	133.90	125.91
PHASE, DEGREES =	.00	152.39	148.13	122.13	146.09	3.58	168.95	145.98	148.77	145.01
FREQUENCY = 656.1, HZ RUN POINT	8									
AMPLITUDE, SPL(DB) =	1.00	126.48	136.71	100.00	129.28	1.01	136.17	137.05	100.00	100.00
PHASE, DEGREES =	.00	313.62	155.64	148.80	140.76	3.78	172.20	163.44	147.18	60.74
FREQUENCY = 663.5, HZ RUN POINT	9									
AMPLITUDE, SPL(DB) =	.99	127.78	137.25	135.89	136.58	.99	139.04	136.57	134.75	132.10
PHASE, DEGREES =	.00	335.97	194.30	215.74	194.43	4.10	208.94	218.60	236.64	351.91
FREQUENCY = 671.5, HZ RUN POINT	10									
AMPLITUDE, SPL(DB) =	1.00	133.74	139.31	140.34	136.02	1.00	139.34	139.58	141.89	126.07
PHASE, DEGREES =	.00	329.99	.20	332.77	27.04	3.89	24.74	351.38	8.24	315.21
FREQUENCY = 678.9, HZ RUN POINT	11									
AMPLITUDE, SPL(DB) =	1.00	160.45	165.06	163.36	162.99	1.00	165.66	164.15	163.20	157.92
PHASE, DEGREES =	.00	112.69	146.70	129.51	155.57	4.04	162.80	154.56	147.79	127.85
FREQUENCY = 687.1, HZ RUN POINT	12									
AMPLITUDE, SPL(DB) =	1.00	170.14	165.44	170.65	156.13	1.00	164.52	159.48	171.00	167.93
PHASE, DEGREES =	.00	339.97	23.78	358.56	47.53	4.17	42.59	23.63	15.31	358.25
FREQUENCY = 693.7, HZ RUN POINT	13									
AMPLITUDE, SPL(DB) =	1.00	168.98	156.54	165.21	162.84	1.01	160.64	160.82	167.54	167.56
PHASE, DEGREES =	.00	142.51	9.61	163.94	22.14	3.91	26.64	189.71	180.59	160.03

FOURIER ANALYSIS RESULTS OF A-TO-D DATA, EXAMPLE CASE, A-TO-D PROGRAM AEDPP, TEST B214-61

	HF-FREQ	HF- 8/9	HF-33/9	HF-19/9	HF-40/9	HF_FREQ	HF-35/9	HF-24/9	HF-17/9	HF- 3/9
FREQUENCY = 702.2, HZ RUN POINT	14									
AMPLITUDE, SPL(DB) =	1.00	166.89	164.58	158.70	164.38	1.00	166.12	144.38	162.48	165.30
PHASE, DEGREES =	.00	247.01	114.03	268.96	127.34	4.18	132.66	113.87	286.21	264.29
FREQUENCY = 710.0, HZ RUN POINT	15									
AMPLITUDE, SPL(DB) =	.99	166.77	167.29	100.00	162.97	.98	167.71	161.24	159.81	167.14
PHASE, DEGREES =	.00	346.07	210.84	23.43	221.65	4.32	228.08	214.83	25.51	5.35
FREQUENCY = 717.1, HZ RUN POINT	16									
AMPLITUDE, SPL(DB) =	1.00	164.80	165.49	155.52	153.79	1.00	164.64	164.26	145.99	166.29
PHASE, DEGREES =	.00	93.90	314.06	286.70	321.98	4.13	330.89	317.99	299.78	112.87
FREQUENCY = 725.0, HZ RUN POINT	17									
AMPLITUDE, SPL(DB) =	1.03	163.96	163.31	162.83	148.44	1.04	160.12	156.94	158.73	166.54
PHASE, DEGREES =	.00	161.69	21.01	358.10	234.95	4.56	39.72	24.19	18.66	181.24
FREQUENCY = 732.8, HZ RUN POINT	18									
AMPLITUDE, SPL(DB) =	1.00	161.49	153.80	164.63	158.91	1.00	100.00	166.32	162.29	165.03
PHASE, DEGREES =	.00	269.56	129.77	110.25	326.39	4.06	320.01	134.59	129.90	289.82
FREQUENCY = 740.6, HZ RUN POINT	19									
AMPLITUDE, SPL(DB) =	1.00	155.64	147.30	163.01	159.60	1.00	155.71	162.75	161.81	162.90
PHASE, DEGREES =	.00	315.78	2.56	154.99	12.56	4.51	16.86	180.35	173.79	335.23
FREQUENCY = 749.3, HZ RUN POINT	20									
AMPLITUDE, SPL(DB) =	1.03	157.17	161.87	158.55	165.46	1.02	165.84	165.30	167.92	167.56
PHASE, DEGREES =	.00	29.04	67.07	223.08	79.25	4.74	84.94	248.62	242.19	44.45
FREQUENCY = 756.2, HZ RUN POINT	21									
AMPLITUDE, SPL(DB) =	.94	144.67	160.34	163.24	158.96	.95	162.46	159.10	163.26	160.93
PHASE, DEGREES =	.00	129.41	152.72	307.72	168.08	3.91	171.98	335.57	326.33	129.67
FREQUENCY = 764.2, HZ RUN POINT	22									
AMPLITUDE, SPL(DB) =	.98	132.57	161.32	162.31	156.31	.99	162.54	154.11	162.94	160.00
PHASE, DEGREES =	.00	168.88	180.35	336.29	195.95	4.38	199.66	7.79	354.93	155.84
FREQUENCY = 771.8, HZ RUN POINT	23									
AMPLITUDE, SPL(DB) =	1.00	151.17	168.59	167.97	156.48	1.00	168.60	150.26	169.35	166.12
PHASE, DEGREES =	.00	25.27	256.49	52.90	271.98	4.71	276.67	91.85	71.84	233.22
FREQUENCY = 781.1, HZ RUN POINT	24									
AMPLITUDE, SPL(DB) =	1.00	150.16	159.85	158.43	100.00	1.00	158.35	139.08	160.83	156.22
PHASE, DEGREES =	.00	105.23	335.38	130.55	110.83	4.54	357.19	330.61	149.97	314.62
FREQUENCY = 787.6, HZ RUN POINT	25									
AMPLITUDE, SPL(DB) =	1.00	152.09	157.84	155.85	147.96	1.00	154.10	148.90	159.55	153.80
PHASE, DEGREES =	.00	133.04	358.39	154.86	185.94	5.22	19.77	356.30	173.88	331.13
FREQUENCY = 794.4, HZ RUN POINT	26									
AMPLITUDE, SPL(DB) =	1.00	160.40	162.23	158.91	159.99	1.00	154.95	161.12	164.29	167.13
PHASE, DEGREES =	.00	168.49	42.55	201.07	237.97	5.21	67.06	44.59	219.78	21.42

FOURIER ANALYSIS RESULTS OF A-TO-D DATA, EXAMPLE CASE, A-TO-D PROGRAM AEDPP, TEST B214-61

	HF-FREQ	HF- 8/9	HF-33/9	HF-19/9	HF-40/9	HF-FREQ	HF-35/9	HF-24/9	HF-17/9	HF- 3/9
FREQUENCY = 802.3, HZ RUN POINT 27										
AMPLITUDE, SPL(DB) =	1.00	156.91	153.10	148.02	157.03	1.00	132.48	158.38	157.58	153.65
PHASE, DEGREES =	.00	280.97	158.65	322.62	349.04	5.00	277.32	153.33	333.14	130.55
FREQUENCY = 810.3, HZ RUN POINT 28										
AMPLITUDE, SPL(DB) =	1.00	153.96	139.97	135.82	153.91	1.00	145.66	155.71	150.97	147.39
PHASE, DEGREES =	.00	305.79	186.16	53.53	9.97	5.18	9.24	172.78	358.81	150.98
FREQUENCY = 817.8, HZ RUN POINT 29										
AMPLITUDE, SPL(DB) =	.96	156.23	142.27	142.73	156.50	.95	154.31	158.95	150.61	150.01
PHASE, DEGREES =	.00	316.90	12.08	132.90	28.98	4.72	32.39	191.58	16.84	173.99
FREQUENCY = 825.0, HZ RUN POINT 30										
AMPLITUDE, SPL(DB) =	1.00	165.46	158.44	156.94	162.79	1.00	164.80	166.61	150.47	153.25
PHASE, DEGREES =	.00	68.84	114.93	266.91	136.93	4.72	138.08	304.68	137.53	289.89
FREQUENCY = 834.3, HZ RUN POINT 31										
AMPLITUDE, SPL(DB) =	1.00	155.78	152.29	149.50	150.45	1.00	155.85	155.79	121.20	142.29
PHASE, DEGREES =	.00	113.12	167.51	320.02	191.14	5.01	189.75	350.73	101.82	324.55
FREQUENCY = 840.5, HZ RUN POINT 32										
AMPLITUDE, SPL(DB) =	1.00	154.42	152.61	150.54	143.94	1.00	155.09	153.51	141.04	135.43
PHASE, DEGREES =	.00	125.33	178.52	325.30	205.05	5.01	200.89	3.10	330.09	29.77
FREQUENCY = 849.5, HZ RUN POINT 33										
AMPLITUDE, SPL(DB) =	1.02	159.43	158.88	157.57	139.39	1.01	159.79	158.29	152.02	131.96
PHASE, DEGREES =	.00	145.37	195.77	352.17	209.87	4.76	216.60	24.52	14.52	79.95
FREQUENCY = 855.9, HZ RUN POINT 34										
AMPLITUDE, SPL(DB) =	.97	163.06	162.25	161.33	140.38	.98	162.00	160.40	156.86	142.65
PHASE, DEGREES =	.00	276.48	328.64	120.88	139.08	5.33	350.82	155.08	138.01	275.17
FREQUENCY = 863.3, HZ RUN POINT 35										
AMPLITUDE, SPL(DB) =	.99	153.45	152.54	153.13	143.47	1.00	150.04	148.54	150.62	139.13
PHASE, DEGREES =	.00	298.85	351.66	143.43	186.54	5.05	15.38	182.71	164.33	310.48
FREQUENCY = 872.6, HZ RUN POINT 36										
AMPLITUDE, SPL(DB) =	1.00	152.16	151.35	152.32	143.86	1.00	147.97	145.37	150.48	139.02
PHASE, DEGREES =	.00	311.94	1.58	147.31	199.51	4.74	26.45	178.87	166.60	328.33
FREQUENCY = 880.6, HZ RUN POINT 37										
AMPLITUDE, SPL(DB) =	1.00	157.07	154.24	157.24	152.34	1.00	146.73	143.10	156.22	145.94
PHASE, DEGREES =	.00	327.00	22.08	170.18	209.98	5.17	54.72	207.90	191.65	337.73
FREQUENCY = 888.0, HZ RUN POINT 38										
AMPLITUDE, SPL(DB) =	1.00	162.20	157.24	161.48	158.03	1.00	144.51	139.15	160.81	151.65
PHASE, DEGREES =	.00	100.64	152.76	302.88	343.26	5.66	206.71	34.42	322.89	113.56
FREQUENCY = 894.9, HZ RUN POINT 39										
AMPLITUDE, SPL(DB) =	1.01	149.54	143.34	151.72	146.86	1.00	131.33	100.00	151.75	140.72
PHASE, DEGREES =	.00	115.07	184.35	327.80	6.82	5.39	322.74	108.65	351.72	130.83

FOURIER ANALYSIS RESULTS OF A-TO-D DATA, EXAMPLE CASE, A-TO-D PROGRAM AEDPP, TEST B214-61

	HF-FREQ	HF- 8/9	HF-33/9	HF-19/9	HF-40/9	HF-FREQ	HF-35/9	HF-24/9	HF-17/9	HF- 3/9
FREQUENCY = 902.5, HZ RUN POINT 40										
AMPLITUDE, SPL(DB) =	1.00	149.12	135.34	148.52	145.45	1.01	139.34	138.70	149.94	143.00
PHASE, DEGREES =	.00	126.25	182.56	331.28	24.99	5.42	31.89	181.61	356.18	146.66
FREQUENCY = 910.6, HZ RUN POINT 41										
AMPLITUDE, SPL(DB) =	1.00	150.80	124.97	149.20	147.11	1.00	146.48	145.45	151.85	146.53
PHASE, DEGREES =	.00	138.34	322.86	340.02	30.15	5.44	32.56	187.59	1.24	144.91
FREQUENCY = 918.4, HZ RUN POINT 42										
AMPLITUDE, SPL(DB) =	1.00	161.79	150.82	160.21	155.73	1.00	160.11	158.66	163.22	157.15
PHASE, DEGREES =	.00	219.19	78.83	63.84	110.87	5.32	110.54	271.72	84.67	236.62
FREQUENCY = 925.3, HZ RUN POINT 43										
AMPLITUDE, SPL(DB) =	1.01	149.67	144.79	145.42	139.42	1.02	149.72	147.37	150.57	145.17
PHASE, DEGREES =	.00	293.80	155.11	148.26	205.18	5.10	186.15	349.09	171.93	322.58
FREQUENCY = 933.6, HZ RUN POINT 44										
AMPLITUDE, SPL(DB) =	.99	141.46	141.08	138.57	128.39	.97	144.47	140.37	144.43	140.78
PHASE, DEGREES =	.00	318.28	176.93	148.64	202.15	5.95	198.99	353.48	169.60	339.43
FREQUENCY = 940.5, HZ RUN POINT 45										
AMPLITUDE, SPL(DB) =	.99	142.10	145.35	136.85	100.00	.98	147.26	145.25	144.27	142.61
PHASE, DEGREES =	.00	307.39	172.58	189.55	218.52	5.81	199.69	2.97	190.17	330.78
FREQUENCY = 948.1, HZ RUN POINT 46										
AMPLITUDE, SPL(DB) =	.99	147.86	151.80	137.21	140.47	.99	152.58	152.61	151.25	150.35
PHASE, DEGREES =	.00	329.72	198.08	172.20	31.40	5.84	224.96	34.39	203.70	349.27
FREQUENCY = 956.0, HZ RUN POINT 47										
AMPLITUDE, SPL(DB) =	1.00	143.95	148.37	100.00	142.74	1.00	146.44	148.81	147.89	148.84
PHASE, DEGREES =	.00	111.24	344.70	289.09	173.55	5.31	13.60	161.83	327.65	132.38
FREQUENCY = 964.0, HZ RUN POINT 48										
AMPLITUDE, SPL(DB) =	1.00	137.40	138.17	100.00	135.78	1.00	133.19	139.99	137.65	143.17
PHASE, DEGREES =	.00	112.95	343.26	99.66	160.56	6.17	35.63	174.28	345.97	136.05
FREQUENCY = 970.3, HZ RUN POINT 49										
AMPLITUDE, SPL(DB) =	1.01	135.51	133.99	100.00	137.13	1.01	128.61	138.43	138.50	141.13
PHASE, DEGREES =	.00	139.95	350.04	222.83	176.14	6.01	56.60	185.26	332.44	129.99
FREQUENCY = 977.7, HZ RUN POINT 50										
AMPLITUDE, SPL(DB) =	1.00	122.87	143.37	135.27	138.81	1.01	136.36	135.67	130.34	142.91
PHASE, DEGREES =	.00	197.21	20.54	141.02	200.57	6.15	62.80	171.73	345.67	140.55
FREQUENCY = 986.1, HZ RUN POINT 51										
AMPLITUDE, SPL(DB) =	.96	140.59	149.42	149.10	149.77	.97	133.92	150.46	135.54	153.27
PHASE, DEGREES =	.00	175.03	71.94	209.03	266.90	6.00	136.78	249.51	80.87	209.49

DATA REDUCTION FINISHED, EXAMPLE CASE, A-TO-D PROGRAM AEDPP, TEST B214-61

EXAMPLE CASE, A-TO-D PROGRAM AEDPP, TEST 8214-61 MACH NUMBER = .080, SVN = 1.841

RUN POINT	FREQ HZ	S	ANGLES ALPHA	ANGLES BETA	ADMITTANCES RE(Y/YS)	ADMITTANCES IM(Y/YS)	YS	ERROR PRMS	PRESSURE DIFFERENCES, DP 1	2	3	4	5	6	7	8	COMBINATIONS
11	678.9	1.8485	.1133	.0396	.3892	.0938	.1565	.241	.3	-.2	-.2	.0	.4	-.3	.1	-.1	35
12	687.1	1.8715	.1288	.1515	.3059	.2071	.1566	.210	.2	-.2	.0	.0	.2	-.2	.2	-.3	35
13	693.7	1.8902	.0000	.2113	.0755	.3037	.1565	.410	.5	-.3	.0	.0	-.2	-.7	.3	.4	35
14	702.2	1.9142	.0121	.2473	.0953	.2864	.1565	.265	.1	-.4	-.3	.0	.1	.0	.4	.1	35
15	710.0	1.9362	.0000	.2999	.0719	.2458	.1564	.193	-.1	-.1	.0	.0	.4	-.1	-.1	-.1	20
16	717.1	1.9561	.0274	.3186	.1120	.2180	.1564	.134	-.2	-.1	-.1	.0	.2	.2	.0	.0	35
17	725.0	1.9782	.0594	.3571	.1526	.1713	.1563	.259	-.3	.1	.2	.0	.2	.3	-.2	-.3	35
18	732.3	1.9999	.0246	.3964	.1014	.1325	.1563	.035	.1	-.0	.0	.0	.0	-.0	.0	-.0	20
19	740.6	2.0213	.0000	.4149	.0660	.1143	.1562	.390	-.5	-.1	.3	.0	-.6	.0	.6	.2	35
20	749.3	2.0461	.0000	.4330	.0644	.0939	.1562	.479	-.5	-.9	.4	.0	-.1	.3	.5	.3	35
21	756.2	2.0655	.0000	.4671	.0633	.0474	.1562	.383	-.1	-.7	.4	.0	-.1	.3	.5	-.3	35
22	764.2	2.0876	.0000	.4714	.0619	.0427	.1561	.459	-.1	-.7	.2	.0	-.0	.7	.4	-.5	35
23	771.3	2.1092	.0219	.4927	.0944	.0112	.1561	.273	.0	-.5	.2	.0	.1	-.0	.4	-.2	35
24	781.1	2.1353	.0000	.4872	.0592	.0205	.1560	2.274	4.6	-.5	.3	.0	-.2	-3.4	.7	-1.5	35
25	787.6	2.1535	.0453	-.4839	.1319	-.0259	.1560	1.438	1.9	-.0	.9	.0	-.3	-2.3	1.4	-1.7	35
26	794.4	2.1724	.0359	-.4530	.1183	-.0782	.1560	.537	.5	-.0	.4	.0	-.1	-.7	.6	-.7	35
27	802.3	2.1945	.0000	-.4045	.0561	-.0962	.1559	.632	1.0	.3	-.3	.0	-.1	-.3	.5	-1.1	35
28	810.3	2.2171	.0217	-.4334	.0944	-.1090	.1559	1.072	1.6	.4	-.1	.0	-1.0	.4	.6	-1.9	35
29	817.8	2.2381	.0283	-.4275	.1072	-.1310	.1559	.639	.3	-1.1	.8	.0	.1	.2	.5	-.8	35
30	825.0	2.2583	.0303	-.3904	.1150	-.2059	.1558	.753	1.1	-1.0	-.2	.0	.4	.3	.5	-1.1	35
31	834.3	2.2842	.0000	-.3921	.0518	-.2090	.1558	.489	1.1	-.4	-.3	.0	.2	-.4	-.0	-.3	35
32	840.5	2.3014	.0232	-.3641	.1037	-.2715	.1558	.426	.7	-.4	-.2	.0	.5	-.6	-.0	.0	35
33	849.5	2.3264	.0129	-.3402	.0818	-.3394	.1557	.291	.0	-.5	-.2	.0	.3	.2	.2	-.0	35
34	855.9	2.3447	.0290	-.3379	.1229	-.3423	.1557	.303	.5	-.6	-.2	.0	.0	.2	.1	-.0	35
35	863.3	2.3654	.0198	-.2985	.1092	-.4583	.1557	.439	-.0	-.7	.1	.0	-.5	.6	.6	-.1	35
36	872.6	2.3914	.0457	-.3167	.1756	-.4028	.1556	.333	-.4	-.4	-.1	.0	.3	.0	.6	-.1	35
37	880.5	2.4135	.0355	-.2838	.1640	-.5118	.1556	.206	-.2	-.3	-.0	.0	.5	-.3	.3	.0	35
38	888.0	2.4346	.0000	-.2981	.0456	-.4815	.1556	1.140	.0	-.8	-.7	.0	2.2	-1.3	-.4	1.0	35
39	894.8	2.4535	.0000	-.2906	.0449	-.5109	.1555	.915	-1.3	-.8	.9	.0	-.2	.0	1.4	-.0	20
40	902.5	2.4753	.0000	-.2679	.0441	-.5972	.1555	.905	.0	-.1	-.3	.0	-1.7	-.1	.6	1.5	35
41	910.6	2.4979	.0000	-.2538	.0433	-.6599	.1555	.800	-.1	-.2	-1.0	.0	-.8	.3	.2	1.5	35
42	918.4	2.5199	.0000	-.2481	.0426	-.6912	.1554	.314	-.0	-.2	-.3	.0	-.4	.2	.4	.4	35
43	925.3	2.5391	.0000	-.2139	.0419	-.8658	.1554	.617	1.0	.2	-.9	.0	.0	-.9	.5	.1	35
44	933.6	2.5624	.0670	-.2160	.3845	-.7742	.1554	1.051	-.1	.3	-.3	.0	.6	-2.3	1.1	.7	35
45	940.5	2.5820	.0000	-.1811	.0406	-1.0964	.1554	.634	-.5	.6	.1	.0	1.2	-.5	-.3	-.6	35
46	948.1	2.6033	.0000	-.1603	.0399	-1.2834	.1553	.520	-.3	-.6	-.2	.0	.3	-.2	1.1	-.2	35
47	956.0	2.6254	.2251	-.0779	1.1036	-.2586	.1553	1.059	-1.3	-.5	.0	.0	-.8	.1	2.0	.4	20
48	964.0	2.6480	.6960	.1382	.8883	1.0130	.1553	1.067	-.4	-1.3	.0	.0	-.7	1.7	1.2	-.5	20
49	970.3	2.6655	.0002	.1260	.0404	1.7295	.1553	2.657	-.3	-2.7	.0	.0	-2.2	3.1	4.0	-2.2	20
50	977.7	2.6863	.0000	-.0853	.0375	-2.6523	.1552	3.775	-5.5	2.7	-.5	.0	5.9	-4.9	1.2	1.0	35
51	986.1	2.7100	.0267	-.0873	.8531	-2.3480	.1552	1.056	2.1	-1.0	.5	.0	.0	-.2	-1.5	.1	35
									.1	-.3	-.0	.0	.1	-.2	.5	-.1	

NORMAL EXIT. EXECUTION TIME: 28933 MILLISECONDS.

@FIN

RUNID: 0188 REF. NO: 51E16617 NAME: SMITH-A-J

LOAD 0399N 472 A-D -1 0188

1-0188*MSG: PLEASE ANSWER G TO ALL TAPE ERRORS

1

TIME: 00:00:28.946 IN: 27 OUT: 0 PAGES: 8

INITIATION TIME: 10:08:46-DEC 3,1971

TERMINATION TIME: 10:13:15-DEC 3,1971

0188 FIN 28.946 8 0

E-16-607

NASA GRANT NGL 11-002-085

BEHAVIOR OF NOZZLES AND ACOUSTIC LINERS IN THREE-DIMENSIONAL ACOUSTIC FIELDS

Progress Report for Period December 1, 1971 to May 31, 1972

Prepared by: Ben T. Zinn, Principal Investigator
W. A. Bell, Graduate Research Assistant
B. R. Daniel, Research Engineer
A. J. Smith, Jr., Research Engineer

School of Aerospace Engineering

Georgia Institute of Technology

Atlanta, Georgia

PROGRESS DURING REPORT PERIOD

Summary

The accuracy of the computer program used to calculate nozzle admittance has been improved and the admittance values of the nozzles under investigation have been recomputed. The sensitivity of the experimental admittance data to errors in frequency measurements has been studied. A computer program which determines the admittances from the phase relatiorship between dynamic pressure measurements has been developed and incorporated into the analog-to-digital data reduction program. To improve the accuracy of the data, two additional channels of dynamic pressure measuring equipment have been added to the data acquisition system; additional microphone port locations have been added along the length of the impedance chamber, and the analog-to-digital data reduction program has been modified to accept fourteen channels of data. Preparation of a final report for the nozzle admittance studies has been initiated, and work has begun on determining the admittances of liner-nozzle configurations. Seventeen nozzle tests have been conducted during this report period.

Theoretical Studies

The theoretical values of the nozzle admittance are obtained from a computer program which uses Crocco's theory[1] to calculate the real and imaginary parts of the admittance. This computer program is used to numerically integrate the complex, nonlinear, Riccati equation

$$\frac{dz}{d\phi} = A(\phi)\, z - B(\phi) - z^2 \qquad (1)$$

where

$$z = \frac{\text{axial dependence of the axial velocity perturbation}}{\text{axial dependence of the radial velocity perturbation}}$$

ϕ = steady state flow potential,

and

$A(\phi)$ and $B(\phi)$ are coefficients whose form depends upon the nondimensional frequency, s, and the nondimensional mean flow velocity, $\bar{q}(\varphi)$.

Once the value of z has been determined at the nozzle entrance, the admittance at this location is obtained from the relation[1]

$$y = \frac{-z}{q^2 z + is} \qquad (2)$$

In checking the previous computer program, it has been found that the calculated nozzle admittances did not correspond to the physical location of the nozzle entrance. With the previous program, the integration of Eq. (1) started at the throat and proceeded until the chamber and nozzle entrance Mach numbers agreed to within 0.0005. Further investigation of this computation has revealed that for some nozzles, this condition was satisfied a short distance before the nozzle entrance was actually reached. To correct for this discrepancy, the computer program has been modified and the integration stops at the exact location of the nozzle entrance. The theoretical predictions obtained with the modified computer program are in better agreement with the experimental data than

the previously calculated predictions, as shown in Figs. 1 and 2.

The sensitivity of the admittance data to errors in frequency was investigated. Admittance data were obtained for a nozzle with a half-angle of 45 degrees, an entrance Mach number of 0.20, and throat and entrance radii of curvature of 2.5 inches. An intentional error of four Hertz was introduced into the data reduction program, and the admittance data were recomputed and compared with the correct results as shown in Figs. 3 and 4. These data indicate that the frequency error has no net effect on the values obtained for the real part of the admittance, but increases the value of the imaginary part by an average value of 0.08. Since the frequency is determined to within ± 2 Hertz with the current experimental apparatus, the effect of errors in frequency on the admittance data is expected to be less than the effect presented in Figs. 3 and 4.

Near the cutoff frequency, large errors in the wavelength occur for errors in frequency of ± 2 Hertz. This phenomenon occurs because the frequency appears in the denominator of the expression for the wavelength, λ, where

$$\lambda = \frac{2\pi\,(1-\bar{M}^2)\,r_c}{\sqrt{s^2 - sv_n^2\,(1-\bar{M}^2)}}$$

and $\bar{M}$ is the chamber Mach number, r_c is the chamber radius, s is the non-dimensional frequency, and $sv_n = 1.8413$ for the first tangential mode. When s equals the cutoff frequency, $sv_n(1-\bar{M}^2)^{\frac{1}{2}}$, the wavelength is infinite. Increasing s by a value of .002, which corresponds to an increase in frequency of 2 Hertz, gives a wave length of 40 feet. Therefore, near

the cutoff frequency relatively small errors in frequency will cause large discrepencies in the computed wave length.

The effects of random experimental errors in the measurement of frequency on the value of the nozzle admittance is a function of where the error occurs in the spectrum of the test frequencies, the geometry of the nozzle, the chamber Mach number, and associated measurement errors in pressure and temperature. At present, no general statements can be made regarding the manner in which all these effect influence the measured nozzle admittances. For example, in Figs. 3 and 4, the admittance data appears to be insensitive to errors in frequency near the cutoff frequency even though large errors in λ occur in this range.

An opposite example is presented in the table below.

Error in Frequency (Hz)	Wavelength (feet)	Real Part of the Admittance	Imaginary Part of the Admittance
-2	14.8	-0.08	-0.26
0	12.1	0.21	-0.10
2	10.4	0.24	0.00

These results were obtained from data taken at a frequency four Hertz above the cutoff frequency of the first tangential mode for a nozzle with a half-angle of 15 degrees, radii of curvature of 5.7 inches, and an entrance Mach number of 0.08. For this geometry and particular set of test conditions the error in frequency of four Hertz changes the value of the real part of the admittance by 0.32 and the imaginary part by 0.26. Further investigations and studies of this problem will continue; however, by using the A-to-D data reduction program, the accuracy

of the frequency measurements should improve which will provide better accuracy in determining the wavelength. Also, the large errors in wavelength are limited to the small range of frequencies very near the cut-off frequency.

The admittance data obtained thus far has been determined from pressure amplitude measurements. To check these data, a different analytical technique, using phase angle data to determine the admittance, has been developed. This technique has been programed and a computer program which uses phase measurements to determine the admittance values is now operational. The accuracy of the measured phase data is currently under investigation. Some of the errors in phase measurements are caused by the phase shifts between individual channels of the tape recorder that is used in the present experimental facility. These shifts are functions of frequency and tape speed, and errors of up to 30 degrees can be encountered when recording at $7\frac{1}{2}$ inches per second and playing back at 1 7/8 inches per second. By recording at 30 inches per second and playing back at 1 7/8 inches per second, the phase shift between the channels is reduced and can be accounted for by proper calibration of the experimental phase measurements. Work on improving the accuracy of the phase measurements is in progress.

The analog-to-digital data reduction program has been extended to include the following fourteen data channels: ten channels of pressure data, two reference frequency channels, and two temperature data channels.

The computer program using phase measurements to calculate admittance values has been incorporated into the A-to-D data reduction program. Preliminary checkouts of this extended A-to-D program are underway. A

computer plotting routine has also been added to the data reduction program. With this routine plots of pressure amplitude and phase versus frequency, and plots of the real and imaginary parts of the admittance versus nondimensional frequency can be obtained. The computer plotting program has been checked out and is presently operational.

A report covering all of the work done to date on the nozzle admittance studies is in preparation. This report is expected to become available this summer.

Experimental Investigations

During this report period 17 tests have been conducted. All of the nozzles previously tested have been retested, and the data stored on analog tape. In addition, the aluminum nozzles with half-angles of 15 and 30 degrees have been remachined for an entrance Mach number of 0.16 and tested. New injector plates for Mach numbers of 0.16 and 0.24 have been fabricated and the nozzle with a 45 degree half-angle has been remachined and tested for entrance Mach numbers of 0.20 and 0.24. This nozzle will be remachined again and tested at entrance Mach numbers of 0.28 and 0.32. This is done to insure that the facility is capable of going to these higher Mach numbers. The data from the 17 tests run so far have not been reduced because of problems with the A-to-D conversion system. These problems have originated because the high sample rates currently being used are close to the limits of the A-to-D conversion system. This system is currently being modified and is expected to be operational shortly. The data recorded in these 17 runs will be reduced as soon as the data reduction system becomes operational. The nozzles

tested to date are presented in Table 1.

In order to obtain more information about the structure of the standing wave in the tube, which would result in more accurate admittance data, additional microphone locations were added along the length of the tube at positions 27, 29, 31, 37, 43, 45, 47, 51, and 56 inches from the nozzle entrance. These additional locations allow the microphones to be placed closer together which, based on previous impedance tube studies, increases the accuracy of the admittance data - especially at higher frequencies. The results of these tests will be available shortly.

A quasi-steady nozzle has been tested and the admittance data is presented in Figs. 5 and 6. These data indicate that the theoretical and experimental results are in agreement up to a value of the nondimensional frequency, s, of 2.6. At values of s greater than 2.6 the theoretical predictions and the experimental results begin to disagree. Based on the good agreement of previous experimental and theoretical data this nozzle will be retested to verify the results.

REFERENCES

1. Crocco, L., and Sirignano, W. A., "Behavior of Supercritical Nozzles under Three-Dimensional Oscillatory Conditions," AGARDograph 117, 1967.

TABLE 1. Nozzles Tested

Nozzle Half-Angle	Chamber Mach Number				
	0.08	0.16	0.20	0.24	0.32
15	1*, 3	9			
30	4	2*, 10			
45	5	6	7	8	

* Radii of Curvature = 5.7 inches
All Others Are 2.5 inches

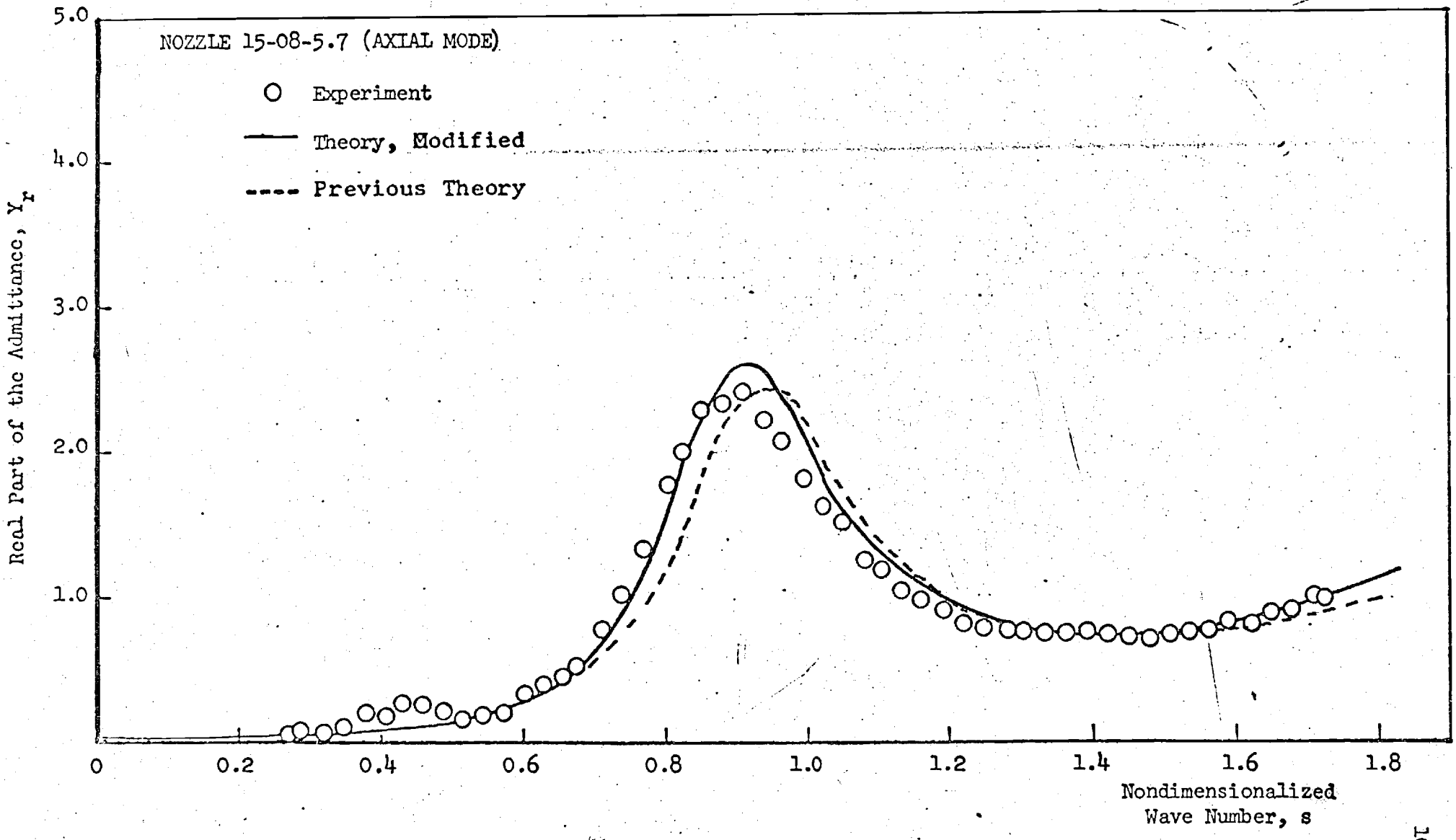

Figure 1. Comparison of the theory and experimental values of the real part of the admittance for the nozzle with a half-angle of 15 degrees, entrance Mach number of .08, and radii of curvature at the throat and entrance of 5.7 inches.

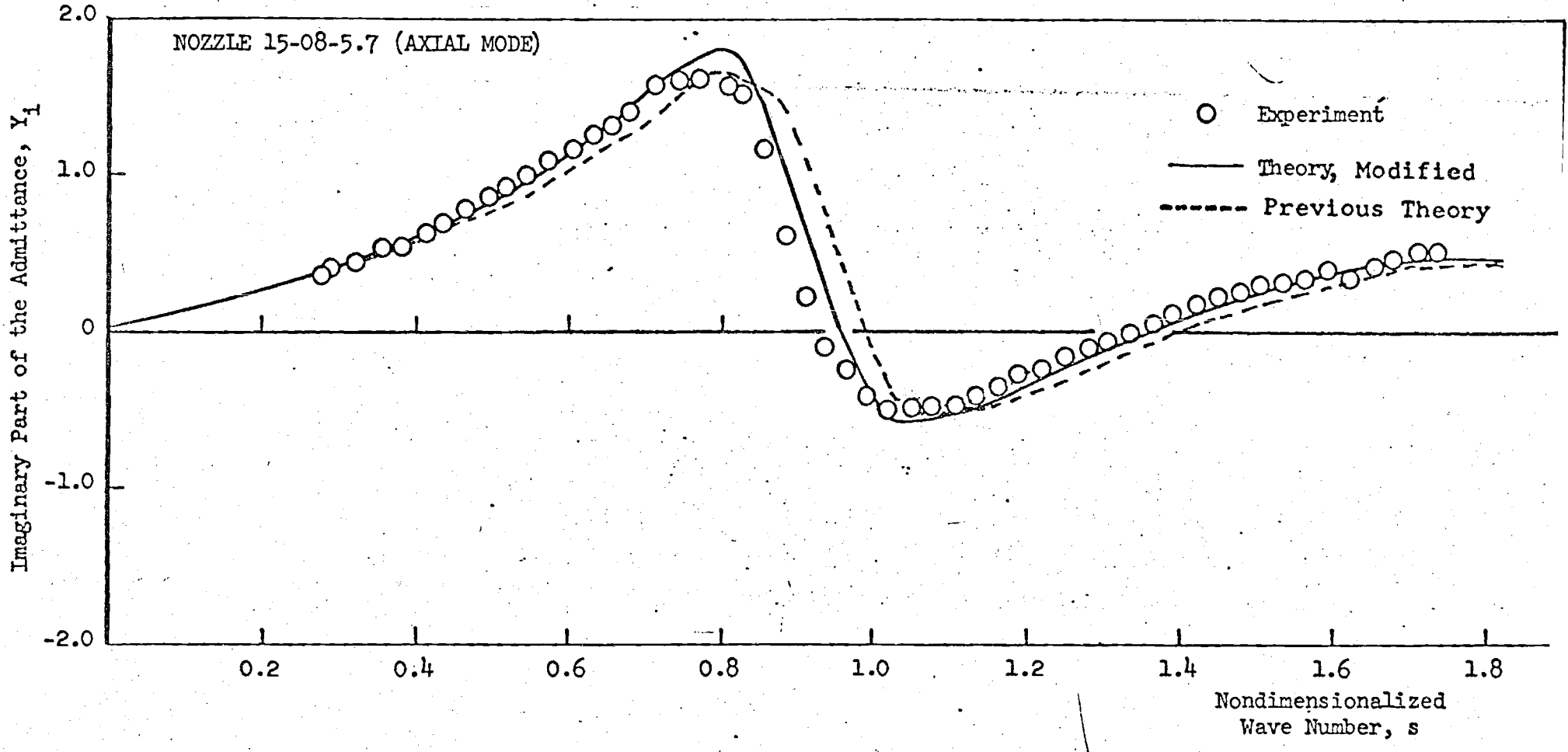

Figure 2. Comparison of the theory and experimental values of the imaginary part of the admittance for the nozzle with a half-angle of 15 degrees, entrance Mach number of .08, and radii of curvature at the throat and entrance of 5.7 inches.

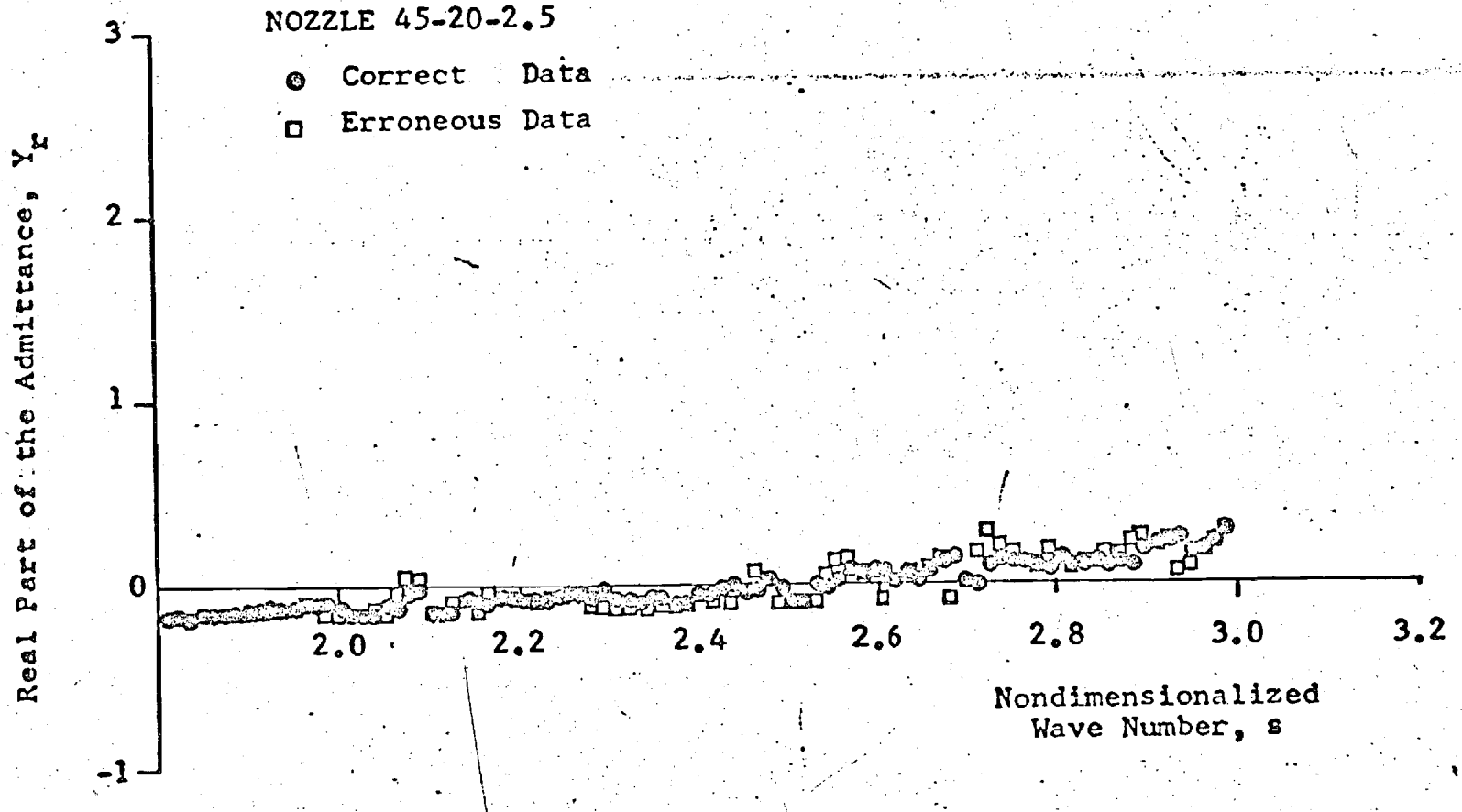

Figure 3. Effect of a four Hertz error in frequency on the real part of the admittance

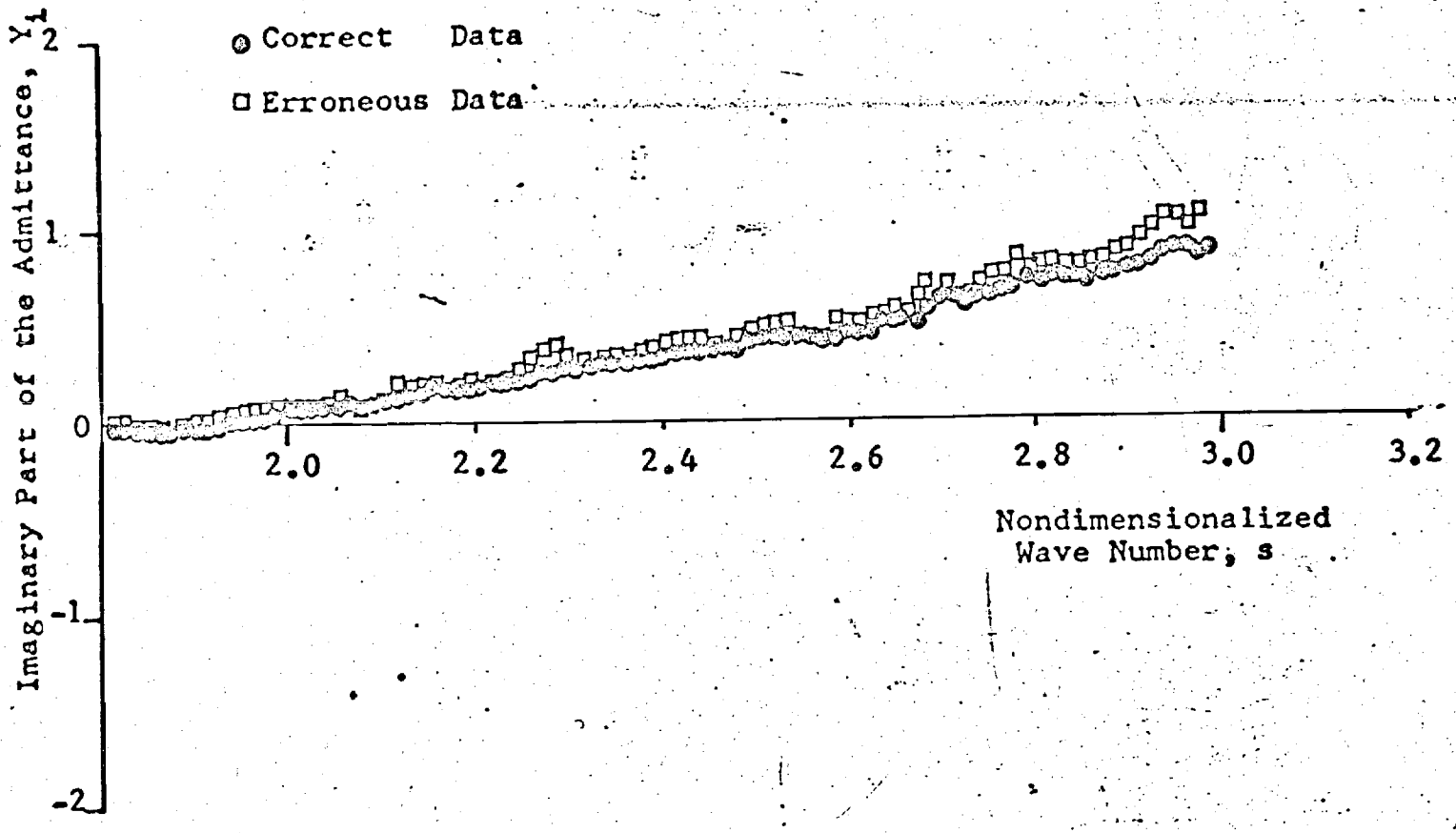

Figure 4. Effect of a four Hertz error in frequency on the imaginary part of the admittance

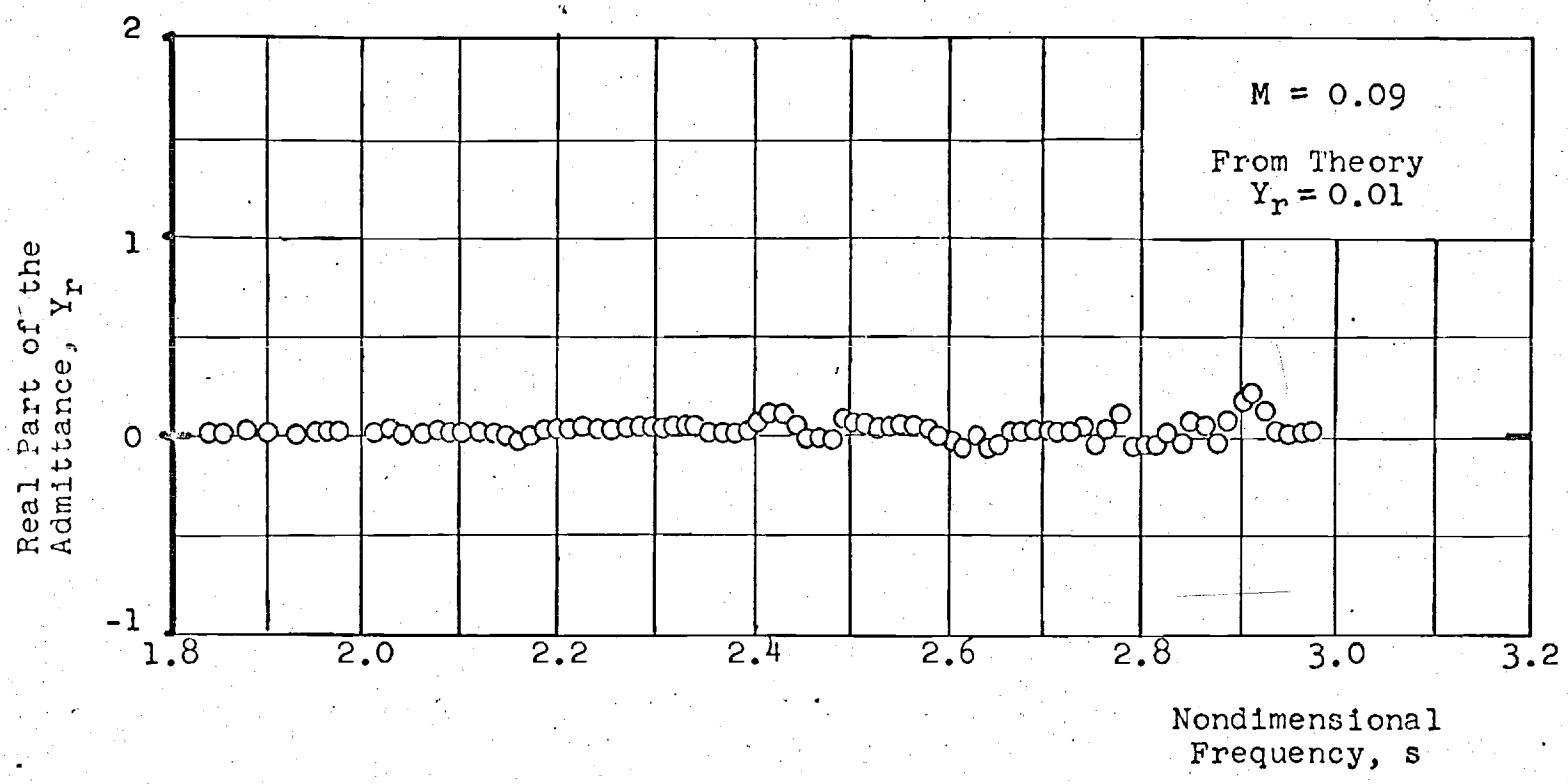

Figure 5. Real Part of the Admittance vs. s for a Multi-orifice, Quasi-steady Nozzle, First Tangential Mixed Modes.

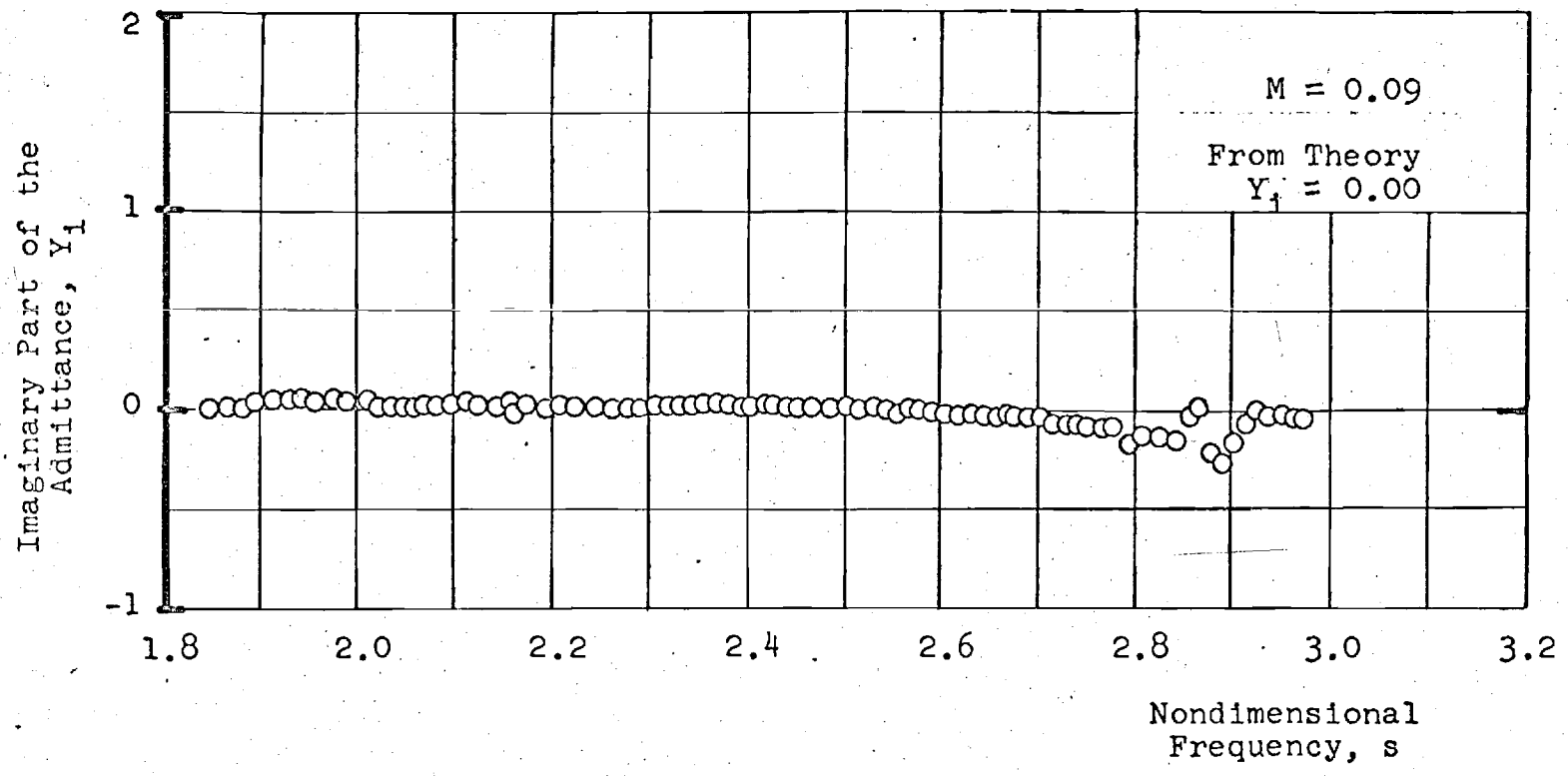

Figure 6. Imaginary Part of the Admittance vs. s for a Multi-orifice, Quasi-steady Nozzle, First Tangential Mixed Modes.

E-16-607

NASA GRANT NGL 11-002-085

BEHAVIOR OF NOZZLES AND ACOUSTIC LINERS IN THREE-DIMENSIONAL ACOUSTIC FIELDS

Semi-Annual Report for Period
June 15, 1972, to December 15, 1972

Prepared by: Ben T. Zinn, Principal Investigator
W. A. Bell, Instructor
B. R. Daniel, Research Engineer
A. J. Smith, Jr., Research Engineer

School of Aerospace Engineering
Georgia Institute of Technology
Atlanta, Georgia

INTRODUCTION

This report consists of a series of monthly progress reports which summarize the work completed under NASA Grant NGL 11-002-085 for the period between June 15, 1972, to December 15, 1972.

During this period nozzle testing was completed, and the nozzle admittance data obtained provide confirmation of the theoretical admittance results predicted from Crocco's three-dimensional nozzle admittance theory. In addition, Crocco's theory was extended to include the effects of a temporal decay coefficient. The extended theory along with experimental admittance data are presented in detail in NASA CR 121129, dated February 1973.

Currently, testing of various liner-nozzle combinations is in progress. The data will be compared with theoretical predictions obtained by Dr. C. E. Mitchell at Colorado State University to evaluate existing liner theories.

July 7, 1972

Dr. R. J. Priem, MS 500-209
NASA
Lewis Research Center
21000 Brookpark Road
Cleveland, Ohio 44135

Dear Dr. Priem:

The following is a summary of work completed under NASA Grant NGR 11-002-085 during the month of June 1972.

The Analog-to-Digital data reduction program is now operational, and experimental nozzle admittance data obtained from this program are presented in Figures 3 through 8.

The program that computes the theoretical values of the nozzle admittance has been modified. This computer program numerically integrates the differential equations necessary for determining the nozzle admittance. Starting at the throat, these equations are integrated until the nozzle entrance is reached. The nozzle entrance was previously taken to be the point at which the Mach number in the nozzle agreed with the chamber Mach number to within ± 0.0005. This program was modified to compute the admittance exactly at the nozzle entrance. Typical results of the modification are shown in Figure 1 for axial modes and Figure 2 for three-dimensional modes.

Analog-to-Digital data reduction program has been used to obtain admittance values from six tests conducted some time ago. Axial and three-dimensional test results have been obtained for the following nozzles: 15-16-2.5, 30-16-2.5, and 45-24-2.5. These test results, along with the corresponding theoretical predictions, are shown in Figures 3 through 8. Examination of these plots shows good agreement between the theoretical and experimental nozzle admittances.

Dr. C. M. Mitchell of Colorado State University has been given the design parameters describing the first manufactured liner and the test conditions at which this liner will be tested. Dr. Mitchell has been asked to use this data to compute the theoretical combustion response and local liner admittance

for tests conducted with three different nozzles. Dr. Mitchell responded by requesting additional data, which must be measured in the liner test. The liner tests will be conducted soon and the data will be sent to Dr. Mitchell shortly thereafter.

The dependence of the measured nozzle admittance on the length of the convergent section of the nozzle is currently under investigation, as you have suggested during your last visit here. This investigation will determine whether the length of the nozzle convergent section can be used in normalizing the frequency in the admittance plots in such a manner that the admittance curves for all the nozzles will coalesce into a single curve. The nozzle admittance theory is also being examined to find the range of parameters at which the peak of the real part of the nozzle admittance "flips" from a positive value to a negative value. The results of these investigations will be presented in the next monthly progress report.

Sincerely,

Ben T. Zinn
Professor

tk

Enclosures

cc: Messrs. W. A. Bell
B. R. Daniel
A. J. Smith, Jr.

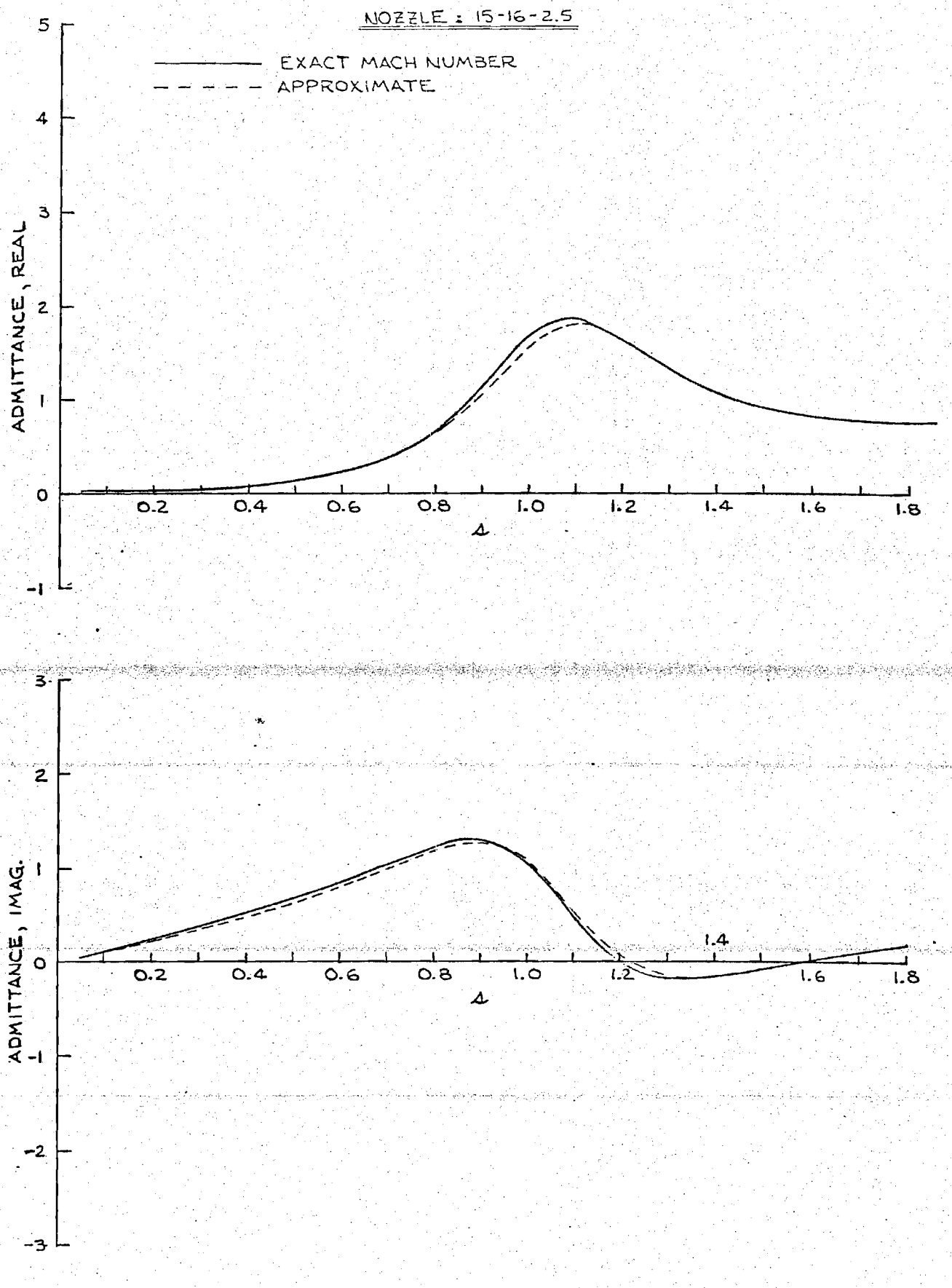

FIGURE 1. THEORETICAL ADMITTANCES FOR AXIAL MODES.

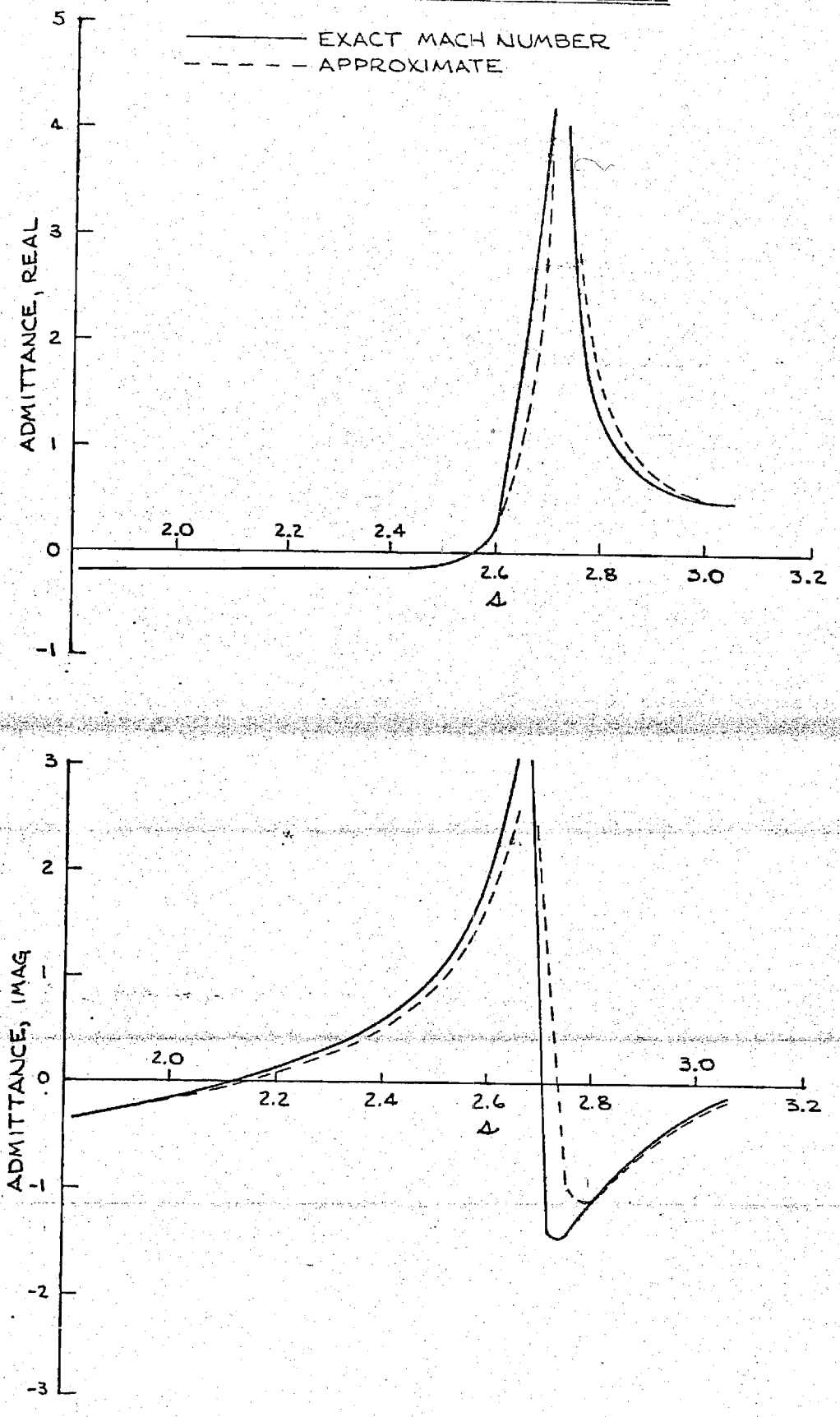

FIGURE 2. THEORETICAL ADMITTANCES FOR THREE-DIMENSIONAL MODES

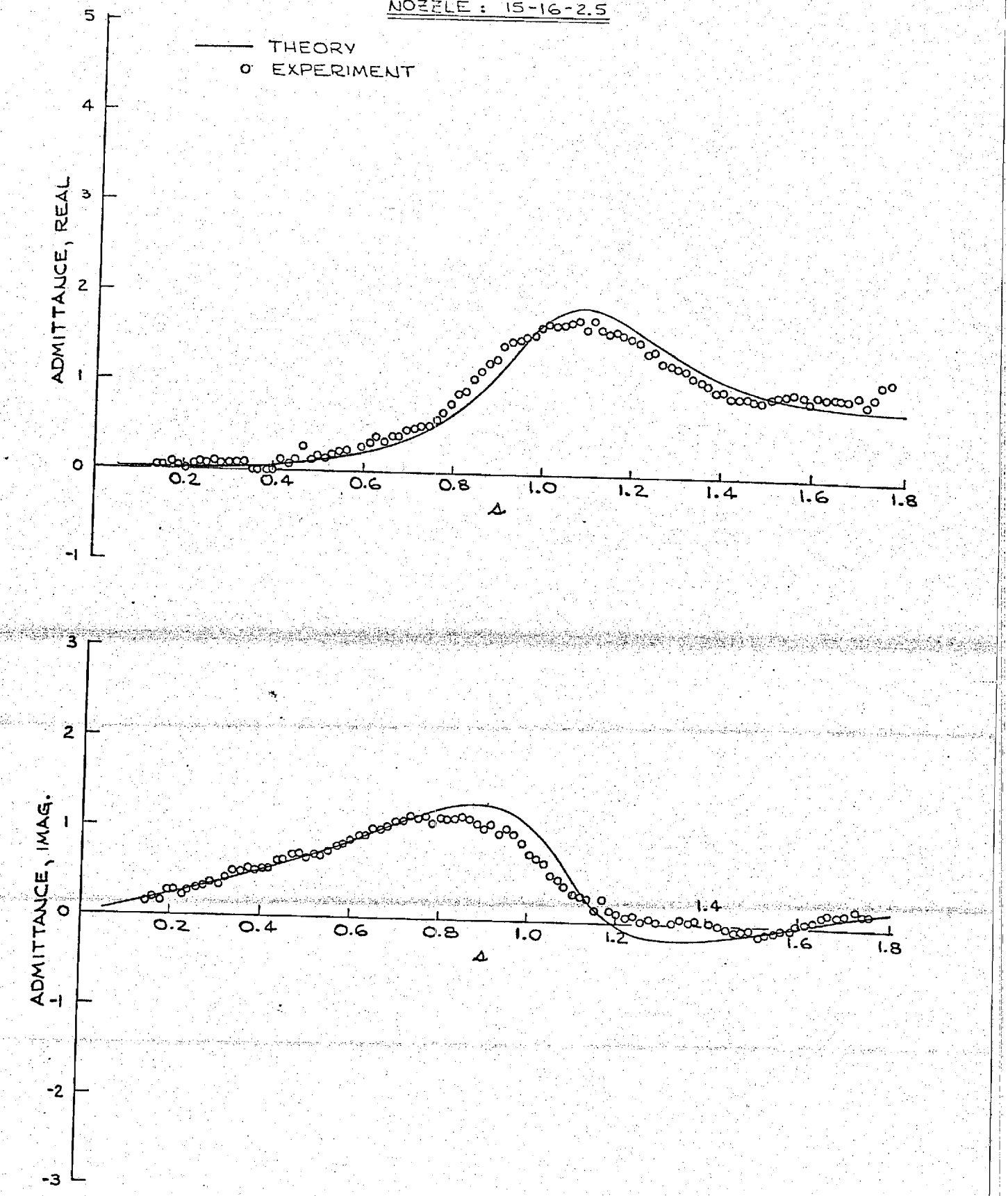

FIGURE 3. AXIAL MODE ADMITTANCES FOR THE 15-16-2.5 NOZZLE.

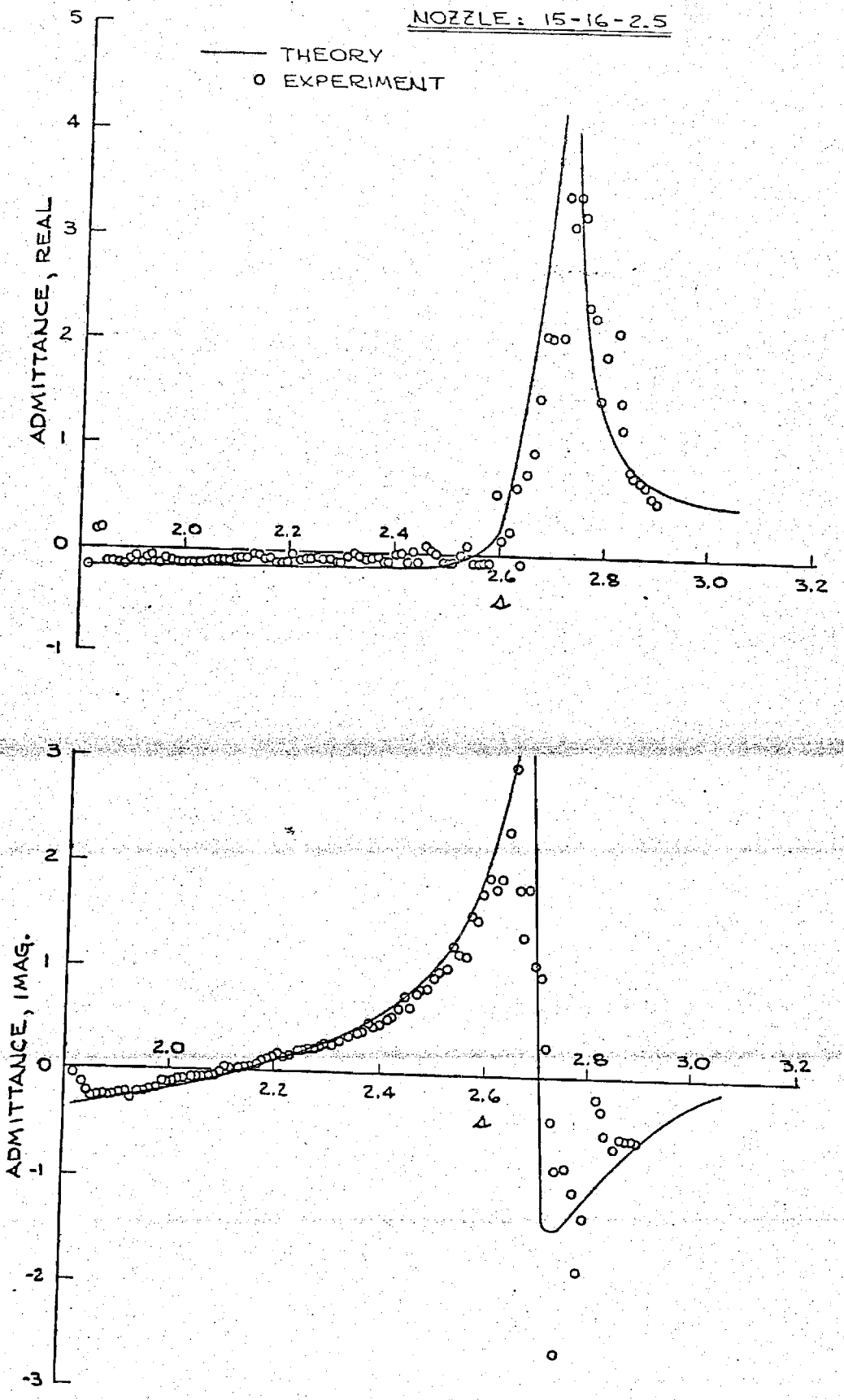

FIGURE 4. THREE-DIMENSIONAL MODE ADMITTANCES FOR THE 15-16-2.5 NOZZLE.

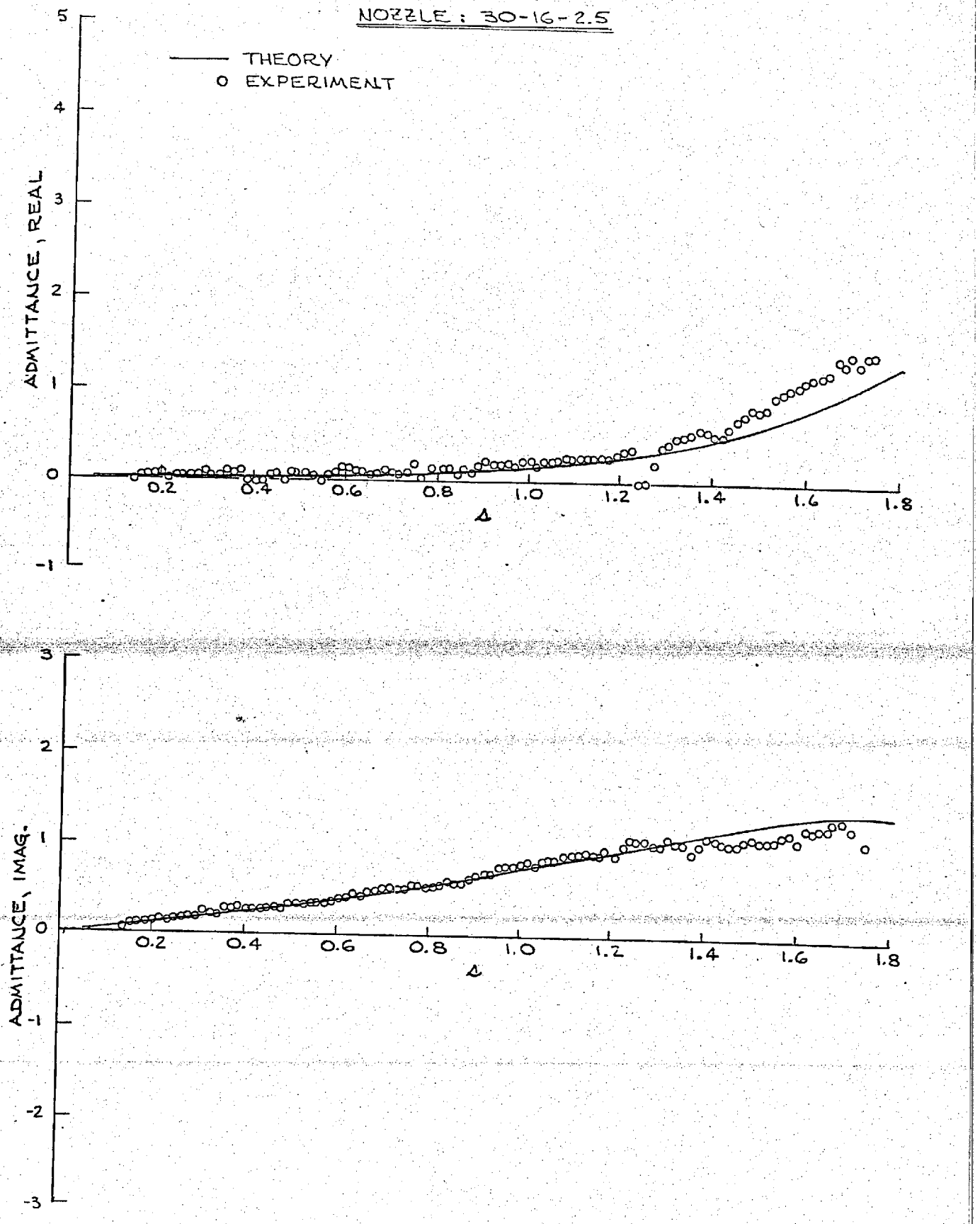

FIGURE 5. AXIAL MODE ADMITTANCES FOR THE 30-16-2.5 NOZZLE.

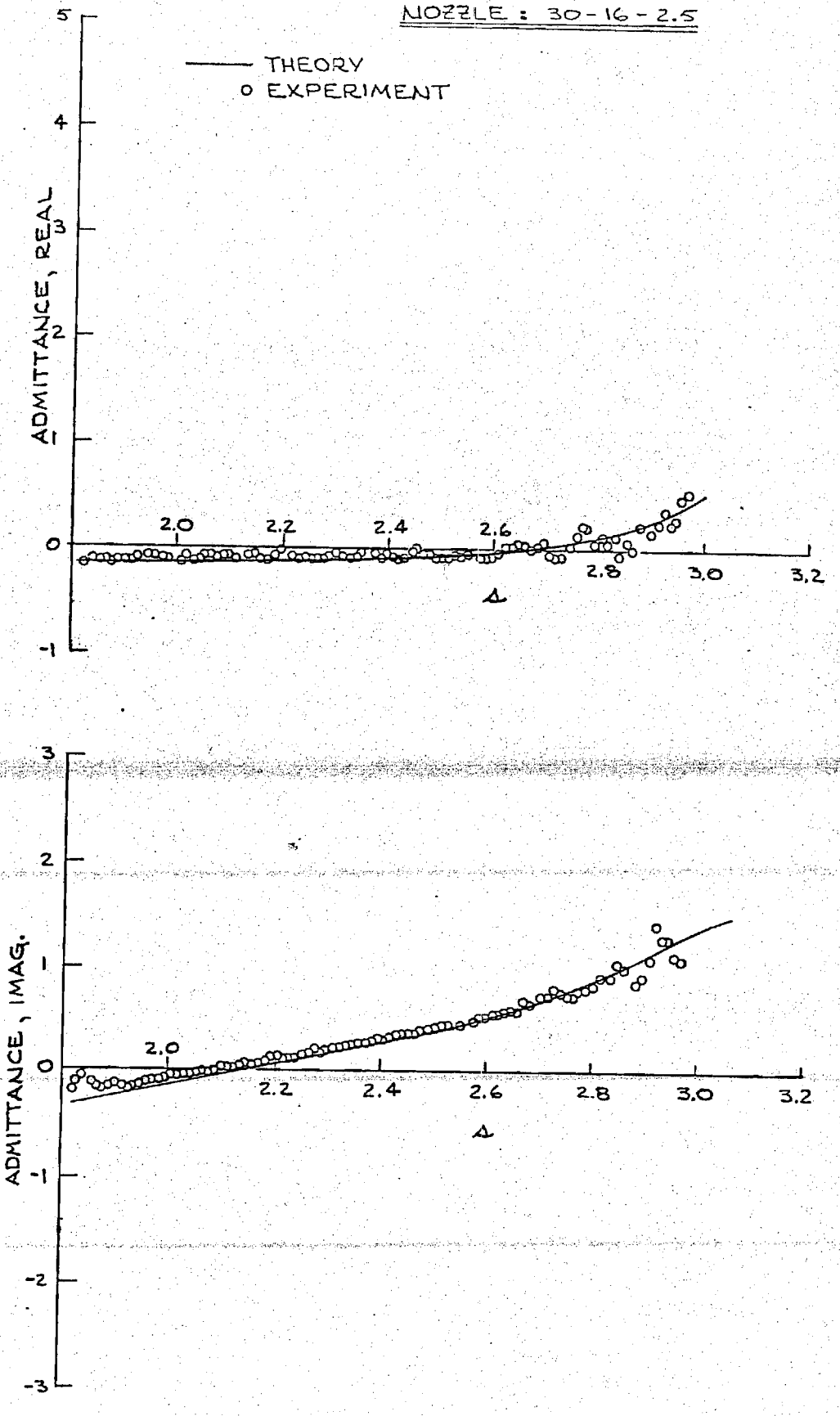

FIGURE 6. THREE-DIMENSIONAL MODE ADMITTANCES FOR THE 30-16-2.5 NOZZLE.

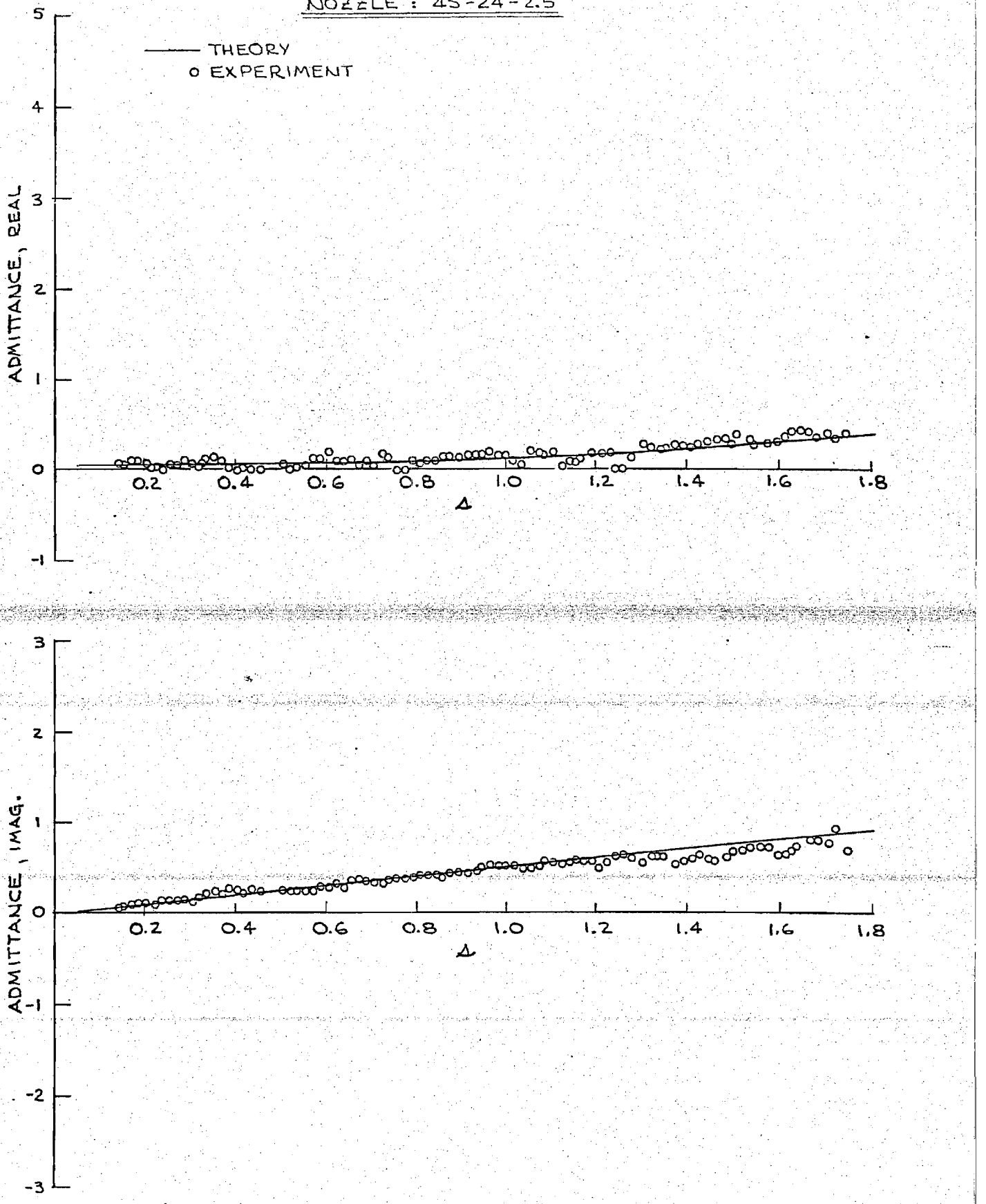

FIGURE 7. AXIAL MODE ADMITTANCES FOR THE 45-24-2.5 NOZZLE.

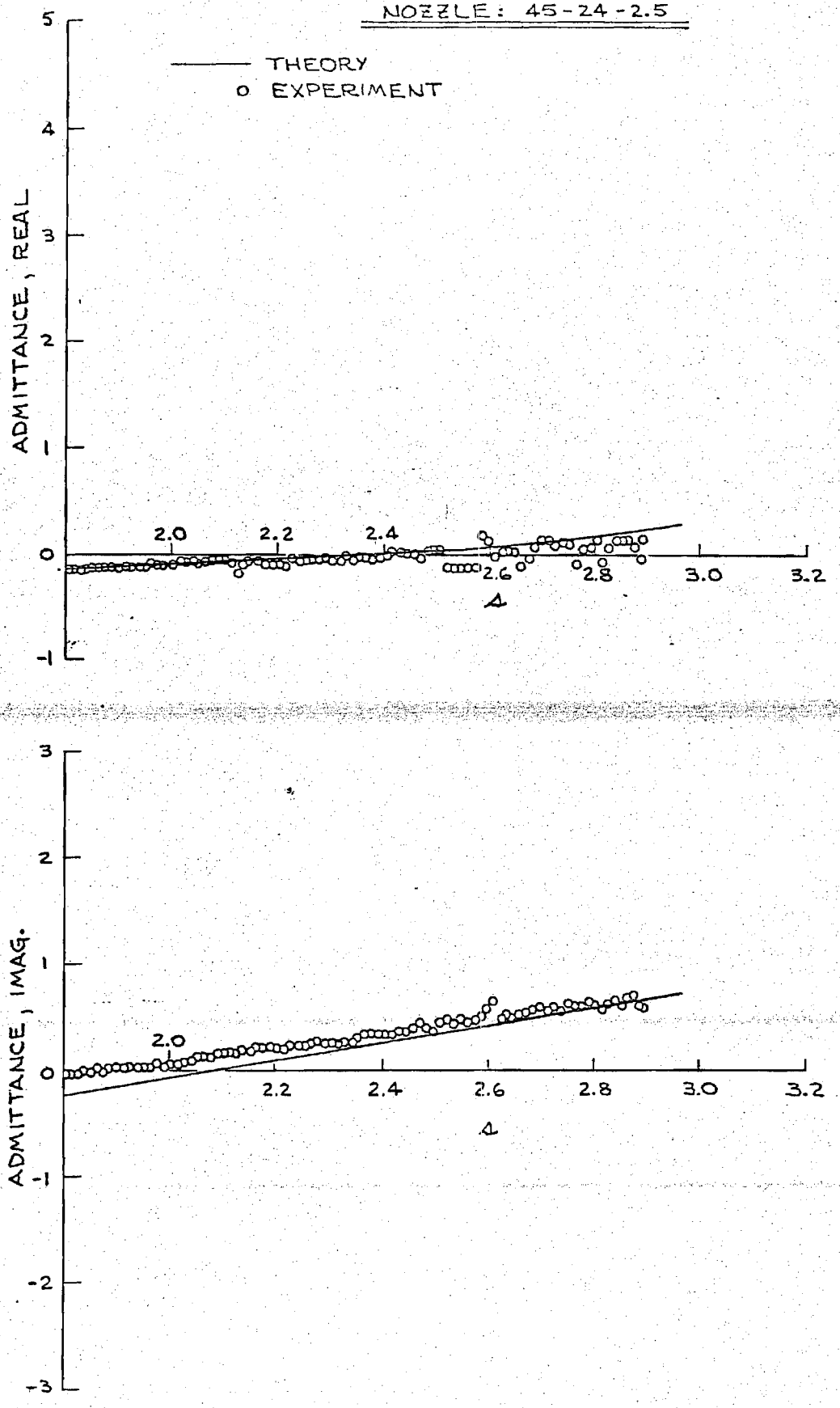

FIGURE 8. THREE-DIMENSIONAL MODE ADMITTANCES FOR THE 45-24-2.5 NOZZLE.

August 9, 1972

Dr. R. J. Priem, MS 500-209
NASA
Lewis Research Center
21000 Brookpark Road
Cleveland, Ohio 44135

Dear Dr. Priem:

The following is a summary of the work completed under NASA Grant NGR 11-002-085 during July 1972.

Testing of new, recently machined nozzles had to be delayed due to a malfunction in the tape transport mechanism of the tape recorder used for data acquisition. The recorder was returned to the manufacturer for repair and is expected to be returned to service this week. The nozzles that have recently been machined include two with half-angles of 15 and 30 degrees and an entrance Mach number of 0.24 and one with a 45 degree half-angle and an entrance Mach number of 0.28. Testing of these nozzles will begin as soon as the tape recorder becomes available.

Preparations for the testing of the first liner, which is now available, is in progress. Attention has been directed on instrumenting the liner to assure accurate determination of pressure amplitude and phase data needed to determine the local liner admittance. Present efforts are directed toward the evaluation and calibration of special adaptors that connect the pressure transducers to the liner. Work is also continuing on the design of two additional liners which will be tested later on in this program.

An investigation of the nozzle admittance theory was made to clarify the reasons for the apparent discontinuity in the real part of the nozzle admittance. This behavior is shown in Figure 1. In the range of nondimensional frequency, S, from 2.6 to 3.0, the real part of the admittance becomes a very large negative value at an entrance Mach number of 0.08; however, at an entrance Mach number of 0.16, the real part of the nozzle admittance assumes large positive values. For both Mach numbers the imaginary part is discontinuous. The effects of varying the nozzle half angle θ_1 is shown in Figure 2. When $\theta_1 = 15^\circ$, a discontinuous behavior exists in the real and imaginary parts of the nozzle admittance in the range of S from 2.6 to 3.0. However, no such behavior is exhibited at nozzle half-angles of 30 and 45 degrees.

To determine the reason for this behavior, the computer program used to calculate the theoretical nozzle admittance values was extended to also determine the values

of α and β from the calculated nozzle admittances. The quantities α and β are defined by the following relationships:

$$e^{-2\pi\alpha} = \left.\frac{\text{Pressure Amplitude of the Reflected Wave}}{\text{Pressure Amplitude of the Incident Wave}}\right|_{\substack{\text{Nozzle}\\ \text{Entrance}}}$$

$\pi(2\beta + 1)$ = Phase difference between the incident and reflected waves at the nozzle entrance

The results of these computations are presented in Tables 1 through 12. Because of the nature of the equations, values of α and β could not be computed for frequencies below the first tangential cutoff frequency. However, as you requested, admittance values for frequencies below the cutoff frequency have been obtained, and they are presented in these tables. By studying the behavior of α and β it was possible to clarify the observed discontinuous behavior of the nozzle admittance.

The expression for the nozzle admittance can be written in the following simplified form:

$$y = c_1 \coth \pi(\alpha - i\beta) - c_2 \qquad (1)$$

where c_1 and c_2 are constant for given values of the frequency, the chamber Mach number, and the value of S_{mn}. The values of α and β are presented in Figure 3 and are obtained from the admittance values plotted in Figure 1. In the range of S from 2.6 to 3.0, the values of α and β are continuous even though the admittance is discontinuous. Notice that in this frequency range β is a small number. Assuming $\beta = 0$, which means that a pressure minimum exists at the nozzle entrance, equation (1) gives

$$y_r = c_1 \coth \pi\alpha - c_2$$

$$y_i = 0$$

For the small negative values of α observed when $\bar{m} = 0.08$, the term $\coth \pi\alpha$ in the expression for the real part of the admittance becomes a large negative value. For the small positive values of α which occur at $\bar{m} = 0.16$, the hyperbolic cotangent term becomes a large positive value. Therefore, the "flip" in y_r from large negative to positive values is caused by the discontinuous behavior of the hyperbolic cotangent function when the argument goes from a small negative to a small positive value. The imaginary part of the admittance

y_i behaves like the trigonometric cotangent function for small values of α. It can be shown from equation (1) that

$$y_i \simeq c_1 \cot \pi\beta + \mathcal{O}\left[(\pi\alpha)^2\right]$$

From Figure 3, for $\bar{m} = 0.08$ β crosses zero at $S = 2.82$. Below this frequency, $\beta \to 0^+$ and so $y_i \to +\infty$. Above this frequency, $\beta \to 0^-$ and $y_i \to -\infty$.

When α or β is not close to zero, discontinuities will not occur in the nozzle admittance as shown in Figure 2 for values of the nozzle half-angle of 30 and 45 degrees. From Tables 5 and 9 it can be seen that for these values of θ_1 and for $\bar{m} = 0.08$, β does not become zero and so the admittance function will be continuous with frequency.

The tables also show that the values of α predicted from theory can be negative. Phase measurements are needed to determine if these negative values are physically possible.

Further work is being done with the theory to determine the effect of the nozzle convergent section length upon the measured nozzle admittance. This work is near completion and the results will be presented in the next monthly report. An amplification factor will also be incorporated into the admittance computations to determine its effect.

Sincerely,

Ben T. Zinn
Professor

tk

Enclosures

cc: Messrs. W. A. Bell
B. R. Daniel
A. J. Smith, Jr.

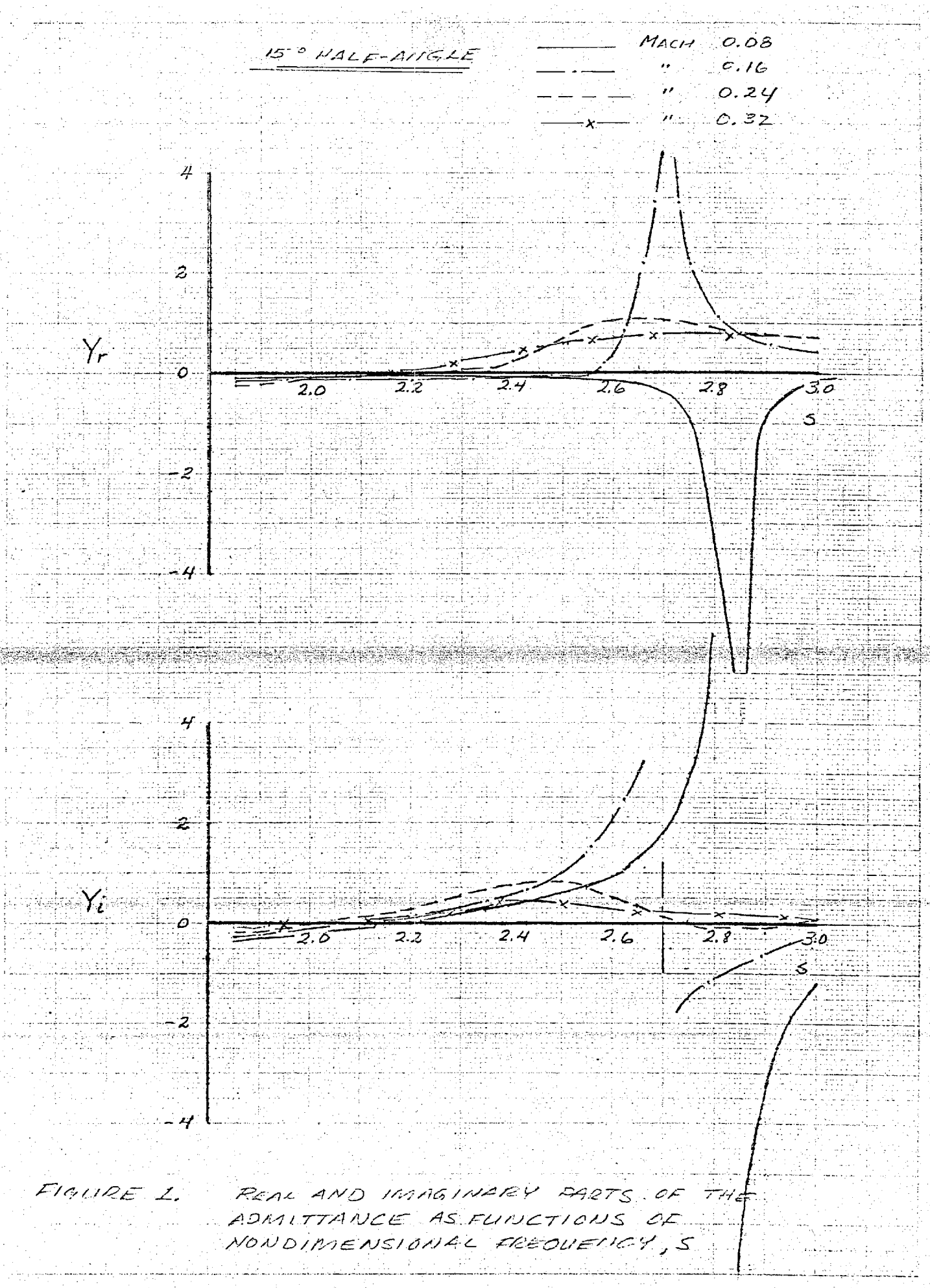

FIGURE 1. REAL AND IMAGINARY PARTS OF THE ADMITTANCE AS FUNCTIONS OF NONDIMENSIONAL FREQUENCY, S

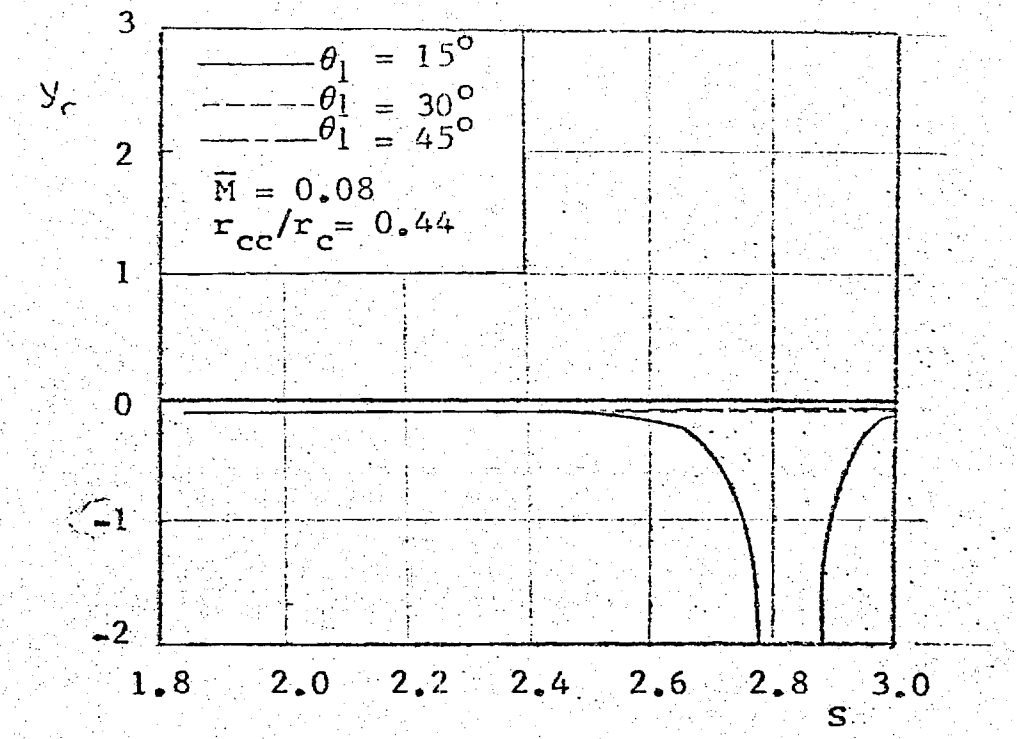

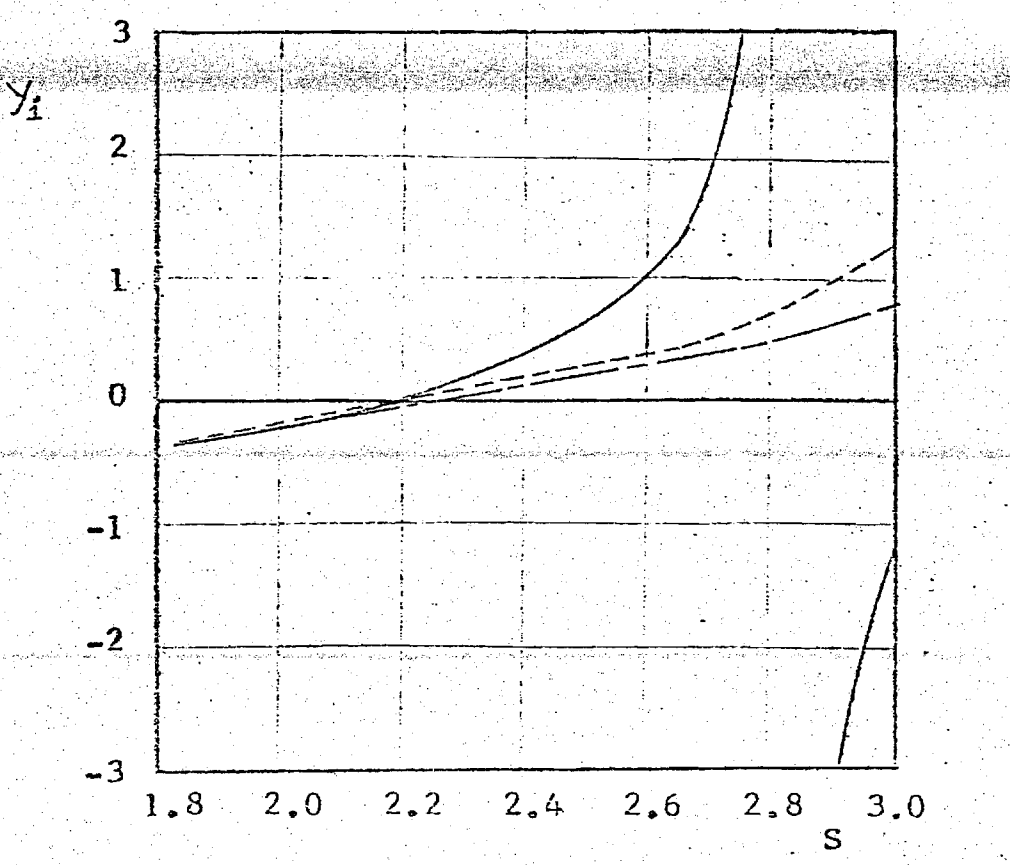

Figure 2. Effect of Nozzle Half-Angle on the Admittance Values Predicted by Theory for Mixed First Tangential-Longitudinal Modes

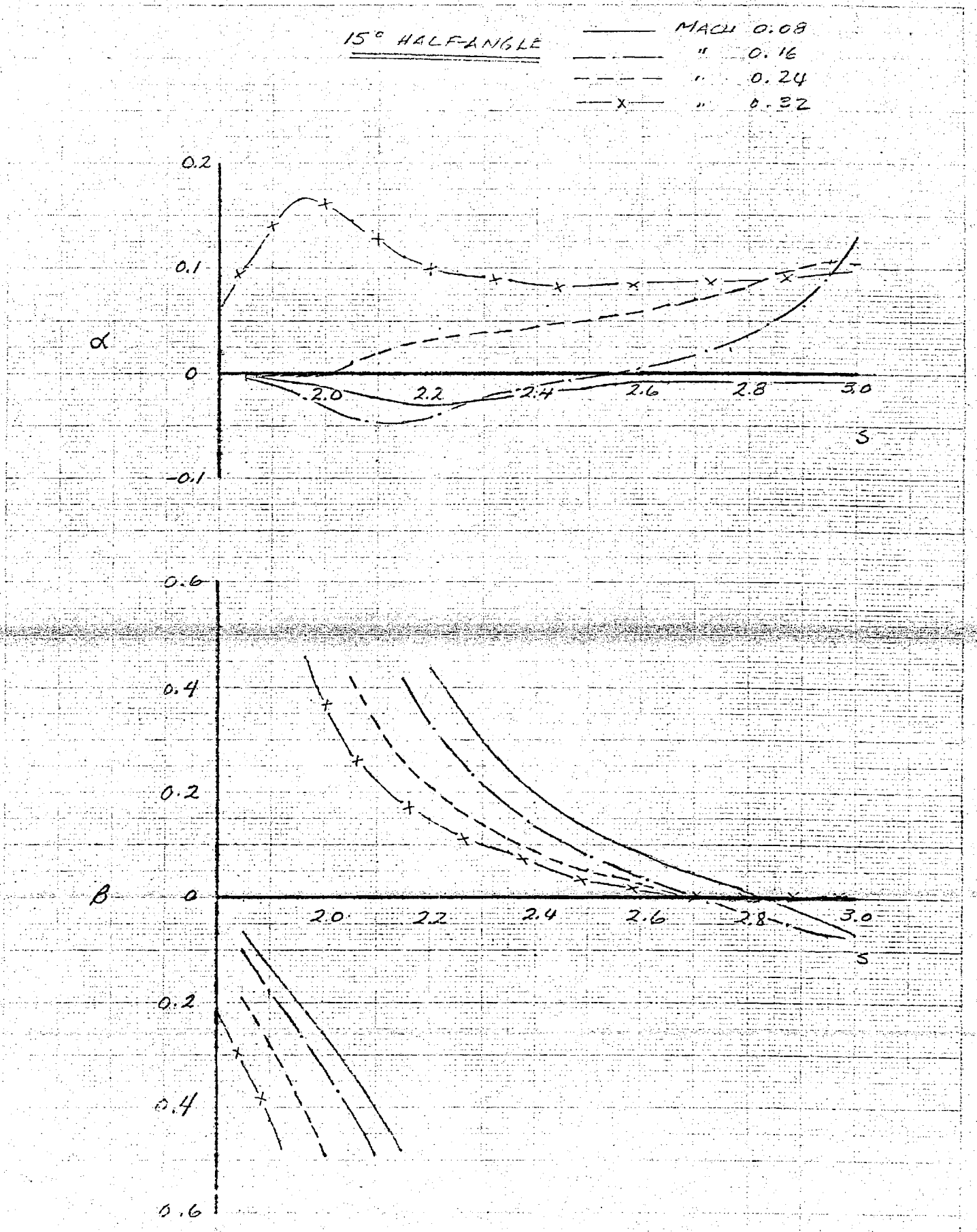

FIGURE 3. ADMITTANCE PARAMETERS, α AND β, AS FUNCTIONS OF NONDIMENSIONAL FREQUENCY, S

THEORETICAL NOZZLE ADMITTANCES

MACH NUMBER = .00 SVN = 1.8413 GAMMA = 1.4

NOZZLE ANGLE = 15.0 RADII OF CURVATURE: THROAT = .4396 ENTRANCE = .4396

WC	YR	YI	W	SYR	SYI	ALPHA	BETA
1.6000	-.07876	-.43499	1.60102	-.10984	-.60666		
1.5500	-.08277	-.47422	1.55099	-.11544	-.66136		
1.6000	-.07876	-.43499	1.60102	-.10984	-.60666		
1.6500	-.07517	-.39660	1.65106	-.10484	-.55312		
1.7000	-.07197	-.35885	1.70109	-.10037	-.50046		
1.7500	-.06912	-.32153	1.75112	-.09639	-.44841		
1.8000	-.06660	-.28444	1.80115	-.09288	-.39670		
1.8500	-.06438	-.24739	1.85118	-.08979	-.34501	-.00200	-.06363
1.9000	-.06247	-.21013	1.90122	-.08713	-.29305	-.00520	-.13047
1.9500	-.06085	-.17242	1.95125	-.08487	-.24046	-.00880	-.19816
2.0000	-.05953	-.13398	2.00128	-.08303	-.18686	-.01331	-.25878
2.0500	-.05852	-.09449	2.05131	-.08161	-.13177	-.01875	-.32535
2.1000	-.05783	-.05354	2.10134	-.08066	-.07467	-.02444	-.39971
2.1500	-.05752	-.01067	2.15137	-.08022	-.01488	-.02883	-.48025
2.2000	-.05763	.03475	2.20141	-.08037	.04846	-.03037	.43842
2.2500	-.05826	.08350	2.25144	-.08125	.11645	-.02883	.36299
2.3000	-.05954	.13665	2.30147	-.08303	.19057	-.02545	.29780
2.3500	-.06169	.19566	2.35150	-.08604	.27288	-.02160	.24370
2.4000	-.06655	.28695	2.40153	-.09281	.40019	-.01680	.18624
2.4500	-.07025	.34083	2.45157	-.09797	.47534	-.01513	.16287
2.5000	-.07828	.43516	2.50160	-.10917	.60689	-.01277	.13238
2.5500	-.09117	.55414	2.55163	-.12715	.77282	-.01092	.10641
2.6000	-.11323	.71325	2.60166	-.15791	.99472	-.00948	.08378
2.6500	-.15513	.94423	2.65169	-.21635	1.31686	-.00836	.06360
2.7000	-.24994	1.32360	2.70173	-.34858	1.84594	-.00751	.04513
2.7500	-.54683	2.08755	2.75176	-.76263	2.91138	-.00689	.02773
2.8000	-2.52309	4.17968	2.80179	-3.51878	5.82774	-.00646	.01082
2.8500	-4.93728	-4.89676	2.85182	-6.88572	-6.82921	-.00624	-.00622
2.9000	-.63325	-2.35623	2.90185	-.88315	-3.28609	-.00622	-.02413
2.9500	-.22193	-1.33704	2.95189	-.30951	-1.86469	-.00648	-.04393
3.0000	-.11628	-.87025	3.00192	-.16217	-1.21368	-.00710	-.06718

$WC = \frac{\omega r_c}{\bar{c}_0}$ $\quad YR = Re\left\{\frac{\bar{\rho}_0 \bar{c}_0}{\gamma}\frac{u'}{p'}\right\}$ $\quad YI = Im\left\{\frac{\bar{\rho}_0 \bar{c}_0}{\gamma}\frac{u'}{p'}\right\}$ $\quad W = \frac{\omega r_c}{\bar{c}} = S$ $\quad SYR = Re\left\{\bar{\rho}\bar{c}\frac{u'}{p'}\right\}$ $\quad SYI = Im\left\{\bar{\rho}\bar{c}\frac{u'}{p'}\right\}$

THEORETICAL NOZZLE ADMITTANCES

MACH NUMBER = .16 SVN = 1.8413 GAMMA = 1.4

NOZZLE ANGLE = 15.0 RADII OF CURVATURE: THROAT = .4396 ENTRANCE = .4396

WC	YR	YI	W	SYR	SYI	ALPHA	BETA
1.6000	-.15446	-.40723	1.60409	-.21296	-.56145		
1.6500	-.16211	-.44620	1.65396	-.22351	-.61519		
1.6700	-.15446	-.40723	1.60409	-.21296	-.56145		
1.6500	-.14759	-.36877	1.65422	-.20349	-.50842		
1.7000	-.14143	-.33062	1.70435	-.19500	-.45583		
1.7500	-.13593	-.29258	1.75447	-.18740	-.40339		
1.8000	-.13102	-.25441	1.80460	-.18064	-.35076		
1.8500	-.12668	-.21586	1.85473	-.17465	-.29760	-.00696	-.10729
1.9000	-.12287	-.17662	1.90486	-.16940	-.24351	-.01374	-.17802
1.9500	-.11957	-.13637	1.95499	-.16485	-.18801	-.02199	-.24518
2.0000	-.11676	-.09467	2.00511	-.16098	-.13052	-.03184	-.31830
2.0500	-.11443	-.05101	2.05524	-.15776	-.07033	-.04168	-.40084
2.1000	-.11256	-.00471	2.10537	-.15519	-.00649	-.04792	-.49101
2.1500	-.11114	.04512	2.15550	-.15323	.06221	-.04744	.41897
2.2000	-.11012	.09972	2.20562	-.15183	.13749	-.04114	.33827
2.2500	-.10942	.16084	2.25575	-.15085	.22175	-.03252	.27121
2.3000	-.10879	.23110	2.30588	-.14999	.31862	-.02416	.21716
2.3500	-.10771	.31459	2.35601	-.14850	.43373	-.01698	.17357
2.4000	-.10408	.41809	2.40614	-.14460	.57643	-.01099	.13785
2.4500	-.09689	.55365	2.45626	-.13359	.76332	-.00588	.10790
2.5000	-.07401	.74461	2.50639	-.10203	1.02660	-.00129	.08213
2.5500	-.00335	1.04067	2.55652	-.00461	1.43479	.00312	.05936
2.6000	.25496	1.54958	2.60665	.35152	2.13643	.00772	.03871
2.6500	1.42521	2.23142	2.65677	1.96496	3.07649	.01288	.01949
2.7000	3.20578	.20521	2.70690	4.41985	.28293	.01911	.00121
2.7500	1.63259	-1.01829	2.75703	2.25087	-1.40393	.02707	-.01648
2.8000	.87446	-.81120	2.80716	1.20563	-1.11841	.03765	-.03362
2.8500	.58183	-.58113	2.85729	.80218	-.80122	.05212	-.04979
2.9000	.44726	-.46985	2.90741	.61665	-.56507	.07203	-.06358
2.9500	.37040	-.37952	2.95754	.52309	-.38537	.09874	-.07177
3.0000	.34593	-.17514	3.00767	.47699	-.24146	.13152	-.06826

THEORETICAL NOZZLE ADMITTANCES

MACH NUMBER = .24 SVN = 1.0413 GAMMA = 1.4

NOZZLE ANGLE = 15.0 RADII OF CURVATURE: THROAT = .4396 ENTRANCE = .4396

XC	YR	YI	W	SYR	SYI	ALPHA	BETA
1.6000	-.21742	-.35507	1.60919	-.29411	-.48031		
1.5500	-.22899	-.39488	1.55890	-.30975	-.53416		
1.6000	-.21742	-.35507	1.60919	-.29411	-.48031		
1.6500	-.20670	-.31526	1.65948	-.27961	-.42638		
1.7000	-.19668	-.27504	1.70976	-.26605	-.37205		
1.7500	-.18718	-.23432	1.76005	-.25320	-.31697		
1.8000	-.17805	-.19274	1.81034	-.24084	-.26072	-.00229	-.09760
1.8500	-.16906	-.14995	1.86063	-.22869	-.20284	-.00456	-.19353
1.9000	-.15996	-.10554	1.91091	-.21638	-.14277	-.00531	-.28267
1.9500	-.15041	-.05902	1.96120	-.20346	-.07983	-.00292	-.37892
2.0000	-.13991	-.00978	2.01149	-.18926	-.01323	.00378	-.48065
2.0500	-.12778	.04287	2.06177	-.17285	.05799	.01317	.42161
2.1000	-.11299	.09977	2.11206	-.15284	.13496	.02201	.33701
2.1500	-.09400	.16186	2.16235	-.12715	.21895	.02865	.26865
2.2000	-.06843	.23006	2.21264	-.09256	.31120	.03332	.21489
2.2500	-.03265	.30497	2.26292	-.04417	.41254	.03681	.17258
2.3000	.01878	.38616	2.31321	.02540	.52228	.03974	.13880
2.3500	.09353	.47014	2.36350	.12651	.63596	.04255	.11132
2.4000	.20857	.54781	2.41378	.27131	.74103	.04549	.08857
2.4500	.34537	.59993	2.46407	.46719	.81153	.04873	.06946
2.5000	.51835	.59827	2.51436	.70118	.80929	.05238	.05323
2.5500	.68381	.52222	2.56465	.92500	.70641	.05652	.03941
2.6000	.80430	.38061	2.61493	1.08799	.51485	.06099	.02686
2.6500	.82625	.23724	2.66522	1.11767	.32091	.06642	.01789
2.7000	.79993	.11743	2.71551	1.08207	.15884	.07214	.00997
2.7500	.74644	.04006	2.76579	1.00972	.05420	.07826	.00396
2.8000	.68878	-.00072	2.81608	.93171	-.00098	.08455	-.00008
2.8500	.63795	-.01588	2.86637	.86296	-.02149	.09069	-.00214
2.9000	.59755	-.01481	2.91666	.80831	-.02003	.09626	-.00227
2.9500	.56776	-.00408	2.96694	.76801	-.00552	.10082	-.00069
3.0000	.54756	.01200	3.01723	.74069	.01623	.10397	.00218

TABLE 4

THEORETICAL NOZZLE ADMITTANCES

MACH NUMBER = .30 SVN = 1.8413 GAMMA = 1.4

NOZZLE ANGLE = 15.0 RADII OF CURVATURE: THROAT = .4396 ENTRANCE = .4396

XC	YR	YI	W	SYR	SYI	ALPHA	BETA
1.6000	-.24760	-.28621	1.61630	-.32619	-.37705		
1.5500	-.26503	-.32676	1.56579	-.34915	-.43047		
1.6000	-.24760	-.28621	1.61630	-.32619	-.37705		
1.6500	-.23052	-.24526	1.66681	-.30369	-.32310		
1.7000	-.21350	-.20375	1.71732	-.28126	-.26841		
1.7500	-.19620	-.16153	1.76783	-.25847	-.21279	.02599	-.11196
1.8000	-.17824	-.11845	1.81834	-.23481	-.15604	.06074	-.21953
1.8500	-.15916	-.07438	1.86885	-.20967	-.09799	.10085	-.31796
1.9000	-.13842	-.02924	1.91936	-.18235	-.03852	.14166	-.42583
1.9500	-.11539	.01700	1.96987	-.15200	.02239	.16516	.45746
2.0000	-.08926	.06423	2.02038	-.11759	.08461	.16158	.35337
2.0500	-.05916	.11215	2.07089	-.07794	.14775	.14499	.27607
2.1000	-.02409	.16020	2.12139	-.03173	.21104	.12814	.22092
2.1500	.01702	.20738	2.17190	.02242	.27320	.11467	.18030
2.2000	.06509	.25218	2.22241	.08575	.33222	.10463	.14913
2.2500	.12072	.29246	2.27292	.15903	.38528	.09735	.12439
2.3000	.18373	.32550	2.32343	.24204	.42881	.09218	.10426
2.3500	.25280	.34828	2.37394	.33304	.45883	.08863	.08756
2.4000	.32513	.35811	2.42445	.42832	.47177	.08632	.07352
2.4500	.39653	.35342	2.47496	.52238	.46560	.08498	.06163
2.5000	.46210	.33467	2.52547	.60877	.44089	.08441	.05152
2.5500	.51745	.30449	2.57598	.68168	.40113	.08446	.04292
2.6000	.55978	.26721	2.62649	.73745	.35202	.08499	.03564
2.6500	.58851	.22767	2.67700	.77530	.29994	.08589	.02956
2.7000	.60503	.19010	2.72751	.79706	.25043	.08706	.02456
2.7500	.61188	.15737	2.77802	.80609	.20732	.08839	.02056
2.8000	.61199	.13095	2.82853	.80624	.17251	.08977	.01747
2.8500	.60804	.11117	2.87904	.80102	.14645	.09110	.01522
2.9000	.60217	.09759	2.92954	.79330	.12856	.09228	.01372
2.9500	.59597	.08940	2.98005	.78513	.11778	.09322	.01289
3.0000	.59051	.08565	3.03056	.77794	.11284	.09384	.01259

TABLE 5

THEORETICAL NOZZLE ADMITTANCES

MACH NUMBER = .08 SVN = 1.8413 GAMMA = 1.4

NOZZLE ANGLE = 30.0 RADII OF CURVATURE: THROAT = .4396 ENTRANCE = .4396

XC	YR	YI	W	SYR	SYI	ALPHA	BETA
1.6500	-.07718	-.42330	1.60102	-.10764	-.59035		
1.5500	-.03080	-.45936	1.55099	-.11269	-.64064		
1.6000	-.07718	-.42330	1.60102	-.10764	-.59035		
1.6500	-.07394	-.38828	1.65106	-.10311	-.54150		
1.7000	-.07104	-.35413	1.70109	-.09907	-.49389		
1.7500	-.06844	-.32073	1.75112	-.09545	-.44730		
1.8000	-.06613	-.28793	1.80115	-.09223	-.40156		
1.8500	-.06408	-.25561	1.85118	-.08937	-.35648	-.00181	-.06164
1.9000	-.06227	-.22364	1.90122	-.08684	-.31190	-.00459	-.13107
1.9500	-.06068	-.19190	1.95125	-.08463	-.26763	-.00747	-.18237
2.0000	-.05930	-.16027	2.00128	-.08270	-.22351	-.01084	-.23043
2.0500	-.05812	-.12861	2.05131	-.08106	-.17936	-.01475	-.27927
2.1000	-.05714	-.09680	2.10134	-.07969	-.13500	-.01909	-.33074
2.1500	-.05635	-.06470	2.15138	-.07858	-.09023	-.02346	-.38548
2.2000	-.05574	-.03215	2.20141	-.07774	-.04484	-.02725	-.44303
2.2500	-.05532	.00101	2.25144	-.07715	.00141	-.02975	.49824
2.3000	-.05509	.03496	2.30147	-.07683	.04876	-.03051	.44069
2.3500	-.05505	.06991	2.35150	-.07678	.09750	-.02960	.38669
2.4000	-.05522	.10610	2.40153	-.07701	.14797	-.02748	.33787
2.4500	-.05560	.14381	2.45157	-.07754	.20056	-.02473	.29489
2.5000	-.05621	.18336	2.50160	-.07840	.25572	-.02182	.25762
2.5500	-.05894	.26654	2.55163	-.08220	.37173	-.01652	.19953
2.6000	-.05823	.26975	2.60166	-.08122	.37620	-.01650	.19782
2.6500	-.05798	.28447	2.65170	-.08086	.39673	-.01578	.18979
2.7000	-.06033	.35041	2.70173	-.08413	.48869	-.01294	.16012
2.7500	-.06368	.42666	2.75176	-.08881	.59503	-.01063	.13480
2.8000	-.06634	.49013	2.80179	-.09252	.68356	-.00916	.11864
2.8500	-.06952	.56175	2.85182	-.09696	.78344	-.00788	.10422
2.9000	-.07321	.64392	2.90185	-.10224	.89812	-.00674	.09125
2.9500	-.07777	.74020	2.95189	-.10847	1.03231	-.00571	.07949
3.0000	-.08297	.85556	3.00192	-.11571	1.19319	-.00478	.06872

THEORETICAL NOZZLE ADMITTANCES

MACH NUMBER = .16 SVN = 1.8413 GAMMA = 1.4

NOZZLE ANGLE = 30.0 RADII OF CURVATURE: THROAT = .4396 ENTRANCE = .4396

XG	YR	YI	W	SYR	SYI	ALPHA	BETA
1.6000	-.14000	-.37806	1.60409	-.19302	-.52123		
1.5500	-.14731	-.41403	1.55396	-.20310	-.57083		
1.6000	-.14000	-.37806	1.60409	-.19302	-.52123		
1.6500	-.13330	-.34284	1.65422	-.18378	-.47268		
1.7000	-.12712	-.30824	1.70435	-.17527	-.42498		
1.7500	-.12141	-.27413	1.75447	-.16739	-.37795		
1.8000	-.11609	-.24037	1.80460	-.16005	-.33140		
1.8500	-.11109	-.20682	1.85473	-.15317	-.28515	.00023	-.11206
1.9000	-.10637	-.17336	1.90486	-.14666	-.23901	-.00039	-.18165
1.9500	-.10186	-.13985	1.95499	-.14044	-.19281	-.00137	-.24273
2.0000	-.09750	-.10614	2.00511	-.13443	-.14634	-.00242	-.30349
2.0500	-.09323	-.07209	2.05524	-.12854	-.09940	-.00323	-.36629
2.1000	-.08898	-.03754	2.10537	-.12268	-.05176	-.00342	-.43102
2.1500	-.08467	-.00231	2.15550	-.11673	-.00319	-.00275	-.49585
2.2000	-.08020	.03378	2.20562	-.11057	.04657	-.00125	.44191
2.2500	-.07547	.07095	2.25575	-.10406	.09782	.00082	.38471
2.3000	-.07035	.10943	2.30588	-.09700	.15087	.00308	.33398
2.3500	-.06468	.14949	2.35601	-.08917	.20610	.00527	.29005
2.4000	-.05823	.19143	2.40614	-.08028	.26393	.00725	.25246
2.4500	-.05074	.23560	2.45626	-.06995	.32483	.00899	.22042
2.5000	-.04186	.28240	2.50639	-.05771	.38935	.01051	.19304
2.5500	-.03112	.33228	2.55652	-.04290	.45812	.01185	.16953
2.6000	-.01790	.38576	2.60665	-.02468	.53185	.01305	.14920
2.6500	.00364	.44998	2.65677	.00502	.67555	.01305	.12017
2.7000	.01964	.50587	2.70690	.02700	.69745	.01520	.11589
2.7500	.04667	.57378	2.75703	.06435	.79108	.01621	.10209
2.8000	.08190	.64766	2.80716	.11292	.89294	.01722	.08970
2.8500	.12832	.72781	2.85729	.17692	1.00345	.01823	.07871
2.9000	.19000	.81387	2.90741	.26196	1.12210	.01927	.06871
2.9500	.27238	.90416	2.95754	.37553	1.24668	.02035	.05961
3.0000	.38226	.99449	3.00767	.52703	1.37111	.02149	.05129

THEORETICAL NOZZLE ADMITTANCES

MACH NUMBER = .20 SVN = 1.8413 GAMMA = 1.4

NOZZLE ANGLE = 30.0 RADII OF CURVATURE; THROAT = .4396 ENTRANCE = .4396

X	YR	YI	W	SYR	SYI	ALPHA	BETA
1.5000	-.17071	-.31512	1.60919	-.23092	-.42627		
1.5500	-.16238	-.35100	1.65890	-.24671	-.47480		
1.6000	-.17071	-.31512	1.60919	-.23092	-.42627		
1.6500	-.15965	-.27976	1.65948	-.21595	-.37843		
1.7000	-.14907	-.24479	1.70976	-.20164	-.33113		
1.7500	-.13885	-.21012	1.76005	-.18783	-.28423		
1.8000	-.12889	-.17563	1.81034	-.17436	-.23758	.02375	-.10113
1.8500	-.11908	-.14123	1.86063	-.16107	-.19104	.04719	-.19270
1.9000	-.10928	-.10681	1.91091	-.14783	-.14449	.06763	-.26847
1.9500	-.09939	-.07228	1.96120	-.13445	-.09777	.08647	-.34303
2.0000	-.08928	-.03753	2.01149	-.12077	-.05077	.10136	-.41916
2.0500	-.07881	-.00248	2.06177	-.10661	-.00335	.10930	-.49481
2.1000	-.06783	.03298	2.11206	-.09176	.04461	.10940	.43463
2.1500	-.05618	.06894	2.16235	-.07600	.09325	.10376	.37298
2.2000	-.04366	.10547	2.21264	-.05907	.14267	.09549	.32127
2.2500	-.03007	.14266	2.26292	-.04068	.19298	.08683	.27855
2.3000	-.01515	.18058	2.31321	-.02050	.24427	.07889	.24322
2.3500	.00136	.21926	2.36350	.00184	.29659	.07205	.21376
2.4000	.01989	.25872	2.41378	.02678	.34998	.06634	.18893
2.4500	.04052	.29896	2.46407	.05481	.40440	.06163	.16775
2.5000	.06395	.33989	2.51436	.08650	.45977	.05778	.14951
2.5500	.09055	.38138	2.56465	.12249	.51589	.05464	.13365
2.6000	.12084	.42318	2.61493	.16346	.57244	.05210	.11973
2.6500	.15539	.46494	2.66522	.21019	.62893	.05004	.10743
2.7000	.19477	.50612	2.71551	.26347	.68463	.04839	.09648
2.7500	.23957	.54600	2.76579	.32407	.73858	.04707	.08668
2.8000	.29030	.58361	2.81608	.39268	.78946	.04604	.07785
2.8500	.34732	.61772	2.86637	.46982	.83559	.04525	.06986
2.9000	.41075	.64686	2.91665	.55563	.87493	.04467	.06261
2.9500	.48033	.66913	2.96694	.64975	.90514	.04427	.05599
3.0000	.55526	.68281	3.01723	.75110	.92364	.04404	.04994

THEORETICAL NOZZLE ADMITTANCES

MACH NUMBER = .30 SVN = 1.8413 GAMMA = 1.4

NOZZLE ANGLE = 30.0 RADII OF CURVATURE: THROAT = .4396 ENTRANCE = .4396

XC	YR	YI	W	SYR	SYI	ALPHA	BETA
1.6000	-.17075	-.25810	1.61630	-.22495	-.34002		
1.5500	-.18684	-.29289	1.56579	-.24614	-.38585		
1.6000	-.17075	-.25810	1.61630	-.22495	-.34002		
1.6500	-.15521	-.22374	1.66681	-.20447	-.29475		
1.7000	-.14007	-.18974	1.71732	-.18453	-.24996		
1.7500	-.12520	-.15605	1.76783	-.16494	-.20558	.05700	-.08516
1.8000	-.11046	-.12262	1.81834	-.14552	-.16154	.11503	-.15871
1.8500	-.09574	-.08939	1.86885	-.12612	-.11777	.17209	-.21996
1.9000	-.08099	-.05633	1.91936	-.10657	-.07421	.23830	-.28964
1.9500	-.06581	-.02340	1.96987	-.08670	-.03083	.30848	-.39415
2.0000	-.05036	.00943	2.02038	-.06634	.01242	.32525	.45749
2.0500	-.03441	.04218	2.07089	-.04533	.05557	.27667	.34927
2.1000	-.01782	.07487	2.12139	-.02347	.09864	.22773	.28858
2.1500	-.00046	.10750	2.17190	-.00061	.14161	.19090	.24908
2.2000	.01781	.14004	2.22241	.02347	.18449	.16346	.21975
2.2500	.03715	.17247	2.27292	.04894	.22721	.14256	.19627
2.3000	.05770	.20474	2.32343	.07602	.26972	.12629	.17665
2.3500	.07963	.23678	2.37394	.10490	.31194	.11339	.15982
2.4000	.10309	.26850	2.42445	.13580	.35372	.10299	.14516
2.4500	.12823	.29976	2.47496	.16893	.39490	.09450	.13221
2.5000	.15522	.33042	2.52547	.20448	.43529	.08750	.12069
2.5500	.18419	.36027	2.57598	.24265	.47462	.08168	.11037
2.6000	.21527	.38909	2.62649	.28360	.51258	.07679	.10106
2.6500	.24857	.41660	2.67700	.32746	.54883	.07266	.09263
2.7000	.28415	.44250	2.72751	.37434	.58294	.06916	.08496
2.7500	.32204	.46641	2.77802	.42426	.61445	.06617	.07796
2.8000	.36221	.48796	2.82853	.47717	.64284	.06361	.07155
2.8500	.40453	.50673	2.87903	.53293	.66757	.06142	.06566
2.9000	.44883	.52230	2.92954	.59128	.68807	.05953	.06024
2.9500	.49482	.53423	2.98005	.65187	.70379	.05790	.05524
3.0000	.54211	.54213	3.03056	.71416	.71419	.05650	.05062

THEORETICAL NOZZLE ADMITTANCES

MACH NUMBER = .08 SVN = 1.8413 GAMMA = 1.4

NOZZLE ANGLE = 45.0 RADII OF CURVATURE; THROAT = .4396 ENTRANCE = .4396

XC	YR	YI	W	SYR	SYI	ALPHA	BETA
1.6000	-.07331	-.39766	1.60102	-.10224	-.55459		
1.5500	-.07663	-.43183	1.55099	-.10687	-.60225		
1.6000	-.07331	-.39766	1.60102	-.10224	-.55459		
1.6500	-.07033	-.36454	1.65106	-.09809	-.50840		
1.7000	-.06765	-.33234	1.70109	-.09435	-.46350		
1.7500	-.06525	-.30095	1.75112	-.09100	-.41972		
1.8000	-.06308	-.27024	1.80115	-.08798	-.37689		
1.8500	-.06114	-.24012	1.85118	-.08527	-.33487	-.00126	-.06554
1.9000	-.05940	-.21047	1.90122	-.08284	-.29353	-.00342	-.13838
1.9500	-.05784	-.18120	1.95125	-.08067	-.25271	-.00577	-.19091
2.0000	-.05645	-.15222	2.00128	-.07873	-.21230	-.00850	-.23876
2.0500	-.05522	-.12345	2.05131	-.07701	-.17216	-.01160	-.28589
2.1000	-.05413	-.09478	2.10134	-.07550	-.13218	-.01493	-.33392
2.1500	-.05318	-.06613	2.15138	-.07417	-.09222	-.01824	-.38343
2.2000	-.05235	-.03740	2.20141	-.07302	-.05216	-.02116	-.43416
2.2500	-.05165	-.00851	2.25144	-.07203	-.01187	-.02329	-.48518
2.3000	-.05105	.02064	2.30147	-.07120	.02879	-.02438	.46484
2.3500	-.05056	.05016	2.35150	-.07051	.06995	-.02437	.41730
2.4000	-.05017	.08015	2.40153	-.06996	.11178	-.02343	.37330
2.4500	-.04987	.11073	2.45157	-.06955	.15443	-.02186	.33347
2.5000	-.04965	.14204	2.50160	-.06925	.19809	-.01994	.29799
2.5500	-.04952	.17420	2.55163	-.06907	.24295	-.01791	.26665
2.6000	-.04947	.20739	2.60166	-.06899	.28923	-.01592	.23911
2.6500	-.04949	.25713	2.65169	-.06972	.35861	-.01332	.20545
2.7000	-.04953	.27753	2.70173	-.06908	.38705	-.01234	.19364
2.7500	-.04965	.31497	2.75176	-.06924	.43926	-.01081	.17483
2.8000	-.04978	.35428	2.80179	-.06943	.49409	-.00944	.15814
2.8500	-.04993	.39581	2.85182	-.06963	.55200	-.00821	.14328
2.9000	-.05004	.43992	2.90185	-.06979	.61352	-.00712	.12996
2.9500	-.05010	.48706	2.95189	-.06987	.67927	-.00614	.11796
3.0000	-.05003	.53777	3.00192	-.06978	.75000	-.00526	.10710

THEORETICAL NOZZLE ADMITTANCES

MACH NUMBER = .16 SVN = 1.0413 GAMMA = 1.4

NOZZLE ANGLE = 45.0 RADII OF CURVATURE: THROAT = .4396 ENTRANCE = .4396

XC	YR	YI	W	SYR	SYI	ALPHA	BETA
1.6000	-.12445	-.34578	1.60409	-.17158	-.47673		
1.5500	-.13140	-.38009	1.55396	-.18116	-.52404		
1.6000	-.12445	-.34578	1.60409	-.17158	-.47673		
1.6500	-.11802	-.31231	1.65422	-.16272	-.43058		
1.7000	-.11206	-.27954	1.70435	-.15449	-.38541		
1.7500	-.10648	-.24738	1.75447	-.14681	-.34106		
1.8000	-.10124	-.21571	1.80460	-.13958	-.29740		
1.8500	-.09627	-.18443	1.85473	-.13273	-.25427	.00925	-.12373
1.9000	-.09153	-.15344	1.90486	-.12619	-.21154	.01413	-.19887
1.9500	-.08696	-.12264	1.95499	-.11989	-.16909	.01768	-.26271
2.0000	-.08252	-.09195	2.00511	-.11378	-.12677	.02049	-.32369
2.0500	-.07817	-.06126	2.05524	-.10778	-.08446	.02260	-.38393
2.1000	-.07385	-.03049	2.10537	-.10182	-.04203	.02393	-.44336
2.1500	-.06952	.00047	2.15550	-.09585	.00064	.02445	.49916
2.2000	-.06512	.03170	2.20562	-.08978	.04371	.02426	.44509
2.2500	-.06059	.06332	2.25575	-.08354	.08730	.02358	.39561
2.3000	-.05588	.09542	2.30588	-.07704	.13155	.02263	.35136
2.3500	-.05091	.12811	2.35601	-.07018	.17662	.02162	.31239
2.4000	-.04560	.16151	2.40614	-.06287	.22268	.02065	.27838
2.4500	-.03987	.19575	2.45626	-.05496	.26988	.01981	.24881
2.5000	-.03360	.23094	2.50639	-.04633	.31841	.01910	.22309
2.5500	-.02668	.26725	2.55652	-.03679	.36846	.01852	.20065
2.6000	-.01896	.30480	2.60665	-.02614	.42024	.01807	.18099
2.6500	-.01027	.34378	2.65677	-.01416	.47397	.01773	.16369
2.7000	-.00039	.38434	2.70690	-.00054	.52989	.01748	.14836
2.7500	.01091	.42667	2.75703	.01504	.58826	.01731	.13473
2.8000	.02395	.47096	2.80716	.03302	.64932	.01722	.12252
2.8500	.03908	.51748	2.85729	.05388	.71340	.01718	.11154
2.9000	.05676	.56626	2.90741	.07825	.78071	.01719	.10162
2.9500	.07752	.61764	2.95754	.10684	.85155	.01725	.09261
3.0000	.10205	.67176	3.00767	.14070	.92617	.01736	.08440

THEORETICAL NOZZLE ADMITTANCES

MACH NUMBER = .24 SVN = 1.8413 GAMMA = 1.4

NOZZLE ANGLE = 45.0 RADIUS OF CURVATURE: THROAT = .4396 ENTRANCE = .4396

XS	YR	YI	W	SYR	SYI	ALPHA	BETA
1.6700	-.14625	-.28945	1.60919	-.19783	-.39155		
1.5500	-.13720	-.32333	1.55090	-.21265	-.43738		
1.6000	-.14525	-.28945	1.60919	-.19783	-.39155		
1.6500	-.13506	-.25622	1.65948	-.18378	-.34660		
1.7000	-.12595	-.22356	1.70976	-.17037	-.30241		
1.7500	-.11640	-.19136	1.76005	-.15746	-.25886		
1.8000	-.10715	-.15956	1.81034	-.14494	-.21584	.03903	-.10207
1.8500	-.09809	-.12808	1.86063	-.13269	-.17325	.07460	-.19354
1.9000	-.08916	-.09683	1.91091	-.12060	-.13099	.10248	-.26868
1.9500	-.08026	-.06576	1.96120	-.10858	-.08895	.12531	-.34256
2.0000	-.07134	-.03479	2.01149	-.09650	-.04706	.14043	-.41772
2.0500	-.06230	-.00386	2.06177	-.08420	-.00522	.14519	-.49122
2.1000	-.05308	.02710	2.11206	-.07180	.03666	.14039	.44200
2.1500	-.04358	.05814	2.16235	-.05895	.07864	.12984	.38494
2.2000	-.03372	.08931	2.21264	-.04561	.12081	.11733	.33759
2.2500	-.02341	.12067	2.26292	-.03166	.16324	.10512	.29842
2.3000	-.01255	.15228	2.31321	-.01697	.20599	.09416	.26574
2.3500	-.00104	.18416	2.36350	-.00140	.24912	.08472	.23815
2.4000	.01124	.21637	2.41378	.01521	.29269	.07672	.21457
2.4500	.02441	.24893	2.46407	.03302	.33674	.07001	.19419
2.5000	.03860	.28188	2.51436	.05221	.38130	.06438	.17642
2.5500	.05395	.31522	2.56465	.07299	.42640	.05965	.16078
2.6000	.07064	.34896	2.61493	.09556	.47204	.05566	.14693
2.6500	.08884	.38308	2.66522	.12018	.51820	.05230	.13457
2.7000	.10874	.41757	2.71551	.14709	.56485	.04944	.12349
2.7500	.13053	.45236	2.76579	.17657	.61191	.04701	.11350
2.8000	.15446	.48738	2.81608	.20894	.65928	.04493	.10446
2.8500	.18076	.52251	2.86637	.24451	.70680	.04315	.09622
2.9000	.20967	.55759	2.91666	.28362	.75426	.04162	.08871
2.9500	.24146	.59243	2.96694	.32663	.80139	.04030	.08182
3.0000	.30114	.66180	3.01723	.40735	.89523	.03763	.07104

MACH NUMBER = .39 SVN = 1.8413 GAMMA = 1.4

NOZZLE ANGLE = 45.0 RADII OF CURVATURE: THROAT = .4396 ENTRANCE = .4396

XC	YR	YI	M	SYR	SYI	ALPHA	BETA
1.6000	-.14936	-.24486	1.61630	-.19677	-.32257		
1.5500	-.16442	-.27807	1.56579	-.21660	-.36633		
1.6000	-.14936	-.24486	1.61630	-.19677	-.32257		
1.6500	-.13488	-.21219	1.66681	-.17769	-.27954		
1.7000	-.12085	-.18001	1.71732	-.15921	-.23714		
1.7500	-.10717	-.14827	1.76783	-.14118	-.19533	.06373	-.07770
1.8000	-.09372	-.11691	1.81834	-.12346	-.15401	.12690	-.14374
1.8500	-.08041	-.08589	1.86885	-.10593	-.11315	.18810	-.19755
1.9000	-.06715	-.05516	1.91936	-.08847	-.07267	.26114	-.25831
1.9500	-.05385	-.02470	1.96987	-.07094	-.03254	.34991	-.35765
2.0000	-.04042	.00554	2.02038	-.05325	.00730	.37856	.46735
2.0500	-.02678	.03559	2.07089	-.03527	.04688	.31024	.34930
2.1000	-.01283	.06546	2.12139	-.01690	.08624	.25080	.29254
2.1500	.00150	.09519	2.17190	.00198	.12540	.20884	.25695
2.2000	.01631	.12477	2.22241	.02149	.16437	.17822	.23045
2.2500	.03167	.15422	2.27292	.04173	.20317	.15498	.20896
2.3000	.04769	.18355	2.32343	.06282	.24180	.13681	.19074
2.3500	.06443	.21273	2.37394	.08488	.28024	.12228	.17489
2.4000	.08201	.24175	2.42445	.10803	.31848	.11046	.16089
2.4500	.10050	.27060	2.47496	.13239	.35648	.10070	.14839
2.5000	.12000	.29922	2.52547	.15809	.39419	.09257	.13714
2.5500	.14061	.32758	2.57598	.18524	.43155	.08571	.12696
2.6000	.16242	.35561	2.62649	.21397	.46847	.07988	.11771
2.6500	.18551	.38323	2.67700	.24440	.50487	.07489	.10926
2.7000	.20999	.41037	2.72751	.27664	.54061	.07059	.10152
2.7500	.23594	.43690	2.77802	.31082	.57557	.06686	.09441
2.8000	.26343	.46271	2.82853	.34703	.60956	.06361	.08786
2.8500	.29253	.48764	2.87904	.38537	.64241	.06076	.08181
2.9000	.32330	.51155	2.92954	.42591	.67391	.05825	.07621
2.9500	.35578	.53424	2.98005	.46870	.70380	.05604	.07101
3.0000	.38999	.55552	3.03056	.51377	.73183	.05408	.06618

September 8, 1972

Dr. R. J. Priem, MS 500-209
NASA
Lewis Research Center
21000 Brookpark Road
Cleveland, Ohio 44135

Dear Dr. Priem:

The following is a summary of the work completed under NASA Grant NGR 11-002-085 during August 1972.

Testing of additional nozzles including two nozzles with half-angles of 15 and 30 degrees and an entrance Mach number of 0.24 and one nozzle with a half-angle of 45 degrees and an entrance Mach number of 0.28 has been completed and the desired nozzle admittances have been obtained. From these tests it was determined that the maximum entrance Mach number attainable with the existing experimental facility is 0.28. However, the admittance data obtained for the nozzles tested to date provide ample information to complete the objectives of the nozzle studies. Plots of these data are being prepared to show the effects of geometry and entrance Mach number on the nozzle admittance values, and to compare the experimental results with theoretical predictions. These plots will be presented in the next monthly report.

Testing of the first liner-nozzle combination was conducted, and the data are being reduced. To obtain accurate phase data necessary for the determination of the local liner admittance, the tape recorder was calibrated to account for the phase shift introduced by head skewing and head stacking offset. This calibration was incorporated into the data reduction computer program to ensure accurate local liner admittance data. Fabrication of the quasi-steady nozzles needed for the liner studies has been initiated.

The nozzle admittance theory has been modified to include the effects of an amplification factor λ. Typical results are shown in Figs. 1 and 2 for representation values of λ obtained from GE-SIP combustion instability studies. The results indicate that varying λ affects the values of the real part of the admittance. Therefore, the amplification factor should be included in the admittance computations where neutrally stable oscillations are not assumed.

In another study, the possibility of correlating admittance data for different nozzles by plotting it versus $S' = \omega L_N/c$, where L_N is the length of the nozzle

convergent section, was investigated. The nozzles examined had an entrance Mach number of 0.08, a radius of curvature to chamber radius ratio of 0.44, and half-angles of 15, 30, and 45 degrees. The results of this study are shown in Figs. 3 and 4 as plots of the real part of the admittance versus the nondimensional frequency S'. According to Figs. 3 and 4, scaling in this manner yields a reasonable correlation of data at low frequencies and a poor correlation of data at high frequencies for both longitudinal and mixed first tangential-longitudinal modes.

Work is in progress on the design of new liners, and additional testing is planned using the existing liner. Results from the liner tests as well as results of the above-mentioned nozzle studies will be included in the next monthly progress report.

Sincerely,

Ben T. Zinn
Professor

tk
Enclosures

cc: Messrs. W. A. Bell
B. R. Daniel
A. J. Smith, Jr.

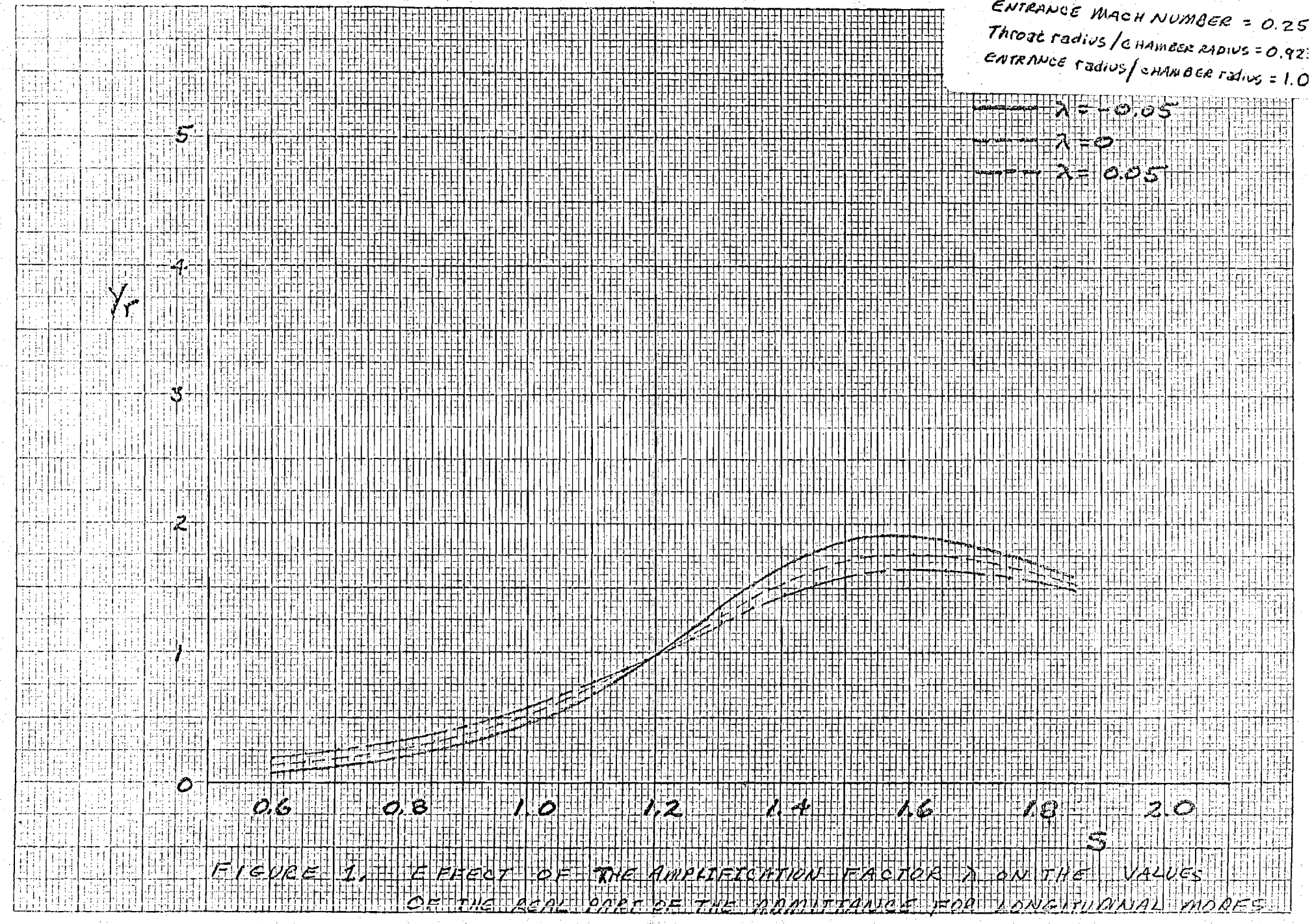

FIGURE 1. - EFFECT OF THE AMPLIFICATION FACTOR λ ON THE VALUES OF THE REAL PART OF THE ADMITTANCE FOR LONGITUDINAL MODES

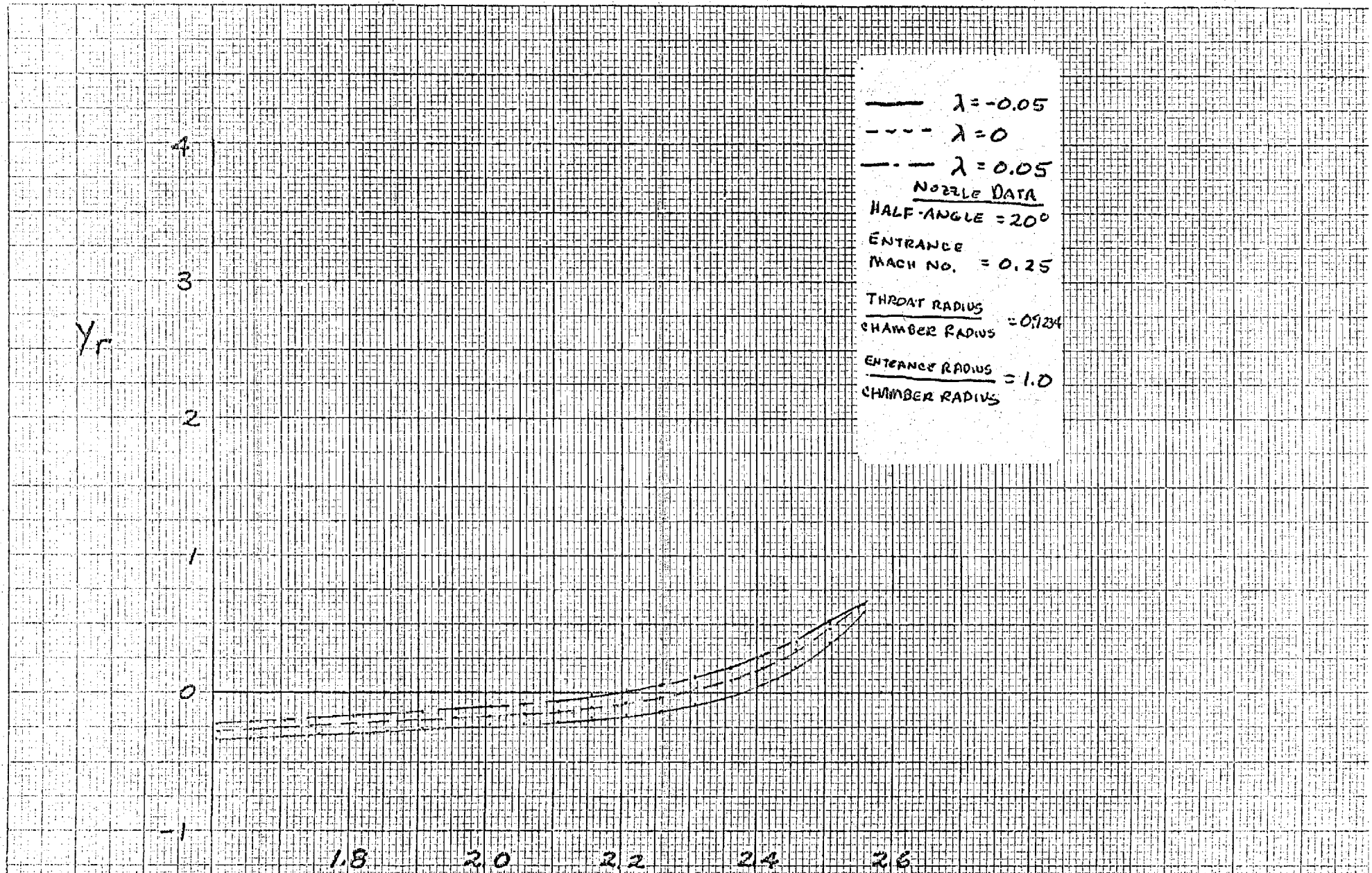

FIGURE 2. EFFECT OF λ ON THE VALUES OF THE REAL PART OF THE ADMITTANCE FOR MIXED FIRST TANGENTIAL-LONGITUDINAL MODES

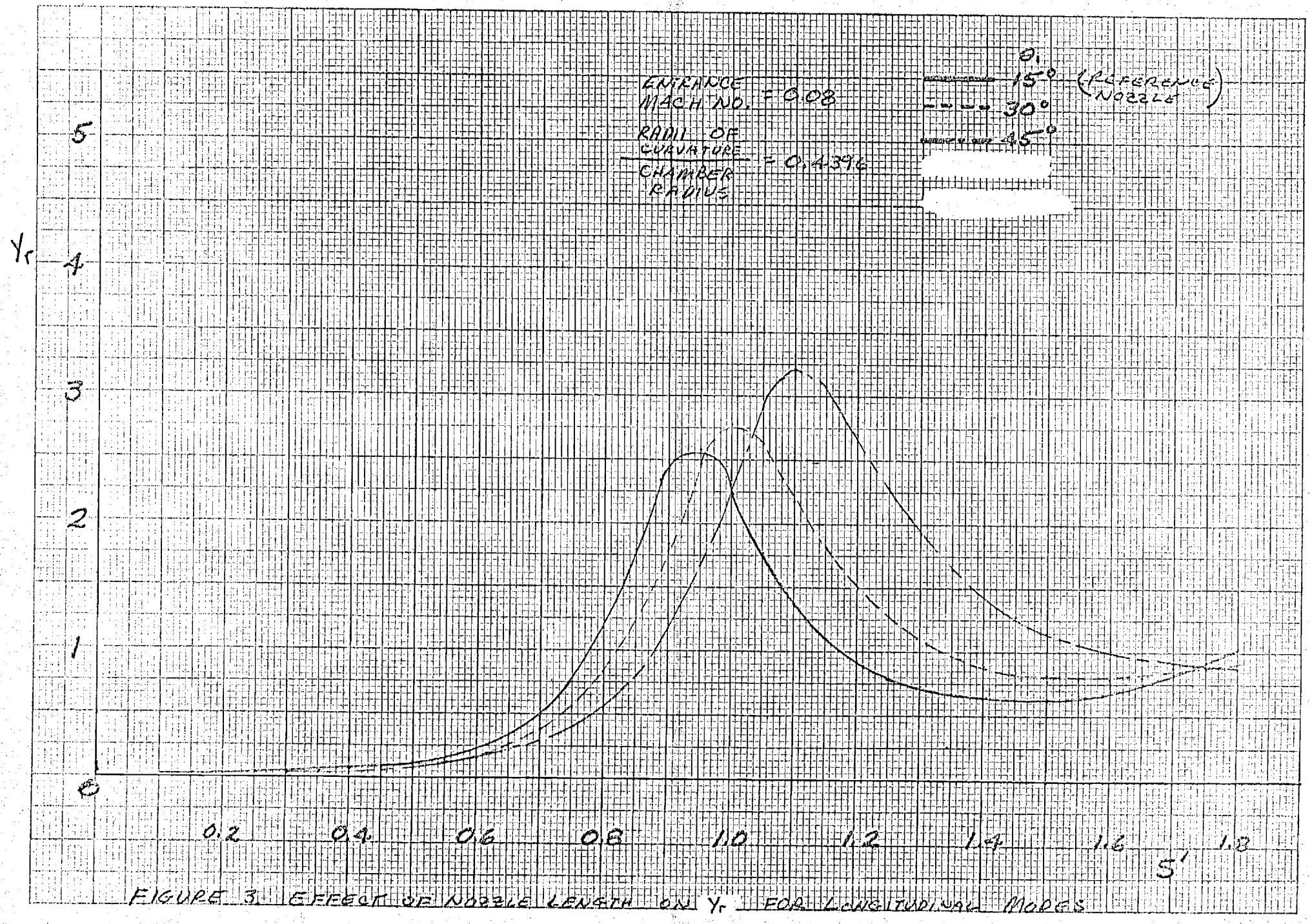

FIGURE 3 EFFECT OF NOZZLE LENGTH ON Y_r FOR LONGITUDINAL MODES

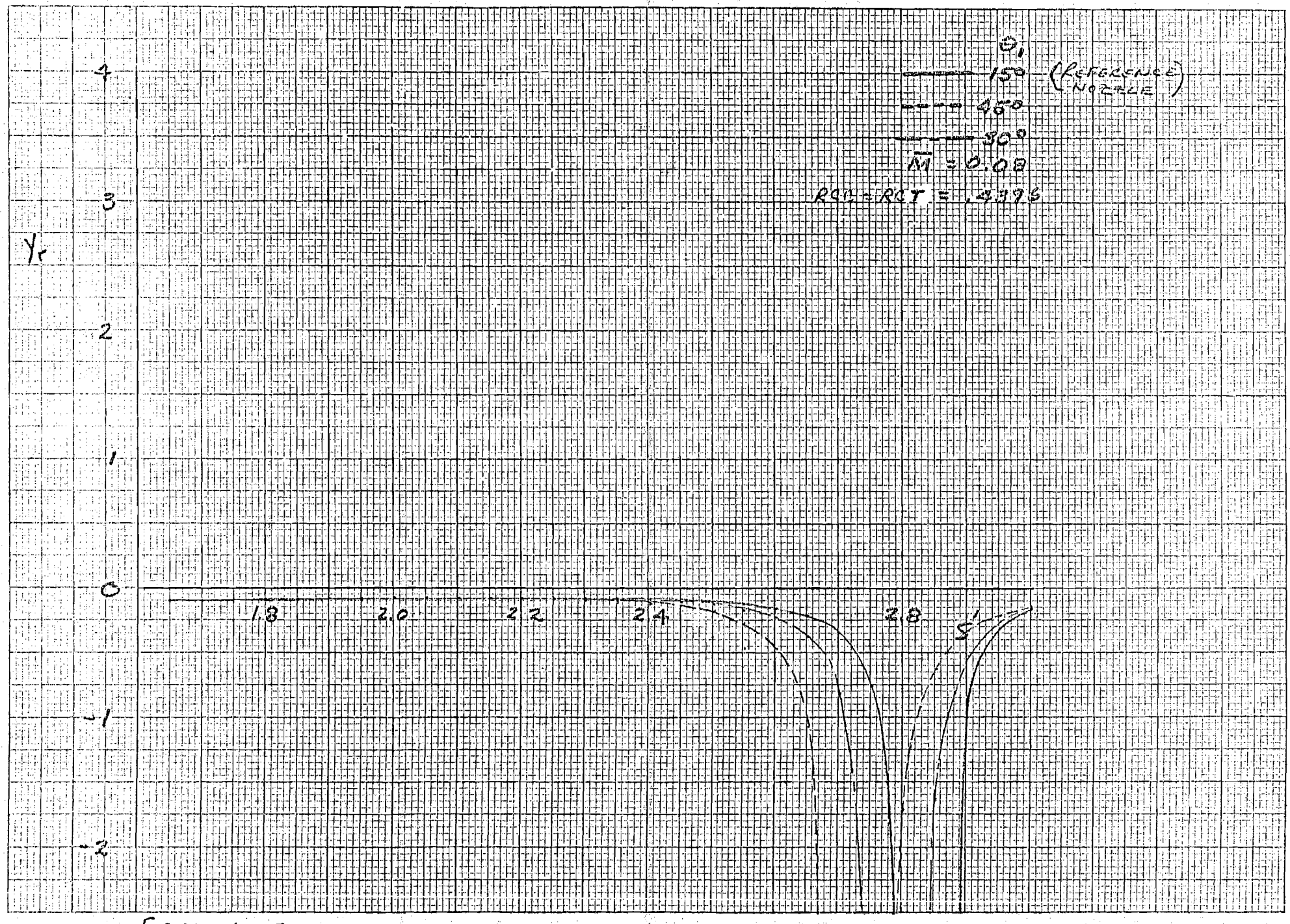

FIGURE 4. EFFECT OF NOZZLE LENGTH ON Y_r FOR MIXED FIRST TANGENTIAL-LONGITUDINAL MODES

October 11, 1972

Dr. R. J. Priem, MS 500-209
NASA
Lewis Research Center
21000 Brookpark Road
Cleveland, Ohio 44135

Dear Dr. Priem:

The following is a summary of the work completed under NASA Grant NGL 11-002-085 during September 1972.

Testing has been completed for the matrix of tested nozzles presented in Table 1. The experimental and theoretical nozzle admittance values for these nozzles are presented as functions of nondimensional frequency S in Figs. 1 through 7. In these figures the effects of nozzle geometry and entrance Mach number are shown for longitudinal and mixed first tangential-longitudinal modes. These data indicate that Crocco's three-dimensional nozzle admittance theory is capable of predicting quantitative nozzle admittance data.

Preliminary test results for the first liner-nozzle combination have been obtained and are currently undergoing analysis. Additional testing on the existing liner is scheduled upon completion of data analysis. Fabrication of the quasi-steady nozzles to be used in the liner studies is in progress. Work is also in progress on the design of new liners. Results from these liner tests will be included in the succeeding monthly progress reports as they become available. In addition, a report discussing the use of Crocco's theory for nozzle admittance determination is currently being prepared.

Sincerely,

William A. Bell
Research Engineer

tk
Enclosures

cc: Dr. B. T. Zinn
Mr. B. R. Daniel
Mr. A. J. Smith, Jr.

Table 1. Tested Nozzles

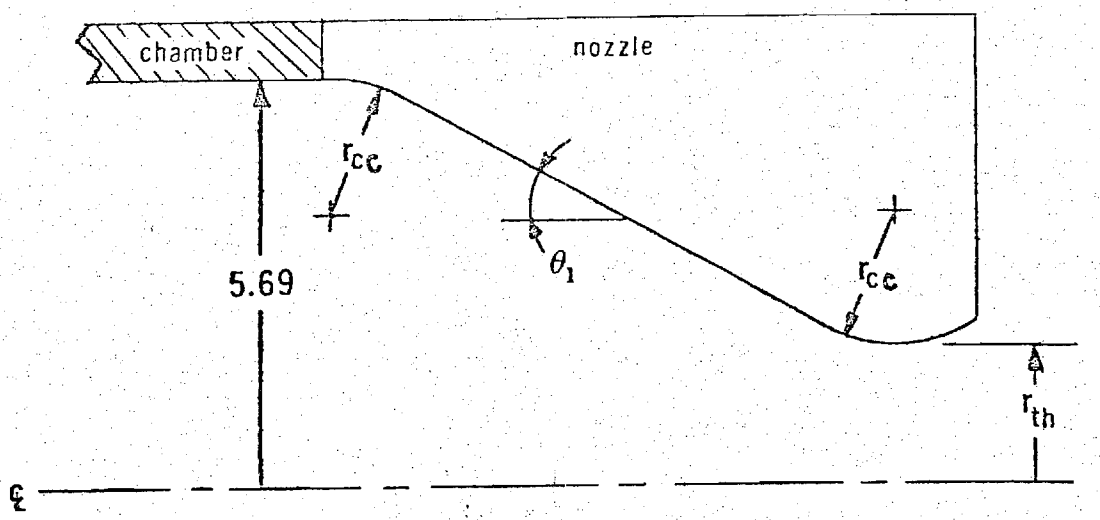

Convergent Half-Angle	Chamber Mach Number			
	0.08	0.16	0.24	0.28
15°	.44,1	.44	.44	
30°	.44	.44,1	.44	
45°	.44	.44	.44	.44

Quantities in boxes indicate values of the ratio r_{cc}/r_c.

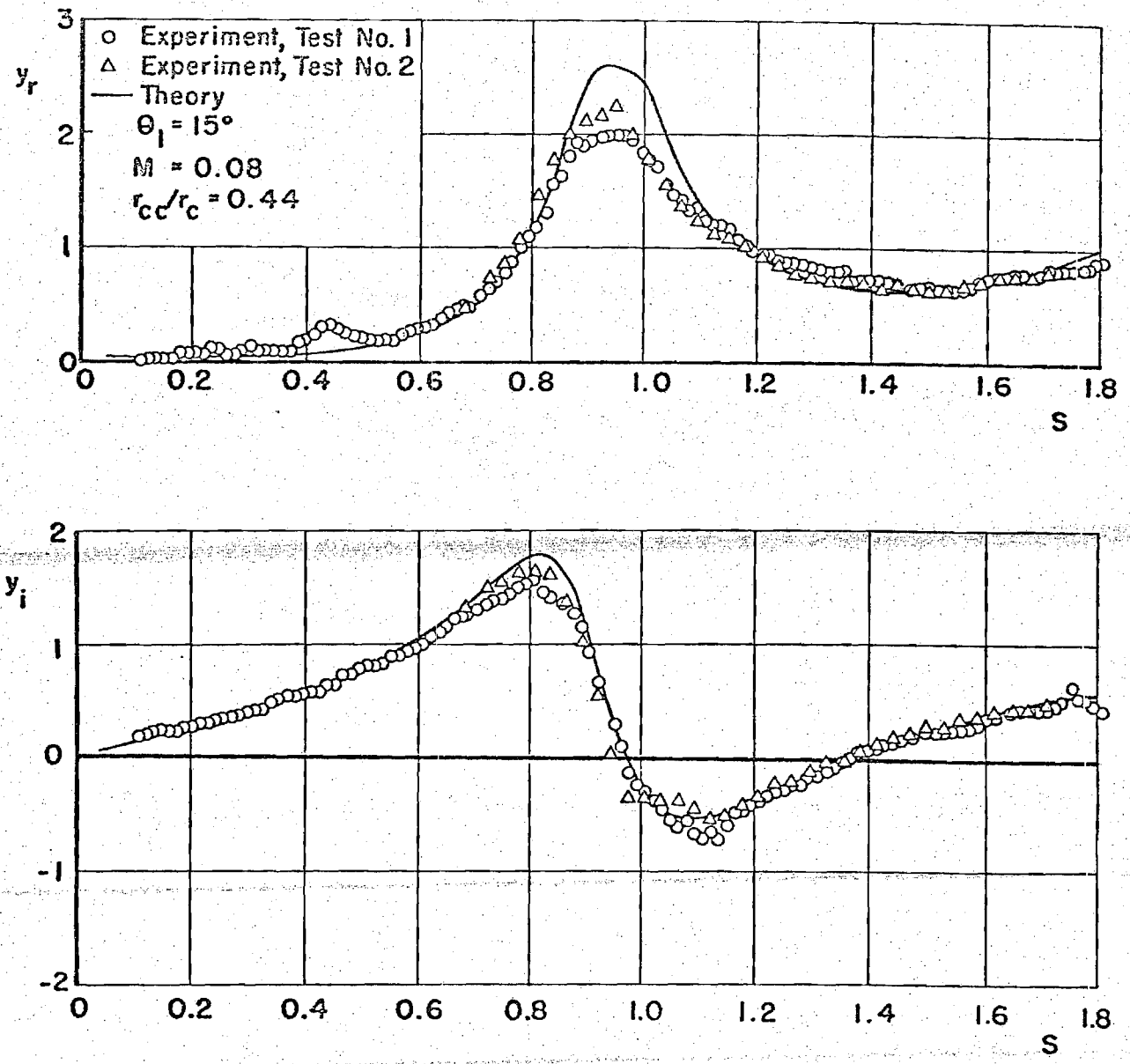

Figure 1. Demonstration of the Test-to-Test Repeatability and Comparison of the Theoretical and Experimental Nozzle Admittance Results for Longitudinal Modes

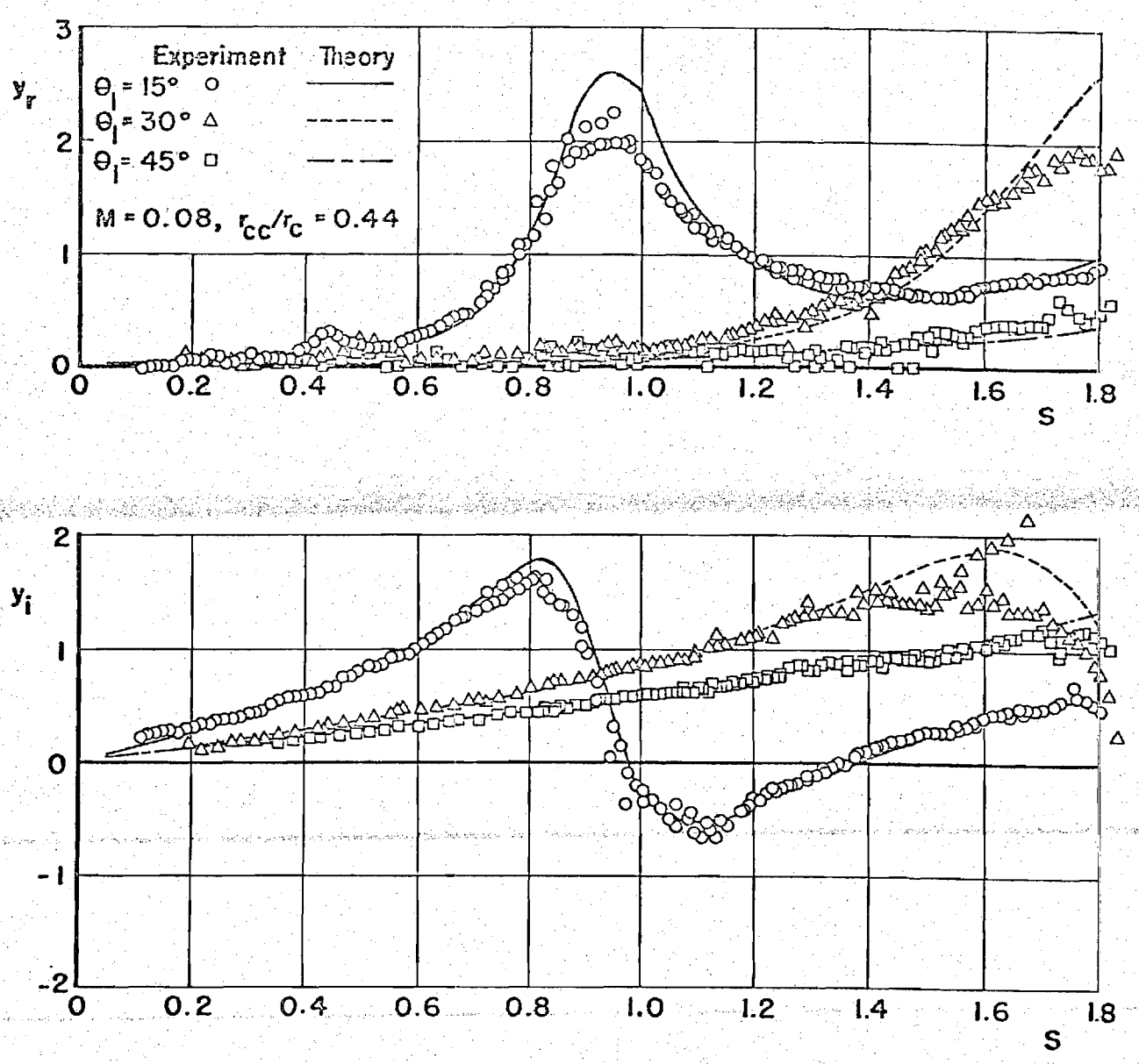

Figure 2. Effect of the Nozzle Half-Angle on the Values of the Admittance for Longitudinal Modes

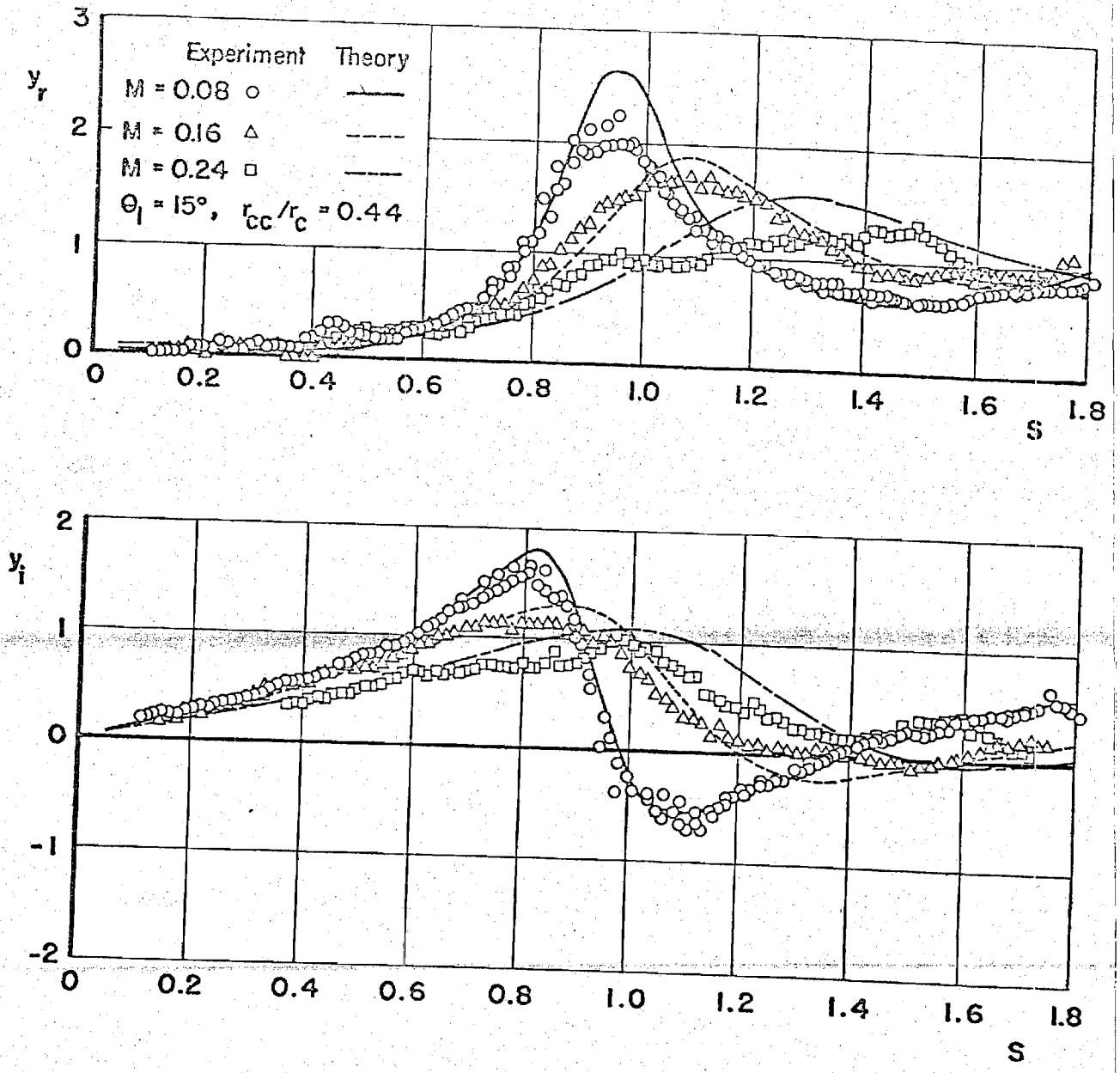

Figure 3. Effect of Chamber Mach Number on the Nozzle Admittance Values for Longitudinal Modes

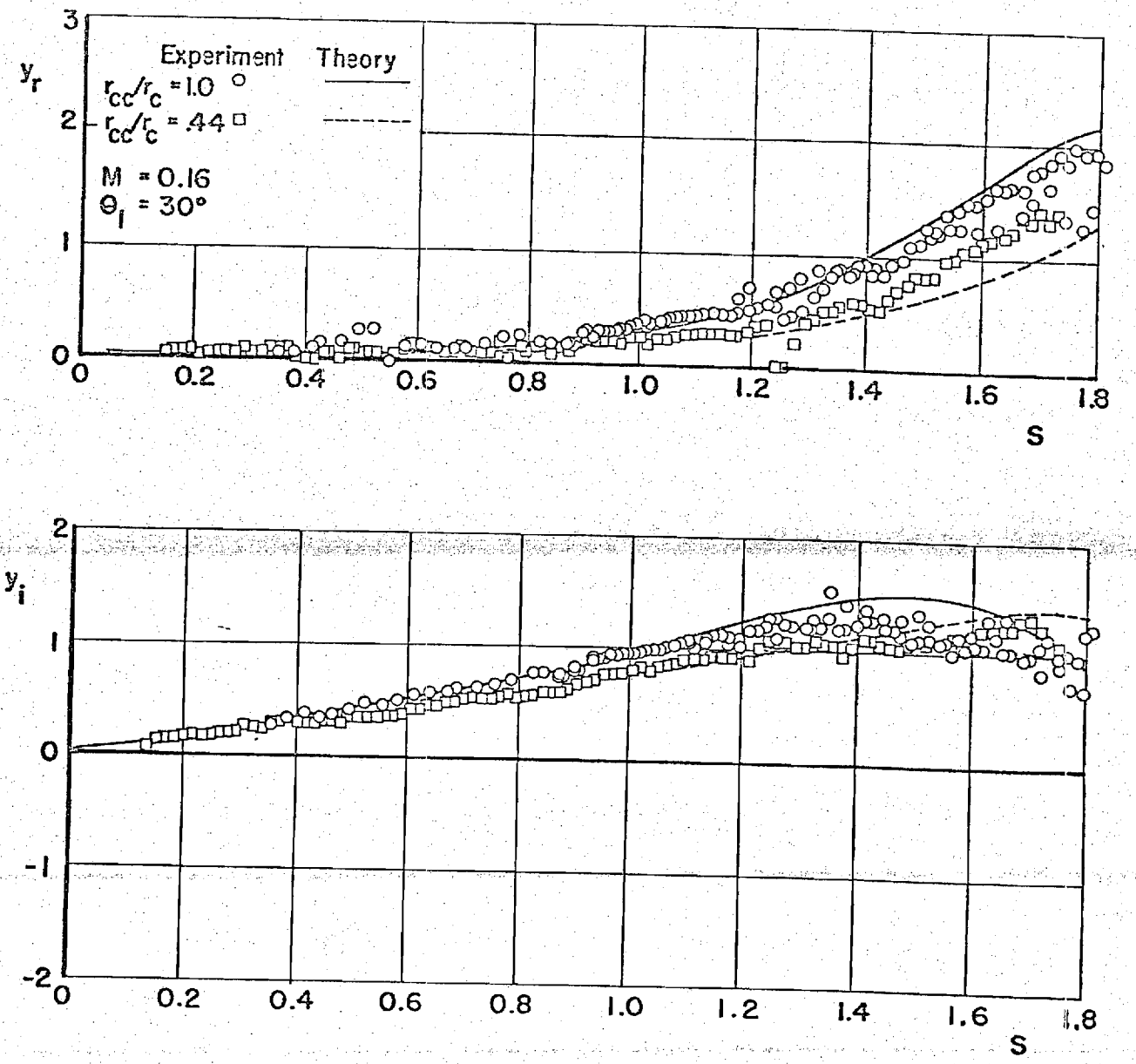

Figure 4. Effect of the Radius of Curvature on the Nozzle Admittance Values for Longitudinal Modes

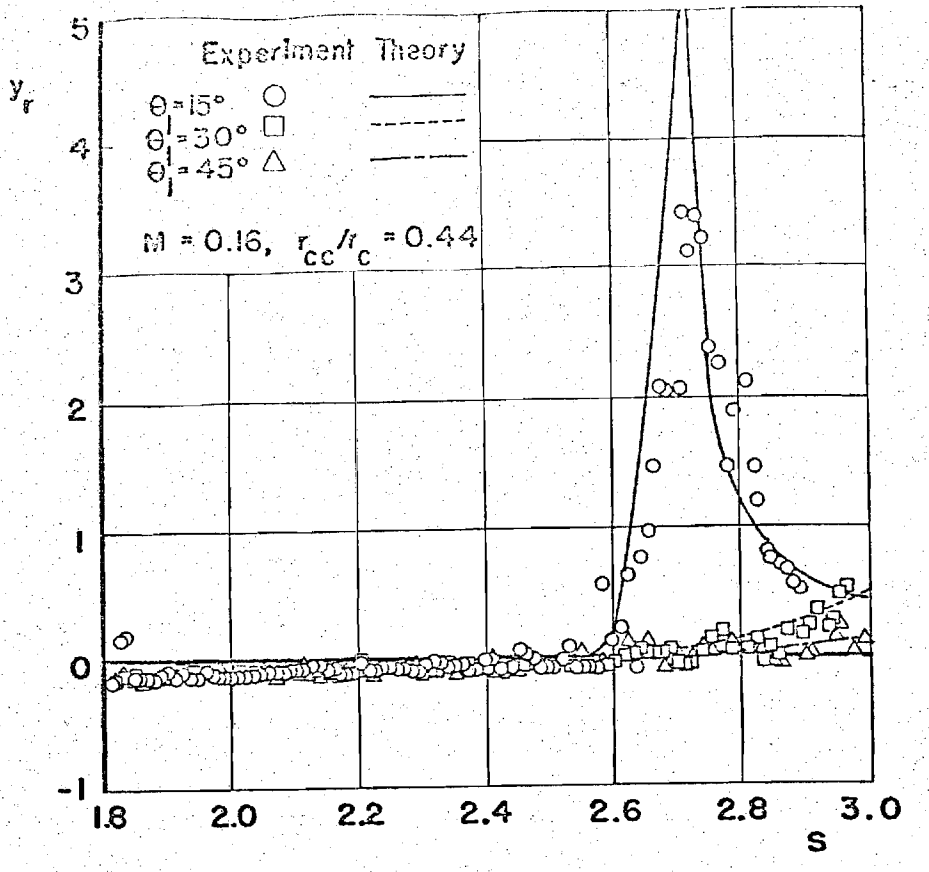

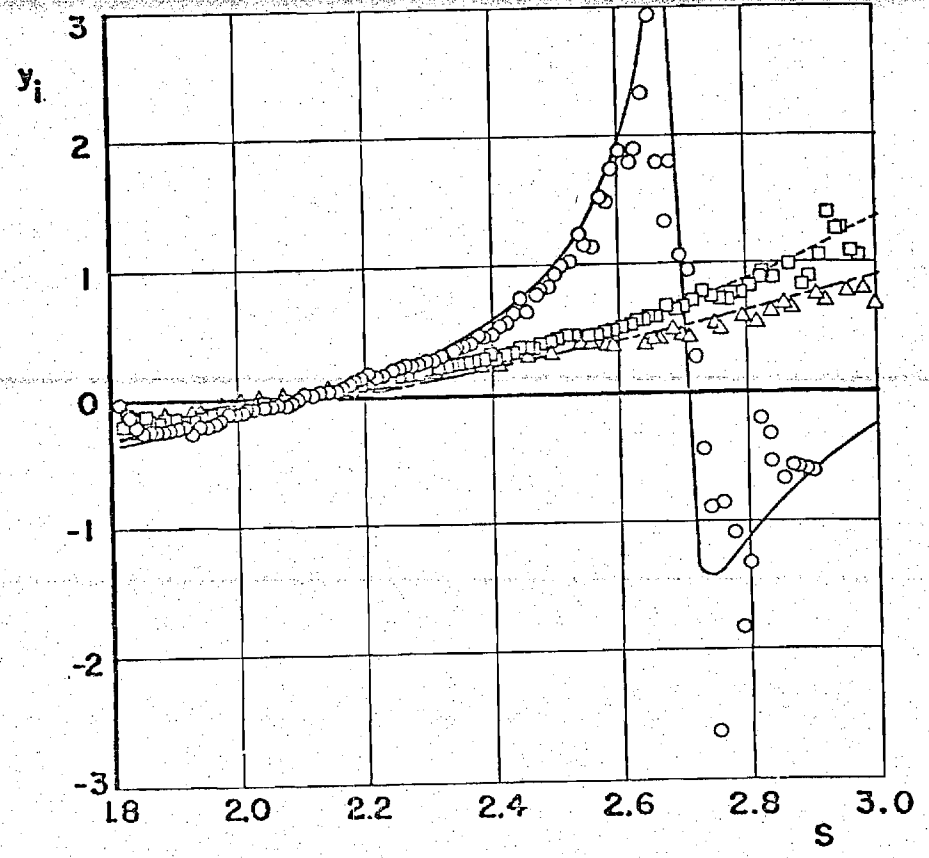

Figure 5. Effect of the Nozzle Half-Angle on the Nozzle Admittance Values for Mixed First Tangential-Longitudinal Modes

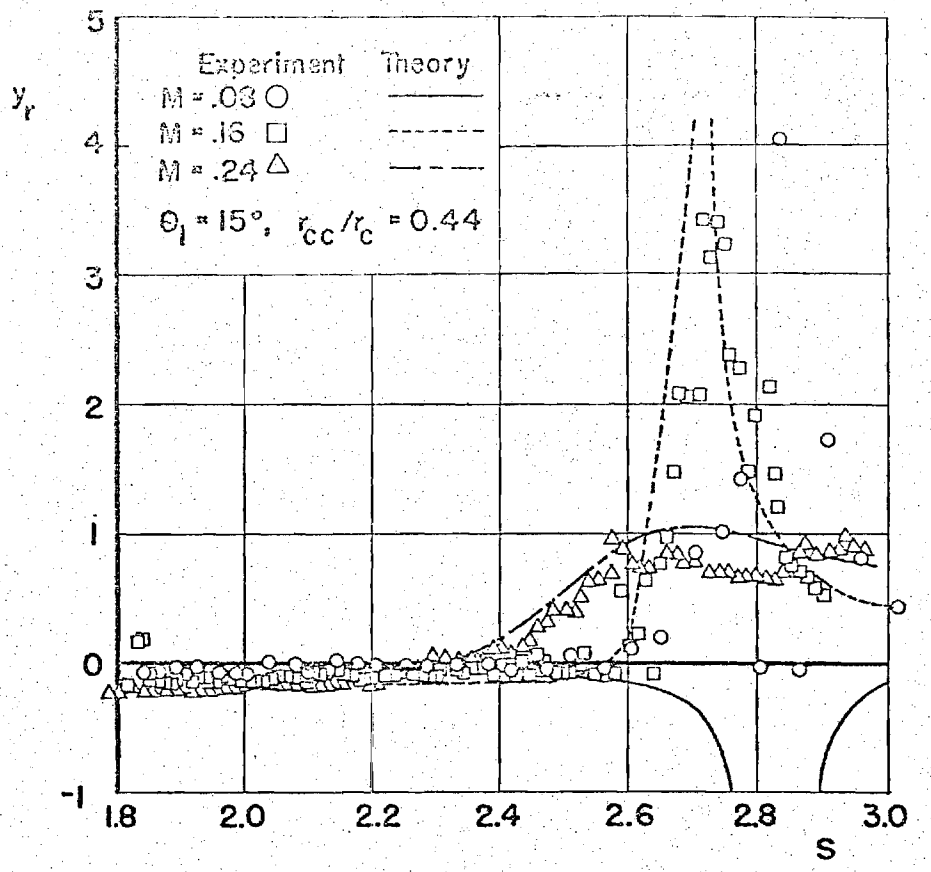

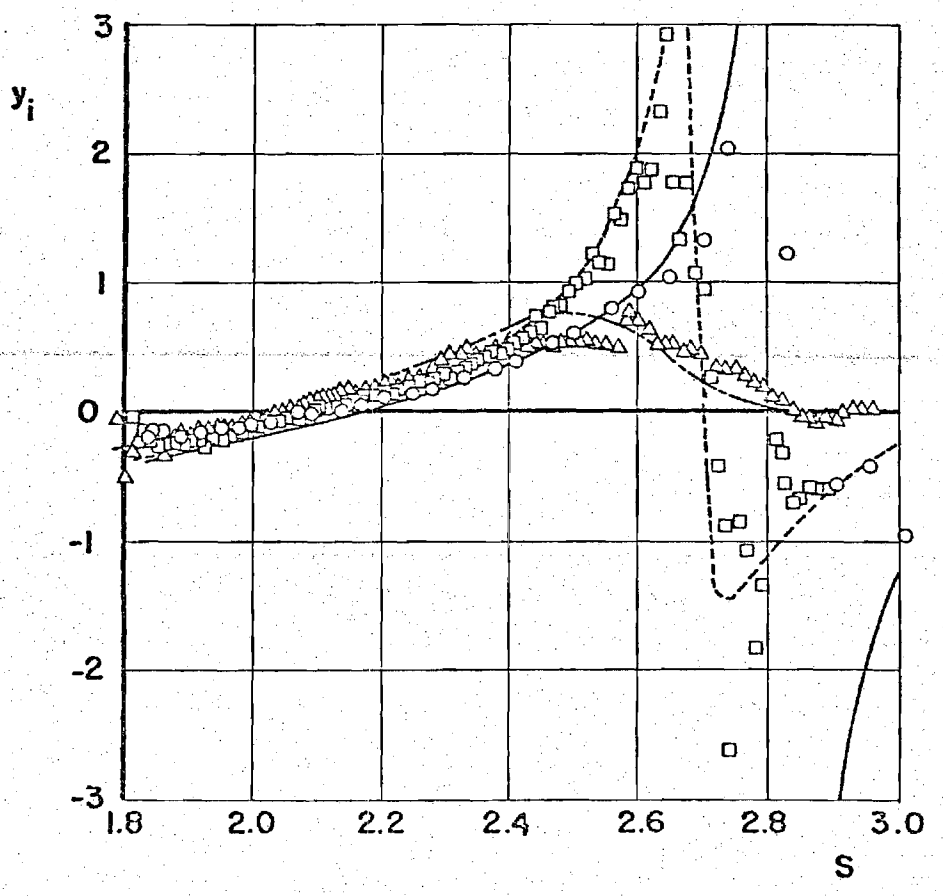

Figure 6. Effect of the Chamber Mach Number on the Nozzle Admittance Values for Mixed First Tangential-Longitudinal Modes

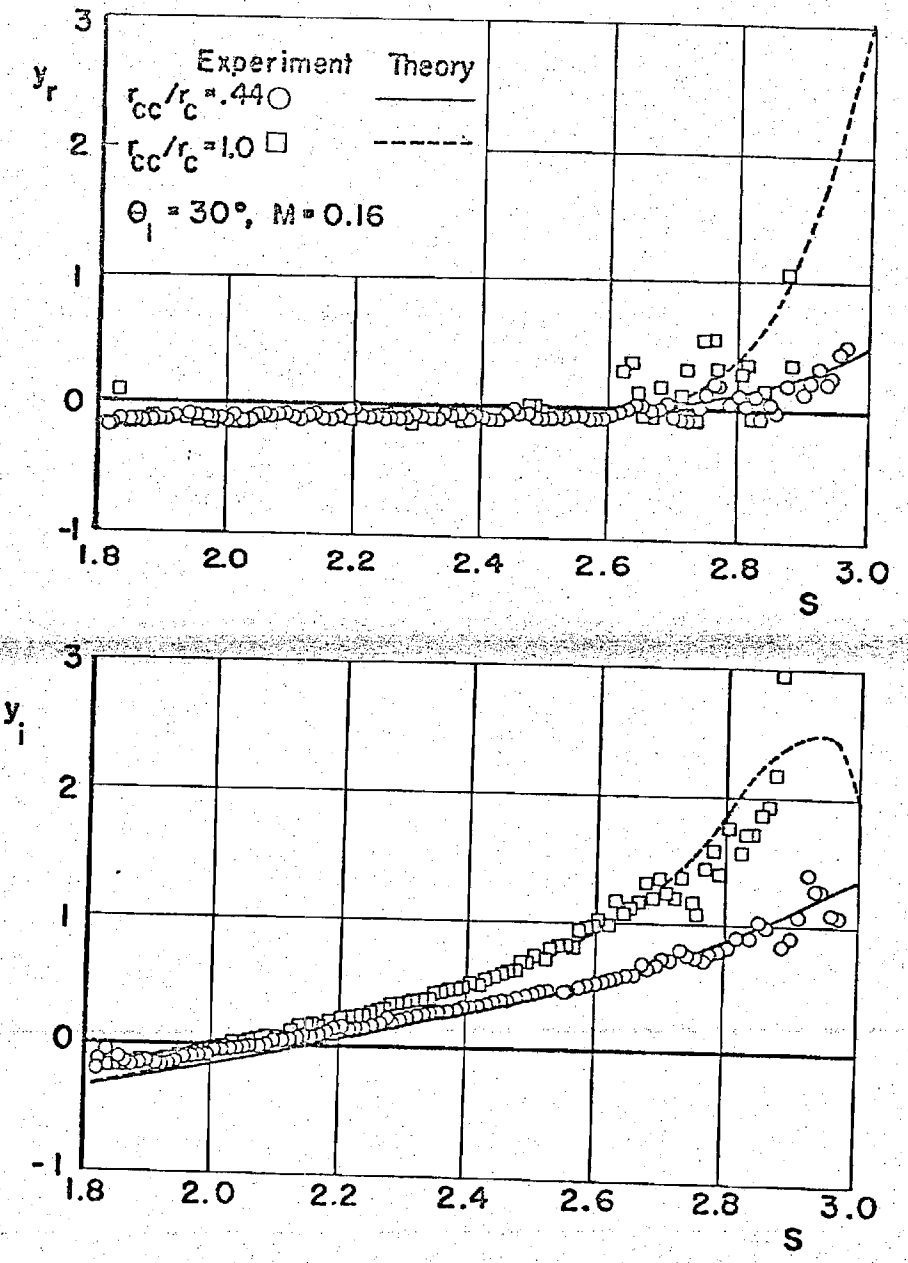

Figure 7. Effect of the Radius of Curvature on the Nozzle Admittance Values for Mixed First Tangential-Longitudinal Modes

November 6, 1972

Dr. R. J. Priem, MS 500-209
NASA
Lewis Research Center
21000 Brookpark Road
Cleveland, Ohio 44135

Dear Dr. Priem:

This report is a summary of the work completed under NASA Grant NGL 11-002-085 during October 1972.

A report is being prepared which describes the analytical technique and computer program used to determine the nozzle admittance. The admittance values are obtained from Crocco's theory which has been modified to include the effects of a decay coefficient. A copy of this report will be sent to you shortly for review.

Data obtained in the tests conducted with the first liner-nozzle combination have been reduced, and they are presented in Figs. 1 through 4, where they are compared with data obtained in the presence of a nozzle only. In Figs. 1 and 2 the influence of the liner on the admittance parameters, α and β, is shown. In inspecting these data it would be helpful to recall that $\exp(-2\pi\alpha)$ is defined as the ratio of the reflected to the incident wave amplitudes at the liner entrance and $\pi(2\beta + 1)$ is the phase shift between the incident and reflected waves. The significant increase in α caused by the presence of the liner indicates that the liner is absorbing a considerable amount of acoustic energy. Plots of the effect of the liner on the real and imaginary parts of the gross liner admittance are presented in Figs. 3 and 4. These data need further study and they will be analyzed in the future.

Preliminary data needed to compute the local liner admittance have been obtained and a computer program needed for reduction of the data is in preparation.

The available nozzle admittance data and the recently measured gross liner-nozzle admittance data will be sent shortly to Dr. C. E. Mitchell for further analysis. These data will be used by Dr. Mitchell to predict the local liner admittances. The predicted local liner admittances will be then compared with

the measured local liner admittance. These comparisons should provide checks on the validity of the theoretical approach developed by Dr. Mitchell as well as the validity of the experimental procedure used in this program.

The design of the two additional liners required for this program has been completed and fabrication of these liners has been initiated. The absorption characteristics of the three liners to be tested during this investigation are shown in Fig. 5. Liner 1 is a low absorption liner designed for a resonant frequency of 650 Hz. Liners 2 and 3 are designed for a resonant frequency of 850 Hz, but Liner 3 has a greater absorption coefficient than Liner 2. The physical properties of these liners are described in the following table.

	Liner		
	1	2	3
Resonant Frequency, Hz	652	845	844
Maximum Absorption at Resonance	0.41	0.42	1.00
Quality Factor, Q	0.95	1.20	2.98
Liner Length, In.	12.0	12.0	12.0
Liner Thickness, In.	0.50	0.50	1.00
Backing Distance, In.	0.44	0.26	0.74
Orifice Diameter, In.	0.159	0.159	0.875
Open Area Ratio	0.03	0.03	0.22
Total Number of Orifices	660	660	192

During the next month, the report concerned with the evaluation of the nozzle admittance from Crocco's theory will be completed. Testing of Liner 1 will continue and the results will be included in the next monthly report.

Sincerely,

Ben T. Zinn
Professor

tk

Enclosures

cc: Messrs. W. A. Bell
B. R. Daniel
A. J. Smith, Jr.

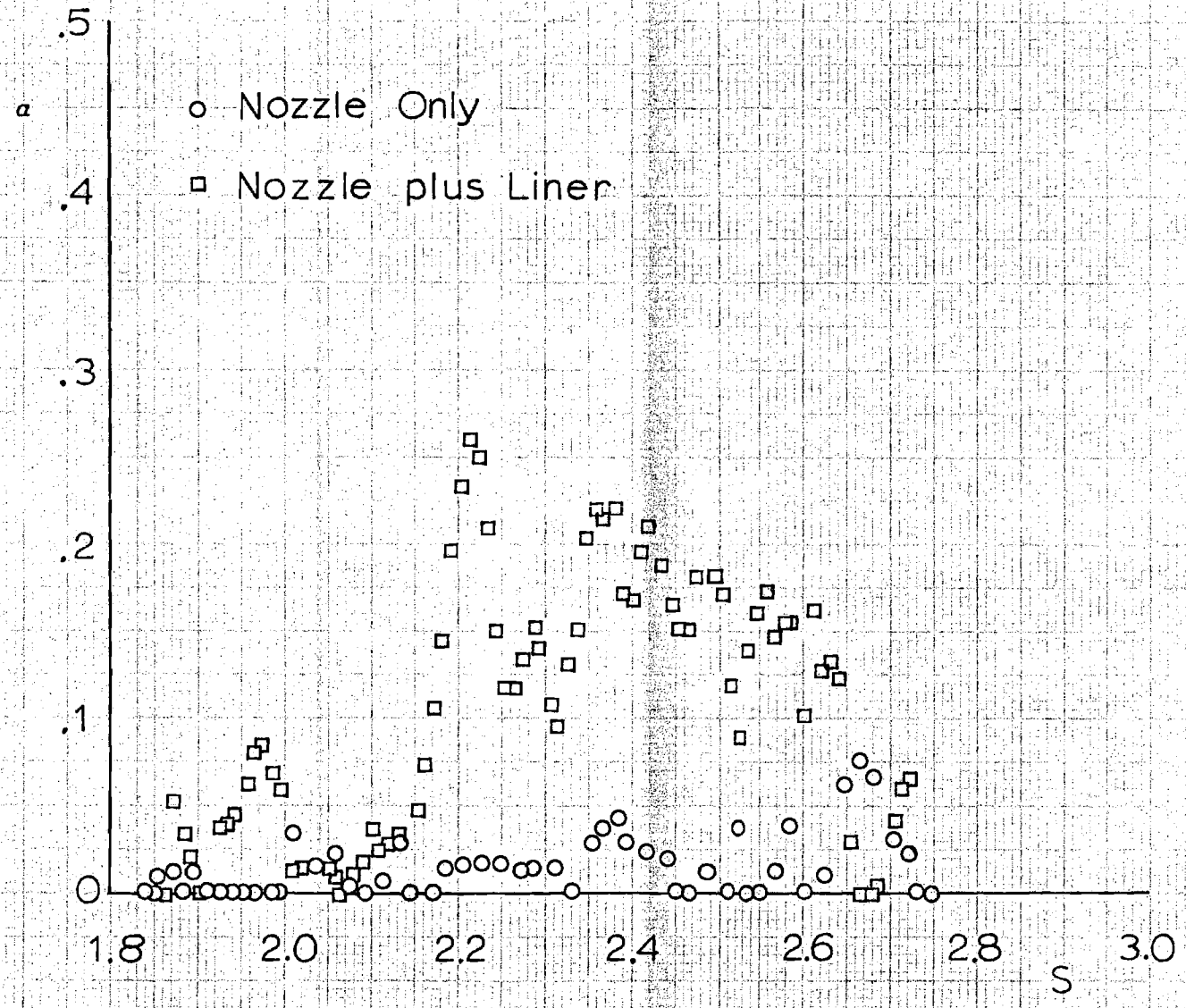

Figure 1. Effect of the Liner on the Values of α

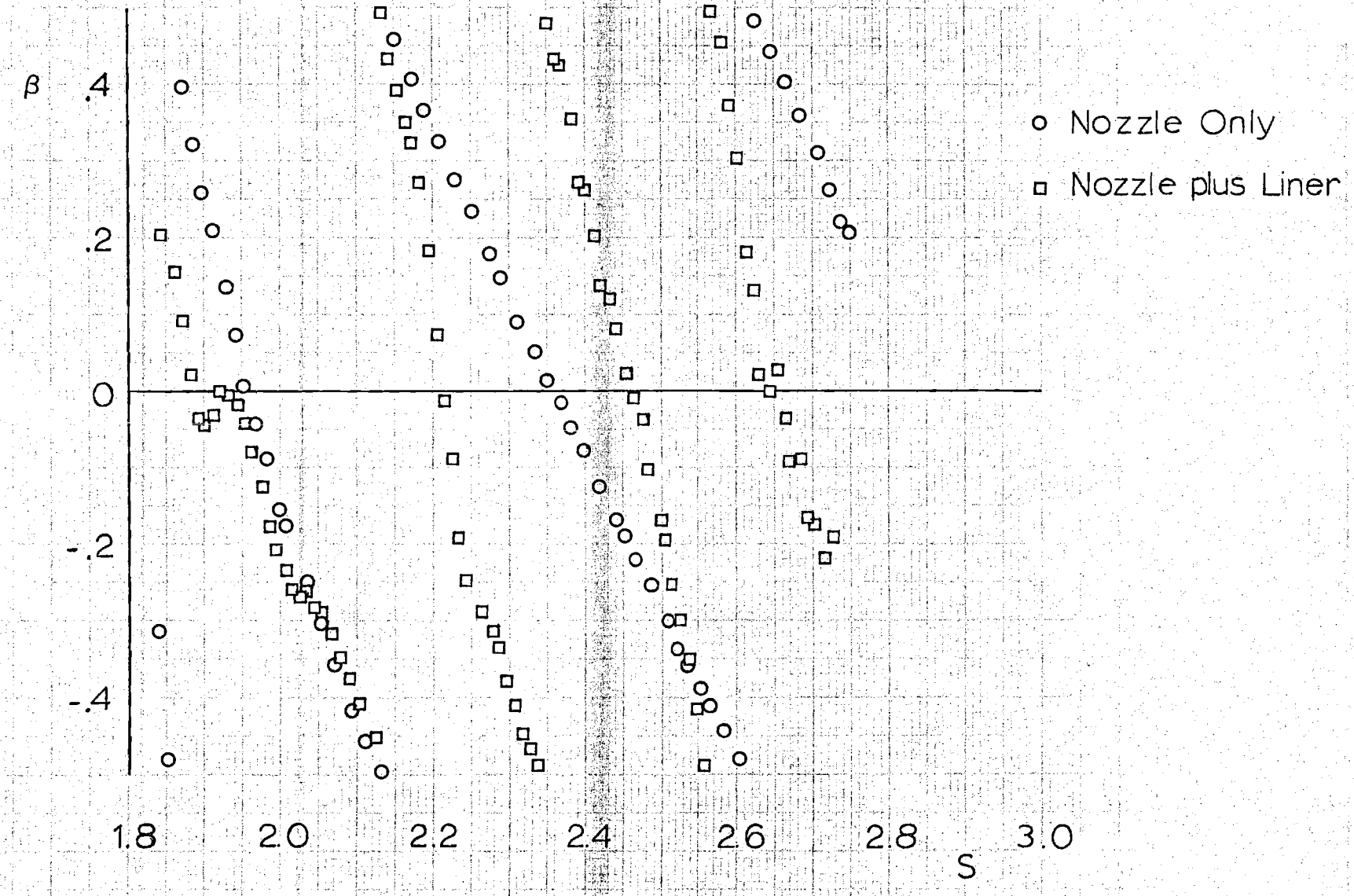

Figure 2. Effect of the Liner on the Values of β

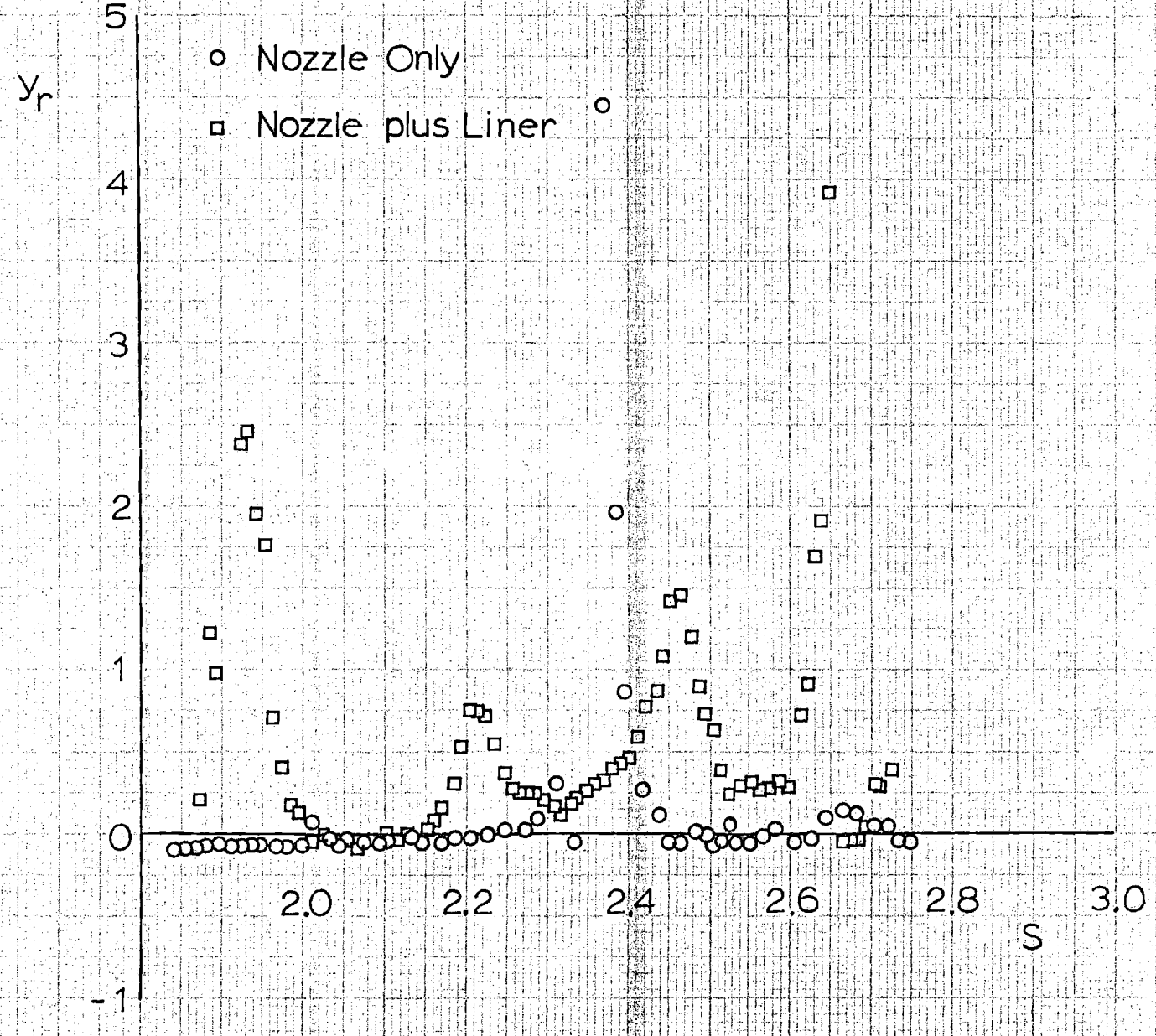

Figure 3. Effect of the Liner on y_r

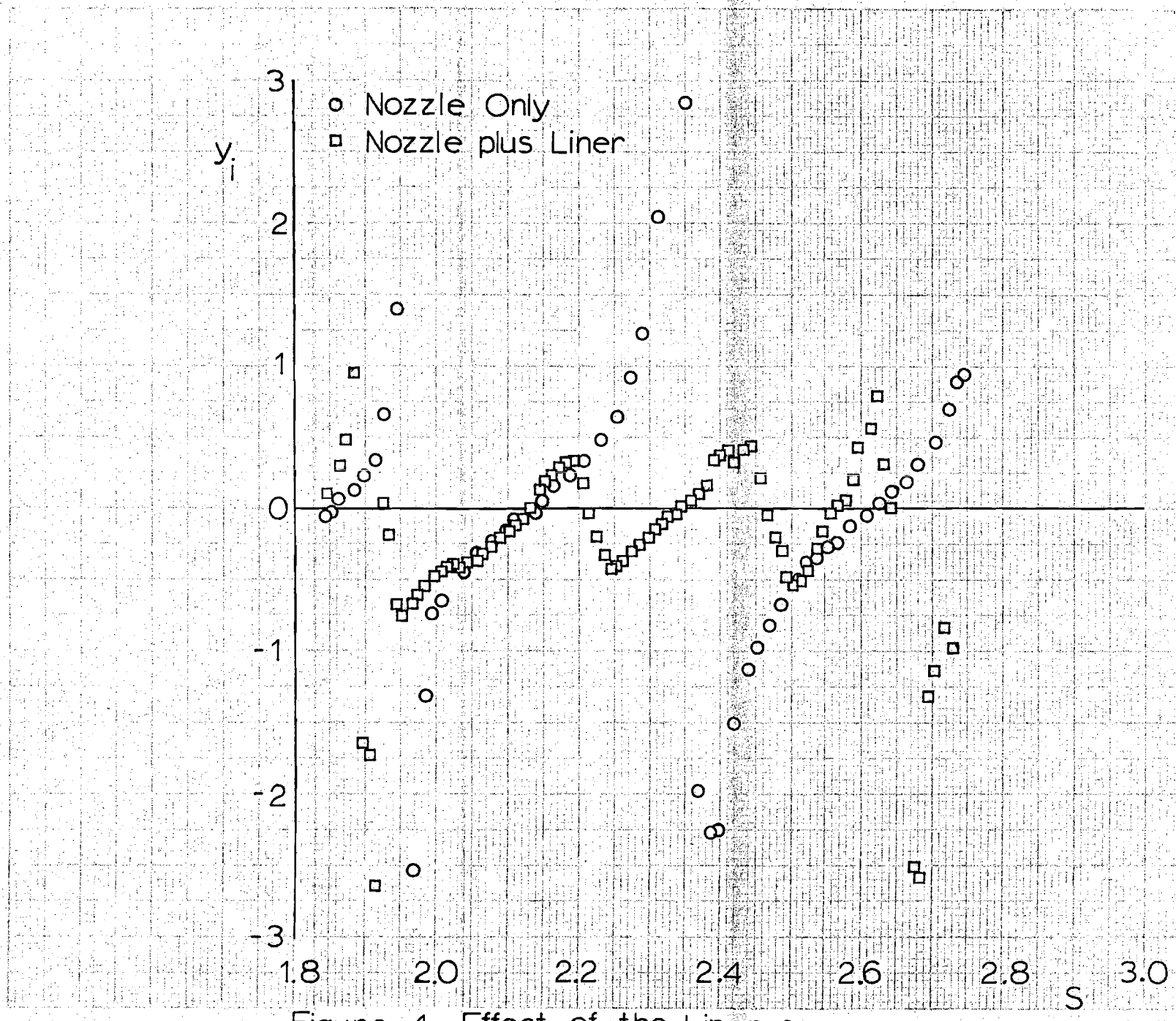

Figure 4 Effect of the Liner on y_i

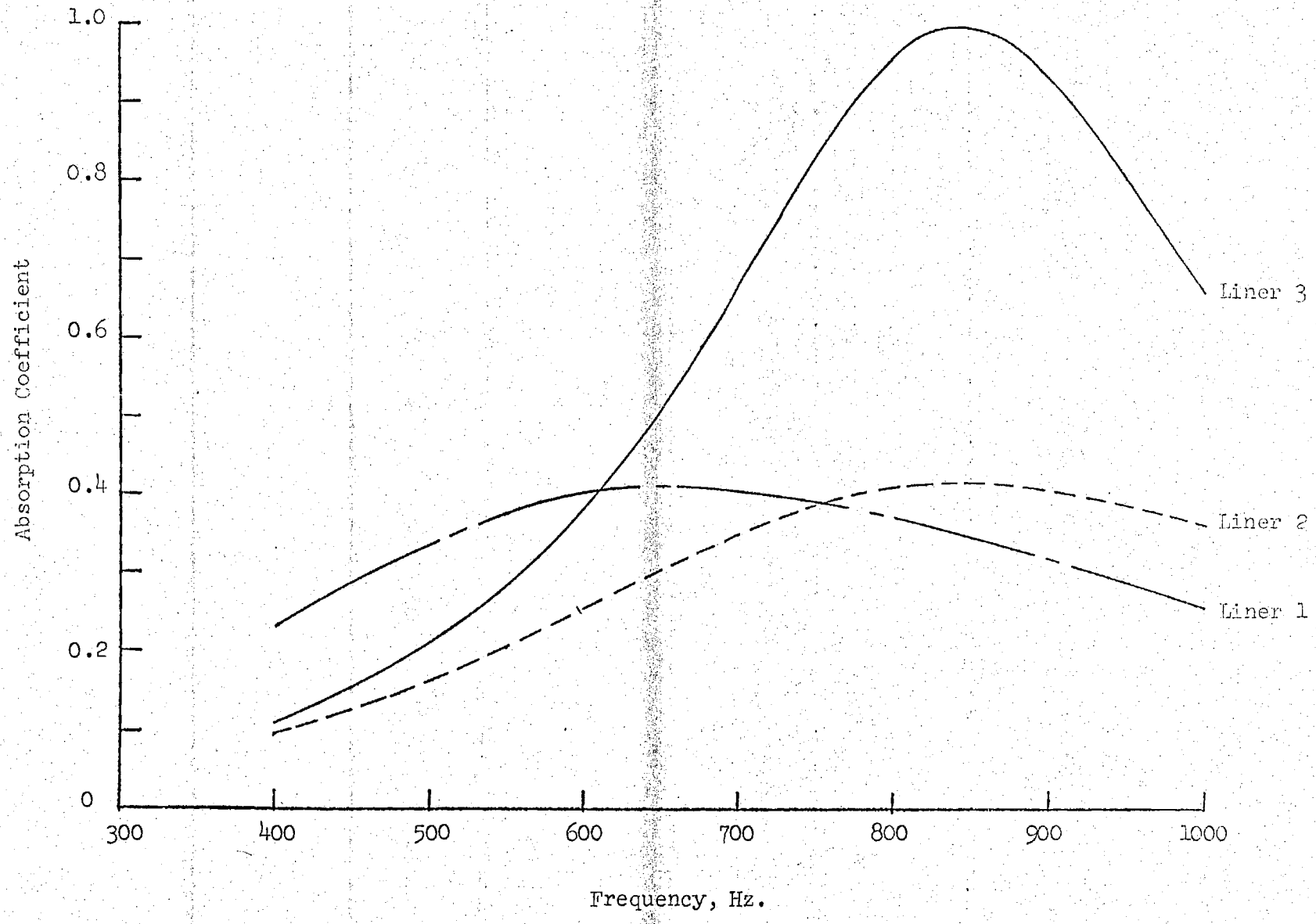

Figure 5. Theoretical Response Characteristics of the Liners to be Tested

December 12, 1972

Dr. R. J. Priem, MS 500-209
NASA
Lewis Research Center
21000 Brookpark Road
Cleveland, Ohio 44135

Dear Dr. Priem:

This report is a summary of the work completed under NASA Grant NGL 11-002-085 during November 1972.

A report has been written which describes the theoretical development, analytical techniques, and computer program used to obtain nozzle admittance values. This report is currently being reviewed, and a rough copy will be sent to you for comments upon completion of this review.

The available nozzle admittance data and the gross liner-nozzle admittance data have been sent to Dr. C. E. Mitchell for further analysis. A copy of these data and the explanatory letter sent to Dr. Mitchell are enclosed. From these data the local liner admittances will be computed analytically and compared with the measured experimental values.

To determine the experimental values of the local liner admittance, a computer program has been written which utilizes the pressure amplitude and phase data to obtain the local admittance. This computer program is currently undergoing its final checkout.

During the past month further testing of liner 1 has been conducted and the data are presently being reduced. Two tests were run; in the first test liner 1 was attached to a quasi-steady nozzle which produced a mean flow Mach number of 0.08; in the second test liner 1 was attached to a Laval nozzle with a half-angle of 15 degrees and an entrance Mach number of 0.24.

During the next month the report describing the determination of the nozzle admittance from Crocco's theory will be sent to you for review. Testing of liner 1 and the fabrication of additional liners will continue. Data

obtained in previous tests will be used to determine local liner admittance.

Sincerely,

Ben T. Zinn
Professor

tk
Enclosures

cc: Dr. W. A. Bell
Mr. B. R. Daniel
Mr. A. J. Smith, Jr.

January 16, 1973

Dr. R.J. Priem, MS 500-209
NASA
Lewis Research Center
21000 Brookpark Road
Cleveland, Ohio 44135

Dear Dr. Priem:

This report is a summary of the work completed under NASA Grant NGL-11-002-085 during December 1972.

The nozzle admittance report has been reviewed, typed, and mailed to you for additional review. It will be prepared for final publication as soon as your comments are received.

The computer program that determines the local liner admittance from experimental measurements of pressure amplitudes and phases was thought to be checked out until an error was recently discovered. The error is being corrected at present and the reduction of the local liner admittance tests will follow thereafter.

Nine liner tests have been conducted to date and are tabulated in Table 1. Three of these tests involved measurements of local liner admittance and four tests involved measurements of gross liner admittance. The remaining two tests involved simultaneous measurements of gross and local liner admittances. All of these tests used the same liner, which is detailed in Fig. 1. Four exhaust nozzles were used for these tests; two Delaval nozzles (Mach numbers of 0.08 and 0.24) and two quasi-steady nozzles (nominal Mach numbers of 0.08 and 0.24). All tests were conducted in the three-dimensional frequency range with the exception of one test, which was tested in the axial mode frequency range.

As shown in Fig. 2, the local liner admittance was measured at four locations during each test; three along the length of the liner and one at a location displaced by 90° from one of the other three transducer locations.

The results obtained in these nine tests are currently being analyzed.

Research plans for the near future call for continuing both the analysis and testing of the available liner and nozzles. Additional liners will be designed, and plans will be made for partitioning the cavity of the existing liner.

Sincerely,

Ben T. Zinn
Professor

tk
Enclosures

cc: Dr. W. A. Bell
Mr. B. R. Daniel
Mr. A. J. Smith, Jr.

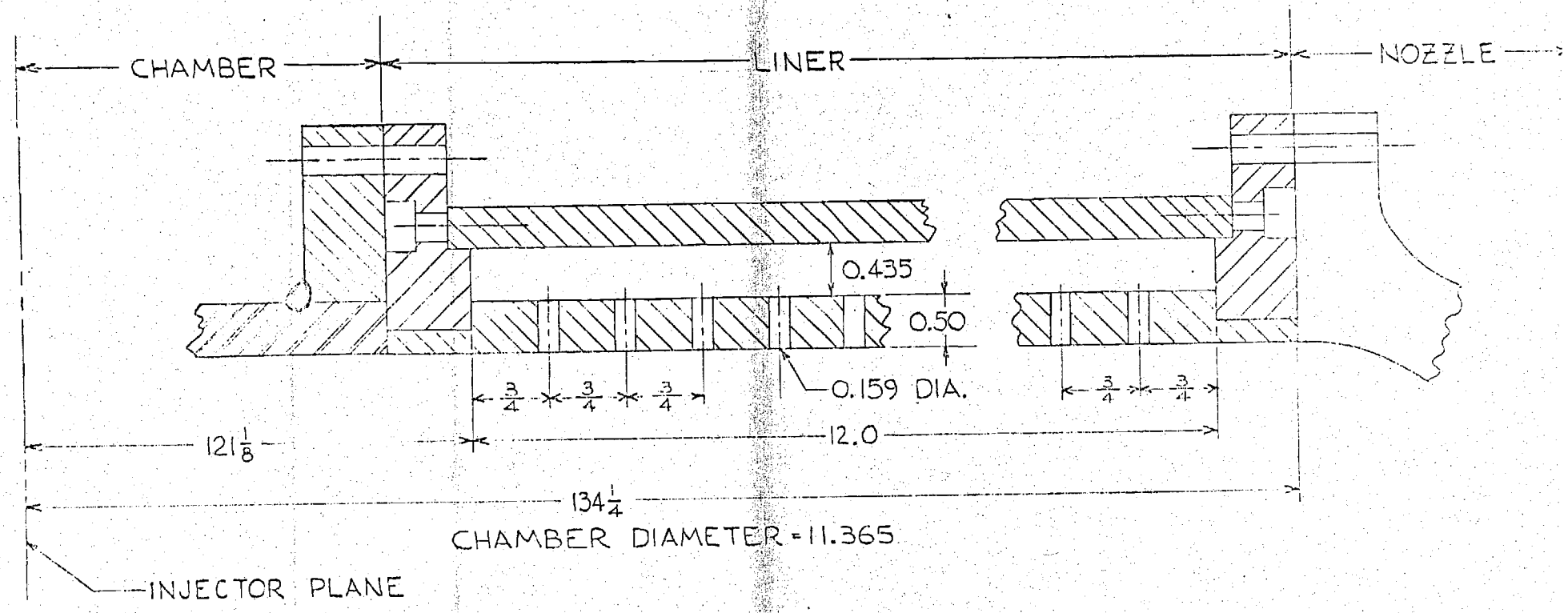

NUMBER OF CIRCUMFERENTIAL ROWS = 15

ORIFICES PER ROW = 44 (EQUALLY SPACED)

TOTAL ORIFICES = 660

ALL DIMENSIONS IN INCHES

Figure 1. Details of Liner 1

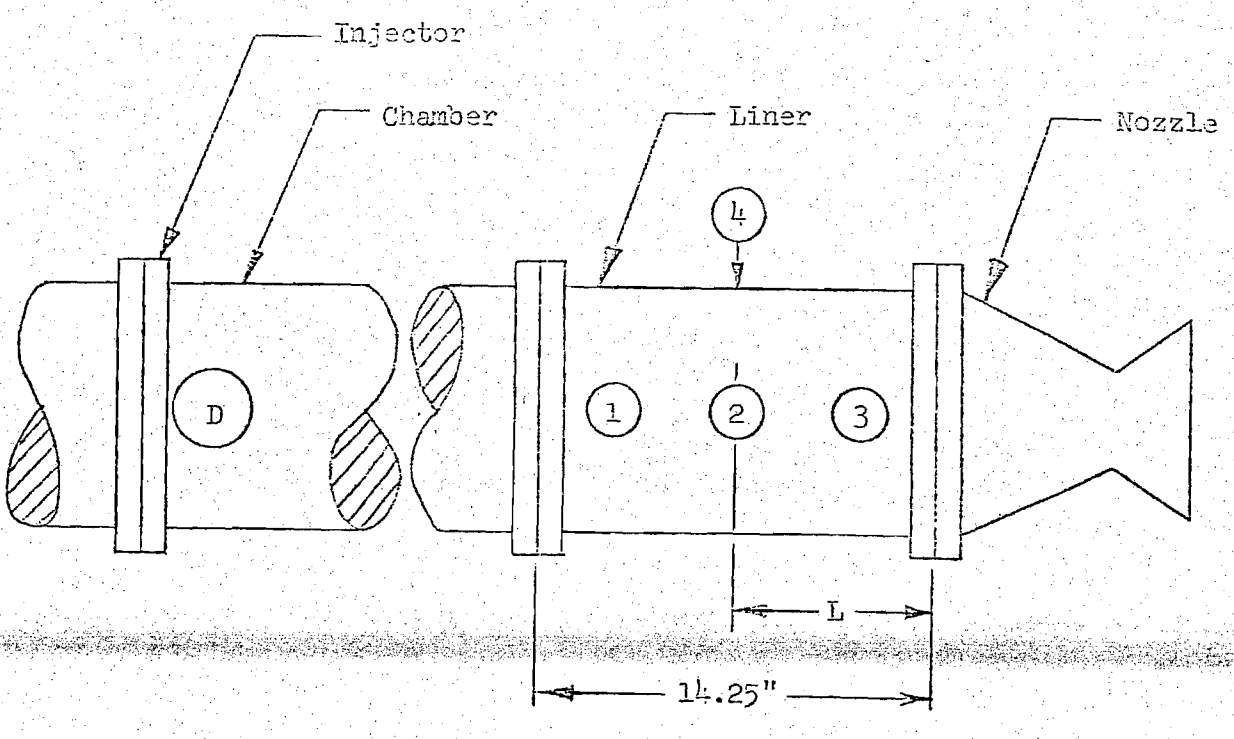

Nomenclature

D : Acoustic Driver

1 : Location L1; L = 12.0"

2 : Location L2; L = 6.75"

3 : Location L3; L = 2.25"

4 : Location L4; L = 6.75"

Figure 2. Acoustic Liner Instrumentation

Table 1. Tabulation of Acoustic Liner Tests

Test Number	Liner Number	Exhaust Nozzle*	Type of Admittance	Frequency Range
1	1	15-08-5.7	Local	3-D
2	1	15-08-5.7	Gross	3-D
3	1	15-24-2.5	Gross	3-D
4	1	15-24-2.5	Local	3-D
5	1	QSN-08	G & L	1-D
6	1	QSN-08	Gross	3-D
7	1	QSN-08	Local	3-D
8	1	QSN-24	Gross	3-D
9	1	QSN-24	G & L	3-D

* Nomenclature

Delaval Nozzle: XX-YY-ZZ

XX: Convergent Half-Angle

YY: Steady-State Mach Number x 100

ZZ: Radius of Curvature

Quasi-Steady Nozzle: QSN-XX

XX: Steady-State Mach Number x 100

E-16-607

NASA GRANT NGL 11-002-085

BEHAVIOR OF NOZZLES AND ACOUSTIC LINERS IN THREE-DIMENSIONAL ACOUSTIC FIELDS

Semi-Annual Progress Report for the Period

1 April 1973 to 30 September 1973

Prepared by: Ben T. Zinn, Principal Investigator
William A. Bell, Instructor
B. Robert Daniel, Research Engineer

School of Aerospace Engineering
Georgia Institute of Technology
Atlanta, Georgia

PROGRESS DURING THE REPORT PERIOD

A. Introduction and Summary

This report summarizes the work completed under NASA Grant NGL 11-002-085 from April 1 to September 30, 1973.

With the completion of the nozzle admittance program, the research conducted under this grant was divided into two major investigations. The first of these studies, which has since been completed, concentrated on the experimental determination of the admittances and the acoustic losses provided by various liner-nozzle combinations under simulated flow conditions which exist inside unstable rocket combustors. Once the acoustic admittance of such a system is known, the damping characteristics of the liner-nozzle combination can be determined. Two types of admittance data were obtained. The local liner admittance was measured using the pressure-phase measurement technique described in Appendix B of Reference 1 and in Reference 2. These data were then compared with predictions obtained from current semi-empirical liner design theories.[1,2]

The second type of admittance data is referred to as gross admittance in this report, and it corresponds to the injector admittance of References 3 and 4. This admittance is a measure of the overall system damping provided by the acoustic liner-nozzle combination. Using the extended impedance tube method developed during the nozzle admittance studies, the gross liner admittance data have been obtained for four liner configurations. The gross and local liner admittance data measured during these studies are summarized in this report. These investigations have led to the publication of two papers - the first is included in the proceedings of the 10th JANNAF Combustion Meeting and the second appears in the October 22nd issue of the Journal of Sound and Vibration. A paper concerning this

work will also be presented in the AIAA 12th Aerospace Sciences Meeting to be held January 30 through February 1, 1974.

The second phase of this research program was concerned with the experimental determination of the admittances of various liquid rocket fuel and oxidizer injector configurations. The measured injector admittances will be compared with available theoretical predictions. During the reporting period the design and fabrication of the experimental facility and the injectors to be tested was completed and preliminary testing to check the system has been completed. The injector admittance data will be obtained during the next report period.

B. Liner Admittance Studies

During this report period, the testing of the acoustic liners has been completed, and the local and gross admittances for several acoustic liner-nozzle combinations have been measured. The purposes of these tests were to assess acoustic liner-nozzle damping capabilities, provide local liner admittance data for comparison with current liner theories, and evaluate existing liner design criteria.

In the majority of the studies conducted to date (e.g., see Reference 1) the performance of acoustic liners has been determined by conventional impedance tube measurements where the tested liner sample is placed normal to the direction of propagation of longitudinal waves. However, in most rocket applications the liner is placed on the walls of the combustor, and the orientation of the liner face relative to the wave motion is entirely different from its orientation in the impedance tube experiment. Also, in many applications the liner is subjected to three-dimensional oscillations and a parallel mean flow whose magnitude and orientation

may also affect liner performance. Although these flow conditions are not simulated in impedance tube experiments, semi-empirical correlations developed from these experiments are widely used in the design of acoustic liners for a variety of practical applications.

The first set of experiments conducted in the present study was designed to measure local liner admittances under flow conditions simulating those observed in rocket combustors experiencing three-dimensional instabilities. These data are used to determine the dependence of the measured local admittance upon liner properties, the amplitude and spatial dependence of the wave motion, and the mean flow Mach number. In addition, these data are used to check the applicability of the empirical correlations currently used in liner design. In the second set of experiments conducted under this program, the overall acoustic performance of various acoustic liner-nozzle combinations was evaluated. These studies were conducted to determine the acoustic energy dissipated in systems consisting of an acoustic liner attached to a choked nozzle, as shown in Figure 1. The data obtained in this set of experiments are also compared with the predictions of Mitchell,[3] who theoretically investigated the performance of such systems.

These experiments have been conducted in the modified impedance tube facility used in the nozzle studies. The acoustic performance of a given liner-nozzle combination was determined by measuring the specific acoustic admittance at the liner entrance plane.

The local liner admittances at several locations along and around the liner face were determined from pressure amplitude and phase measurements

taken by pairs of transducers located in the liner cavity and at the liner face. The dependence of the local liner admittance upon the local pressure amplitude was included in the data reduction program to account for the nonlinear behavior of the liner.

Several liner designs including an unpartitioned liner, a partitioned liner, a liner consisting of an array of single Helmholtz resonators and a liner consisting of single orifices with common annular cavities were tested. These liners were tested in combination with several multi-orifice (i.e., quasi-steady) and deLaval nozzles to determine the effects of liner design, nozzle design and chamber mean flow Mach number upon the measured admittances.

Real and imaginary parts of the local liner admittance modes were measured and compared over the frequency range covering mixed first tangential-longitudinal modes with the corresponding theoretical predictions. The local liner admittance results can be summarized as follows:

(1) Poor agreement exists between the theoretical and experimental data for unpartitioned liners and for partitioned liners as shown in Figures 2 and 3.

(2) For liners consisting of individual resonators and orifices with a common annular cavity, the theoretical admittance values are generally in good agreement with the experimental data as shown in Figures 4 and 5. The theory is capable of predicting the tuning frequency of these liners to within two per cent.

(3) Mean flow increases the tuning frequency of the liner since the flow turbulence decreases the effective length of the orifice. From Figure 6, the effective length decreases with increasing Mach number.

(4) Mean flow also increases the frequency range over which the liner is effective and increases the resistance of the liner.

To determine the "overall" effectiveness of a given liner, the measured real and imaginary parts of the admittance of the entrance plane of a given liner-nozzle combination are compared with corresponding values of the admittances measured when the liner is replaced by a solid wall. These comparisons show that the presence of a liner increases the wave attenuation provided by a choked nozzle only and that increasing the liner length increases the wave attenuation. The attenuation for different liner-nozzle combinations was determined and compared with one another and with the predictions of available liner design theories. Due to the length of the required computations, only limited comparisons between these experimental data and Mitchell's theoretical predictions[3] have been conducted. For partitioned liners, reasonable agreement exists at some frequencies and poor agreement exists at others. Mitchell's theory is currently being used to determine the acoustic performance of liners with individual resonators and liners with annular cavities.

The goals for the next report period include:

(1) The presentation of the liner program results in a special report.

(2) The completion of the injector response studies which will include the comparison of the experimental data with existing theoretical predictions.

REFERENCES

1. Garrison, G. D., "Suppression of Combustion Oscillations with Mechanical Damping Devices," Interim Report, PWA FR-3299, August 1969.
2. Oberg, C. L., "Improved Design Techniques for Acoustic Liners," Rocketdyne Technical Report RR-68-5, May 1968.
3. Mitchell, C. E., Espander, W. R., and Baer, M. R., "Determination of Decay Coefficients for Combustors with Acoustic Absorbers," NASA CR 120836, January 1972.
4. Priem, R. J. and Rice, E. S., "Combustion Instability with Finite Mach Number Flow and Acoustic Liners," NASA TM X-52412, 1968.

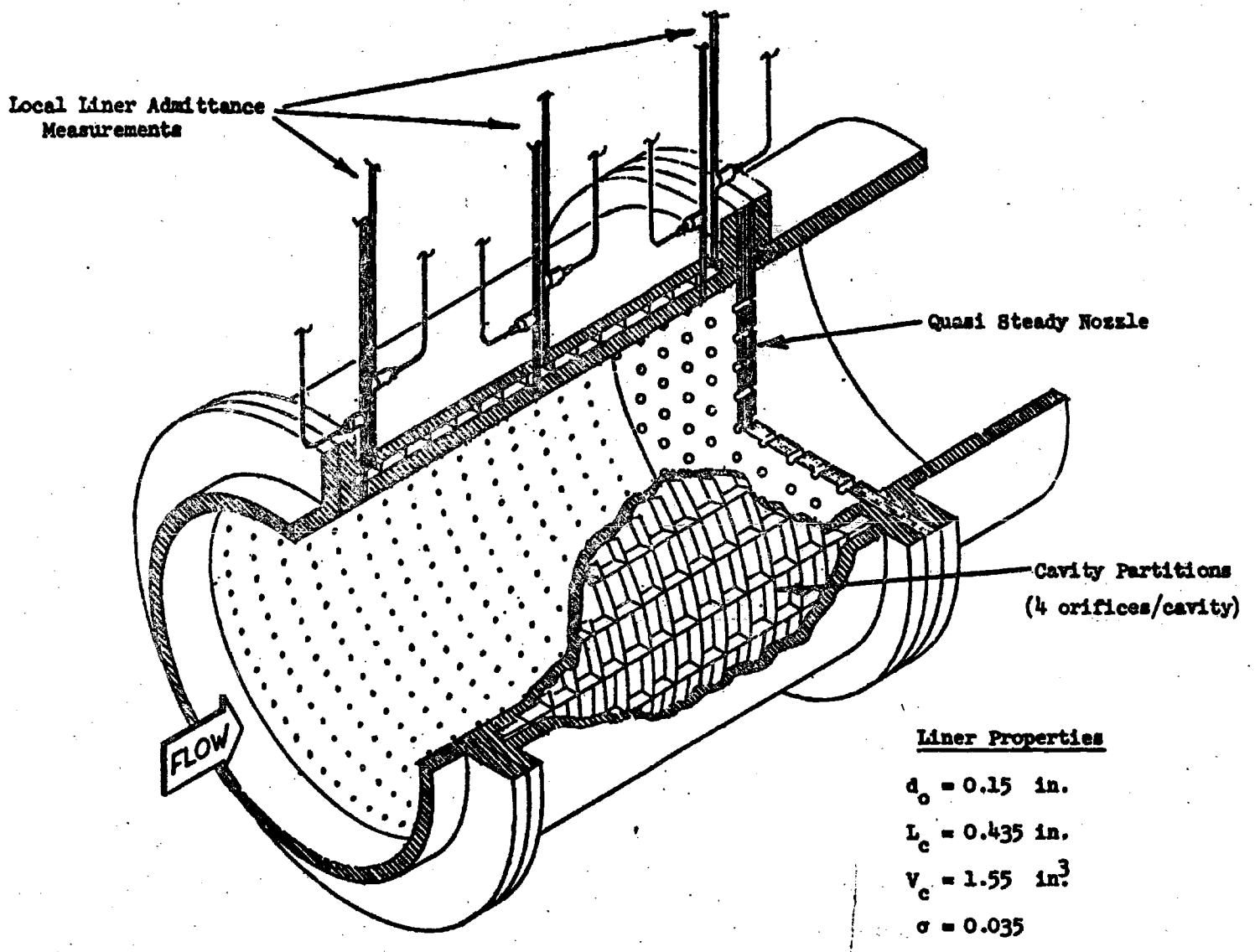

Figure 1. Partitioned Liner - Quasi Steady Nozzle Combination.

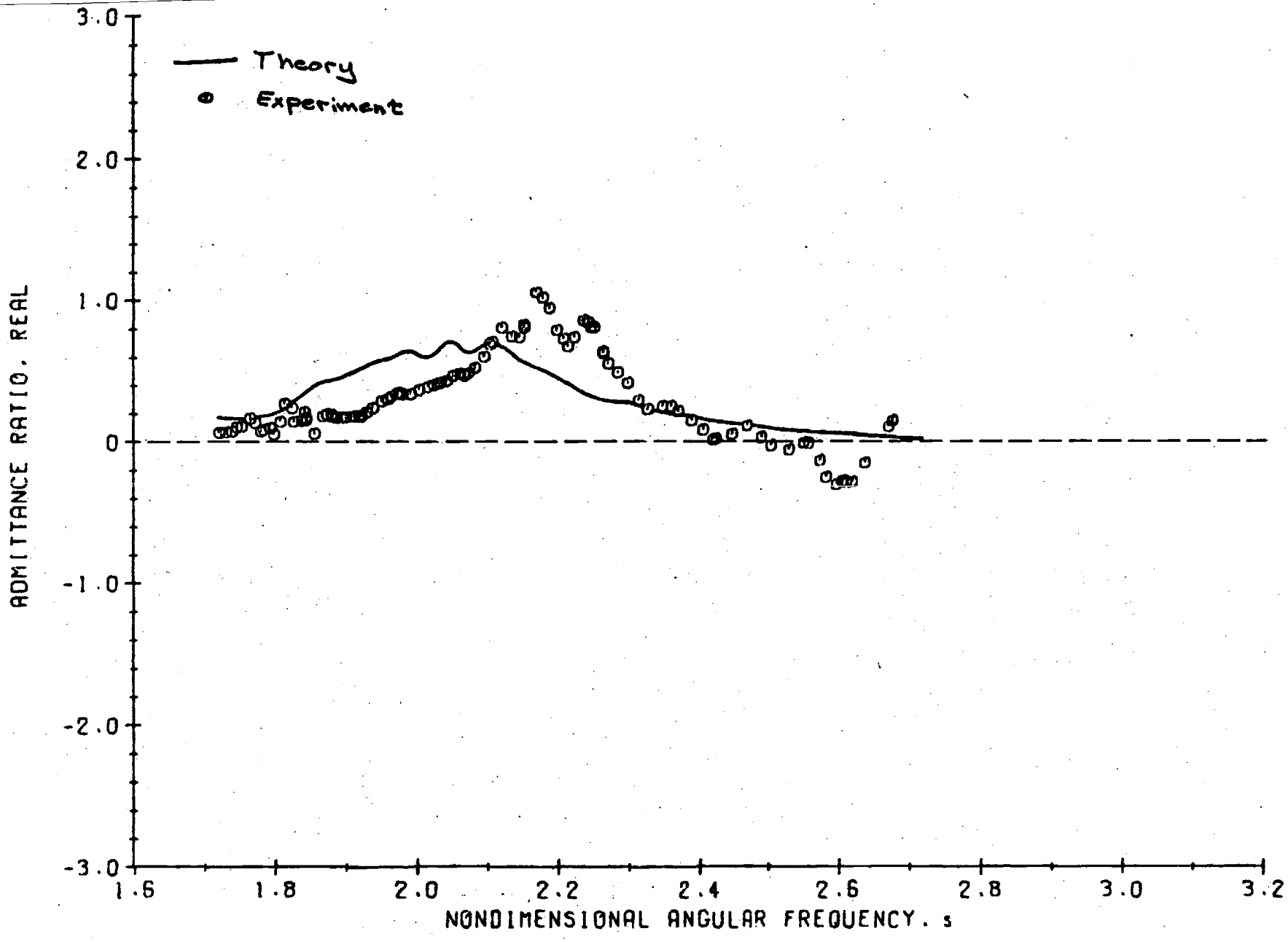

Figure 2. Comparison of Theoretical and Experimental Values of the Real Part of the Local Liner Admittance for a Partitioned Liner.

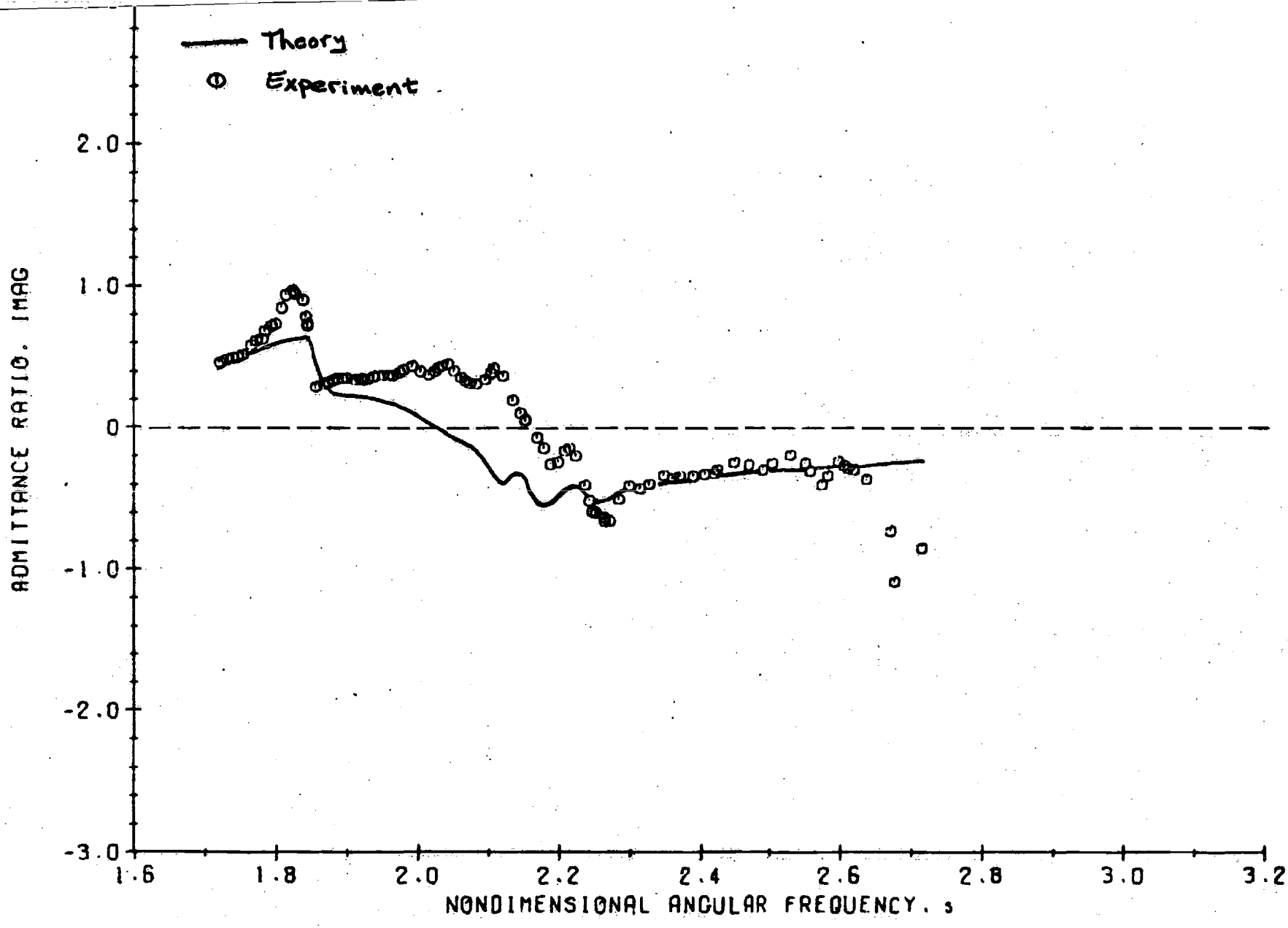

Figure 3. Comparison of Theoretical and Experimental Values of the Imaginary Part of the Local Liner Admittance for a Partitioned Liner.

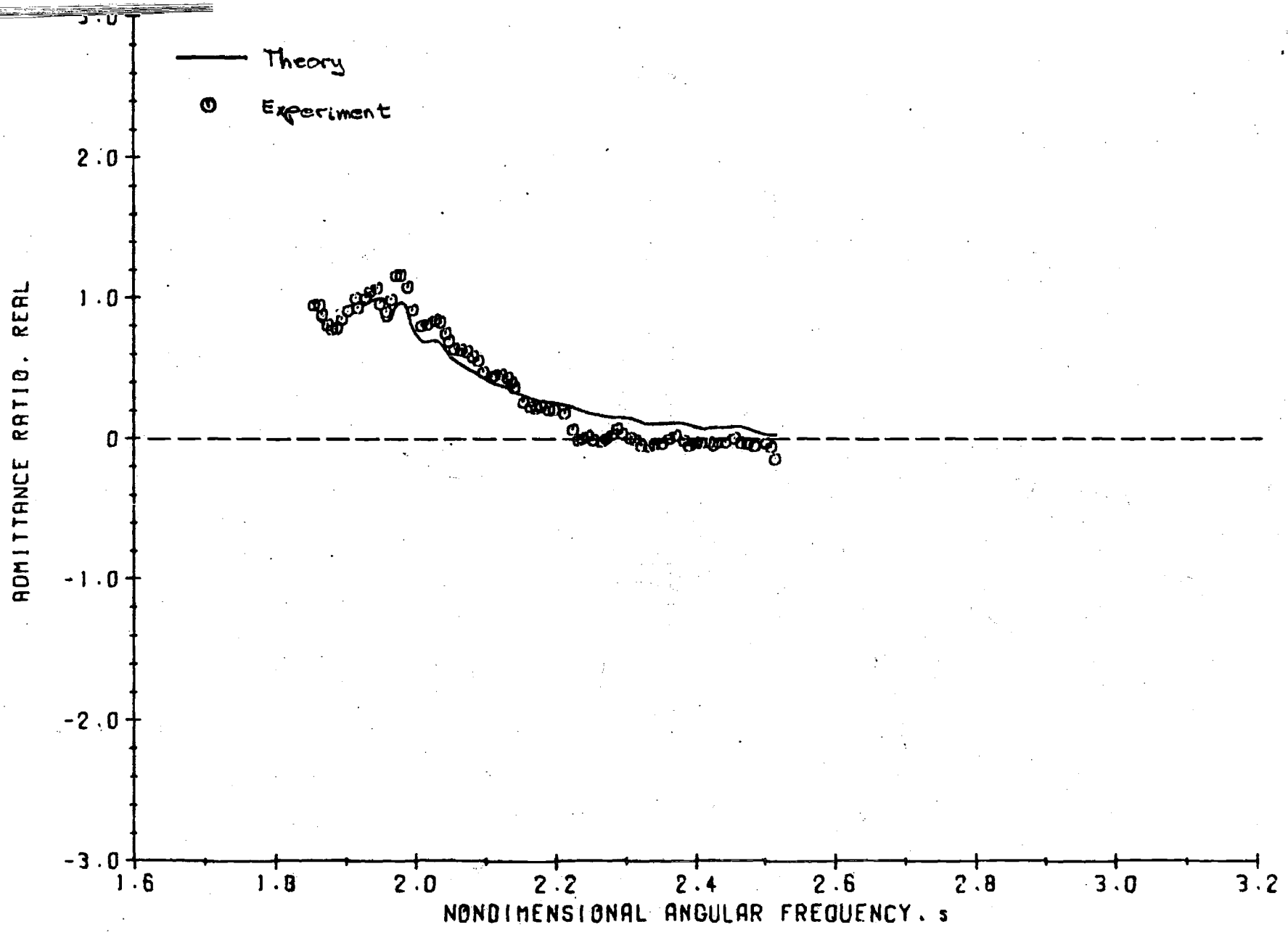

Figure 4. Comparison of the Theoretical and Experimental Values of the Real Part of the Local Liner Admittance for a Liner Consisting of Individual Resonators.

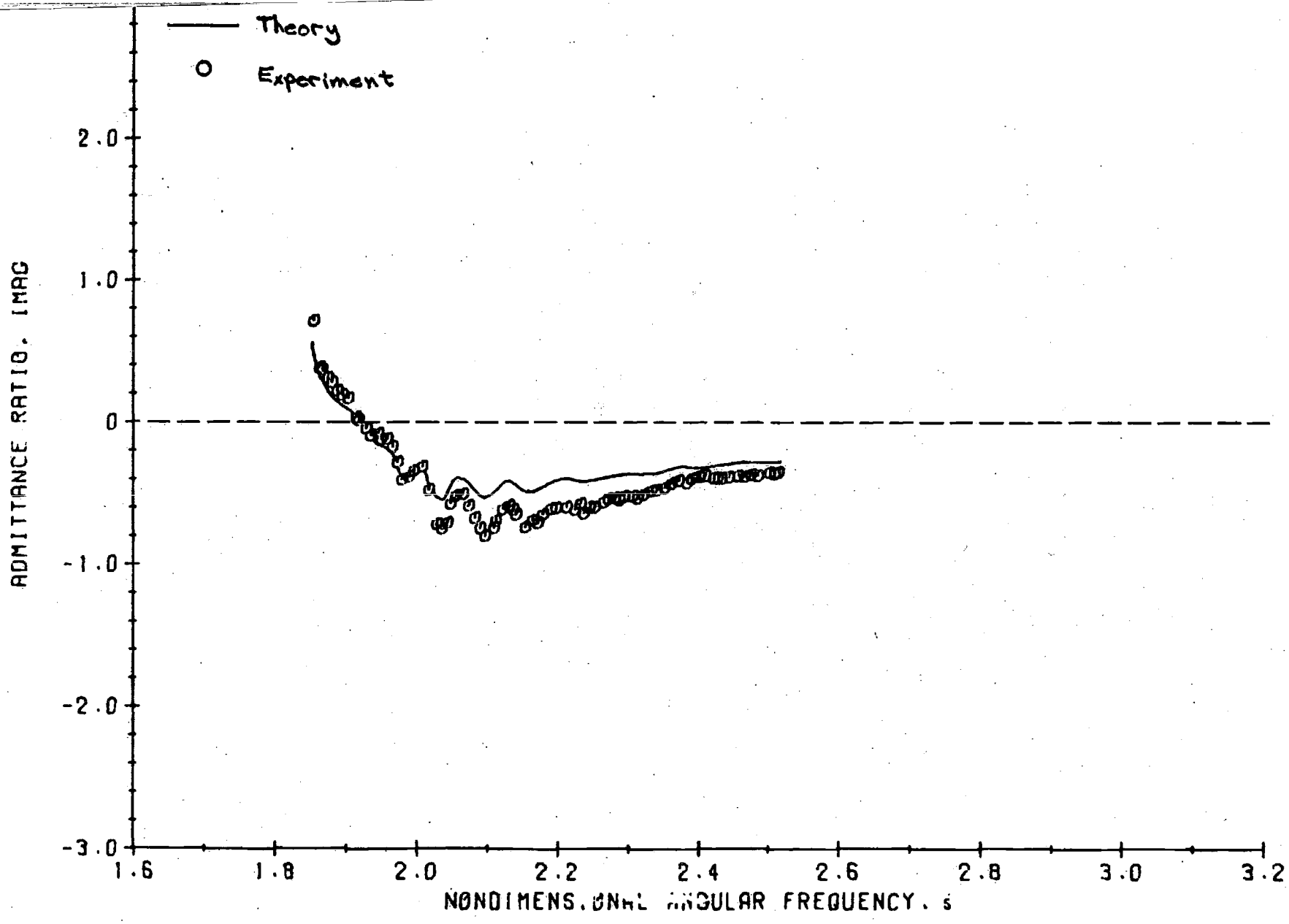

Figure 5. Comparison of the Theoretical and Experimental Values of the Imaginary Part of the Local Liner Admittance for a Liner Consisting of Individual Resonators.

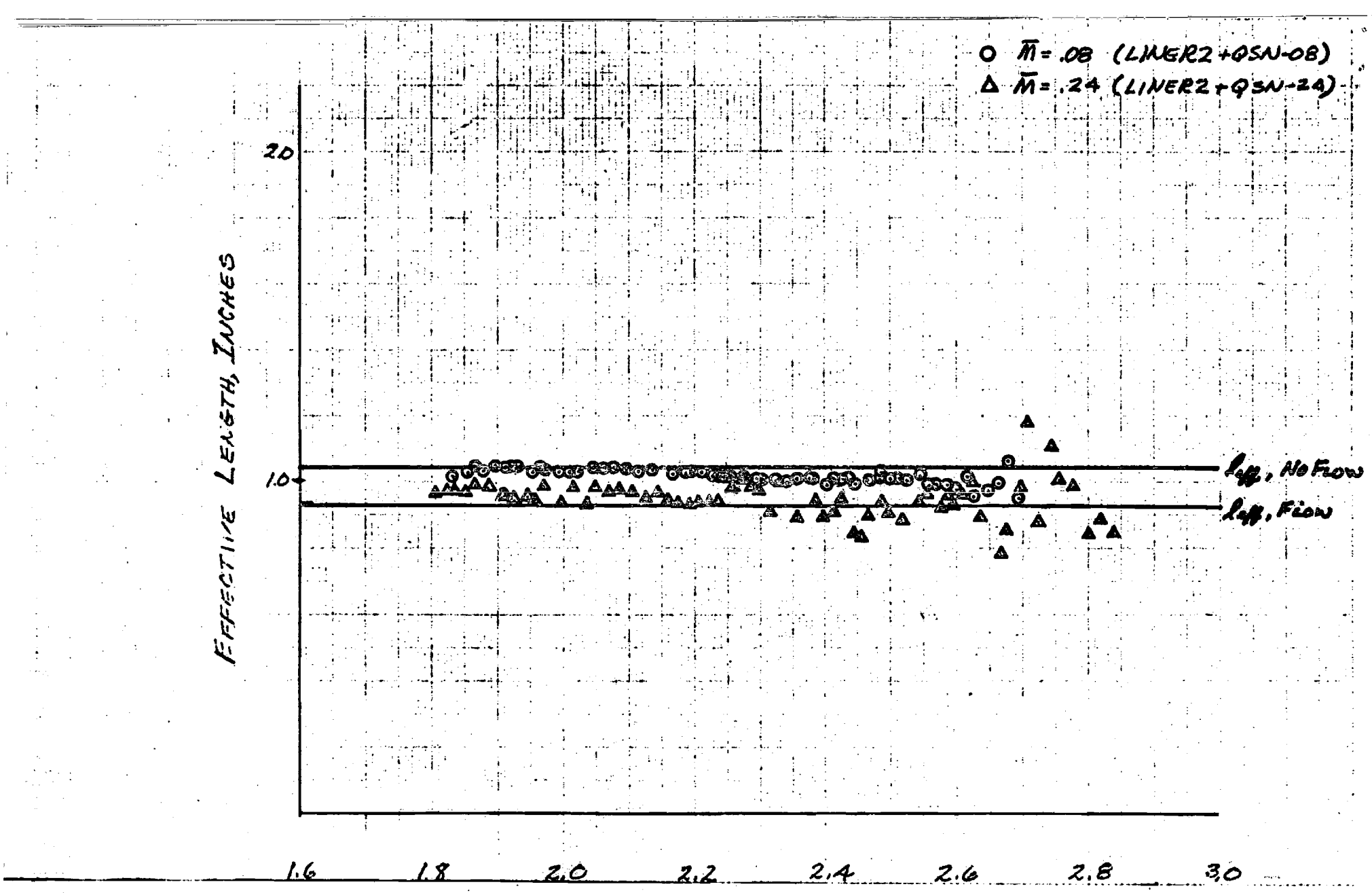

Figure 6. Effect of Mean Flow on the Effective Length.

E-16-601

NASA GRANT NGL 11-002-085

THE RESPONSE FACTORS OF COAXIAL INJECTORS IN UNSTABLE GASEOUS PROPELLANT ROCKET MOTORS

Semi-Annual Progress Report 3

For the Period

1 April 1974 to 30 September 1974

Prepared by: B. T. Zinn, Principal Investigator
B. A. Janardan, Research Engineer
B. R. Daniel, Research Engineer

School of Aerospace Engineering
Georgia Institute of Technology
Atlanta, Georgia

PROGRESS DURING THE REPORT PERIOD

A. Introduction

This report summarizes the work done under NASA Grant NGL 11-002-085 during the period 1 April 1974 to 30 September 1974. This investigation concerning the determination of the response factors of various gaseous rocket injector configurations was initiated on April 1, 1973. During the first year of investigation the required experimental apparatus was developed and the necessary injector configurations were designed and fabricated. Detailed descriptions of the experimental facility, the various injector configurations, along with preliminary admittance data were reported in the annual progress report submitted to NASA in April 1974.

Some of the results obtained during the present investigation were presented at the 11th JANNAF Conference held at JPL, Pasadena, during September 9-13, 1974. Also, another paper based on the results of this investigation has been accepted and will be presented at the 13th Aerospace Sciences Meeting scheduled to be held in January 1975.

During the present reporting period the admittances and response factors of the designed injector configurations were determined over a range of experimental conditions. The measured response factors were then used to check the applicability of the Feiler and Heidmann study[1] that investigated this problem analytically. The results obtained during this period are briefly discussed in this report. In preparation for the next phase of this program, two new injector configurations, designed to determine the dependence of the injector response factor upon the injector open area ratio and the injector orifice length, have been designed. Brief

descriptions of these injector configurations, which are presently being fabricated, are also presented in this report.

B. Injector Response Measurement

For a stability analysis of a liquid rocket motor the data describing the losses provided by the nozzle and acoustic liners must be supplemented by data that quantitatively describes the influence of the injector on the stability of the engine. Customarily the effect of the injector is described by means of a response factor which is defined as the complex ratio of the burning rate perturbation to the chamber pressure perturbation. In Reference 1, the response of a coaxial injector element has been studied theoretically in an attempt to determine the dependence of the injector response factor upon injector design parameters. The present investigation had been undertaken with the objective of providing experimental data that could be used to check the applicability of the predictions of Reference 1.

The injector admittance data, from which the required response factors can be determined, was measured in this study by employing the modified impedance-tube technique. The experimental facility and the injector configurations used are described in detail in Reference 2.

During the period under consideration in this report, the frequency dependence of the admittances and response factors of the three injector configurations shown in Figure 1 were investigated. Configurations 1 and 2 were designed to simulate the flow behavior in gaseous fuel and oxidizer coaxial injector elements, respectively. Configuration 3, which is a combination of configurations 1 and 2, simulates the flow behavior in a coaxial injector element of a gaseous rocket motor.

The measured admittances of the injector surfaces are presented in Figures 2 through 4 along with the admittance data predicted by the Feiler and Heidmann model. The experimental data include admittances of the test injectors measured with pressure drops of 0.025, 0.05 and 1 psi. The measured admittance data of injector configuration 1 (with open area ratio, $\sigma = 0.047$) and 2 (with $\sigma = 0.017$) are presented in Figures 2 and 3 and those of injector configuration 3 are presented in Figure 4. The total predicted admittances of injector configuration 3 were obtained by combining the individually predicted admittances of the fuel and oxidizer elements (i.e., configuration 1 and 2). An examination of these figures indicates reasonably good agreement between the measured and theoretically predicted admittance data. The scatter observed, particularly in the measured values of the imaginary part of the admittance, is due to the fact that at the corresponding frequencies the standing wave in the impedance tube has a flat minima and hence its axial location could not be precisely measured.

The measured admittance, y_s, which represents an average value of the nondimensional specific admittance of the injector surface is used to compute the nondimensional specific admittance, y_o, at the injector element opening. The required relationship between these two admittances is

$$y_s = \sigma\, y_o \tag{1}$$

This expression has been obtained from the perturbed form of the mass conservation law after neglecting the term $\frac{\partial}{\partial t}\int_V \rho' dV$ in a small volume in front of the injector face where the injector streams are supposed to mix. The nondimensional injector response factor N is then calculated

from the nondimensional orifice admittance y_o and the relationship

$$N = -\frac{1}{\gamma}\left[1 + \frac{y_o}{M_o}\right] \tag{2}$$

where M_o is the mean flow Mach number at the injector orifice. The above relationship is obtained by relating the definitions of N and y_o to one-another and assuming that gas is perfect and the oscillation is isentropic.

The frequency dependence of the response factor of the injector configuration 3 was calculated using the measured admittance data, presented in Figure 4, and Eqs. (1) and (2); this data is presented in Figure 5. The total predicted response factor, N_t, for injector configuration 3 was determined from the theoretically[1] predicted responses of injector configurations 1 and 2 (see Figures 2 and 3) and the following expression suggested by Feiler and Heidmann[1]:

$$N_t = \frac{\bar{W}_1}{\bar{W}_t} N_1 + \frac{\bar{W}_2}{\bar{W}_t} N_2; \quad \bar{W}_t = \bar{W}_1 + \bar{W}_2 \tag{3}$$

where N_1 and N_2 respectively represent the individual response factors of injectors 1 and 2. In Eq. (3) $\bar{W}_1/\bar{W}_t$ and $\bar{W}_2/\bar{W}_t$ respectively represent the mean fractions of the mass flow rates in injector configurations 1 and 2. An examination of Figure 5 indicates a good agreement between the measured and theoretically predicted response factor data. This agreement suggests that Eq. (3) may be used to calculate total response factors of coaxial injectors, containing both fuel and oxidizer elements, from the response factors of the individual elements.

Two new injector configurations, designed to determine the dependence of the injector response factors upon the injector open area ratio and the injector orifice length have been designed and are being fabricated.

These injectors, planned to be tested during the next phase of this investigation, have each 13 individual elements simulating gaseous oxidizer injector elements. One of the injectors has been designed with an open area ratio σ = 10% and injector orifice length L = 0.875" while the other has been designed with σ = 10% and L = 1.75 inches.

C. Conclusion

The injector response data measured to date indicates that under the flow conditions encountered in this study there is a good agreement between the measured admittances and those predicted by the Feiler and Heidmann analysis. Also, based upon the agreement obtained so far the expression suggested by Feiler and Heidmann for calculating the total response factors of coaxial injectors containing both fuel and oxidizer elements seems to be valid.

The studies planned for the next reporting period are

(1) Determine the frequency dependence of the response factors of the two new injector configurations in order to check the ability of the theory to predict the dependence of the injector response factor upon the injector geometry.

(2) Investigate the feasibility of determining the injector admittance and response data under "hot" conditions.

The determination of the injector responses in the presence of combustion should determine the capabilities of different injectors to "drive" combustion instability. The attainment of such data should considerably improve our understanding of combustion instability in liquid and gaseous rocket motors.

References

1. Feiler, C. E. and Heidmann, M. F., "Dynamic Response of Gaseous-Hydrogen Flow Systems and its Application to High Frequency Combustion Instability," NASA TN D-4040, June 1967.
2. Annual Progress Report for Period 1 April 1973 to 31 March 1974 of NASA Grant NGL 11-002-085, April 1974.

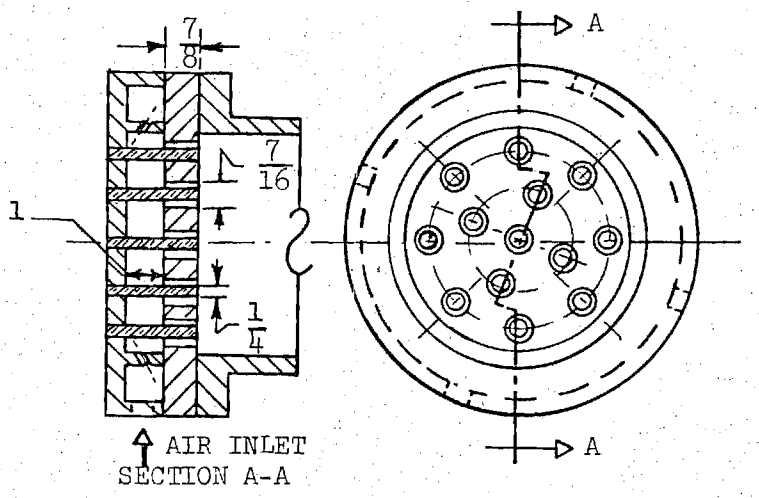

CONFIGURATION 1

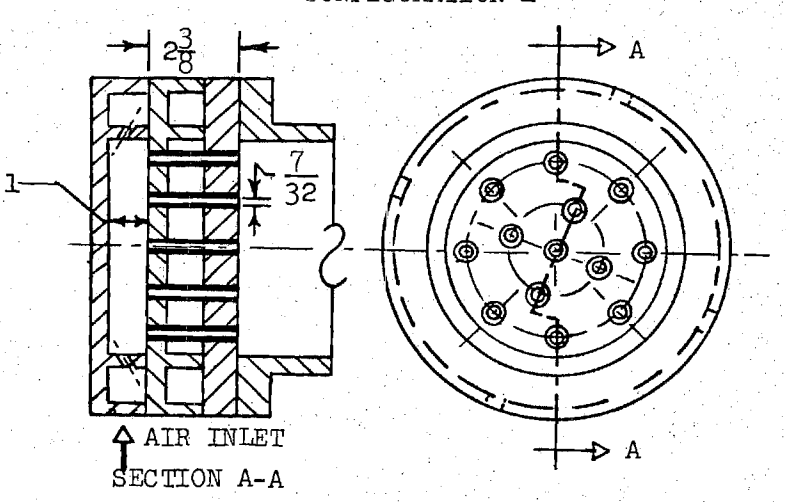

CONFIGURATION 2

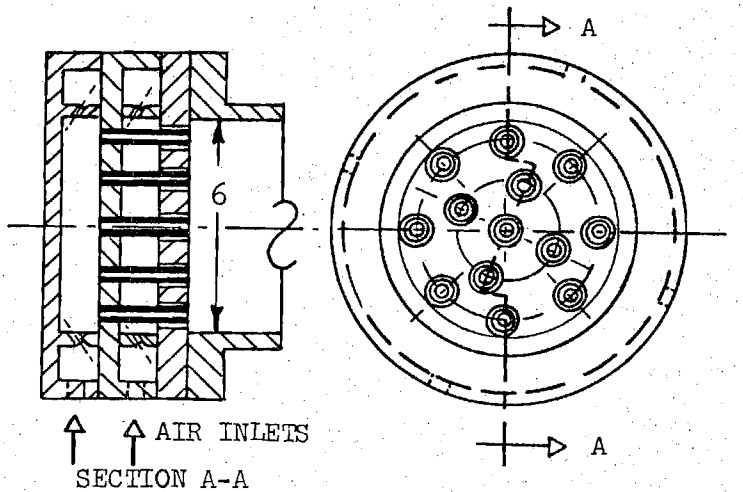

CONFIGURATION 3

(ALL DIMENSIONS IN INCHES)

Figure 1. Tested Injector Configurations

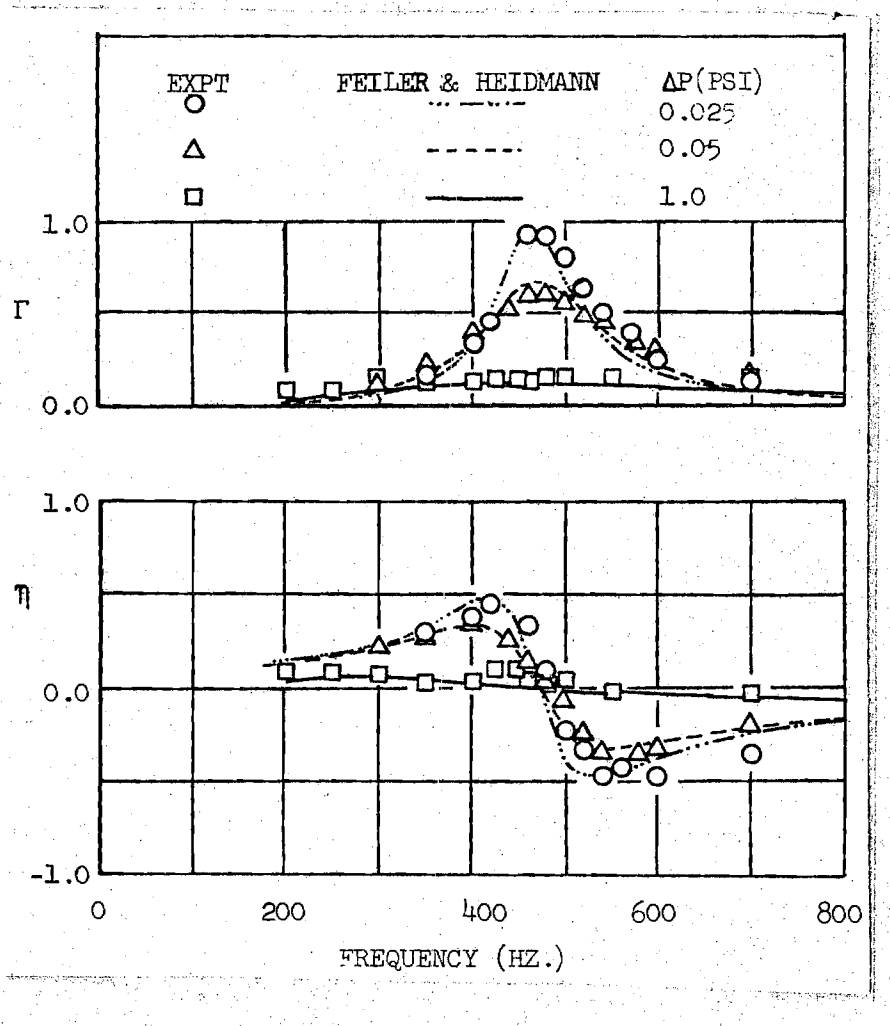

Figure 2. Frequency Dependence of Admittances of Injector Configuration 1

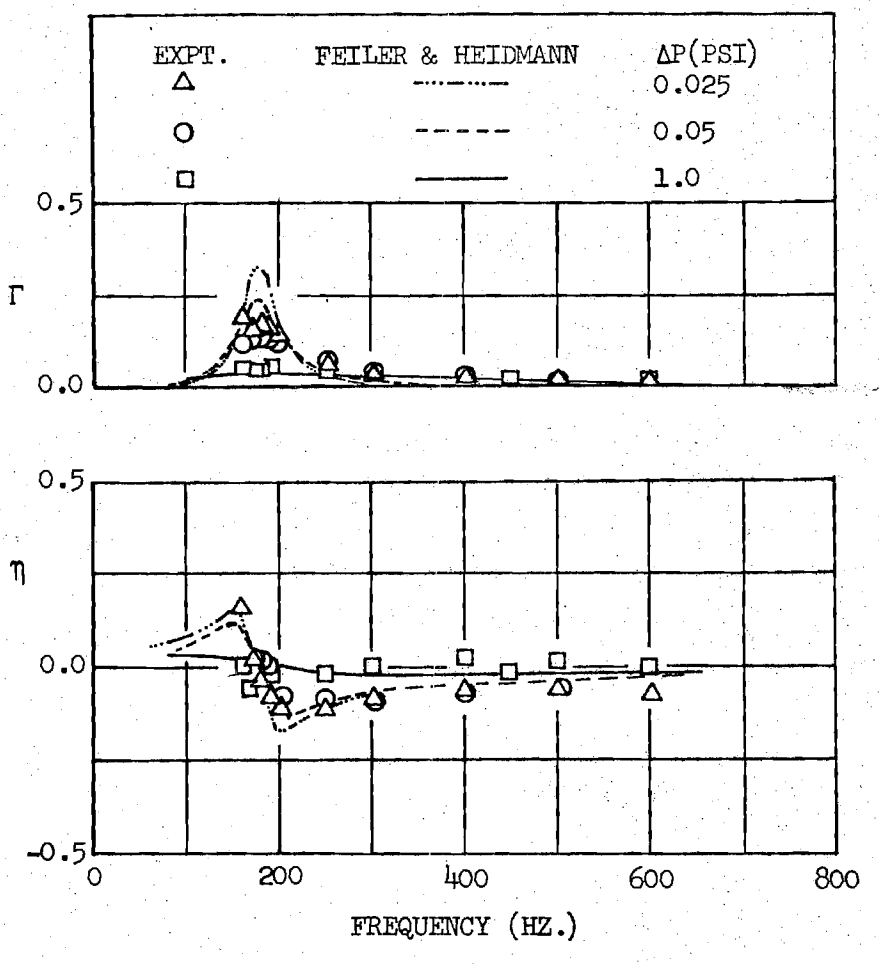

Figure 3. Frequency Dependence of Admittances of Injector Configuration 2

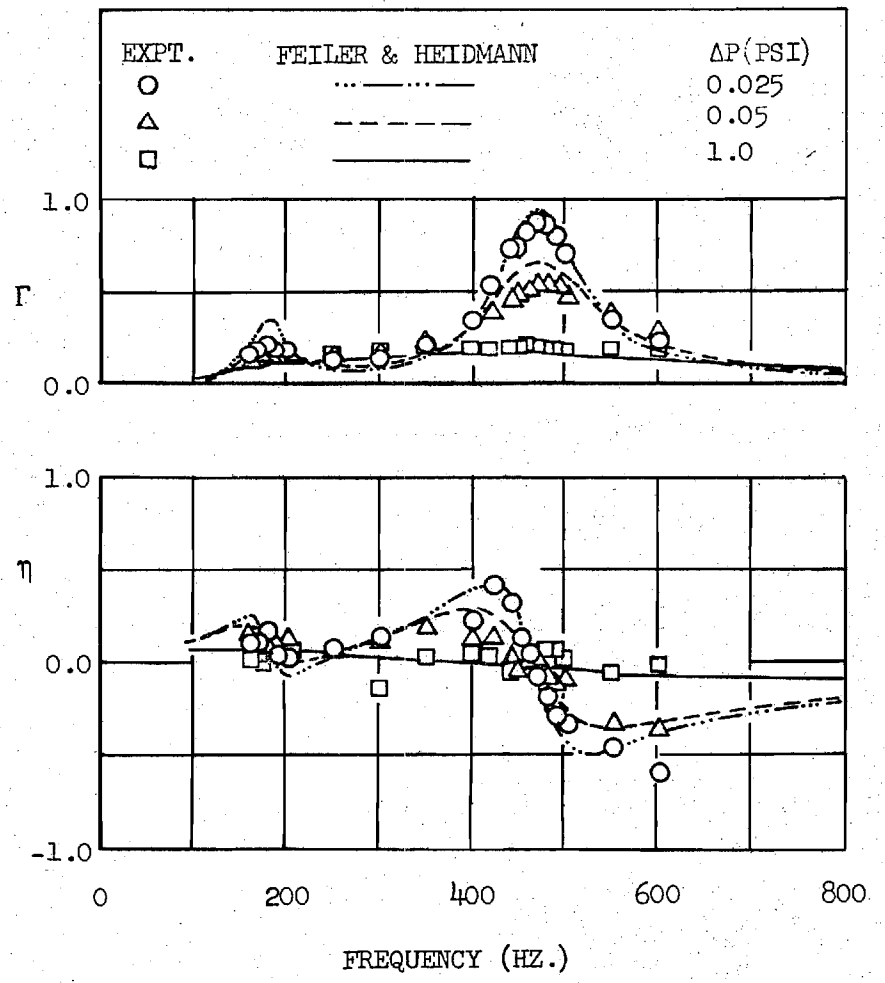

Figure 4. Frequency Dependence of Injector Surface Admittances of Configuration 3

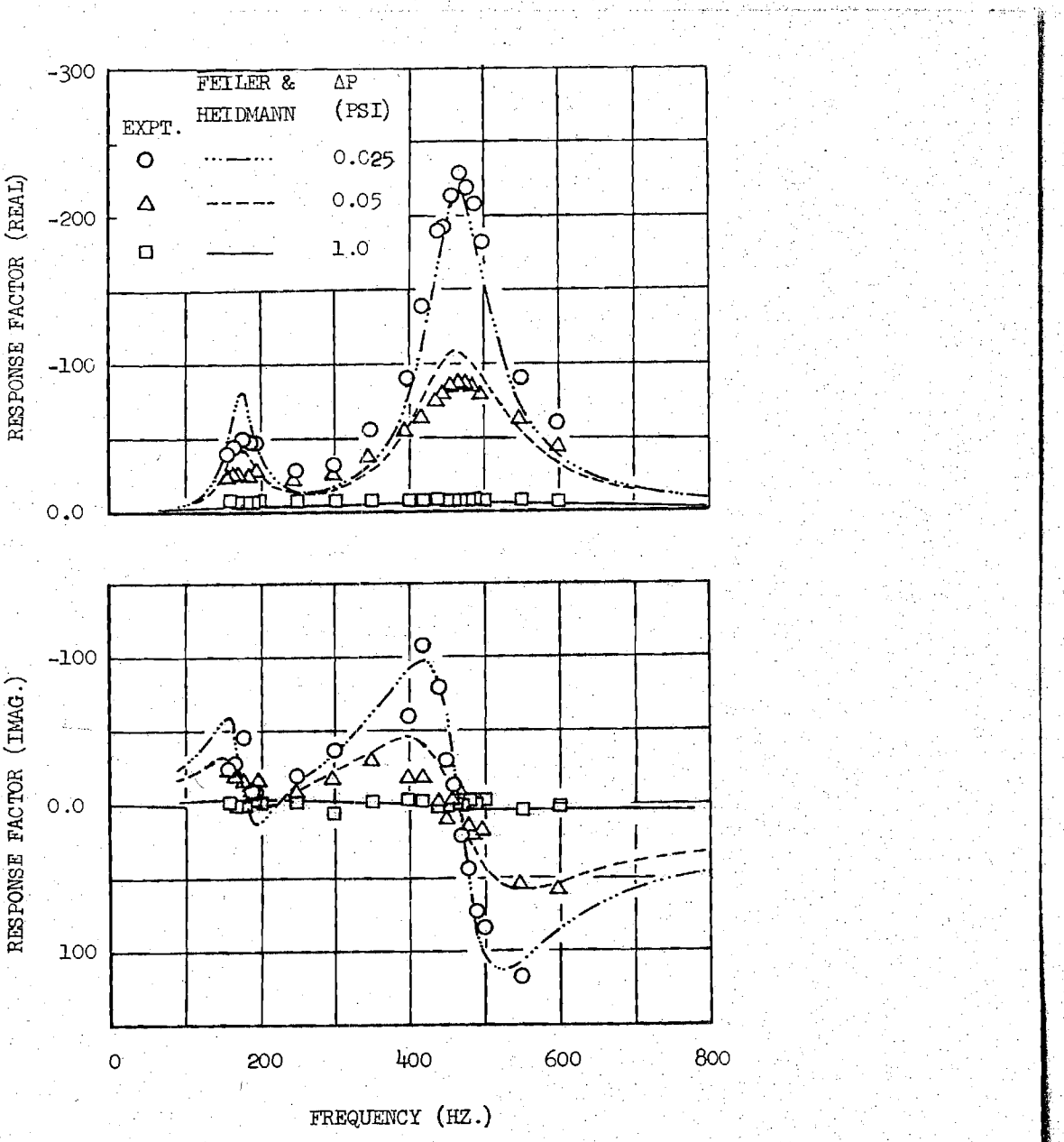

Figure 5. Frequency Dependence of Injector Orifice Response Factor of Configuration 3

E-16-607

NASA GRANT NGL 11-002-085

BEHAVIOR OF NOZZLES AND ACOUSTIC LINERS IN THREE-DIMENSIONAL ACOUSTIC FIELDS

Yearly Progress Report for Period 1 April 1972 to 31 March 1973

Prepared by: Ben T. Zinn, Principal Investigator
William A. Bell, Instructor
B. Robert Daniel, Research Engineer

School of Aerospace Engineering
Georgia Institute of Technology
Atlanta, Georgia

PROGRESS DURING THE REPORT PERIOD

A. Introduction and Summary

This report summarizes the work done under NASA Grant NGL 11-002-085 during the year 1 April 1972 to 31 March 1973.

The research conducted under this grant is divided into three major tasks. The first task consists of experimentally determining the admittances of a family of Laval nozzles and comparing the results with available theoretical predictions. Since the admittance is often used as a boundary condition in combustion instability analyses,[1,2,3] it is important that reliable nozzle admittance data be available. To date, the nozzle admittance measurements have been completed and the data show that Crocco's three-dimensional nozzle admittance theory provides accurate admittance values. The experimental data compare favorably with the theoretical predictions over a wide range of frequencies and nozzle entrance Mach numbers. Also, during this past year, Crocco's theory has been extended to evaluate the nozzle admittance in situations where the amplitude of the oscillation in the nozzle increases or decreases with time. The extended theory, a description of the associated computer program, and a comparison of the theoretical predictions with relevant experimental data were published as a NASA technical report (NASA CR-121129) and distributed to the persons on a mailing list provided by NASA.

The second major task of this research consists of evaluating the damping capabilities of various liner-nozzle combinations. This task has been initiated during the past year and preliminary data have been obtained. An outline of the results is briefly discussed in this report.

The last task of this research consists of experimentally determining the admittance of various injector configurations for comparison with available theoretical predictions. Work on this project has only recently begun, and results will be presented in future reports.

A brief outline of the results obtained from the nozzle and liner studies will now be presented.

B. Nozzle Admittance Studies

This investigation was undertaken to provide experimental nozzle admittance data for comparison with the values computed from Crocco's theory.[4] When this research began, the theoretical predictions had not been verified experimentally although these predictions had been used in several combustion instability analyses.[1,5]

To obtain experimental nozzle admittance values, the classical impedance tube technique[6] was extended to include three-dimensional waves and a constant, one-dimensional, mean flow. The experimental setup consists of a cylindrical tube with a sound source at one end and the choked nozzle under investigation at the other end. During an experiment, the incident wave from the sound source combines with the wave reflected back from the nozzle to form a standing wave pattern in the tube. The structure of the standing wave pattern depends upon the nozzle admittance. By taking pressure amplitude and phase measurements at several locations along the tube, the nozzle admittance value which gives the best fit between the standing wave pattern computed from theory and the measured experimental points is determined.

To improve the experimental technique, an analog-to-digital data reduction computer program was developed during this past year. This program decreased the time required for data reduction by previously used methods by several orders of magnitude. This computer program calculates pressure amplitudes and phases from the analog signals recorded by the pressure transducers during a test. Although the admittance can be determined from either pressure amplitude or phase data, optimum accuracy was achieved by using both amplitude and phase data in the determination of the nozzle admittances. The experimental nozzle admittance values obtained using this technique were in excellent agreement with the theoretical predictions. Several nozzle configurations were tested at entrance Mach numbers ranging from 0.08 to 0.24 and at frequencies covering the range of longitudinal and mixed first tangential-longitudinal modes. A portion of the results of this investigation were published in the March 1973 edition of the AIAA Journal.

In addition to the experimental work, theoretical investigations led to the extension of Crocco's theory to include the effects of a temporal decay coefficient. The extended theory and the associated computer program are described in NASA CR-121129, and the computer program has recently been sent to the NASA Computer Program Library. These studies indicated that variations of wave amplitude should be accounted in the prediction of the nozzle admittance.

Based on the theoretical and experimental results, the following general conclusions can be made.

(1) The nozzle provides less damping for three-dimensional oscillations than for longitudinal modes. In fact, for three-dimensional waves, the real part of the nozzle admittance can assume negative values, which indicates that the nozzle exerts a destabilizing influence upon the chamber oscillations.

(2) The temporal decay coefficient can have a significant influence on the computed nozzle admittance values.

(3) For longitudinal modes, increasing the nozzle length increases the value of the real part of the nozzle admittance and thus tends to have a stabilizing influence upon chamber oscillations. For mixed first tangential-longitudinal modes, the opposite effect is observed.

(4) Increasing the Mach number increases nozzle damping for both longitudinal and three-dimensional modes.

Additional tests have been conducted with quasi-steady nozzle configurations, and the data are currently undergoing analysis. The results will be presented in future reports.

C. Liner Admittance Studies

During the past year testing of acoustic liners has been initiated to determine the local liner admittance and the gross admittance of various liner-nozzle combinations. These tests are being performed in order to assess liner damping capabilities, provide data for comparison with current liner theories, and evaluate existing design criteria.

To date, one liner has been extensively tested. This liner consists of a perforated cylindrical inner shell and a rigid outer shell with the annular gap between forming the resonator cavity. During a test, the liner is inserted between the end of the impedance tube and the nozzle entrance. The gross admittance of the liner-nozzle combination is measured using the experimental technique and data reduction computer program developed in the nozzle admittance studies. Recently, this computer program was extended to determine local liner admittances from pressure amplitude and phase measurements taken inside the liner cavity and in the chamber.

Experimental results obtained with the above-mentioned liner are in poor agreement with available theoretical predictions. This disagreement can be attributed to the fact that there is wave motion inside the non-partitioned annular liner cavity. Therefore, the assumption of spatially uniform pressure in the cavity, which is used in the development of the liner theory, is violated. To overcome this difficulty, the liner cavity has been partitioned in order to eliminate the cavity wave motion and minimize the spatial variation in pressure. The experimental response of this liner is presently being investigated. Based on the results of this testing, at least two additional liners will be designed, built, and tested.

Major goals for next year's studies include:

(1) The completion of the liner program and presentation of the results in a special report.

(2) The experimental determination of the responses of various injector designs. The measured admittance date will be compared with the predictions of existing theories.

REFERENCES

1. Crocco, L., "Theoretical Studies on Liquid Propellant Rocket Instability," Tenth Symposium (International) on Combustion, Combustion Institute, pp. 1101-1128, June 1965.

2. Priem, R. J. and Rice, E. J., "Combustion Instability with Finite Mach Number Flow and Acoustic Liners," NASA TMX-52412, 1968.

3. Mitchell, C.E., Expander, W. R., and Baer, M. R., "Determination of Decay Coefficients for Combustors with Acoustic Absorbers," NASA CR-120836, January 1972.

4. Crocco, L., and Sirignano, W. A., "Behavior of Supercritical Nozzles under Three-Dimensional Oscillatory Conditions," AGARDograph 117, Butterworth Publications Limited, 1967.

5. Zinn, B. T. and Savell, C. T., "A Theoretical Study of Three-Dimensional Combustion Instability in Liquid Propellant Rocket Engines," Tenth Symposium (International) on Combustion, Combustion Institute, pp. 139-147, June 1965.

6. Scott, R. A., "An Apparatus for Accurate Measurement of the Acoustic Impedance of Sound Absorbing Materials," Proceedings of the Physical Society, Vol. 58, p. 253, 1946.

File/ E-16-607

NASA GRANT NGL 11-002-085

THE RESPONSE FACTORS OF ACOUSTIC LINERS AND THE UNSTEADY COMBUSTION PROCESS IN UNSTABLE LIQUID PROPELLANT ROCKET MOTORS

Yearly Progress Report for the Period

1 April 1973 to 31 March 1974

Prepared by: Ben T. Zinn, Principal Investigator
William A. Bell, Instructor
B. Robert Daniel, Research Engineer
B. A. Janardan, Post-Doctoral Fellow
Stanley P. Poynor, Graduate Research Assistant

School of Aerospace Engineering
Georgia Institute of Technology
Atlanta, Georgia

PROGRESS DURING THE REPORT PERIOD

A. Introduction

This report summarizes the work done under NASA Grant NGL 11-002-085 during the year 1 April 1973 to 31 March 1974.

The research work conducted during the reporting period was divided into two major studies. The first study, which has since been completed, concentrated on the determination of the behavior and damping of various acoustic liner designs and the capabilities of various acoustic liner-nozzle combinations used in liquid rockets. The performance of four different liner configurations was tested in an impedance tube containing three-dimensional wave motion and a one-dimensional mean flow past the liner surface. Both the local liner admittance and the overall wave attenuation provided by various acoustic liner-nozzle combinations were measured. A comparison was made between the experimental data and predictions from current theoretical analyses to evaluate the applicability of these theories.

The second investigation conducted under this program was concerned with the determination of the response factors of various liquid and gaseous rocket injector configurations. The measured injector response factor data were then used to check the applicability of the predictions of the Feiler and Heidmann study[1] that investigated this problem analytically. During the reporting period, the required experimental setup was developed and its operation was checked out. Also, all the required injector configurations were designed, fabricated and their admittances determined over a range of experimental conditions. The above-mentioned experimental facility and the data obtained in these tests are briefly discussed in this report.

B. Liner Admittance Studies

The liner admittance studies have been completed and the results were reported in two publications[2,3] which were presented at the 10th JANNAF Combustion Conference and the AIAA 12th Aerospace Sciences meeting. The objectives of these studies were to: (1) evaluate the performance of practical acoustic liner designs under conditions simulating those observed in unstable liquid rockets; i.e., with three-dimensional oscillations superimposed upon a one-dimensional mean flow moving past the liner face; (2) determine the overall damping provided by various liner-nozzle combinations; and (3) compare the experimental data with available theoretical predictions to evaluate the applicability of the theories.

At the time when this investigation was undertaken, the design equations used to determine acoustic liner damping and tuning frequencies were semi-empirical and they were based upon theoretical considerations of the behavior of a single Helmholtz resonator and data obtained from impedance tube experiments. In these experiments, one-dimensional waves were excited in the tube by an acoustic driver located at one end and the liner sample under investigation attached to the other end. With this experimental arrangement, the effects of mean flow past the liner face and three-dimensional wave motion, often encountered during liquid rocket combustion instability, could not be evaluated. Also, in practice, the acoustic liners used in rocket motors are placed on the combustor's walls, where their orientation is either parallel or oblique to the direction of wave motion. In the impedance tube experiments, the tested liner sample is placed normal to the direction of wave propagation. Thus, the capability of the above-mentioned semi-empirical liner design equations to adequately describe the performance of a liner under practical rocket motor flow conditions was open to question.

In the studies carried out under this grant, the performance of the acoustic liners was evaluated under conditions simulating those encountered in an unstable rocket motor experiencing three-dimensional instability in mixed first tangential-longitudinal modes. The parameters measured in this study were (1) the local liner admittance, from which the absorption coefficient and tuning frequency of the liner can be obtained and (2) the overall admittance (or damping) of various acoustic liner-nozzle combinations. The measured data were compared with the predictions of available design equations. The configurations tested in this program included four different acoustic liner geometries at mean flow Mach numbers of 0.08 and 0.24 using both quasi-steady and Laval nozzles to exhaust the flow. A typical test configuration is shown in Figure 1 and the tested liners are described in Table I. The details of the theory and experimental apparatus are presented in Reference 3.

The results of these investigations can be summarized as follows:

(1) The theoretical and experimental local liner admittance results are in good agreement for both spinning and standing three-dimensional modes for liners 1, 2, and 3 of Table I. However, poor agreement was obtained for liner 4, for which the cavities are unpartitioned, because of wave motion in the liner cavity which is not accounted for in the theory.

(2) For low mean flow Mach numbers (i.e., $\bar{M} \leq 0.08$) the mean flow has negligible effect on the damping characteristics of the liner. For high subsonic Mach numbers ($\bar{M} \geq 0.24$) the major effect of the mean flow is to increase the tuning frequency of the liner because of a decrease in the effective length of the liner orifice. In the Mach number range of 0.08 to 0.24 further

studies are necessary to quantitatively determine the influence of the Mach number on the effective length. No detectable influence of the mean flow on the local liner admittance was measured.

(3) The measured data indicate that the assumption of spatially uniform liner admittance, often used in analytical studies, can result in serious errors. The local liner admittance values can vary by as much as 50 percent at different locations on the liner face because of the dependence of the liner damping on wave amplitude.

C. Injector Response Studies

For a stability analysis of a liquid rocket motor the data describing the losses provided by the nozzle and acoustic liners must be supplemented by data that quantitatively describes the influence of the injector on the stability of the engine. Customarily the effect of the injector is described by means of a response factor which is defined as the complex ratio of the burning rate perturbation to the chamber pressure perturbation. In Reference 1, the response of a coaxial injector element has been studied theoretically, in an attempt to determine the dependence of the injector response factor upon injector design parameters. The present investigation had been undertaken with the object of providing experimental data that could be used to check the applicability of the predictions of Reference 1.

The injector admittance data, from which the required response factors can be determined, is measured in this investigation by using the modified impedance tube technique. The experimental facility shown in Figure 2 consists of a 6 inch diameter cylindrical tube with a sound source

capable of generating harmonic waves of desired frequency placed at one end and the injector element under investigation placed at the other end. During an experiment, the flow of a gaseous propellant through the injector is simulated by the flow of air. Regulating values are provided to ensure that the pressure drop across the injector orifices is maintained at a required value. By means of the acoustic driver, a standing wave pattern of a given frequency is excited in the tube and a microphone probe is traversed along the tube to measure the axial variation of the standing wave pattern. The admittance of the injector surface is then determined by measuring (a) the distance of the first pressure amplitude minimum or maximum from the injector surface and (b) the ratio of the minimum pressure amplitude to the maximum pressure amplitude. The response factor N of the tested injector is then calculated from the measured admittance y using the following relationship:

$$N = \frac{1}{\gamma}\left(1 + \frac{y}{\bar{M}}\right)$$

where $\bar{M}$ is the mean flow Mach number at the injector orifice. The frequency dependence of the admittance and the response factor of the tested injector is then determined by repeating the experiment at different frequencies.

During the reporting period the admittances of four injector configurations shown in Figures 3 through 6 were investigated under three different tasks. The objective of Task I is to determine the admittances of the experimental configurations, shown in Figures 3 and 4, that simulate the behavior of a gaseous fuel injector. In Task II, the admittances of the injector configuration shown in Figure 5, which simulates the behavior of the oxidizer flow element of a coaxial injector, is being investigated.

In Task III, the admittances of the injector configuration shown in Figure 6, which contains both the fuel and oxidizer injector elements of Tasks I and II, are investigated. The total injector response N_t of this configuration is first calculated using the response factor data measured in Tasks I and II and using the following expression which has been used in Reference 1:

$$N_t = \frac{\bar{w}_f}{\bar{w}_t} N_f + \frac{\bar{w}_{ox}}{\bar{w}_t} N_{ox}$$

In the above expression N_f and N_{ox} respectively represent the response factors of the fuel and oxidizer injector elements while $\bar{w}_f/\bar{w}_t$ and $\bar{w}_{ox}/\bar{w}_t$ represent the mean fractions of the fuel and oxidizer flow rates, respectively. The injector response factors obtained by use of the above expression will be compared with the response factor measured using the Task III injector configuration. Such a comparison will provide a check upon the validity of the above expression.

To date measurements have been made using the injector elements of Tasks I and II and the admittance data obtained is presented in this report. Tests with the Task III injector configuration are in progress and the resulting data will be presented in future progress reports.

Before presenting the results, it is necessary to point out a difference between the geometrical configurations of the injector elements whose admittances are measured in this study and the injector configurations considered in the theoretical model of Feiler and Heidmann.[1] The theoretical analysis considers the behavior of a single injector element and its predictions provide a response factor that is valid at the exit plane of the injector orifice. It would be extremely difficult to directly measure the response factor of a single injector element; instead, this study undertook the measurement of the response factors of injector configurations

containing a number of injector elements. The admittances measured in this study represent "average" admittances over the tested injector surface. Hence, before any meaningful comparisons between the predicted and the measured sets of admittance data can be made, the above-mentioned difference must be suitably taken into consideration. Using mass conservation considerations, this difference can be accounted for by multiplying the theoretically predicted admittances by the open area ratio σ (defined as the ratio of the sum of the orifice cross-sectional areas to the impedance tube cross-sectional area) of the injector configuration. This step "averages" the predicted admittance over the injector surface. To illustrate this point the theoretically predicted frequency dependence of the admittances of the Task I 13-orifice injector configuration with a pressure drop of 1 psi across the injector orifices is presented in Figure 7. The broken lines in this figure describe the admittances at the exit of the injector orifices while the solid lines represent the "average" admittances of the injector surface. It is this "average" data which has to be compared with the measured admittances.

An examination of Figure 7 also indicates that the "average" admittances of the injector surface with pressure drop of 1 psi across the injector orifice are small in magnitude. These admittances further decrease in magnitude upon increasing the pressure drop across the injector orifices and/or decreasing the open area ratio of the injector configuration. This observation indicates that with the injector configurations shown in Figures 3 through 6 it would be difficult to experimentally differentiate between admittance data measured with large pressure drops across the injector orifices. Hence, in order to obtain admittance data for the purposes of a meaningful comparison with the theoretically predicted data, it was

decided to determine the frequency dependence of the admittances of the above-mentioned injector configurations with pressure drops of less than 0.1 psi across the injector orifices. The magnitudes of the predicted admittances at the injector surfaces with such pressure drops across the injector orifices are well within the measurable range of the experimental setup.

The measured admittances of the injector surfaces are presented in Figures 8 through 10 along with the admittance data predicted using the Feiler and Heidmann analysis. The frequency dependence of the admittance of the Task I 13-orifice injector (σ = 0.0465) with pressure drops of 0.025 and 0.05 psi and of the Task I 5-orifice injector (σ = 0.0179) with pressure drops of 0.04 and 0.06 psi are presented in Figures 8 and 9 respectively. In Figure 10 the frequency dependence of the admittance of the Task II 13-orifice injector (σ = 0.0172) with pressure drops of 0.025 and 0.05 psi is presented. For comparison purposes the admittance data of each of the above injector configurations measured with no flow present are also presented in Figures 8 through 10. An examination of these figures indicates reasonably good agreement between the measured and theoretically predicted admittance data. The scatter observed, particularly in the measured values of the imaginary part of the admittance, is due to the fact that at the corresponding frequencies the standing wave in the impedance tube has a fairly flat minima and hence a precise measurement of the axial location on this minima becomes difficult.

The studies planned for the next reporting period are:

(a) Investigation of the response factor behavior of the Task III injector configuration

(b) Continue a present study concerned with the determination of whether injector admittance data with higher pressure drops across the injector orifices can be obtained with suitable modifications to the existing experimental setup.

(c) As a part of the continuation of this research program, new injectors will be designed, fabricated and their admittances measured in order to determine the dependence of the injector response factor upon injector design parameters.

REFERENCES

1. Feiler, C. E. and Heidmann, M. F., "Dynamic Response of Gaseous-Hydrogen Flow Systems and its Application to High Frequency Combustion Instability," NASA TN D-4040, June 1967.

2. Bell, W. A., Daniel, B. R., Smith, A. J., Jr. and Zinn, B. T., "Experimental Determination of Acoustic Liner Attenuation Under Simulated Engine Flow Conditions," Proceedings of the 10th JANNAF Combustion Meeting, CPIA Publication 243, Vol. II, December 1973, pp. 285-298.

3. Bell, W. A., Daniel, B. R. and Zinn, B. T., "Acoustic Liner Performance in the Presence of a Mean Flow and Three-Dimensional Wave Motion," AIAA Paper No. 74-61, January 31, 1974.

Table 1

Liner Characteristics

	Liner 1*	Liner 2**	Liner 3#	Liner 4##
Cavity Diameter	1.000	-----	-----	-----
Orifice Length	0.866	0.688	0.500	0.500
Orifice Diameter	0.250	0.250	0.159	0.159
$\sigma = \frac{\text{Orifice Area}}{\text{Cavity Area}}$	0.0625	0.032	0.035	0.027
Backing Distance	0.500	0.313	0.435	0.435
Effective Length	1.041	0.873	0.610	0.619
Nondimensional Tuning Frequency	1.971	1.945	2.058	~2.0
Linear Resistance @ 32°F	0.0966	0.158	0.165	0.199
Aperture Mach Number @ 155 db	0.0582	0.0588	0.0584	0.0586
Nonlinear Resistance	0.8177	1.617	1.476	1.905
Cavity Width	------	0.750	0.625	12

All Dimensions in Inches

Values Based on Equations (1) - (9) of Reference (3)

*Individual Resonators

**Annular Cavity

#Partitioned

##Unpartitioned

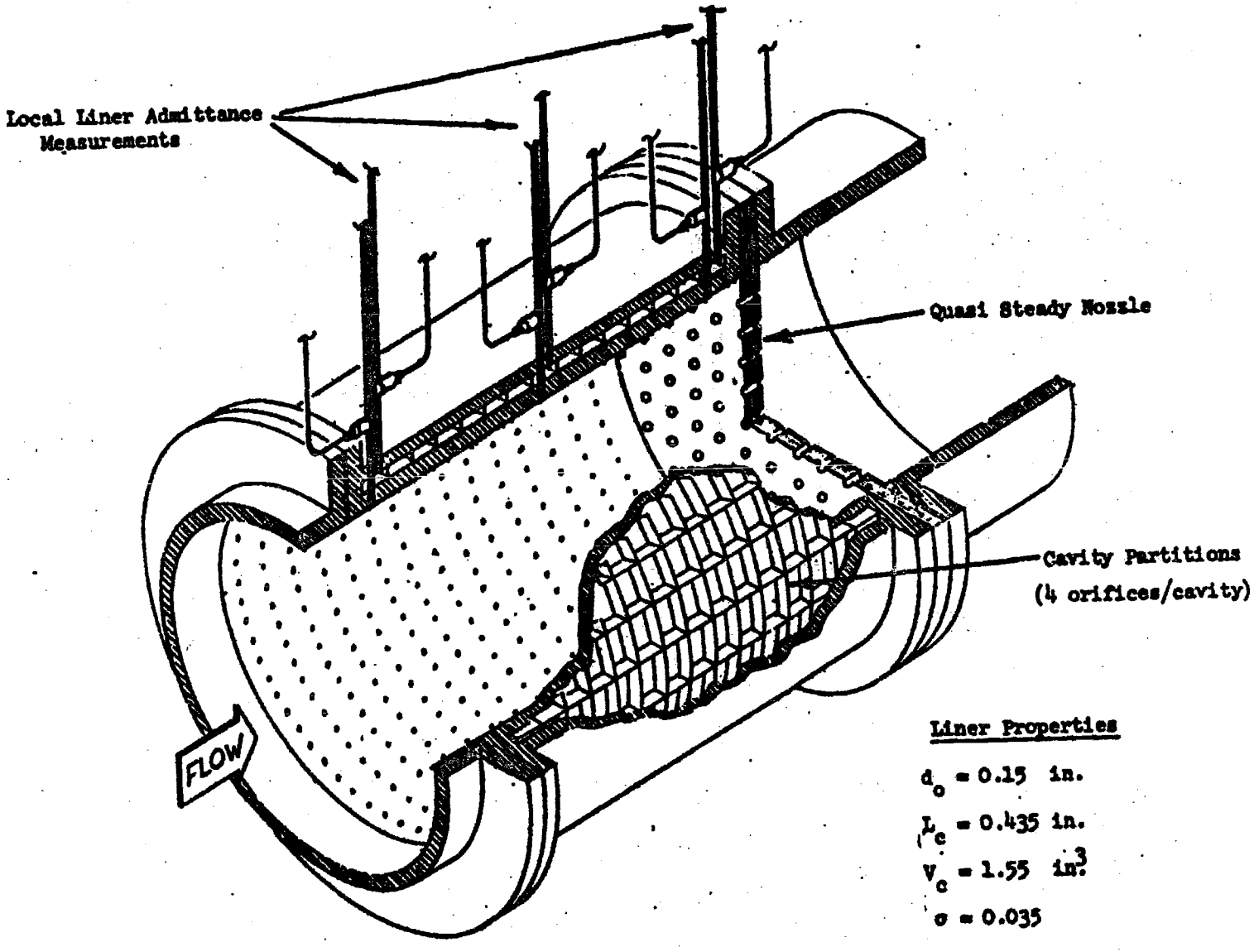

Figure 1. Partitioned Liner - Quasi Steady Nozzle Combination.

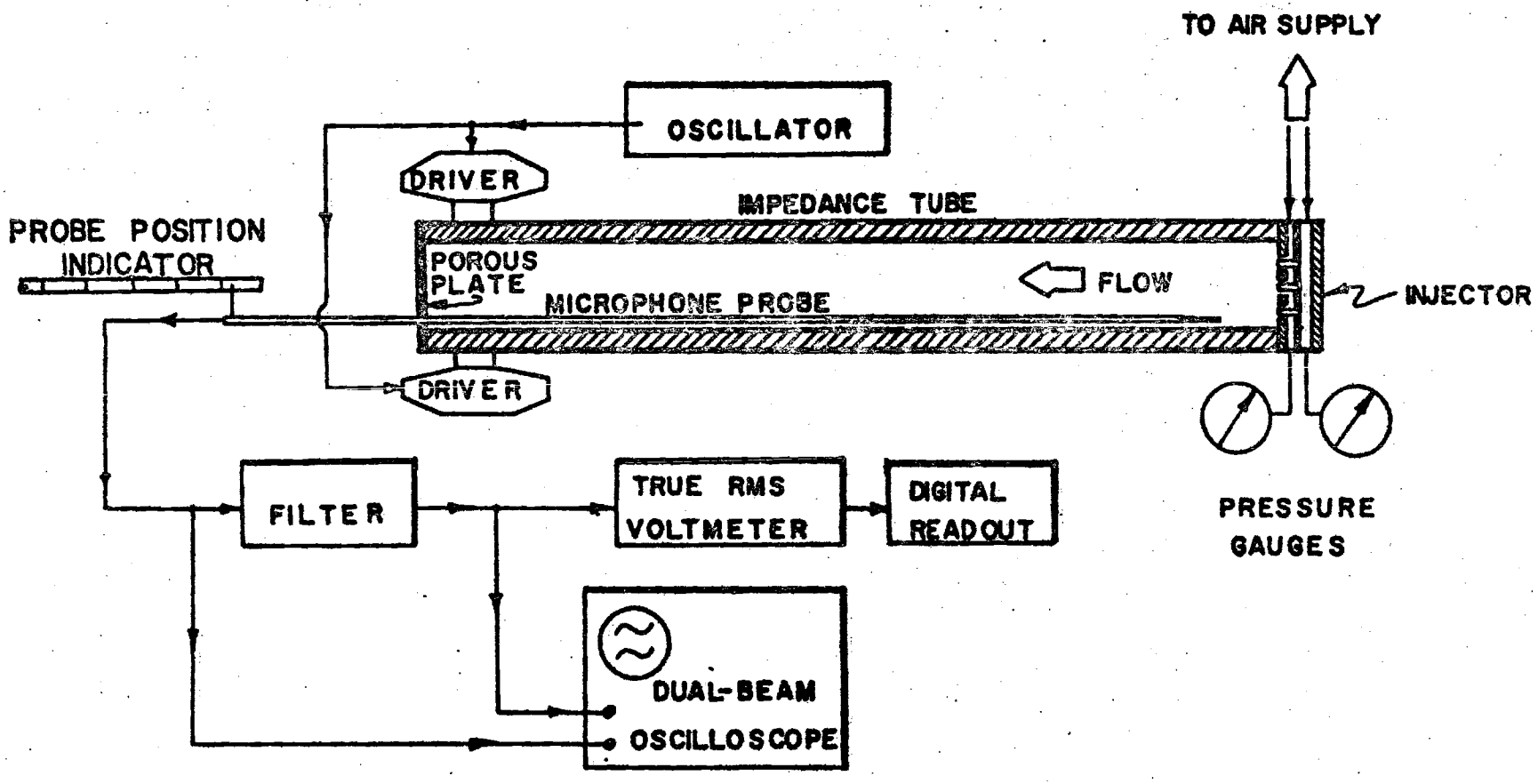

Figure 2. Experimental Apparatus

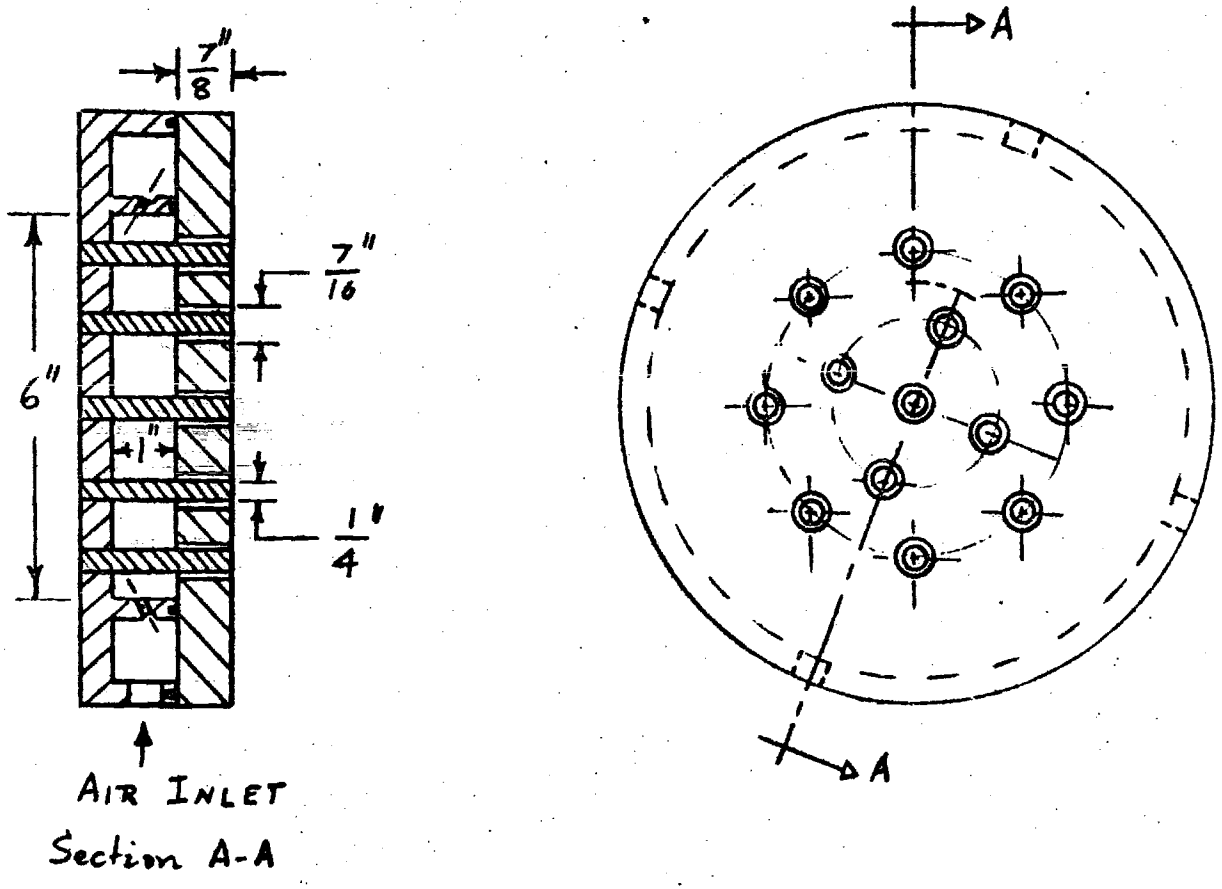

Figure 3. Task I, 13 Orifice Injector (σ = 0.0465).

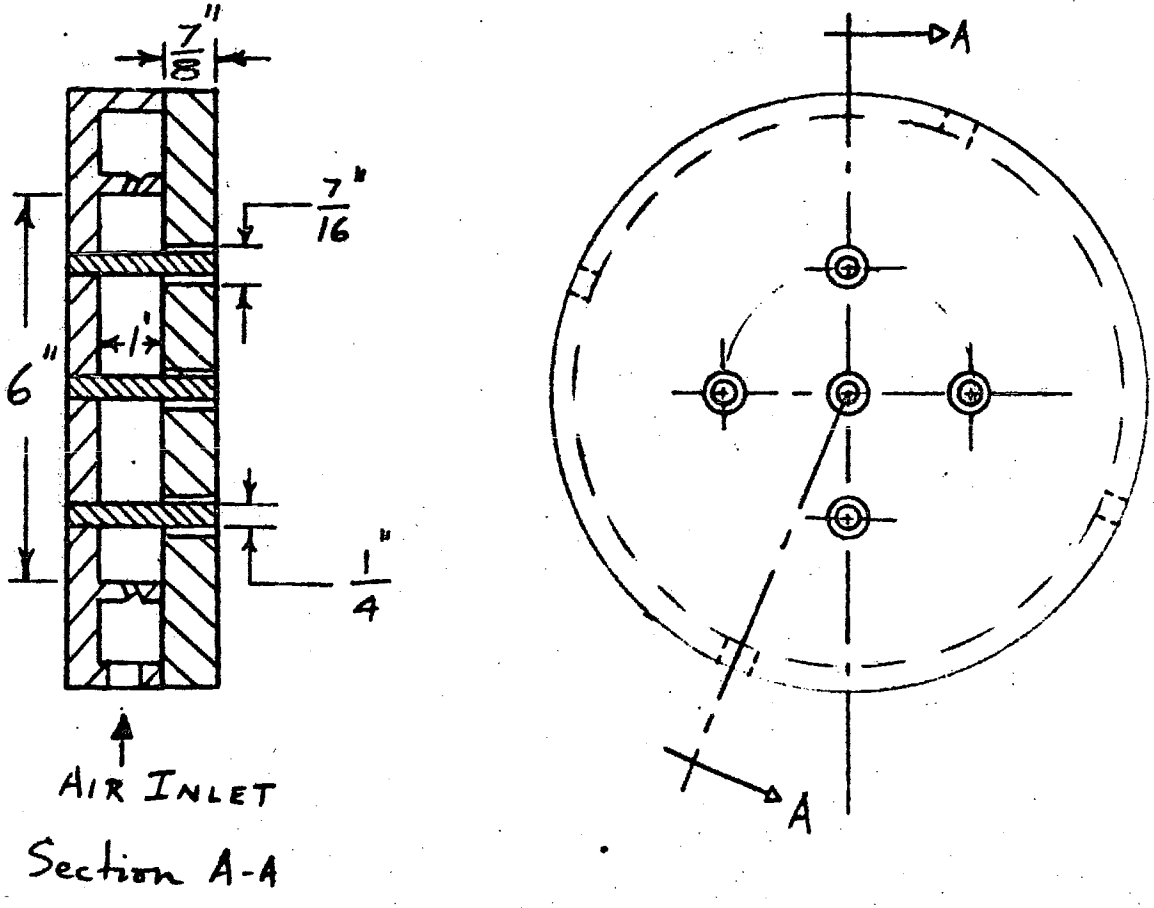

Figure 4. Task I, 5 Orifice Injector (σ = 0.0179).

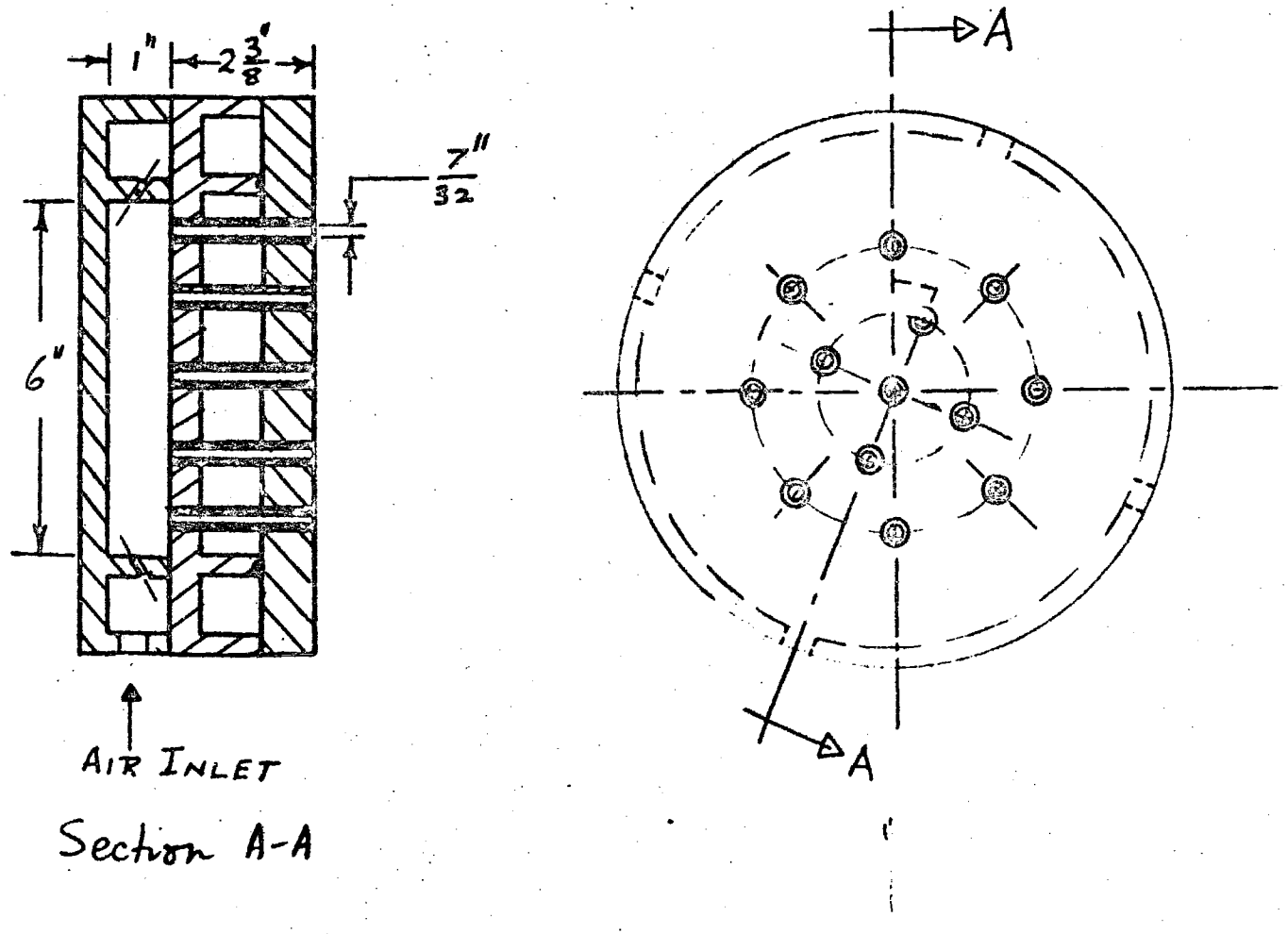

Figure 5. Task II, 13 Orifice Injector (σ = 0.0172).

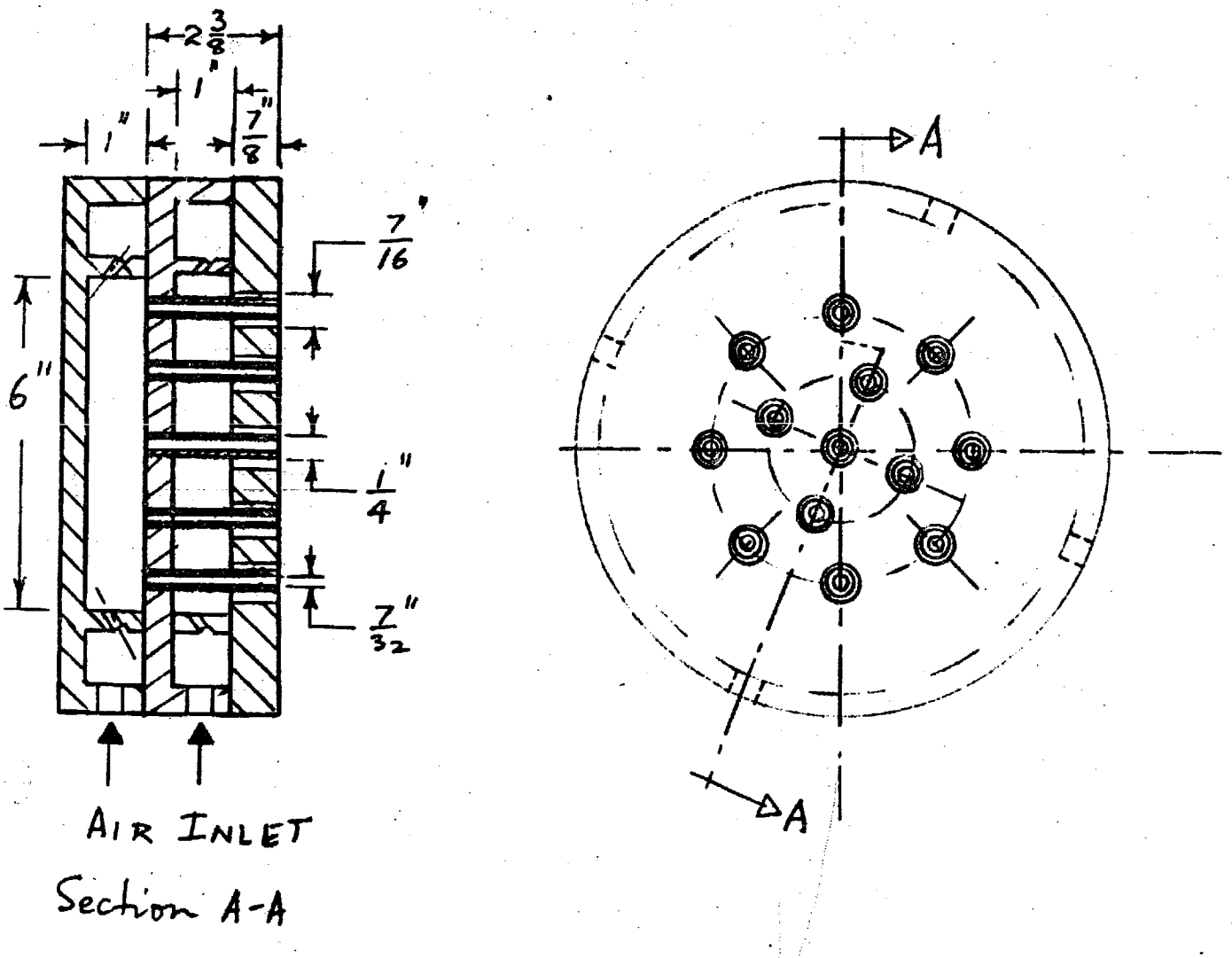

Figure 6. Task III, 13 Orifice Injector.

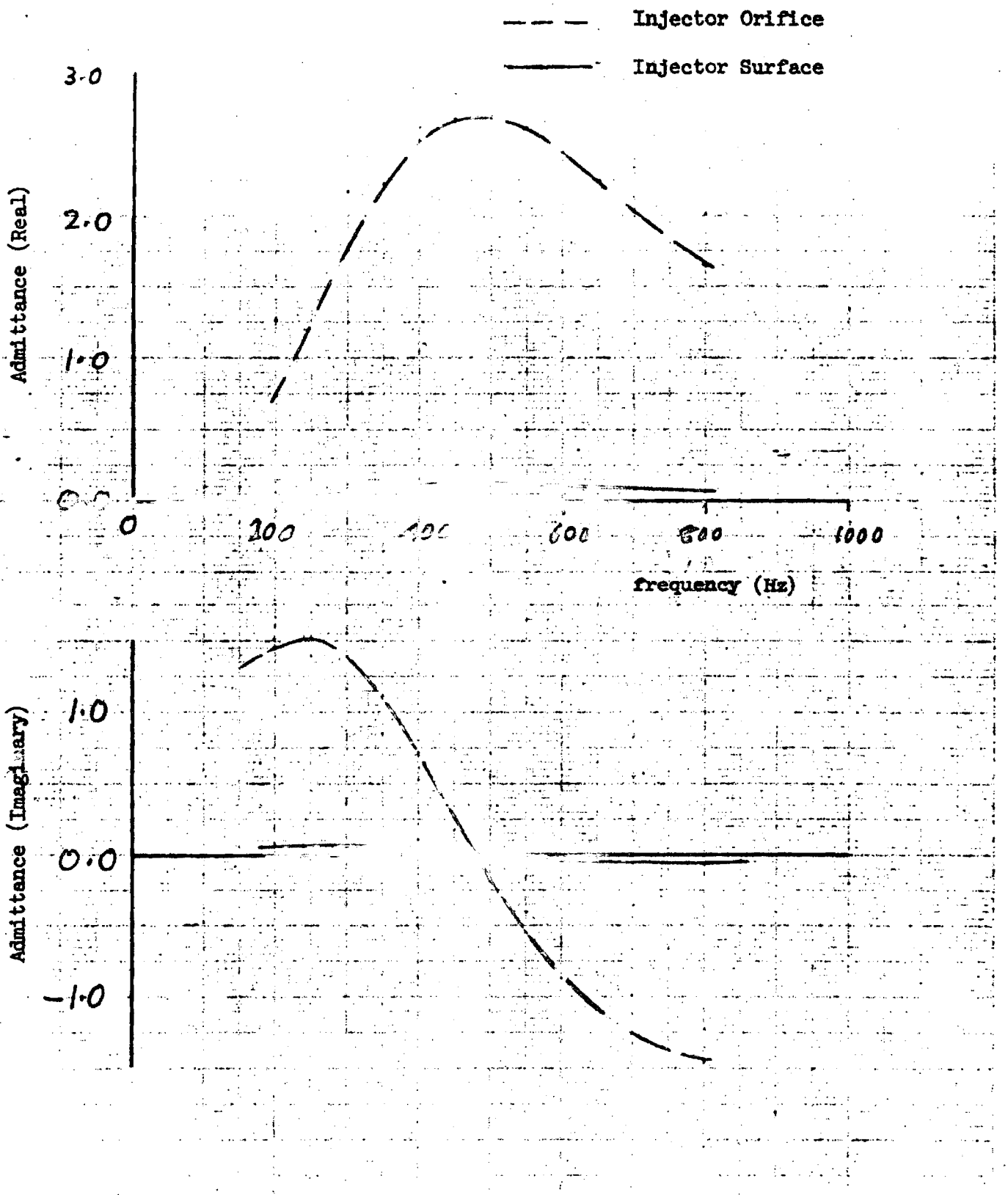

Figure 7. Task I, 13 Orifice Injector, Δp = 1 psi (σ = 0.0465).

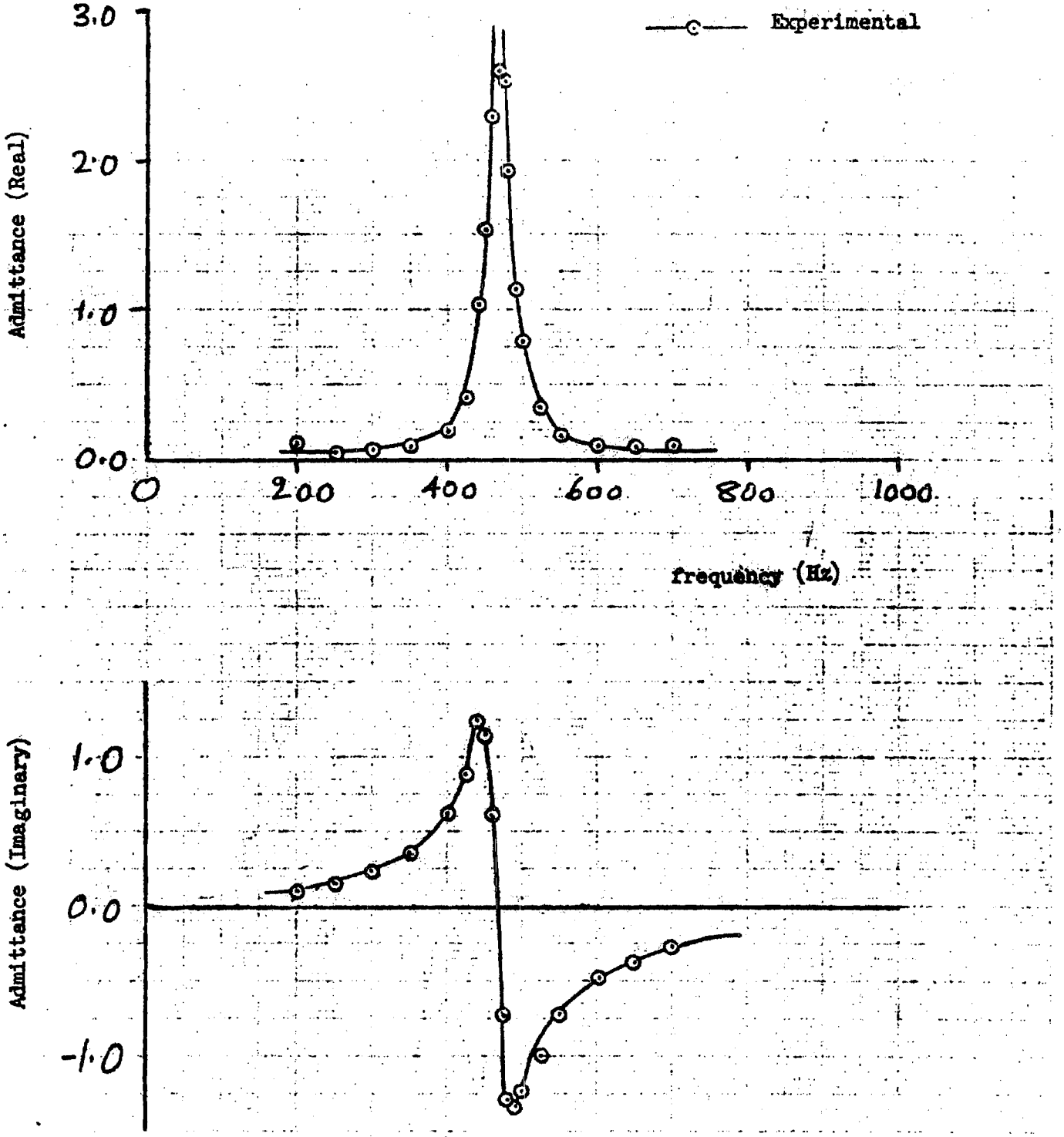

Figure 8(a). Task I, 13 Orifice Injector, NO FLOW.

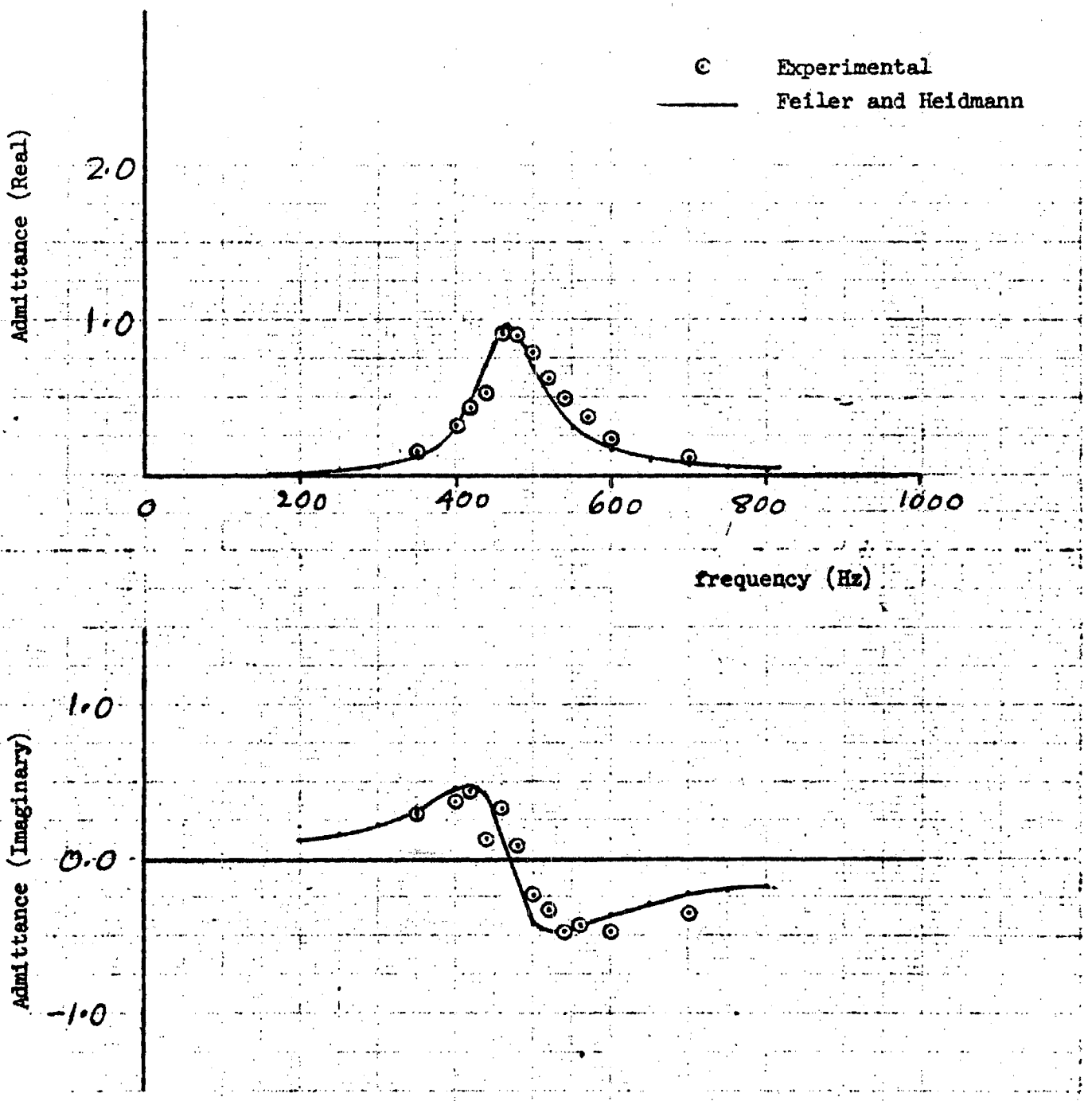

Figure 8(b). Task I, 13 Orifice Injector, $\Delta p = 0.025$ psi.

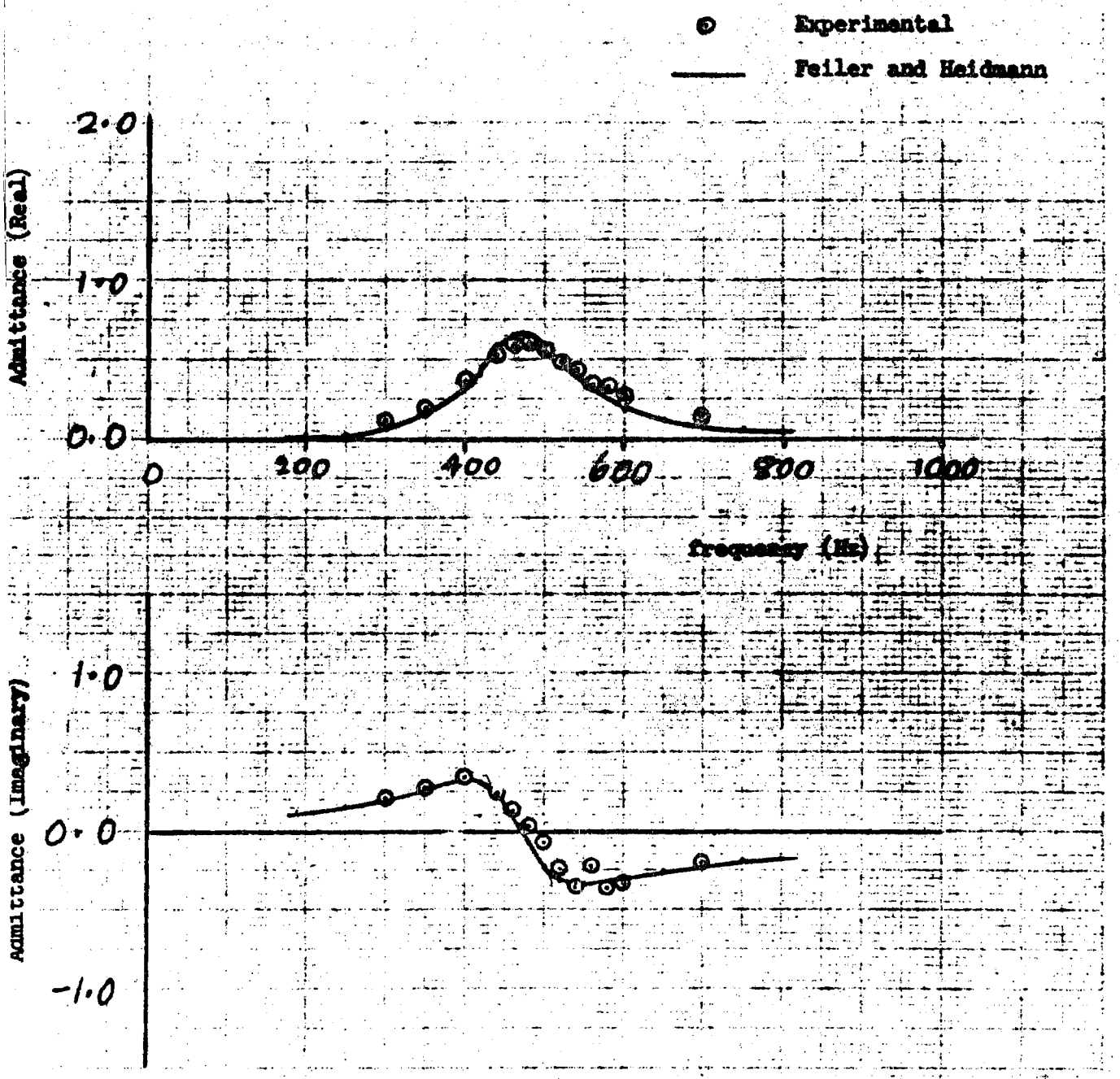

Figure 8(c). Task I, 13 Orifice Injector, $\Delta p = 0.05$ psi.

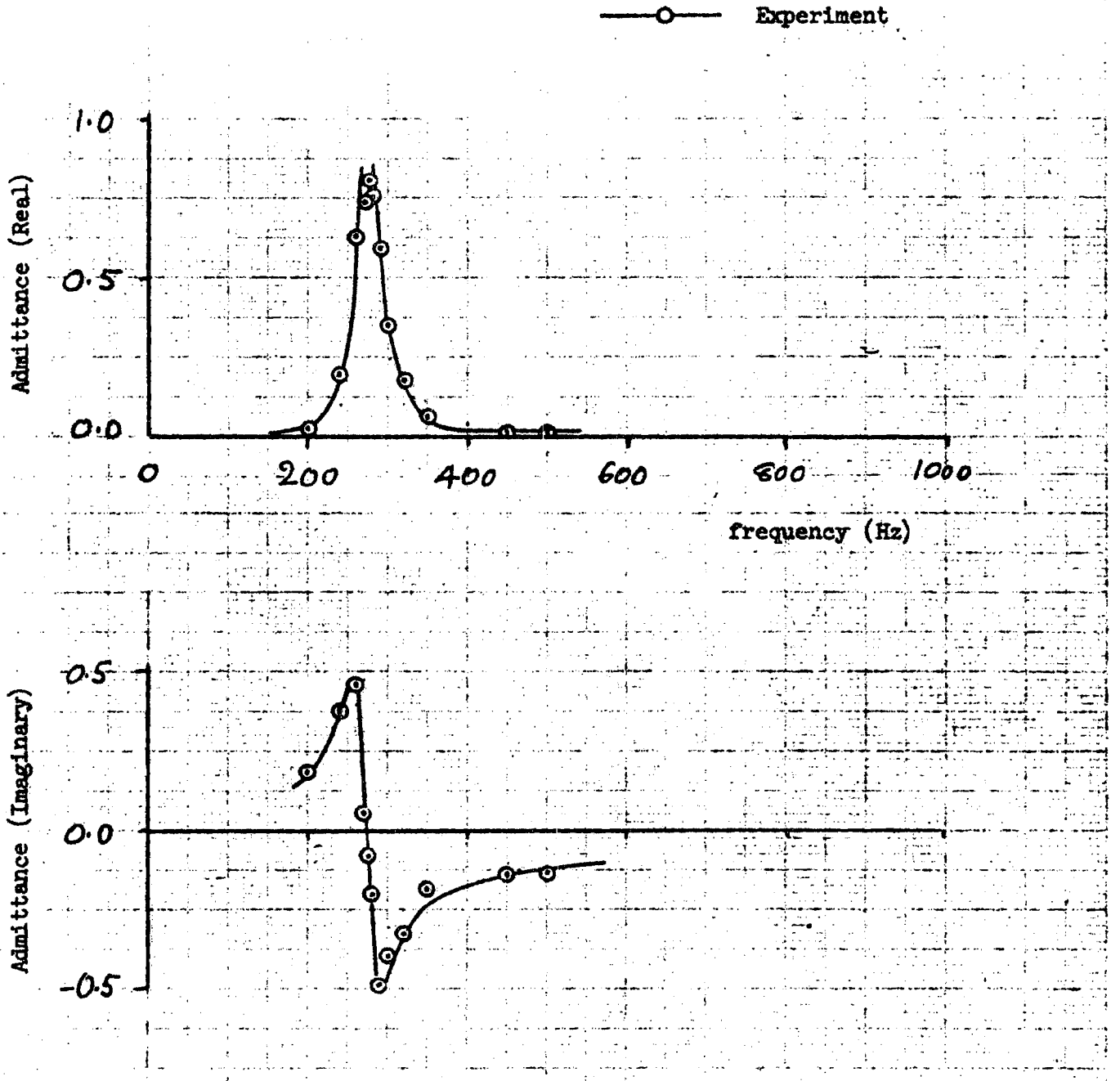

Figure 9(a). Task I, 5 Orifice Injector, NO FLOW.

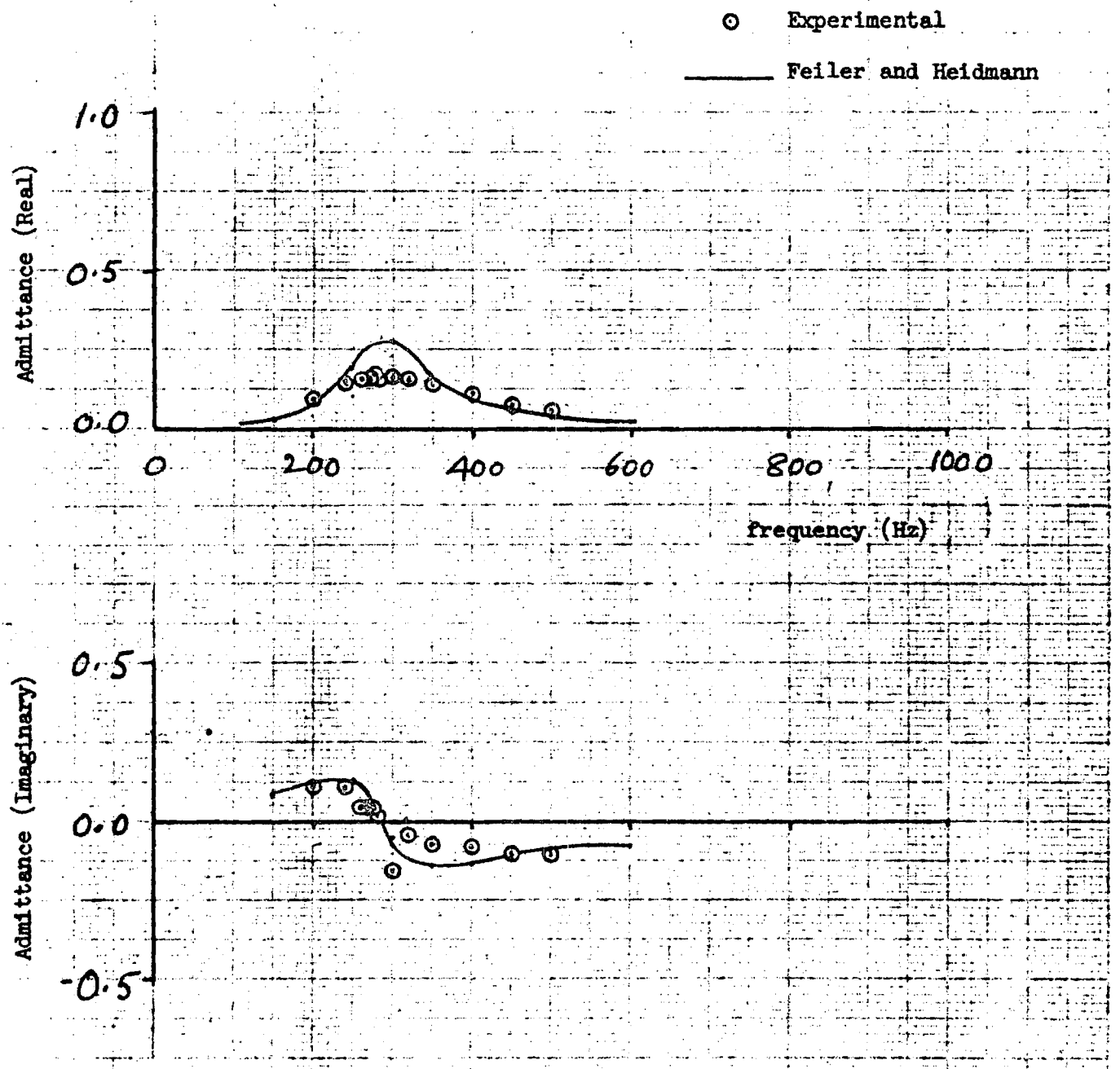

Figure 9(b). Task I, 5 Orifice Injector, $\Delta p = 0.04$ psi.

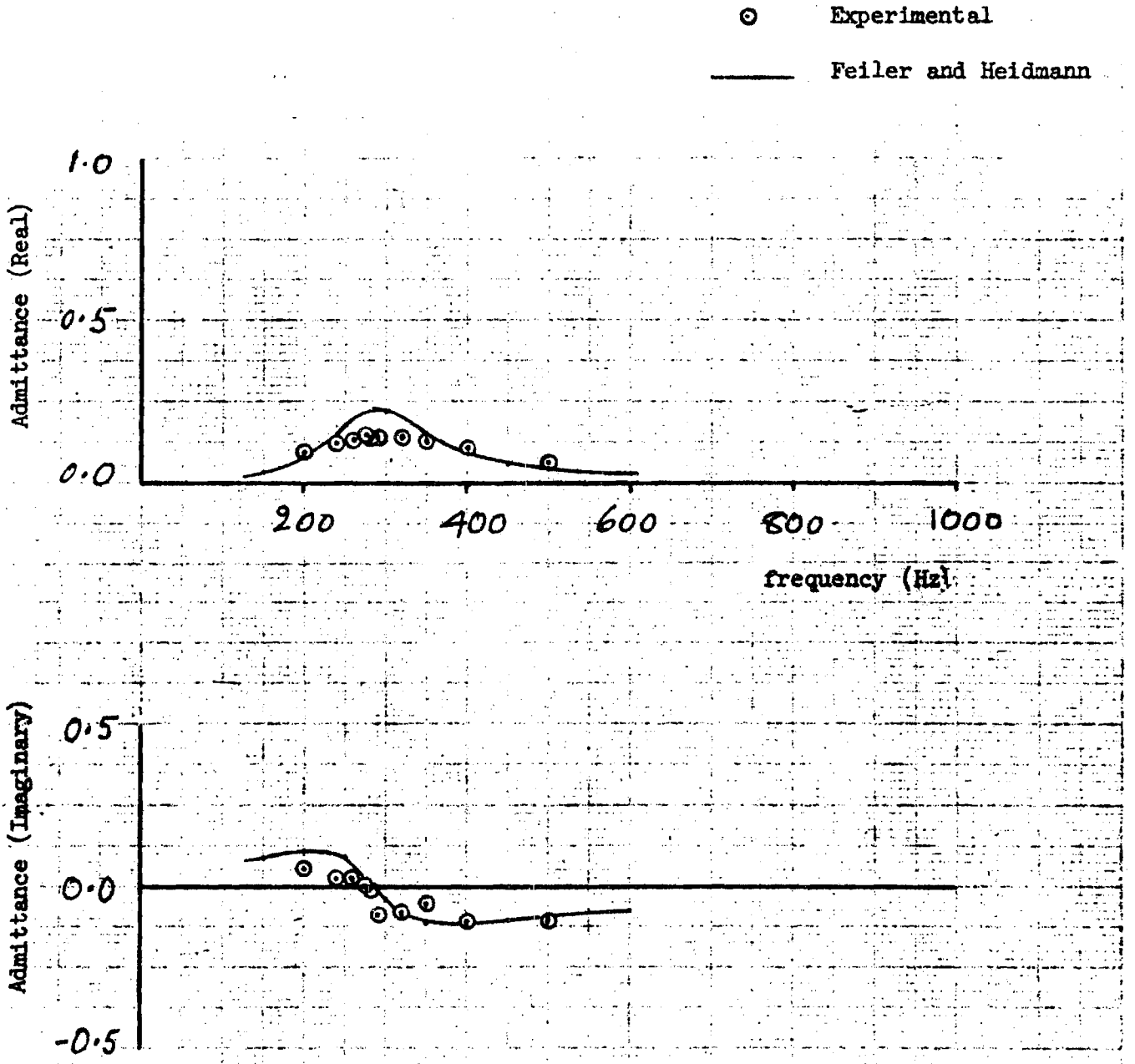

Figure 9(c). Task I, 5 Orifice Injector, $\Delta p = 0.06$ psi.

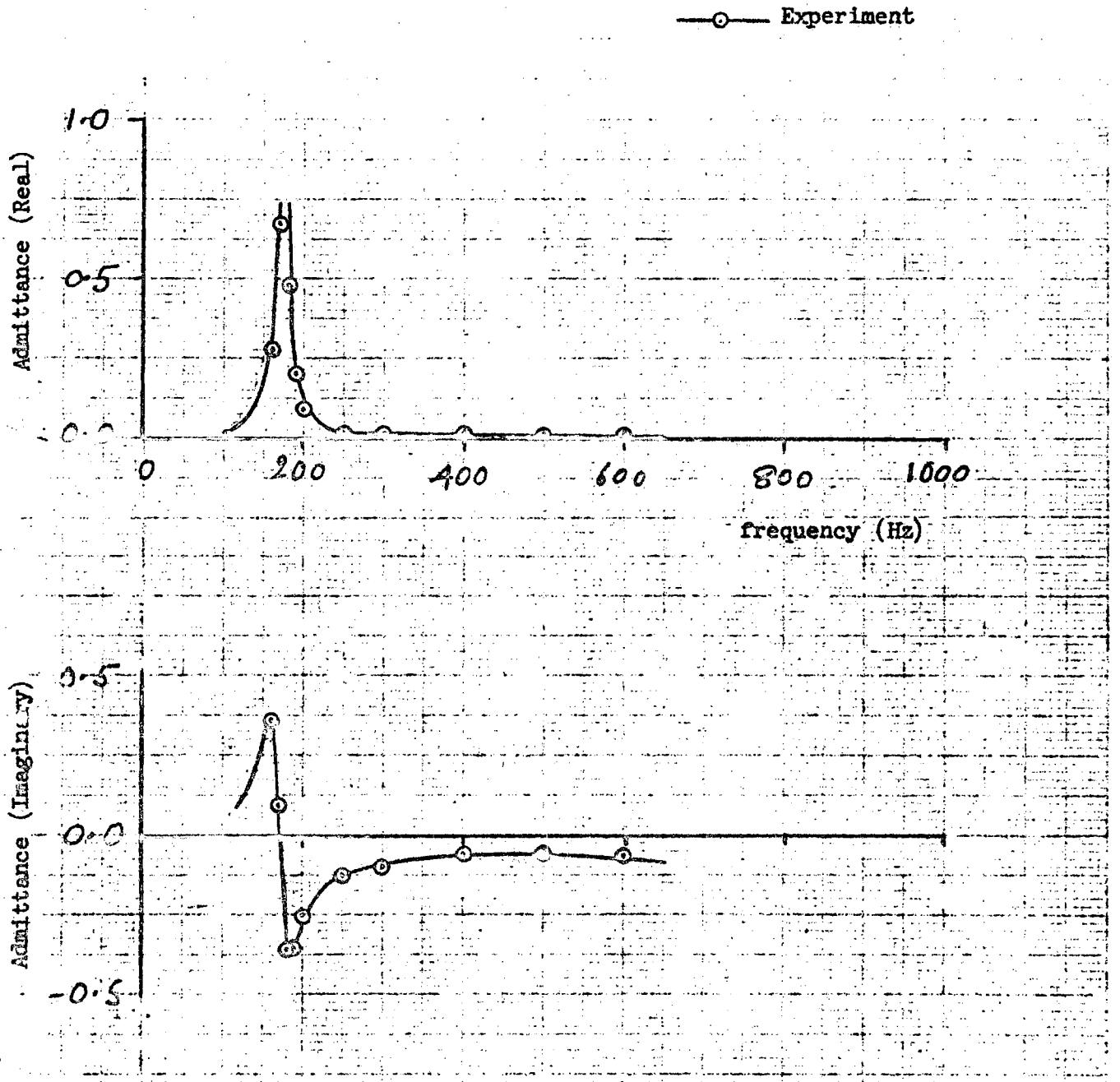

Figure 10(a). Task II, 13 Orifice Injector, NO FLOW.

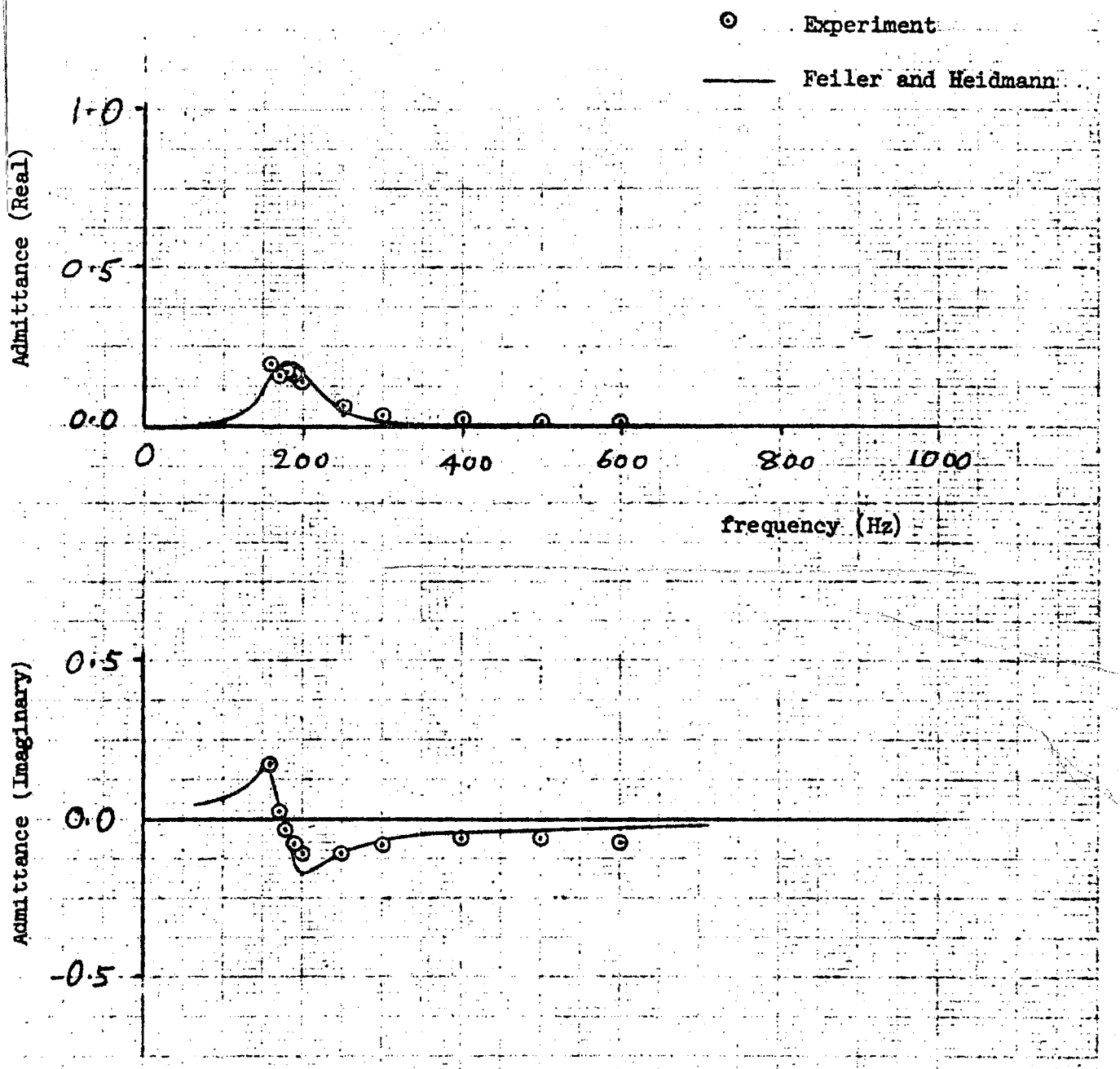

Figure 10(b). Task II, 13 Orifice Injector, $\Delta p = 0.025$ psi.

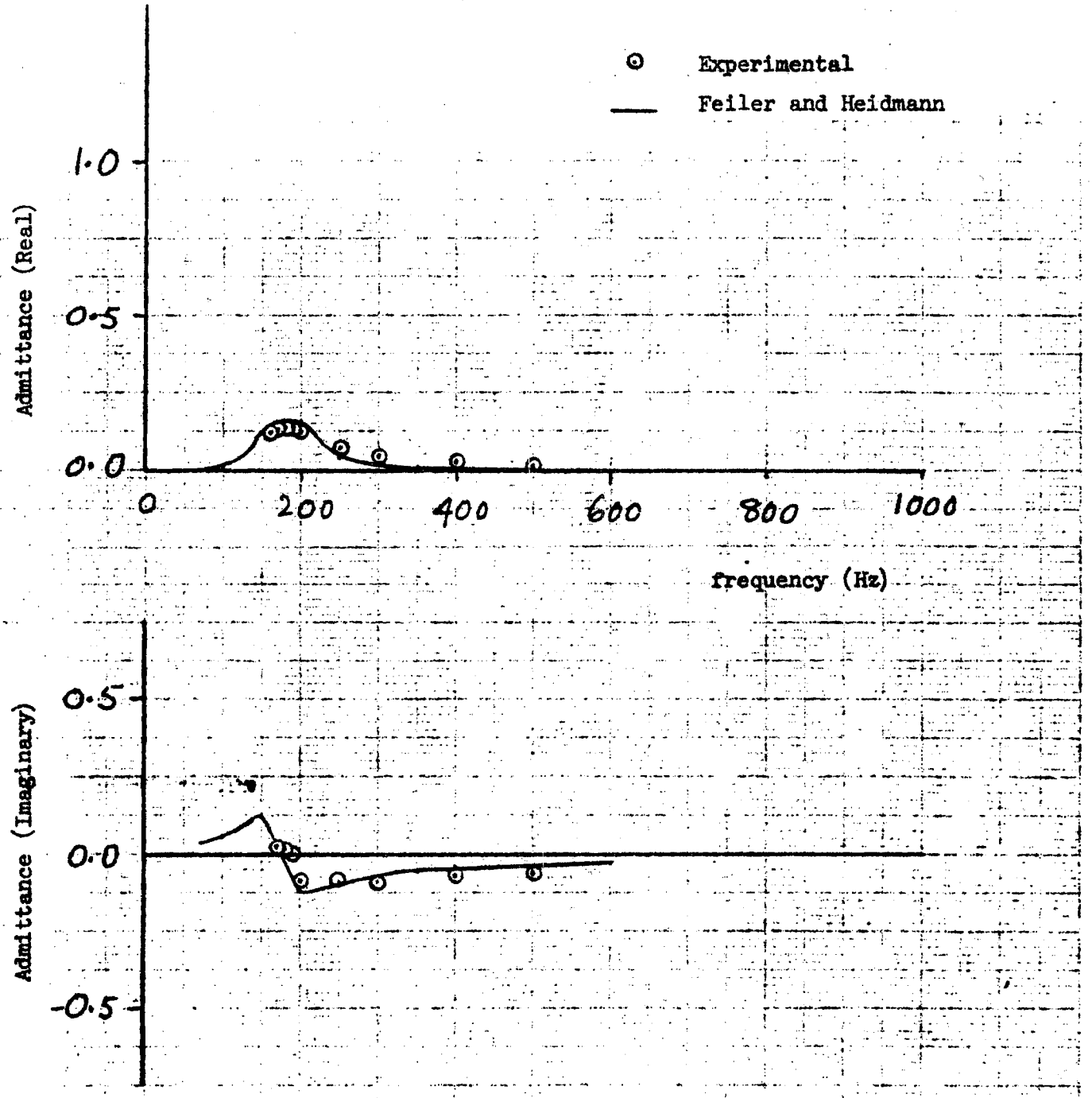

Figure 10(c). Task II, 13 Orifice Injector, $\Delta p = 0.05$ psi.

NASA CR-121129

THE PREDICTION OF THREE-DIMENSIONAL LIQUID-PROPELLANT ROCKET NOZZLE ADMITTANCES

by

W. A. Bell and B. T. Zinn

GEORGIA INSTITUTE OF TECHNOLOGY

prepared for

NATIONAL AERONAUTICS AND SPACE ADMINISTRATION

NASA Lewis Research Center
Grant NGL 11-002-085
Richard J. Priem, Project Manager

Requests for copies of this report should be referred to:

National Aeronautics and Space Administration
Scientific and Technical Information Facility
P. O. Box 33
College Park, Md. 20740

Report No.	2. Government Accession No.	3. Recipient's Catalog No.
NASA CR-121129		

Title and Subtitle	5. Report Date
THE PREDICTION OF THREE-DIMENSIONAL LIQUID-PROPELLANT ROCKET NOZZLE ADMITTANCES	February 1973
	6. Performing Organization Code

Author(s)	8. Performing Organization Report No.
W. A. Bell and B. T. Zinn	
	10. Work Unit No.

Performing Organization Name and Address	11. Contract or Grant No.
Georgia Institute of Technology Atlanta, Georgia 30332	NGL 11-002-085
	13. Type of Report and Period Covered
Sponsoring Agency Name and Address	Contractor Report
National Aeronautics and Space Administration Washington, D. C. 20546	14. Sponsoring Agency Code

Supplementary Notes

Technical Officer, Richard J. Priem, NASA Lewis Research Center, 21000 Brookpark Road, Cleveland, Ohio 44135

Abstract

Crocco's three-dimensional nozzle admittance theory is extended to be applicable when the amplitudes of the combustor and nozzle oscillations increase or decrease with time. An analytical procedure and a computer program for determining nozzle admittance values from the extended theory are presented and used to compute the admittances of a family of liquid-propellant rocket nozzles. The calculated results indicate that the nozzle geometry, entrance Mach number and temporal decay coefficient significantly affect the nozzle admittance values. The theoretical predictions are shown to be in good agreement with available experimental data.

Key Words (Suggested by Author(s))	18. Distribution Statement
Combustion instability Liquid rockets Nozzles	Unclassified - unlimited

Security Classif. (of this report)	20. Security Classif. (of this page)	21. No. of Pages	22. Price*
Unclassified	Unclassified	55	$3.00

* For sale by the National Technical Information Service, Springfield, Virginia 22151

ABSTRACT

Crocco's three-dimensional nozzle admittance theory is extended to be applicable when the amplitudes of the combustor and nozzle oscillations increase or decrease with time. An analytical procedure and a computer program for determining nozzle admittance values from the extended theory are presented and used to compute the admittances of a family of liquid-propellant rocket nozzles. The calculated results indicate that the nozzle geometry, entrance Mach number and temporal decay coefficient significantly affect the nozzle admittance values. The theoretical predictions are shown to be in good agreement with available experimental data.

TABLE OF CONTENTS

LIST OF ILLUSTRATIONS

LIST OF TABLES

INTRODUCTION

The interaction between the pressure oscillations inside an unstable rocket combustion chamber and the wave motion in the convergent section of the exhaust nozzle can have a significant effect on the stability characteristics of the rocket motor and is an important consideration in analytical studies concerned with the prediction of the stability of liquid-propellant rocket engines. This report is concerned with the investigation of this interaction.

To determine the stability of a liquid-propellant rocket engine, the equations describing the behavior of the oscillatory flow field throughout the rocket motor must be solved. To simplify the problem, it is convenient to analyze the oscillations in the combustion chamber and the nozzle separately. For such an analysis, the combustion chamber extends from the injector face to the nozzle entrance as shown in Fig. 1. All the combustion is assumed to take place in the combustion chamber where the mean flow Mach number is generally assumed to be low. On the other hand, no combustion is assumed to take place in the nozzle and its mean flow Mach number increases from a low value at the nozzle entrance to unity at the throat. Downstream of the throat the flow is supersonic and disturbances in this region cannot propagate upstream and affect the chamber conditions. Therefore, in combustion instability studies it is only necessary to consider the behavior of the oscillations in the converging section of the nozzle since only these oscillations can influence the conditions in the combustion chamber.

The nozzle admittance[1,2] is the boundary condition that must be satisfied by the combustor flow oscillations at the nozzle entrance. Defined as the ratio of the axial velocity perturbation to the pressure perturbation at the nozzle entrance, the nozzle admittance can also be used to determine whether wave motion in the nozzle under consideration adds or removes energy from the combustor oscillations. Furthermore, this boundary condition influences the structures and resonant frequencies of the natural modes of the combustor under investigation.

To theoretically determine the nozzle admittance, the equations which describe the behavior of the waves in the convergent section of the exhaust nozzle must be solved. These equations have been developed by

Crocco[2] and were solved numerically to obtain admittance values for one- and three-dimensional oscillations. These values were tabulated over a wide range of frequencies and entrance Mach numbers for a specific nozzle geometry. By applying the scaling technique developed in Ref. 2, the admittances of related nozzles can be determined. It was pointed out,[2] however, that interpolation of the tabulated values can result in large errors in the predicted nozzle admittances; furthermore, the accuracy of the scaling procedure is open to question. In addition, Crocco's theory is only applicable to constant amplitude periodic wave motions, and in its present form it cannot be applied to cases where the amplitude of the oscillations varies in time.

In this report, the equations needed for computing the nozzle admittance are presented and their solutions are outlined. Crocco's theory is extended to account for wave-amplitude variation with time. Typical theoretical predictions are shown and compared with available experimental data. The effects of the nozzle geometry and chamber Mach number on the nozzle admittance are presented in plots showing frequency dependence of the real and imaginary parts of the nozzle admittance. The effects of the decay coefficient are also assessed. A manual describing the use of the computer program which calculates nozzle admittance values along with a program listing is presented in the appendix.

SYMBOLS

A, B, C	variable coefficients defined below Eq. (14)
c	nondimensional speed of sound, $c^*/\bar{c}^*_o$
$\underline{e}_\varphi$, $\underline{e}_\psi$, $\underline{e}_\theta$	unit vectors
i	$\sqrt{-1}$
J_m	Bessel function of the first kind of order m
$K(\psi,\theta,t)$	a function having the following space and time dependence:

$$J_m\left[S_{mn}\left(\frac{\psi}{\psi_w}\right)^{\frac{1}{2}}\right]e^{i\omega t \pm im\theta}$$

M	Mach number at the nozzle entrance

m number of mode diametral nodal lines

n number of mode tangential nodal lines

p nondimensional pressure, $p^*/\bar{p}^*_o$

q nondimensional velocity, $\vec{q}^*/\bar{c}^*_o$

r nondimensional radius, r^*/r^*_c

r_{cc} nondimensional radius of curvature at the nozzle entrance, r^*_{cc}/r^*_c

r_{ct} nondimensional radius of curvature at the nozzle throat, r^*_{ct}/r^*_c

S nondimensional frequency, $\omega^* r^*_c/\bar{c}^*$

S_{mn} the nth root of the equation

$$\frac{dJ_m(x)}{dx} = 0$$

t nondimensional time, $t^*\bar{c}^*_o/r^*_o$

u nondimensional axial velocity component, $u^*/\bar{c}^*_o$

v nondimensional radial velocity component, $v^*/\bar{c}^*_o$

w nondimensional tangential velocity component, $w^*/\bar{c}^*_o$

y irrotational specific nozzle admittance defined in Eq. (13)

$$y = \bar{\rho}^*\bar{c}^* \frac{u'^*}{p'^*} = \gamma\bar{\rho}\bar{c}\,\frac{u'}{p'}$$

z nondimensional axial coordinate, z^*/r^*_c

γ ratio of specific heats

ζ a function used to compute the nozzle admittance; defined below Eq. (13)

θ tangential coordinate, radians

θ_1 nozzle half-angle, degrees

λ nondimensional temporal decay coefficient, $\lambda^* r^*_c/\bar{c}^*_o$

ρ nondimensional density, $\rho^*/\bar{\rho}^*_o$

τ a function used to compute the nozzle admittance; $\tau = 1/\zeta$

φ nondimensional steady state velocity potential, $\varphi^*/\bar{c}^*_o r^*_c$

Φ a function describing the φ-dependence of the radial velocity perturbation

ψ nondimensional steady state stream function, $\frac{1}{2}\bar{\rho}(\varphi)\bar{q}(\varphi)r^2$

ω nondimensional frequency, $\omega^* r^*_c/\bar{c}^*_o$

Subscripts:

c	evaluated at the chamber wall
i	imaginary part of a complex quantity
o	stagnation value
r	real part of a complex quantity
th	evaluated at the nozzle throat
w	evaluated at the nozzle wall
$\rightarrow$	vector quantity

Superscripts:

$'$	perturbation quantity
$-$	steady state value
$*$	dimensional quantity

ANALYSIS

Derivation of the Wave Equations

The equations used by Crocco[2] to compute the nozzle admittance will be developed from the conservation equations. To keep the problem mathematically tractable and yet physically meaningful, the following assumptions were employed.

(1) The nozzle flow is a calorically perfect gas consisting of a single species.

(2) Viscosity and heat conduction are negligible.

(3) The steady state flow is one-dimensional; this assumption implies that the nozzle is slowly converging.

(4) The amplitudes of the waves are small so that only linear terms in the perturbed quantities need to be retained in the conservation equations.

(5) The oscillations are assumed to be irrotational.

Using these assumptions, the equations of motion in nondimensional form become

Continuity

$$\frac{\partial \rho}{\partial t} + \nabla \cdot (\rho q) = 0 \qquad (1)$$

Momentum

$$\frac{\partial \vec{q}}{\partial t} + \tfrac{1}{2}\nabla q^2 = -\frac{1}{\rho}\nabla p \tag{2}$$

and, from the isentropic conditions, $c^2 = p/\rho$ and $p = \rho^\gamma$.

To obtain the linearized wave equations, the dependent variables are expressed in the following form:

$$\vec{q} = \bar{\vec{q}} + q', \quad p = \bar{p} + p', \quad \rho = \bar{\rho} + \rho' \tag{3}$$

Substituting these expressions into Eqs. (1) and (2), neglecting all non-linear terms involving primed quantities, and separating the resulting system of equations into a set of steady state equations and a set of unsteady equations yield the system of steady state equations:

$$\nabla\cdot(\bar{\rho}\bar{\vec{q}}) = 0; \quad \bar{c}^2 = \bar{\rho}^{\gamma - 1} = 1 - \frac{\gamma - 1}{2}\bar{q}^2; \quad \bar{p} = \bar{\rho}^\gamma \tag{4}$$

and the following system of unsteady linear equations that describe the wave motion:

$$\frac{\partial \rho'}{\partial t} + \nabla\cdot(\bar{\vec{q}}\rho' + \bar{\rho}\vec{q}') = 0 \tag{5}$$

$$\frac{\partial \vec{q}'}{\partial t} + \nabla(\bar{\vec{q}}\cdot q') = -\nabla\left(\frac{p'}{\gamma\bar{\rho}}\right) \tag{6}$$

$$p' = \bar{c}^2\rho' \tag{7}$$

To simplify the application of the boundary conditions at the nozzle walls, these wave equations are solved in the orthogonal coordinate system shown in Fig. 1. In this coordinate system the steady state velocity potential φ replaces the axial coordinate z, the steady state stream function ψ replaces the radial coordinate r and the angle θ is used to denote azimuthal variations. Using this coordinate system the velocity vectors can be expressed as follows:

$$\vec{\bar{q}} = \bar{q}(\varphi)\, \vec{e}_{\varphi}$$

$$\vec{q}' = u'\vec{e}_{\varphi} + v'\vec{e}_{\psi} + w'\vec{e}_{\theta}$$

Using the definitions of the steady state velocity potential and stream function for a one-dimensional mean flow, it can be shown[2] that

$$q(\varphi) = \frac{d\varphi}{dz}$$

$$\psi = \tfrac{1}{2}\bar{\rho}(\varphi)\,\bar{q}(\varphi)\,r^2$$

Rewriting Eqs. (5) and (6) in the (φ,ψ,θ) coordinate system yields the following system of equations[2]:

Continuity

$$\frac{\partial}{\partial t}\left(\frac{p'}{\bar{\rho}}\right) + \bar{q}^2\,\frac{\partial}{\partial\varphi}\left(\frac{\rho'}{\bar{\rho}} + \frac{u'}{\bar{q}}\right) + 2\bar{\rho}\bar{q}\,\frac{\partial}{\partial\psi}\left(\frac{v'}{r\bar{\rho}\bar{q}}\right) + \frac{\bar{\rho}\bar{q}}{2\psi}\,\frac{\partial(rw')}{\partial\theta} = 0 \tag{8}$$

Momentum

φ-component

$$\frac{\partial\left(\frac{u'}{\bar{q}}\right)}{\partial t} + \frac{\partial}{\partial\varphi}\left(\bar{q}^2\,\frac{u'}{\bar{q}}\right) + \frac{\partial}{\partial\varphi}\left(\frac{p'}{\gamma\bar{\rho}}\right) = 0 \tag{9}$$

ψ-component

$$\frac{\partial}{\partial t}\left(\frac{v'}{r\bar{\rho}\bar{q}}\right) + \bar{q}^2\,\frac{\partial}{\partial\varphi}\left(\frac{v'}{r\bar{\rho}\bar{q}}\right) + \frac{\partial}{\partial\psi}\left(\frac{p'}{\gamma\bar{\rho}}\right) = 0 \tag{10}$$

θ-component

$$\frac{\partial}{\partial t}(rw') + \bar{q}^2\,\frac{\partial}{\partial\varphi}(rw') + \frac{\partial}{\partial\theta}\left(\frac{p'}{\gamma\bar{\rho}}\right) = 0 \tag{11}$$

Equations (7) through (11) constitute a system of five equations in the five unknowns -- $\rho'/\bar{\rho}$, $u'/\bar{q}$, $v'/r\bar{\rho}\bar{q}$, rw', and $p'/\gamma\bar{\rho}$. These equations are solved by the method of separation of variables and the solutions are

$$\frac{u'}{\bar{q}} = \frac{d\Phi(\varphi)}{d\varphi} K(\psi,\theta,t)$$

$$\frac{v'}{r\bar{\rho}\bar{q}} = \Phi(\varphi) \frac{\partial}{\partial\psi}\left[K(\psi,\theta,t)\right]$$

$$rw' = \Phi(\varphi) \frac{\partial}{\partial\theta}\left[K(\psi,\theta,t)\right]$$

$$\frac{p'}{\bar{p}} = -\left[i(\omega - i\lambda)\Phi(\varphi) + \bar{q}^2(\varphi) \frac{d\Phi(\varphi)}{d\varphi}\right] K(\psi,\theta,t)$$

$$\frac{\rho'}{\bar{\rho}} = -\frac{1}{\bar{c}^2}\left[i(\omega - i\lambda) \Phi(\varphi) + \bar{q}^2(\varphi) \frac{d\Phi(\varphi)}{d\varphi}\right] K(\psi,\theta,t)$$

where

$$K(\psi,\theta,t) = \begin{cases} J_m\left[S_{mn}\left(\frac{\psi}{\psi_w}\right)^{\frac{1}{2}}\right] \cos m\theta\, e^{i(\omega - i\lambda)t} & \text{for standing waves} \\ J_m\left[S_{mn}\left(\frac{\psi}{\psi_w}\right)^{\frac{1}{2}}\right] e^{\pm im\theta}\, e^{i(\omega - i\lambda)t} & \text{for spinning waves} \end{cases}$$

These solutions identically satisfy the momentum and energy equations. Substituting these solutions into Eq. (8) and eliminating variables give the following differential equation for the function Φ:

$$\bar{q}^2(\bar{c}^2 - \bar{q}^2) \frac{d^2\Phi}{d\varphi^2} - \bar{q}^2\left[\frac{1}{\bar{c}^2} \frac{d\bar{q}^2}{d\varphi} + 2i(\omega - i\lambda)\right] \frac{d\Phi}{d\varphi}$$

$$+ \left[(\omega - i\lambda)^2 - \frac{\gamma - 1}{2} i(\omega - i\lambda) \frac{\bar{q}^2}{\bar{c}^2} \frac{d\bar{q}^2}{d\varphi} - \frac{S_{mn}^2 \bar{c}^2}{r_w^2}\right] \Phi = 0 \qquad (12)$$

The function Φ can be related to the specific acoustic admittance by the formula[2]

$$y = \gamma\bar{\rho}\bar{c} \frac{u'}{p'} = -\frac{\gamma\bar{\rho}\bar{c}\zeta}{\bar{q}^2\zeta + i(\omega - i\lambda)} \qquad (13)$$

where $\zeta = \frac{1}{\Phi}\frac{d\Phi}{d\varphi}$. Using the definition of ζ and Eq. (12), the following differential equation for ζ is derived:

$$\frac{d\zeta}{d\varphi} - \frac{B}{A}\zeta + \zeta^2 = -\frac{C}{A} \tag{14}$$

where

$$A = \bar{q}^2(\bar{c}^2 - \bar{q}^2)$$

$$B = \bar{q}^2\left[\frac{1}{\bar{c}^2}\frac{d\bar{q}^2}{d\varphi} + 2i(\omega - i\lambda)\right]$$

$$C = \left[(\omega - i\lambda)^2 - \frac{S_{mn}^2\bar{c}^2}{r_w^2} - i(\omega - i\lambda)\frac{\gamma - 1}{2}\frac{\bar{q}^2}{\bar{c}^2}\frac{d\bar{q}^2}{d\varphi}\right]$$

Equation (14) is a complex Riccati equation which must be solved numerically to obtain ζ. Once the value of ζ is determined at the nozzle entrance, the nozzle admittance can be computed directly from Eq. (13). Inspection of Eq. (14) shows that the value of ζ depends upon its coefficients A, B, and C which in turn depend upon ω, λ, S_{mn}, and the space dependence of $\bar{q}$ and $\bar{c}$ in the nozzle. The behavior of $\bar{q}$ and $\bar{c}$ in the nozzle can be computed once the value of γ and the nozzle contour are specified.

To determine ζ for given values of ω, λ, S_{mn} and γ and a specific nozzle contour, Eq. (14) must be integrated numerically. A major difficulty which can occur during this integration is that ζ becomes unbounded whenever Φ approaches zero, which causes numerical difficulties in the integration scheme. Crocco and Sirignano[2] noted that this phenomenon occurred for low Mach numbers and high values of ω/S_{mn}. At these Mach numbers and frequencies they developed asymptotic solutions for ζ.

Instead of using the asymptotic solution, an exact numerical solution is obtained in this study. The problem is resolved by introducing a new dependent variable

$$\tau = \frac{1}{\zeta} = \frac{\Phi}{\frac{d\Phi}{d\varphi}}$$

As Φ approaches zero and the magnitude of ζ becomes large, τ becomes small. Introducing the definition of τ into Eq. (14) gives the following Riccati equation for τ

$$\frac{d\tau}{d\varphi} + \frac{B}{A}\tau - \frac{C}{A}\tau^2 = 1 \tag{15}$$

At those regions where ζ becomes unbounded, Eq. (15) is integrated instead of Eq. (14).

Method of Solution

To obtain the nozzle admittance from Eq. (13), values of ζ and τ are computed by numerically integrating Eq. (14) or (15). To evaluate the coefficients A, B, and C, a differential equation that describes the variations of the steady state velocity in the subsonic portion of the nozzle must be derived. Differentiating the continuity equation

$$\bar{\rho}\bar{r}^2\bar{q} = \bar{\rho}_{th}\, r_{th}^2\, \bar{q}_{th} = \text{constant} \tag{16}$$

where $\bar{q}_{th}^2 = \bar{c}_{th}^2 = 2/(\gamma + 1)$, and using Eq. (4) yield the following differential equation

$$\frac{d\bar{q}^2}{dr} = \frac{1}{dr/d\bar{q}^2} = -\frac{4}{r_{th}}\left(\frac{2}{\gamma + 1}\right)^{\frac{-\gamma - 1}{4(\gamma - 1)}}\left[\frac{(\bar{q}^2)^{\frac{5}{4}}\left(1 - \frac{\gamma - 1}{2}\bar{q}^2\right)^{\frac{2\gamma - 1}{2(\gamma - 1)}}}{1 - \frac{\gamma + 1}{2}\bar{q}^2}\right] \tag{17}$$

Using Eq. (17) and the specified nozzle contour in terms of $r(z)$, the quantity $d\bar{q}/d\varphi$ can be obtained from the relationship

$$\frac{d\bar{q}^2}{d\varphi} = \frac{dq^2}{dr}\frac{dr}{dz}\frac{dz}{d\varphi} = 2\frac{d\bar{q}}{dr}\frac{dr}{dz} \tag{18}$$

Once $\bar{q}^2$ is known the corresponding value of $\bar{c}^2(\varphi)$ can be obtained by use of Eq. (4). To evaluate dr/dz in Eq. (18), the nozzle contour shown in Fig. 2 is used. Starting at the combustion chamber the contour is generated by a circular arc of radius r_{cc} turned through an angle θ_1, the nozzle half-angle. This arc connects smoothly to a straight line which is inclined

at an angle θ_1 to the nozzle axis. This straight line then joins with another circular arc of radius r_{ct} which turns through an angle θ_1 and ends at the throat. Using this nozzle contour, in regions I, II and III of Fig. 2

$$\left.\frac{dr}{dz}\right|_I = - \frac{\left[2r_{ct}(r - r_{th}) - (r - r_{th})^2\right]^{\frac{1}{2}}}{r_{ct} + r_{th} - r}$$

$$\left.\frac{dr}{dz}\right|_{II} = - \tan \theta_1$$

$$\left.\frac{dr}{dz}\right|_{III} = \frac{\left[2r_{cc}(1 - r) - (1 - r)^2\right]^{\frac{1}{2}}}{1 - r_{cc} - r}$$

Utilizing the appropriate expression for dr/dz, Eq. (18) can now be solved simultaneously with Eq. (14) or (15) to determine the nozzle admittance.

The numerical integration of these equations must start at some initial point where the initial conditions are known. Since the equation for ζ is singular at the throat[2], the integration is initiated at a point that is located a short distance upstream of the throat. The needed initial conditions are obtained by expanding the dependent variables in a Taylor series about the throat. To obtain this Taylor series, its coefficients $\zeta(0) = \zeta_0$ and $\zeta_1 = \left.\frac{d\zeta}{d\varphi}\right|_{\varphi = 0}$ must be evaluated at the throat where $\varphi = 0$. These coefficients are evaluated by substituting the series

$$\zeta = \zeta_0 + \zeta_1\varphi + \ldots$$

into Eq. (14) and taking the limit as $\varphi \to 0$. The results are

$$\zeta_0 = \zeta(0) = \frac{C_0}{B_0}$$

$$\zeta_1 = \left.\frac{d\zeta}{d\varphi}\right|_{\varphi = 0} = \left[B_1\left(\frac{C_0}{B_0}\right) - A_1\left(\frac{C_0}{B_0}\right)^2 - C_1\right]/(A_1 - B_0)$$

where

$$C_0 = C\Big|_{\varphi = 0} = \left[(\omega - i\lambda)^2 - i\,\frac{2(\gamma - 1)(\omega - i\lambda)}{(\gamma + 1)\sqrt{r_{th} r_{ct}}} - \frac{S_{mn}^2}{r_{th}^2}\left(\frac{2}{\gamma + 1}\right)\right]$$

$$B_0 = B\Big|_{\varphi = 0} = \frac{4}{\gamma + 1}\left[\frac{1}{\sqrt{r_{th} r_{ct}}} + i(\omega - i\lambda)\right]$$

$$B_1 = \left.\frac{dB}{d\varphi}\right|_{\varphi = 0} = \frac{4}{\gamma + 1}\left[\frac{6 + \gamma}{3 r_{th} r_{ct}} + i\,\frac{2(\omega - i\lambda)}{\sqrt{r_{th} r_{ct}}}\right]$$

$$A_1 = \left.\frac{dA}{d\varphi}\right|_{\varphi = 0} = \frac{-4}{(\gamma + 1)\sqrt{r_{th} r_{ct}}}$$

$$C_1 = \left.\frac{dC}{d\varphi}\right|_{\varphi = 0} = 2\left(\frac{\gamma - 1}{\gamma + 1}\right)\left[\frac{S_{mn}^2}{r_{th}^2\sqrt{r_{th} r_{ct}}} - \frac{i(\omega - i\lambda)}{3 r_{th} r_{ct}}(6 + \gamma)\right]$$

The following relations are used in the evaluation of the above quantities:

$$\bar{q}^2\Big|_{\varphi = 0} = \frac{2}{\gamma + 1}$$

$$\left.\frac{d\bar{q}^2}{d\varphi}\right|_{\varphi = 0} = \frac{4}{(\gamma + 1)\sqrt{r_{th} r_{ct}}}$$

Once ζ_0 and ζ_1 are known, the initial condition at $\varphi = \varphi_1$ is obtained from the expression $\zeta(\varphi_1) = \zeta_0 + \zeta_1 \varphi_1$.

The numerical solution is obtained by use of a modified Adams predictor-corrector scheme, and employing a Runge-Kutte scheme of order four to start the numerical integration. Initially, Eqs. (14) and (18) are integrated to determine ζ; if the magnitude of ζ exceeds a specified value at which numerical difficulties can occur, the integration of Eq. (14) is terminated. Using the value of ζ at that point, τ is computed and the

integration proceeds using Eq. (15). Similarly, should the magnitude of τ become excessively large, the integration of Eq. (15) is terminated, ζ is computed from the value of τ at that point, and the integration proceeds using Eq. (14). This process is repeated until the nozzle entrance is reached. A computer program utilizing this procedure has been written in FORTRAN V for use on the UNIVAC 1108 computer and it is presented in the Appendix.

RESULTS AND DISCUSSION

Using the previously mentioned computer program, theoretical values of the real and imaginary parts of the nozzle admittance have been computed for several nozzle configurations having contours similar to the one presented in Fig. 2. In these computations the radii of curvature, r_{cc} and r_{ct}, are assumed to be equal. The admittance values are presented as functions of the nondimensional frequency S in Figs. 3 through 9 where they are compared with available experimental data obtained from Ref. 3. In these figures, the frequency has been nondimensionalized by the ratio of the steady state speed of sound at the nozzle entrance to the chamber radius r_c.

Admittances for Longitudinal Modes

Longitudinal-type instabilities in general occur in the range of S from 0 to approximately 1.8 which is in the vicinity of the cutoff frequency of the first tangential modes. The cutoff frequency of a particular transverse mode is $S_{mn}\sqrt{(1 - M^2)}$ where S_{mn} is the transverse mode eigenvalue and the subscripts m and n respectively denote the number of diametral nodal lines and the number of tangential nodal lines. Values of S_{mn} are given in Table 1 for several values of m and n.

For longitudinal modes good agreement exists between the experimental and theoretical values of the real and imaginary parts of the admittance as shown in Figs. 3 through 5. The effect of changing the nozzle half-angle is presented in Fig. 3 for a nozzle with an entrance Mach number M of 0.08 and $r_{cc}/r_c = 0.44$. The data indicate that increasing θ_1 increases the frequency at which the real and imaginary parts of the admittance attain maximum values. These data also indicate that the assumption of a one-dimensional mean flow

Table 1. Values of Transverse Mode Eigenvalues; S_{mn}

Transverse Wave Pattern	m	n	S_{mn}
Longitudinal	0	0	0
First Tangential (1T)	1	0	1.8413
Second Tangential (2T)	2	0	3.0543
First Radial (1R)	0	1	3.8317
Third Tangential (3T)	3	0	4.2012
Fourth Tangential (4T)	4	0	5.3175
First Tangential, First Radial (1T,1R)	1	1	5.3313
Fifth Tangential (5T)	5	0	6.4154
Second Tangential, First Radial (2T,1R)	2	1	6.7060
Second Radial (2R)	0	2	7.0156

used in the development of the theory appears to be valid. Even for nozzles with half-angles as high as 45 degrees, for which it has been shown that the mean flow is two-dimensional,[4] the experimental and theoretical nozzle admittance values are in good agreement.

Examination of Fig. 4 shows that the entrance Mach number M has a significant effect on the admittance values for $\theta_1 = 15$ degrees and $r_{cc}/r_c = 0.44$. However, increasing the nozzle half-angle appears to decrease the influence of the entrance Mach number, and for $\theta_1 = 45$ degrees variations in M has little effect.[3] The dependence of the nozzle admittance upon the radius of curvature for a nozzle with $M = 0.16$ and $\theta_1 = 30$ degrees is shown in Fig. 5.

The data presented in Figs. 3 through 5 show that for longitudinal modes the real part of the nozzle admittance is always positive. As indicated by Crocco[1,2] positive values of the real part of the nozzle admittance imply that the nozzle removes acoustic energy from the combustor wave system which implies that the nozzle exerts a stabilizing influence upon the chamber oscillations.

In combustion instability analyses of liquid-propellant rocket motors, it is often assumed that the nozzle is short. This assumption implies that the nozzle length and throat diameter are much smaller than the chamber length and diameter so that the wave travel time in the nozzle is much shorter than the wave travel time in the chamber. For a short nozzle the real and imaginary

parts of the admittance are independent of frequency and are given by the expressions[5]

$$y_r = \frac{\gamma - 1}{2} M \; ; \quad y_i = 0$$

These theoretical short nozzle admittance results do not agree with the results obtained for typical liquid rocket nozzles presented in Figs. 3 through 5. The disagreement is especially evident for nozzles with low values of θ_1, which imply that the nozzle is long, and for high values of S where the wave length of the oscillation becomes of the same order of magnitude as a characteristic nozzle dimension.

Admittances for Mixed First Tangential-Longitudinal Modes

The mixed first tangential-longitudinal modes are those three-dimensional modes which exist between the cutoff frequencies of the first tangential ($S \simeq 1.8$) and second tangential ($S \simeq 3.0$) modes. Theoretical and experimental nozzle admittance data for these modes are presented in Figs. 6 through 8.

In Fig. 6 the influence of the nozzle half-angle on the admittance values is shown. The theoretical and experimental results are in good agreement and they indicate that increasing θ_1 increases the frequency at which the real and imaginary parts of the admittance reach maximum values.

The effect of Mach number on the admittance values is presented in Fig. 7 for $\theta_1 = 15$ degrees and $r_{cc}/r_c = 0.44$. Mach number effects are especially significant at the higher frequencies. However, as shown in Ref. 3, increasing the nozzle half-angle decreases the dependence of the admittance values on the Mach number. The effect of changing the radii of curvature on the admittance values is presented in Fig. 8.

The results presented in Figs. 6 through 8 show that for mixed first tangential-longitudinal modes the real part of the nozzle admittance can be negative which means that the nozzle radiates wave energy back into the combustor; this process exerts a destabilizing influence on the oscillations in the chamber.[2] These negative values occur only for three-dimensional modes and, as shown by Crocco,[2] their cause can be traced to the term involving S_{mn} in Eq. (12). For longitudinal modes, for which S_{mn}

is zero, the real part of the nozzle admittance is always positive, and for those modes the nozzle always exerts a stabilizing influence upon the combustor oscillations.

Effect of Decay Coefficient upon Admittance Data

The nozzle admittance theory has been modified to include the effects of a temporal decay coefficient, λ. Typical results are shown in Figs. 9 and 10 for values of λ of -0.05, 0, and 0.05. These results indicate that varying λ affects both the real and imaginary parts of the admittance. Therefore, the decay coefficient should be included in the nozzle admittance computations when the oscillations are not neutrally stable.

SUMMARY AND CONCLUSIONS

The equations necessary to determine the nozzle admittance for one- and three-dimensional oscillations have been developed. The analytical approach used in solving the nozzle wave equations is outlined and employed to obtain nozzle admittance data for typical nozzle configurations. These data show the dependence of the nozzle admittance values upon nozzle geometry, nozzle Mach number, mode of oscillation, and the temporal damping coefficient.

The results can be summarized as follows for longitudinal and mixed first tangential-longitudinal modes. Decreasing the nozzle length by increasing the nozzle half-angle and Mach number or by decreasing the throat and entrance radii of curvature decreases the frequency dependence of the nozzle admittance. Good agreement exists between the theoretical predictions and available experimental data. However, the nozzle admittance values for typical liquid rocket nozzles are not in agreement with the values obtained from short nozzle theory. Including the effects of a temporal damping coefficient in the nozzle admittance computations changes the admittance values. Therefore, when the oscillations are not neutrally stable, the temporal decay coefficient should be accounted for in the computations.

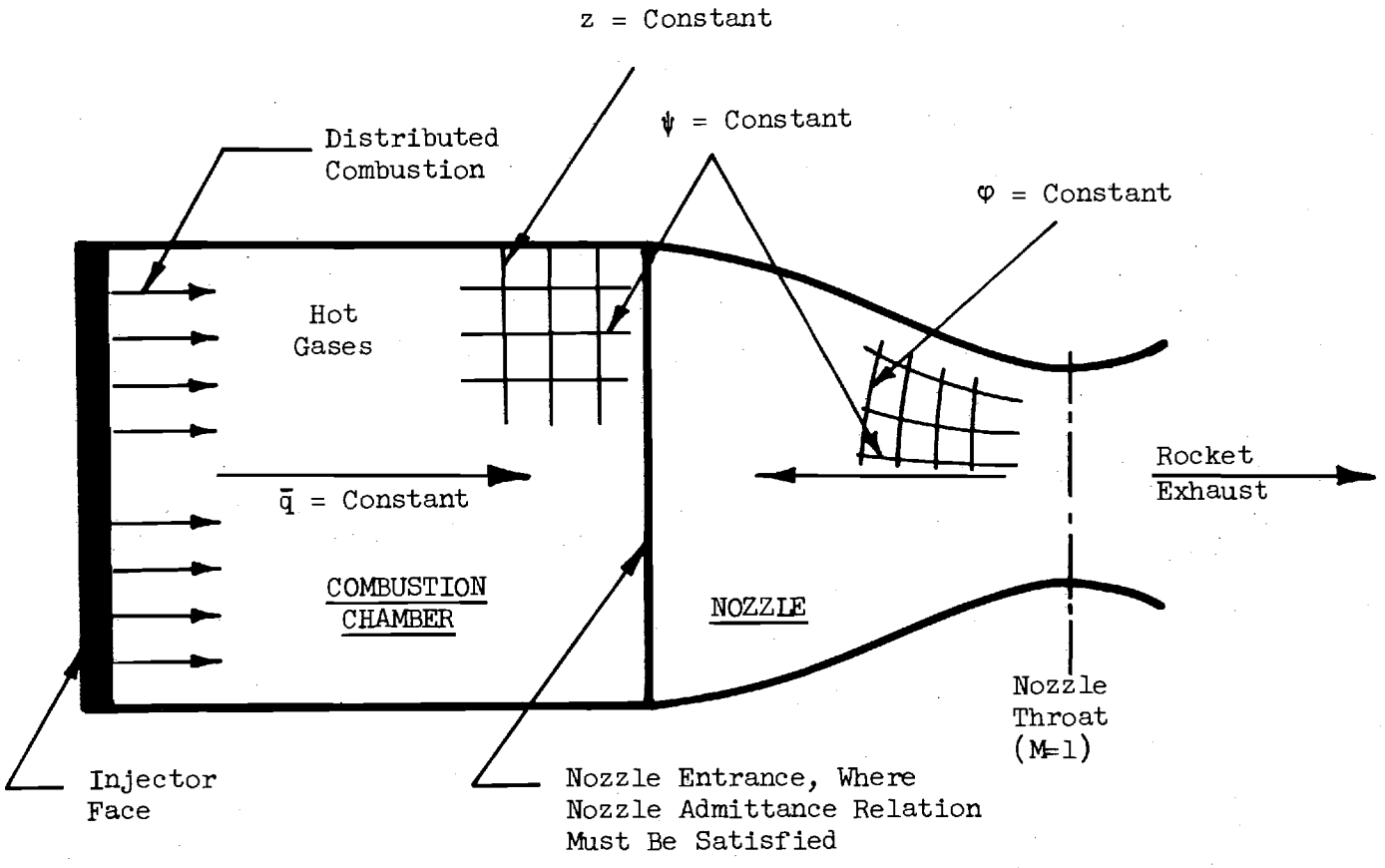

Figure 1. Typical Mathematical Model of a Liquid Rocket Engine

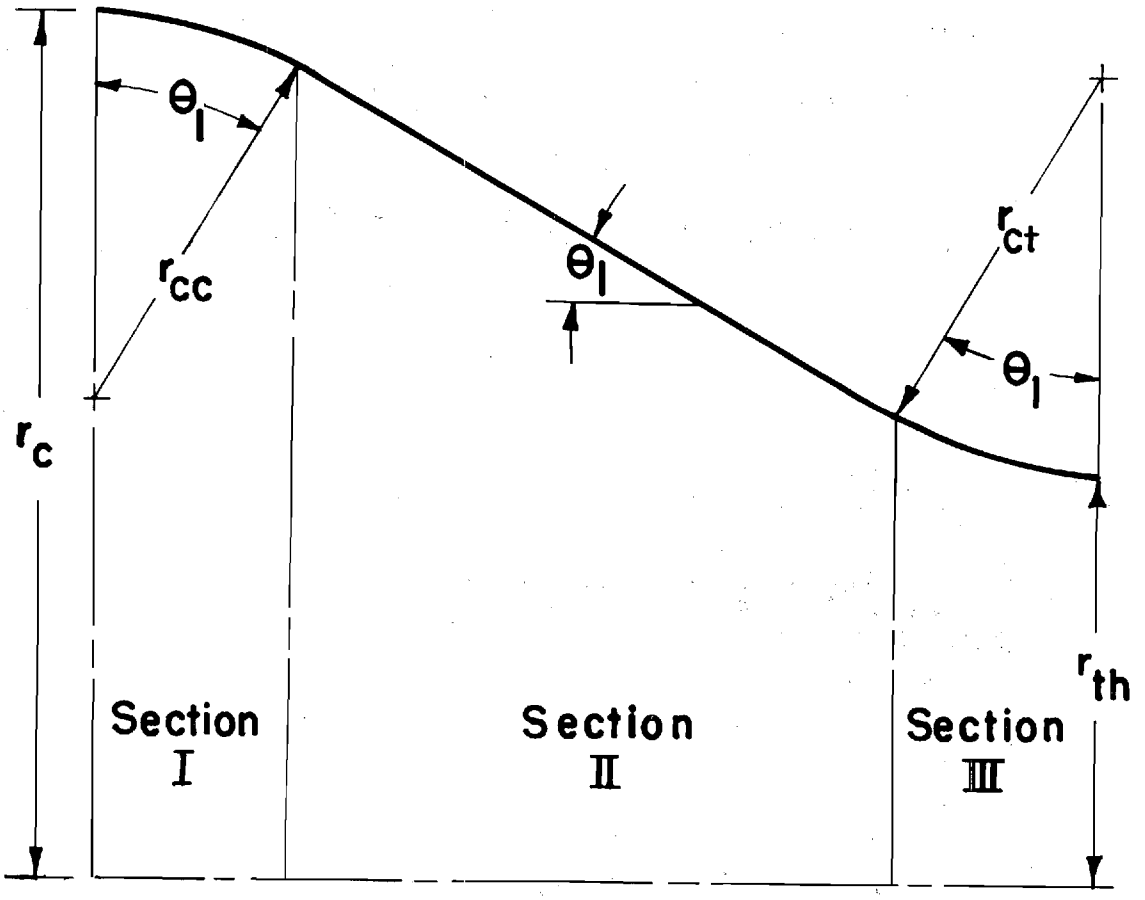

Figure 2. Nozzle Contour

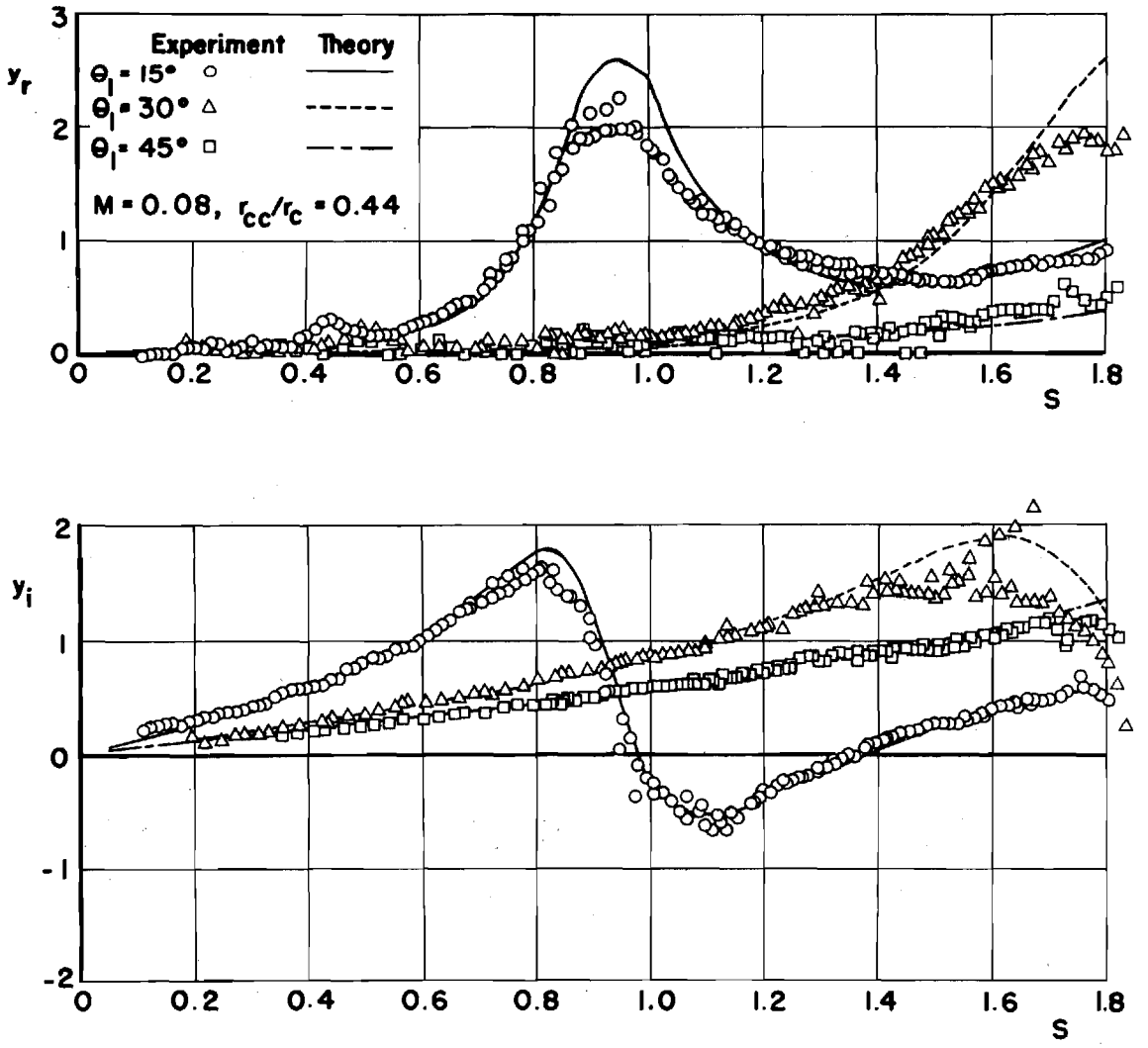

Figure 3. The Effect of Nozzle Half-Angle on the Theoretical and Experimental Nozzle Admittance Values for Longitudinal Modes

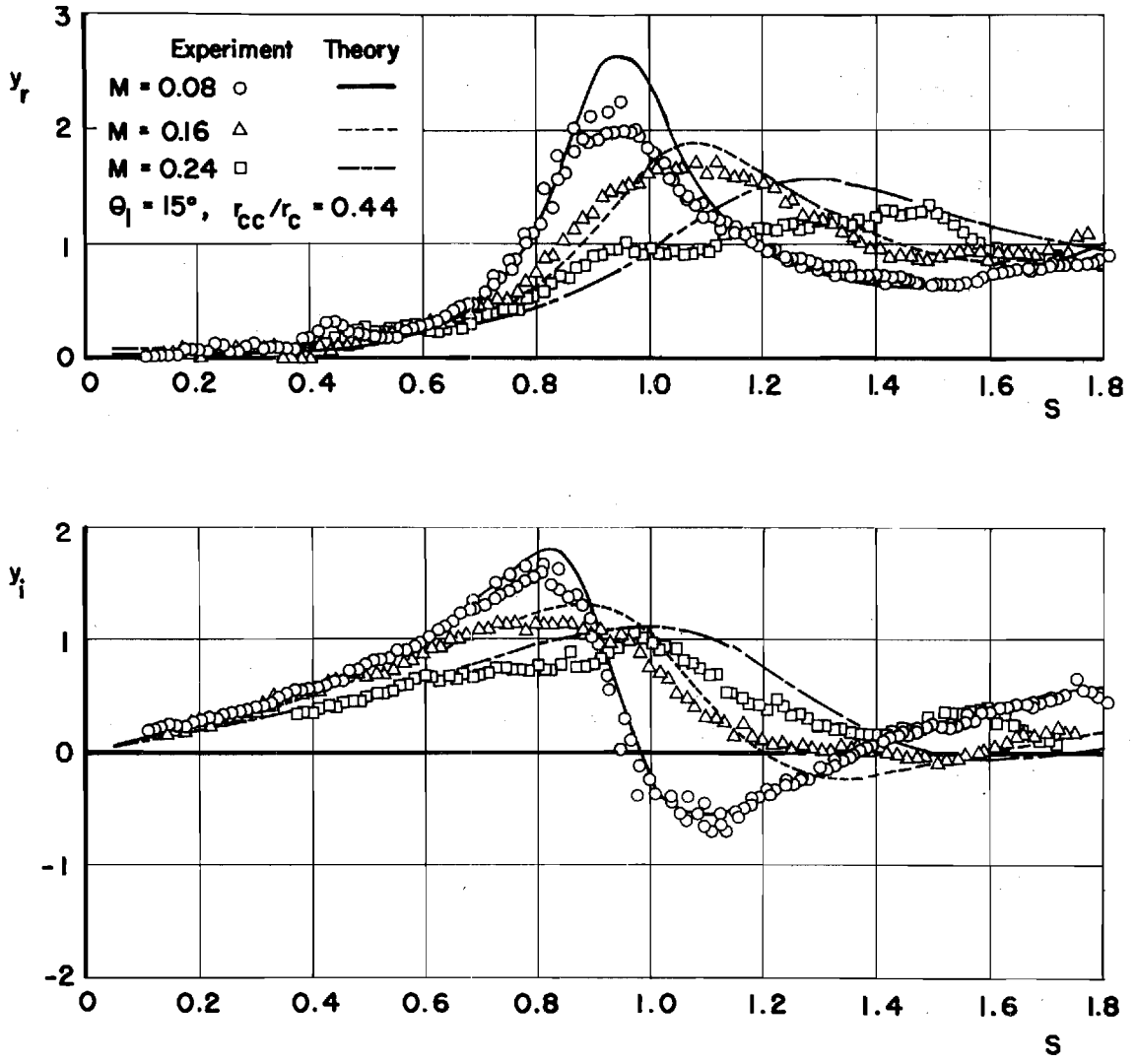

Figure 4. The Effect of Entrance Mach Number on the Theoretical and Experimental Nozzle Admittance Values for Longitudinal Modes

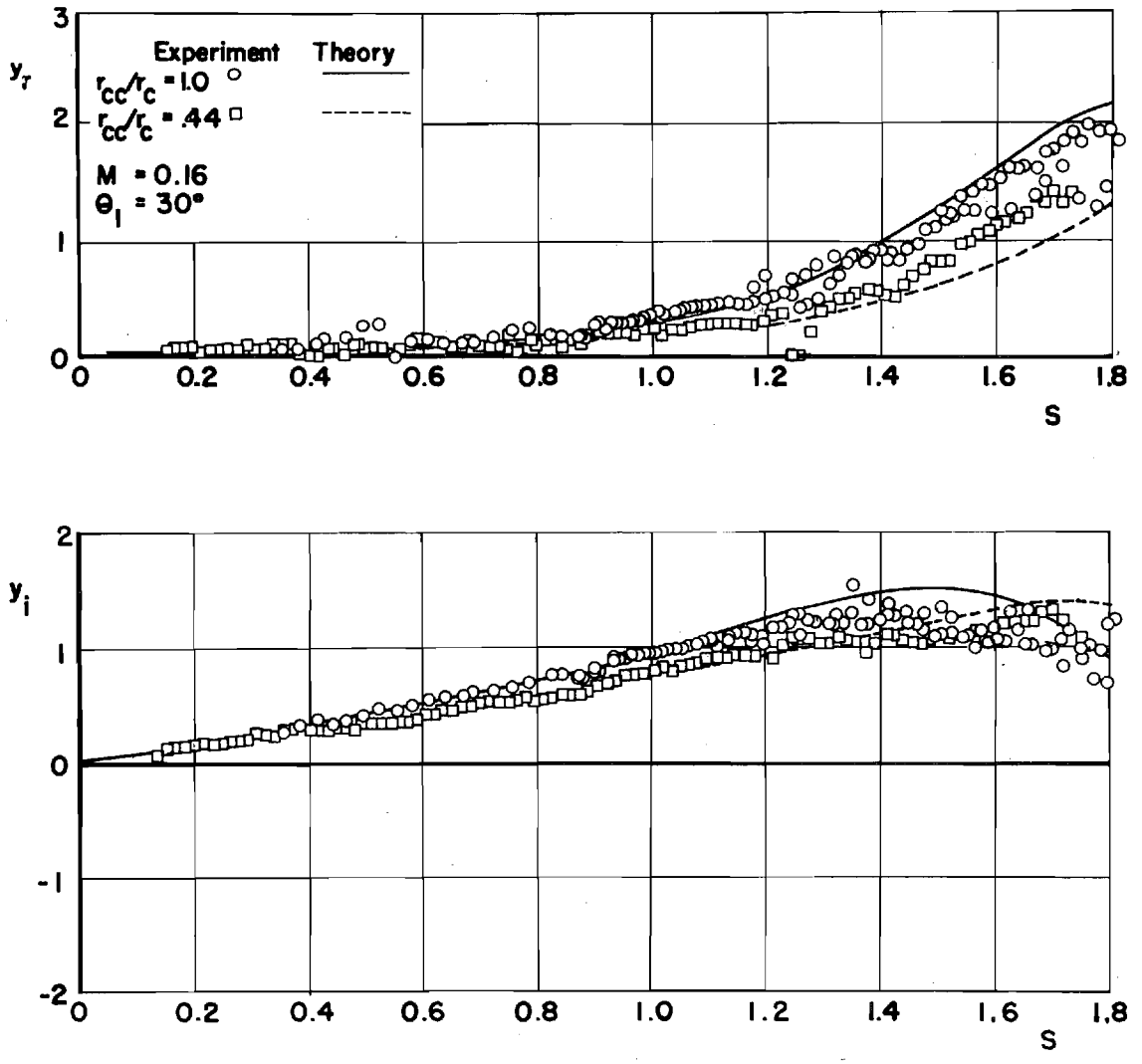

Figure 5. The Effect of the Radii of Curvature on the Theoretical and Experimental Nozzle Admittance Values for Longitudinal Modes

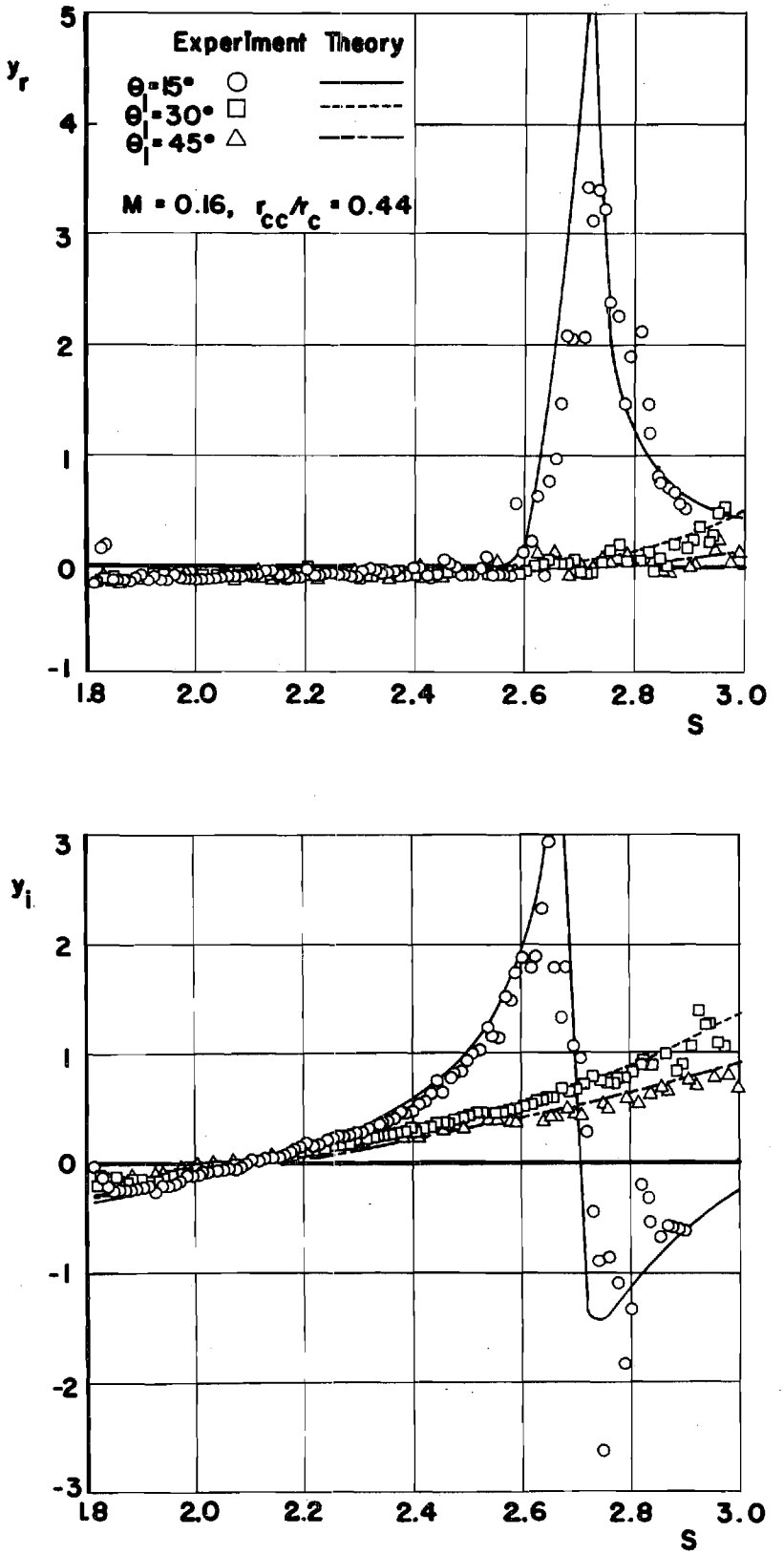

Figure 6. The Effect of the Nozzle Half-Angle on the Theoretical and Experimental Nozzle Admittance Values for Mixed First Tangential-Longitudinal Modes

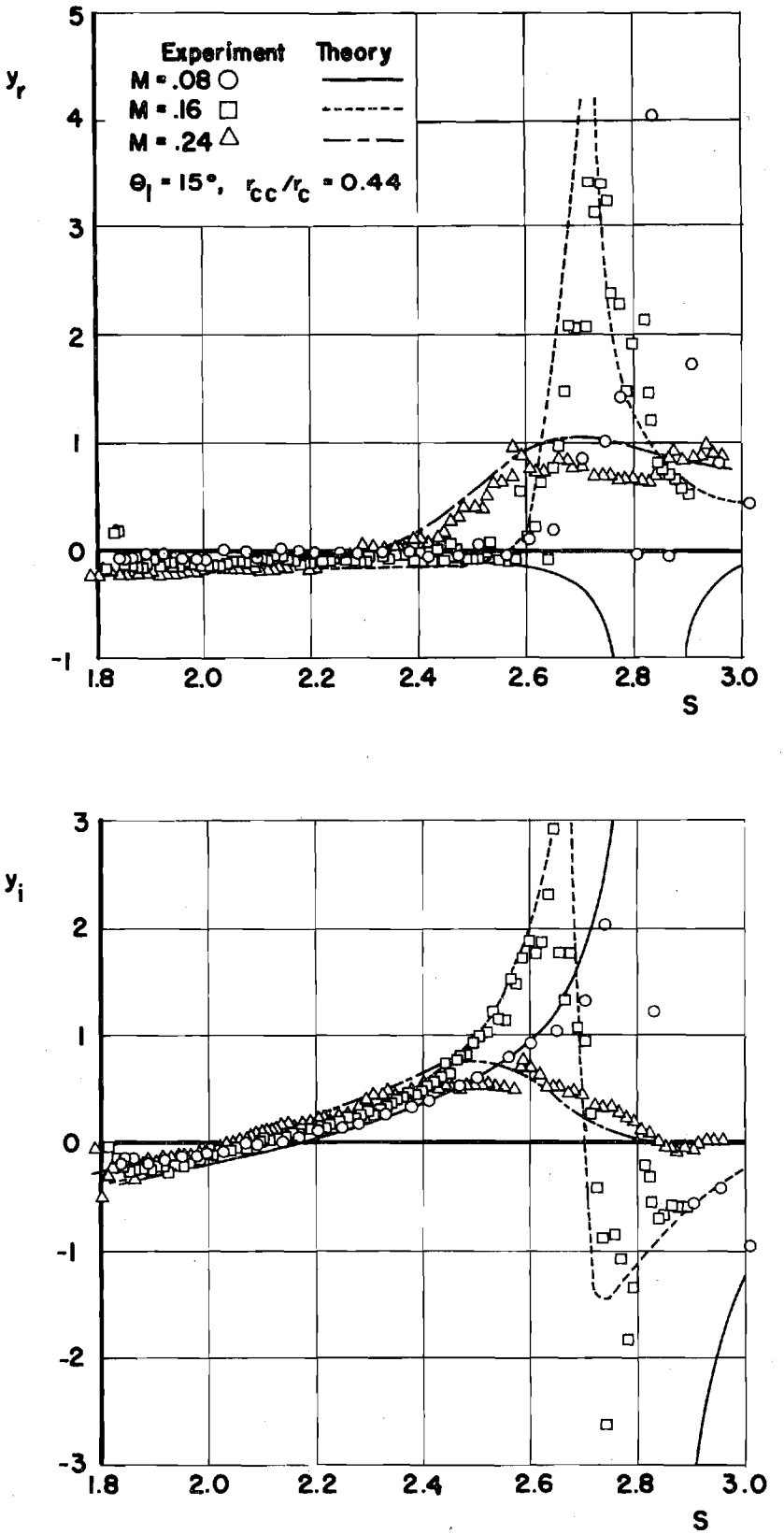

Figure 7. The Effect of Entrance Mach Number on the Theoretical and Experimental Nozzle Admittance Values for Mixed First Tangential-Longitudinal Modes

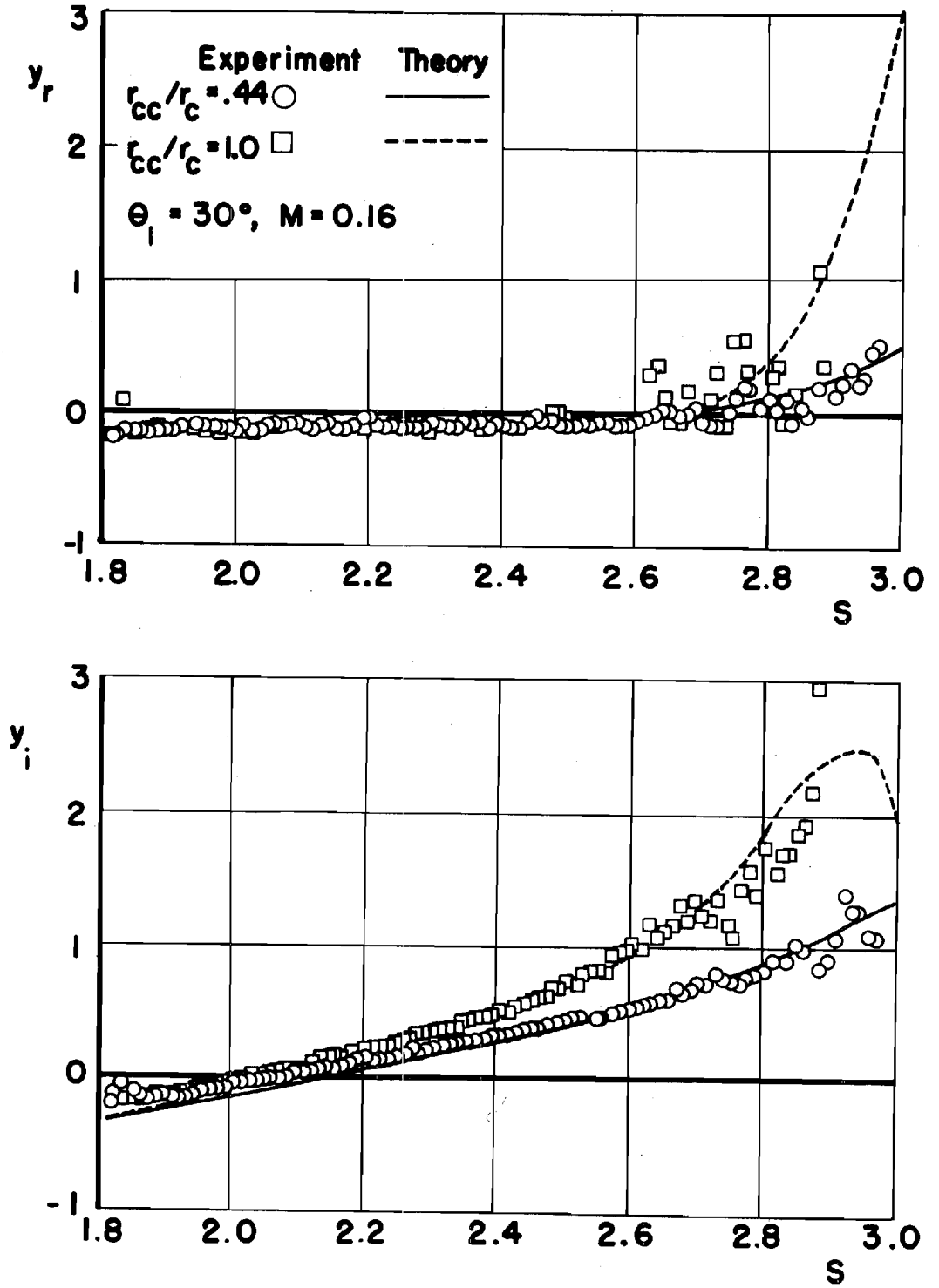

Figure 8. The Effect of the Radii of Curvature on the Theoretical and Experimental Nozzle Admittance Values for Mixed First Tangential-Longitudinal Modes

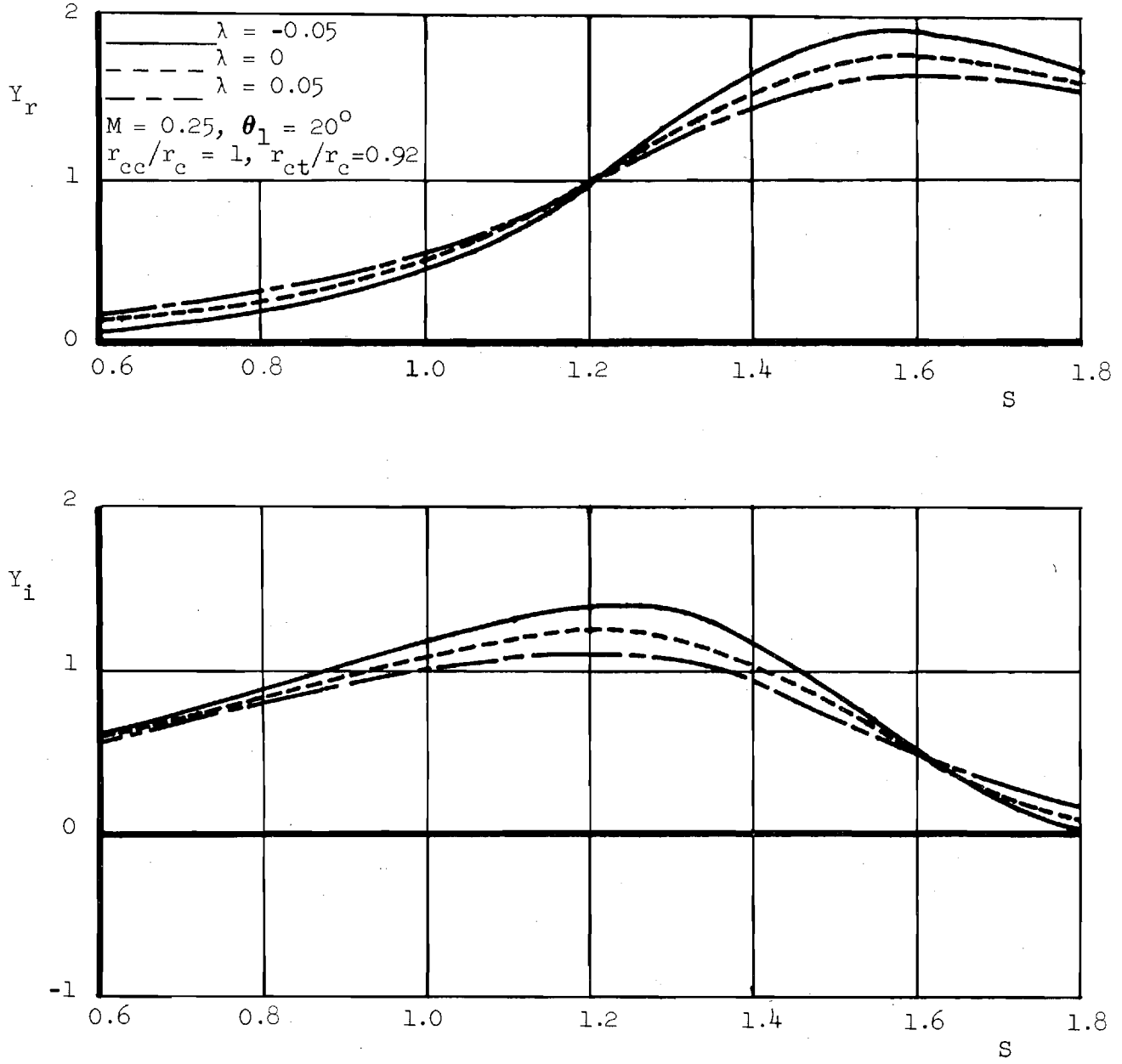

Figure 9. Effect of the Temporal Decay Coefficient on the Theoretical Nozzle Admittance Values for Longitudinal Modes

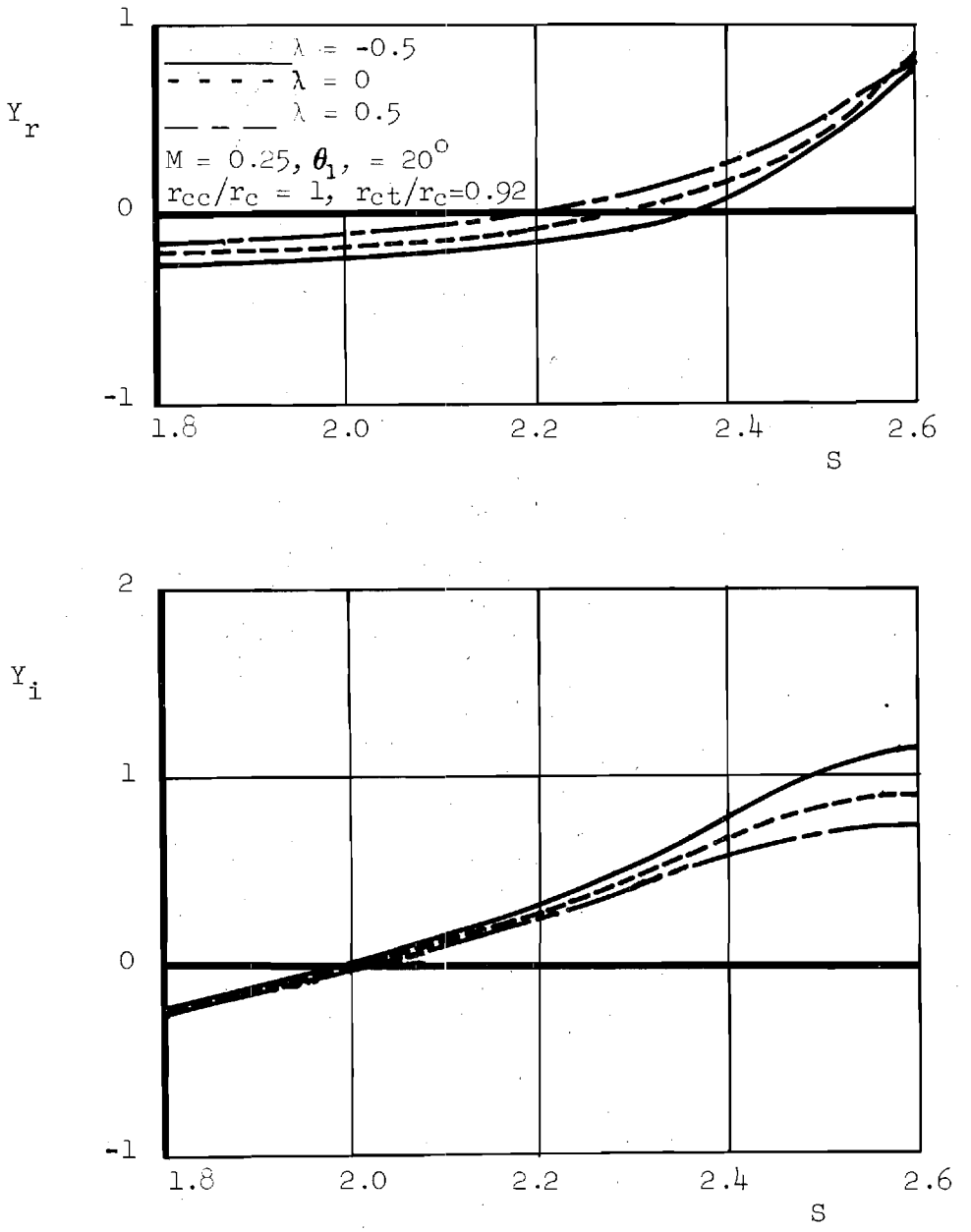

Figure 10. Effect of the Temporal Decay Coefficient on the Theoretical Nozzle Admittance Values for Mixed First Tangential-Longitudinal Modes

APPENDIX

COMPUTER PROGRAM USED TO DETERMINE THE IRROTATIONAL NOZZLE ADMITTANCE

The computer program for calculating the irrotational nozzle admittance from Crocco's theory[2] which is extended to account for temporal damping is written in FORTRAN V interpretive language compatible with the UNIVAC 1108 machine language compiler. This program consists of seven routines - the main or control program and six subroutines. The names of the routines are listed in Table A-1 in sequential order. The FORTRAN symbols used in these routines and their definitions are presented in Table A-2 in alphabetical order. The input parameters necessary for the admittance computations must be specified in the main program and are listed in Table A-3. The output parameters and their definitions are listed in Table A-4. A detailed flow chart of the computer program is shown in Fig. A-1, and the program listing and sample output are presented in Tables A-5 and A-6, respectively.

This computer program has been written to predict nozzle admittances for nozzle contours shown in Fig. 2. The run time required depends upon the number of admittance values desired and the nozzle length. To obtain 40 admittance values at different frequencies for the nozzles investigated in this study, one to two minutes of run time on the UNIVAC 1108 computer are required.

Table A-1. List of Subroutines in the Computer Program Used to Determine the Irrotational Nozzle Admittance

Subroutine	Description
MAIN	Specifies the nozzle geometry and operating conditions in the converging section of the nozzle
NOZADM	Specifies initial conditions at the throat, computes the final nozzle admittance values, and contains all output formats
RKTZ	Uses the Runge-Kutta of order four to obtain initial values for the modified Adams integration routine
RKZDIF	Computes the differential element in the converging section of the nozzle used to solve Eq. (14)
RKTDIF	Computes the differential element in the converging section of the nozzle used to solve Eq. (15)
ZADAMS	Numerically integrates Eq. (14) using the modified Adams numerical integration scheme
TADAMS	Numerically integrates Eq. (15) using the modified Adams numerical integration scheme

Table A-2. Definition of FORTRAN Variables
(Page 1 of 4)

Variable	Definition
A	Real coefficient A of Eqs. (14) and (15)
A(5)	Coefficients of the Runge-Kutta formulas of order four
AF	Nondimensional temporal damping coefficient λ
ANGLE	Nozzle half-angle, degrees
A1R	Derivative of the coefficient A evaluated at the throat
BI	Imaginary part of the coefficient B in Eqs. (14) and (15)
BR	Real part of the coefficient B in Eqs. (14) and (15)
BOI	Value of BI at the throat
BOR	Value of BR at the throat
B1I	Derivative of BI evaluated at the throat
B1R	Derivative of BR evaluated at the throat
C	Nondimensional speed of sound squared, c^2
CI	Imaginary part of the coefficient C in Eqs. (14) and (15)
CM	Mach number at the nozzle entrance
COR(5)	Formula for the corrector in the modified Adams integration routine
CR	Real part of the coefficient C in Eqs. (14) and (15)
COI	Value of CI at the throat
COR	Value of CR at the throat
C1I	Derivative of CI evaluated at the throat
C1R	Derivative of CR evaluated at the throat
DP	Integration stepsize
DP(5)	Derivative used in the corrector formula in the modified Adams integration routine
DR	Derivative of the local wall radius with respect to axial distance
DU	Derivative of the nondimensional velocity $\bar{q}^2$ with respect to the wall radius r
DWC	Increment of the nondimensional frequency ω

Table A-2. Definition of FORTRAN Variables
(Page 2 of 4)

Variable	Definition
DY(5,4)	Derivative used in the modified Adams integration scheme
F	Constant given as $\bar{q}/\gamma\bar{p}$ evaluated at the nozzle entrance
FZ(4,5)	Derivative used in the Runge-Kutta method
F1	Lumped parameter determined by the conditions at the throat
F2	Lumped parameter determined by the conditions at the throat
GAM	Ratio of specific heats γ
G(5)	Dependent variable in the Runge-Kutta integration routine
H	Integration stepsize
I	Integer counter
IP	Integer constant. If IP = 0 the nozzle admittance is output. If IP $\neq$ 0 the amplitude and phase of the pressure oscillation are output along the length of the nozzle
IQ	If IQ = 2, the integration of Eq. (15) for τ is complete
IQZ	= 1: Eq. (15) for τ is integrated = 2: Eq. (14) for ζ is integrated
J	Integer variable
JOPT	= 1: Eq. (15) for τ is integrated = 2: Eq. (14) for ζ is integrated
K	Integer variable
N	Integer variable
NU	Number of differential equations to be solved by the Runge-Kutta or the modified Adams integration routine
NWC	Number of frequency points
P	Value of the steady state velocity potential
PARG	Phase of the pressure oscillation in the nozzle
PHII	Imaginary part of Φ
PHIR	Real part of Φ

Table A-2. Definition of FORTRAN Variables
(Page 3 of 4)

Variable	Definition
PI	Imaginary part of the pressure oscillation
PMAG	Magnitude of the pressure oscillation
PR	Real part of the pressure oscillation
PRED(5)	Predictor formula for the modified Adams integration routine
Q	Constant given as $(r_{th}/4)\left(\frac{2}{\gamma + 1}\right)^{\frac{\gamma + 1}{4(\gamma - 1)}}$
QBAR	Nondimensional steady state velocity $\bar{q}$
R	Local wall radius r
RCC	Ratio of the radius of curvature at the nozzle entrance to the radius at the nozzle entrance
RCT	Ratio of the radius of curvature at the throat to the radius at the nozzle entrance
RHO	Nondimensional, steady-state density $\bar{\rho}$
RT	Nondimensional throat radius
R1	Nondimensional radius at the entrance to Section 2 of the converging portion of the nozzle
R2	Nondimensional radius at the entrance to Section 3 of the converging portion of the nozzle
SRTR	Constant give as $\sqrt{r_{th} r_{cc}}/r_c$
SVN	S_{mn}
SVNR	$S_{mn} r_c / r_{th}$
SYI	Imaginary part of the specific admittance y
SYR	Real part of the specific admittance y
T	Nozzle half-angle, in radians
TDN	Inverse of the square of the magnitude of ζ
TI	Imaginary part of τ
TMAG	Magnitude of τ
TPI	Derivative of TI with respect to φ

Table A-2. Definition of FORTRAN Variables
(Page 4 of 4)

Variable	Definition
TPR	Derivative of TR with respect to φ
TR	Real part of τ
TZ	Value of φ at the nth integration point
T2	Square of the magnitude of τ
U	Steady state velocity squared, $\bar{q}^2$
UZ	Dependent variable in the Runge-Kutta integration scheme
W	Nondimensional frequency S
WC	Nondimensional frequency ω
X	Value of φ at the nth integration point
Y(5)	Dependent variable used in the modified Adams integration scheme
YI	Imaginary part of the irrotational nozzle admittance defined by Crocco in Ref. 2
YR	Real part of the nozzle admittance defined by Crocco in Ref. 2
ZDN	Inverse of the square of the magnitude of ζ
ZI	Imaginary part of ζ
ZMAG	Magnitude of ζ
ZPI	Derivative of ZI with respect to φ
ZPR	Derivative of ZR with respect to φ
ZR	Real part of ζ
ZOI	Value of ZI at the throat
ZOR	Value of ZR at the throat
Z1I	Value of ZPI at the throat
Z1R	Value of ZPR at the throat
Z2	Square of the magnitude of ζ

Table A-3. Input Parameters

Variable	Definition
GAM	Ratio of specific heats, γ
CM	Mach number at the nozzle entrance
SVN	Nth root of the equation $\frac{dJ_V(x)}{dx} = 0$. Corresponds to S_{mn}. Values of S_{mn} are given in Table 1 for various acoustic modes
WC	Initial value of ω
DWC	Increment of frequency
NWC	Number of frequency points desired
ANGLE	Nozzle half-angle, degrees
RCT	Radius of curvature at the throat nondimensionalized with respect to the chamber radius
RCC	Radius of curvature at the nozzle entrance nondimensionalized with respect to the chamber radius
IP	= 0: nozzle admittances are printed $\neq$ 0: pressure magnitude and phase are printed at each point along the nozzle
AF	Temporal damping coefficient λ

Table A-4. Output Parameters

Variable	Definition
WC	Nondimensional frequency, ω
YR	Real part of the admittance as defined by Crocco in Ref. 2
YI	Imaginary part of the admittance as defined by Crocco in Ref. 2
W	Nondimensional frequency
SYR	Real part of the specific admittance y
SYI	Imaginary part of the specific admittance y

Table A-5. Listing of the Computer Program Used to Determine the Irrotational Nozzle Admittance (Page 1 of 10)

```
 1*          COMMON/X1/GAM, SVN, ANGLE, RCT, RCC /X2/T,RT, Q, R1, R2, IP, WC,AF
 2*          COMMON/X3/Z1R, Z1I
 3*          COMMON/X4/ CM
 4*          GAM = 1.233
 5*          AF = 0
 6*          IP=0
 7*          RCC = 1
 8*          RCT = 5.457*2/11.82
 9*          NWC = 40
10*          DWC = 0.05
11*          ANGLE = 20
12*          CM = .25
13*          DO 100 I = 1,2
14*          IF(I.EQ.2) GO TO 5
15*          SVN = 0
16*          NWC = 27
17*          GO TO 20
18*        5 SVN = 1.84129
19*          NWC = 20
20*       20 CONTINUE
21*          DO 200 J = 1,3
22*          AF = 0.05*(J-2)
23*          IF (I .EQ.2) GO TO 25
24*          WC = 0.55
25*          GO TO 30
26*       25 WC = 1.55
27*       30 CONTINUE
28*          IF(IP .EQ. 0) GO TO 10
29*          WRITE(6, 1000) CM, SVN, GAM, ANGLE, RCT, RCC
30*       10 CALL NOZADM(CM,     NWC, DWC)
31*      200 CONTINUE
32*      100 CONTINUE
33*     1000 FORMAT(46X, 28HPRESSURE MAGNITUDE AND PHASE, //, 38X,
34*         1       14HMACH NUMBER = , F3.2, 7H SVN = , F6.4, 9H GAMMA = , F3.1
35*         2       , /, 22X, 15HNOZZLE ANGLE = , F4.1, 21H RADII OF CURVATURE:
36*         3       , 9HTHROAT = , F6.4, 12H ENTRANCE = , F6.4, //, 46X,
37*         4       2H X, 7X, 4HPMAG, 10X, 4HPARG, /)
38*          STOP
39*          END
```

Table A-5. Continued (Page 2 of 10)

```
1*            SUBROUTINE NOZADM(CM,     NWC, DWC)
2*            DIMENSION DY(5,4), G(5), GP(5), Y(5)
3*            COMMON/X1/GAM,SVN,ANGLE,RCT,RCC/X2/T,RT,Q,R1,R2,IP,WC, AF
4*            COMMON/X3/Z1R,Z1I
5*            DP = -0.001
6*             T = 3.1415927 * ANGLE / 180
7*            WRITE(6,1000) CM, SVN, GAM, AF, ANGLE, RCT, RCC
8*            DO 10 N = 1, NWC
9*       20        WC = WC + DWC
10*      25        RT =(CM**0.5)*((1+ (GAM-1)*CM*CM/2)**((-GAM-1)/(4*(GAM-1)))
11*       1           )*((2/(GAM+1))**((-GAM-1)/(4*(GAM-1))))
12*                 Q = (0.25*RT)*((2/(GAM+1))**((GAM+1)/(4*(GAM-1))))
13*              PHIR = 1
14*              PHII = 0
15*                R1 = RT + RCT*(1 - COS(T))
16*                R2 = 1  - RCC*(1 - COS(T))
17*                 R = RT
18*                 P = 0
19*                 U = 2 / (GAM+1)
20*              SRTR = (RT * RCT)**0.5
21*               A1R = -4 /((GAM+1)*SRTR)
22*               B0R = -A1R +4*AF/(GAM+1)
23*               B0I = 4 * WC /(GAM+1)
24*              SVNR = SVN/RT
25*               C0R = WC * WC -((SVNR*SVNR) * 2 / (GAM+1))
26*       1           - AF*AF - 2*AF*(GAM-1)/((GAM+1)*SRTR)
27*               C0I = -2 * WC * (GAM-1) / ((GAM+1)*SRTR) - 2*AF*WC
28*               B1R = (24 + 4*GAM)/(3*RCT*RT*(GAM+1)) - 8*AF/(SRTR*(GAM+1))
29*               B1I = 8 * WC / (SRTR*(GAM+1))
30*               C1R = 2 * (GAM - 1) * SVNR * SVNR /(SRTR * (GAM+1))
31*       1           - AF* (B1R+8*AF/(SRTR*(GAM+1)))*(GAM-1)*0.5
32*               C1I = -B1R * WC * (GAM - 1) * 0.5
33*               Z0R = (B0R*C0R + B0I*C0I) / (B0R*B0R + B0I*B0I)
34*               Z0I = (B0R*C0I - B0I*C0R) / (B0R*B0R + B0I*B0I)
35*                F1 = B1R*Z0R - B1I*Z0I - Z0R*Z0R*A1R + A1R*Z0I*Z0I - C1R
36*                F2 = B1I*Z0R + B1R*Z0I - 2*A1R*Z0I*Z0R - C1I
37*               Z1R = (F1*(A1R - B0R) - F2*B0I) / ((A1R-B0R)*(A1R-B0R) +
38*       1              B0I*B0I)
39*               Z1I = (F2*(A1R - B0R) + F1*B0I) / ((A1R-B0R)*(A1R-B0R) +
40*       1              B0I*B0I)
41*                 C = U
42*              G(1) = U
43*              G(2) = Z0R
44*              G(3) = Z0I
45*              G(4) = PHIR * Z0R - PHII * Z0I
46*              G(5) = PHII * Z0R + Z0I * PHIR
47*            DY(1,1) = -A1R
48*            DY(2,1) = Z1R
49*            DY(3,1) = Z1I
50*            DY(4,1) = PHIR
51*            DY(5,1) = PHII
52*                IQZ = 2
53*               DO 30 I = 2,4
54*                    CALL RKT7(5,DP,P,G,GP,IQZ)
55*                       P = P + DP
56*                       U = G(1)
57*                      ZR = G(2)
58*                      ZI = G(3)
59*                    PHIR = G(4)
60*                    PHII = G(5)
```

Table A-5. Continued (Page 3 of 10)

```
61*                   DY(1,I) = GP(1)
62*                   DY(2,I) = GP(2)
63*                   DY(3,I) = GP(3)
64*                   DY(4,I) = GP(4)
65*        30         DY(5,I) = GP(5)
66*                 Y(1) = U
67*                 Y(2) = ZR
68*                 Y(3) = ZI
69*                 Y(4) = PHIR
70*                 Y(5) = PHII
71*                 CALL ZADAMS(5,DP,P,Y,DY,IQZ)
72*                 IF(IP .EQ. 1) GO TO 10
73*                    U = Y(1)
74*                   ZR = Y(2)
75*                   ZI = Y(3)
76*           PHIR = Y(4)
77*           PHII = Y(5)
78*                 QSAR = U**0.5
79*                    C = 1 - U*0.5*(GAM-1)
80*                  RHO = C**(1/(GAM-1))
81*                    F = QSAR / (GAM*RHO)
82*                 IF(IQZ .EQ. 1) GO TO 35
83*                  ZDN = (U*ZR+AF)*(U*ZR+AF) + (WC+U*ZI)*(WC+U*ZI)
84*                   YR = -(ZR*(U*ZR+AF) + ZI*(WC+U*ZI))*F/ZDN
85*                   YI = F*(WC*ZR - AF*ZI)/ZDN
86*                 GO TO 40
87*        35         TR = Y(2)
88*                   TI = Y(3)
89*                  TDN = (U+AF*TR-WC*TI)*(U+AF*TR-WC*TI)+(WC*TR)*(WC*TR)
90*                   YR = -F*(U-WC*TI+AF*TR)/TDN
91*                   YI = F*(WC*TR+AF*TI)/TDN
92*                   YI = F * WC * TR / TDN
93*        40         SYR = GAM*(C**((GAM+1)/(2*(GAM-1))))*YR
94*                   SYI = GAM*(C**((GAM+1)/(2*(GAM-1))))*YI
95*                     W = WC *(C**-.5)
96*        50       WRITE(6,1005) WC, YR, YI, W, SYR, SYI
97*        10 CONTINUE
98*      1000 FORMAT(1H1, 45X, 30HTHEORETICAL NOZZLE ADMITTANCES, //, 25X,
99*         1       14HMACH NUMBER = , F3.2, 7H SVN = , F6.4, 9H GAMMA = , F3.1
100*        1       ,21H DECAY COEFFICIENT = , F6.4, //,
101*        2       22X, 15HNOZZLE ANGLE = , F4.1, 2X, 21HRADII OF CURVATURE:
102*        3       , 9HTHROAT = , F6.4, 12H ENTRANCE = , F6.4, //, 34X, 2HWC,
103*        4       7X, 2HYR, 8X, 2HYI, 8X, 1HW, 8X, 3HSYR, 8X, 3HSYI, /)
104*     1005 FORMAT(31X, F6.4, 5F10.5)
105*          RETURN
106*          END
```

Table A-5. Continued (Page 4 of 10)

```
      SUBROUTINE RKTZ(NU, H, T1, U, DUM, JOPT)
      COMMON/X2/T,RT,Q,R1,R2,IP,WC,AF
      DIMENSION U(5), A(5), UZ(5), FZ(4,5),DUM(5)
      A(1) = 0
      A(2) = 0
      A(3) = 0.5
      A(4) = 0.5
      A(5) = 1.0
        TZ = T1
      DO 10 J = 1, NU
          UZ(J) = U(J)
   10   DUM(J) = FZ(1,J)
      IF(JOPT .EQ. 2) GO TO 15
      CALL RKTDIF(TZ,UZ,DUM)
      GO TO 20
   15 CALL RKZDIF(TZ,UZ,DUM)
   20 DO 25 J = 1, NU
   25   FZ(1,J) = DUM(J)
      DO 30 I = 2,4
            TZ = T1 + A(I+1)*H
          DO 35 J = 1, NU
              UZ(J) = U(J) + A(I+1)*H*FZ(I-1,J)
   35         DUM(J) = FZ(I,J)
          IF(JOPT .EQ. 2) GO TO 40
          CALL RKTDIF(TZ,UZ,DUM)
          GO TO 45
   40     CALL RKZDIF(TZ,UZ,DUM)
   45     DO 50 J = 1, NU
   50       FZ(I,J) = DUM(J)
   30 CONTINUE
      DO 55 J = 1, NU
   55     U(J) = U(J) + H*(FZ(1,J)+2*(FZ(2,J)+FZ(3,J))+FZ(4,J)) / 6.0
      GO TO (60,65),JOPT
   60 CALL RKTDIF(TZ,U ,DUM)
      GO TO 70
   65 CALL RKZDIF(TZ,U ,DUM)
   70 IF(IP.EQ.0) GO TO 75
        PR = WC*U(5)- U(1)*DUM(4) - AF*U(4)
        PI = -WC*U(4) - U(1)*DUM(5) - AF*U(5)
      PMAG = SQRT(PR*PR + PI*PI)
      PARG = ATAN(PI/PR)
      WRITE(6,1000) TZ, PMAG, PARG
 1000 FORMAT(4X, F6.4, 1X, F10.5, 3X, F10.5)
   75 RETURN
      END
```

Table A-5. Continued (Page 5 of 10)

```
      SUBROUTINE RKZDIF(P,G,GP)
      COMMON/X1/GAM,SVN,ANGLE,RCT,RCC/X2/T,RT,Q,R1,R2,IP,WC,AF
      COMMON/X3/Z1R,Z1I
      DIMENSION G(5), GP(5)
         U = G(1)
        ZR = G(2)
        ZI = G(3)
      PHIR = G(4)
      PHII = G(5)
      IF(P) 15, 10, 15
   10 GP(1) = 4/((GAM+1)*((RCT*RT)**0.5))
      GP(2) = Z1R
      GP(3) = Z1I
      GP(4) = Z1R
      GP(5) = Z1I
      GO TO 20
   15    C = 1 - (GAM - 1) * U * 0.5
         R = Q * ((C)**(-1/(2*(GAM-1)))) * (U**-0.25) *4.0
      IF(R-1) 22, 22, 50
   22 IF(R - R1) 25, 30, 30
   25   DR = -((2*RCT*(R-RT) - (R-RT)*(R-RT))**0.5)/(RT+RCT-R)
      GO TO 45
   30 IF(R-R2) 35, 40, 40
   35   DR = -TAN(T)
      GO TO 45
   40   DR = ((2*RCC*(1-R) - (R-1)*(R-1))**0.5)/(1-R-RCC)
   45   DU = -(U**0.75)*(C**((2*GAM-1)/(2*(GAM-1))))/(Q*(1-(GAM+1)*U*.5)
     1       )
      GP(1)= DU*DR
      GO TO 55
   50 GP(1) = 0
   55    A = U*(C-U)
         BR = U*GP(1)/C + 2*AF*U
         BI = 2*WC*U
         CR = WC*WC - SVN*SVN*C/(R*R) - AF*AF
     1       -(GAM-1)*AF*U*GP(1)*0.5*(1/C)
         CI = -(GAM-1)*WC*U*GP(1)*0.5*(1/C) - 2*AF*WC
      GP(2)= ((BR*ZR - BI*ZI - CR) / A) - ZR*ZR + ZI*ZI
      GP(3)= ((BI*ZR + BR*ZI - CI) / A) - 2*ZR*ZI
      GP(4)= ZR*PHIR - ZI*PHII
      GP(5)= ZR*PHII + ZI*PHIR
   20 RETURN
      END
```

Table A-5. Continued (Page 6 of 10)

```
1*          SUBROUTINE RKTDIF(P,G,GP)
2*          COMMON/X1/GAM,SVN,ANGLE,RCT,RCC/X2/T,RT,Q,R1,R2,IP,WC,AF
3*          DIMENSION G(5), GP(5)
4*             U = G(1)
5*            TR = G(2)
6*            TI = G(3)
7*          PHIR = G(4)
8*          PHII = G(5)
9*             C = 1 - (GAM-1)*U*0.5
10*            R = Q * (1/C)**(-1/(2*(GAM-1)))) * (U**-0.25) *4.0
11*         IF(R-1) 22,22,50
12*      22 IF(R-R1) 25, 30, 30
13*      25    DR = -((2*RCT*(R-RT) - (R-RT)*(R-RT))**0.5)/(RT+RCT-R)
14*         GO TO 45
15*      30 IF(R-R2) 35,40,40
16*      35    DR = -TAN(T)
17*         GO TO 45
18*      40    DR = ((2*RCC*(1-R) - (R-1)*(R-1))**0.5)/(1-R-RCC)
19*      45    DU = -(U**0.75)*(C**((2*GAM-1)/(2*(GAM-1)))) / (Q*(1-(GAM+1)*U*
20*        1          0.5))
21*         GP(1)= DU*DR
22*         GO TO 55
23*      50 GP(1) = 0
24*      55    A = U*(C-U)
25*            BR = U*GP(1)/C + 2*AF*U
26*            BI = 2*WC*U
27*            CR = WC*WC - SVN*SVN*C/(R*R) - AF*AF
28*        1       -(GAM-1)*AF*U*GP(1)*0.5*(1/C)
29*            CI = -(GAM-1)*WC*U*GP(1)*0.5*(1/C) - 2*AF*WC
30*         GP(2)= 1 - (BR*TR-BI*TI) - (CR*(TR*TR-TI*TI)-2*CI*TR*TI))/ A
31*         GP(3)= (-BR*TI - BI*TR + CI*(TR*TR-TI*TI) + 2*CR*TR*TI) /A
32*            T2 = TR*TR + TI*TI
33*         GP(4)= (TR*PHIR - TI*PHII)/T2
34*         GP(5)= (TR*PHII + TI*PHIR)/T2
35*         RETURN
36*         END
```

Table A-5. Continued (Page 7 of 10)

```
      SUBROUTINE ZADAMS(N,H,X,Y,DY,IQZ)
      COMMON/X1/GAM,SVN,ANGLE,RCT,RCC/X2/T,RT,Q,R1,R2,IP,WC,AF
      COMMON/X4/ CM
      DIMENSION COR(5), DP(5), DY(5,4), PRED(5), Y(5), Q(5), GP(5)
   10 CONTINUE
      DO 15 I = 1,N
        PRED(I) = Y(I)+H*(55.*DY(I,4)-59.*DY(I,3)+37.*DY(I,2)-9.*DY(I,1)
     1                  )/24.0
   15 CONTINUE
        X = X+H
        U = PRED(1)
       ZR = PRED(2)
       ZI = PRED(3)
     PHIR = PRED(4)
     PHII = PRED(5)
        C = 1 - (GAM-1)*U*0.5
        R = Q * ((C)**(-1/(2*(GAM-1)))) * (U**-0.25) *4.0
      IF(R-1) 17,17,100
   17 IF(R-R1) 20, 25, 25
   20   DR = -((2*RCT*(R-RT)-(R-RT)*(R-RT))**0.5) / (RT+RCT-R)
      GO TO 40
   25 IF(R-R2) 30, 35, 35
   30   DR = -TAN(T)
      GO TO 40
   35   DR = ((2*RCC*(1-R) - (1-R)*(1-R))**0.5) / (1-R-RCC)
   40   DU = -(U**0.75)*(C**((2*GAM-1)/(2*(GAM-1))))/(Q*(1-(GAM+1)*U*0.5
     1       ))
      DP(1)= DR*DU
        A = U*(C-U)
       BR = U*DP(1)/C+ 2*AF*U
       BI = 2*WC*U
       CR = WC*WC - (SVN*SVN*C)/(R*R) - AF*AF
     1        -(GAM-1)*AF*U*DP(1)*0.5/C
       CI = -(GAM-1)*WC*U*DP(1)*0.5/C - 2*AF*WC
      DP(2)= ((BR*ZR - BI*ZI - CR)/A) - ZR*ZR + ZI*ZI
      DP(3)= ((BI*ZR + BR*ZI - CI)/A) - 2*ZR*ZI
      DP(4)= ZR*PHIR - ZI*PHII
      DP(5)= ZR*PHII + ZI*PHIR
      DO 45 I = 1,N
        COR(I) = Y(I)+H*(DY(I,2)-5.*DY(I,3)+19.*DY(I,4)+9.*DP(I))/24.0
   45   Y(I) = (251.*COR(I) + 19.*PRED(I)) / 270.
        U = Y(1)
       ZR = Y(2)
       ZI = Y(3)
     PHIR = Y(4)
     PHII = Y(5)
        C = 1 - (GAM-1)*U*0.5
   52 DO 55 I = 1,N
        DY(I,1) = DY(I,2)
        DY(I,2) = DY(I,3)
   55   DY(I,3) = DY(I,4)
      ZMAG = (ZR*ZR + ZI*ZI)**0.5
      IF(ZMAG - 10 ) 60, 90, 90
   60   R = Q * ((C)**(-1/(2*(GAM-1)))) * (U**-0.25) *4.0
      IF(R-1) 62, 62, 100
   62 IF(R-R1) 65,70,70
   65   DR = -((2*RCT*(R-RT) - (R-RT)*(R-RT))**0.5)/(RT+RCT-R)
      GO TO 85
   70 IF(R-R2) 75,80,80
   75   DR = -TAN(T)
      GO TO 85
```

Table A-5. Continued (Page 8 of 10)

```
      80    DR = ((2*RCC*(1-R) - (1-R)*(1-R))**0.5)/(1-R-RCC)
      85    DU = -(U**0.75)*(C**((2*GAM-1)/(2*(GAM-1))))/(Q*(1-(GAM+1)*U/2))
         DY(1,4)= DR*DU
            A = U*(C-U)
           BR = U*DY(1,4)/C + 2*AF*U
           BI = 2*WC*U
           CR = WC*WC - (SVN*SVN*C)/(R*R) - AF*AF
     1          -(GAM-1)*AF*U*DY(1,4)*0.5/C
           CI = -(GAM-1)*WC*U*DY(1,4)*0.5/C -2*AF*WC
         DY(2,4)= (BR*ZR - BI*ZI -CR)/A - ZR*ZR + ZI*ZI
         DY(3,4)= (BI*ZR + BR*ZI -CI)/A - 2*ZR*ZI
         DY(4,4)= ZR*PHIR - ZI*PHII
         DY(5,4)= ZR*PHII + ZI*PHIR
         IF(IP .EQ. 0) GO TO 87
           PR = WC*PHII - U*DY(4,4) - AF*PHIR
           PI = -WC*PHIR -U*DY(5,4)   - AF*PHII
         PMAG = (PR*PR + PI*PI)**.5
         PARG = ATAN(PI/PR)
         WRITE(6,1000) X, PMAG, PARG
      87 GO TO 10
      90  IQZ = 1
           Z2 = ZMAG*ZMAG
         Y(2) = ZR/Z2
         Y(3) = -ZI/Z2
          ZPR = DY(2,4)
          ZPI = DY(3,4)
         DY(2,4)= -(ZPR*(ZR*ZR - ZI*ZI) + 2*ZR*ZI*ZPI)/(Z2*Z2)
         DY(3,4)= (2*ZPR*ZR*ZI - ZPI*(ZR*ZR - ZI*ZI))/(Z2*Z2)
         G(1) = U
         G(2) = Y(2)
         G(3) = Y(3)
         G(4) = PHIR
         G(5) = PHII
         DY(1,1)= DY(1,4)
         DY(2,1)= DY(2,4)
         DY(3,1)= DY(3,4)
         DY(4,1)= PHIR*ZR - PHII*ZI
         DY(5,1)= PHII*ZR + PHIR*ZI
         DO 95 I = 2,4
              CALL RKTZ(5,H,X,G,GP,IQZ)
                 X = X+H
                 U = G(1)
                TR = G(2)
                TI = G(3)
              PHIR = G(4)
              PHII = G(5)
           DY(1,I) = GP(1)
           DY(2,I) = GP(2)
           DY(3,I) = GP(3)
           DY(4,I) = GP(4)
      95   DY(5,I) = GP(5)
         Y(1) = U
         Y(2) = TR
         Y(3) = TI
         Y(4) = PHIR
         Y(5) = PHII
         CALL TADAMS(N,H,X,Y,DY,IQZ,IQ)
         GO TO (10, 100),IQ
     1000 FORMAT(46X,F6.4,1X,F10.5,3X,F10.5)
      100 RETURN
         END
```

Table A-5. Continued (Page 9 of 10)

```
      SUBROUTINE TADAMS(N,H,X,Y,DY,IQZ,IQ)
      COMMON/X1/GAM,SVN,ANGLE,RCT,RCC/X2/T,RT,Q,R1,R2,IP,WC,AF
      COMMON/X4/ CM
      DIMENSION COR(5), DP(5), DY(5,4), PRED(5), Y(5), G(5), GP(5)
   10 CONTINUE
      DO 15 I = 1,N
        PRED(I) = Y(I)+H*(55*DY(I,4)-59.*DY(I,3)+37.*DY(I,2)-9*DY(I,1))/
     1            24.0
   15 CONTINUE
         X = X+H
         U = PRED(1)
        TR = PRED(2)
        TI = PRED(3)
      PHIR = PRED(4)
      PHII = PRED(5)
         C = 1 - (GAM-1)*U*.5
         R = Q * (1/C)**(-1/(2*(GAM-1))) * (U**-0.25) *4.0
      IF(R-1) 17,17,100
   17 IF(R-R1) 20, 25, 25
   20    DR = -((2*RCT*(R-RT) - (R-RT)*(R-RT))**.5)/(RT+RCT-R)
         GO TO 40
   25 IF(R-R2) 30, 35, 35
   30    DR = -TAN(T)
         GO TO 40
   35    DR = ((2*RCC*(1-R) - (1-R)*(1-R))**.5)/(1-R-RCC)
   40    DU =-(U**.75)*(C**((2*GAM-1)/(2*(GAM-1))))/(Q*(1-(GAM+1)*U**.5))
      DP(1)= DR*DU
         A = U*(C-U)
        BR = U*DP(1)/C+ 2*AF*U
        BI = 2*WC*T
        CR = WC*WC - (SVN*SVN*C)/(R*R) - AF*AF
     1       -(GAM-1)*AF*U*DP(1)*0.5/C
        CI = -(GAM-1)*WC*U*DP(1)*0.5/C - 2*AF*WC
      DP(2)= 1 + (-BR*TR+BI*TI+CR*(TR*TR-TI*TI)-2*CI*TR*TI)/A
      DP(3)= (-BR*TI - BI*TR + CI*(TR*TR - TI*TI) + 2*CR*TR*TI)/A
        T2 = TR*TR + TI*TI
      DP(4)= (TR*PHIR - TI*PHII)/T2
      DP(5)= (TR*PHII + TI*PHIR)/T2
      DO 45 I = 1,N
         COR(I) = Y(I)+H*(DY(I,2)-5.*DY(I,3)+19.*DY(I,4)+9.*DP(I))/24.0
   45    Y(I) = (251.*COR(I) + 19.*PRED(I))/270.
         U = Y(1)
        TR = Y(2)
        TI = Y(3)
      PHIR = Y(4)
      PHII = Y(5)
         C = 1 - (GAM-1)*U*.5
   52 DO 55 I = 1,4
        DY(I,1) = DY(I,2)
        DY(I,2) = DY(I,3)
   55   DY(I,3) = DY(I,4)
        T2 = TR*TR + TI*TI
      TMAG = T2**.5
      IF(TMAG - 10 ) 60, 90, 90
   60    R = Q * (1/C)**(-1/(2*(GAM-1))) * (U**-0.25) *4.0
      IF(R-1) 62, 62, 100
   62 IF(R-R1) 65,70,70
   65    DR = -((2*RCT*(R-RT)-(R-RT)*(R-RT))**.5)/(RT+RCT-R)
         GO TO 85
   70 IF(R-R2) 75,80,80
   75    DR = -TAN(T)
         GO TO 85
```

Table A-5. Continued (Page 10 of 10)

```
63*        80   DR = ((2*RCC*(1-R) - (1-R)*(1-R))**.5)/(1-R-RCC)
64*        85   DU = -(U**.75)*(C**((2*GAM-1)/(2*(GAM-1))))/(Q*(1-(GAM+1)*U*.5))
65*           DY(1,4)= DR*DU
66*              A = U*(C-U)
67*             BR = U*DY(1,4)/C + 2*AF*U
68*             BI = 2*WC*U
69*             CR = WC*WC - (SVN*SVN*C)/(R*R) - AF*AF
70*          1       -(GAM-1)*AF*U*DY(1,4)*0.5/C
71*             CI = -(GAM-1)*WC*U*DY(1,4)*0.5/C -2*AF*WC
72*           DY(2,4)= 1 + (-BR*TR + BI*TI + CR*(TR*TR - TI*TI) - 2*CI*TR*TI)/A
73*           DY(3,4)= (-BR*TI - BI*TR + CI*(TR*TR - TI*TI) + 2*CR*TR*TI)/A
74*           DY(4,4)= (TR*PHIR - PHII*TI)/T2
75*           DY(5,4)= (TR*PHII + PHIR*TI)/T2
76*           IF(IP .EQ. 0) GO TO 87
77*             PR = WC*PHII - U*DY(4,4) - AF*PHIR
78*             PI = -WC*PHIR -U*DY(5,4)   - AF*PHII
79*           PMAG = (PR*PR + PI*PI)**.5
80*           PARG = ATAN(PI/PR)
81*           WRITE(6,1000) X, PMAG, PARG
82*        87 GO TO 10
83*        90  IQZ = 2
84*           Y(2) = TR/T2
85*           Y(3) = -TI/T2
86*            TPR = DY(2,4)
87*            TPI = DY(3,4)
88*           DY(2,4)= -(TPR*(TR*TR - TI*TI) + 2*TR*TI*TPI)/(T2*T2)
89*           DY(3,4)=(2*TPR*TR*TI-TPI*(TR*TR-TI*TI))/(T2*T2)
90*           G(1) = U
91*           G(2) = Y(2)
92*           G(3) = Y(3)
93*           G(4) = PHIR
94*           G(5) = PHII
95*           DY(1,1)= DY(1,4)
96*           DY(2,1)= DY(2,4)
97*           DY(3,1)= DY(3,4)
98*           DY(4,1)= (PHIR*TR - PHII*TI)/T2
99*           DY(5,1)= (PHII*TR - PHIR*TI)/T2
100*          DO 95 I = 2,4
101*               CALL RKTZ(5,H,X,G,GP,IQZ)
102*                  X = X+H
103*                  U = G(1)
104*                 ZR = G(2)
105*                 ZI = G(3)
106*               PHIR = G(4)
107*               PHII = G(5)
108*             DY(1,I) = GP(1)
109*             DY(2,I) = GP(2)
110*             DY(3,I) = GP(3)
111*             DY(4,I) = GP(4)
112*       95    DY(5,I) = GP(5)
113*          Y(1) = U
114*          Y(2) = ZR
115*          Y(3) = ZI
116*          Y(4) = PHIR
117*          Y(5) = PHII
118*           IQ  = 1
119*          GO TO 105
120*       100   IQ = 2
121*      1000 FORMAT(46X, F6.4, 1X, F10.5, 3X, F10.5)
122*       105 RETURN
123*           END
```

Table A-6. Sample Output

THEORETICAL NOZZLE ADMITTANCES

MACH NUMBER = .25 SVM = 1.8413 GAMMA = 1.2 DECAY COEFFICIENT = -.0500

NOZZLE ANGLE = 20.0 RADII OF CURVATURE: THROAT = .9234 ENTRANCE = 1.0000

R	YR	YI	M	SYR	SYI
1.6000	-.28273	-.35483	1.60581	-.33670	-.42732
1.6500	-.27001	-.31495	1.65600	-.32154	-.37507
1.7000	-.25820	-.27857	1.70618	-.30749	-.32221
1.7500	-.24715	-.22543	1.75636	-.29433	-.26845
1.8000	-.23669	-.17922	1.80654	-.28186	-.21343
1.8500	-.22661	-.13161	1.85672	-.26986	-.15673
1.9000	-.21667	-.08219	1.90690	-.25803	-.09788
1.9500	-.20659	-.03048	1.95709	-.24603	-.03630
2.0000	-.19598	.02407	2.00727	-.23339	.02867
2.0500	-.18432	.08216	2.05745	-.21950	.09784
2.1000	-.17087	.14458	2.10763	-.20348	.17217
2.1500	-.15459	.21227	2.15781	-.18410	.25279
2.2000	-.13397	.28633	2.20799	-.15954	.34098
2.2500	-.10675	.36791	2.25818	-.12713	.43814
2.3000	-.06962	.45811	2.30836	-.08291	.54555
2.3500	-.01763	.55747	2.35854	-.02100	.66387
2.4000	.05634	.66508	2.40872	.06709	.79202
2.4500	.16198	.77657	2.45890	.19290	.92479
2.5000	.31059	.88672	2.50908	.36967	1.04883
2.5500	.49692	.94600	2.55927	.59165	1.12557

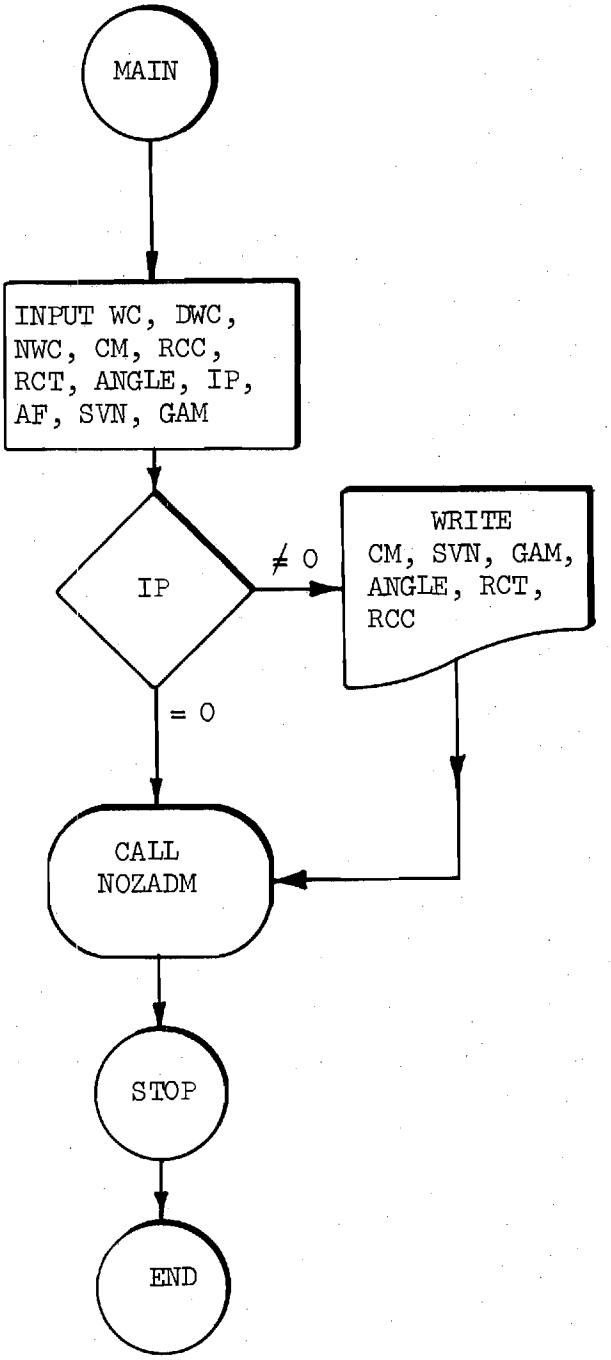

Figure A-1. Flow Chart for the Nozzle Admittance Computer Program (Page 1 of 10)

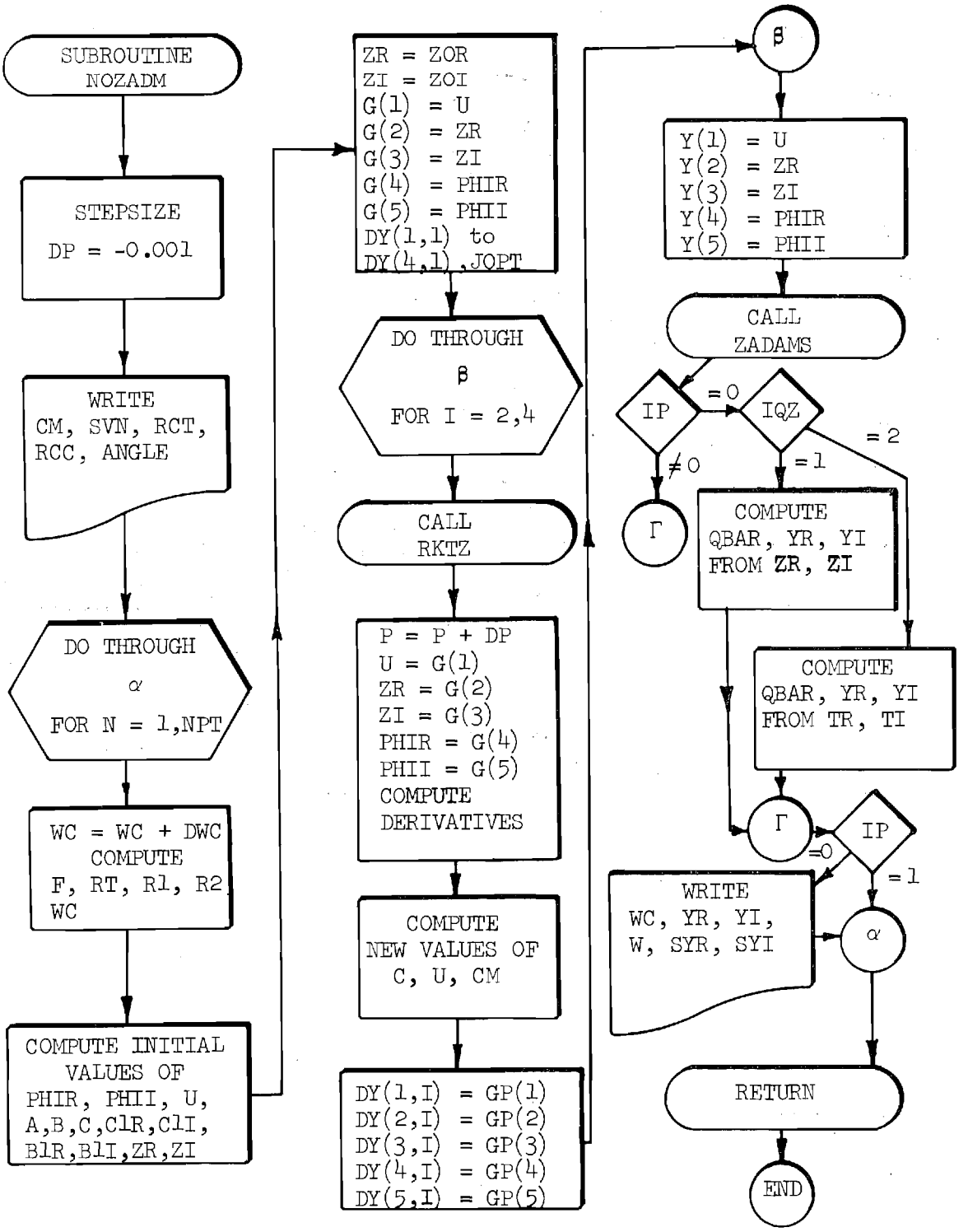

Figure A-1. Continued (Page 2 of 10)

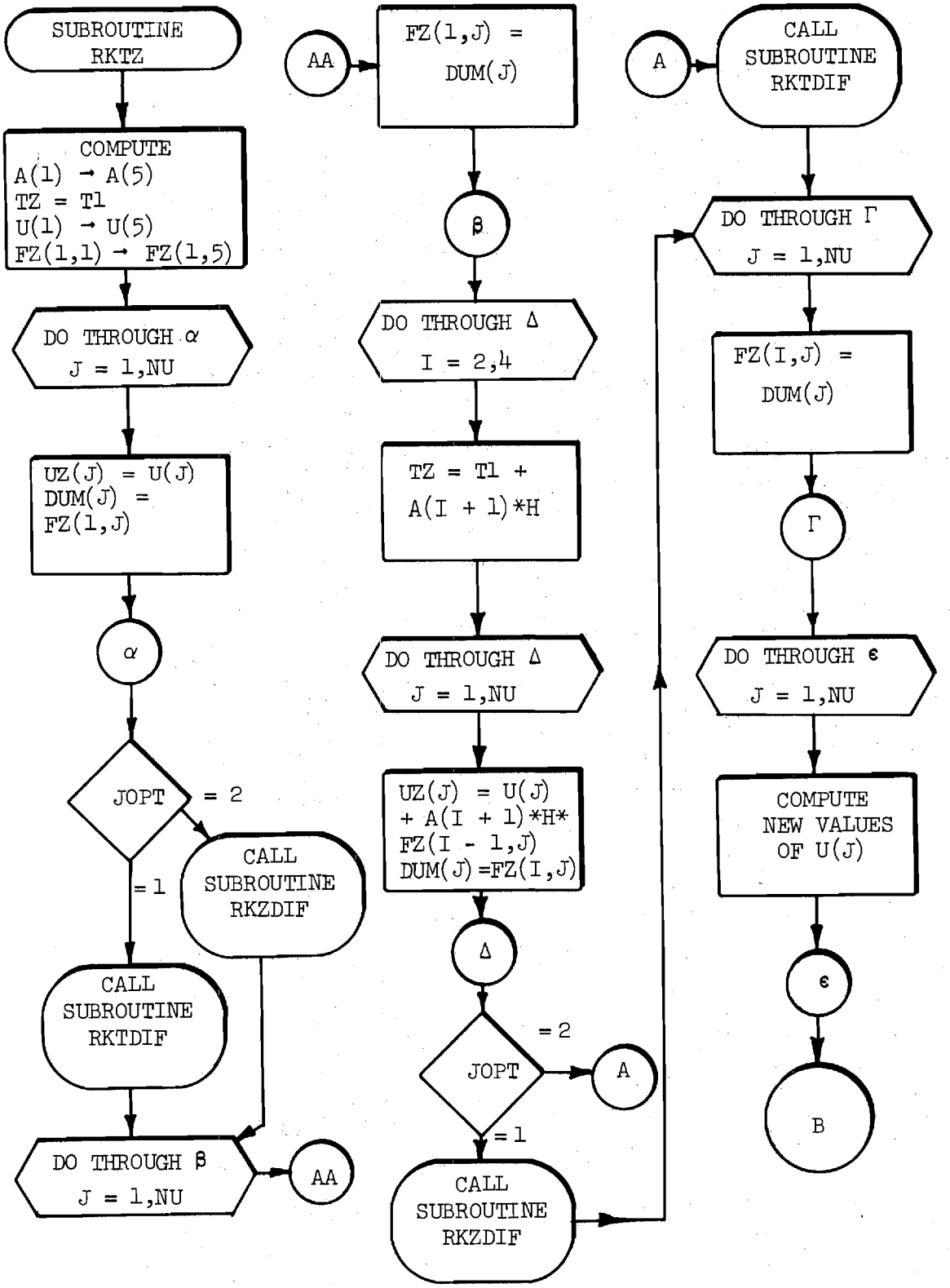

Figure A-1. Continued (Page 3 of 10)

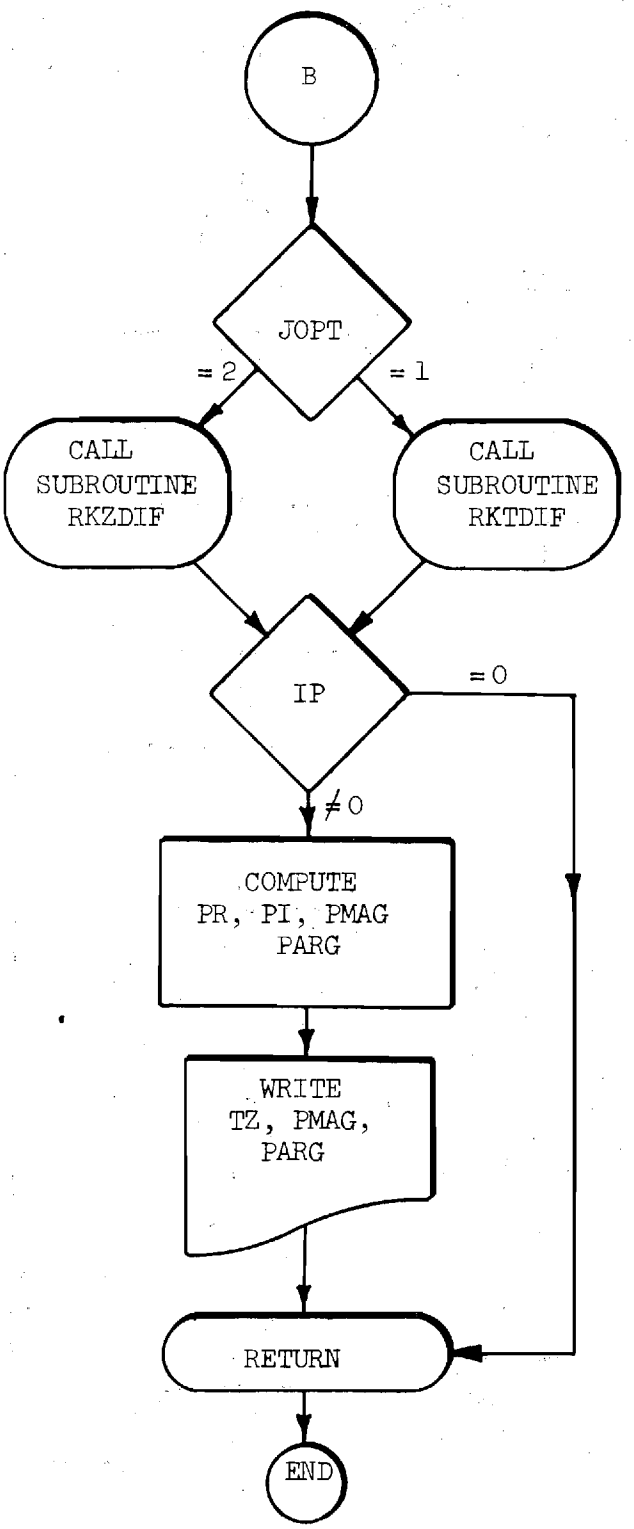

Figure A-1. Continued (Page 4 of 10)

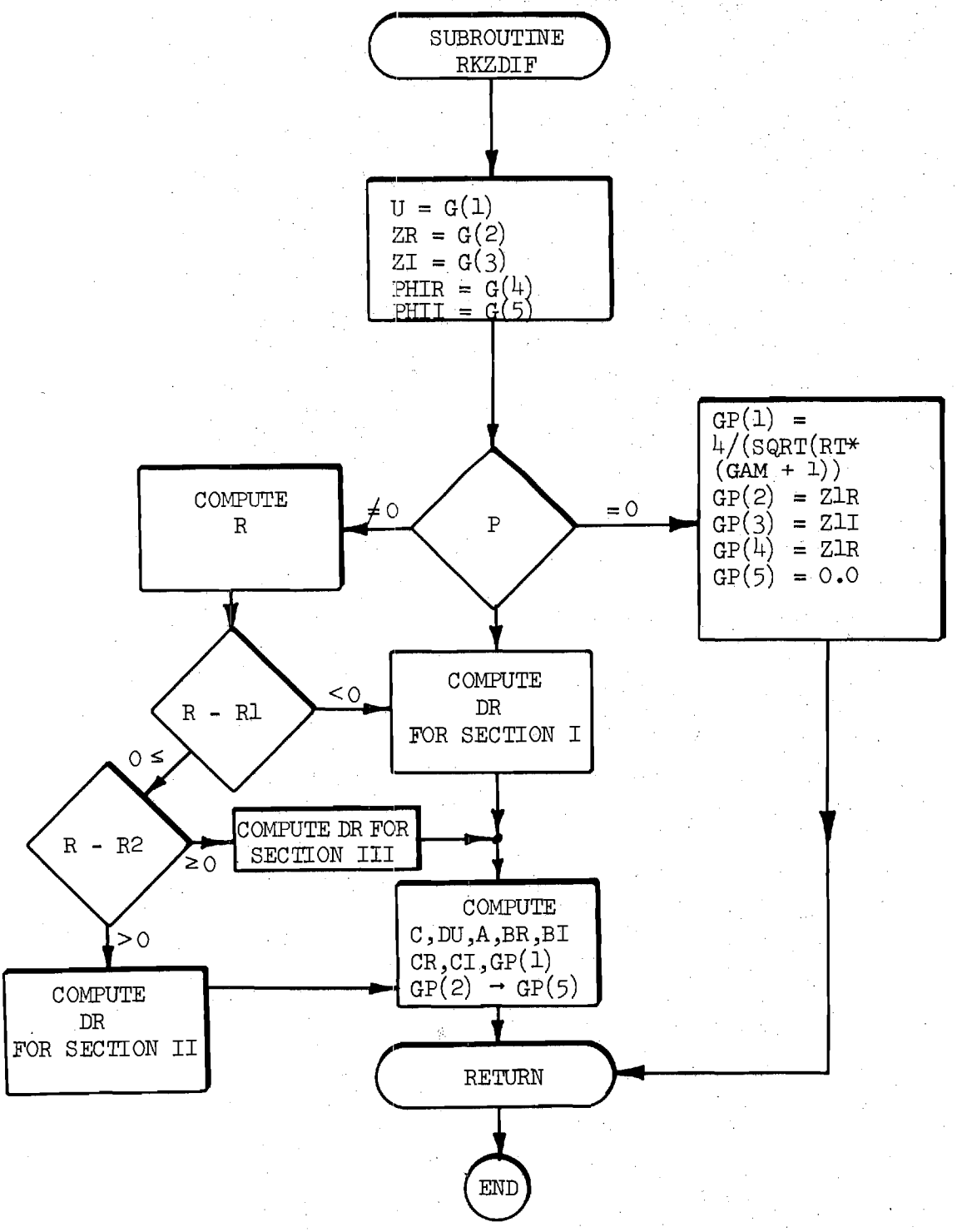

Figure A-1. Continued (Page 5 of 10)

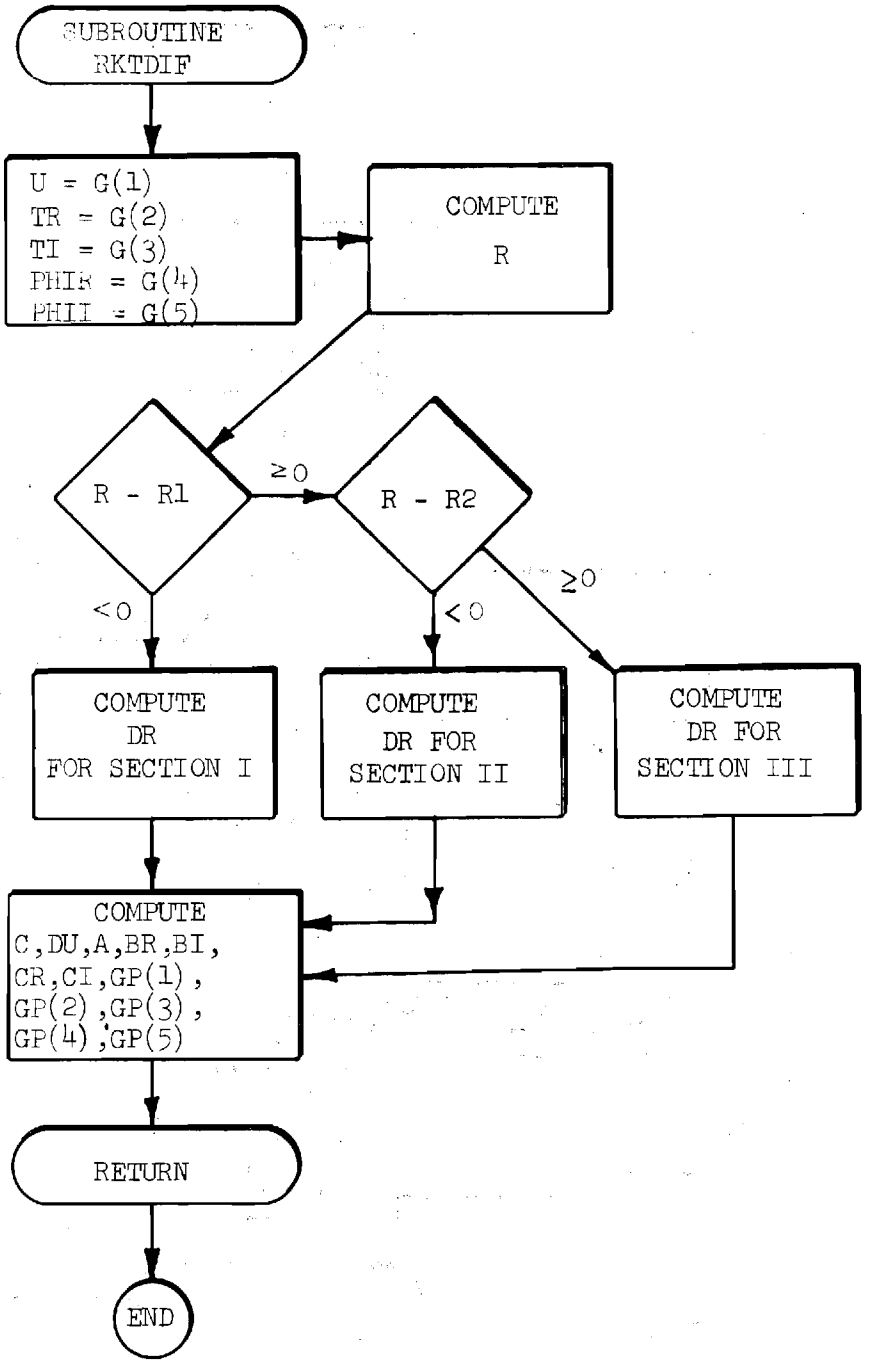

Figure A-1. Continued (Page 6 of 10)

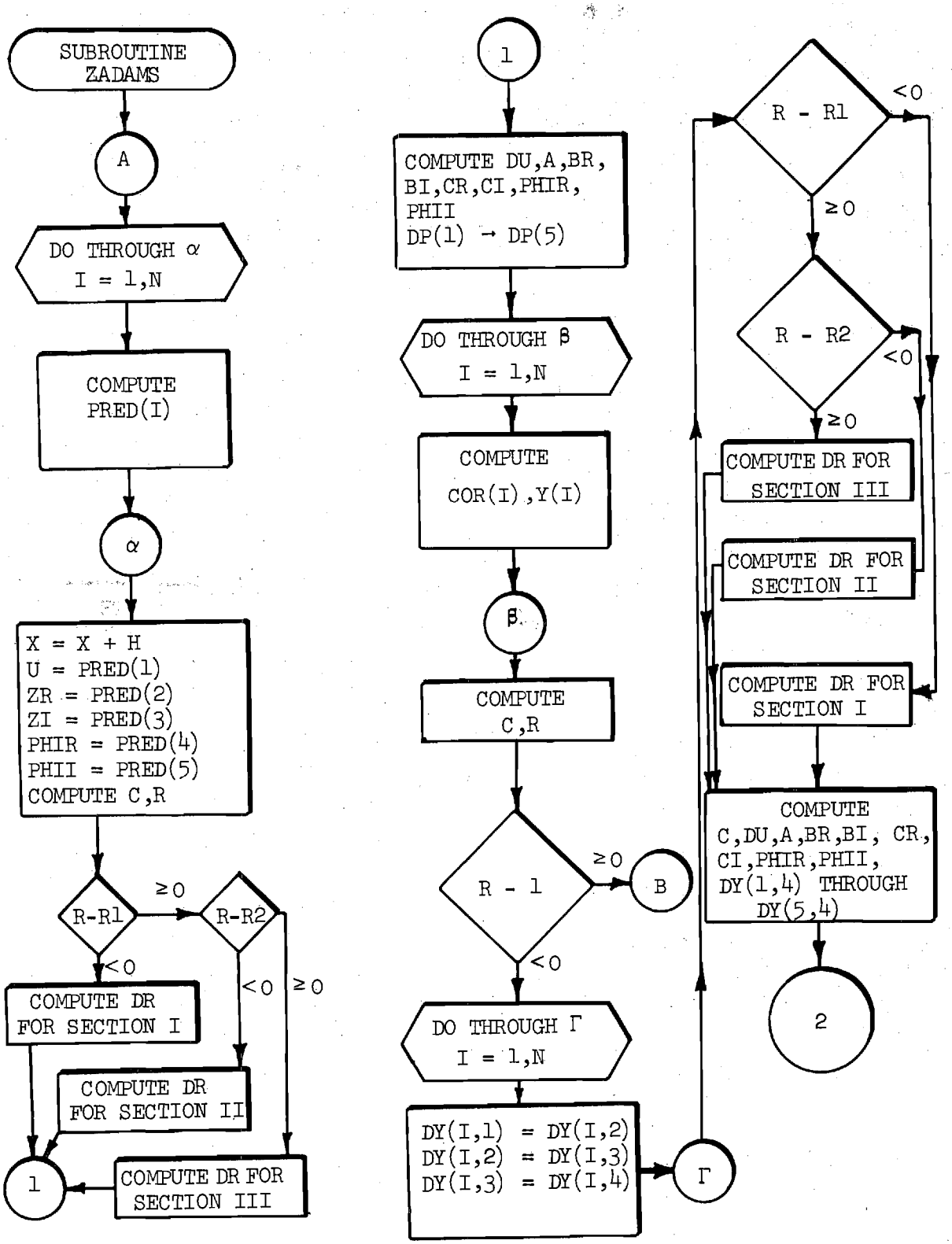

Figure A-1. Continued (Page 7 of 10)

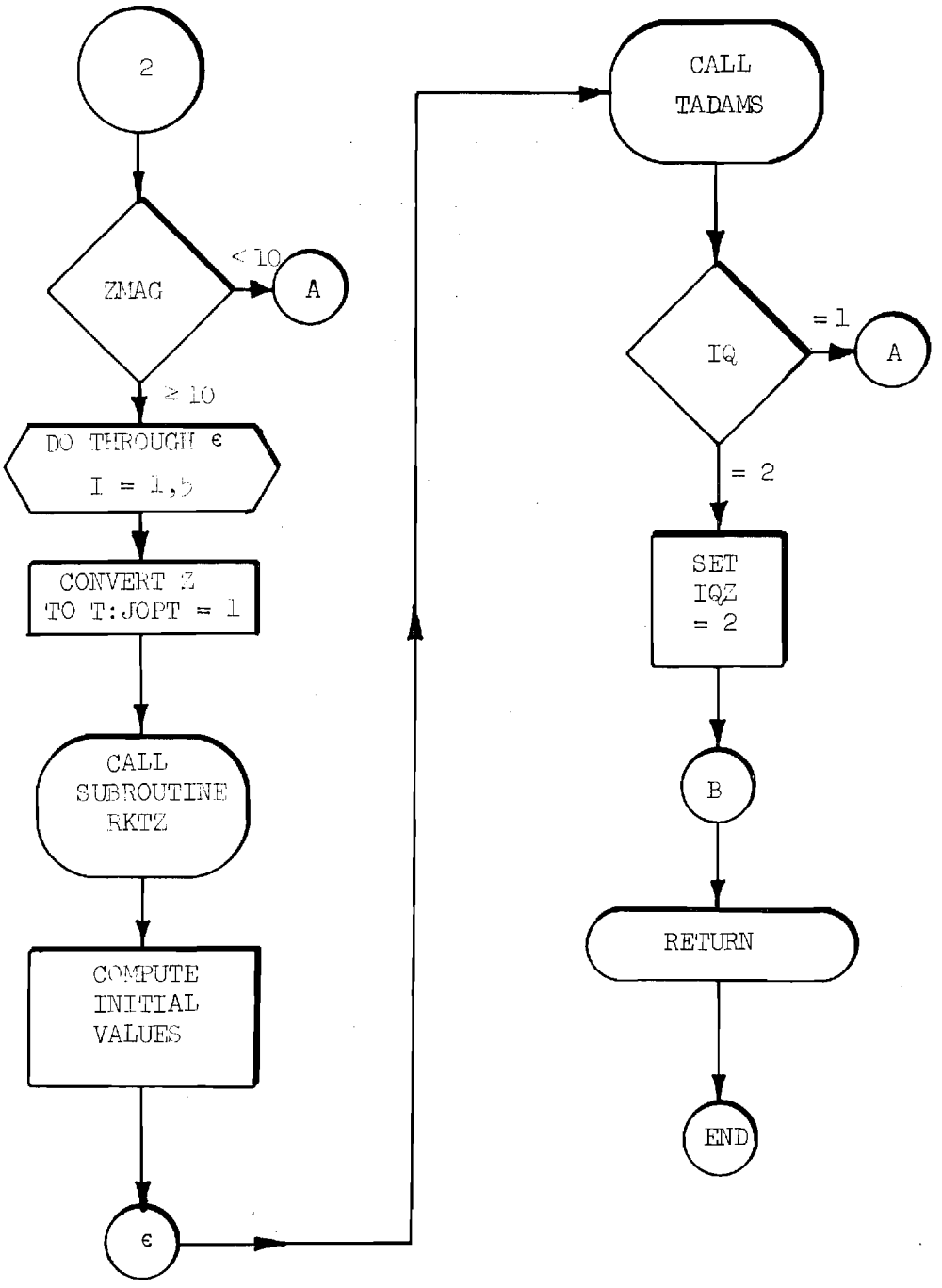

Figure A-1. Continued (Page 8 of 10)

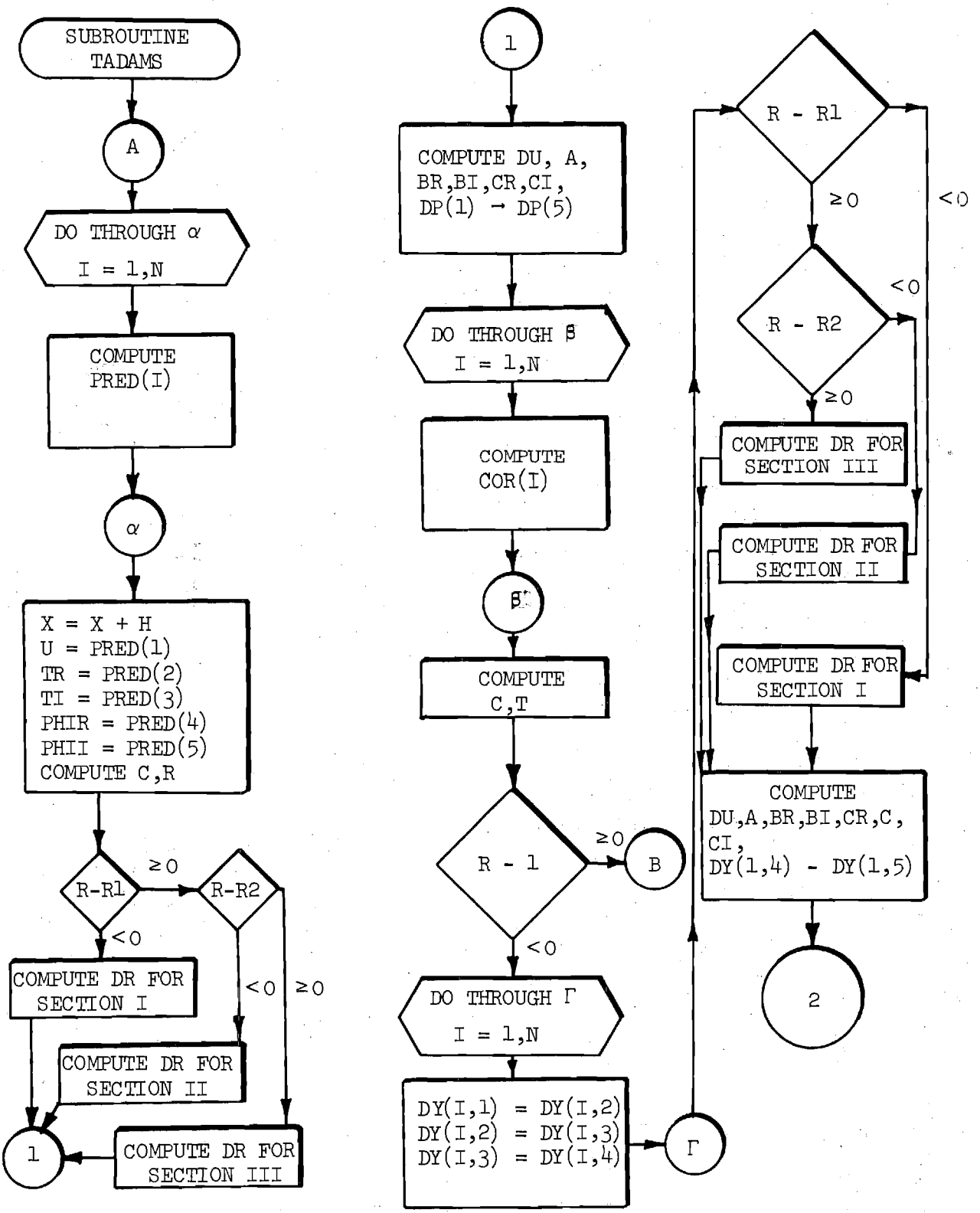
SUBROUTINE TADAMS
A
DO THROUGH α
I = 1,N
COMPUTE PRED(I)
α
X = X + H
U = PRED(1)
TR = PRED(2)
TI = PRED(3)
PHIR = PRED(4)
PHII = PRED(5)
COMPUTE C,R
R-R1
≥0
R-R2
<0
<0
≥0
COMPUTE DR FOR SECTION I
COMPUTE DR FOR SECTION II
COMPUTE DR FOR SECTION III
1
1
COMPUTE DU, A, BR,BI,CR,CI, DP(1) → DP(5)
DO THROUGH β
I = 1,N
COMPUTE COR(I)
β
COMPUTE C,T
R - 1
≥0
B
<0
DO THROUGH Γ
I = 1,N
DY(I,1) = DY(I,2)
DY(I,2) = DY(I,3)
DY(I,3) = DY(I,4)
Γ
R - R1
≥0
<0
R - R2
<0
≥0
COMPUTE DR FOR SECTION III
COMPUTE DR FOR SECTION II
COMPUTE DR FOR SECTION I
COMPUTE DU,A,BR,BI,CR,C, CI, DY(1,4) - DY(1,5)
2

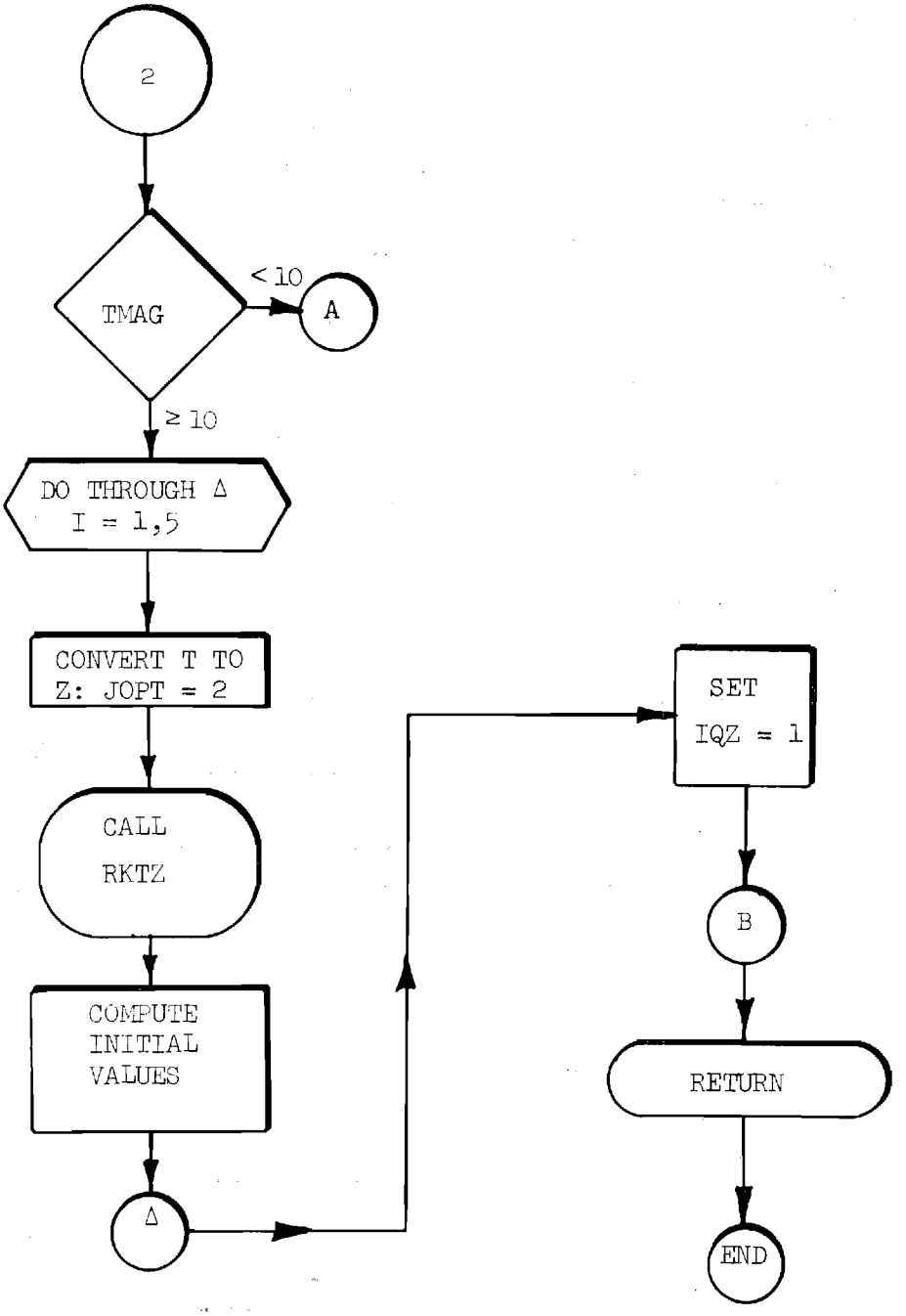

Figure A-1. Concluded (Page 10 of 10)

REFERENCES

1. Crocco, L., and Cheng, S. I., Theory of Combustion Instability in Liquid Propellant Rocket Motors, AGARDograph 8, Butterworth Publications Limited, London, 1956.
2. Crocco, L., and Sirignano, W. A., Behavior of Supercritical Nozzles under Three-Dimensional Oscillatory Conditions, AGARDograph 117, Butterworth Publications Limited, London, 1967.
3. Bell, W. A., "Experimental Determination of Three-Dimensional Liquid Rocket Nozzle Admittances," PH.D. Thesis, School of Aerospace Engineering, Georgia Institute of Technology, Atlanta, Georgia, July 1972.
4. Serra, R. A., "Determination of Internal Gas Flows by a Transient Numerical Technique," AIAA Journal, Vol. 10, May 1972, p. 603.
5. Zinn, B. T., "Longitudinal Mode Acoustic Losses in Short Nozzles," J. of Sound and Vibration, 22(1), pp. 93-105, 1972.

REPORT DISTRIBUTION LIST

Dr. R. J. Priem, MS 500-209
NASA Lewis Research Center
21000 Brookpark Road
Cleveland, Ohio 44135 (2)

Norman T. Musial
NASA Lewis Research Center
21000 Brookpark Road
Cleveland, Ohio 44135

Library
NASA Lewis Research Center
21000 Brookpark Road
Cleveland, Ohio 44135 (2)

Report Control Office
NASA Lewis Research Center
21000 Brookpark Road
Cleveland, Ohio 44135

Brooklyn Polytechnic Institute
Attn: V. D. Agosta
Long Island Graduate Center
Route 110
Farmingdale, New York 11735

Chemical Propulsion Information Agency
Johns Hopkins University/APL
Attn: T. W. Christian
8621 Georgia Avenue
Silver Spring, Maryland 20910

NASA
Lewis Research Center
Attn: E. W. Conrad, MS 500-204
21000 Brookpark Road
Cleveland, Ohio 44135

North American Rockwell Corporation
Rocketdyne Division
Attn: L. P. Combs, D/991-350, Zone 11
6633 Canoga Park, California 91304

National Technical Information Service
Springfield, Virginia 22151
(40 Copies)

Aerospace Corporation
Attn: O. W. Dykema
Post Office Box 95085
Los Angeles, California 90045

Ohio State University
Department of Aeronautical and Astronautical Engineering
Attn: R. Edse
Columbus, Ohio 43210

TRW Systems
Attn: G. W. Elverum
One Space Park
Redondo Beach, California 90278

Bell Aerospace Company
Attn: T. F. Ferger
Post Office Box 1
Mail Zone J-81
Buffalo, New York 14205

Pratt & Whitney Aircraft
Florida Research & Development Center
Attn: G. D. Garrison
Post Office Box 710
West Palm Beach, Florida 33402

NASA
Lewis Research Center
Attn: L. Gordon, MS 500-209
21000 Brookpark Road
Cleveland, Ohio 44135

Purdue University
School of Mechanical Engineering
Attn: R. Goulard
Lafayette, Indiana 47907

Air Force Office of Scientific Research
Chief Propulsion Division
Attn: Lt. Col. R. W. Haffner (NAE)
1400 Wilson Boulevard
Arlington, Virginia 22209

NASA Representative
NASA Scientific and Technical
Information Facility
P. O. Box 33
College Park, Maryland 20740
(2 Copies with Document Release
Authorization Form)

University of Illinois
Aeronautics/Astronautic Engineering
Department
Attn: R. A. Strehlow
Transportation Building, Room 101
Urbana, Illinois 61801

NASA
Manned Spacecraft Center
Attn: J. G. Thibadaux
Houston, Texas 77058

Massachusetts Institute of Technology
Department of Mechanical Engineering
Attn: T. Y. Toong
77 Massachusetts Avenue
Cambridge, Massachusetts 02139

Illinois Institute of Technology
Attn: T. P. Torda
Room 200 M. H.
3300 S. Federal Street
Chicago, Illinois 60616

AFRPL
Attn: R. R. Weiss
Edwards, California 93523

U. S. Army Missile Command
AMSMI-RKL, Attn: W. W. Wharton
Redstone Arsenal, Alabama 35808

University of California
Aerospace Engineering Department
Attn: F. A. Williams
Post Office Box 109
LaJolla, California 92037

Georgia Institute of Technology
School of Aerospace Engineering
Attn: B. T. Zinn
Atlanta, Georgia 30332

Pennsylvania State University
Mechanical Engineering Department
Attn: G. M. Faeth
207 Mechanical Engineering Bldg.
University Park, Pennsylvania 16802

TISIA
Defense Documentation Center
Cameron Station
Building 5
5010 Duke Street
Alexandria, Virginia 22314

Office of Assistant Director
(Chemical Technician)
Office of the Director of Defense
Research and Engineering
Washington, D. C. 20301

D. E. Mock
Advanced Research Projects Agency
Washington, D. C. 20525

Dr. H. K. Doetsch
Arnold Engineering Development Center
Air Force Systems Command
Tullahoma, Tennessee 37389

Library
Air Force Rocket Propulsion
Laboratory (RPR)
Edwards, California 93523

Library
Bureau of Naval Weapons
Department of the Navy
Washington, D. C.

Library
Director (Code 6180)
U. S. Naval Research Laboratory
Washington, D. C. 20390

APRP (Library)
Air Force Aero Propulsion Laboratory
Research and Technology Division
Air Force Systems Command
United States Air Force
Wright-Patterson AFB, Ohio 45433

Marshall Industries
Dynamic Science Division
2400 Michelson Drive
Irvine, California 92664

Mr. Donald H. Dahlene
U. S. Army Missile Command
Research, Development, Engineering
and Missile Systems Laboratory
Attn: AMSMI-RK
Redstone Arsenal, Alabama 35809

Library
Bell Aerosystems, Inc.
Box 1
Buffalo, New York 14205

Report Library, Room 6A
Battelle Memorial Institute
505 King Avenue
Columbus, Ohio 43201

D. Suichu
General Electric Company
Flight Propulsion Laboratory
Department
Cincinnati, Ohio 45215

Library
Ling-Temco-Vought Corporation
Post Office Box 5907
Dallas, Texas 75222

Marquardt Corporation
16555 Saticoy Street
Box 2013 - South Annex
Van Nuys, California 91409

P. F. Winternitz
New York University
University Heights
New York, New York

R. Stiff
Propulsion Division
Aerojet-General Corporation
Post Office Box 15847
Sacramento, California 95803

Technical Information Department
Aeronutronic Division of Philco
Ford Corporation
Ford Road
Newport Beach, California 92663

Library-Documents
Aerospace Corporation
2400 E. El Segundo Boulevard
Los Angeles, California 90045

Library
Susquehanna Corporation
Atlantic Research Division
Shirley Highway and Edsall Road
Alexandria, Virginia 22314

STL Tech. Lib. Doc. Acquisitions
TRW System Group
One Space Park
Redondo Beach, California 90278

Dr. David Altman
United Aircraft Corporation
United Technology Center
Post Office Box 358
Sunnyvale, California 94088

Library
United Aircraft Corporation
Pratt & Whitney Division
Florida Research and Development
Center
Post Office Box 2691
West Palm Beach, Florida 33402

Library
Air Force Rocket Propulsion
Laboratory (RPM)
Edwards, California 93523

Allan Hribar, Assistant Professor
Post Office Box 5014
Tennessee Technological University
Cookeville, Tennessee 38501

NASA
Lewis Research Center
Attn: E. O. Bourke, MS 500-209
21000 Brookpark Road
Cleveland, Ohio 44135

Library, Department 596-306
Rocketdyne Division of Rockwell
North American Rockwell, Inc.
6633 Canoga Avenue
Canoga Park, California 91304

Library
Stanford Research Institute
333 Ravenswood Avenue
Menlo Park, California 94025

Rudy Reichel
Aerophysics Research Corp.
Post Office Box 187
Bellevue, Washington 98009

Princeton University
James Forrestal Campus Library
Attn: D. Harrje
Post Office Box 710
Princeton, New Jersey 08540

U. S. Naval Weapons Center
Attn: T. Inouye, Code 4581
China Lake, California 93555

Office of Naval Research
Navy Department
Attn: R. D. Jackel, 473
Washington, D. C. 20360

Air Force Aero Propulsion Laboratory
Attn: APTC Lt. M. Johnson
Wright-Patterson AFB, Ohio 45433

Naval Underwater Systems Center
Energy Conversion Department
Attn: Dr. R. S. Lazar, Code TB 131
Newport, Rhode Island 02840

NASA
Langley Research Center
Attn: R. S. Levine, MS 213
Hampton, Virginia 23365

Aerojet General Corporation
Attn: David A. Fairchild, Mech. Design
Post Office Box 15847 (Sect. 9732)
Sacramento, California 95809

NASA
Lewis Research Center, MS 500-313
Rockets & Spacecraft Procurement Section
21000 Brookpark Road
Cleveland, Ohio 44135

NASA
Lewis Research Center
Attn: H. W. Douglass, MS 500-205
21000 Brookpark Road
Cleveland, Ohio 44135

University of Michigan
Aerospace Engineering
Attn: J. A. Nicholls
Ann Arbor, Michigan 48104

Tulane University
Attn: J. C. O'Hara
6823 St. Charles Avenue
New Orleans, Louisiana 70118

University of California
Department of Chemical Engineering
Attn: A. K. Oppenheim
6161 Etcheverry Hall
Berkeley, California 94720

Army Ballistics Laboratories
Attn: J. R. Osborn
Aberdeen Proving Ground, Maryland 21005

Sacramento State College
School of Engineering
Attn: F. H. Reardon
6000 J. Street
Sacramento, California 95819

Purdue University
School of Mechanical Engineering
Attn: B. A. Reese
Lafayette, Indiana 47907

NASA
George C. Marshall Space Flight Center
Attn: R. J. Richmond, SNE-ASTN-PP
Huntsville, Alabama 35812

Colorado State University
Mechanical Engineering Department
Attn: C. E. Mitchell
Fort Collins, Colorado 80521

University of Wisconsin
Mechanical Engineering Department
Attn: P. S. Myers
1513 University Avenue
Madison, Wisconsin 53706

North American Rockwell Corporation
Rocketdyne Division
Attn: J. A. Nestlerode,
AC46 D/596-121
6633 Canoga Avenue
Canoga Park, California 91304

Jet Propulsion Laboratory
California Institute of Technology
Attn: J. H. Rupe
4800 Oak Grove Drive
Pasadena, California 91103

University of California
Mechanical Engineering Thermal Systems
Attn: Professor R. Sawyer
Berkeley, California 94720

ARL (ARC)
Attn: K. Scheller
Wright-Patterson AFB, Ohio 45433

E-16-607
Fluid Tech.

NASA CR-134788

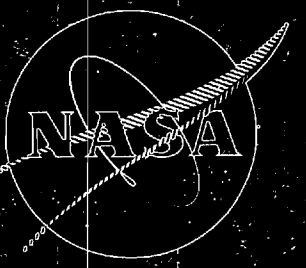

CHARACTERISTICS OF RESPONSE FACTORS OF COAXIAL GASEOUS ROCKET INJECTORS

by

B. A. Janardan
B. R. Daniel
B. T. Zinn

GEORGIA INSTITUTE OF TECHNOLOGY
ATLANTA, GEORGIA 30332

prepared for
NATIONAL AERONAUTICS AND SPACE ADMINISTRATION

NASA Lewis Research Center
Grant NGL 11-002-085
Richard J. Priem, Project Manager

1. Report No.	2. Government Accession No.	3. Recipient's Catalog No.
NASA CR-134788		

4. Title and Subtitle	5. Report Date
CHARACTERISTICS OF RESPONSE FACTORS OF COAXIAL GASEOUS ROCKET INJECTORS	March 1975
	6. Performing Organization Code
7. Author(s)	8. Performing Organization Report No.
B. A. Janardan, B. R. Daniel and B. T. Zinn	
	10. Work Unit No.
9. Performing Organization Name and Address	
Georgia Institute of Technology Atlanta, Georgia 30332	11. Contract or Grant No. NGL 11-002-085
	13. Type of Report and Period Covered
12. Sponsoring Agency Name and Address	Contractor Report
National Aeronautics and Space Administration Washington, D. C. 20546	14. Sponsoring Agency Code

15. Supplementary Notes

Technical Monitor, Richard J. Priem, NASA Lewis Research Center, 21000 Brookpark Road, Cleveland, Ohio 44135

16. Abstract

In this report the results of an experimental investigation undertaken to determine the frequency dependence of the response factors of various gaseous propellant rocket injectors subject to axial instabilities are presented. The injector response factors were determined, using the modified impedance-tube technique, under cold-flow conditions simulating those observed in unstable rocket motors. The tested injectors included a gaseous-fuel injector element, a gaseous-oxidizer injector element and a coaxial injector with both fuel and oxidizer elements. Emphasis was given to the determination of the dependence of the injector response factor upon the open-area ratio of the injector, the length of the injector orifice, and the pressure drop across the injector orifices. The measured data are shown to be in reasonable agreement with the corresponding injector response factor data predicted by the Feiler and Heidmann model.

17. Key Words (Suggested by Author(s))	18. Distribution Statement
Combustion instability Gaseous rocket Injector Response factor	Unclassified - unlimited

19. Security Classif. (of this report)	20. Security Classif. (of this page)	21. No. of Pages	22. Price*
Unclassified	Unclassified	36	$3.00

* For sale by the National Technical Information Service, Springfield, Virginia 22151

SUMMARY

In this report the results of an experimental investigation undertaken to determine the frequency dependence of the response factors of various gaseous propellant rocket injectors subject to axial instabilities are presented. The injector response factors were determined, using the modified impedance-tube technique, under cold-flow conditions simulating those observed in unstable rocket motors. The tested injectors included a gaseous-fuel injector element, a gaseous-oxidizer injector element and a coaxial injector with both fuel and oxidizer elements. Emphasis was given to the determination of the dependence of the injector response factor upon the open-area ratio of the injector, the length of the injector orifice, and the pressure drop across the injector orifices. The measured data are shown to be in reasonable agreement with the corresponding injector response factor data predicted by the Feiler and Heidmann model.

TABLE OF CONTENTS

LIST OF ILLUSTRATIONS

INTRODUCTION

The stability of the combustor of a rocket motor depends upon the wave-energy balance between the various gain and loss mechanisms that are present in the system. The primary source of wave-energy gain is the combustion process. Wave-energy losses are provided by the mean flow, the nozzle, and mechanical damping devices (e.g., acoustic liners) which may be present in the system. As the stability of a rocket motor depends upon the difference between the gain and loss mechanisms, it is of utmost importance that quantitative data capable of describing the damping provided by the loss mechanisms and the driving provided by the unsteady combustion process must be available. Furthermore, an understanding of the dependence of these gain and loss mechanisms upon engine design parameters and operating conditions is needed. The investigation described in this report was undertaken for the purpose of obtaining a better understanding of the driving provided by the unsteady combustion process; specifically, this investigation was concerned with the acquisition of experimental data that quantitatively describes the manner in which various injector designs affect the energy gain provided by the unsteady combustion process.

The injector elements of a gaseous rocket motor control the steady state gas flow and heat transfer patterns inside the combustion chamber. In addition, the injector design influences the response of the flow rate through the injector to combustion chamber disturbances. The characteristics of this response have a profound effect upon engine stability. Customarily, the influence of the injector upon the chamber stability is described by an injector response factor which describes the manner in which the propellants' burning rate responds to a given pressure oscillation in the chamber. The injector response factor basically accounts for the dependence of the unsteady burning rate upon both the unsteady combustion process and unsteady flow of propellants through the injector elements. This response factor can be used to evaluate the energy added by the combustion process into the disturbance in the combustion chamber. It can also be used as the injector

end boundary condition that needs to be satisfied in a stability analysis of a gaseous rocket combustion chamber.

Most of the available experimental investigations[1-7] on the behavior of gaseous propellant injectors were concerned with the steady operation of these devices with little or no consideration being given to the corresponding unsteady problem. In contrast, the analytical studies of Feiler and Heidmann were concerned with the predictions of the characteristics of the response factor of a gaseous injector element. In the Feiler and Heidmann analysis,[8,9] a single gaseous hydrogen injector element is modeled as a combination of lumped flow elements. The desired expressions for the injector response factor are then obtained by solving the conservation equations that describe the unsteady flow inside the various components of the injector. The resulting expressions describe the dependence of the injector response factor upon the injector geometry and the flow conditions in the chamber and the injector. In this analytical model, combustion is assumed to be concentrated in front of the injector face and the effects of mixing and chemical reactions are accounted for by the introduction of an as yet unknown time delay τ_b^*. The period τ_b^* describes the time required for the gaseous oxidizer and fuel streams to mix and burn. In Ref. 10, the Feiler and Heidmann predictions[8] have been modified to account for the compressibility of the gaseous streams flowing through the injector elements.

The results of Refs. 8 and 10 indicate that for a given frequency range and for certain ranges of the parameter τ_b^*, various injector designs can indeed result in the amplification of chamber disturbances. When τ_b^* is identically zero, which corresponds to the case of no combustion present in the system, the results of Refs. 8 and 10 indicate that under these conditions the injector acts as a mechanical damping device; a situation that is to be expected from related studies of Helmholtz resonators and acoustic liners.

Although the predictions of the Feiler and Heidmann analysis have been known for a number of years, they have never been verified experimentally. It is one of the objectives of this investigation to provide

experimental data that could be used to check the validity of the Feiler and Heidmann model. In addition, this investigation is concerned with providing experimental data that will quantitatively describe the manner in which various coaxial injector designs affect the stability of gaseous propellant rocket motors. In pursuit of the above-mentioned objectives, the response factors of a number of gaseous rocket injector configurations have been measured under cold-flow conditions simulating those observed in rocket motors experiencing axial instabilities. Specifically, the response factor of configurations that simulate the flow conditions in a gaseous-fuel injector element, a gaseous-oxidizer injector element, and a coaxial injector with both fuel and oxidizer elements have been determined using the modified impedance-tube technique. The measured injector response factor data are presented and the results discussed in this report.

NOMENCLATURE

A	area
C	Capacitance, defined by Eq. (4)
c	speed of sound
I	Inductance, defined by Eq. (4)
L	length of the injector orifice
l_{eff}	effective orifice length given by Eq. (14)
M	Mach number
N	nondimensional injector response factor
P	pressure
R	Resistance, defined by Eq. (4)
V	injector dome volume
W	mass flow rate of propellant
Y	admittance
y	nondimensional admittance
α	admittance parameter defined by Eq. (7)
β	admittance parameter defined by Eq. (8)

γ	specific heat ratio
δ	equal to $(\bar{P}^*_d - \bar{P}^*_c)/\bar{P}^*_c$
λ	wavelength
ρ	density
σ	open-area ratio of the injector
τ	time lag
ω	angular frequency

Superscripts

$(\bar{})$	steady state quantity
$()^*$	dimensional quantity
$()'$	perturbation quantity

Subscripts

$()_b$	associated with the combustion process
$()_c$	evaluated in the chamber
$()_d$	evaluated in the injector dome
$()_f$	associated with the fuel
$()_{ox}$	associated with the oxidizer
$()_s$	evaluated at the injector surface
$()_1$	evaluated at injector orifice entrance
$()_2$	evaluated at injector orifice exit

ANALYTICAL CONSIDERATIONS

The ability to quantitatively describe the injector response factor is of great practical importance since the combined response of the injector flow rate and the combustion process to chamber disturbances is the mechanism responsible for amplifying and maintaining combustion instability oscillations. In an effort to develop an analytical technique for the prediction of the response factor of a gaseous injector,

Feiler and Heidmann [8, 9] analyzed in detail the unsteady flow through the gaseous hydrogen injector element shown in Fig. 1. Combustion is assumed to occur a certain distance downstream of the injector exit plane and the response of the injector flow rate to a small amplitude pressure oscillation in the chamber is determined by analyzing the linearized conservation equations for each of the injector components. Assuming that each of the injector components behaves as a lumped element, and applying the Laplace transform to the linearized conservation equations, the relationships presented in Fig. 1 are obtained. By appropriate manipulations of these equations and setting the Laplace operator s equal to $i\omega$, which implies a sinusoidal time dependence of the perturbations, the following expression for the injector response factor was obtained:

$$N = \frac{W_b'}{P_c'} = \left(\frac{W_{b_{max}}'}{P_{c_{max}}'}\right) e^{i\theta} \tag{1}$$

where

$$\frac{W_{b_{max}}'}{P_{c_{max}}'} = \frac{-1}{R_2 \left\{ \left[\frac{R_1}{C^* \omega^*} - I^* \omega^* \right]^2 + \left[2 \left(\frac{R_1 \Delta P_1^*}{\bar{P}_d^*} + \frac{\Delta P_2^*}{\bar{P}_2^*} \right) \right]^2 \right\}^{\frac{1}{2}}} \tag{2}$$

$$\theta = \frac{\pi}{2} - \omega^* \tau_b^* - \arctan \frac{2 \left\{ \frac{R_1 \Delta P_1^*}{\bar{P}_d^*} + \frac{\Delta P_2^*}{\bar{P}_2^*} \right\}}{\left\{ \frac{R_1}{C^* \omega^*} - I^* \omega^* \right\}} \tag{3}$$

and

$$C^* \omega^* = \left(\bar{\rho}_d^* V^* / \gamma \bar{W}^* \right) \omega^* \quad ; \quad I^* \omega^* = \left[\bar{W}^* \left(L^* / A_1^* \right) / g \bar{P}_2^* \right] \omega^* \tag{4a}$$

$$\frac{\Delta P_1^*}{\bar{P}_d^*} = \left(\bar{P}_d^* - \bar{P}_1^*\right)/\bar{P}_d^* \quad ; \quad \frac{\Delta P_2^*}{\bar{P}_2^*} = \left(\bar{P}_2^* - \bar{P}_c^*\right)/\bar{P}_2^* \tag{4b}$$

$$R_1 = \frac{\bar{P}_d^*}{\bar{P}_1^* - \left(\Delta P_1^*/\gamma\right)} \quad ; \quad R_2 = \frac{\bar{P}_2^*}{\bar{P}_c^* - \left(\Delta P_2^*/\gamma\right)} \tag{4c}$$

The quantity τ_b^* appearing in Eq. (3) is the residence time of a propellant mass element in the combustor prior to its combustion; τ_b^* is identically zero when there is no combustion in the system. The parameters appearing in Eq. (4) depend upon the injector geometry and engine operating conditions, and their influence upon the injector element response factor is also of interest to rocket designers.

Expressions similar to those developed above for the gaseous-fuel injector element can also be developed for the gaseous-oxidizer injector element. The total response, N_t, of a coaxial gaseous injector element can then be obtained, by substituting the expressions for the fuel and oxidizer response factors into the following equation:

$$N_t = \frac{W_t'}{P'} = \frac{\left(W_t^*\right)'/\bar{W}_t^*}{\left(P^*\right)'/\bar{P}^*} = \frac{\left\{\left(W_{ox}^*\right)' + \left(W_f^*\right)'\right\}/\bar{W}_t^*}{\left(P^*\right)'/\bar{P}^*} \tag{5}$$

$$= \left[\frac{\bar{W}_{ox}^*}{\bar{W}_t^*}\right] N_{ox} + \left[\frac{\bar{W}_f^*}{\bar{W}_t^*}\right] N_f \tag{5}$$

where N_{ox} and N_f respectively represent the response factors of the oxidizer and fuel injector elements while $\bar{W}_{ox}^*/\bar{W}_t^*$ and $\bar{W}_f^*/\bar{W}_t^*$ represent the ratios of the mean oxidizer and fuel flow and the total mean flow, respectively.

RESPONSE FACTOR DETERMINATION

The required injector response factor data were determined in this investigation from injector admittance data measured by use of the modified impedance-tube technique. The impedance tube setup shown in Fig. 2, consists of a 6-inch diameter cylindrical tube with a sound source capable of generating harmonic waves of desired frequency placed at one end. The injector element under investigation is placed at the other end. During an experiment, the flow of a gaseous propellant through the injector is simulated by the flow of air. Regulating valves are provided to ensure that the pressure drop across the injector orifices is maintained at a required value. By means of an acoustic driver, a standing wave pattern of a given frequency is excited in the tube and a microphone probe is traversed along the tube to measure the axial variation of the standing pressure wave pattern. As explained in the next section, the admittance of the injector end of the impedance-tube is determined from the measured axial variation of the standing pressure wave. The frequency dependence of the admittance and the response factor of the injector is determined by repeating the experiment at different frequencies.

The first step in the determination of the injector response factor N consists of the measurement of the "average" surface admittance Y_s^* at the injector end of the modified impedance tube. The "average" surface admittance is defined as the ratio of the "average" normal velocity perturbation across the injector surface and the local pressure perturbation; that is:

$$Y_s^* = \frac{\vec{u}_s^{*\prime} \cdot \vec{n}}{p_s^{*\prime}} \tag{6}$$

The admittance Y_s^* is a complex number whose real and imaginary parts describe the relationships that exist at the location under consideration between the amplitudes and phases of the velocity and pressure perturbations.

From a physical point of view it is more satisfying to describe the admittance by means of two parameters α and β which respectively describe changes in amplitudes and phases between the incident and reflected pressure waves at the location under consideration; that is:

$$\left[\frac{\text{Amplitude of Reflected Pressure Wave}}{\text{Amplitude of Incident Pressure Wave}}\right]_{\substack{\text{Injector}\\\text{Face}}} = e^{-2\pi\alpha} \qquad (7)$$

$$\left[\begin{matrix}\text{Phase change Between Incident and}\\\text{Reflected Pressure Waves}\end{matrix}\right]_{\substack{\text{Injector}\\\text{Face}}} = \pi(1 + 2\beta) \qquad (8)$$

The parameter β appearing above satisfies the condition $|\beta| \leq 0.5$.

The expressions required for the calculation of the injector surface admittance are obtained from solutions of the system of conservation equations which describe the behavior of small amplitude, one-dimensional waves inside an impedance-tube containing a steady one-dimensional flow. These solutions are required to satisfy an admittance boundary condition at the injector surface in terms of the as yet unknown parameters α and β. The resulting expressions (See Ref. 12 for detailed derivations of these solutions), describing the time and space dependence of the pressure and velocity perturbations at the injector surface, are substituted into Eq. (6) to obtain an expression for the injector surface admittance. Normalizing the resulting expression with the characteristic admittance $Y_g^* = 1/\bar{\rho}^*\bar{c}^*$ of the gas medium, the following expression for the nondimensional injector surface admittance y_s is obtained[12]:

$$y_s = \frac{Y_s^*}{Y_g^*} = \Gamma + i\eta = \coth \pi(\alpha - i\beta) \qquad (9)$$

It can also be shown[12] that the parameters α and β, which appear in Eqs. (7), (8) and (9) must satisfy the following relationships be-

tween variables describing the characteristics of the standing wave pattern:

$$\alpha = \frac{1}{\pi} \tanh^{-1}\left[\frac{|P^*_{min}|}{|P^*_{max}|}\right]; \quad \beta = \frac{2Z^*_{min}}{\lambda^*} \tag{10}$$

In impedance-tube experiments and in the present study, the relationships presented in Eq. (10) are used to determine the admittance variables α and β. The procedure leading to the determination of α and β consists of measuring (a) the distance Z^*_{min} from the injector surface to the first pressure amplitude minimum and (b) the ratio of $|P^*_{min}|/|P^*_{max}|$ of the minimum pressure amplitude to the maximum pressure amplitude. The resulting values of α and β are then substituted into Eq. (9) to obtain the injector surface admittance.

From the measured injector surface admittance y_s, the injector orifice admittance y_2 is determined by using the following relationship obtained from the perturbed form of mass conservation law:

$$(u^*)'_s A^*_s = (u^*)'_2 A^*_2$$

which upon dividing by $(P^*)'_s$ gives

$$y_2 = y_s/\sigma \tag{11}$$

where $\sigma = A^*_2/A^*_s$ is the injector open-area ratio. In deriving Eq. (11) the gas has been assumed to be incompressible; an allowable assumption for the situation under consideration.

An expression relating the nondimensional response factor N to the nondimensional admittance y is obtained from the definitions of these two quantities as follows:

$$N = \frac{\vec{W}^{*\prime} \cdot \vec{n}/\bar{W}^{*}}{P^{*\prime}/\bar{P}^{*}} = \frac{\bar{P}^{*}}{\bar{\rho}^{*}\bar{u}^{*}}\left[\bar{\rho}^{*}\frac{\vec{u}^{*\prime} \cdot \vec{n}}{P^{*\prime}} + \frac{\rho^{*\prime}}{P^{*\prime}}\bar{u}^{*} \cdot \vec{n}\right]$$

$$= \frac{1}{\gamma \bar{M}}\left[\bar{\rho}^{*}\bar{c}^{*}\frac{\vec{u}^{*\prime} \cdot \vec{n}}{P^{*\prime}} + \bar{M} \cdot \vec{n}\right]$$

$$= \frac{1}{\gamma \bar{M}}\left(y + \bar{M} \cdot \vec{n}\right) \qquad (12)$$

In deriving Eq. (12) it has been assumed that the gas is perfect and that the oscillations are isentropic. The response factor N of the test injectors is finally obtained by substituting the measured orifice admittance y_2 into Eq. (12) which can be rewritten in the following form for the experimental setup of this investigation:

$$N = \frac{1}{\gamma}\left[-\frac{y_2}{\bar{M}_2} + 1\right] \qquad (13)$$

TEST INJECTORS

In order to obtain the needed data, the frequency dependence of the response factors of the injector configurations shown in Figs. 3 through 6 have been determined. The characteristic dimensions of these injectors, namely, the injector orifice open-area ratio, the orifice length, and the injector dome volume are also presented in the above-mentioned figures.

Injector configurations 1 and 2 were designed to simulate the flow behavior through gaseous-fuel injector elements. The dimensions of these configurations were chosen to provide data capable of determining the effect of the injector open-area ratio upon the injector response factor. Injector configurations 3 through 5 were designed to simulate the flow behavior in gaseous-oxidizer injector elements, and their

dimensions were chosen to allow the determination of the dependence of the injector response factor upon the orifice length. Injector configuration 6, shown in Fig. 6, consists of a combination of configurations 1 and 3. This configuration was designed to simulate the flow behavior in a coaxial injector of a gaseous rocket motor. This injector configuration was tested to check the validity of Eq. (5) by comparing its measured response factors with predicted response factor data obtained by substituting the individually-predicted response factors of configurations 1 and 3 into Eq. (5).

RESULTS

Introduction

The results presented in this section were obtained by measuring the admittances and response factors of the test injectors over the frequency range of 150 to 800 Hz which included their resonant frequency. To establish the repeatability of the experimental data, the frequency dependence of the response factor one of the test injectors was measured on two different occasions and the response factor data obtained in these tests are presented in Fig. 7. An examination of this figure indicates that the measurement technique yields repeatable data. The scatter observed in the measured values of the imaginary part of the response factor is due to the fact that at the corresponding frequencies the standing wave in the impedance tube had a flat minima and hence its axial location could not be precisely measured.

Before presenting the results, it is necessary to point out a difference between the geometrical configurations of the injector elements whose admittances were measured in this study and the injector configurations considered in the theoretical model of Feiler and Heidmann.[8] The theoretical analysis considers the behavior of a single injector element and its predictions provide a response factor that is valid at the exit plane of the injector orifice. As it would be extremely difficult to directly measure the response factor of a single injector element, this study undertook the measurement of the response

factors of configurations containing either 5 or 13 injector elements. As stated earlier, the admittances measured in this study represent "average" admittances over the tested injector surface. Hence, before any meaningful comparisons between the predicted and the measured sets of admittance data can be made, the above-mentioned difference must be suitably taken into consideration. This point was discussed in the previous section where it was shown that by using mass conservation considerations, this difference can be accounted for by multiplying the theoretically predicted orifice admittances by the open-area ratio σ of the injector configuration. This step "averages" the predicted orifice admittance over the injector surface. To illustrate this point, the theoretically predicted frequency dependence of the admittances of injector configuration 1 with a pressure drop δ of 0.068 across the injector orifices is presented in Fig. 8. The broken lines in this figure describe the admittances at the exit plane of the injector orifices while the solid lines represent the "average" admittances of the injector surface. It is this "average" data which has to be compared with the admittances measured during this investigation.

In the present study, the expressions provided by Feiler and Heidmann[8] have been slightly modified when used to compute the predicted admittances and response factors of the test injector configurations. This was necessitated by the observation that the measured resonant frequencies of the tested injectors did not coincide with their predicted values. This is illustrated by the data presented in Fig. 9. The broken line in this figure describes the theoretically predicted frequency dependence of the real and imaginary parts of the response factor of one of the test injectors. An examination of this figure indicates that while the two sets of data are similar in magnitude and shape, the observed injector resonant frequency is lower than its predicted value. In an effort to explain this frequency shift, use was made of knowledge developed in studies concerned with the behavior of Helmholtz resonators and acoustic liners[13, 14] where it has been well known that the effective length of the slug of the gaseous mass oscillating within the orifice is longer than the orifice length.

It is also well known that the resonant frequencies of Helmholtz resonators and acoustic liners are inversely proportional to the square root of the orifice length. This suggests that the actual length L^* of the injector orifices should be replaced by an effective length l^*_{eff} whenever it appears in the analytical expressions of the Feiler and Heidmann analysis. From experimental reactance data of acoustic liners with apertures of various thicknesses, Garrison[13] developed the following empirical relation for the effective length l^*_{eff}:

$$l^*_{eff} = L^* + 0.85\left[1 - 0.70\sqrt{\sigma}\right]\left(D^*_o - D^*_i\right) \qquad (14)$$

where D^*_o and D^*_i are respectively the outer and inner diameters of the orifices. Computing the predicted response factor data of the test injector with L^* replaced by the effective length l^*_{eff}, the result indicated by the solid line in Fig. 9 was obtained. The experimental resonant frequency now is in better agreement with the predicted resonant frequency than the original Feiler and Heidmann prediction. Based on this result all of the theoretically predicted data presented in the remainder of this report was obtained by suitably incorporating Eq. (14) into the expressions of Ref. 8.

Comparison of Measured and Predicted Injector Admittances

The injector admittances measured during the course of the present study are presented in Figs. 10 through 14 along with admittance data predicted by the Feiler and Heidmann model. These figures describe, respectively, the frequency dependence of the real and imaginary parts of the surface admittances of injector configurations 1 through 5. An examination of these figures indicates a reasonable agreement between the measured and predicted admittances. The discrepancy observed in the data may be, among other factors, due to the fact that radial pressure gradients were measured in the domes of some of the tested injectors. These pressure gradients resulted in different pressure drops across different injector elements. The possibility of such pressure

gradients is not considered in the theoretical model[8] and their effect cannot be accounted for in predicting the injectors' response factors. The theoretical admittances obtained in this study were computed assuming that the pressure drops across all of the injector orifices were equal to the pressure drop measured across one of the outer injector elements; an assumption that is contrary to the above-mentioned observations.

The response factors of injector configurations 1 through 5 were obtained by substituting the measured admittance data into Eq. (13). As suggested in Ref. 8, the response factor data for the injectors tested in this program, with different pressure drops, are plotted in Fig. 15 in terms of a generalized response factor φ defined as

$$\varphi = N_{Real} \left\{ 2R_2 \left(\frac{R_1 \Delta P_1^*}{\bar{P}_d^*} + \frac{\Delta P_2^*}{\bar{P}_2^*} \right) \right\} \tag{15}$$

and a generalized reactance Ψ defined as

$$\Psi = \left(\frac{R_1}{C^* \omega^*} - I^* \omega^* \right) / 2 \left(\frac{R_1 \Delta P_1^*}{\bar{P}_2^*} + \frac{\Delta P_2^*}{\bar{P}_2^*} \right) \tag{16}$$

An examination of Fig. 15 indicates a reasonable agreement between the experimental data and the predictions of the Feiler and Heidmann model. Furthermore, this plot points to a convenient way for correlating and plotting injector response factor data.

Effect of Injector Design Parameters Upon Injector Response Factors

During this investigation, the dependence of the injector response factors upon the pressure drop across the injector orifices, the open-area ratio of the injector and the length of the injector orifices were investigated. The dependence of the injector response upon the pressure drop across the injector orifices is demonstrated by the data presented earlier in Figs. 10 through 14. An examination of these figures

indicates that the injector admittances and response factors decrease rapidly in magnitude with increase in pressure drop across the orifices. Increase in pressure drop results in an increase in the resistance of the injector plate. This decreases the coupling between the pressure oscillation inside the injector dome and the pressure oscillation in the combustor in front of the injector plate. The increase in the injector pressure drop is observed, however, to have little effect upon the resonant frequency of the injector.

In order to determine the dependence of the injector response factor upon the injector characteristic dimensions, the admittance data measured with test configurations 1, 4 and 5 were substituted into Eq. (13) and the response factors obtained are presented in Figs. 16 and 17. The data presented in Fig. 16 describes the effect of the open-area ratio upon the injector response factor for a given orifice length and mass flux through the injector orifices. An examination of Fig. 16 indicates that an increase in the open-area ratio of the injector results in an increase in the damping provided by the injector. In addition, the data indicates an increase in the resonant frequency which is to be expected from results of studies on Helmholtz resonantors. The increase in the injector damping is due to the fact that for a given mass flux an increase in the open-area ratio results in a decrease in the pressure drop across the orifices. This in turn decreases the injector resistance. From a stability point of view this seems to suggest that, for a given mass flow across the injector plate, an injector should be designed with as large an open-area ratio as possible. However, in contemplating such changes in actual systems, one should also consider how an increase in the open-area ratio would affect other gain or loss mechanism in the system. For example, in an actual gaseous propellant rocket motor a decrease in the pressure drop across the injector orifices also affects the mixing rate and hence the propellants burning rate.

For a given open-area ratio and pressure drop across the orifices, data describing the effect of the orifice length upon the injector response factor is presented in Fig. 17. An examination of this figure

indicates that an increase in the orifice length from 0.875" to 1.75" resulted in a decrease in the resonant frequency of the injector. Further examination of Fig. 17 indicates that although there is no observable change in the magnitude of the response factor at resonance, an increase in the orifice length decreases the band width of the response curve.

CONCLUSIONS

The measured data indicates that under the test conditions encountered in this study, there is reasonable agreement between the measured injector response factors and those predicted by the Feiler and Heidmann model. The good agreement observed between the measured and predicted total response factors of coaxial injectors containing both fuel and oxidizer elements suggests that the procedure suggested by Feiler and Heidmann for calculating the total response factors from individual injector response factor data is indeed valid.

The measured response factor data indicates that the orifice length can be varied to shift the resonant frequency of the injector without any change in the magnitude of the response factor at resonance. However, changes in pressure drop across the orifices and the open-area ratio of the injector were found to have a considerable effect on the injector response factor.

The injector configurations investigated in this program were similar to Helmholtz Resonators with a steady through flow. The interaction of such a configuration with a sound wave is not expected to produce any wave amplification, as was recognized by Feiler and Heidmann and confirmed by the data reported in this report. When a time delay, τ_b^*, due to combustion is added to the theoretical model, the phase relationship between the pressure and velocity perturbations required for wave amplification (and instability) is obtained. To test the latter hypothesis, and in the process measure the characteristic combustion time, τ_b^*, additional studies that will measure the response factors of "reacting" gaseous rocket injectors, under a variety of conditions simulating those observed in unstable engines, are needed.

REFERENCES

1. Falkenstein, G. L. and Domokos, S. J., "High Pressure Gaseous Hydrogen/Gaseous Oxygen Thrusters," AIAA/SAE 7th Propulsion Conference, Salt Lake City, Utah, AIAA Paper No. 71-737, June 1971.
2. Gregory, J. W. and Herr, P. N., "Hydrogen-Oxygen Space Shuttle ACPS Thruster Technology Review," AIAA/SAE 8th Propulsion Conference, New Orleans, Louisiana, AIAA Paper No. 72-1158, November 1972.
3. Paster, R. D., Lauffer, J. R., and Domokos, S. J., "Low Pressure Gaseous Hydrogen/Gaseous Oxygen Auxiliary Rocket Engines," AIAA/SAE 7th Propulsion Conference, Salt Lake City, Utah, AIAA Paper No. 71-738, June 1971.
4. Nagai, C. K., Gurnitz, R. N., and Clapp, S. D., "Cold-Flow Optimization of Gaseous Oxygen/Gaseous Hydrogen Injectors for the Space Shuttle APS Thrustor," AIAA/SAE 7th Propulsion Conference, Salt Lake City, Utah, AIAA Paper No. 71-673, June 1971.
5. Kors, D. L. and Calhoon, D. F., "Gaseous Oxygen/Gaseous Hydrogen Injector Element Modeling," AIAA/SAE 7th Propulsion Conference, Salt Lake City, Utah, AIAA Paper No. 71-674, June 1971.
6. Calhoon, D. F., Ito, J. I., and Kors, D. L., "Investigation of Gaseous Propellant Combustion and Associated Injector/Chamber Design Guidelines," NASA CR-121234, July 1973.
7. Burick, R. J., "Optimum Design of Space Storable Gas/Liquid Coaxial Injectors," Journal of Spacecraft and Rockets, Vol. 10, No. 10, pp. 663-670, October 1973.
8. Feiler, C. E. and Heidmann, M. F., "Dynamic Response of Gaseous Hydrogen Flow System and its Application to High Frequency Combustion Instability," NASA TN D-4040, June 1967.
9. Harrje, D. T., Editor, Liquid Propellant Rocket Combustion Instability, NASA SP-194, 1972.
10. Priem, R. J. and Yang, J. Y. S., "Technique for Predicting High Frequency Stability Characteristics of Gaseous Propellant Combustors," NASA TN D-7406, October 1973.
11. Morse, P. M. and Ingard, K. V., Theoretical Acoustics, McGraw Hill,

New York, 1968.

12. Bell, W. A., Daniel, B. R., and Zinn, B. T., "Experimental and Theoretical Determination of Admittances of a Family of Nozzles Subjected to Axial Instabilities," Journal of Sound and Vibration, Vol. 30, No. 2, pp. 179-190, September 1973.
13. Garrison, G. D., "Suppression of Combustion Oscillations with Mechanical Damping Devices," Interim Report PA FR-3299, Pratt and Whitney Aircraft Florida Research and Development Center, West Palm Beach, Florida, August 1969.
14. Lewis, G. D. and Garrison, G. D., "The Role of Acoustic Absorbers in Preventing Combustion Instability," AIAA/SAE 7th Propulsion Conferences, Salt Lake City, Utah, AIAA Paper No. 71-699, June 1971.

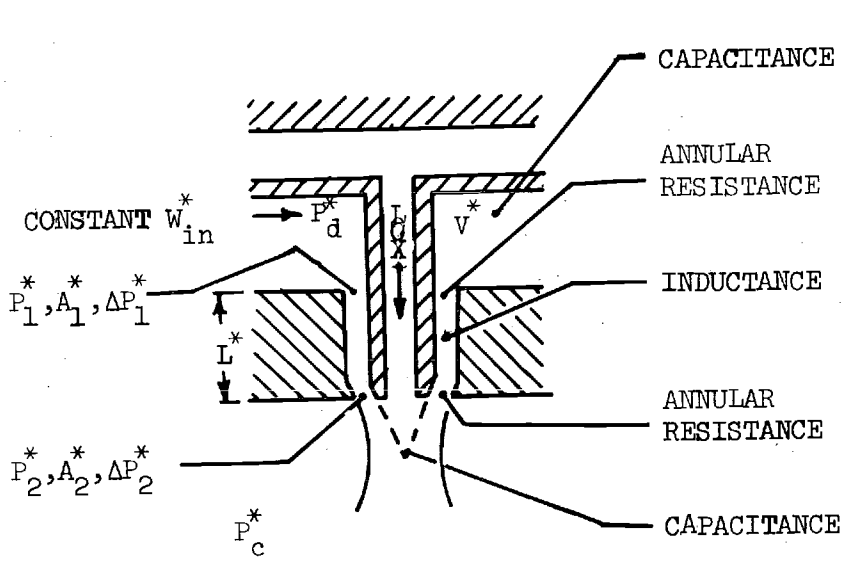

$$\frac{\bar{\rho}^*_d V^*}{\gamma \bar{W}^*} s P'_d = -W'$$

$$W' = \frac{1}{2}\left[\frac{\bar{P}^*_d}{\Delta P^*_1} P'_d + \left(\frac{1}{\gamma} - \frac{\bar{P}^*_1}{\Delta P^*_1}\right) P'_1\right]$$

$$P'_1 - P'_2 = \frac{\bar{W}^* L^*}{g \bar{P}^*_2 A^*_1} sW'$$

$$W' = \frac{1}{2}\left[\frac{\bar{P}^*_2}{\Delta P^*_2} P'_2 + \left(\frac{1}{\gamma} - \frac{\bar{P}^*_c}{\Delta P^*_2}\right) P'_c\right]$$

$$W'_b = W' e^{-\tau^*_b s}$$

Figure 1. Gaseous Hydrogen Injector.

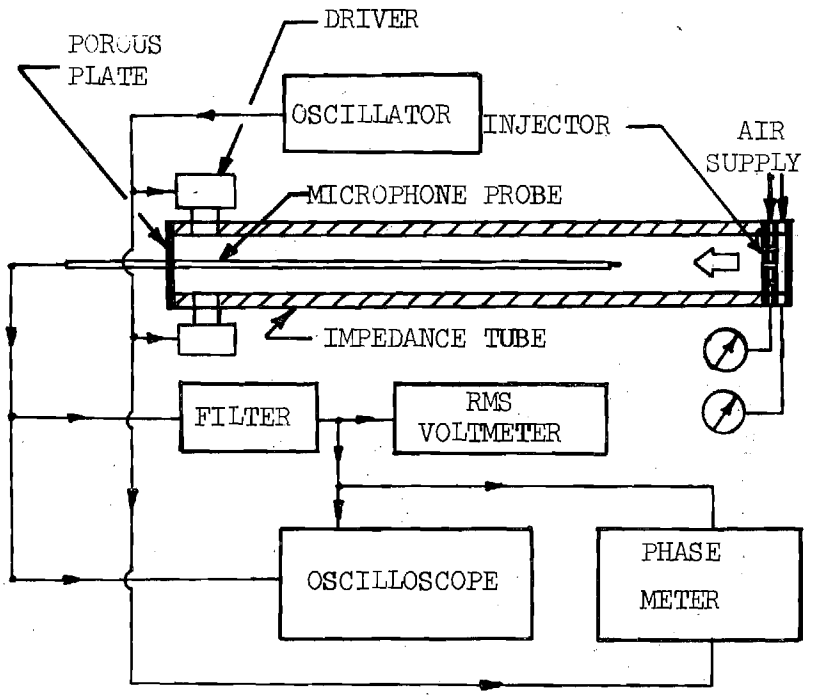

Figure 2. Experimental Apparatus

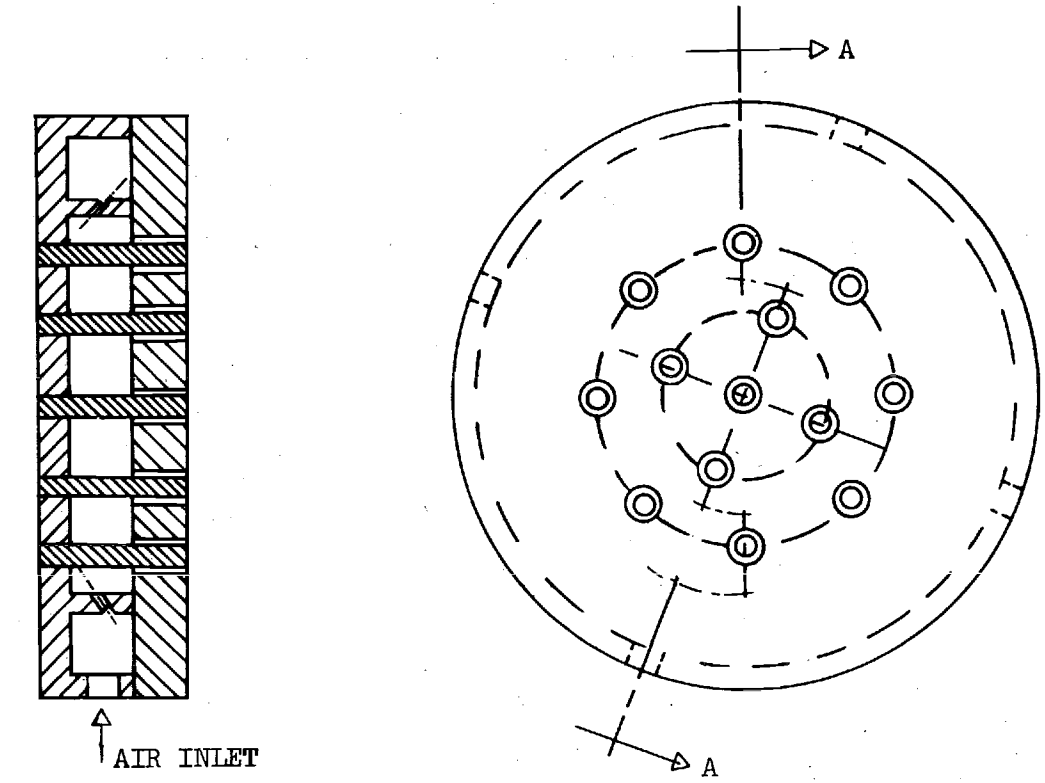

SECTION A-A

CONFIGURATION	σ (%)	L (IN.)	V (IN^3)
1	4.7	0.875	27.6

Figure 3. Description of Injector Configuration 1.

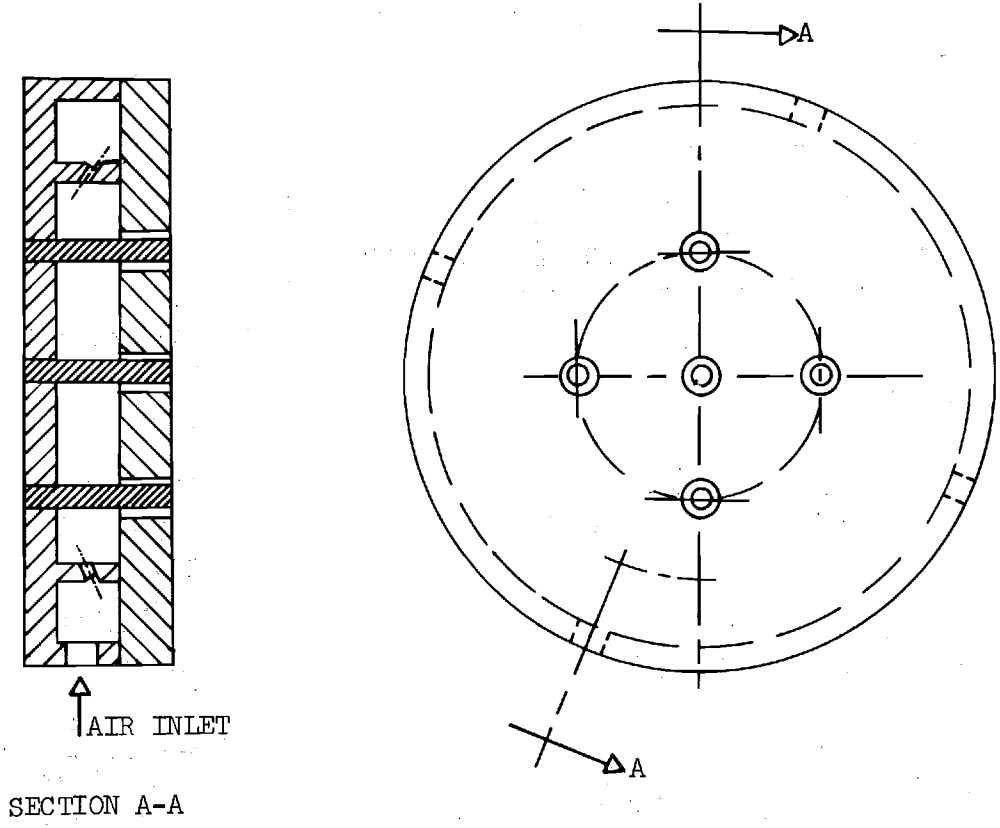

SECTION A-A

CONFIGURATION	σ (%)	L (IN.)	V (IN^3)
2	1.8	0.875	28.0

Figure 4. Description of Injector Configuration 2.

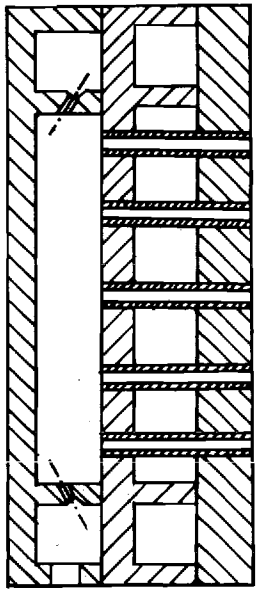

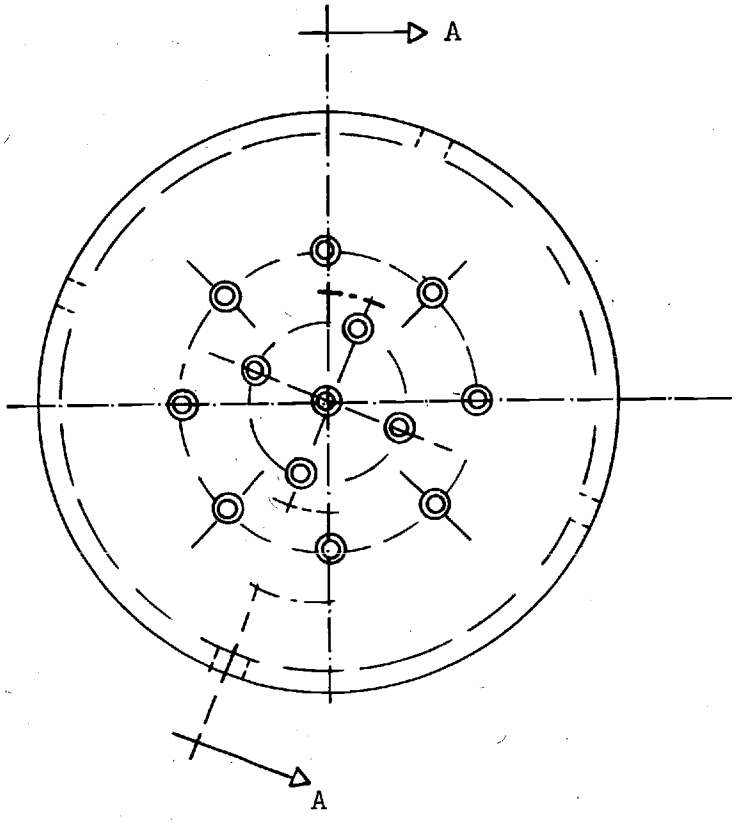

CONFIGURATION	σ (%)	L (IN.)	V(IN.^{3})
3	1.7	2.38	28.2
4	10.2	0.875	28.2
5	10.2	1.75	28.2

Figure 5. Descriptions of Injector Configurations 3, 4 and 5.

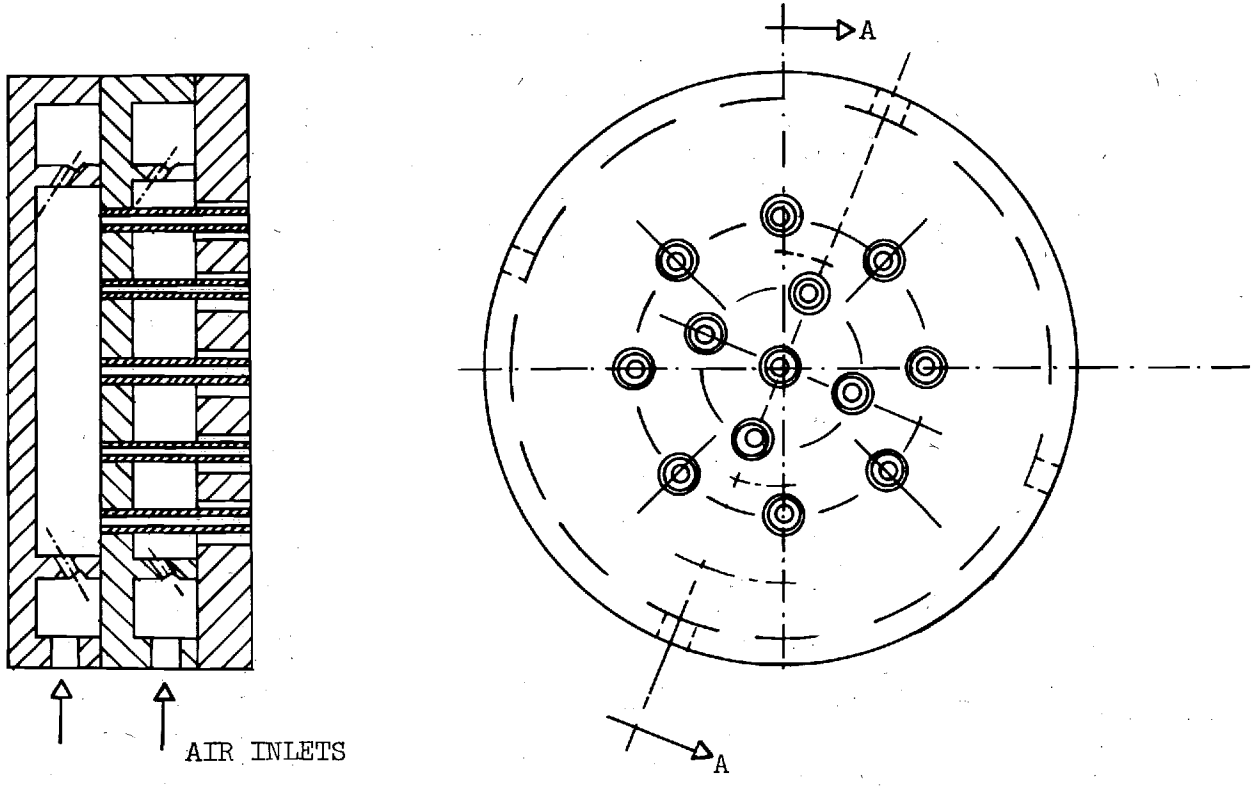

SECTION A-A

CONFIGURATION		σ (%)	L (IN.)	V(IN.^{3})
6	1	4.7	0.875	27.6
	3	1.7	2.38	28.2

Figure 6. Description of Injector Configuration 6.

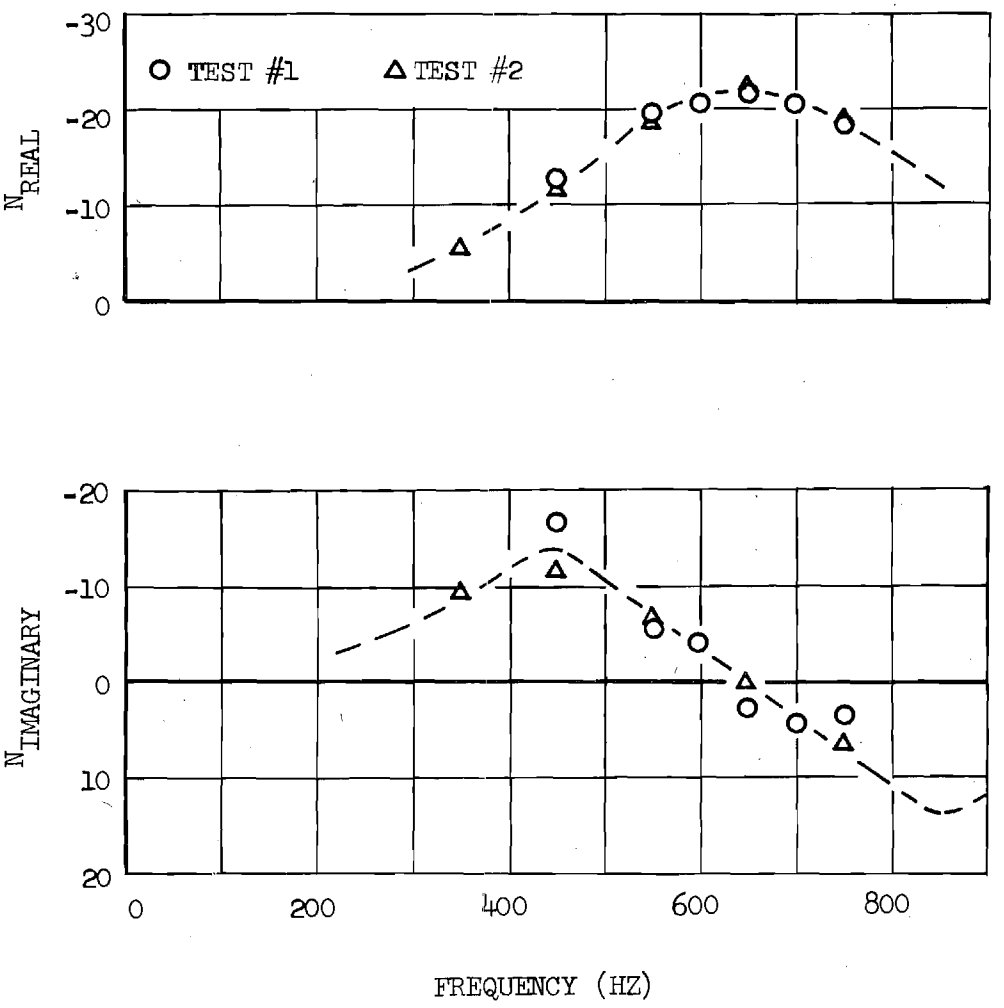

Figure 7. Repeatability of the Measured Response Factor Data.

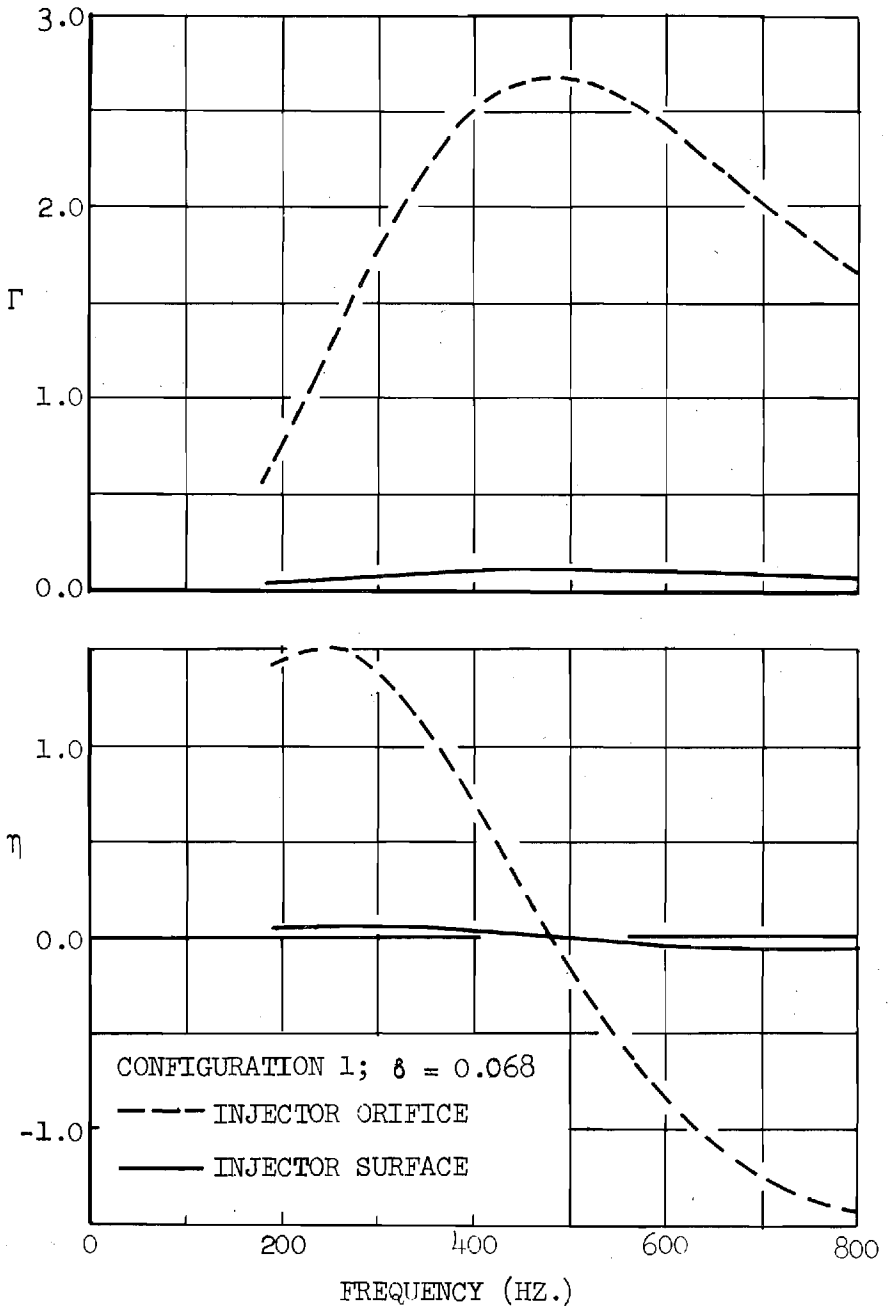

Figure 8. Predicted Admittances for the Injector Configuration 1.

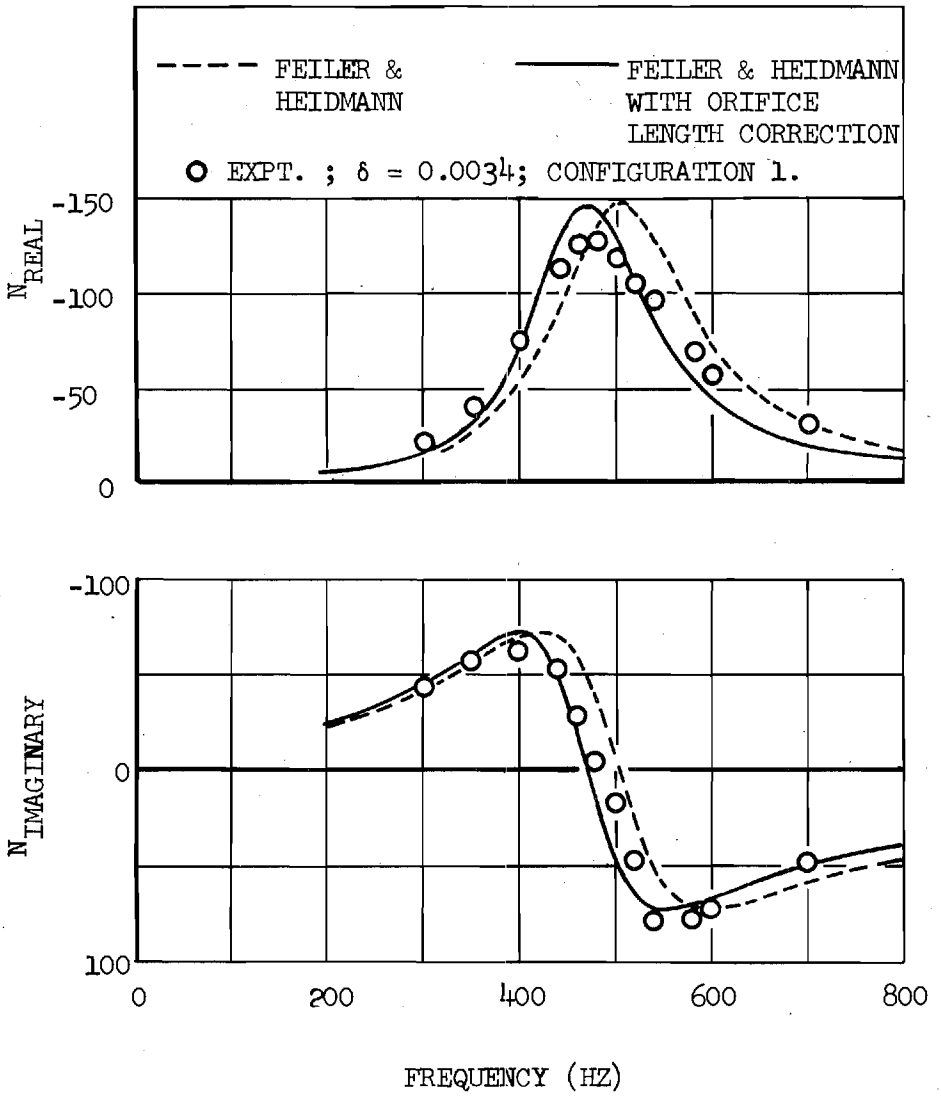

Figure 9. Feiler and Heidmann Predicted Response Factor Data with and without Orifice Length Correction.

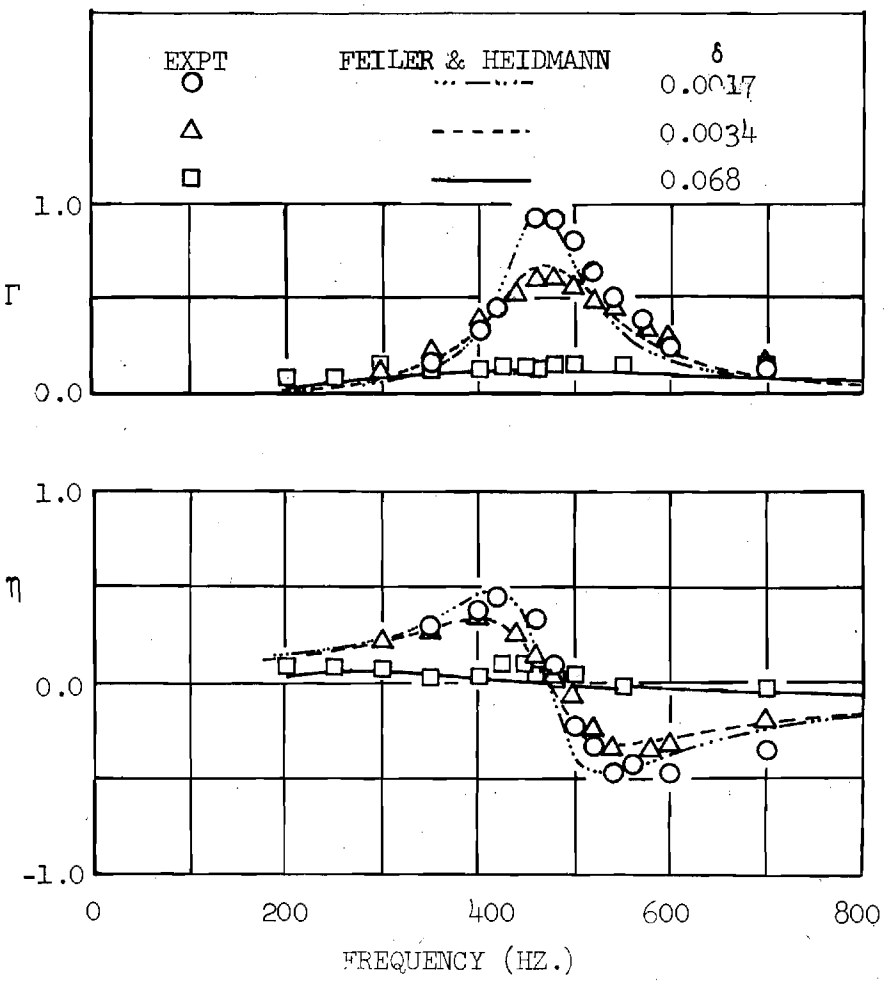

Figure 10. Frequency Dependence of the Surface Admittances of Injector Configuration 1.

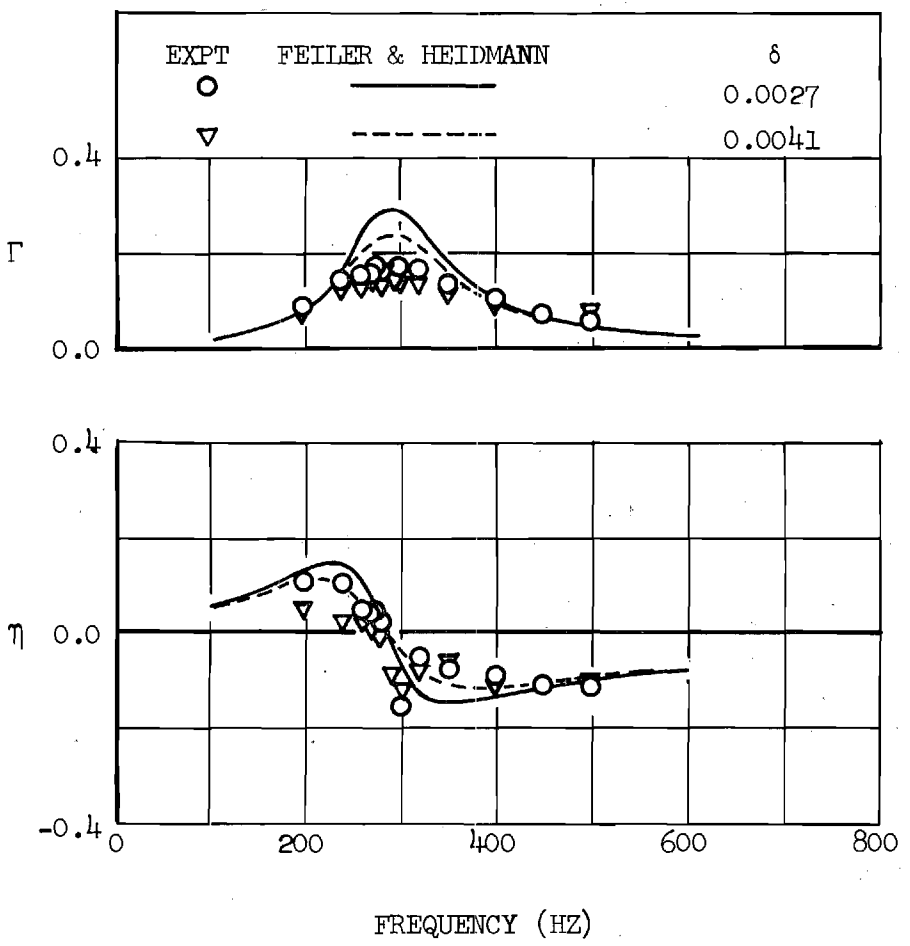

Figure 11. Frequency Dependence of the Surface Admittances of Injector Configuration 2.

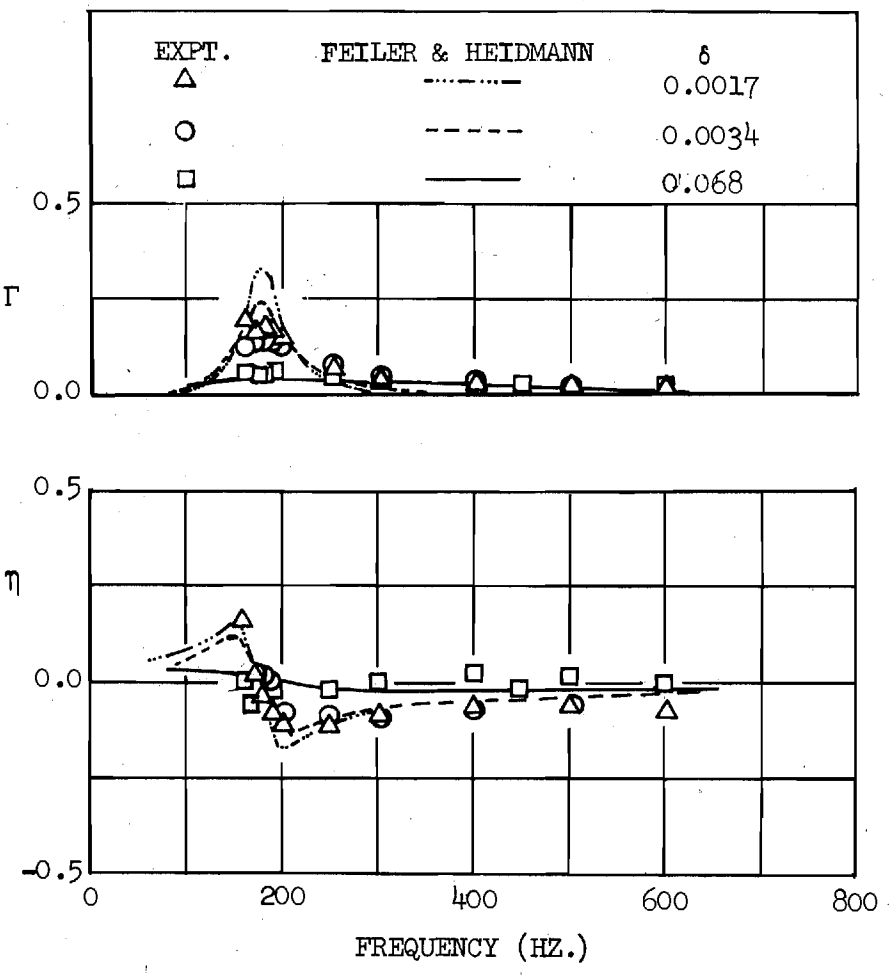

Figure 12. Frequency Dependence of the Surface Admittances of Injector Configuration 3.

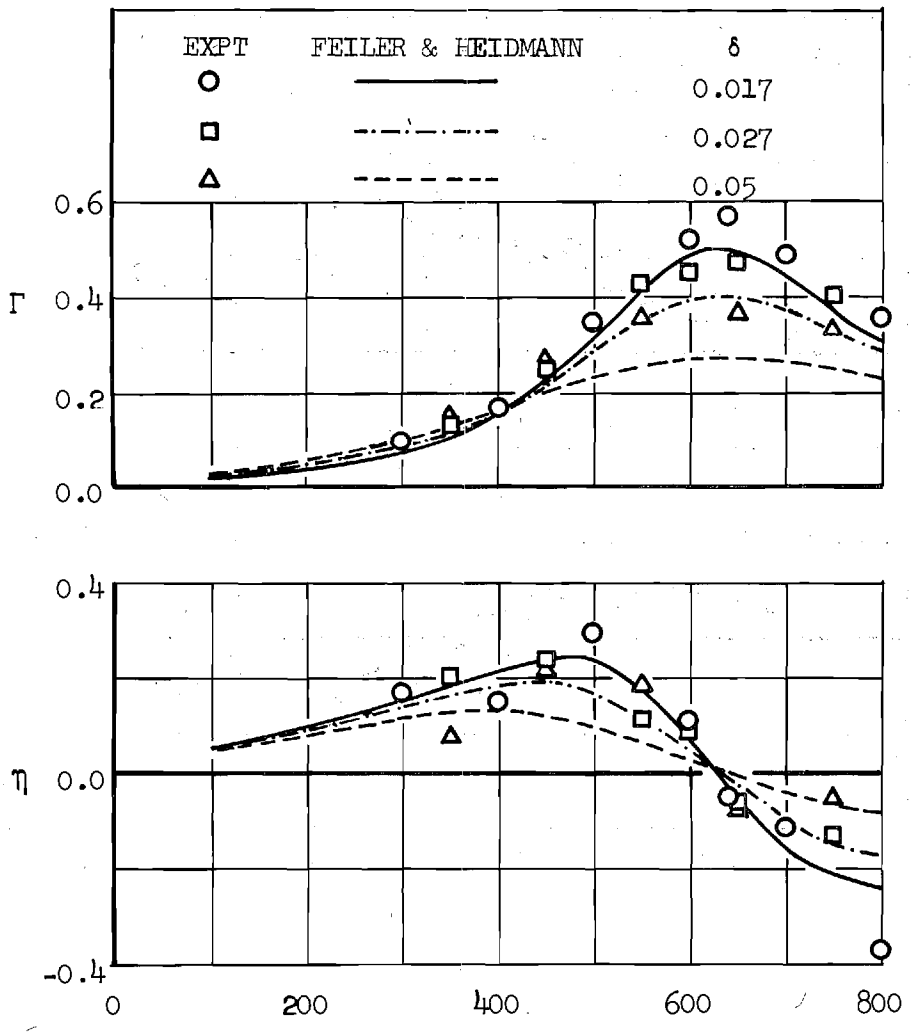

Figure 13. Frequency Dependence of the Surface Admittances of Injector Configuration 4.

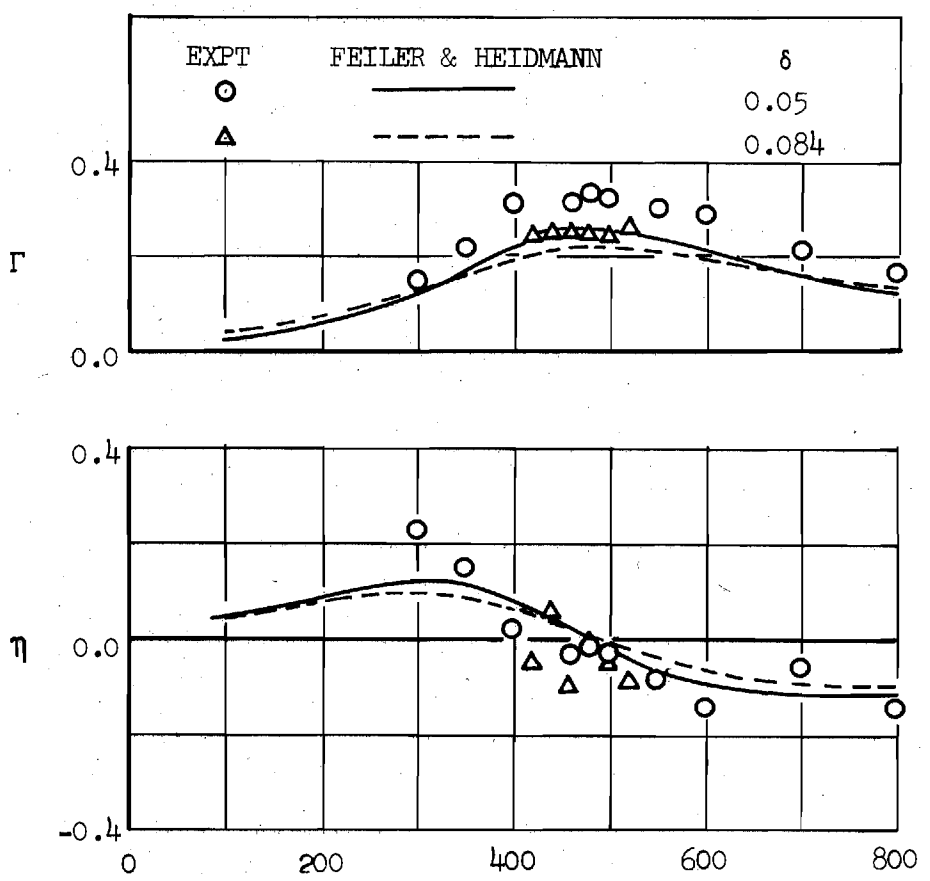

Figure 14. Frequency Dependence of the Surface Admittances of Injector Configuration 5.

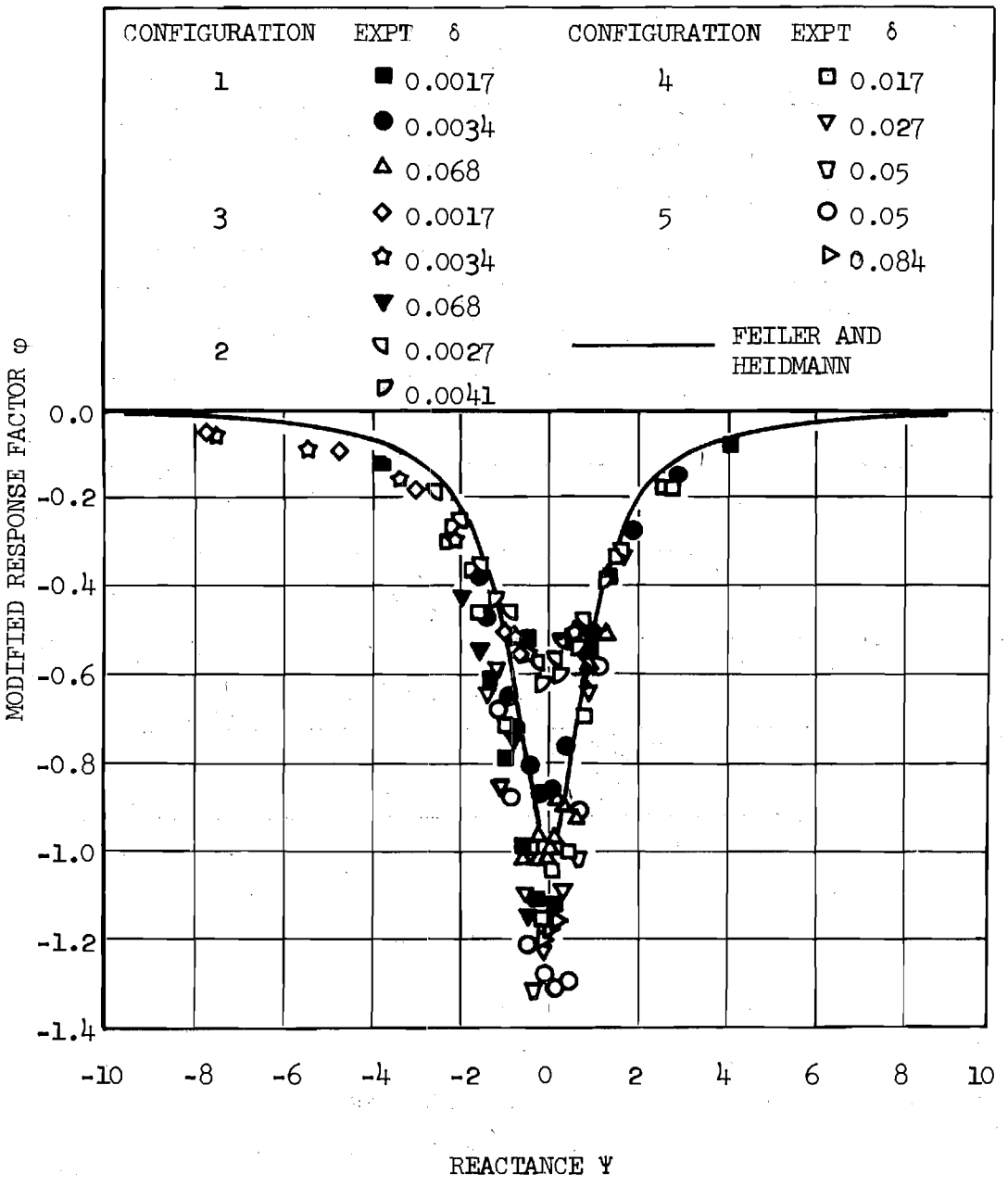

Figure 15. Generalized Response Factor Data Plotted Against Reactance.

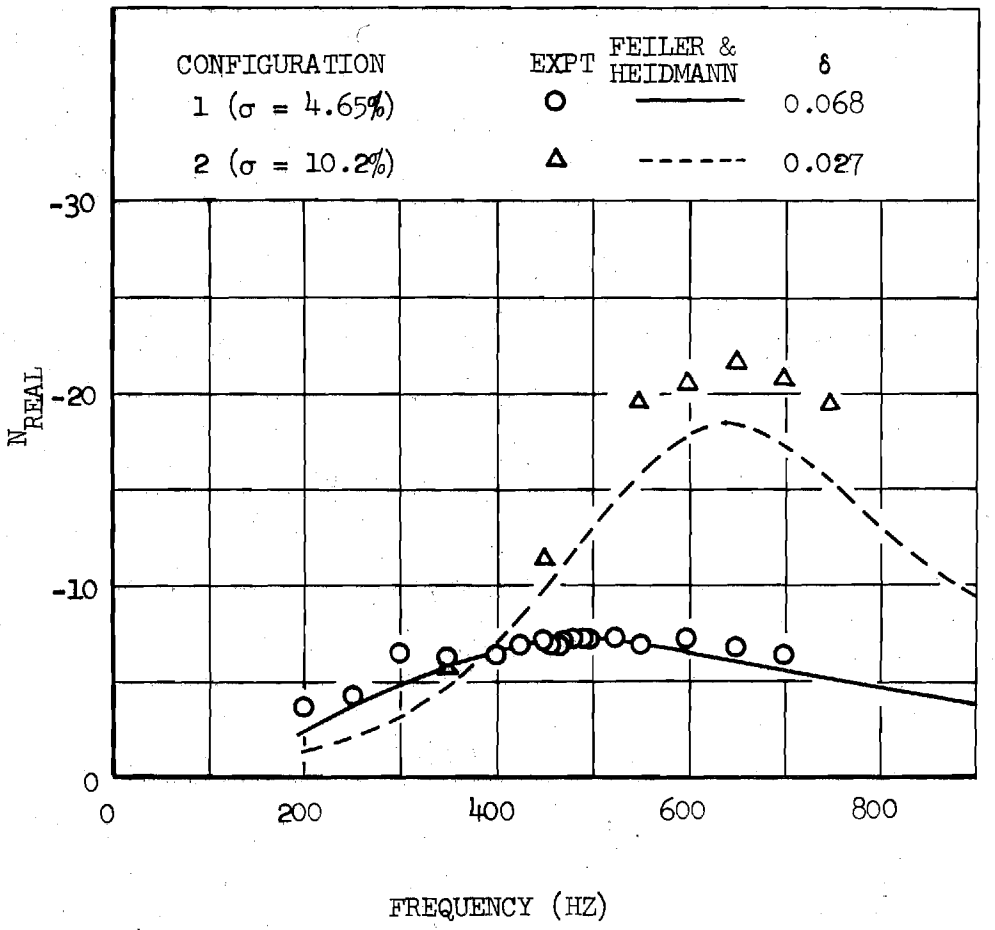

Figure 16. Effect of Open-Area Ratio on Injector Response Factor.

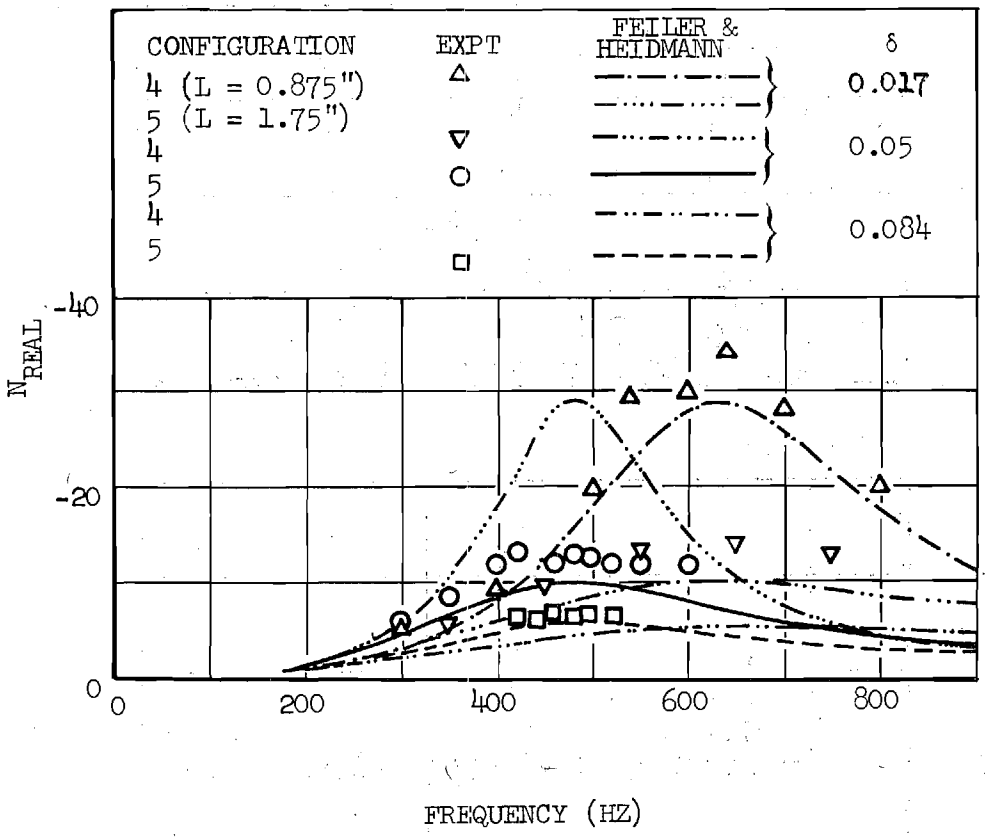

Figure 17. Effect of Orifice Length on Injector Response Factor.

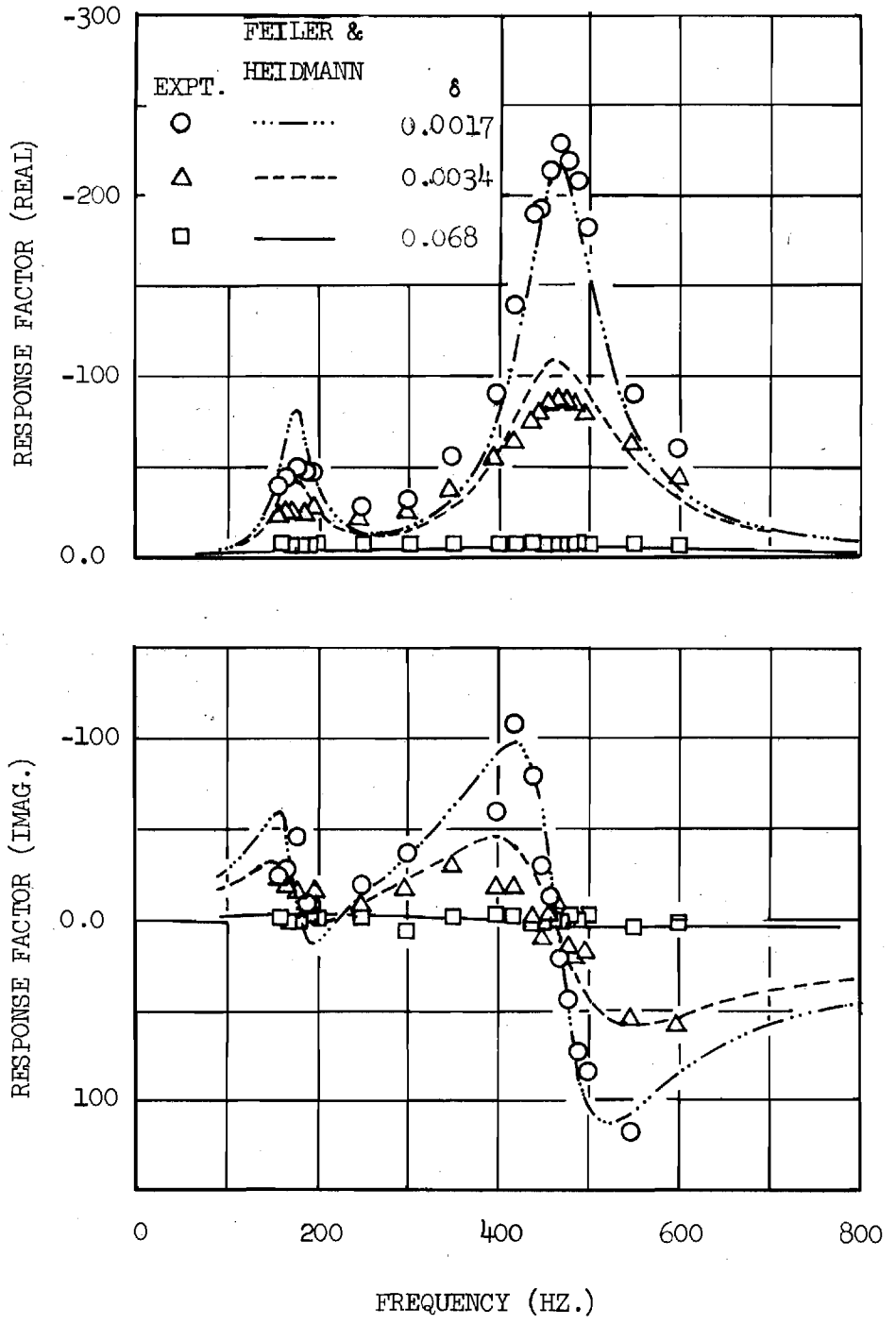

Figure 18. Frequency Dependence of Response Factors of Injector Configuration 6.

REPORT DISTRIBUTION LIST

NASA-Lewis Research Center
Attn: Dr. R. J. Priem/MS 500-204
21000 Brookpark Road
Cleveland, OH 44135
(2 copies)

NASA-Lewis Research Center
Attn: N. T. Musial/MS 500-311
21000 Brookpark Road
Cleveland, OH 44135

NASA-Lewis Research Center
Attn: Library/MS 60-3
21000 Brookpark Road
Cleveland, OH 44135

NASA-Lewis Research Center
Attn: Report Control Office/MS 5-5
21000 Brookpark Road
Cleveland, OH 44135

NASA-Lewis Research Center
Attn: E. A. Bourke/MS 500-205
21000 Brookpark Road
Cleveland, OH 44135

NASA Headquarters
Attn: RPS/Robert A. Wasel
600 Independence Ave., SW, Rm 526
Washington, DC 20546

NASA-Lewis Research Center
Attn: Procurement Section
Mail Stop 500-313
21000 Brookpark Road
Cleveland, OH 44135

NASA-Lyndon B. Johnson Space Center
Attn: EP/Joseph G. Thibodaux
Houston, TX 77058

NASA-George C. Marshall Space
Flight Center
Attn: S&E-ASTN-PP/R. J. Richmond
Huntsville, AL 35812

Aerojet Liquid Rocket Company
Attn: David A. Fairchild
Bldg. 20001/Sec. 9732
P. O. Box 13222
Sacramento, CA 95813

Aerojet General Corporation
Propulsion Division
Attn: R. Stiff
P. O. Box 15847
Sacramento, CA 95803

Aerospace Corporation
Attn: O. W. Dykema
P. O. Box 92957
Los Angeles, CA 90045

Aerospace Corporation
Attn: Library-Documents
2400 E. El Segundo Boulevard
Los Angeles, CA 90045

Air Force Rocket Propulsion
Lab. (RPM)
Attn. Library
Edwards, CA 93523

Air Force Office of Scientific
Research
Chief Propulsion Division
Attn: Dr. J. F. Masi (NAE)
1400 Wilson Boulevard
Arlington, VA 22209

Air Force Rocket Propulsion Lab.
Attn: Daweel George
Edwards, CA 93523

AFAPL
Research & Technology Division
AF Systems Command
U. S. Air Force
Attn: Library/APRP
Wright Patterson AFB, OH 45433

NASA Scientific & Technical Information Facility - Acquisitions Br.
P. O. Box 33
College Park, MD 20740 (10 copies)

Army Ballistics Research Labs.
Attn: Austin W. Barrows
Code AMXBR-1B
Aberdeen Proving Grounds, MD 21005

Army Ballistic Research Labs.
Attn: Ingo W. May
Code AMXBR-1B
Aberdeen Proving Grounds, MD 21005

Army Material Command
Missile Systems Div.
Attn: Stephen R. Matos
Code AMCRD-MT
5001 Eisenhower Ave.
Alexandria, VA 22304

Air Force Systems Command
Arnold Engineering Development Center
Attn: Dr. H. K. Doetsch
Tullahoma, TN 37389

Aeronutronic Div. of Philco Ford Corporation
Technical Information Dept.
Ford Road
Newport Beach, CA 92663

Battelle Memorial Institute
Attn: Report Library, Room 6A
505 King Avenue
Columbus, OH 43201

Bell Aerosystems, Inc.
Attn: Library
Box 1
Buffalo, NY 14205

Bell Aerospace Company
Attn: T. F. Ferger
P. O. Box 1
Mail Zone, J-81
Buffalo, NY 14205

Air Force Rocket Propulsion Lab
Attn: Richard R. Weiss
Edwards, CA 93523

AFAPL
Attn: Frank D. Stull (RJT)
Wright Patterson AFB, OH 45433

California Institute of Technology
Jet Propulsion Laboratory
Attn: Fred E. C. Culick
4800 Oak Grove Drive
Pasadena, CA 91103

California Institute of Technology
Jet Propulsion Laboratory
Attn: Jack H. Rupe
4800 Oak Grove Drive
Pasadena, CA 91103

California State University
Sacramento School of Engineering
Attn: Frederick H. Reardon
6000 J. Street
Sacramento, CA 95819

Chemical Propulsion Information Agency
Johns Hopkins University/APL
Attn: T. W. Christian
8621 Georgia Avenue
Silver Spring, MD 20910

Colorado State University
Attn: Charles E. Mitchell
Fort Collins, CO 80521

Frankford Arsenal
Attn: Martin Visnov
NDP-R, Bldg. 64-2
Bridge & Tacony Streets
Philadelphia, PA 19137

General Electric Company
Flight Propulsion Lab. Dept.
Attn: D. Suichu
Cincinnati, OH 45215

Bureau of Naval Weapons
Department of the Navy
Attn: Library
Washington, DC

Brooklyn Polytechnic Institute
Long Island Graduate Center
Attn: V. D. Agosta
Route 110
Farmingdale, NY 11735

Marquardt Corporation
16555 Saticory Street
Box 2013 - South Annex
Van Nuys, CA 91409

Massachusetts Institute of Tech.
Department of Mechanical Engr.
Attn: T. Y. Toong
77 Massachusetts Avenue
Cambridge, MA 02139

McDonald Douglas Corporation
McDonnell Douglas Astronautics Co.
Attn: William T. Webber
5301 Bolsa Ave.
Huntington Beach, CA 92647

D. E. Mock
Advanced Research Projects Agency
Washington, DC 20525

Lockheed Aircraft Corporation
Lockheed Propulsion Co., Div.
Attn: Norman S. Cohen
P. O. Box 111
Redlands, CA 92373

Naval Postgraduate School
Department of Aeronautics
Attn: David W. Netzer
Monterey, CA 93940

Naval Underwater Systems Center
Energy Conversion Dept.
Attn: Robert S. Lazar, Code 5B331
Newport, RI 02840

Georgia Institute of Technology
School of Aerospace Engineering
Attn: Warren C. Strahle
Atlanta, GA 30332

Georgia Institute of Technology
School of Aerospace Engineering
Attn: Ben T. Zinn
Atlanta, GA 30322

Melvin Gerstein
P. O. Box 452
Altadena, CA 91001

Ohio State University
Department of Aeronautical and
Astronautical Engineering
Attn: R. Edse
Columbus, OH 43210

Pennsylvania State University
Mechanical Engineering Dept.
Attn: G. M. Faeth
207 Mechanical Engineering Bldg.
University Park, PA 16802

Princeton University
Forrestal Campus Library
Attn: Irvin Glassman
P. O. Box 710
Princeton, NJ 08450

Princeton University
Forrestal Campus Library
Attn: David T. Harrje
P. O. Box 710
Princeton, NJ 08540

Princeton University
Forrestal Campus Library
Attn: Martin Summerfield
P. O. Box 710
Princeton, NJ 08540

Propulsion Sciences, Inc.
Attn: Vito Agosta
P. O. Box 814
Melville, NY 11746

Georgia Institute of Technology
School of Aerospace Engineering
Attn: Edward W. Price
Atlanta, GA 30332

Naval Weapons Center
Attn: Charles J. Thelan, Code 4305
China Lake, CA 93555

Naval Postgraduate School
Department of Aeronautics
Attn: Allen F. Fuhs
Monterey, CA 93940

Research and Development Associates
Attn: Raymond B. Edelman
P. O. Box 3580
525 Wilshire Blvd.
Santa Monica, CA 90402

Rockwell International Corp.
Rocketdyne Division
Attn: L. P. Combs, D/991-350
Zone 11
6633 Canoga Avenue
Canoga Park, CA 91304

Rockwell International Corp.
Rocketdyne Division
Attn: James A. Nestlerode
Dept. 596-124, AC46
6633 Canoga Ave.
Canoga Park, CA 91304

Rockwell International Corp.
Rocketdyne Division
Attn: Carl L. Oberg
Dept. 589-197-SS11
6633 Canoga Ave.
Canoga Park, CA 91304

Rockwell International Corp.
Rocketdyne Division
Attn: Library Dept. 596-306
6633 Canoga Avenue
Canoga Park, CA 91304

Purdue University
Jet Propulsion Laboratory
Project Squid
Attn: Robert Goulard
West Lafayette, IN 47907

Purdue University Res. Foundation
School of Mechanical Engineering
Attn: John R. Osborn
Thermal Sci. Propulsion Center
West Lafayette, IN 47906

Purdue University Res. Foundation
School of Mechanical Engineering
Attn: Bruce A. Reese
Thermal Sci. Propulsion Center
West Lafayette, IN 47906

Tennessee Technological University
Dept. of Mech. Engrg.
Attn: Kenneth R. Purdy
P. O. Box 5014
Cookeville, TN 38501

Textron, Inc.
Bell Aerospace, Div.
Research Department
Attn: John R. Morgenthaler, C-84
P. O. Box One
Buffalo, NY 14240

TRW, Inc.
TRW Systems Gp.
Attn: A. C. Ellings
One Space Park
Redondo Beach, CA 90278

TRW Systems
Attn: G. W. Elveran
One Space Park
Redondo Beach, CA 90278

TRW Systems Group
STL Tech. Lib. Doc. Acquisitions
One Space Park
Redondo Beach, CA 90278

Stanford Research Institute
333 Ravenswood Avenue
Menlo Park, CA 94025

Susquehanna Corporation
Atlantic Research Division
Attn: Library
Shirley Highway and Edsall Rd.
Alexandria, VA 22314

TISIA
Defense Documentation Center
Cameron Station, Bldg. 5
5010 Duke Street
Alexandria, Va. 22314

United Aircraft Corporation
Pratt & Whitney Aircraft Div.
Attn: Thomas C. Mayes
P. O. Box 2691
West Palm Beach, FL 33402

United Aircraft Corporation
United Technology Center
Attn: Library
P. O. Box 358
Sunnyvale, CA 94088

University of California, Berkeley
Dept. of Mechanical Engineering
Attn: A. K. Oppenheim
Berkeley, CA 94720

University of Michigan
Attn: James A. Nicholls
P. O. Box 622
Ann Arbor, MI 48107

University of Wisconsin
Mechanical Engineering Dept.
Attn: P. S. Myers
1513 University Avenue
Madison, WI 53706

Office of Assistnat Director
(Chemical Technician)
Office of the Director of Defense
Research & Engineering
Washington, DC 20301

Tulane University
Attn: J. C. O'Hara
6823 St. Charles Ave.
New Orleans, LA 70118

Ultrasystems, Inc.
Attn: Thomas J. Tyson
500 Newport Center Dr.
Newport Beach, CA

United Aircraft Corp.
Pratt & Whitney Division
Florida Research & Development
Center
Attn: Library
West Palm Beach, FL 33402

United Aircraft Corporation
Attn: R. H. Woodward Waesche
400 Main Street
East Hartford, CT 06108

University of California
Aerospace Engineering Dept.
Attn: F. A. Williams
P. O. Box 109
LaJolla, CA 92037

University of Illinois
Aeronautics/Astronautic Eng. Dept.
Attn: R. A. Strehlow
Trans. Bldg., Room 101
Urbana, IL 61801

University of Utah
Dept. of Chemical Engineering
Attn: Alva D. Baer
Bark Bldg., Room 307
Salt Lake City, UT 84112

U. S. Naval Research Laboratory
Director (Code 6180)
Attn: Library
Washington, DC 20390

Virginia Polytechnic Institute
State University
Attn: J. A. Schetz
Blacksburg, VA 24061

Journal of Sound and Vibration (1973) **30**(2), 179–190

EXPERIMENTAL AND THEORETICAL DETERMINATION OF THE ADMITTANCES OF A FAMILY OF NOZZLES SUBJECTED TO AXIAL INSTABILITIES†

W. A. BELL, B. R. DANIEL AND B. T. ZINN
Georgia Institute of Technology,
School of Aerospace Engineering, Atlanta, Georgia 30332, *U.S.A.*

(*Received* 3 *March* 1973)

In combustion instability analyses of rocket engines, it is necessary to determine the interaction between the oscillations in the combustor and the wave system in the nozzle. This interaction can be specified once the nozzle admittance is known. The present paper is concerned with the experimental and theoretical determination of the admittances of practical nozzles that are subjected to axial oscillations. The impedance tube technique, modified to account for the presence of a mean flow, was used to experimentally measure the one-dimensional nozzle admittances. The modified impedance tube theory and experimental facility used to evaluate the nozzle admittance are briefly discussed in this paper. Crocco's nozzle admittance theory is used to predict the admittances of the tested nozzles for comparison with the experimental data. The theoretical and experimental nozzle admittances are obtained for a family of nozzles having Mach numbers from 0·08 to 0·28, different angles of convergence, and different radii of curvature at the throat and entrance sections. The analytical and experimental results are presented as curves showing the frequency dependence of the real and imaginary parts of the nozzle admittances. Examination of these data shows that the theoretical and experimental admittance values are in good agreement with one another which indicates that existing nozzle admittance theories may be used in practice to predict one-dimensional nozzle admittances.

1. INTRODUCTION

Combustion instability studies are concerned with analyzing the behavior of disturbances (i.e., waves) which may occur in the combustors of rocket engines as a result of such phenomena as local explosions that result from uneven distribution of unburned propellants, malfunction of the feed system in liquid rockets, turbulence, and so on. To determine the stability characteristics of a rocket engine, the interaction between the disturbance and the various processes occurring inside the combustor (e.g., the unsteady combustion process, the mean flow, etc.) and various system components (e.g., the nozzle) must be evaluated to ascertain whether the amplitude of the disturbance will grow or decay with time. Previous studies [1] of combustion instability indicate that the interaction between the nozzle and the combustor wave systems can significantly affect the stability characteristics of the rocket motor. Therefore, the influence of the nozzle on the disturbance inside the combustor is an important consideration in combustion instability analyses. This paper is concerned with both the theoretical and experimental determinations of the effects of various nozzle designs upon the stability of combustors experiencing longitudinal type of instability. Their effects on the three-dimensional instabilities are discussed in reference [2].

† Sponsored under NASA grant NGL 11-002-085; Dr R. J. Priem grant monitor.

The interaction between the combustor and nozzle wave systems may be described by specifying the nozzle admittance which is defined as the complex ratio of the axial velocity perturbation to the pressure perturbation, evaluated at the nozzle entrance. Once the nozzle admittance is known, it can be used to describe the nozzle boundary condition in analytical combustion instability studies and to evaluate the mean wave-energy flux that is crossing the nozzle entrance plane.

In linear combustion instability analyses it is generally assumed that the time dependence of the disturbance is exponential (e.g., $p \propto \exp(\lambda_1 t)$) and the analysis usually attempts to determine how various phenomena affect the magnitude and sign of λ_1. Such an analysis usually establishes the dependence of λ_1 upon the nozzle admittance. For example, Crocco's investigation [3] of linear axial instabilities in liquid propellant rocket motors yielded the following relationship:†

$$\lambda_1 z_e = -(y_r + \gamma M) + \left(\frac{\gamma}{\pi P_{00}}\right) \int_0^{z_e} \frac{dQ_r}{dz} \cos \frac{\omega r_c z}{c} dz +$$

$$+ (2 - \gamma) \frac{\omega r_c}{c} \int_0^{z_e} M \sin \frac{2\omega r_c z}{c} dz.$$

In the above equation, the terms involving Q_r, M, and y_r, respectively, represent the dependence of λ_1 upon the unsteady combustion process, the mean flow Mach number and the oscillations in the nozzle. From the expression for λ_1, it can be seen that when the real part of the nozzle admittance y_r is positive the interaction between the oscillation in the combustor and the oscillation in the nozzle will tend to decrease λ_1 and thus exert a stabilizing influence on the rocket motor; the opposite occurs when y_r is negative.

The prediction of the nozzle admittance has been the subject of several theoretical analyses. In these investigations the mean flow in the nozzle is assumed to be one-dimensional, and the gas is assumed to be ideal and non-reacting. Tsien [4] was the first to study the response of a choked nozzle under the influence of axial pressure and velocity perturbations superimposed upon the steady-state flow. To account for the effect of the nozzle upon engine stability, Tsien introduced a transfer function defined as the ratio of the mass flow perturbation to the chamber pressure perturbation evaluated at the nozzle entrance. Assuming isothermal perturbations and a linear steady-state velocity distribution in the nozzle, Tsien restricted his studies to the limiting cases of very high and very low frequency oscillations. Later, Crocco [1, 5] removed the assumption of isothermal oscillations, extended Tsien's work to include the entire frequency range, and introduced the concept of admittance to study the influence of the nozzle on the combustor oscillations. By assuming a linear steady-state velocity profile and isentropic perturbations in the nozzle, Crocco obtained a hypergeometric equation which he then solved to determine the nozzle admittance. In 1967, Crocco extended his earlier analysis to consider the admittances of choked nozzles with three-dimensional flow oscillations [6]. By numerically integrating the equations governing the wave motion in the nozzle Crocco was able to evaluate the admittances of various nozzle configurations over the frequency range of interest in combustion instability studies. All of the analytical nozzle admittance investigations predict that in the range of frequencies which is of interest in longitudinal combustion instability studies, the real part of the nozzle admittance is positive, implying that the nozzle exerts a stabilizing influence on axial instabilities.

Although the predictions of reference [6] have been widely used in analyses of various axial combustion instability problems (e.g., see reference [7]), the accuracy of these predictions

† A list of nomenclature is given in the Appendix.

has never been fully determined. It is the objective of the present investigation to experimentally and theoretically determine the admittances of a variety of nozzle designs that are of interest in combustion instability studies. In the following sections, the experimental technique and apparatus used to measure nozzle admittances for longitudinal oscillations are discussed. The procedure used to numerically calculate the nozzle admittance from Crocco's theory [6] is then presented. Finally, the theoretical and experimental admittance results are presented for a family of practical nozzles having entrance Mach numbers from 0·08 to 0·24 with different convergent half-angles and different radii of curvature at the throat and entrance sections.

2. EXPERIMENTAL TECHNIQUES

Two techniques have been used previously to measure the one-dimensional nozzle admittance. In 1961, Crocco, Monti and Grey [8] determined the real and imaginary parts of the admittance from direct measurements of the pressure and velocity perturbations at the nozzle entrance. However, the accuracy of the data was limited by wave distortion at higher frequencies, a low signal-to-noise ratio, and difficulties in measuring the velocity perturbations with hot-wire anemometers. The second method, often referred to as the half-power bandwidth technique, was developed by Buffum, Dehority, Slates and Price [9]. The limitations of this technique were later discussed by Culick and Dehority [10], who in conclusion recommended that the classical impedance tube method [11, 12, 13] be adopted for nozzle admittance measurements. In an independent investigation, Bell [14] also concluded that the impedance tube method should be used in the experimental determination of nozzle admittances.

Based on the analyses of references [10] and [14], a modification of the classical impedance tube method was developed for this investigation. The apparatus used in the classical impedance tube technique consists of a smooth-walled cylindrical tube with a sound source at one end and the sample, whose admittance is to be measured, at the other end. The sound source is used to generate a standing wave pattern in the tube. The shape of the resulting standing wave pattern depends upon the admittance of the tested sample. By measuring the spatial dependence of the amplitude of the standing wave in the tube, the admittance of the sample can be determined. In this investigation, the classical impedance tube technique is extended to account for the presence of a one-dimensional mean flow in the tube.

To determine the nozzle admittance in a modified impedance tube experiment, an expression describing the behavior of the standing wave pattern in the tube must first be derived. This expression is obtained by solving the wave equation describing the behavior of a one-dimensional pressure oscillation superimposed upon an axial mean flow. This wave equation is [13]

$$\left(\frac{1}{c}\frac{\partial}{\partial t} + M\frac{\partial}{\partial z}\right)^2 p = \frac{\partial^2 p}{\partial z^2}. \tag{1}$$

The solution of equation (1) can be expressed as follows:

$$p = \exp\left\{i\left(\omega t + \frac{kMz}{1-M^2}\right)\right\}\left[A_+ \exp\left\{\frac{-ikz}{1-M^2}\right\} + A_- \exp\left\{\frac{ikz}{1-M^2}\right\}\right]. \tag{2}$$

Equation (2) describes a standing wave pattern formed by a combination of two simple harmonic waves traveling along the tube; the wave with amplitude A_+ travels in the positive z direction, while the one with amplitude A_- travels in the negative z direction. In impedance

tube analyses, it is convenient to express the axial dependence of the waves in terms of hyperbolic functions. Introducing the relationship

$$A_{\pm} = \tfrac{1}{2}A \exp\{\pm[\pi\alpha - i\pi(\beta + \tfrac{1}{2})]\} \tag{3}$$

into equation (2) yields

$$p = A \exp\left\{i\left(\omega t + \frac{kMz}{1-M^2}\right)\right\} \cosh\left[\pi\alpha - i\pi\left(\beta + \tfrac{1}{2} + \frac{2z}{\lambda}\right)\right]. \tag{4}$$

By letting $z = 0$ at the nozzle entrance, the non-dimensional specific admittance y can be expressed in terms of the parameters α and β. From the definition of the specific admittance,

$$y = \rho c \frac{u}{p}\bigg|_{z=0},$$

and the axial component of the linearized momentum equation [13],

$$\rho c\left(ik + M\frac{\partial}{\partial z}\right)u = -\frac{\partial p}{\partial z},$$

the following expression for y is obtained:

$$y = \coth \pi(\alpha - i\beta) \tag{5}$$

To compute the nozzle admittance from equation (5), α and β must be determined. These parameters can be computed from either pressure amplitude or phase measurements taken axially along the tube. From equation (4) the pressure can be written in the form

$$p = |p|\, e^{i(\omega t + \delta)},$$

where the pressure amplitude $|p|$ is given by

$$|p| = A\left[\cosh^2 \pi\alpha - \cos^2 \pi\left(\beta + \frac{2z}{\lambda}\right)\right]^{1/2} \tag{6}$$

and the phase δ is

$$\delta = \frac{kMz}{1-M^2} + \arctan\left[\tanh \pi\alpha \cot \pi\left(\beta + \frac{2z}{\lambda}\right)\right]. \tag{7}$$

In this study, pressure amplitude measurements are used to obtain values of α and β from which the nozzle admittance is determined. The pressure amplitude measurements are taken at several axial positions along the tube as shown in Figure 1. Knowing the Mach number from the nozzle contraction ratio, and measuring the frequency and temperature directly, one can then determine the wavelength λ from the following relation:

$$\lambda = \frac{c(1-M^2)}{f},$$

where $c = (\gamma RT)^{1/2}$. As shown in Figure 1, increasing α decreases the difference in amplitude between the maxima and minima along the standing wave. Varying β changes the positions of the minima or maxima relative to the location of the nozzle entrance. By taking several pressure amplitude measurements along the length of the tube, it is possible to determine α and β.

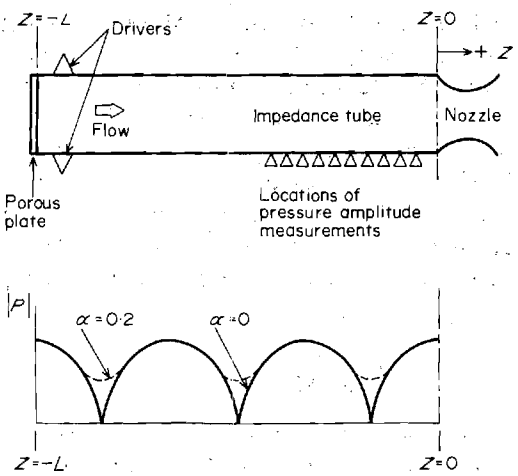

Figure 1. Modified impedance tube experiment.

In principle, only three amplitude measurements at different axial locations are required to solve for the three unknowns α, β, and A by use of equation (6). However, Gately and Cohen [15] have shown that large errors in α may result from relatively small errors in pressure amplitude measurements when only three pressure amplitudes are used. This observation was verified in this study, and it was attributed to the fact that three amplitude measurements do not yield enough information about the shape of the standing wave pattern from which α and β are determined. To improve the accuracy of the measured nozzle admittances, it is desirable to take as many pressure amplitude measurements as possible, at different axial locations, to better diagnose the shape of the standing wave pattern. In the experiments conducted in this investigation, ten pressure amplitude measurements have been taken.

To compute α and β from the measured amplitude data the method of non-linear regression [16] is used. This method consists of finding the values of α, β, and A which provide the best fit between the experimental amplitude data and equation (6). This is accomplished by computing the values of α, β, and A which minimize the r.m.s. deviation between the theoretical amplitude predictions and the corresponding experimental data. To determine the minimum r.m.s. deviation, the following function F is minimized:

$$F = \sum_{i=1}^{n} [E_i - T_i(\alpha, \beta, A)]^2. \tag{8}$$

In the above expression, n is the number of pressure amplitude measurements; $3 \leqslant n \leqslant 10$ for the present experiment. For a given pressure amplitude measurement E_i taken at a distance z_i from the nozzle entrance, the corresponding theoretical pressure amplitude is T_i, and it is obtained from equation (6); that is,

$$T_i = A\left[\cosh^2 \pi\alpha - \cos^2 \pi\left(\beta + \frac{2z_i}{\lambda}\right)\right]^{1/2}. \tag{9}$$

At the location where F is a minimum

$$\frac{\partial F}{\partial \alpha} = \frac{\partial F}{\partial \beta} = \frac{\partial F}{\partial A} = 0. \tag{10}$$

Equation (10) yields three non-linear equations which are solved numerically for the three unknowns α, β, and A.

Equation (10) is solved numerically by use of Marquardt's algorithm [16, 17]. This algorithm is an extension of the Newton–Raphson iteration scheme which keeps the rapid convergence properties of the Newton–Raphson method and improves its stability characteristics at the same time. To start the iteration, equation (8) is solved explicitly for α, β, and A, combinations of three amplitude measurements being used. For ten amplitude measurements taken axially along the tube, 120 combinations of three different pressure amplitudes can be obtained. The computed set of values of α, β, and A which gives the minimum value of F in equation (8) is then used to start the numerical iteration. The values of α and β obtained from the iteration are then used to compute the real and imaginary parts of the admittance from equation (5).

3. APPARATUS

The experimental apparatus, described in detail in reference [14], is a modified impedance tube apparatus designed to accommodate a one-dimensional mean flow through the tube. As shown in Figure 1, the regulated air flow enters the 10 ft long, 12 inch diameter impedance tube through a porous plate at the driven end and is exhausted through the nozzle under investigation, which is attached to the other end of the tube. The pressure in the impedance tube is maintained at a sufficiently high level to assure sonic flow at the nozzle throat throughout the test.

A standing wave pattern is superimposed upon the mean flow by two electropneumatic drivers which are positioned opposite to one another on the walls of the tube immediately downstream of the injector plate. To measure the pressure amplitude of the standing wave pattern in the tube, pressure transducers are located from 1 to 60 inches from the nozzle entrance along the length of the tube. Provisions have also been made for the installation of thermocouples and for static pressure monitoring.

During a test the frequency of the generated axial waves is varied linearly by a sweep oscillator. The signals from the sweep oscillator, pressure transducers, and thermocouple are continuously recorded during testing by a 14-channel tape recorder. Upon completion of a test, the pressure amplitude data is Fourier analysed (i.e., filtered), the signal from the sweep oscillator being used as a reference signal. For each frequency of interest the filtered pressure amplitude data together with the measured temperature data, used to compute the speed of sound, are input into a computer program which employs the non-linear regression method to obtain the nozzle admittance values over a range of the non-dimensional frequency S.

In this study, nozzle admittance data are obtained for a series of axisymmetric nozzles. The contour of these nozzles, shown in Figure 2, is generated by a circular arc of radius r_{cc}

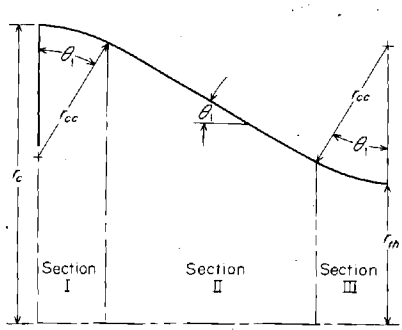

Figure 2. Nozzle contour geometry.

TABLE 1

Parameters of nozzles tested

	M		
θ_1	0·08	0·16	0·24
15	0·44, 1·0†	0·44	0·44
30	0·44	0·44, 1·0	0·44
45	0·44	0·44	0·44

† r_{cc}/r_c.

which starts at the impedance tube and is turned through the nozzle half-angle θ_1. This arc smoothly connects to a conical nozzle section of half-angle θ_1. This conical section then joins with a circular arc of radius r_{cc} that is also turned through an angle θ_1. The properties of the nozzles tested in this investigation are described in Table 1 which presents the value of the ratio of the radius of curvature to the chamber radius, for each nozzle with a given half-angle θ_1 and a given entrance Mach number M. By testing this group of nozzles, the dependence of the nozzle admittance upon the half-angle, entrance Mach number, and radii of curvature can be determined.

4. NOZZLE ADMITTANCE THEORY

Crocco's theory [6] was used to obtain theoretical nozzle admittance values for comparison with the experimental data. In this study Crocco developed the following expression for the nozzle admittance:

$$y = \frac{-(\rho/\rho_0)\zeta}{(c/c_0)M^2\zeta + iS}, \tag{11}$$

where ζ is a complex quantity whose behavior is governed by the non-linear Riccati equation

$$\frac{d\zeta}{d\varphi} + \zeta^2 = A(\varphi)\zeta + B(\varphi), \tag{12}$$

where

$$A(\varphi) = \left[\left(\frac{c_0}{c}\right)^2 \frac{d(q/c_0)^2}{d\varphi} + 2i\frac{\omega r_c}{c_0}\right] \Big/ \left[\left(\frac{c}{c_0}\right)^2 - \left(\frac{q}{c_0}\right)^2\right],$$

$$B(\varphi) = -\left[\left(\frac{\omega r_c}{c_0}\right)^2 - i\frac{\gamma-1}{2}\left(\frac{\omega r_c}{c_0}\right)M^2\frac{d(q/c_0)^2}{d\varphi}\right] \Big/ \left[\left(\frac{c}{c_0}\right)^2 - \left(\frac{q}{c_0}\right)^2\right]$$

and φ is the non-dimensional steady-state velocity potential. Once ζ is determined from the integration of equation (12), the specific nozzle admittance is readily obtained from equation (11).

To determine ζ for given values of the non-dimensional frequency S and a specific nozzle contour, equation (12) must be numerically integrated. The major difficulty in this integration is that ζ can assume large values over certain ranges of φ, which causes numerical difficulties in the integration scheme. Crocco and Sirignano [6] noted this behavior and developed asymptotic solutions for ζ for use when these difficulties are encountered.

Instead of using the asymptotic theory, a different approach is employed in this study. The problem is resolved by defining a new independent variable

$$\tau = \frac{1}{\zeta}.$$

Thus, as ζ takes on very large values, τ tends toward zero. Introducing the definition of τ into equation (12) gives the following Riccati equation for τ:

$$\frac{d\tau}{d\phi} + A(\phi)\tau + B(\phi)\tau^2 = 1. \tag{13}$$

At those points where ζ becomes very large, equation (13) is integrated instead of equation (12) or (13). Equations (12) and (13) are singular at the throat; consequently the numerical integration must start at that point. Following the procedure used in reference [5], ζ, the mean flow variables, and the coefficients A and B are evaluated at the throat. These values are then used to obtain initial values for the initiation of the numerical integration. Equation (12) and the equations describing the behavior of the mean flow (6) are then integrated by a modified Adams predictor–corrector scheme, a Runge–Kutta scheme of order four being used to start the integration. During the integration the value of ζ is monitored. If the magnitude of ζ exceeds a value at which instabilities can occur in the integration scheme, the integration of equation (12) is terminated, the value of τ at that point is computed, and the integration proceeds with equation (13) being used. Similarly, should the magnitude of τ become excessively large, then the value of ζ is determined at that point and the integration proceeds with equation (12) being used. This process is repeated until the nozzle entrance plane is reached. A computer program which employs this procedure was written and used to calculate the theoretical nozzle admittance values for the nozzles investigated in this study.

5. RESULTS

The experimental values of the nozzle admittance are presented as functions of non-dimensional frequency S in Figures 3 through 6. The range of S covered in this investigation is from zero to the cut-off frequency of the first tangential mode (i.e., $S \simeq 1{\cdot}8$). For values of

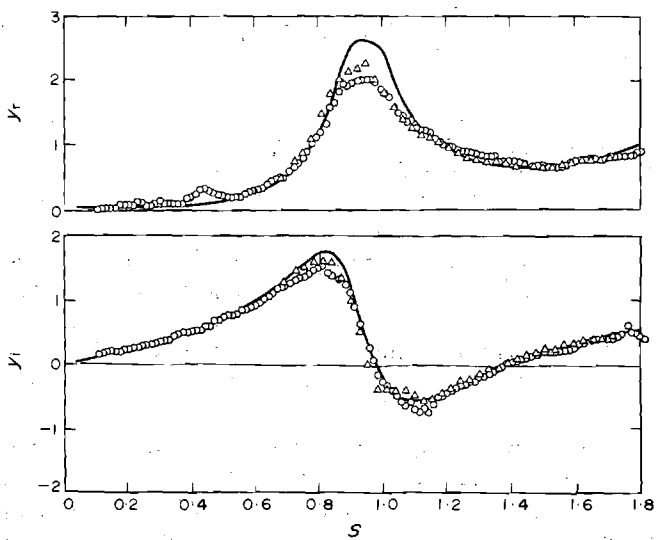

Figure 3. Test-to-test repeatability of experimental nozzle admittance data and comparison with theoretical predictions. $\theta_1 = 15°$, $M = 0{\cdot}08$, $r_{cc}/r_c = 0{\cdot}44$. ○, Experiment, test no. 1; △, experiment, test no. 2; ——, theory.

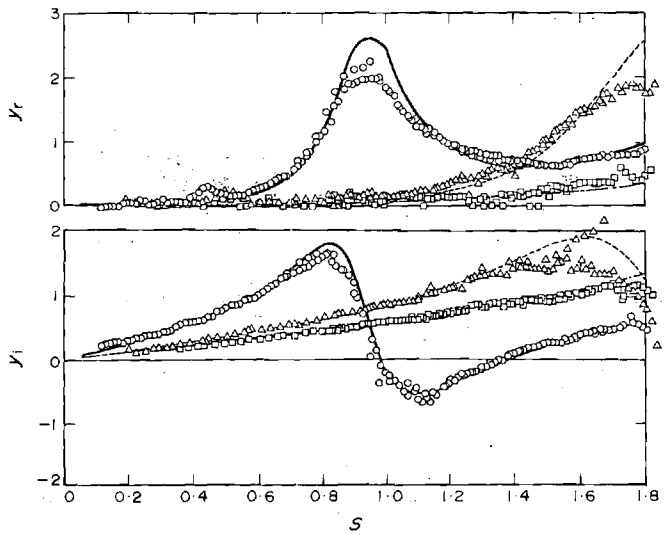

Figure 4. Effect of nozzle half-angle on the experimental and theoretical nozzle admittance values. $M = 0{\cdot}08$, $r_{cc}/r_c = 0{\cdot}44$. $\theta_1 = 15°$: ○, experiment; ——, theory. $\theta_1 = 30°$: △, experiment; – – –, theory. $\theta_1 = 45°$: □, experiment; —·—, theory.

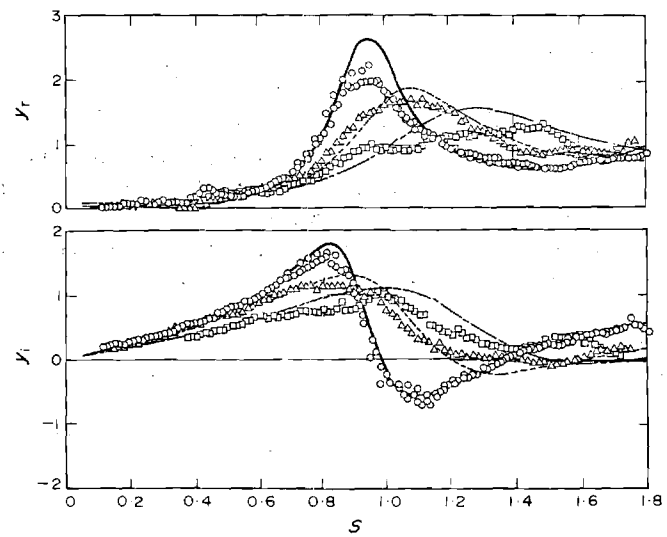

Figure 5. Effect of entrance Mach number on the experimental and theoretical nozzle admittance values. $\theta_1 = 15°$, $r_{cc}/r_c = 0{\cdot}44$. $M = 0{\cdot}08$: ○, experiment; ——, theory. $M = 0{\cdot}16$: △, experiment; – – –, theory. $M = 0{\cdot}24$: □, experiment; ———, theory.

S higher than 1·8, the oscillations in the tube become three-dimensional and purely one-dimensional oscillations cannot be maintained in the impedance tube. The determination of nozzle admittances when the oscillations are three-dimensional is discussed in reference [2]. To indicate the repeatability and reliability of the experimental technique, data from two different tests are compared in Figure 3; the two sets of data are in close agreement. It is also shown in Figure 3 that the theoretical predictions compare quite well with the experimental data.

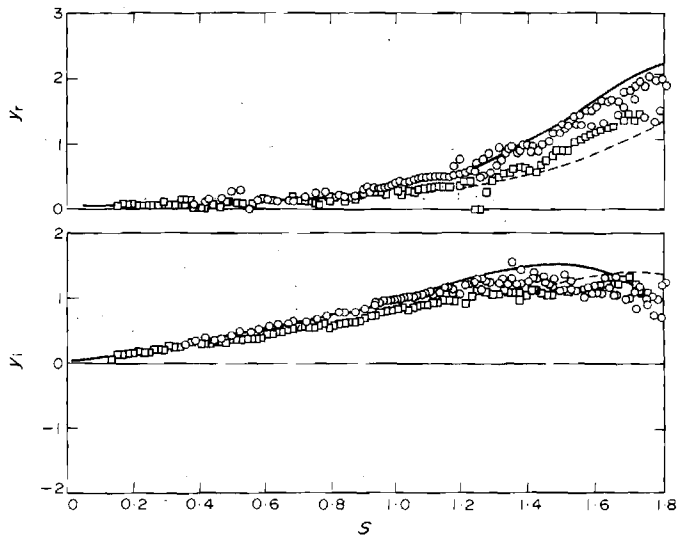

Figure 6. The effect of the ratio of the radius of curvature to chamber radius on the experimental and theoretical nozzle admittance values. $M = 0{\cdot}16$, $\theta_1 = 30°$. $r_{cc}/r_c = 1{\cdot}0$: ○, experiment; ——, theory. $r_{cc}/r_c = 0{\cdot}44$: □, experiment; – – –, theory.

The effects of changing the nozzle geometry and entrance Mach number on the admittance values are presented in Figures 4, 5, and 6. For $M = 0{\cdot}08$ and $r_{cc}/r_c = 0{\cdot}44$, increasing θ_1 tends to increase the frequency at which the maximum values of the real and imaginary parts of the admittance occur, as shown in Figure 4. The effect of varying the entrance Mach number is shown in Figure 5 for $\theta_1 = 15°$ and $r_{cc}/r_c = 0{\cdot}44$. The effect of changing the ratio r_{cc}/r_c from 0·44 to 1·0 is shown in Figure 6 for nozzles with $\theta_1 = 30°$ and $M = 0{\cdot}08$. Examination of Figures 3 through 6 shows that the theoretical and experimental results are, in general, in good agreement to within experimental error and the limitations of the impedance tube theory.† These data also show that at low frequencies where the ratio of the length of the nozzle convergent section to the wavelength is small, the nozzle admittances are almost independent of frequency. At these frequencies these nozzles respond in a quasi-steady manner.

6. CONCLUSIONS

Based on the results of this investigation, the modified impedance tube technique can be used to determine the admittance of a duct termination in the presence of a mean flow. In the present study, quantitative nozzle admittance data were obtained using this technique for a family of nozzles with different entrance Mach numbers, different convergence angles, and different radii of curvature. The theoretical and experimental nozzle admittance data are in close agreement, indicating that Crocco's nozzle admittance theory can be used to predict nozzle admittances needed for longitudinal stability analyses

† For example, in the theory a uniform velocity profile across the tube is assumed, and the presence of a boundary layer near the walls is neglected. However, the good agreement between the theoretical and experimental data obtained in this study suggests that when the impedance tube diameter is large the shear flow near the wall has little effect upon the measured data.

REFERENCES

1. L. Crocco and S. I. Cheng 1956 *AGARDograph No.* 8, *Chapter* I *and Appendix B.* Theory of combustion instability and its experimental verification. London: Butterworth Publications.
2. B. T. Zinn, W. A. Bell, B. R. Daniel and A. J. Smith, Jr. 1973 *American Institute of Aeronautics and Astronautics Journal* **11**, 267. Experimental determination of three-dimensional liquid rocket nozzle admittances.
3. L. Crocco 1965 *Tenth Symposium (International) on Combustion, Pittsburgh, Pennsylvania: Combustion Institute*, 1101–1128. Theoretical studies on liquid-propellant rocket instability.
4. H. S. Tsien 1952 *American Rocket Society Journal* **22**, 139. The transfer function of rocket motors.
5. L. Crocco 1953 *Aerotecnica Roma* **33**, 46. Supercritical gaseous discharge with high frequency oscillations.
6. L. Crocco and W. A. Sirignano 1967 *AGARDograph No.* 117. Behavior of supercritical nozzles under three-dimensional oscillatory conditions. London: Butterworth Publications.
7. A. J. Smith and F. H. Reardon 1968 *Aerojet-General Technical Report No. AFRPL-TR*-67-314, *Vol.* I. The sensitive time lag theory and its application to liquid rocket combustion instability problems.
8. L. Crocco, R. Monti and J. Grey 1961 *American Rocket Society Journal* **31**, 771. Verification of nozzle admittance theory by direct measurement of the admittance parameter.
9. F. G. Buffum, G. L. Dehority, R. O. Slates and E. W. Price 1966 *China Lake, California: Naval Ordnance Test Station, NOTS TP* 3932. Acoustic losses of a subscale cold-flow rocket motor for various "J" values.
10. F. E. C. Culick and G. L. Dehority 1968 *China Lake, California: Naval Weapons Center, NWC Report No.* 4544. An analysis of axial acoustic waves in a cold-flow rocket.
11. R. A. Scott 1946 *Proceedings of the Physical Society* **58**, 253. An apparatus for accurate measurement of the acoustic impedance of sound absorbing materials.
12. W. K. R. Lippert 1953 *Acustica* **3**, 153. The practical representation of standing waves in an acoustic impedance tube.
13. R. M. Morse and K. U. Ingard 1968 *Theoretical Acoustics.* New York: McGraw-Hill Book Company, Inc. See pp. 467 ff.
14. W. A. Bell 1972 *Ph.D. Thesis, Georgia Institute of Technology.* Experimental determination of three-dimensional liquid rocket nozzle admittances.
15. W. S. Gately and R. Cohen 1969 *Journal of the Acoustical Society of America* **46**, 6. Methods for evaluating the performance of small acoustic filters.
16. R. C. Pfahl and B. J. Mitchel 1970 *American Institute of Aeronautics and Astronautics Journal* **8**, 1046. Nonlinear regression methods for simultaneous property measurement.
17. D. W. Marquardt 1963 *Journal of the Society for Industrial and Applied Mathematics* **11**, 431. An algorithm for least-squares estimation of nonlinear parameters.

APPENDIX

NOMENCLATURE

A	constant defined by equation (3), lbf/in^2
A_+	amplitude of a pressure wave moving in the positive z direction, lbf/in^2
A_-	amplitude of a pressure wave moving in the negative z direction, lbf/in^2
$A(\varphi)$, $B(\varphi)$	variable coefficients defined in equation (12)
c	steady-state speed of sound, ft/s
E_i	experimentally measured pressure amplitude at the ith location along the impedance tube, lbf/in^2
f	frequency, Hz
i	$\sqrt{-1}$, imaginary unit
k	wave number $= \omega/c$, radian/ft